BEILSTEIN JOURNAL OF ORGANIC CHEMISTRY

Total synthesis: an enabling science

Edited by Bastien Nay

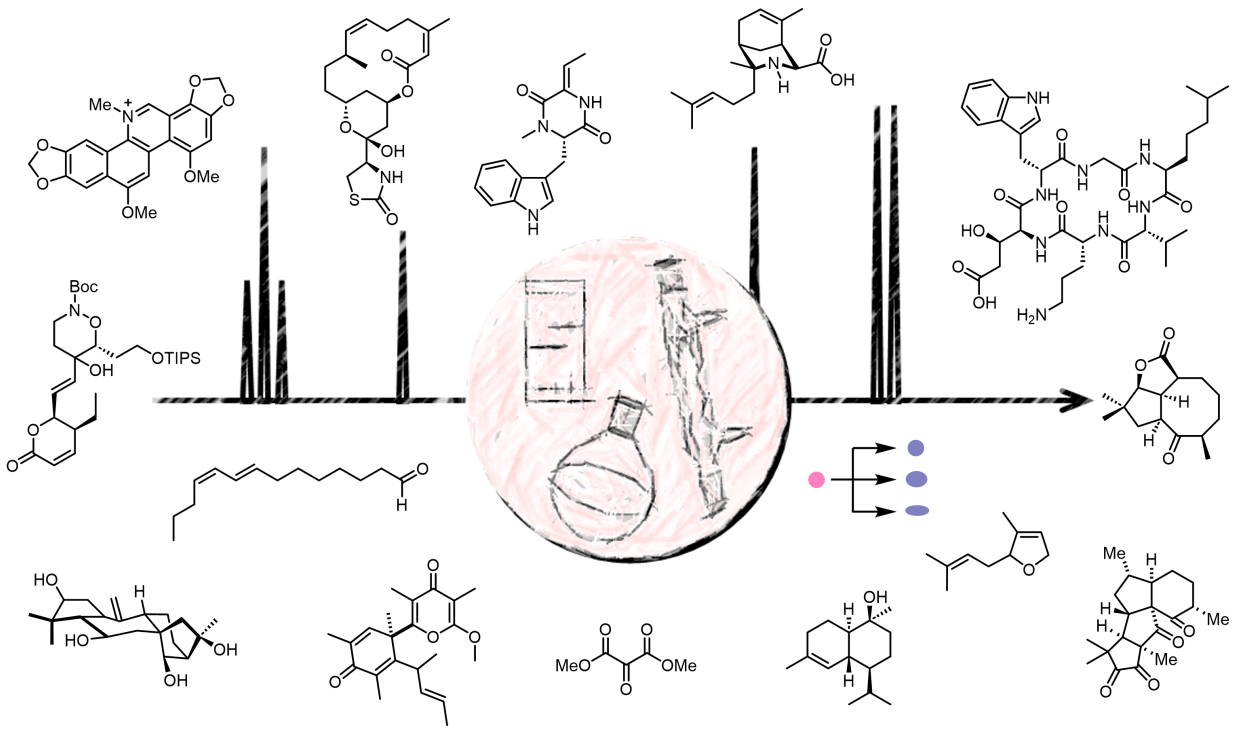

Imprint

Beilstein Journal of Organic Chemistry
www.bjoc.org
ISSN 1860-5397
Email: journals-support@beilstein-institut.de

The *Beilstein Journal of Organic Chemistry* is published by the Beilstein-Institut zur Förderung der Chemischen Wissenschaften.

Beilstein-Institut zur Förderung der Chemischen Wissenschaften
Trakehner Straße 7–9
60487 Frankfurt am Main
Germany
www.beilstein-institut.de

BEILSTEIN JOURNAL OF ORGANIC CHEMISTRY

Total synthesis: an enabling science

Bastien Nay

Editorial

Open Access

Address:
Laboratoire de Synthèse Organique, École Polytechnique, CNRS, ENSTA, Institut Polytechnique de Paris, 91128 Palaiseau, France

Email:
Bastien Nay - bastien.nay@polytechnique.edu

Keywords:
chemical complexity; natural products; synthetic methodologies; total synthesis

Beilstein J. Org. Chem. **2023,** *19,* 474–476.
https://doi.org/10.3762/bjoc.19.36

Received: 06 April 2023
Accepted: 12 April 2023
Published: 19 April 2023

This article is part of the thematic issue "Total synthesis: an enabling science".

Associate Editor: B. Nay

Total synthesis is a topic strongly related to synthetic methodology developments and to natural product isolation or biosynthesis. Thus, thematic issues dealing with total synthesis in the *Beilstein Journal of Organic Chemistry* have naturally been published in these fields, such as "Transition-metal and organocatalysis in natural product synthesis" (edited by D. Chen and D. Ma) [1] or "Natural products in synthesis and biosynthesis" (edited twice by J. Dickschat) [2,3]. Previously, the early thematic issue "Indolizidines and quinolizidines: natural products and beyond" (edited by J. P. Michael) from 2007 [4] displayed some of the very first total syntheses ever published in the *Beilstein Journal of Organic Chemistry*, such as those of frog indolizidine alkaloids [5,6]. However, no thematic issue specifically related to total synthesis has been published before, and we thought it would be time to fill this gap. Although innovative developments are constantly needed to improve methods and strategy, keeping in mind the difficulty of performing transformations on highly functionalized compounds, the total synthesis of complex natural products is indeed mature in terms of efficiency, practicality, economy, and scalability. In short, it has become an enabling science.

Total synthesis is the science of constructing molecules from simple starting materials. It often deals with complex molecular architectures that require a thorough retrosynthetic problem-solving analysis [7]. Total synthesis and the discovery of new synthetic methodologies have always been intimately related. Specific methodologies have often been developed to synthesize valuable compounds, while total synthesis has often been a pretext to demonstrate the value of a new synthetic reaction [8,9]. Old and recent achievements show that connections to other disciplines are important to the success of total synthesis and can be a source of new discoveries. Indeed, as a science allowing the preparation of useful functional compounds, it is strongly connected to biological and medicinal studies, while the development of natural-product-based tools for chemical biology often requires the construction of complex molecules [10,11]. Incidentally, the term "total synthesis" is not limited to natural products but also, sometimes, targets complex drugs [12,13]. Furthermore, it is possible to test biosynthetic hypotheses concerning natural products through synthetic approaches (biomimetic synthesis) [14]. In addition, total syntheses have also been achieved with enzymes, strengthening the links to biology [15].

Total synthesis is not limited to academic laboratories but rather also pursued in industry, where a particular efficiency and economy of tasks is of paramount importance [12], as illus-

trated in this thematic issue with the synthesis of pheromones [16]. This requires permanent technological progress. Thus, the recent boom of artificial intelligence, machine learning, and computational chemistry for retrosynthetic analyses and beyond foreshadows a renewed interest in harvesting increasingly complex synthetic strategies for industrial processes. Although it can be useful in operating routine processes, AI will not replace human creativity [17]. In terms of discoveries in organic chemistry, total synthesis is a fruitful feed, and serendipity has well been exploited. Even dead ends, yet always heartbreaking for synthetic chemists, still provide a wealth of useful information for the chemical community [18]. Finally, this is not to forget that organic chemistry, which is above all an experimental science, is performed daily by researchers in the laboratory, and some of these lives can be truly inspiring to current and future generations.

It was the aim of this thematic issue to cover any of the previous remarks. Thanks to the contributions of talented and enthusiastic authors, we were able to gather articles on total synthesis (Figure 1), not only illustrating the utility but also the vitality of this field.

I warmly thank all the authors of this thematic issue for their beautiful contributions. I also thank the Editorial Team of the *Beilstein Journal of Organic Chemistry* for their significant efforts in checking, formatting, and finally subtilizing all these articles.

Bastien Nay

Palaiseau, April 2023

ORCID® iDs

Bastien Nay - https://orcid.org/0000-0002-1209-1830

References

1. Transition-metal and organocatalysis in natural product synthesis. https://www.beilstein-journals.org/bjoc/series/32 (accessed April 12, 2023).
2. Natural products in synthesis and biosynthesis. https://www.beilstein-journals.org/bjoc/series/36 (accessed April 12, 2023).
3. Natural products in synthesis and biosynthesis II. https://www.beilstein-journals.org/bjoc/series/57 (accessed April 12, 2023).
4. Indolizidines and quinolizidines: natural products and beyond. https://www.beilstein-journals.org/bjoc/series/2 (accessed April 12, 2023).
5. Toyooka, N.; Zhou, D.; Nemoto, H.; Garraffo, H. M.; Spande, T. F.; Daly, J. W. *Beilstein J. Org. Chem.* **2007,** *3,* No. 29. doi:10.1186/1860-5397-3-29

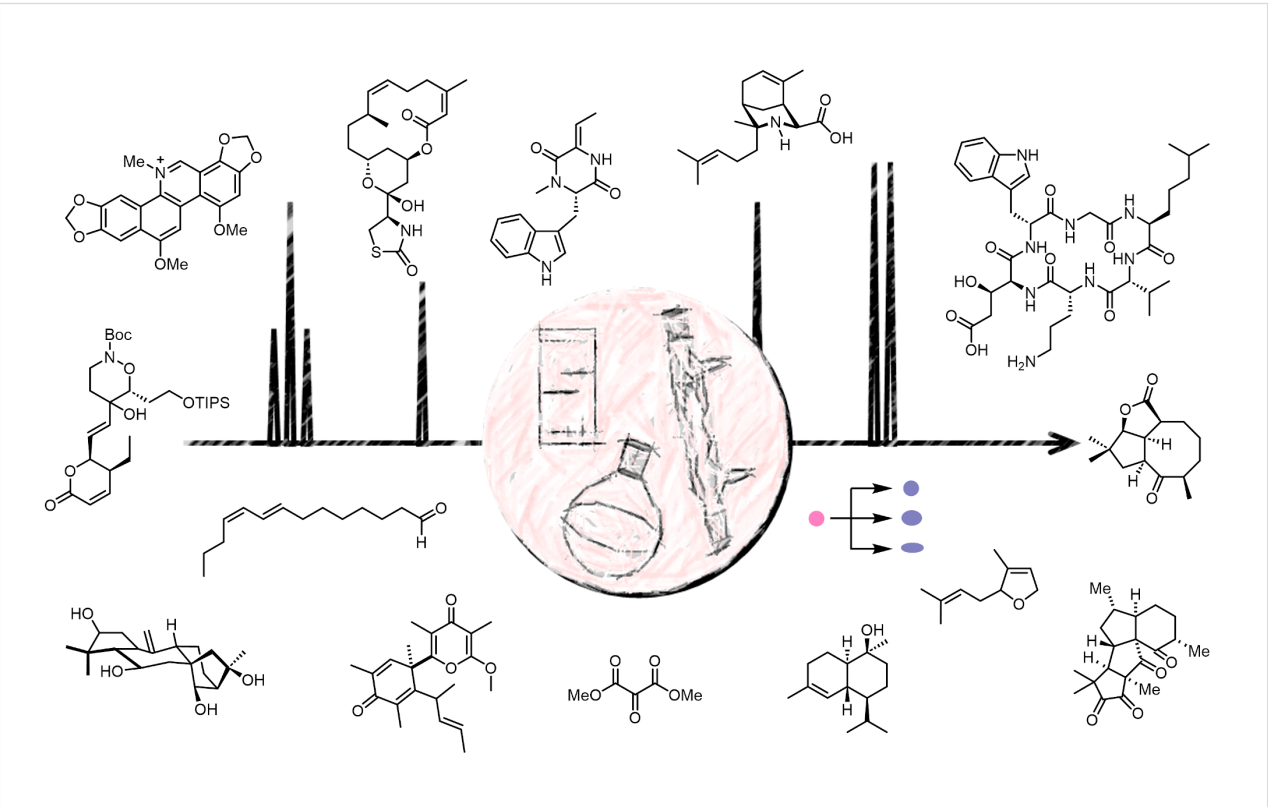

Figure 1: A summary of compounds targeted in this thematic issue.

6. Kobayashi, S.; Toyooka, N.; Zhou, D.; Tsuneki, H.; Wada, T.; Sasaoka, T.; Sakai, H.; Nemoto, H.; Garraffo, H. M.; Spande, T. F.; Daly, J. W. *Beilstein J. Org. Chem.* **2007,** *3,* No. 30. doi:10.1186/1860-5397-3-30
7. Corey, E. J.; Cheng, X.-M. *The Logic of Chemical Synthesis;* Wiley: Hoboken, NJ, USA, 1995.
8. Brown, D. G.; Boström, J. *J. Med. Chem.* **2016,** *59,* 4443–4458. doi:10.1021/acs.jmedchem.5b01409
9. Nicolaou, K. C.; Rigol, S.; Yu, R. *CCS Chem.* **2019,** *1,* 3–37. doi:10.31635/ccschem.019.20190006
10. Wetzel, S.; Bon, R. S.; Kumar, K.; Waldmann, H. *Angew. Chem., Int. Ed.* **2011,** *50,* 10800–10826. doi:10.1002/anie.201007004
11. Wu, Z.-C.; Boger, D. L. *Nat. Prod. Rep.* **2020,** *37,* 1511–1531. doi:10.1039/d0np00060d
12. Yu, M. J.; Zheng, W.; Seletsky, B. M. *Nat. Prod. Rep.* **2013,** *30,* 1158–1164. doi:10.1039/c3np70051h
13. Hayashi, Y.; Ogasawara, S. *Org. Lett.* **2016,** *18,* 3426–3429. doi:10.1021/acs.orglett.6b01595
14. Poupon, E.; Nay, B., Eds. *Biomimetic Organic Synthesis;* Wiley-VCH: Weinheim, Germany, 2011. doi:10.1002/9783527634606
15. Roberts, A. A.; Ryan, K. S.; Moore, B. S.; Gulder, T. A. M. Total (Bio)Synthesis: Strategies of Nature and of Chemists. In *Natural Products via Enzymatic Reactions;* Piel, J., Ed.; Topics in Current Chemistry, Vol. 297; Springer: Berlin, Heidelberg, 2010; pp 149–203. doi:10.1007/128_2010_79
16. Gayon, E.; Lefèvre, G.; Guerret, O.; Tintar, A.; Chourreu, P. *Beilstein J. Org. Chem.* **2023,** *19,* 158–166. doi:10.3762/bjoc.19.15
17. Empel, C.; Koenigs, R. M. *Angew. Chem., Int. Ed.* **2019,** *58,* 17114–17116. doi:10.1002/anie.201911062
18. Sierra, M. A.; de la Torre, M. C.; Cossío, F. P. *More Dead Ends and Detours: En Route to Successful Total Synthesis;* Wiley-VCH: Weinheim, Germany, 2013. doi:10.1002/9783527654628

License and Terms

BEILSTEIN JOURNAL OF ORGANIC CHEMISTRY

Synthesis of tryptophan-dehydrobutyrine diketopiperazine and biological activity of hangtaimycin and its co-metabolites

Houchao Xu[1], Anne Wochele[2], Minghe Luo[3], Gregor Schnakenburg[4], Yuhui Sun[3], Heike Brötz-Oesterhelt[2] and Jeroen S. Dickschat[*1]

Letter

Open Access

Address:
[1]Kekulé-Institute of Organic Chemistry and Biochemistry, University of Bonn, Gerhard-Domagk-Straße 1, 53121 Bonn, Germany, [2]Interfaculty Institute of Microbiology and Infection Medicine, Department of Microbial Bioactive Compounds, University of Tübingen, Auf der Morgenstelle 28, 72076 Tübingen, Germany, [3]Key Laboratory of Combinatorial Biosynthesis and Drug Discovery, Ministry of Education, and School of Pharmaceutical Sciences, Wuhan University, No. 185 East Lake Road, Wuhan, 430071, People's Republic of China and [4]Institute of Inorganic Chemistry, University of Bonn, Gerhard-Domagk-Straße 1, 53121 Bonn, Germany

Email:
Jeroen S. Dickschat[*] - dickschat@uni-bonn.de

* Corresponding author

Keywords:
antibiotics; enantioselective synthesis; peptides; racemisation; *Streptomyces*

Beilstein J. Org. Chem. **2022,** *18,* 1159–1165.
https://doi.org/10.3762/bjoc.18.120

Received: 12 July 2022
Accepted: 29 August 2022
Published: 07 September 2022

This article is part of the thematic issue "Total synthesis: an enabling science".

Associate Editor: B. Nay

Abstract

An improved synthesis for tryptophan-dehydrobutyrine diketopiperazine (TDD), a co-metabolite of the hybrid polyketide/non-ribosomal peptide hangtaimycin, starting from L-tryptophan is presented. Comparison to TDD isolated from the hangtaimycin producer *Streptomyces spectabilis* confirmed its *S* configuration. The X-ray structure of the racemate shows an interesting dimerisation through hydrogen bridges. The results from bioactivity testings of hangtaimycin, TDD and the hangtaimycin degradation product HTM_{222} are given.

Introduction

Hangtaimycin (**1**, Scheme 1) was first isolated from *Streptomyces spectabilis* and shown to possess weak antimicrobial activity against *Bacillus subtilis* [1]. Together with a structural revision from 29*Z* to 29*E* configuration and further biological evaluation of its hepatoprotective properties, its biosynthetic gene cluster was recently identified [2]. The biosynthetic machinery is composed of a hybrid *trans*-acyltransferase (*trans*-AT, [3,4]) polyketide synthase (PKS) and non-ribosomal peptide synthase (NRPS) [2] with a dehydrating bimodule [5,6] involved in the installation of the remaining *Z*-configured double bond within the polyketide backbone [7]. Furthermore, a cytochrome P450 monooxygenase was recently shown to be responsible for the oxidation of deoxyhangtaimycin (**3**), a compound with antiviral activity, to **1** [8]. The thereby installed

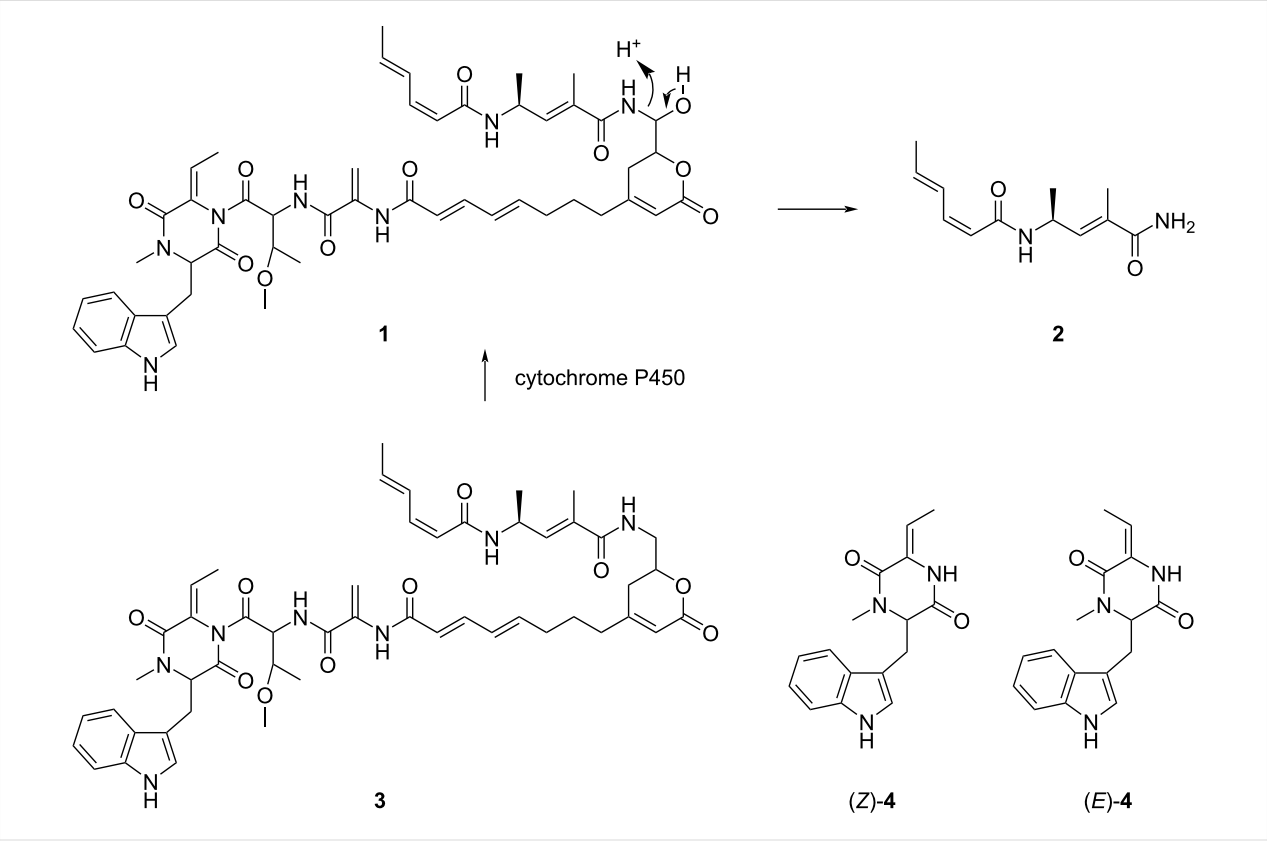

Scheme 1: Structures of hangtaimycin (**1**) and its co-metabolites.

hemiaminal function is also the breaking point for **1** into a larger lactone-polyene peptide fragment and a smaller fragment HTM_{222} (**2**, named after its molecular mass of 222 Da) [2]. Another hangtaimycin co-metabolite in *S. spectabilis* [9] is tryptophan-dehydrobutyrine diketopiperazine (TDD, **4**) that was already isolated several decades before the discovery of **1**, and likewise reported to have no antibacterial activity [9]. The initially published structure was that of (*E*)-**4** [9], but later revised as that of (*Z*)-**4**. The same compound is also observed in *S. olivaceus* [10] and was reported to function as a competitive inhibitor of glutathione *S*-transferase [11], which may be a result of a thiol addition of glutathione to the Michael acceptor in **4**. While the relative and absolute configuration of hangtaimycin have not yet firmly been established, **2** is known to be *S*-configured and is derived from an L-alanine unit [2]. TDD (**4**) was recently suggested to be *R*-configured, containing a D-tryptophan unit, based on a comparison of the optical rotation of the isolated compound ($[\alpha]_D^{20}$ = −12.67, *c* 1.1, 95% EtOH [1]) to **4** synthesised from L-tryptophan ($[\alpha]_D^{21}$ = +13, *c* 0.03, EtOH [12]), but the melting point of the synthetic material (mp 191–192 °C, for the compound numbered (*Z*)-**32** in ref. [12]) did not match that of isolated TDD (mp 121–123 °C [9]), and conclusively the compounds that have been compared cannot be the same. This prompted the authors of the synthetic study to conclude on the need for a structural revision of **4** [12], with unclear reasoning for the newly assigned structure. However, this newly suggested structure of **4** is not reflected in the structure of **1** [1,2] and not supported by bioinformatic analysis of its biosynthetic gene cluster [2], although it seems reasonable to consider **4** as a degradation product of **1**. Moreover, the originally reported optical rotation of **4** is positive ($[\alpha]_D^{24.5}$ = +10.0, *c* 1.1, 95% EtOH [9]), in contrast to the later reported negative value mentioned above [1]. In order to resolve the confusion, we have reisolated **4** from *S. spectabilis* and report on an improved synthesis. Furthermore, the results from bioactivity testings with **1**, **2** and **4** are discussed.

Results and Discussion

Synthesis of TDD

The first synthetic route towards **4** started from L-tryptophan (**5**) that was converted through a standard transformation into the methyl ester **6** and then through sequential reductive aminations with benzaldehyde and paraformaldehyde into **7** (Scheme 2) [13]. Cleavage of the benzyl group by catalytic hydrogenation afforded **8** that was coupled with *tert*-butyloxycarbonyl (Boc)-protected threonine using bis(2-oxo-3-oxazolidinyl)phosphinic chloride (BOP-Cl) [14,15] and Hünig's base to give **9**. Cleavage of the Boc group with 5% TFA followed by

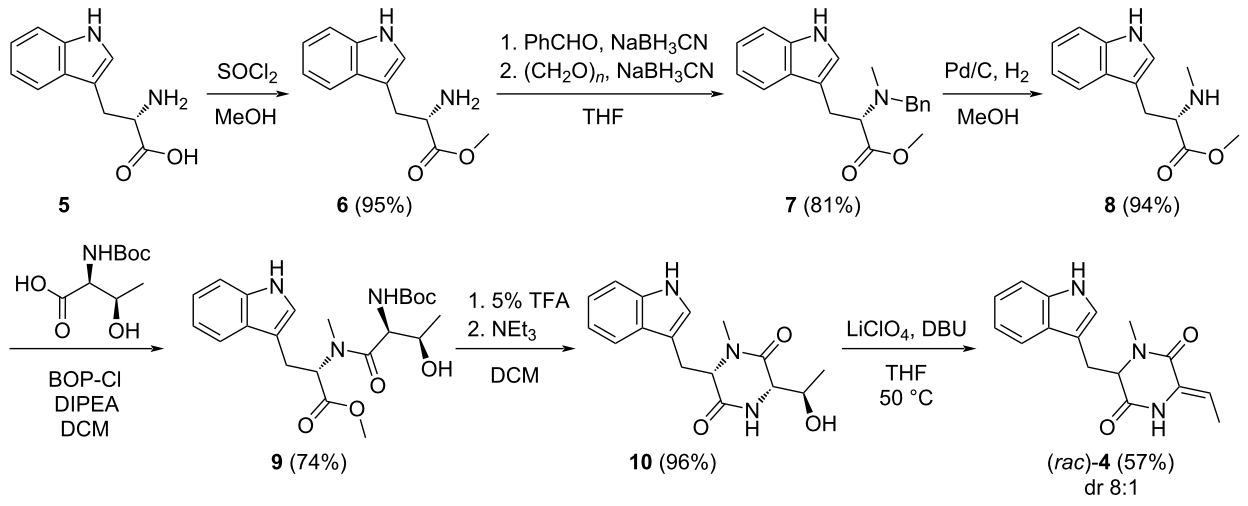

Scheme 2: First synthetic route towards TDD (**4**).

basic treatment resulted in the cyclisation to the dioxopiperazine **10**. Acetylation and subsequent treatment with $LiClO_4$ and DBU is a common strategy for the dehydration of serine and threonine units in peptides [16], but unfortunately the acetylation of **10** failed. Interestingly, the direct treatment of **10** with $LiClO_4$ and DBU under prolonged reaction times (3 days) resulted in the elimination of water. This reaction proceeded with a high diastereoselectivity (*Z*/*E* = 8:1), giving access to **4** in a satisfactory yield of 29% over 6 steps. However, the optical rotation of the obtained material showed only a small positive value ($[\alpha]_D^{25}$ = +1.9, *c* 0.27, EtOH), suggesting that **4** had undergone racemisation during the prolonged basic treatment with DBU in the last step. This was confirmed by HPLC analysis on a chiral stationary phase, showing that the obtained target compound **4** was nearly racemic (Figure 1A).

Because of the configurational instability of **4** under base treatment, we aimed at an approach for the final elimination step

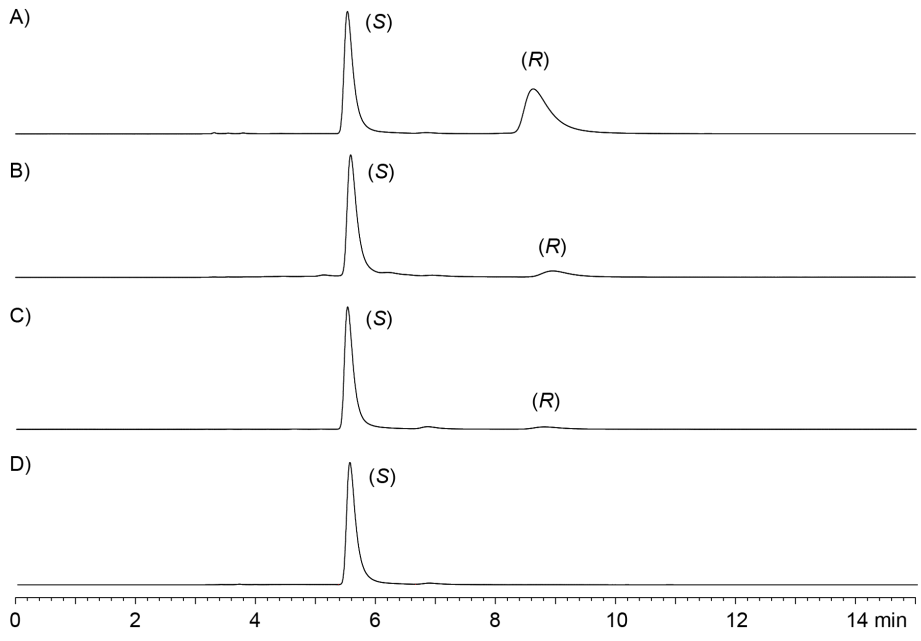

Figure 1: HPLC analyses of (*Z*)-**4** on a chiral stationary phase. A) Nearly racemic **4** from the first synthetic route (Scheme 2), B) enantiomerically enriched **4** (80% ee) from the second synthetic approach (Scheme 3), C) enantiomerically enriched **4** (90% ee) obtained under optimised conditions for the elimination reaction of **14** (Scheme 3), and D) natural enantiomerically pure (*S*)-TDD isolated from *S. spectabilis*.

using milder conditions (Scheme 3). The newly developed synthesis started from **7** that was Boc-protected at the indole to yield **11**. Removal of the benzyl group by catalytic hydrogenation to **12** was followed by coupling with benzyloxycarbonyl (Cbz) and methoxymethyl (MOM)-protected threonine to give **13**. Removal of the Cbz group by catalytic hydrogenation proceeded with spontaneous cyclisation to **14**. With this material, the elimination of the MOM group smoothly proceeded by treatment with KH and 18-crown-6 in THF at 25 °C to **15**, that upon removal of the Boc group with TFA and 1,3-dimethoxybenzene [17] gave (*Z*)-**4** as a single diastereomer through *anti* elimination. Overall, TDD was obtained from L-tryptophan in a high yield of 37% over eight linear steps. HPLC analysis on a chiral stationary phase showed that **4** obtained through this second route was enantiomerically enriched (80% ee by peak integration, Figure 1B). Further improvement of the enantiomeric excess of **4** (90% ee, Figure 1C) was possible by performing the elimination reaction with **14** and KH and 18-crown-6 under ice cooling. This helped to suppress basic racemisation of **4**, but required prolonged reaction times and gave a slightly diminished yield for **15** (70%), lowering the overall yield of TDD to 33% over eight steps. The major enantiomer of **4** obtained from this second route was identical to natural TDD (Figure 1D) which is thus *S*-configured, i.e., derived from L-tryptophan. Moreover, the olefinic double bond in **4** is *Z*-configured as indicated by a strong NOESY correlation between the amide NH and the neighbouring methyl group.

The structure of TDD

These findings not only challenge the originally assigned structure of (*E*)-**4** [9] and confirm the structural revision of (*Z*)-**4** [1], but also question the suggested structural revision that placed the *N*-methyl group at the other nitrogen of the dioxopiperazine moiety [12]. Moreover, the confusing situation about the absolute configuration and optical rotation are resolved through this work, clearly showing *S*-configuration for **4** that exhibits a negative optical rotation ($[\alpha]_D^{25}$ = –15.5, *c* 0.102, MeOH). The reason for the varying melting points for **4** in the literature is unclear, but we noticed a pronounced difference in the crystallisation behaviour of racemic and enantiomerically pure **4**. While (*rac*)-**4** readily formed crystals (mp 134–136 °C), several attempts to crystallise (*S*)-**4**, a material that was obtained as a viscous oil, failed. The X-ray crystallographic analysis of (*rac*)-**4** showed an interesting dimer interaction of its enantiomers through hydrogen bridges between the amide (NH-CO) groups (Figure 2, for crystallographic parameters cf. Supporting Information File 1, Table S1), that may support its easy crystallisation in comparison to enantiomerically enriched **4**.

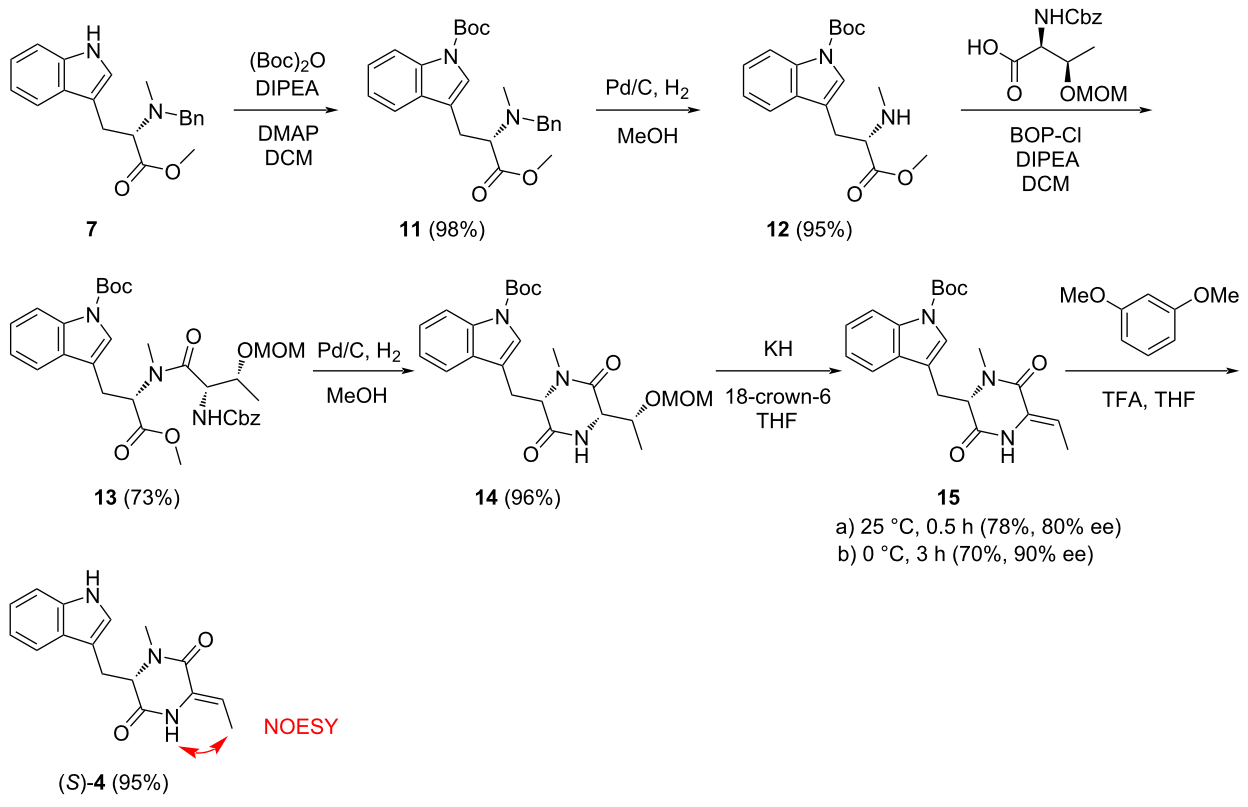

Scheme 3: Second synthetic route towards TDD ((*Z*)-**4**).

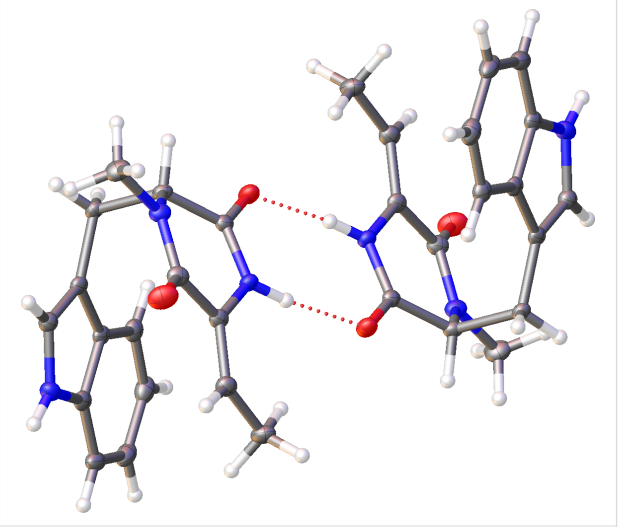

Figure 2: X-ray structure of (*rac*)-**4**.

Note that the dimer between the two enantiomers of **4** is achiral which allows for a regular packing of (*rac*)-**4** in the crystal. In contrast, a hypothetical similar interaction between two molecules of the same enantiomer can only lead to a chiral dimer that, if formed at all, may crystallise less efficiently.

Bioactivity testing

Previous reports have mentioned that TDD (**4**) exhibits no antibacterial activity, without providing information about the test organisms used [9]. For this reason, and because of the above-mentioned confusions about the true nature of **4** in the previous literature, the bioactivity of natural (enantiomerically pure) **4** isolated from *S. spectabilis* was reinvestigated. For comparison, synthetic (*rac*)-(*Z*)-**4** and its stereoisomer (*rac*)-(*E*)-**4** (Scheme 2) were included in the bioactivity testing, as well as the previously synthesised HTM_{222} (**2**) and **1** isolated from *S. spectabilis*. Neither **2** nor any of the stereoisomers of **4** showed antibacterial effects against a panel of Gram-positive and Gram-negative organisms (Supporting Information File 1, Table S2). Only **1** exhibited concentration-dependent growth retardation of the Gram-positive species *Bacillus subtilis* 168 and *Acinetobacter baumannii* 09987 (Figure 3A and B). However, growth inhibition was not strong enough to yield a clear MIC value, as the determination of a MIC requires complete

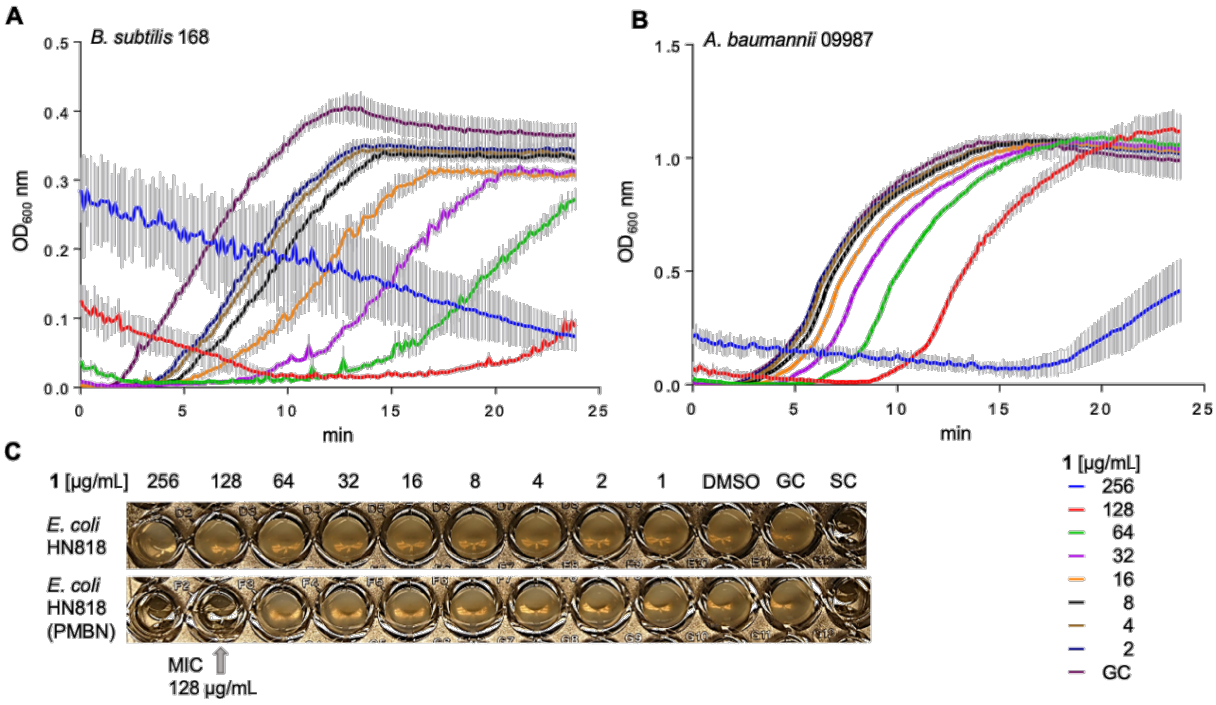

Figure 3: Bioactivity testing with hangtaimycin (**1**). A) Growth retardation of model species *B. subtilis* 168 and of B) nosocomial pathogen *A. baumannii* 09987 monitored by recording the turbidity increase of growing culture aliquots exposed to a concentration series of **1** every 10 min over 24 h. An increase in the optical density at 600 nm (OD_{600}) reflects biomass production. At concentrations of ≥64 µg/mL **1** precipitated, leading to elevated OD_{600} values at the beginning of the experiment that were unrelated to growth. The curves reflect the mean values of three separate cultures and standard deviations are depicted by black bars. C) MIC assay against *E. coli*. The MIC is defined as the lowest concentration of an antibacterial agent inhibiting visible bacterial growth (no turbidity detected by the naked eye) after overnight incubation. Only when the outer membrane was permeabilised by polymyxin B nonapeptide (PMBN), **1** inhibited growth of *E. coli* sufficiently to yield a clear MIC. GC, growth control (no inhibitor), SC, sterile control (no bacteria), DMSO, culture medium supplemented with 1% DMSO, reflecting the DMSO concentrations in the hangtaimycin-containing samples.

inhibition of visible bacterial growth and residual growth occurred up to the highest concentration tested (256 µg/mL). In the Gram-negative *Escherichia coli*, the outer membrane protects the cells from the impact of **1**. When the integrity of the outer membrane was compromised by adding the outer-membrane permeabilizing polymyxin B nonapeptide (PMBN, 10 µg/mL), a MIC of 128 mg/mL was achieved (Figure 3C).

We also investigated whether the reported inhibition of glutathione *S*-transferase [11] is a result of a Michael addition of glutathione to TDD. However, no reaction occurred between glutathione and TDD in DMF/H_2O (1:1) under prolonged stirring at room temperature. Also the addition of base (NEt_3) did not promote the reaction. Therefore, the mode of action of TDD towards glutathione *S*-transferase needs further investigation.

Conclusion

We have established an efficient synthesis of TDD that makes this compound available from L-tryptophan with a high yield of 33% (90% ee) over eight linear steps, establishing *S* configuration for the natural product from *S. spectabilis* that is likely reflected in the corresponding portion of hangtaimycin. A key step in the synthesis is the elimination of a MOM group using KH and 18-crown-6 that must be carried out with care, because TDD easily undergoes racemisation under basic conditions. The X-ray analysis showed an interesting dimer interaction of the enantiomers in racemic TDD through hydrogen bridges, that may support its much easier crystallisation in comparison to enantiomerically pure or enriched TDD. In fact, the obtained viscous oils did not crystallise, suggesting that the previously reported melting point of 121–123 °C [9] that is close to our measured melting point for (*rac*)-**4** (134–136 °C) may have been measured for isolated material after it had undergone (partial) racemisation. The reported inactivity of **4** against bacteria was confirmed in this study, and also **2** is an inactive metabolite of *S. spectabilis*, while for **1** moderate growth retardation against *A. baumannii* and *B. subtilis*, and growth inhibition against PMBN-treated *E. coli* was observed. However, the low activity of **1** in these assays suggests that the natural function of this structurally remarkable compound awaits future clarification.

Supporting Information

Supporting Information File 1

Experimental, analytical and X-ray data as well as copies of NMR spectra.
[https://www.beilstein-journals.org/bjoc/content/supplementary/1860-5397-18-120-S1.pdf]

Acknowledgements

We thank Andreas Schneider for HPLC analyses.

Funding

This work was funded by the Deutsche Forschungsgemeinschaft DFG (TRR 261, project ID 398967434). H. B.-O. received infrastructural support by the Cluster of Excellence EXC2121 Controlling Microbes to Fight Infection project, ID 390838134).

ORCID® iDs

Houchao Xu - https://orcid.org/0000-0002-4480-2035
Gregor Schnakenburg - https://orcid.org/0000-0001-6489-2106
Yuhui Sun - https://orcid.org/0000-0001-5720-9620
Heike Brötz-Oesterhelt - https://orcid.org/0000-0001-9364-1832
Jeroen S. Dickschat - https://orcid.org/0000-0002-0102-0631

References

1. Zuo, L.; Jiang, B.; Jiang, Z.; Zhao, W.; Li, S.; Liu, H.; Hong, B.; Yu, L.; Zuo, L.; Wu, L. *J. Antibiot.* **2016,** *69,* 835–838. doi:10.1038/ja.2016.29
2. Luo, M.; Xu, H.; Dong, Y.; Shen, K.; Lu, J.; Yin, Z.; Qi, M.; Sun, G.; Tang, L.; Xiang, J.; Deng, Z.; Dickschat, J. S.; Sun, Y. *Angew. Chem., Int. Ed.* **2021,** *60,* 19139–19143. doi:10.1002/anie.202106250
3. Piel, J. *Proc. Natl. Acad. Sci. U. S. A.* **2002,** *99,* 14002–14007. doi:10.1073/pnas.222481399
4. Helfrich, E. J. N.; Piel, J. *Nat. Prod. Rep.* **2016,** *33,* 231–316. doi:10.1039/c5np00125k
5. Moldenhauer, J.; Chen, X.-H.; Borriss, R.; Piel, J. *Angew. Chem., Int. Ed.* **2007,** *46,* 8195–8197. doi:10.1002/anie.200703386
6. Wagner, D. T.; Zeng, J.; Bailey, C. B.; Gay, D. C.; Yuan, F.; Manion, H. R.; Keatinge-Clay, A. T. *Structure* **2017,** *25,* 1045–1055.e2. doi:10.1016/j.str.2017.05.011
7. Yin, Z.; Dickschat, J. S. *Nat. Prod. Rep.* **2021,** *38,* 1445–1468. doi:10.1039/d0np00091d
8. Li, X.; Fu, J.; Li, Y.; Liu, J.; Gao, R.; Shi, Y.; Li, Y.; Sun, H.; Wang, L.; Li, Y.; Jiang, B.; Wu, L.; Hong, B. *Org. Lett.* **2022,** *24,* 1388–1393. doi:10.1021/acs.orglett.2c00242
9. Kakinuma, K.; Rinehart, K. L., Jr. *J. Antibiot.* **1974,** *27,* 733–737. doi:10.7164/antibiotics.27.733
10. Fiedler, H.-P.; Nega, M.; Pfefferle, C.; Growth, I.; Kempter, C.; Stephan, H.; Metzger, J. W. *J. Antibiot.* **1996,** *49,* 758–764. doi:10.7164/antibiotics.49.758
11. Komagata, D.; Sawa, R.; Kinoshita, N.; Imada, C.; Sawa, T.; Naganawa, H.; Hamada, M.; Okami, Y.; Takeuchi, T. *J. Antibiot.* **1992,** *45,* 1681–1683. doi:10.7164/antibiotics.45.1681
12. Santamaría, A.; Cabezas, N.; Avendaño, C. *Tetrahedron* **1999,** *55,* 1173–1186. doi:10.1016/s0040-4020(98)01095-3
13. White, K. N.; Konopelski, J. P. *Org. Lett.* **2005,** *7,* 4111–4112. doi:10.1021/ol051441w
14. Diago-Meseguer, J.; Palomo-Coll, A. L.; Fernández-Lizarbe, J. R.; Zugaza-Bilbao, A. *Synthesis* **1980,** 547–551. doi:10.1055/s-1980-29116
15. Tung, R. D.; Rich, D. H. *J. Am. Chem. Soc.* **1985,** *107,* 4342–4343. doi:10.1021/ja00300a051

16. Sommerfeld, T. L.; Seebach, D. *Helv. Chim. Acta* **1993,** *76,* 1702–1714. doi:10.1002/hlca.19930760427
17. Schmidt, U.; Lieberknecht, A.; Bökens, H.; Griesser, H. *J. Org. Chem.* **1983,** *48,* 2680–2685. doi:10.1021/jo00164a010

License and Terms

BEILSTEIN JOURNAL OF ORGANIC CHEMISTRY

Vicinal ketoesters – key intermediates in the total synthesis of natural products

Marc Paul Beller and Ulrich Koert*

Review

Open Access

Address:
Fachbereich Chemie, Philipps-Universität Marburg,
Hans-Meerwein-Straße 4, 35032 Marburg, Germany

Email:
Ulrich Koert* - koert@chemie.uni-marburg.de

* Corresponding author

Keywords:
aldol addition; ketoesters; natural products; total synthesis

Beilstein J. Org. Chem. **2022,** *18,* 1236–1248.
https://doi.org/10.3762/bjoc.18.129

Received: 19 July 2022
Accepted: 30 August 2022
Published: 15 September 2022

This article is part of the thematic issue "Total synthesis: an enabling science".

Associate Editor: B. Nay

Abstract

This review summarizes examples for the application of vicinal ketoesters such as α-ketoesters, mesoxalic esters, and α,β-diketoesters as key intermediates in the total synthesis of natural products utilizing their electrophilic keto group as reactive site. Suitable key reactions are, e.g., aldol additions, carbonyl ene reactions, Mannich reactions, and additions of organometallic reagents. The vicinal arrangement of carbonyl groups allows the stabilization of reactive conformations by chelation or dipole control.

Introduction

Vicinal ketoesters contain a carbonyl group adjacent to an ester group. One keto group results in α-ketoesters **1** and two vicinal keto groups lead to α,β-diketo esters **2** (Scheme 1). On the other hand, two carboxylic acid functionalities adjacent to a keto group result in mesoxalic diesters **3**, or mesoxalic ester amides **4**. The increased electrophilicity of the keto group and the high density of these complex functional groups make such structures attractive as key intermediates for the total synthesis of natural products [1]. Thus, the high electrophilicity of the central carbonyl group in α,β-diketoesters **2** allows the formation of stable hydrates **5**. In case of an enolizable position enolization (**2**→**6**) is facilitated.

The chemistry of vicinal polycarbonyl compounds such as *vic*-diketoesters has been investigated in depth by Wasserman, Parr [2] and Gleiter, Rubin [3]. Important contributions for the use of α,β-diketoesters in stereoselective transformations came from Doyle's group [4,5]. One remarkable example is the diastereoselective intramolecular aldol addition of ketones such as **7** (Scheme 2) [5]. Brønsted-acid catalysis leads via a transition state **8** to the aldol **9**, while the use of chelating Lewis acids results via **10** in the epimeric aldol **11**.

This review is a collection of total syntheses of natural products where vicinal keto esters were used as key intermediates.

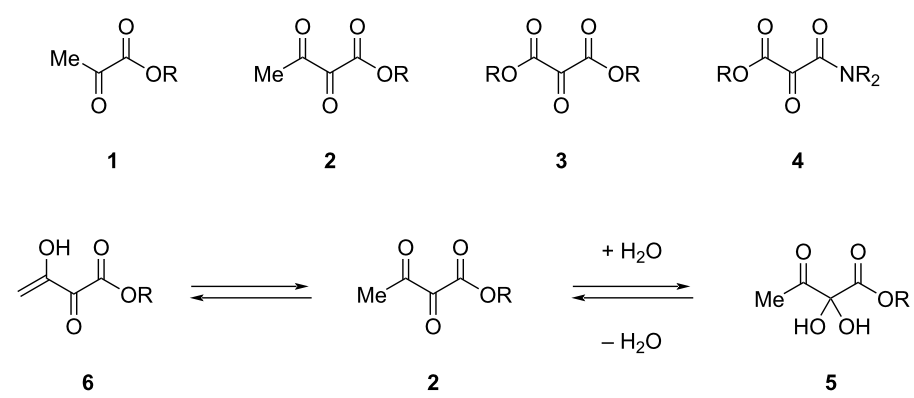

Scheme 1: Structures of vicinal ketoesters and examples for their typical reactivity.

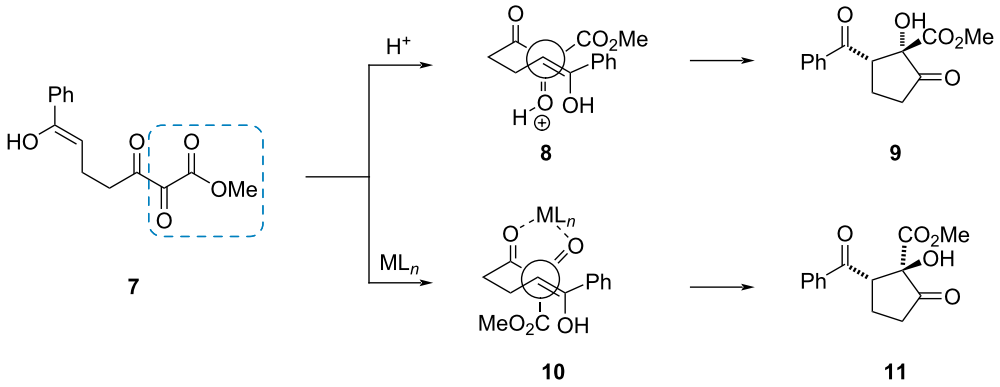

Scheme 2: Doyle's diastereoselective intramolecular aldol addition of α,β-diketoester.

For reasons of clarity and better comparability all syntheses are strongly summarized highlighting the key step only.

The presentation of the examples is structured in three parts:

1. **α-Ketoesters** as key intermediates: (+)-euphorikanin A, (−)-preussochromone A, (−)-preussochromone D, (−)-jiadifenoxolane A, palau'amine, jatrophen, (−)-hopeanol, (+)-campthotecin, isoretronecanol, corynoxine, (+)-gracilamine, (−)-irofulven.
2. **Mesoxalic** diester and ester amides as key intermediates: (+)-awajanomycin, (−)-aplaminal, cladoniamide G.
3. **α,β-Diketoesters** as key intermediates: preussochromones E and F.

Review

1. α-Ketoesters as key intermediates:

(+)-Euphorikanin A

In the final step of the synthesis of (+)-euphorikanin A (**16**), an ingenane-derived diterpenoid with a 5/6/7/3-fused tetracyclic carbon skeleton, Carreira et al. used an intramolecular nucleophilic addition of an alkenyl metal species to the α-ketoester **15** (Scheme 3) [6]. The ketoester **15** was synthesized by a chiral pool approach starting from (+)-3-carene derived cycloheptenone **13** [7,8] and aldehyde **12** (accessible from (*R*)-Roche ester [9]) via the γ-lactone **14**. The ketoester moiety was established by an enolate hydroxylation with Davis' oxaziridine and subsequent oxidation using Dess–Martin periodinane. Initial attempts for the key step (**15** → **16**) like a Nozaki–Hiyama–Kishi reaction failed, but lithium–halogen exchange using *t*-BuLi at low temperatures gave the desired vinyllithium intermediate **I** which successfully added to the desired α-carbonyl group.

(−)-Preussochromone A

In 2020, the Koert group disclosed the synthesis of (−)-preussochromone A (**24**), a fungal metabolite with a highly substituted tetrahydrothiopyrane core annulated to a chromenone [10]. The tetrahydrothiopyrane ring was closed by a Lewis-acid-promoted cycloisomerization of the α-ketoester **22**, which can be described as a Friedel–Crafts-type reaction or an aldol reaction of an *S*,*O*-ketene acetal (Scheme 4). The re-

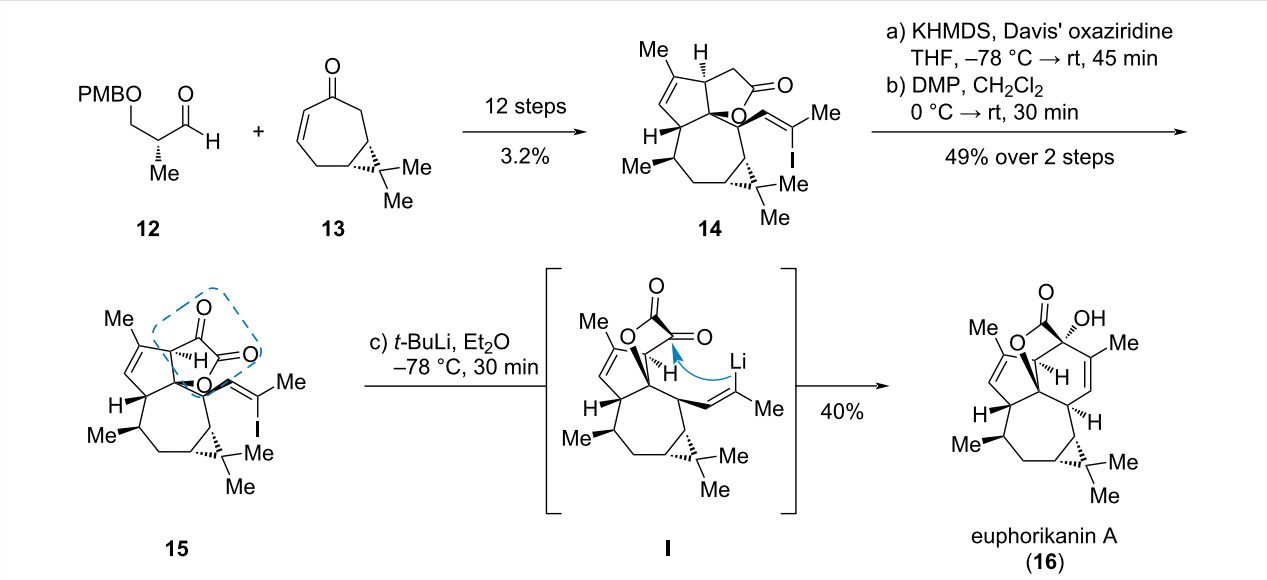

Scheme 3: Synthesis of euphorikanin A (**16**) by intramolecular, nucleophilic addition [6].

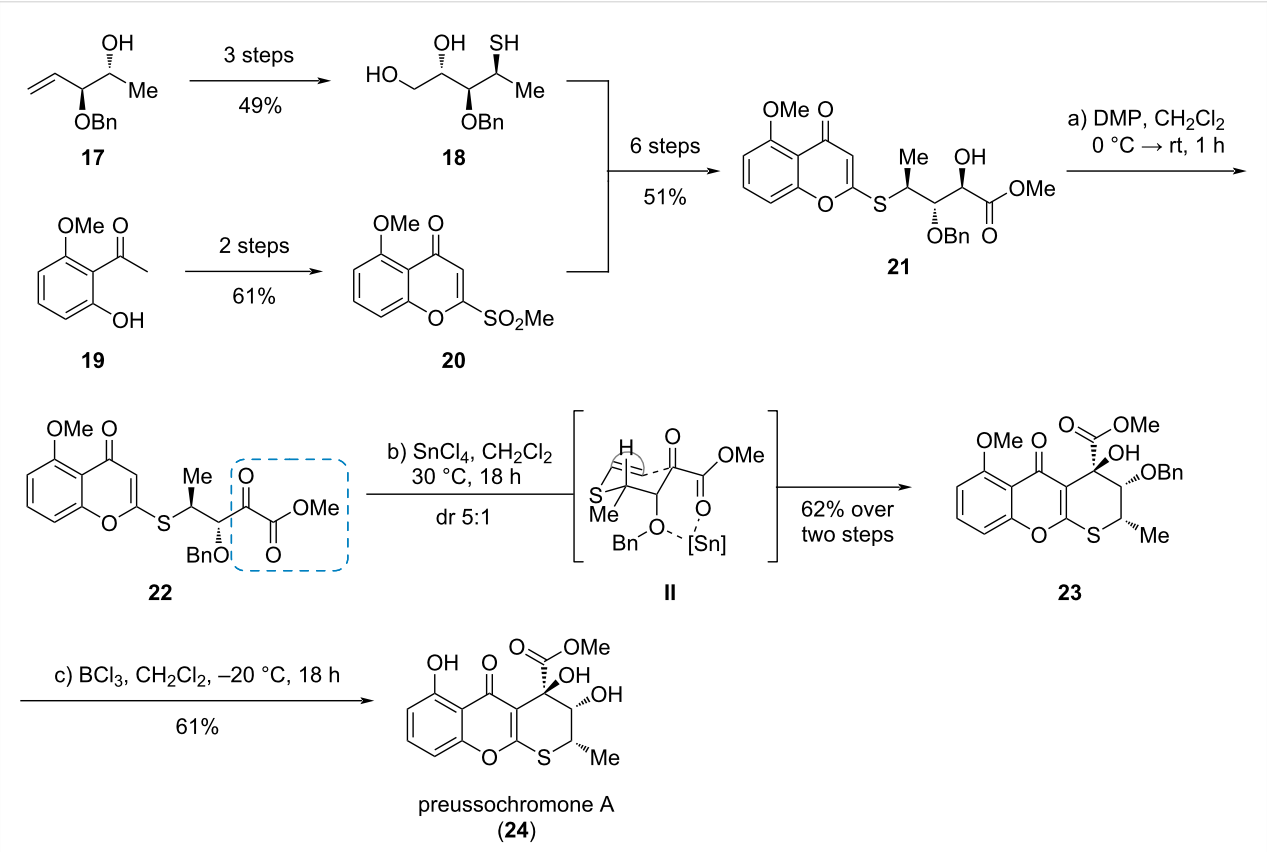

Scheme 4: Ketoester cycloisomerization for the synthesis of preussochromone A (**24**) [10].

quired ketoester **22** was synthesized from sulfonylchromenone **20**, accessible from dihydroxyacetophenone **19** and thiol **18** derived from known alcohol **17** [11,12]. DMP oxidation of α-hydroxyester **21** and subsequent cycloisomerization led to the desired cyclization product **23** via transition state **II** in a dr of 5:1. Final deprotection gave preussochromone A (**24**).

(–)-Preussochromone D

A similar approach was chosen in the synthesis of the structurally related natural product preussochromone D (**30**) reported by Koert et al. [13]. The synthesis commenced with the efficient production of alcohol **26** from 5-hydroxy-4*H*-chromen-4-one (**25**, Scheme 5) [14]. The ketoester moiety was build up via oxidation and nucleophilic addition of methyl diazoacetate, yielding alcohol **27**. Subsequent oxidation gave α-ketoester **28** which was used in an intramolecular, Lewis acid-mediated aldol reaction, presumably via tridentate complex transition state **III**, to give diol **29** as a single diastereomer. Inversion of the secondary alcohol and deprotection gave preussochromone D (**30**).

(–)-Jiadifenoxolane A

The *Illicium* sesquiterpenes containing a *seco*-prezizaane carbon framework are highly oxidized, structurally complex natural products. Maimone et al. published a remarkable synthesis of the *Illicium* sesquiterpene (−)-jiadifenoxolane A (**36**), starting from the abundant sesquiterpene (+)-cedrol (**31**, Scheme 6) [15]. Through a series of finely tuned CH oxidations, cedrol (**31**) was converted to the lactone **32**. In a single step, using Riley oxidation conditions, the methyl ketone moiety was transferred to the α-ketoester **33**. Reduction, lactonization, and elimination gave the ketoesters-derived enol **34**. Oxidation of the latter compound to the α-keto-β-hydroxy ester **IV** using DMDO and subsequent heating in $PhCF_3$ triggered an α-ketol rearrangement which led to ketol **V**. Diastereoselective reduction gave α,β-dihydroxyester **35** which was converted to (−)-jiadifenoxolane A (**36**) in five further steps.

Palau'amine

Palau'amine (**45**), a dimeric pyrrole-imidazole-bisguanidine alkaloid, was first isolated from the marine sponge *Stylotella aurantium* in 1993 [16,17]. It received considerable attention from the synthetic community because of its broad range of biological activities and complex structure. In an early endeavour of L. Overman et al. in 1997 [18] towards the originally proposed structure of palau'amine (**44**), a [3 + 2]-dipolar cycloaddition of α-ketoester **41** and the thiosemicarbazide **42**-derived azomethine imine **VI** to the triazacyclopenta[*cd*]pentalene **43** was utilized as a key step (Scheme 7) [18-21].

The α-ketoester **41** was accessible from amide **38**, which in turn was obtained from allylic alcohol **37**. Oxidation and Horner–Wadsworth–Emmons reaction with phosphonate **39** delivered the silyl enol ether **40**, which was deprotected and

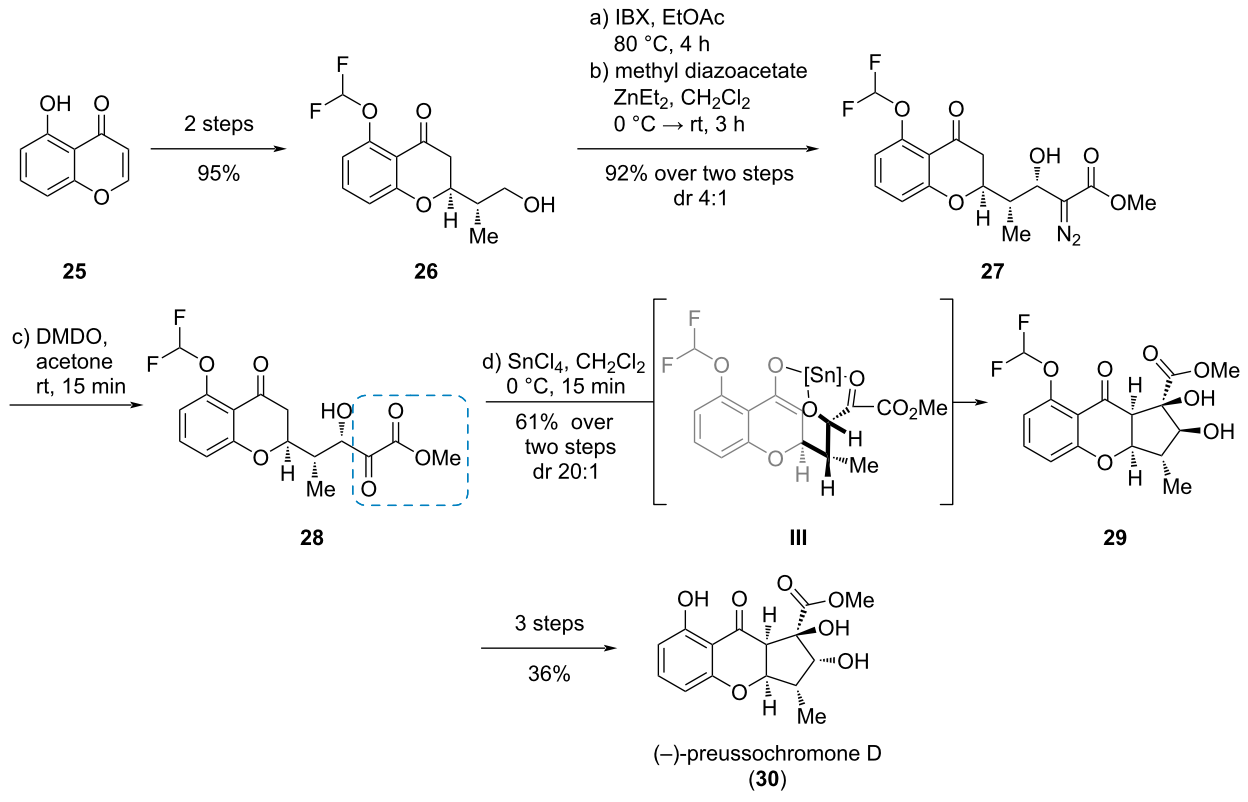

Scheme 5: Diastereoselective, intramolecular aldol reaction of an α-ketoester **28** in the synthesis of (–)-preussochromone D (**30**) [13,14].

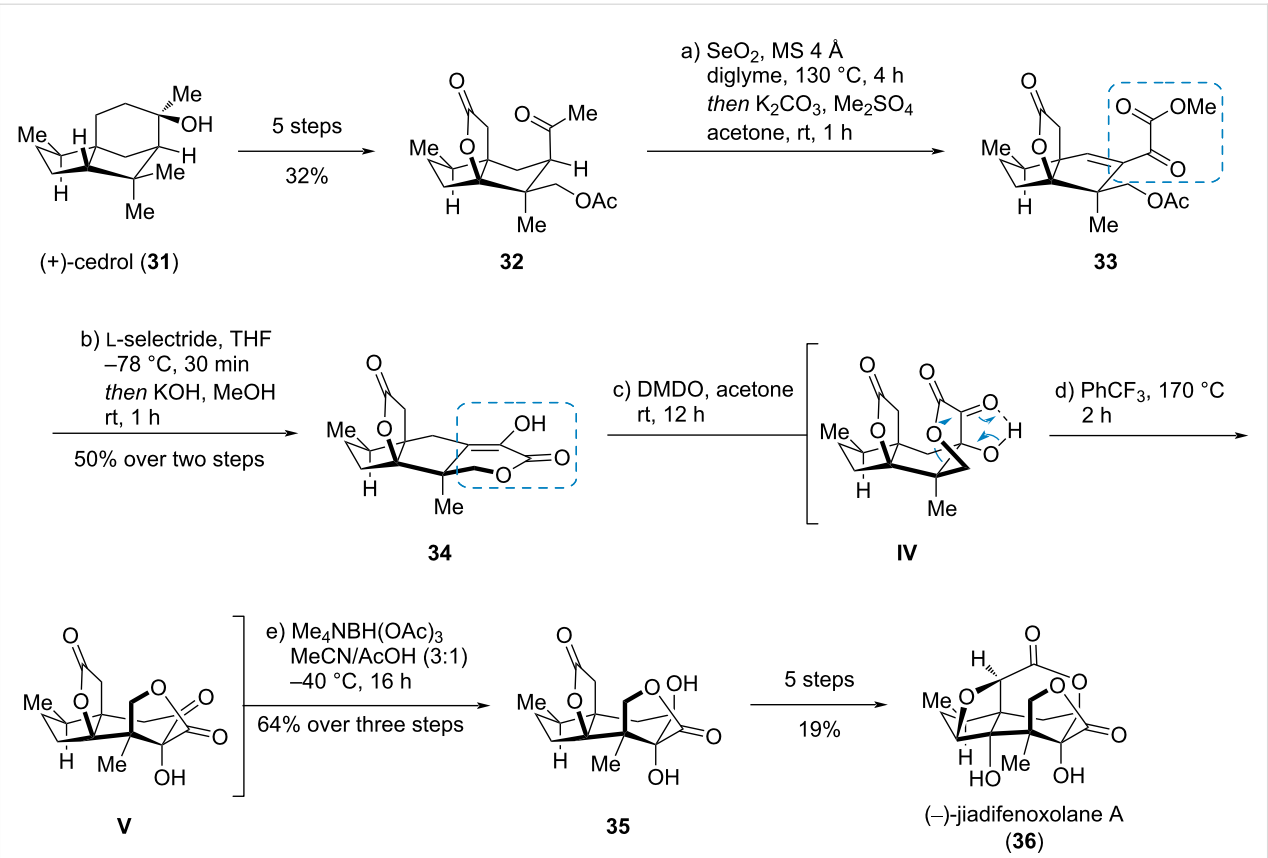

Scheme 6: Synthesis of an α-ketoester through Riley oxidation and its use in an α-ketol rearrangement in the synthesis of (–)-jiadifenoxolane A (**36**) [15].

cyclized via a Grubbs metathesis to α-ketoester **41**. Subsequent cycloaddition delivered the advanced intermediate **43** in an efficient and elegant way.

Jatropha-5,12-diene

Towards the total synthesis of natural and unnatural jatrophane diterpenes, Hiersemann et al. used a highly efficient, intramolecular carbonyl-ene reaction of α-ketoester **49** (Scheme 8) [22]. The ketoester was synthesized by a Horner–Wadsworth–Emmons reaction of phosphonate **48** with aldehyde **47**. Enantiopure aldehyde **47** was easily accessible from oxazolidinone **46** via Evans-aldol chemistry [23]. Heating of the α-ketoester **49** led to the highly substituted cyclopentanol **50** in a good dr of ≈5:1 (minor diastereomer not shown) via transition state **VII** where pseudo-1,3-strain is minimized. Nineteen further steps were necessary to give the naturally occurring jatrophen **51**.

(–)-Hopeanol

In the synthesis of the polyphenolic natural product (−)-hopeanol (**59**), Nicolaou et al. used an α-ketoester moiety as a precursor for an intramolecular Friedel–Crafts cyclization (Scheme 9) [24]. Therefore, phenylacetaldehyde **52** was converted to the alcohol **53**, which was esterified with the α-ketoacid **54** to give ketoester **55**. Grignard addition to the keto carbonyl and subsequent TBS deprotection delivered the tertiary alcohol **56**, which was dehydroxylated to the diastereomeric cations **VIII** and **IX**. Friedel–Crafts reaction gave diastereomeric lactones **57** and **58**. The major diastereomer **58** could be converted to the complex polyphenol (−)-hopeanol (**59**) in seven further steps.

(+)-Camptothecin

In the formal synthesis of the pentacyclic, antiproliferative quinoline alkaloid camptothecin (**65**), Peters et al. used an α-ketoester moiety in an auxiliary controlled approach towards the only stereogenic center present in the natural product (Scheme 10) [25]. First, the ketoacid **60** was esterified with 8-phenylmenthol (**61**) to yield the α-ketoester **62**, followed by nucleophilic addition of isopropenylmagnesium bromide to give α-hydroxyester **63** in excellent yield and diastereoselectivity. Eight additional steps gave the bicyclic compound **64** which was already known from previous camptothecin syntheses.

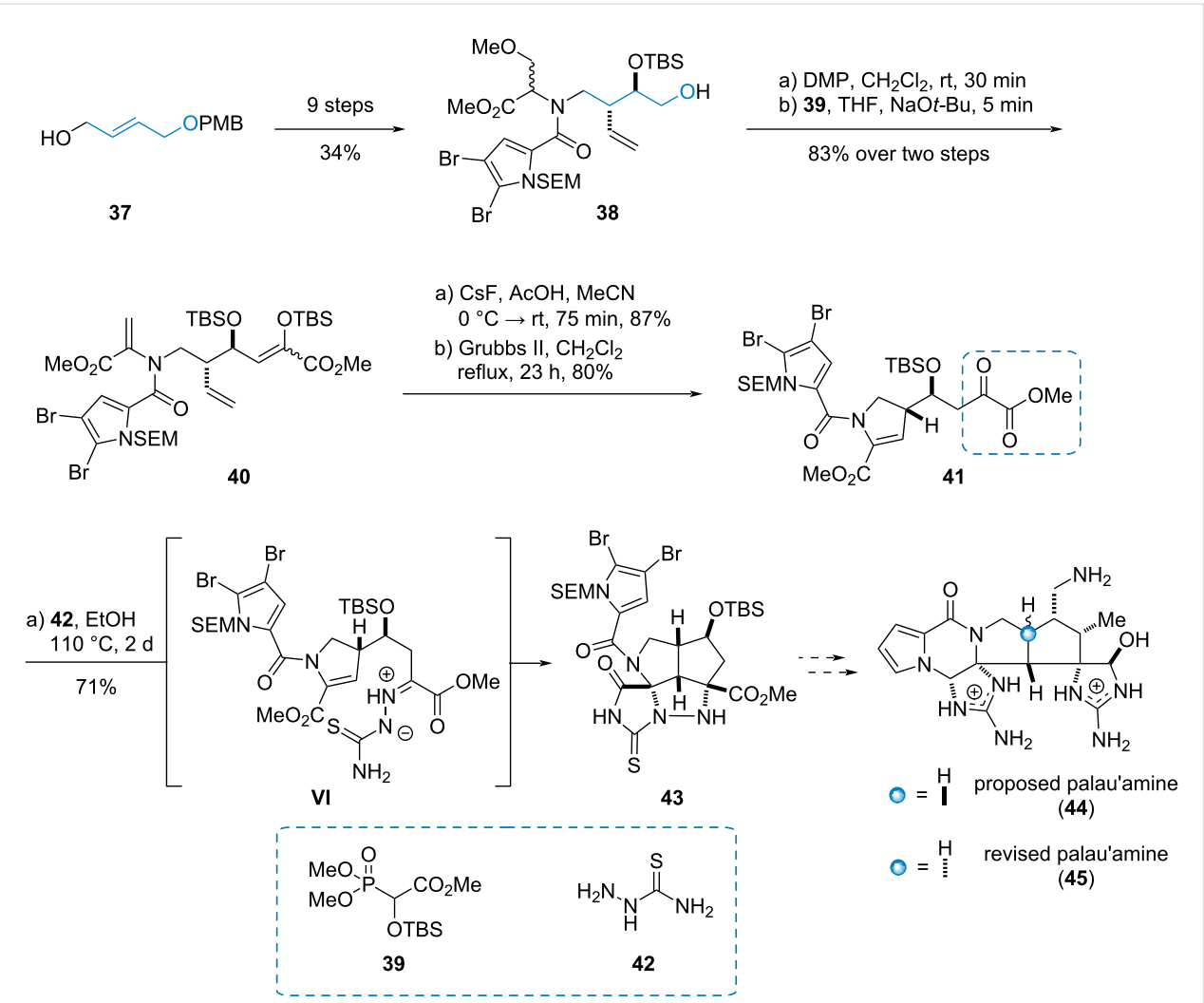

Scheme 7: Azomethine imine cycloaddition towards the synthesis of the proposed structure of palau'amine (**44**) [19].

Isoretronecanol

The α-ketoester moiety can also be used in photochemical reactions, as shown by Gramain et al. in the synthesis of the pyrrolizidine alkaloid (*rac*)-isoretronecanol (**69**, Scheme 11) [26]. A Claisen condensation of the lithium enolate of *N*-acetylpyrrolidine (**66**) with diethyl oxalate gave the ketoester **67**. Irradiation of compound **67** with a medium pressure mercury lamp in Pyrex® glassware triggered a 1,6-HAT leading to biradical **X** which combined to the racemic pyrrolizidine **68** as a 1:1 mixture of diastereomers. Three more steps gave the target compound **69** in 31% overall yield.

Corynoxine

Hiemstra et al. used the α-ketoester moiety for different purposes in the syntheses of a range of oxindole alkaloids. The start of the synthesis of (*rac*)-corynoxine (**76**) was the conversion of tryptamine (**70**) to oxindole **71**, which was used in a chemoselective Mannich reaction with aldehyde **72**, introducing the α-ketoester moiety (Scheme 12) [27].

The major *trans*-isomer **73** was further converted to the natural products corynoxine and rychnophylline. The minor *cis*-isomer **74** was used in an intramolecular Tsuji–Trost reaction, where the ketoester served as a nucleophile, which build up the piperidine ring and selectively set the desired *cis*-substitution. Subsequent transesterification gave the α-ketoester **75**, which was used in a Wittig reaction. The undesired *Z*-configured double bond was isomerized to the *E*-alkene and final hydrogenation delivered corynoxine (**76**).

(+)-Gracilamine

The Mannich reaction was also used by Nagasawa et al. as a key step in the synthesis of (+)-gracilamine (**83**), a penta-

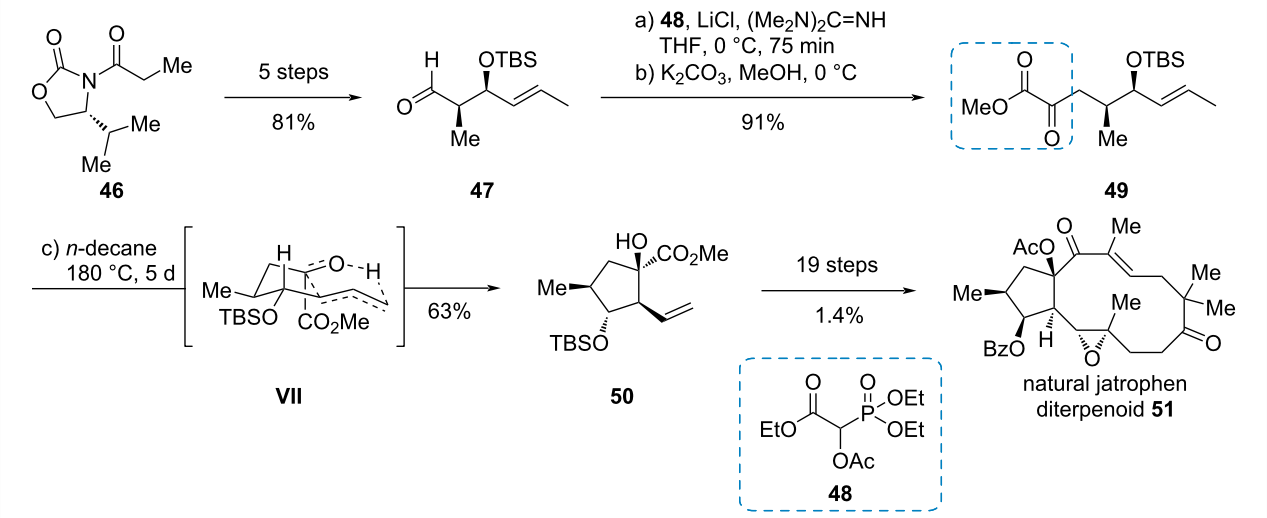

Scheme 8: Intramolecular diastereoselective carbonyl-ene reaction of an α-ketoester in the synthesis of jatrophane diterpenoids [22].

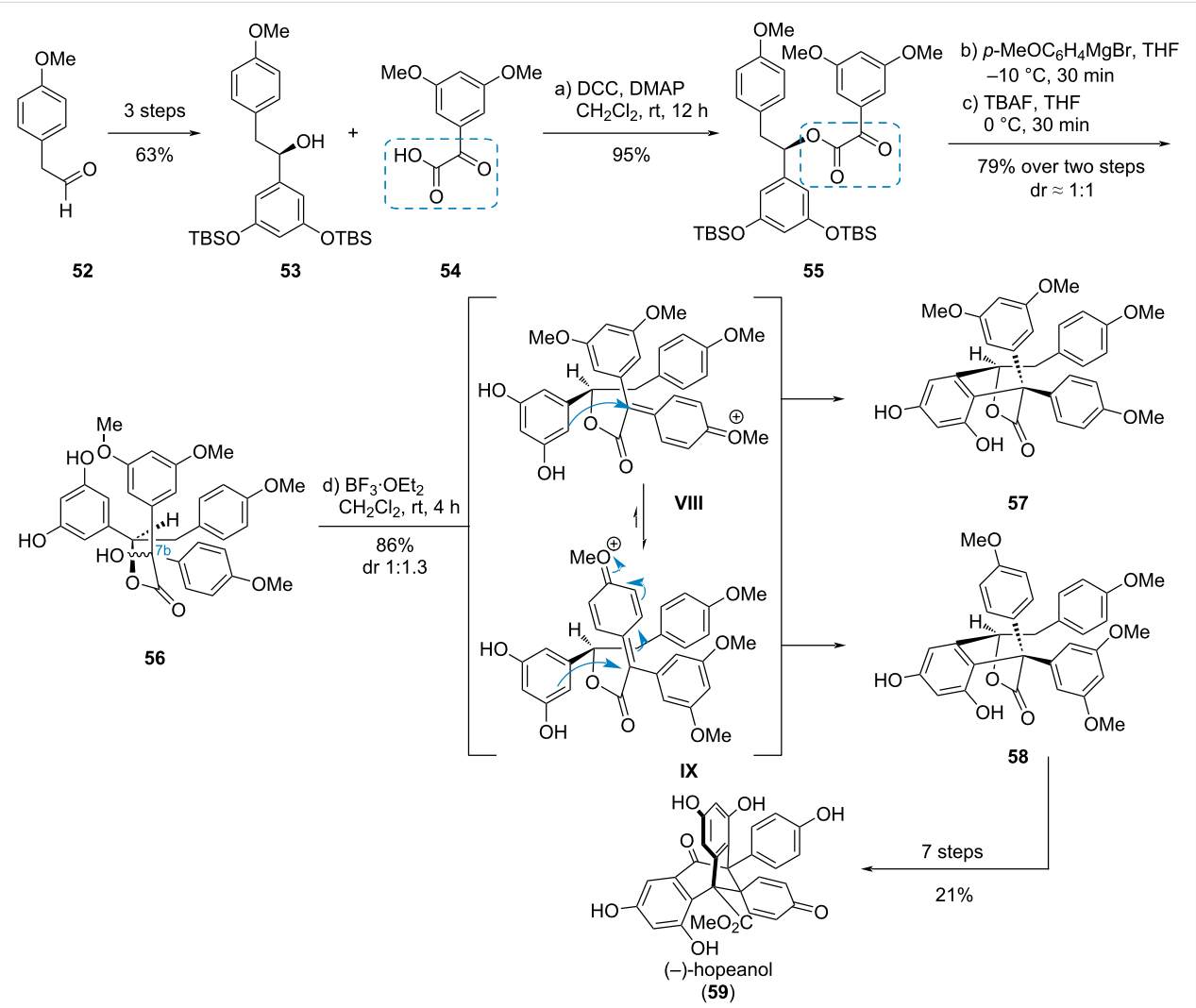

Scheme 9: Grignard addition to an α-ketoester and subsequent Friedel–Crafts cyclization in the synthesis of (–)-hopeanol (**59**) [24].

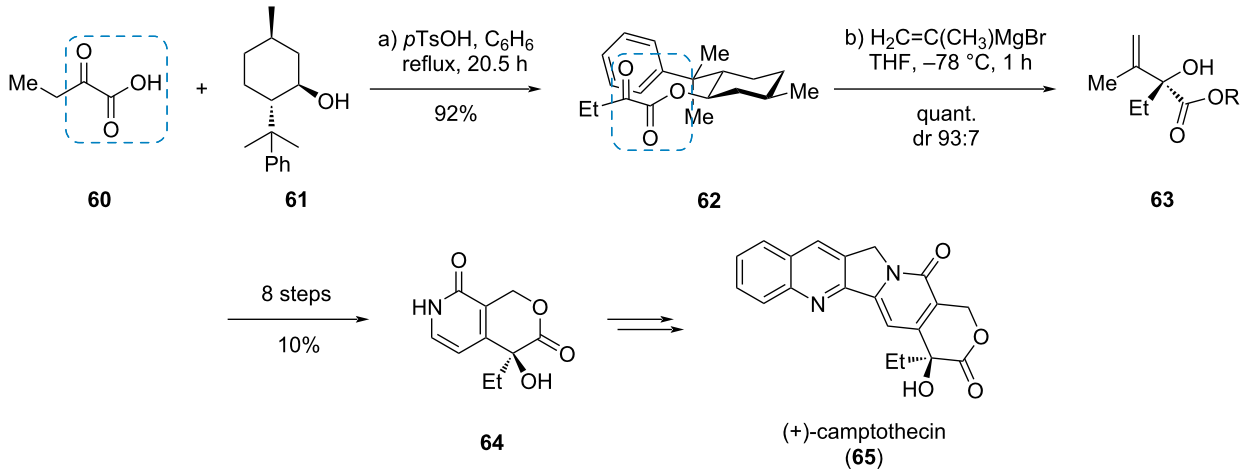

Scheme 10: Diastereoselective addition to an auxiliary modified α-ketoester in the formal synthesis of (+)-campthotecin (**65**) [25].

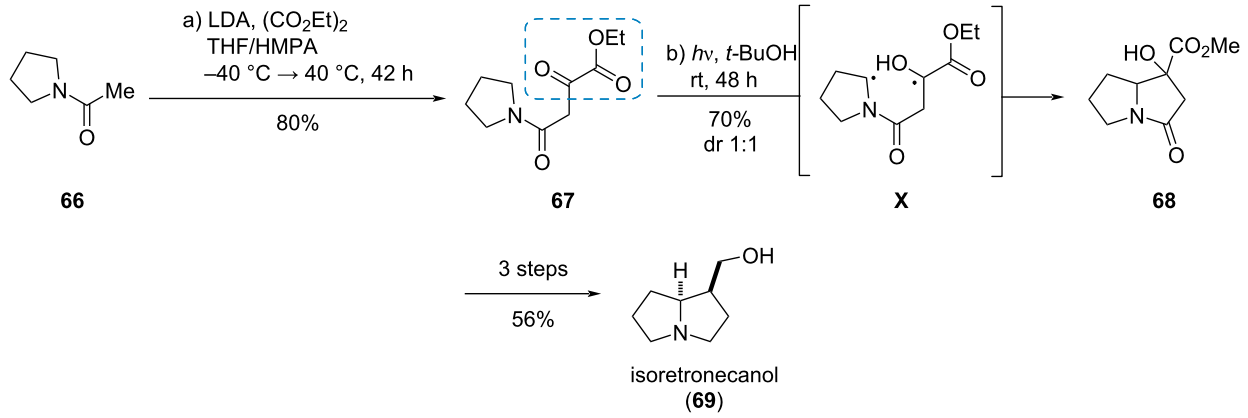

Scheme 11: Intramolecular photoreduction of an α-ketoester in the synthesis of (*rac*)-isoretronecanol (**69**) [26].

cyclic alkaloid isolated from the plant *Galanthus gracilis*, (Scheme 13) [28]. The synthesis started from readily available sesamol (**79**) and imine **78** which gave the advanced intermediate **80** in ten steps. An intramolecular Mannich reaction of compound **80** with α-ketoester **81** furnished compound **82** with the last ring of the target (+)-gracilamine (**83**), which was accessible after two further steps.

(–)-Irofulven

Irofulven (**87**) is a highly cytotoxic, semisynthetic drug obtained from the illudin sesquiterpene family. In a de novo synthesis towards (−)-irofulven (**87**), Movassaghi et al. used a Cu^{II}-catalyzed asymmetric aldol reaction of *O*-silyl ketene *S*,*O*-acetal **84** with methyl pyruvate (**85**) to enantioselectively install the crucial tertiary TMS-protected alcohol in ester **86** (Scheme 14) [29]. Eleven further steps gave (−)-irofulven (**87**).

2. Mesoxalic diesters and ester amides as key intermediates

(+)-Awajanomycin

Diethyl mesoxalate (**90a**) is a valuable building block due to the high density of carbon atoms in high oxidation states. As a *vic*-tricarbonyl compound, its central keto group is an especially potent electrophile. The Koert group used this reactivity in their synthesis of (+)-awajanomycin (**92**), a marine natural product with a γ-lactone-δ-lactam core structure (Scheme 15) [30,31]. Key step was an asymmetric allylboration of diethyl mesoxalate (**90a**) with boronate **89**, which was easily accessible through a Matteson homologation of dichloromethyl boronate **88**. The reaction of (*Z*)-alkenyl boronate **89** with mesoxalate **90a** delivered product **91** through the six-membered transition state **XI**. Eight further steps accomplished the total synthesis of (+)-awajanomycin (**92**).

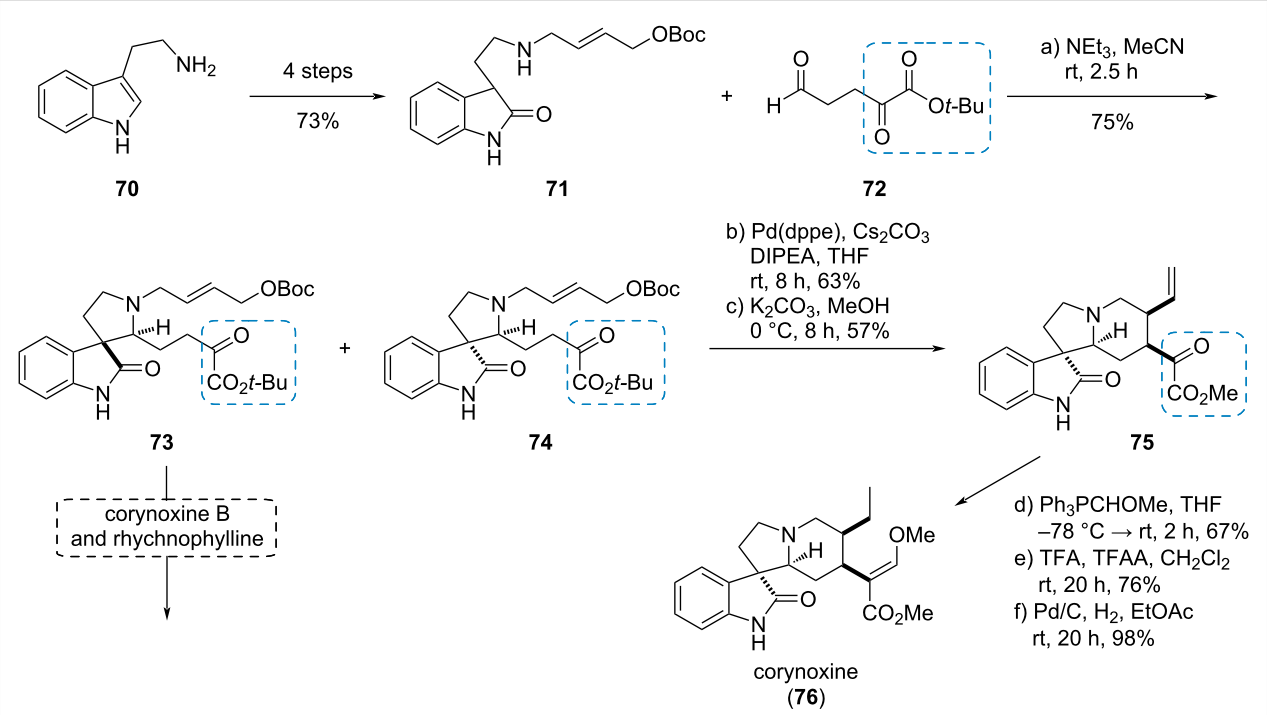

Scheme 12: α-Ketoester as nucleophile in a Tsuji–Trost reaction in the synthesis of (*rac*)-corynoxine (**76**) [27].

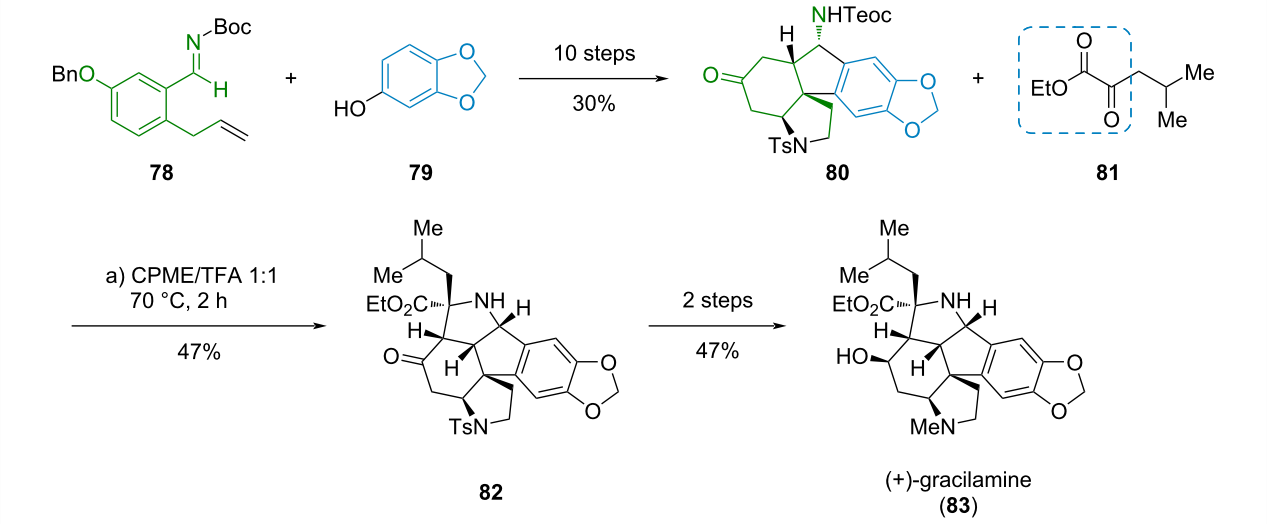

Scheme 13: Mannich reaction of an α-ketoester in the synthesis of (+)-gracilamine (**83**) [28].

(–)-Aplaminal

Dimethyl mesoxalate (**90b**) was used by Smith and Liu in the synthesis of the cytotoxic metabolite (−)-aplaminal (**96**), which was isolated from the sea hare *Aplysia kurodai* [32]. The natural product is characterized by a triazabicyclo[3.2.1]octane, where each bridge possesses a nitrogen atom. The synthesis commenced with *N*-Boc-serine (**93**) which was converted to secondary aniline **94** in three steps (Scheme 16). Subsequent deprotection and condensation with dimethyl mesoxalate (**90b**) gave imidazolidine **95**. With compound **95** at hands, five further steps gave (−)-aplaminal (**96**) in a good overall yield of 19%.

Cladoniamide G

The unsymmetrical mesoxalic acid amide **102** was used by Koert et al. in the racemic synthesis of the bisindole alkaloid (*rac*)-cladoniamide G (**103**, Scheme 17) [33]. The synthesis

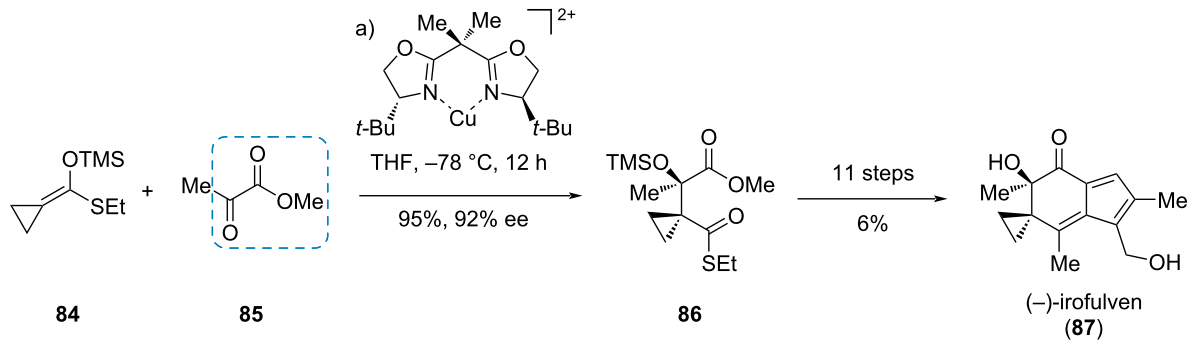

Scheme 14: Enantioselective aldol reaction using an α-ketoester in the synthesis of (–)-irofulven (**87**) [29].

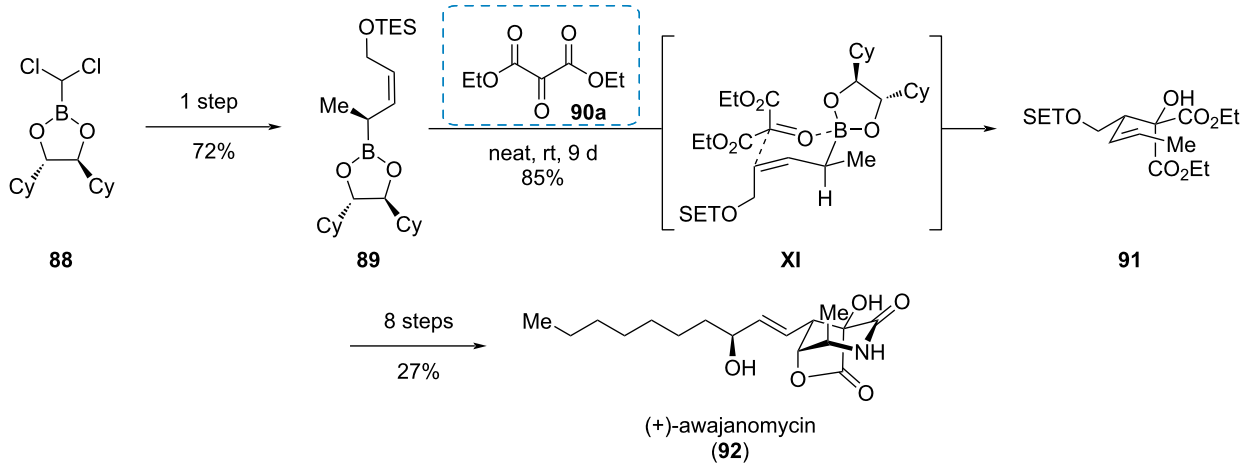

Scheme 15: Allylboration of a mesoxalic acid ester in the synthesis of (+)-awajanomycin (**92**) [30,31].

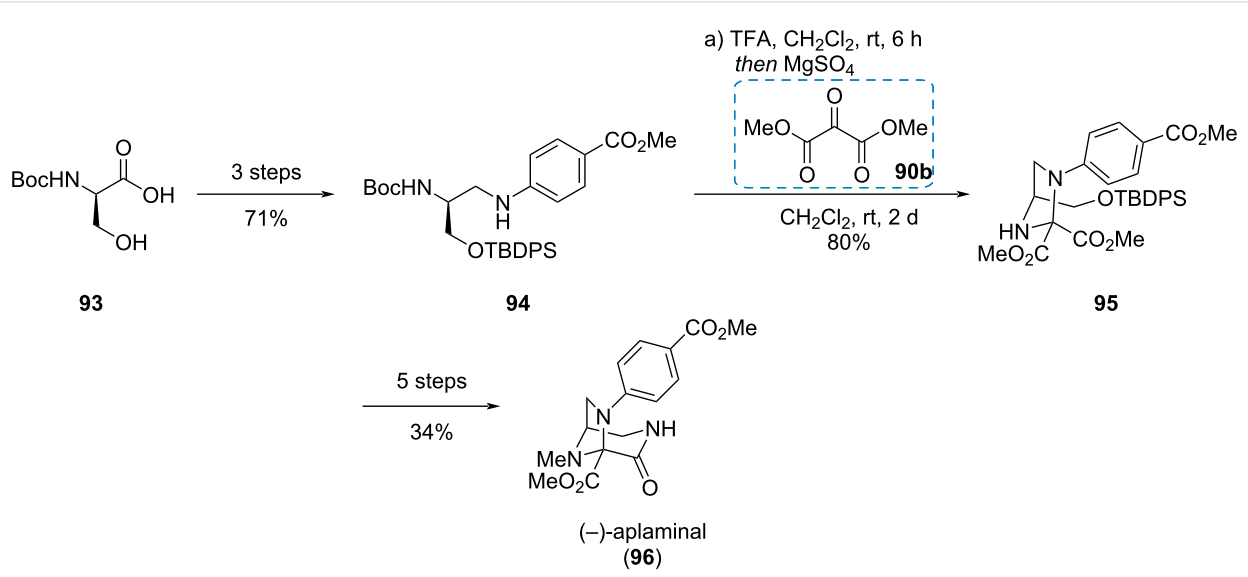

Scheme 16: Condensation of a diamine with mesoxolate in the synthesis of (–)-aplaminal (**96**) [32].

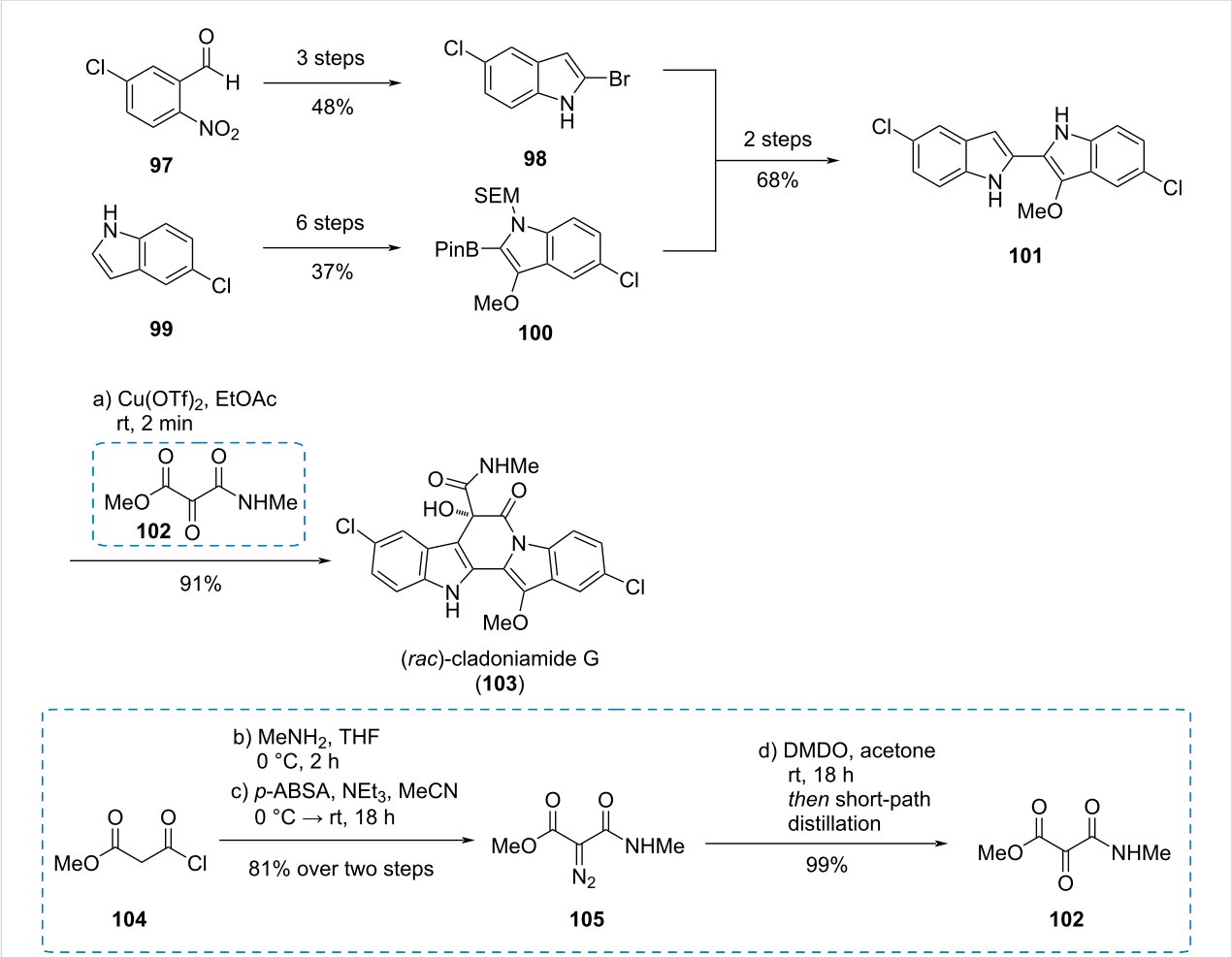

Scheme 17: Synthesis of mesoxalic ester amide **102** and its use in the synthesis of (*rac*)-cladoniamide G (**103**) [33].

started with benzaldehyde **97** and indole **99** which were converted to the indole building blocks **98** and **100**, respectively. These were connected to bisindole **101**, which reacted with mesoxalic ester amide **102** in a Friedel–Crafts reaction followed by a spontaneous lactamization to give (*rac*)-cladoniamide G (**103**). The mesoxalic ester amide **102** was synthesized from malonyl chloride **104** through amidation and Regitz diazotransfer, yielding diazo compound **105**. Subsequent oxidation and dehydration of the resulting hydrate through short-patch distillation gave the desired *vic*-tricarbonyl compound **102**.

3. α,β-Diketoesters as key intermediates

Preussochromone E and F

In a short and enantioselective total synthesis of preussochromone E (**110**) and F (**109**), Koert et al. used the complex *vic*-tricarbonyl compound **108** to set two stereogenic centers and correct one via an intramolecular aldol addition (**108** → **109**; Scheme 18) [34]. The *vic*-tricarbonyl compound **108** was synthesized via DMDO oxidation from α-diazo-β-ketoester **107**, which was easily accessible from 5-methoxy-4*H*-chromen-4-one (**106**). The thermodynamically controlled basic intramolecular aldol addition of compound **108** using the bulky amine base 2,6-di-*tert*-butyl-4-methylpyridine (DTBMP) led to epimerization of the methyl group and cyclization, giving preussochromone F (**109**) as single isolable diastereomer probably via transition state **XII**. The subsequent reduction of compound **109** gave preussochromone E (**110**).

Conclusion

The variety of examples prove that vicinal ketoesters are valuable synthetic intermediates for the synthesis of complex target structures such as natural products. α-Ketoesters, mesoxalic esters, and α,β-diketoesters can be used bearing an electrophilic keto group as reactive site. The vicinal arrangement of carbonyl groups allows the stabilization of reactive conformations by chelation or dipole control. Suitable key reactions are e.g., aldol additions, carbonyl ene reactions, Mannich reactions, and addi-

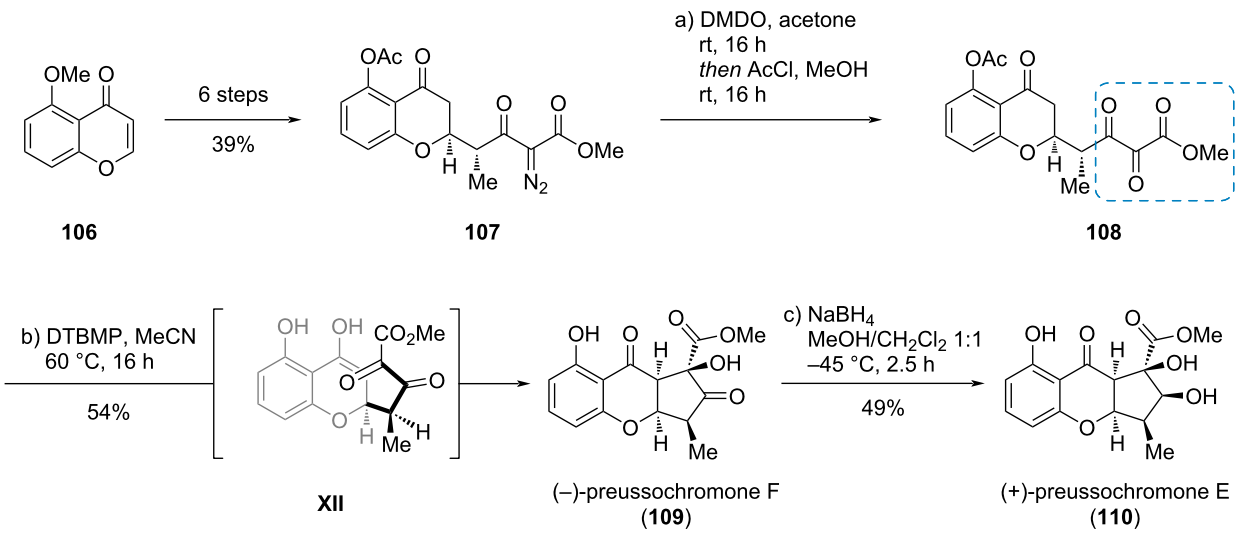

Scheme 18: The thermodynamically controlled, intramolecular aldol addition of a *vic*-tricarbonyl compound in the synthesis of preussochromones E (**110**) and F (**109**) [34].

tions of organometallic reagents. The presented examples may encourage the use of vicinal ketoesters in future applications, in particular in the field of natural product synthesis.

Funding

Financial support by the Deutsche Forschungsgemeinschaft (Ko 1349/20-1) is gratefully acknowledged.

ORCID® iDs

Ulrich Koert - https://orcid.org/0000-0002-4776-8549

References

1. Selter, L.; Zygalski, L.; Kerste, E.; Koert, U. *Synthesis* **2016,** *49,* 17–28. doi:10.1055/s-0035-1562623
2. Wasserman, H. H.; Parr, J. *Acc. Chem. Res.* **2004,** *37,* 687–701. doi:10.1021/ar0300221
3. Rubin, M. B.; Gleiter, R. *Chem. Rev.* **2000,** *100,* 1121–1164. doi:10.1021/cr960079j
4. Truong, P. M.; Zavalij, P. Y.; Doyle, M. P. *Angew. Chem., Int. Ed.* **2014,** *53,* 6468–6472. doi:10.1002/anie.201402233
5. Truong, P.; Shanahan, C. S.; Doyle, M. P. *Org. Lett.* **2012,** *14,* 3608–3611. doi:10.1021/ol301317a
6. Classen, M. J.; Böcker, M. N. A.; Roth, R.; Amberg, W. M.; Carreira, E. M. *J. Am. Chem. Soc.* **2021,** *143,* 8261–8265. doi:10.1021/jacs.1c04210
7. Satoh, T.; Kaneko, Y.; Okuda, T.; Uwaya, S.; Yamakawa, K. *Chem. Pharm. Bull.* **1984,** *32,* 3452–3460. doi:10.1248/cpb.32.3452
8. Jackson, R. K., III; Wood, J. L. *Org. Lett.* **2021,** *23,* 1243–1246. doi:10.1021/acs.orglett.0c04219
9. Chen, T.; Altmann, K.-H. *Chem. – Eur. J.* **2015,** *21,* 8403–8407. doi:10.1002/chem.201501252
10. Beller, M. P.; Harms, K.; Koert, U. *Org. Lett.* **2020,** *22,* 6127–6131. doi:10.1021/acs.orglett.0c02197
11. Pavan Kumar, C.; Ravinder, M.; Kumar, S.; Rao, V. *Synthesis* **2011,** 1320. doi:10.1055/s-0030-1259985
12. Ramulu, U.; Ramesh, D.; Rajaram, S.; Reddy, S. P.; Venkatesham, K.; Venkateswarlu, Y. *Tetrahedron: Asymmetry* **2012,** *23,* 117–123. doi:10.1016/j.tetasy.2012.01.014
13. Kerste, E.; Harms, K.; Koert, U. *Org. Lett.* **2019,** *21,* 4374–4377. doi:10.1021/acs.orglett.9b01594
14. Kerste, E.; Beller, M. P.; Koert, U. *Eur. J. Org. Chem.* **2020,** 3699–3711. doi:10.1002/ejoc.202000465
15. Condakes, M. L.; Hung, K.; Harwood, S. J.; Maimone, T. J. *J. Am. Chem. Soc.* **2017,** *139,* 17783–17786. doi:10.1021/jacs.7b11493
16. Kinnel, R. B.; Gehrken, H. P.; Scheuer, P. J. *J. Am. Chem. Soc.* **1993,** *115,* 3376–3377. doi:10.1021/ja00061a065
17. Kinnel, R. B.; Gehrken, H.-P.; Swali, R.; Skoropowski, G.; Scheuer, P. J. *J. Org. Chem.* **1998,** *63,* 3281–3286. doi:10.1021/jo971987z
18. Overman, L. E.; Rogers, B. N.; Tellew, J. E.; Trenkle, W. C. *J. Am. Chem. Soc.* **1997,** *119,* 7159–7160. doi:10.1021/ja9712985
19. Bélanger, G.; Hong, F.-T.; Overman, L. E.; Rogers, B. N.; Tellew, J. E.; Trenkle, W. C. *J. Org. Chem.* **2002,** *67,* 7880–7883. doi:10.1021/jo026282y
20. Katz, J. D.; Overman, L. E. *Tetrahedron* **2004,** *60,* 9559–9568. doi:10.1016/j.tet.2004.06.140
21. Lanman, B. A.; Overman, L. E.; Paulini, R.; White, N. S. *J. Am. Chem. Soc.* **2007,** *129,* 12896–12900. doi:10.1021/ja074939x
22. Schnabel, C.; Sterz, K.; Müller, H.; Rehbein, J.; Wiese, M.; Hiersemann, M. *J. Org. Chem.* **2011,** *76,* 512–522. doi:10.1021/jo1019738
23. Helmboldt, H.; Köhler, D.; Hiersemann, M. *Org. Lett.* **2006,** *8,* 1573–1576. doi:10.1021/ol060115t
24. Nicolaou, K. C.; Kang, Q.; Wu, T. R.; Lim, C. S.; Chen, D. Y.-K. *J. Am. Chem. Soc.* **2010,** *132,* 7540–7548. doi:10.1021/ja102623j
25. Peters, R.; Althaus, M.; Nagy, A.-L. *Org. Biomol. Chem.* **2006,** *4,* 498–509. doi:10.1039/b514147h

26. Gramain, J. C.; Remuson, R.; Vallee, D. *J. Org. Chem.* **1985,** *50,* 710–712. doi:10.1021/jo00205a037
27. Wanner, M. J.; Ingemann, S.; van Maarseveen, J. H.; Hiemstra, H. *Eur. J. Org. Chem.* **2013,** 1100–1106. doi:10.1002/ejoc.201201505
28. Odagi, M.; Yamamoto, Y.; Nagasawa, K. *Angew. Chem., Int. Ed.* **2018,** *57,* 2229–2232. doi:10.1002/anie.201708575
29. Movassaghi, M.; Piizzi, G.; Siegel, D. S.; Piersanti, G. *Angew. Chem., Int. Ed.* **2006,** *45,* 5859–5863. doi:10.1002/anie.200602011
30. Wohlfahrt, M.; Harms, K.; Koert, U. *Angew. Chem., Int. Ed.* **2011,** *50,* 8404–8406. doi:10.1002/anie.201103679
31. Wohlfahrt, M.; Harms, K.; Koert, U. *Eur. J. Org. Chem.* **2012,** 2260–2265. doi:10.1002/ejoc.201200059
32. Smith, A. B., III; Liu, Z. *Org. Lett.* **2008,** *10,* 4363–4365. doi:10.1021/ol801794f
33. Schütte, J.; Kilgenstein, F.; Fischer, M.; Koert, U. *Eur. J. Org. Chem.* **2014,** 5302–5311. doi:10.1002/ejoc.201402531
34. Beller, M. P.; Ivlev, S.; Koert, U. *Org. Lett.* **2022,** *24,* 912–915. doi:10.1021/acs.orglett.1c04261

License and Terms

BEILSTEIN JOURNAL OF ORGANIC CHEMISTRY

Enantioselective total synthesis of putative dihydrorosefuran, a monoterpene with an unique 2,5-dihydrofuran structure

Irene Torres-García, Josefa L. López-Martínez, Rocío López-Domene, Manuel Muñoz-Dorado, Ignacio Rodríguez-García and Miriam Álvarez-Corral*

Full Research Paper

Open Access

Address:
Departamento Química Orgánica, Universidad de Almería, ceiA3. E04120 Almería, Spain

Email:
Miriam Álvarez-Corral* - malvarez@ual.es

* Corresponding author

Keywords:
Ag(I) cyclization; allenylation; $CpTiCl_2$; 2,5-dihydrofurans; monoterpenes

Beilstein J. Org. Chem. **2022,** *18,* 1264–1269.
https://doi.org/10.3762/bjoc.18.132

Received: 28 July 2022
Accepted: 09 September 2022
Published: 19 September 2022

This article is part of the thematic issue "Total synthesis: an enabling science".

Associate Editor: B. Nay

Abstract

An original synthesis of the structure of dihydrorosefuran, a compound allegedly identified in *Artemisia pallens* and *Tagetes mendocina*, has been developed. The key steps in the five-step 36% overall yield synthesis are a $CpTi^{III}Cl_2$ mediated Barbier-type allenylation of a linear aldehyde and the formation of a 2,5-dihydrofuran scaffold through a Ag(I)-mediated cyclization. Neither of the reported spectral data for dihydrorosefuran match those of the synthetic product, suggesting that the isolated compound from *Tagetes mendocina* is in fact the natural product rosiridol, while the real structure of the product from *Artemisia pallens* remains unknown.

Introduction

Artemisia pallens is an aromatic plant from southern India whose essential oil, known as Davana oil, has shown increasing interest mainly for its use in some beverages, cakes, pastries, etc., as well as in the perfumery industry [1]. In addition, *A. pallens* has been used in Indian traditional medicine (Ayurveda) for the treatment of measles, cough, cold, depression, diabetes, and high blood pressure [2]. More recently other biological activities have been reported, such as the blood glucose lowering effect of *A. pallens* [3,4], and its anti-asthmatic potential [5].

A component responsible for the fresh and floral odor of the essential oil was isolated from Davana oil and was assigned as a 2,5-dihydrofuranic monoterpenoid (compound **1** in Scheme 1) and named dihydrorosefuran [6-8]. Furthermore, the same structure was attributed to an isolated substance from the Argentinean herb *Tagetes mendocina* [9], although not all of its spectroscopic features did match point by point with those previously reported. This made us think that this could be a case of misassigned natural product [10], hence we decided to perform its total synthesis.

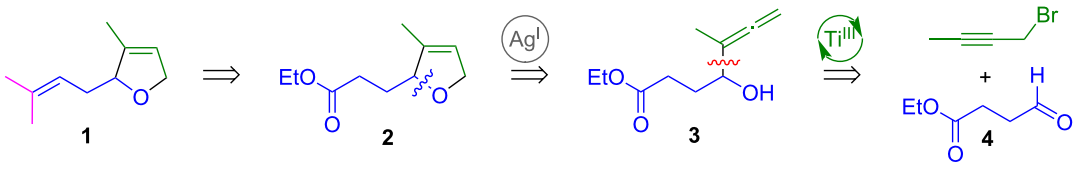

Scheme 1: Retrosynthetic scheme of the target molecule **1**.

Results and Discussion

Our synthetic strategy is based on two metal-mediated steps (Scheme 1). In this way, we thought that the 2,5-dihydrofuran structural motif that is found in the target molecule **1** could be prepared through a Ag(I)-induced intramolecular addition of the hydroxy group to the terminal double bond of the allene in compound **3**. Another key step is the Ti(III)-mediated straightforward synthesis of this α-hydroxyallene, which could be achieved through a regioselective Barbier-type coupling of a propargylic halide (1-bromo-2-butyne) with the aldehyde **4** mediated by the organometallic half-sandwich complex [$CpTi^{III}Cl_2$] [11,12].

Following this retrosynthetic proposal, our route starts from ethyl 4-oxobutanoate (**4**) [13] which was prepared by ozonolysis of commercially available ethyl pent-4-enoate (Scheme 2). Coupling of the aldehyde **4** with 1-bromobut-2-yne in the presence of $CpTi^{III}Cl_2$ (generated in situ by reduction of $CpTiCl_3$ with Mn) afforded α-hydroxyallene **3**. We have recently described that this Barbier-type reaction affords α-hydroxyallenes as major products, mixed with smaller amounts of homopropargylic alcohols, either if the reaction is performed with stoichiometric amounts of $CpTiCl_3$ or if catalytic amounts are used [12]. However, using the particular substrates in this approach, the allenic compound **3** was exclusively formed, in a satisfactory 81% yield [14]. It is also important to control the pH during the reaction workup, as some contamination of the product with lactone **5** can arise at low pH values, which goes in detriment of the yield. The 2,5-dihydrofuran ring in target compound **1** was obtained through a Ag(I)-mediated intramolecular addition of the hydroxy to the allene group, a process that transformed allene **3** into compound **2**. The isopropenyl residue of the target compound **1** was assembled through a two-step sequence. The first one was the addition of an excess of methylmagnesium bromide to the ester **2**, that completed the carbon skeleton. The second step was the pH-controlled regioselective dehydration of the tertiary alcohol **6** with amberlyst-15® leading to the monoterpene **1**. Other systems tested for the elimination of the hydroxy group in **6** were pyridinium *p*-toluenesulfonate (PPTS) and camphorsulfonic acid (CSA), that gave poorer results, failing to afford a single product. On the other hand, lactone **5** could also be transformed into alcohol **6** through a simple change in the order of the reactions: addition of methylmagnesium bromide to **5** afforded **7**, which was then transformed into **6** by the Ag(I)-mediated cyclization (Scheme 2).

Once we had synthesized racemic compound **1**, we designed a chiral version using a stereoselective kinetic resolution of allenol **3** via lipase AK-catalyzed acetylation [15]. In this way, unaltered, (−)-hydroxyallene **3** could be separated from (+)-acetyl derivative **9** through standard column chromatogra-

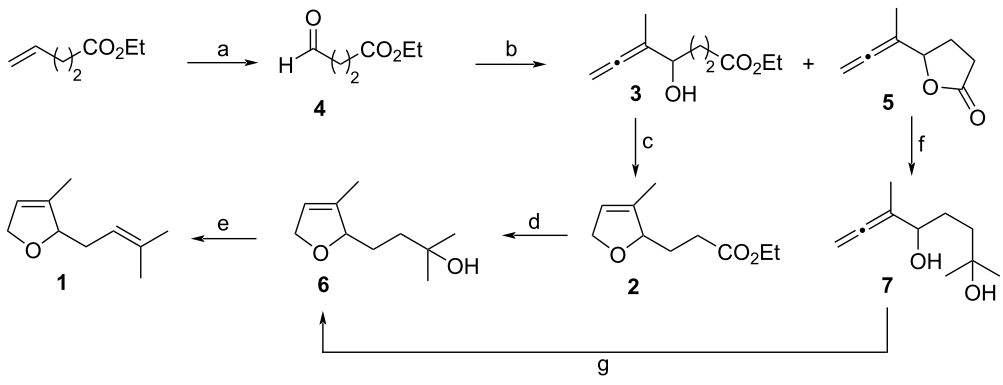

Scheme 2: Synthesis of dihydrofuran-monoterpenoid **1**. a) i. O_3, −78 °C; ii. PPh_3, rt, 76%; b) 1-bromobut-2-yne, $CpTiCl_3$, Mn and THF (**3**: 71–81%, **5**: 0–10%); c) $AgNO_3$, Me_2CO, 88%; d) MeMgBr, Et_2O, 90%; e) Amberlyst®-15, DCM, 74%; f) MeMgBr, Et_2O, 83%; g) $AgNO_3$, Me_2CO, 75%.

phy (Scheme 3). Enantiomeric excesses of (−)-**3** and (+)-**9** were determined by chiral HPLC analyses. Analysis of the NMR data of the Mosher's derivatives of **8** suggested (*S*) configuration for the alcohol (−)-**3** [16].

On the other hand, enantiopure acetate (+)-(*R*)-**9** was transformed into diol (+)-(*R*)-**7** by the addition of an excess of MeMgBr. Finally, these enantiopure compounds, α-hydroxyallene (−)-(*S*)-**3** and diol (+)-(*R*)-**7**, can be used to prepare both enantiomers of compound **1** following the procedures shown in Scheme 2.

Unfortunately, once the racemic synthesis was successfully completed and the chiral design was fulfilled, it was found that the spectroscopic data of compound **1** did not match neither with those published for the allegedly dihydrorosefuran isolated from *Artemisia pallens* nor with those reported for the compound from *Tagetes mendocina* (see Table 1 and Table 2). The ^{13}C NMR data of compound **1** are quite similar to those of the natural product isolated from *T. mendocina,* except for the signals of the oxygenated carbons (C2 and C5). The same behavior pattern can be observed in the ^{1}H NMR data. This made us think that the natural product of *T. mendocina* could have an acyclic skeleton instead of a dihydrofuran one. For this reason, we propose this compound should be the diol called rosiridol (Table 1), a substance that has been isolated from other natural sources [18,19], whose structure was also confirmed by total synthesis some years ago [20]. Comparison of NMR data (Table 1) confirmed the initial suspicion. We are still intrigued about the real structure of the natural product isolated from *A. pallens*. However, it must be considered that this product was elucidated using low frequency NMR machines, which suggests that further research on the chemical composition of this oil is needed.

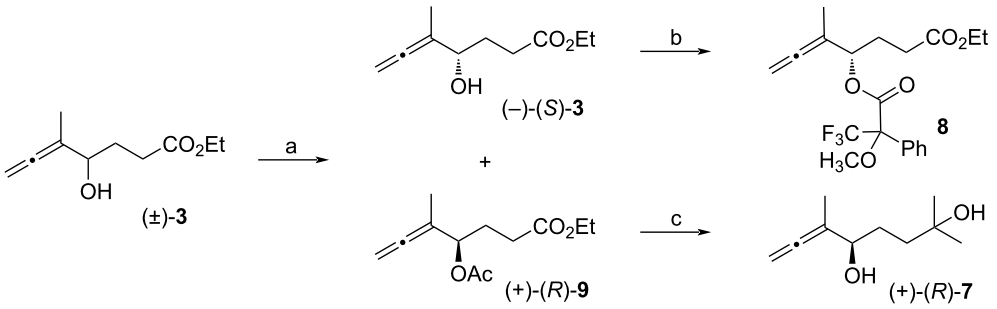

Scheme 3: Racemic resolution of allenol **3** and synthesis of derivatives. a) Lipase AK, vinyl acetate, *t*-BuOMe, 30 °C, ((–)-(*S*)-**3**: 46%, 90% ee, (+)-(*R*)-**9**: 39%, 95% ee); b) *N*,*N*'-dicyclohexylcarbodiimide (DCC), dimethylaminopyridine (DMAP), (*S*) or (*R*)-(–)-α-methoxy-α-(trifluoromethyl)phenylacetic acid, 66% [17], c) MeMgBr (5 equiv), Et_2O, 67%.

Table 1: ^{1}H NMR data of isolated and synthetic products.[a]

	sources of claimed dihydrorosefuran		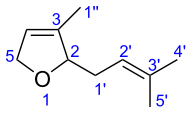 **1**	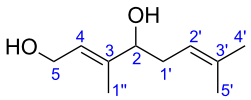 rosiridol[b]
	A. pallens[a,c] [7,8]	*T. mendocina*[d] [9]	this work synthesis[e]	literature synthesis[d] [20]
H2	4.04 (td, *J* = 8.0, 1.0 Hz)	4.03 (t, *J* = 8 Hz)	4.67 (br s)	4.02–3.99 (m)
H4	5.07 (td, *J* = 8.0, 1.0 Hz)	5.66 (t, *J* = 8 Hz)	5.51 (br s)	5.67–5.62 (m)
H5	4.55 (d, *J* = 7.0 Hz)	4.21 (dd)	4.62–4.53 (m)	4.24–4.15 (m)
H1'	2.30 (m)	2.24 (m)	2.41 (m), 2.20 (ddd, *J* = 14.0, 7.0, 6.5 Hz)	2.28–2.19 (m)
H2'	5.32 (t, *J* = 7.0 Hz)	5.13 (t, *J* = 8 Hz)	5.21 (t, hept, *J* = 6.9, 1.5 Hz)	5.13–5.09 (m)
H4'	1.67 (s)	1.75 (s)	1.74 (s)	1.73 (d, *J* = 1.1 Hz)
H5'	1.60 (s)	1.66 (s)	1.66 (s)	1.64 (s)
H1"	2.05 (s)	1.69 (s)	1.72 (s)	1.67 (s)

[a]$CDCl_3$ in all cases; [b]arbitrary numbering for comparison purposes; [c]80 MHz; [d]400 MHz; [e]500 MHz.

Table 2: ^{13}C NMR data of isolated and synthetic products[a].

	sources of claimed dihydrorosefuran		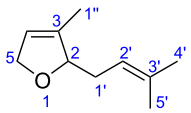 **1**	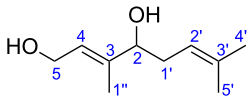 rosiridol[b]
	A. pallens[a,c] [7,8]	*T. mendocina*[d] [9]	this work synthesis[e]	literature synthesis[d] [20]
C2	64.0	76.4	87.5	76.4
C3	145.5	140.4	138.1	140.2
C4	129.3	124.5	120.7	124.5
C5	61.0	59.1	74.5	59.0
C1'	39.8	34.2	32.9	34.1
C2'	118.0	119.7	119.7	119.8
C3'	142.0	135.3	133.6	135.0
C4'	26.2	25.9	25.9	25.8
C5'	24.8	18.0	18.0	18.0
C1"	17.5	12.2	12.5	12.0

[a]$CDCl_3$ in all cases; [b]arbitrary numbering for comparison purposes; [c]80 MHz; [d]100 MHz; [e]125 MHz.

Conclusion

In summary, we have proved that the two-step sequence Ti^{III} allenylation–Ag^{I} cyclization is a simple and efficient strategy for the preparation of the 2,5-dihydrofuran moiety present in many natural products. In fact, we have achieved the total synthesis of the 2,5-dihydrofuran structure **1**. After systematic data analysis of our prepared compound and those in the literature, it can be concluded that the proposed structure of the product isolated from *Artemisia pallens* oil, dihydrorosefuran, is not correct. In addition, it is clear that the compound isolated from *Tagetes mendocina* is the acyclic diol named rosiridol.

Experimental

Ti-induced allenylation of ethyl 4-oxobutanoate (**4**)

Under an Ar atmosphere, dry THF (8 mL) that was deoxygenated prior to use was added to a mixture of $CpTiCl_3$ (329 mg, 1.50 mmol) and Mn dust (165 mg, 3.00 mmol) resulting in a green suspension. Then, a solution of ethyl 4-oxobutanoate (**4**, 196 mg, 1.50 mmol) and 1-bromobut-2-yne (0.27 mL, 3.00 mmol) in THF (2 mL) was dripped and the mixture was stirred for 2.5 hours. The mixture was filtered, diluted with EtOAc, washed with 3% HCl and brine, and dried (anhydrous $MgSO_4$), and the solvent was removed. The residue was purified by flash chromatography (*n*-hexane/EtOAc 8:2) to afford ethyl 4-hydroxy-5-methylhepta-5,6-dienoate (**3**, 225 mg, 81%) isolated as light yellow oil. IR (ATR) ν (cm^{-1}): 3434, 2972, 2928, 1958, 1723, 1436, 1374, 1172, 1028, 925, 853; ^{1}H NMR (300 MHz, $CDCl_3$) δ 4.77 (dq, J = 2.3, 3.2 Hz, 2H), 4.12 (q, J = 7.1 Hz, 2H), 4.05 (m, 1H), 2.42 (t, J = 7.2 Hz, 2H), 2.18 (s, 1H), 2.04–1.77 (m, 2H), 1.70 (td, J = 0.5, 3.2 Hz, 3H), 1.25 (t, J = 7.1 Hz, 3H) ppm; ^{13}C NMR (75 MHz, $CDCl_3$, DEPT) δ 204.8 (C), 174.0 (C), 101.6 (C), 77.0 (CH_2), 71.5 (CH), 60.5 (CH_2), 30.4 (CH_2), 30.0 (CH_2), 14.5 (CH_3), 14.2 (CH_3) ppm; HRMS–ESI (Q-TOF, *m/z*): $[M + H]^+$ calcd for $C_{10}H_{17}O_3$, 185.1178; found, 185.1158. A lactone is formed as side product (0–10%) when the HCl solution used for the workup has a concentration higher than 3%. Compound **5**: IR (ATR) ν (cm^{-1}): 2982, 2927, 1960, 1772, 1427, 1331, 1162, 974, 918, 855; ^{1}H NMR (300 MHz, $CDCl_3$) δ 4.89 (m, 1H), 4.86 (m, 2H), 2.55 (m, 2H), 2.30 (m, 2H), 1.79 (t, J = 3.1 Hz, 3H) ppm; ^{13}C{^{1}H} NMR (75 MHz, $CDCl_3$, DEPT) δ 206.0 (C), 177.0 (C), 98.0 (C), 80.4 (CH), 77.5 (CH_2), 28.5 (CH_2), 26.1 (CH_2), 15.0 (CH_3) ppm; HRMS–ESI (Q-TOF, *m/z*): $[M + H]^+$ calcd for $C_8H_{11}O_2$,139.0759; found, 139.0782.

Silver(I)-promoted cyclization of ethyl 4-hydroxy-5-methylhepta-5,6-dienoate (**3**)

A solution of the allenol **3** (65 mg, 0.35 mmol) in acetone (2 mL) was added to a suspension of $AgNO_3$ (120 mg, 0.70 mmol) in acetone (1.5 mL) in the absence of light, and the mixture was stirred at 40 °C overnight. Brine was added and the mixture was extracted with Et_2O. The organic phase was dried over anhydrous $MgSO_4$, and concentrated under reduced pressure. The residue was purified by silica gel flash column chromatography (*n*-hexane/EtOAc 9:1) to afford ethyl 3-(3-methyl-2,5-dihydrofuran-2-yl)propanoate (**2**, 57 mg, 88%) isolated as colorless oil. IR (ATR) ν (cm^{-1}): 2969, 2927, 2849, 1731, 1442, 1376, 1251, 1160, 1092, 1026, 895, 734. ^{1}H NMR (300 MHz,

$CDCl_3$) δ 5.53 (m, 1H), 4.69 (br s, 1H), 4.56 (m, 2H), 4.15 (q, *J* = 7.1 Hz, 2H), 2.39 (m, 2H), 2.12–2.06 (m, 1H), 1.83–1.74 (m, 1H), 1.72 (br s, 3H), 1.27 (t, *J* = 7.1 Hz, 3H) ppm; $^{13}C\{^1H\}$ NMR (75 MHz, $CDCl_3$, DEPT) δ 173.9 (C), 137.2 (C), 121.3 (CH), 86.4 (CH), 74.7 (CH_2), 60.3 (CH_2), 29.4 (CH_2), 28.9 (CH_2), 14.2 (CH_3), 12.3 (CH_3) ppm; HRMS–ESI (Q-TOF, *m/z*): $[M + H]^+$ calcd for $C_{10}H_{17}O_3$,185.1172; found, 184.1162.

Synthesis of 2-methyl-4-(3-methyl-2,5-dihydrofuran-2-yl)butan-2-ol (**6**)

Under an N_2 atmosphere, methylmagnesium bromide (3 M in Et_2O, 0.075 mL, 0.23 mmol) was diluted with dry Et_2O (1.5 mL). A solution of ethyl 3-(3-methyl-2,5-dihydrofuran-2-yl)propanoate (**2**, 16 mg, 0.087 mmol) in Et_2O (1 mL) was added dropwise and the reaction mixture was stirred for 3 hours at room temperature. The reaction was quenched with saturated NH_4Cl and extracted with EtOAc. The combined organic layer was washed with saturated $NaHCO_3$, brine, and dried over anhydrous $MgSO_4$. The solvent was evaporated in vacuum and the residue was purified using column chromatography (*n*-hexane/EtOAc 7:3) to give 2-methyl-4-(3-methyl-2,5-dihydrofuran-2-yl)butan-2-ol (**6**, 169 mg, 90%) isolated as colorless oil. IR (ATR) *ν* (cm^{-1}): 3425, 2969, 2922, 2852, 1636, 1444, 1382, 1089, 1057, 1025; ^1H NMR (300 MHz, $CDCl_3$) δ 5.51 (br s, 1H), 4.68 (br s, 1H), 4.58 (m, 2H), 2.05 (br s, 1H), 1.82 (m, 1H), 1.72 (br s, 3H), 1.57 (m, 3H), 1.24 (s, 6H) ppm; $^{13}C\{^1H\}$ NMR (75 MHz, $CDCl_3$, DEPT) δ 137.8 (C), 120.7 (CH), 87.7 (CH), 74.5 (CH_2), 70.4 (C), 38.5 (CH_2), 29.5 (CH_3), 29.4 (CH_3), 28.3 (CH_2), 12.5 (CH_3) ppm; HRMS–ESI (Q-TOF, *m/z*): $[M + H]^+$ calcd for $C_{10}H_{19}O_2$, 171.1385; found, 171.1368.

Synthesis of 3-methyl-2-(3-methylbut-2-en-1-yl)-2,5-dihydrofuran (**1**)

The reaction of amberlyst®-15 (dry, 97 mg) and 2-methyl-4-(3-methyl-2,5-dihydrofuran-2-yl)butan-2-ol (**6**, 97 mg, 0.57 mmol), based on the previously reported literature procedure [21], afforded 3-methyl-2-(3-methylbut-2-en-1-yl)-2,5-dihydrofuran (**1**, 64 mg, 74%) isolated as colorless oil. IR (ATR) *ν* (cm^{-1}): 3066, 2965, 2918, 2843, 1668, 1445, 1377, 1080, 975, 850, 778; ^1H NMR (500 MHz, $CDCl_3$) δ 5.51 (br s, 1H, H4), 5.21 (t, hept, *J* = 7.0, 1.5 Hz, 1H, H2'), 4.67 (br s, 1H, H2), 4.62–4.53 (m, 2H, H5), 2.41 (m, 1H, H1'a), 2.20 (ddd, *J* = 14.0, 7.0, 6.5 Hz, 1H, H1'b), 1.74 (d, *J* = 1.5 Hz, 3H, H4'*), 1.72 (m, 3H, H1''), 1.66 (br s, 3H, H5'*) ppm; $^{13}C\{^1H\}$ NMR (125 MHz, $CDCl_3$, DEPT) δ 138.1 (C, C3), 133.6 (C, C3'), 120.7 (CH, C4), 119.7 (CH, C2'), 87.5 (CH, C2), 74.5 (CH_2, C5), 32.9 (CH_2, C1'), 25.9 (CH_3, C4'*), 18.0 (CH_3, C5'*), 12.5 (CH_3, C1'') ppm (*may be interchanged); HRMS–ESI (Q-TOF, *m/z*): $[M + H]^+$ calcd for $C_{10}H_{17}O$, 153.1274; found, 153.1262.

Supporting Information

Supporting Information File 1

Experimental procedures, characterization of other substances, and copies of IR, NMR spectra and HPLC chromatograms.
[https://www.beilstein-journals.org/bjoc/content/supplementary/1860-5397-18-132-S1.pdf]

Funding

We are grateful for the financial support received from Junta de Andalucía (Conserjería de Economía, Conocimiento, Empresas, y Universidad CTEICU) and Fondo Europeo de Desarrollo Regional (FEDER) for the Project UAL2020-FQM-B1989.

ORCID® iDs

Irene Torres-García - https://orcid.org/0000-0003-0967-4311
Josefa L. López-Martínez - https://orcid.org/0000-0003-2598-1573
Manuel Muñoz-Dorado - https://orcid.org/0000-0002-2679-270X
Ignacio Rodríguez-García - https://orcid.org/0000-0002-2985-8567
Miriam Álvarez-Corral - https://orcid.org/0000-0002-4300-4680

References

1. Hellivan, P.-J. *Perfum. Flavor.* **2011,** *36,* 38–43.
2. Kulkarni, R. N. Artemisia pallens. In *Artemisia;* Wright, C. W., Ed.; Taylor & Francis: London, UK, 2002; Vol. 18, pp 119–137.
3. Subramoniam, A.; Pushpangadan, P.; Rajasekharan, S.; Evans, D. A.; Latha, P. G.; Valsaraj, R. *J. Ethnopharmacol.* **1996,** *50,* 13–17. doi:10.1016/0378-8741(95)01329-6
4. Pavithra, K. S.; Annadurai, J.; Ragunathan, R. *J. Pharmacogn. Phytochem.* **2018,** *7,* 664–675.
5. Mukherjee, A. A.; Kandhare, A. D.; Rojatkar, S. R.; Bodhankar, S. L. *Biomed. Pharmacother.* **2017,** *94,* 880–889. doi:10.1016/j.biopha.2017.08.017
6. Chandra, A.; Misra, L. N.; Thakur, R. S. *Tetrahedron Lett.* **1987,** *28,* 6377–6380. doi:10.1016/s0040-4039(01)91378-4
7. Misra, L. N.; Chandra, A.; Thakur, R. S. *Phytochemistry* **1991,** *30,* 549–552. doi:10.1016/0031-9422(91)83725-z
8. Misra, L. N.; Chandra, A.; Thakur, R. S. *Phytochemistry* **1991,** *30,* 4212–4213. doi:10.1016/0031-9422(91)83512-j
9. Lima, B.; Agüero, M. B.; Zygadlo, J.; Tapia, A.; Solis, C.; Rojas De Arias, A.; Yaluff, G.; Zacchino, S.; Feresin, G. E.; Schmeda-Hirschmann, G. *J. Chil. Chem. Soc.* **2009,** *54,* 68–72. doi:10.4067/s0717-97072009000100016
10. Nicolaou, K. C.; Snyder, S. A. *Angew. Chem., Int. Ed.* **2005,** *44,* 1012–1044. doi:10.1002/anie.200460864
11. López-Martínez, J. L.; Torres-García, I.; Rodríguez-García, I.; Muñoz-Dorado, M.; Álvarez-Corral, M. *J. Org. Chem.* **2019,** *84,* 806–816. doi:10.1021/acs.joc.8b02643
12. Torres-García, I.; López-Martínez, J. L.; Martínez-Martínez, R.; Oltra, J. E.; Muñoz-Dorado, M.; Rodríguez-García, I.; Álvarez-Corral, M. *Appl. Organomet. Chem.* **2020,** *34,* 10.1002/aoc.5244. doi:10.1002/aoc.5244

13. Smith, A. B., III; Fukui, M.; Vaccaro, H. A.; Empfield, J. R. *J. Am. Chem. Soc.* **1991,** *113,* 2071–2092. doi:10.1021/ja00006a029
14. Reaction performed with stoichiometric amounts of $CpTiCl_2$.
15. Li, W.; Lin, Z.; Chen, L.; Tian, X.; Wang, Y.; Huang, S.-H.; Hong, R. *Tetrahedron Lett.* **2016,** *57,* 603–606. doi:10.1016/j.tetlet.2015.12.098
16. Hoye, T. R.; Jeffrey, C. S.; Shao, F. *Nat. Protoc.* **2007,** *2,* 2451–2458. doi:10.1038/nprot.2007.354
17. Under this standard esterification conditions, some lactonization leading to compound **5** is observed.
18. Ali, Z.; Fronczek, F. R.; Khan, I. A. *Planta Med.* **2008,** *74,* 178–181. doi:10.1055/s-2008-1034288
19. Yoshikawa, M.; Nakamura, S.; Li, X.; Matsuda, H. *Chem. Pharm. Bull.* **2008,** *56,* 695–700. doi:10.1248/cpb.56.695
20. Schöttner, E.; Simon, K.; Friedel, M.; Jones, P. G.; Lindel, T. *Tetrahedron Lett.* **2008,** *49,* 5580–5582. doi:10.1016/j.tetlet.2008.07.018
21. Frija, L. M. T.; Afonso, C. A. M. *Tetrahedron* **2012,** *68,* 7414–7421. doi:10.1016/j.tet.2012.06.083

License and Terms

BEILSTEIN JOURNAL OF ORGANIC CHEMISTRY

Preparation of an advanced intermediate for the synthesis of leustroducsins and phoslactomycins by heterocycloaddition

Anaïs Rousseau, Guillaume Vincent and Cyrille Kouklovsky*

Full Research Paper

Open Access

Address:
Institut de Chimie Moléculaire et des Matériaux d'Orsay, Université Paris-Saclay, CNRS, F-91405 Orsay, France

Email:
Cyrille Kouklovsky* - cyrille.kouklovsky@universite-paris-saclay.fr

* Corresponding author

Keywords:
cycloaddition; organolithium; stereoselective; total synthesis

Beilstein J. Org. Chem. **2022,** *18,* 1385–1395.
https://doi.org/10.3762/bjoc.18.143

Received: 23 August 2022
Accepted: 23 September 2022
Published: 04 October 2022

This article is part of the thematic issue "Total synthesis: an enabling science".

Associate Editor: B. Nay

Abstract

A convergent strategy for the synthesis of leustroducsins and phoslactomycins has been designed, relying on the synthesis and the coupling of three main fragments. The central fragment was synthesized via a regio-and stereoselective nitroso Diels–Alder reaction with an enol phosphate, followed by reductive cleavage of the phosphate to the ketone **11b**. Coupling studies of this fragment with the lactone fragment was accomplished in a stereoselective fashion through a vinyllithium intermediate. An advanced synthetic intermediate was then obtained after functional group transformation.

Introduction

Leustroducsins **1a–c** and phoslactomycins **2a–f** are a family of closely related natural products extracted from *Streptomyces platensis* (leustroducsins) or *Streptomyces nigresens* (phoslactomycins) [1-4]. The main difference within this large family is the presence of an additional ester substituent on the terminal cyclohexane ring. Common structural motifs include a polyunsaturated acyclic chain with an unsaturated lactone ring and an amine-containing side chain (Figure 1).

These natural products have attracted much attention due to their original structure and to their activity as inhibitors of the serine/threonine phosphatase enzyme PP2A [5,6]. Therefore, phoslactomycins [7-12] and leustroducsins [13-17] have been subject of extensive synthetic studies.

In a project related to the synthesis of leustroducins and phoslactomycins, we have designed a convergent synthetic strategy involving the preparation and the coupling of three main fragments (Figure 2): the lactone fragment **3**, the central fragment **4** and the cyclohexane fragment **5**. We have previously described the enantioselective synthesis of the lactone fragment **3** [18]; we now disclose the synthesis of the oxazi-

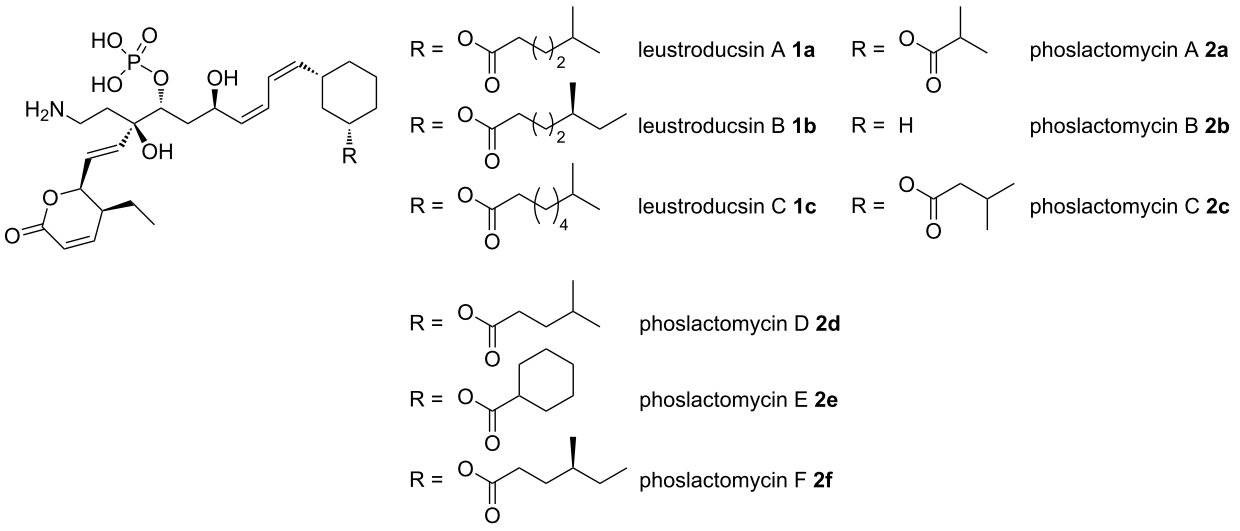

Figure 1: Structures of leustroducsins and phoslactomycins.

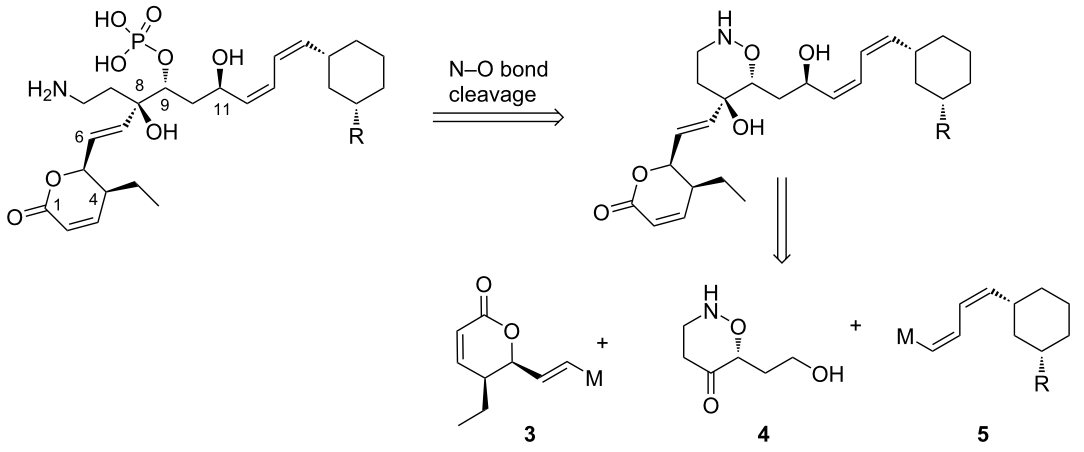

Figure 2: Synthetic strategy for the leustroducins and phoslactomycins.

none **4** and attempts for coupling both fragments for the synthesis of an advanced intermediate.

The synthetic strategy for the synthesis of the central fragment takes advantage of the proximity between the terminal amino function and the hydroxy function at C9. It was anticipated that both functions could arise from the cleavage of a N–O bond from an 1,2-oxazine, itself obtained by a nitroso Diels–Alder reaction from a chiral nitroso derivative and a functionalized diene (Figure 3). The nitroso Diels–Alder cycloaddition reaction has been well studied and has been used as a powerful tool for synthesis [19-22].

We have reported extensive studies on the regio-and stereoselectivity of nitroso Diels–Alder reactions between various nitroso derivatives and functionalized dienes [23]. These studies led to the selection of enol phosphates as ketone precursors for the diene functionalization. Enol phosphates display several advantages over the related enol silyl ethers [24,25]: they are more stable towards acidic conditions, their electronic character contributes to high regioselectivity in cycloaddition reactions, and they can be converted to many other functions, including their hydrolysis to ketones [26]. In the other hand, we have shown that the Wightman reagent **6**, a chiral chloronitroso derivative [27], led to a complete regio- and stereoselective reaction with functionalized dienes (Scheme 1). The chiral auxiliary contributes to both regioselectivity and stereoselectivity. After hydrolysis of the chiral auxiliary and Boc-protection of the nitrogen atom, cycloadduct **8** was obtained in 55% yield and 90% ee. Therefore, the combination of both these reagents

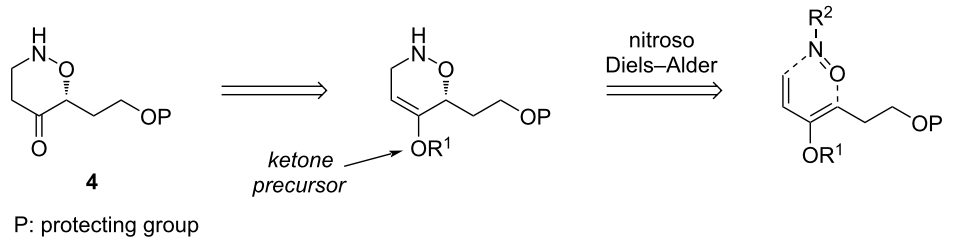

Figure 3: strategy for the synthesis of central fragment **4**: nitroso Diels–Alder reaction.

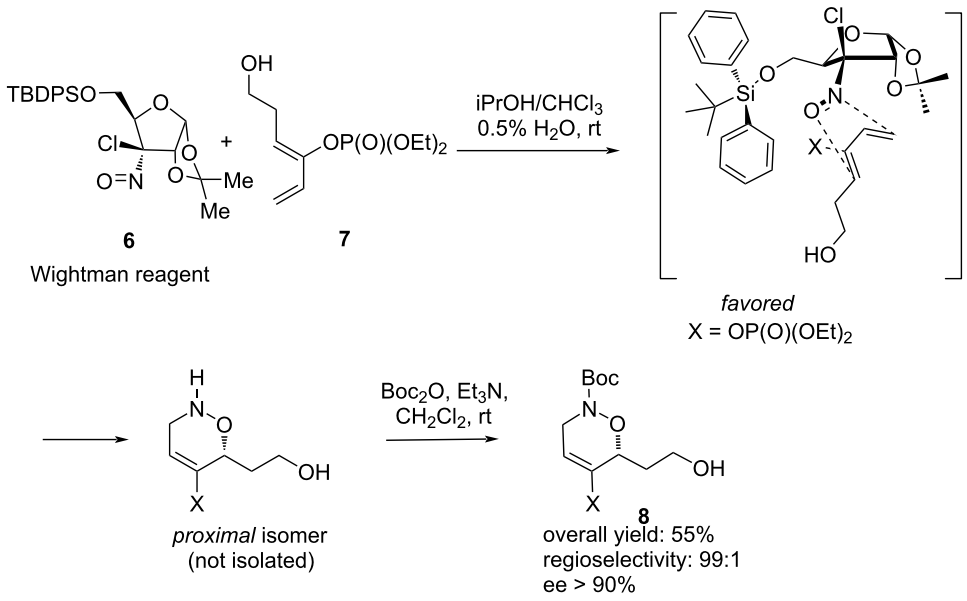

Scheme 1: A highly regio-and stereoselective nitroso Diels–Alder cycloaddition between Wightman's reagent **6** and a dienic enol phosphate.

should provide a quick and selective access to the central fragment of leustroducsins/phoslactomycins.

Results and Discussion

Asymmetric cycloaddition

Preliminary studies for the conversion of enol phosphate to the corresponding ketone were accomplished using an unprotected primary alcohol. However, it appeared that hydroxy group protection was necessary: control experiments made on the racemic cycloadduct **8** showed that basic hydrolysis of the enol phosphate led to the cyclic hemiacetal **9** in modest yield (Scheme 2).

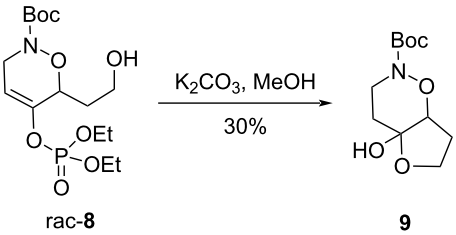

Scheme 2: Hydrolysis of enol phosphate in the unprotected cycloadduct.

Therefore, compound **8** was protected as silyl or benzyl ether using standard techniques. Unfortunately, no hydrolysis under several basic conditions provides the target ketone, no conversion and/or decomposition being observed (Scheme 3).

Enol phosphates can be hydrolysed under basic, acidic or reductive conditions [26]. Although acidic conditions could not be used due to the lability of the nitrogen Boc-protecting group, we found that the TIPS-protected cycloadduct **10b** could be cleanly transformed into the ketone **11b** with excess Red-Al [28], together with a small amount of the over reduced alcohol **12b**,

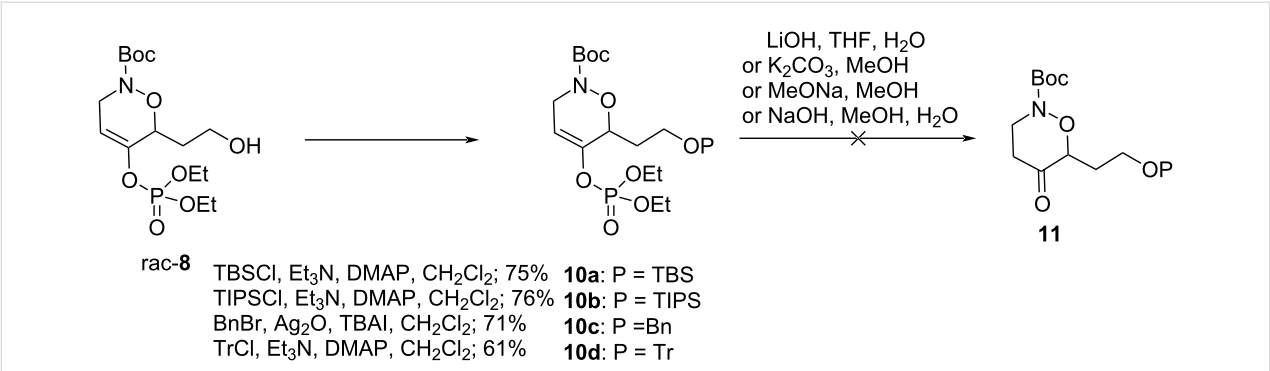

Scheme 3: Attempts for hydrolysis of the enol phosphate under basic conditions.

which could be reoxidized to **11b** (Scheme 4). Other substrates failed to deliver appreciable yields of the ketone under the same conditions.

These studies validate the role of TIPS ether as protecting group for the primary alcohol. At this stage we wondered whether it was possible to perform the whole synthetic sequence with this protecting group. Accordingly, the enol phosphate **13** was synthesized in five steps (26% overall yield) from 1,4-butanediol (Scheme 5). Since cycloaddition with the Wightman reagent **6** releases hydrogen chloride in the reaction medium, it was found necessary to add a small amount of calcium carbonate. Optically active cycloadduct **10b** was obtained in 73% yield and 86% ee after nitrogen protection as its Boc-carbamate. Ketone

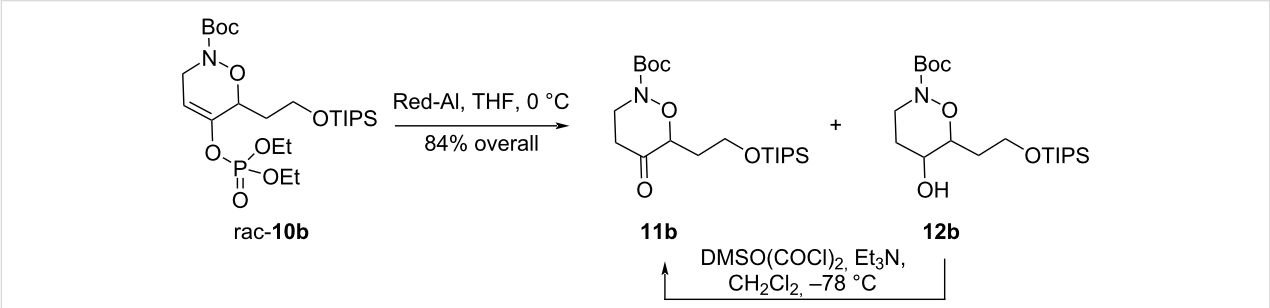

Scheme 4: Cleavage of enol phosphate with Red-Al.

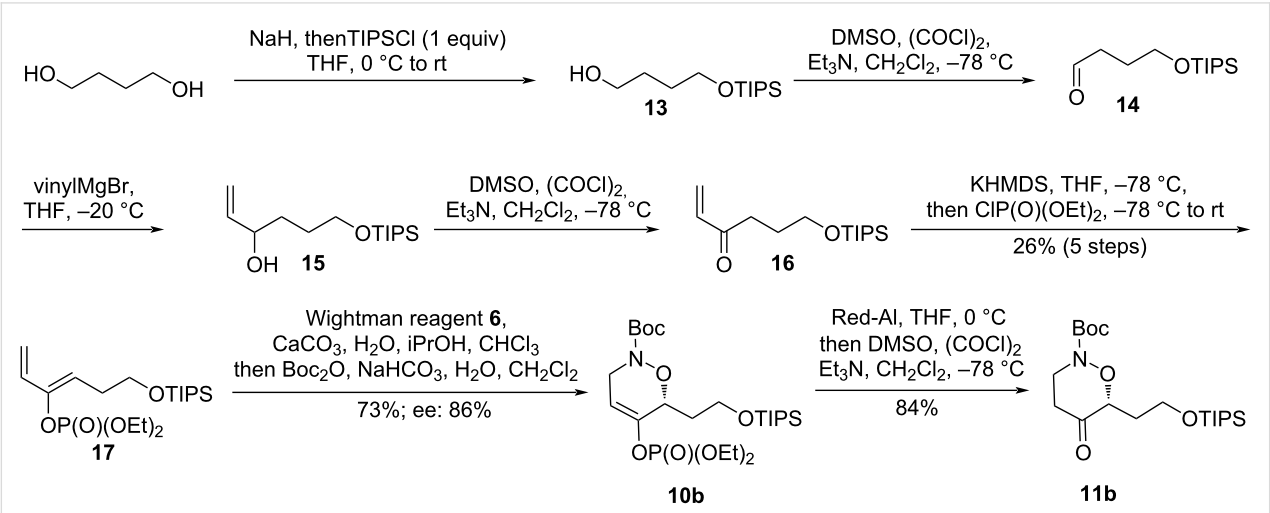

Scheme 5: Synthesis of the protected central fragment **11b**.

11b was obtained by Red-Al reduction in identical yield to the racemic equivalent.

We have therefore completed a quick, efficient and selective access to the central core of leustroducsins/phoslactomycins using an asymmetric nitroso Diels–Alder reaction. This fragment displays a ketone function that will be used for coupling with the lactone fragment **3** by generation of the tertiary alcohol.

Studies in fragment coupling

We have previously reported the synthesis of the lactone fragment by catalytic asymmetric [2 + 2] cycloaddition followed by ring extension [18]. The initial product was the TMS-acetylene **18** which could be easily desilylated to give **21**. However, model studies for coupling revealed the incompatibility of the lactone function; therefore, it was reduced with DIBAL-H then transformed into **19** by a one pot acetalization–desilylation procedure (91:9 mixture of diastereomers) [17]. Hydrozirconation followed by treatment with iodine furnished the target vinyl iodide **20** (Scheme 6); iodination with NIS, as previously described [29], gave lower yields.

We first attempted the coupling with the terminal alkyne **19**, anticipating the possibility of reducing the triple bond after coupling reaction. In agreement with literature precedents, we chose LiHMDS for deprotonation of **19** [30,31]. However, condensation of the corresponding lithium acetylide to the ketone **11b** gave modest and non-reproducible yields of the desired product **22** (Scheme 7, Table 1). The configuration of the newly created stereogenic center was undetermined.

Table 1: Coupling reaction between alkyne **19** and ketone **11b**.

entry	n_1	n_2	conditions	yield
1	1	1,2	–78 °C, 15 min, then rt, 8 h	21%
2	1	1,2	–78 °C, 2 h, then rt, 16 h	16%
3	1,5	1,8	–78 °C, 2 h, then rt, 3 h	24%
4	1,5	1,6	–78 °C, 2 h, then rt, 4 h	39%

These experiments showed the necessity to perform a fast reaction in order to avoid degradation. The optimal amount of base was found to be 1.6 equivalents (Table 1, entry 4). Higher

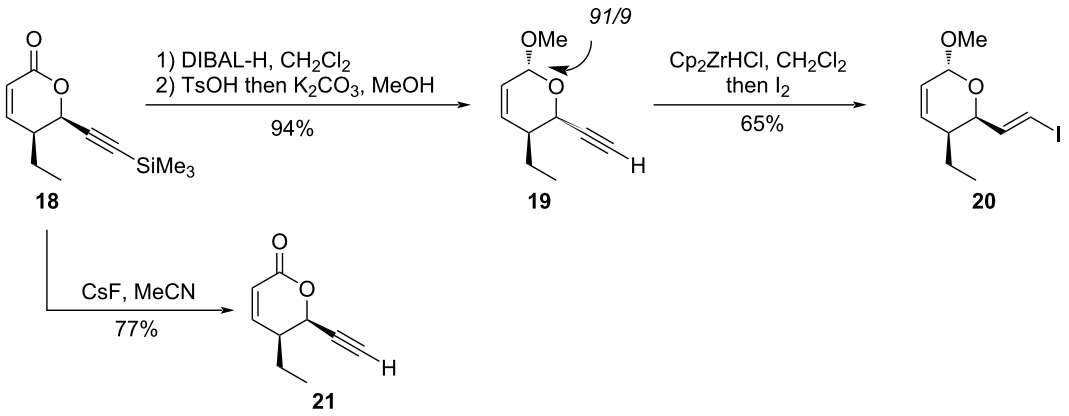

Scheme 6: Synthesis and derivatization of the lactone fragment.

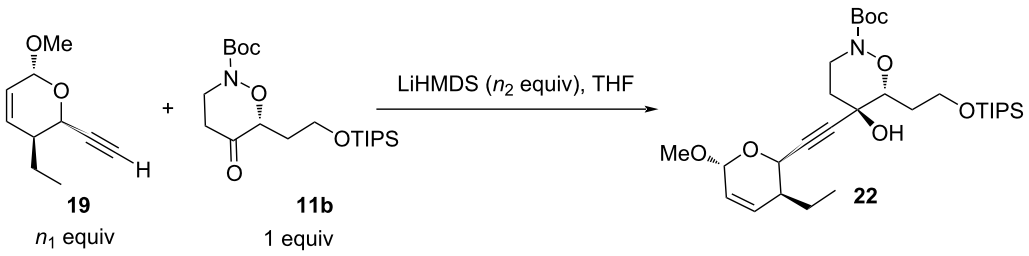

Scheme 7: Coupling reaction between alkyne **19** and ketone **11b**.

amounts lowered the yields (Table 1, entry 3), probably due to competitive enolization of the cyclic ketone. Excess alkyne was also necessary, as low yields were obtained when using equimolar amounts of both **19** and **11b** (Table 1, entries 1 and 2).

These disappointing results with alkyne **19** prompted us to investigate the coupling with an organometallic reagent derived from vinyl iodide **20**. This reagent was already synthesized and coupled with acyclic ketones in previous syntheses of leustroducsins or phoslactomycins [7-17]. Thus, treatment of **20** with *n*-butyllithium in THF gave the organometallic intermediate which was condensed onto ketone **11b** (Scheme 8, Table 2). Since no product was obtained under these standard conditions, we considered the use of additives in order to make the organolithium intermediate more nucleophilic. However, no reaction was observed when $ZnMe_2$ (which was used in the synthesis of leustroducsin B by Trost and co-workers [17]) was added; trimethylaluminum and cerium chloride also failed to promote the reaction. However, switching the solvent from THF to toluene afforded 21% of product **23** with $CeCl_3$ as additive. It appeared that the solvent had more influence on the course of the reaction than the metal. Indeed, reaction between vinyl iodide and ketone with *n*-BuLi in toluene [32] without any additive gave a reproducible 46% yield of **23**. Optimal conditions were obtained using 1.8 equivalents of vinyl iodide and 1.7 equivalents of BuLi (Table 2, entry 6).

It was difficult at this stage to determine the stereoselectivity of the coupling reaction since the starting acetal in **20** was a mixture of diastereomers. Therefore, we decided to oxidize the acetal in **23** to the corresponding lactone (Scheme 9). The acetal was first hydrolyzed to the hemiacetal **24** in quantitative yield. Oxidation of **24** proved delicate due to the lability of the tertiary allylic alcohol, and the presence of acid-sensitive protecting groups. Several conditions were tested: silver oxide on celite [33] failed to give any conversion. PCC with sodium acetate [34] gave only traces of the target lactone **25**. However, the use of the Jones' reagent gave reproducible yields of **25**, together with the deprotected alcohol **26**. Under optimized conditions (1.15 equiv, 15 min) a combined 46% yield could be obtained. Higher equivalents of the oxidizing reagents or longer reaction time considerably lowered the yields.

NMR analysis of products **25** and **26** showed these compounds were obtained as single diastereomers, thus indicating the complete stereoselectivity of the coupling reaction. This validates the overall strategy for the synthesis of leustroducsins or phoslactomycins by the synthesis of a central cyclic core and its coupling with the other fragments.

Conclusion

We have synthesized an advanced intermediate for the total synthesis of leustroducsins and phoslactomycins using a highly regio- and stereoselective nitroso Diels–Alder reaction, and a coupling reaction between a ketone and a vinyllithium reagent. This strategy offered quick and stereoselective access to an advanced precursor to these natural products. Further studies concerning the completion of the total synthesis via the preparation and coupling of the fragment **5** is under study in our laboratory.

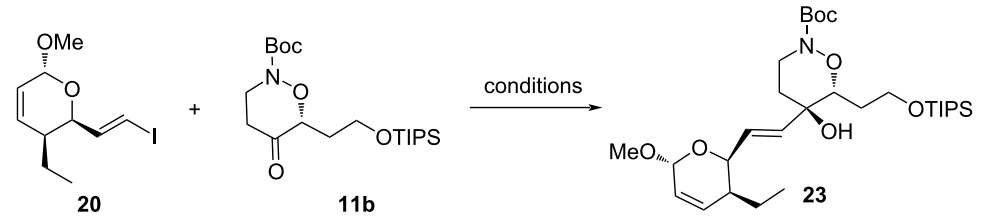

Scheme 8: Coupling reaction between vinyl iodide **20** and ketone **11b**.

Table 2: Coupling reaction between vinyl iodide **20** and ketone **11b**.

entry	conditions	yield
1	2 equiv **20**, 1.8 equiv *n*-BuLi, THF, –78 °C to rt	0%
2	2 equiv **20**, 1.8 equiv *n*-BuLi, 2 equiv $ZnMe_2$, THF, –78 °C to rt	0%
3	2 equiv **20**, 1.8 equiv *n*-BuLi, 2 equiv $AlMe_3$, THF, –78 °C to rt	0%
4	2 equiv **20**, 1.8 equiv *n*-BuLi, 2 equiv $CeCl_3$, THF, –78 °C to rt	0%
5	2 equiv **20**, 1.8 equiv *n*-BuLi, 2 equiv $CeCl_3$, **toluene**, –78 °C to rt	21%
6	1.8 equiv **20**, 1.7 equiv *n*-BuLi, **toluene**, –78 °C to rt	46%

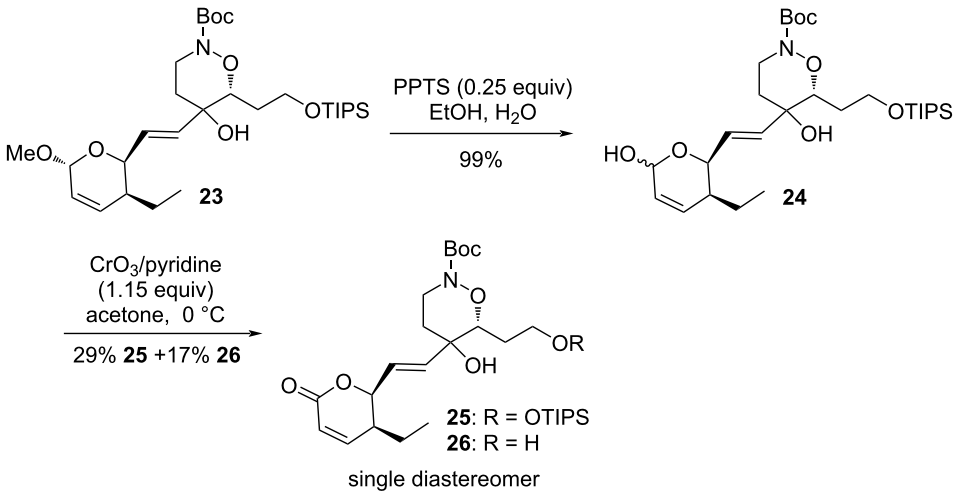

Scheme 9: Oxidation of the acetal to the lactone.

Experimental

Unless otherwise stated, all reactions were conducted in oven-dried glassware under an atmosphere of dry argon. Tetrahydrofuran was distilled over sodium/benzophenone ketyl under argon. Acetonitrile, dichloromethane, DMSO, DMF and toluene were distilled over calcium hydride under argon. All other reagents were used as received. Chromatographic purifications refer to flash chromatography on silica gel. ^{1}H NMR spectra were measured at 250, 300, 360 or 400 MHz using $CDCl_3$ as solvent using residual chloroform (7.26 ppm) as an internal reference. ^{13}C NMR spectra were measured at 62.5, 75 or 90 MHz using residual chloroform (77.1 ppm) as an internal reference. High-resolution mass spectrometry (HRMS) analyses were conducted with electro spray ionization (ESI).

6-Triisopropylsilyloxyhex-1-en-3-one (16): A solution of oxalyl chloride (0.49 mL, 5.75 mmol, 1.5 equiv) in dichloromethane (12 mL) was cooled to −78 °C and DMSO (0.82 mL, 11.49 mmol, 3 equiv) was added over 5 min. After 15 min, a solution of the alcohol **15** [35] (1.044 g, 3.83 mmol) in dichloromethane (5 mL) was added over 5 min. The reaction mixture was stirred for 30 min at −78 °C before addition of triethylamine (2.7 mL, 19.15 mmol, 5 equiv). The cooling bath was removed and the solution was allowed to warm to rt in 30 min. It was then poured into diethyl ether (50 mL) and the solution was successively washed with saturated aqueous $CuSO_4$ solution (4 × 12.5 mL), saturated aqueous NH_4Cl solution (3 × 12.5 mL), dried ($MgSO_4$), filtered and concentred under reduced pressure to give a brown oil (1.021 g, 99%). R_f: 0,59 (10% AcOEt/cyclohexane); ^{1}H NMR (300 MHz, $CDCl_3$) δ 6.32 (dd, J = 17.7, 10.2 Hz, 1H), 6.19 (dd, J = 17.7, 1.5 Hz, 1H), 5.78 (dd, J = 10.2, 1.5 Hz, 1H), 3.68 (t, J = 6 Hz, 2H), 2.68 (t, J = 7.2 Hz, 2H), 1.86–1.77 (m, 2H), 1.00 (m, 21H) ppm; ^{13}C NMR (75 MHz, $CDCl_3$) δ 200.8, 136.7, 127.9, 62.4, 35.9, 27.2, 18.0, 12.0 ppm; HRMS (*m*/*z*): [M + Na]$^+$ calcd 293.1907; found, 293.1898.

(3*Z*)-3-Diethylphosphoryloxy-6-triisopropylsilyloxyhexa-1,3-dien (17): A 0.5 M solution of potassium hexamethyldisilazide in toluene (4.4 mL, 2.22 mmol, 1.2 equiv) was added to a cooled (−78 °C) solution of diethyl chlorophosphate (0.27 mL, 1.85 mmol) in anhydrous THF (7 mL). A solution of the enone **16** (500 mg, 1.85 mmol) in THF (6 mL) was then slowly added. The solution was stirred 30 min at −78 °C, then 1 h at 0 °C and then 1 h at rt, before being poured in diethyl ether (35 mL). The solution was washed with 5% aqueous ammonia solution (18 mL). The aqueous layer was extracted with diethyl ether (3 × 35 mL) and the combined organic layers were dried ($MgSO_4$), filtered and concentred under reduced pressure to give a brown oil. Purification by column chromatography (25% AcOEt/cyclohexane) gave the enol phosphate **17** as a yellow oil (200 mg, 26%). R_f: 0.47 (30% AcOEt/cyclohexane); ^{1}H NMR (360 MHz, $CDCl_3$) δ 6.15 (dd, J = 17.3, 10.8 Hz, 1H), 5.47 (d, J = 17.3 Hz, 1H), 5.29 (dt, J = 7.2, 1.4 Hz, 1H), 5.08 (d, J = 10.8 Hz, 1H), 4.15–4.12 (m, 4H), 3.71 (t, J = 6.5 Hz, 2H), 2.48 (2dt, J = 7.2, 6.5 Hz, 2H), 1.31 (dt, J = 6.8, 1.1 Hz, 6H), 1.01 (m, 21H) ppm; ^{13}C NMR (90 MHz, $CDCl_3$) δ 146.2, 131.9, 118.0, 114.2, 64.4, 62.4, 30.0, 18.0, 16.2, 12.0 ppm; HRMS (*m*/*z*): [M + H]$^+$ calcd 407.2377; found, 407.2359.

(6*R*)-*tert*-Butyl 5-(diethoxyphosphoryloxy)-6-(2-((triisopropylsilyl)oxy)ethyl)-3,6-dihydro-2*H*-1,2-oxazine-2-carboxylate (10b): A solution of the enol phosphate **17** (420 mg, 1.03 mmol) in chloroform (1.8 mL) was added to a solution of the Wightman reagent **6** (981 mg, 2.06 mmol, 2 equiv), calcium carbonate (206 mg, 2.06 mmol, 2 equiv) and water (40 µL,

2.06 mmol, 2 equiv) in isopropanol (1.8 mL). The mixture was stirred at rt for 30 h. Water (0.75 mL) was added and the solution stirred for additional 1 h. The pH was adjusted to 8 by addition of saturated aqueous $NaHCO_3$ solution (1,6 mL), and a solution of Boc_2O (899 mg, 4.12 mmol, 4 equiv) in chloroform (0.8 mL) was added. The solution was stirred at rt for 64 h and poured into a mixture of water (37 mL) and dichloromethane (74 mL); the layers were separated and the aqueous layer extracted with dichloromethane (3 × 74 mL). The combined organic layers were dried ($MgSO_4$), filtered and concentred under reduced pressure. Purification of the crude product by column chromatography (30% AcOEt/cyclohexane) gave the cycloadduct **10b** as a yellow oil (404 mg, 73%). R_f: 0.42 (30% AcOEt/cyclohexane); ^{1}H NMR (360 MHz, $CDCl_3$) δ 5.69 (m, 1H), 4.57 (broad d, J = 9.4 Hz, 1H), 4.16 (q, J = 7.2 Hz, 4H), 4.12–4.00 (m, 2H), 3.99–3.82 (m, 2H), 2.03–1.85 (m, 2H), 1.47 (s, 9H), 1.34 (t, J = 7.2 Hz, 6H), 1.05 (m, 21H) ppm; ^{13}C NMR (90 MHz, $CDCl_3$) δ 154.8, 146.8, 105.1, 81.7, 75.2, 64.8, 59.3, 43.7, 33.7, 28.4, 18.1, 16.2, 12.1 ppm; HRMS (*m*/*z*): $[M + Na]^+$ calcd 560.2779; found, 560.2775; $[\alpha]^{20}_D$: +5.8 (*c* 1.0, CH_2Cl_2); ee: 8% (Whelk-O1, 1 mL/min, 95:5 hexane/EtOH, t_r (*R*) = 14.9 min, t_r (*S*) = 16.2 min).

(6*R*)-*tert*-Butyl 5-oxo-6-(2-((triisopropylsilyl)oxy)ethyl)-1,2-oxazinane-2-carboxylate (11b): A solution of the cycloadduct **10b** (404 mg, 0.751 mmol) in anhydrous THF (12 mL) was cooled to 0 °C and a 3 M solution of Red-Al® in toluene (1 mL, 3 mmol, 4 equiv) was rapidly added. After stirring 30 min at 0 °C, the reaction was hydrolyzed by addition of an saturated aqueous NH_4Cl solution (4 mL). The solution was concentred under reduced pressurre, the residue taken up with dichloromethane (10 mL) and filtered, washing with dichloromethane (3 × 5 mL). The filtrate was concentred under reduced pressure to give a yellow oil (300 mg) consisting in a mixture of the ketone **11b** and the over-reduced alcohol. This mixture was carried into the next step without further purification.

DMSO (0.16 mL, 2.241 mmol, 3 equiv) was added dropwide to a cooled (−78 °C) solution of oxalyl chloride (0.1 mL, 1.121 mmol, 1.5 equiv) in dichloromethane (3.4 mL). After stirring 15 min at −78 °C, a solution of the crude product from reduction reaction (300 mg) in dichloromethane (2 mL) was added dropwise. After 30 min at −78 °C, triethylamine (0.52 mL, 3.735 mmol, 5 equiv) was added. The colling bath was removed and the solution stirred at rt for 40 min, before being poured into diethyl ether (45 mL). The solution was succesively washed with saturated aqueous $CuSO_4$ solution (4 × 10 mL) and saturated aqueous NH_4Cl solution (3 × 10 mL), then dried ($MgSO_4$), filtered and concentred under reduced pressure. The residue was purified by filtration through a short plug of silica gel, eluting with ethyl acetate. Concentration under reduced pressure gave the pure ketone **11b** as an orange oil (255 mg, 84% over two steps). R_f: 0.29 (10% AcOEt/cyclohexane); ^{1}H NMR (250 MHz, $CDCl_3$) δ 4.49 (dd, J = 8.3, 3.8 Hz, 1H), 4.18–4.08 (m, 1H), 3.94 (m, 4H), 2.67 (t, J = 7.0 Hz, 2H), 2.16–2.03 (m, 1H), 1.99–1.85 (m, 1H), 1.51 (s, 9H), 1.05 (m, 21H) ppm; ^{13}C NMR (90 MHz, $CDCl_3$) δ 206.6, 154.9, 85.1, 82.3, 59.0, 45.0, 36.5, 32.2, 28.4, 18.1, 12.1 ppm; HRMS (*m*/*z*): $[M + Na]^+$ calcd 424.2490; found, 424.2480; $[\alpha]_D^{20}$ +37.4 (*c* 0.5, CH_2Cl_2).

(5*S*,6*R*)-5-Ethyl-6-ethynyl-5,6-dihydro-2*H*-pyran-2-one (21): Caesium fluoride (290 mg, 1.91 mmol, 1.3 equiv) was added to a solution of the lactone **18** [6] (327 mg, 1.47 mmol) in anhydrous acetonitrile (15 mL). The solution was stirred at rt; after 2 h 20 min, additional CsF (112 mg, 0.74 mmol, 0.5 equiv) was added. After a total time of 3 h 30 min, the solution was partioned between diethyl ether (70 mL) and water (35 mL). The layers were separated, the organic layer was washed with saturated aqueous NaCl solution (35 mL). The combined aqueous layers were extracted with diethyl ether (2 × 70 mL). The organic layers were combined, dried ($MgSO_4$), filtered and concentred under reduced pressure. Purification of the residue by column chromatography (25% Et_2O/pentane) gave **21** as a yellow oil (171 mg, 77%). R_f: 0.33 (30% Et_2O/pentane); ^{1}H NMR (250 MHz, $CDCl_3$) δ 6.79 (dd, J = 9.8, 3.5 Hz, 1H), 6.05 (dd, J = 10.0, 2.0 Hz, 1H), 5.16 (dd, J = 4.8, 2.3 Hz, 1H), 2.68–2.59 (m, 1H), 2.56 (d, J = 2.0 Hz, 1H), 1.86–1.62 (m, 2H), 1.04 (t, J = 7.3 Hz, 3H) ppm; ^{13}C NMR (90 MHz, $CDCl_3$) δ 162.5, 148.8, 120.3, 77.4, 76.6, 70.7, 38.7, 22.6, 10.9 ppm; HRMS (*m*/*z*): $[M + Na]^+$ calcd 173.0573; found, 173.0572; $[\alpha]_D^{20}$ +132.0 (*c* 1.0, CH_2Cl_2).

(2*R*,3*S*,6*RS*)-3-Ethyl-2-ethynyl-6-methoxy-3,6-dihydro-2*H*-pyran (19): This compound was prepared according to reference [18].

A solution of the lactone **18** (1.23 g, 5.53 mmol) in anhydrous dichloromethane (10 mL) was cooled to −78 °C and a solution of DIBAL-H in toluene (1.2 M, 6 mL, 7.19 mmol, 1.3 equiv) was added dropwise. The reaction mixture was stirred at −78 °C for 30 min then poured into a $NaHCO_3$ solution (5 mL). The layers were separated and the aqueous layer extracted with ethyl acetate (3 × 10 mL). The combined organic layers were dried ($MgSO_4$), filtered and concentred under reduced pressure. The residue (1.3 g) was redissolved in anhydrous methanol (25 mL) and paratoluenesulfonic acid hydrate (53 mg, 0.277 mmol, 0.05 equiv) was added. After stirring 1 h at rt, solid K_2CO_3 (1.53 g, 11.06 mmol, 2 equiv) was added and the mixture stirred overnight at rt. Diethyl ether (50 mL) was added and the solution washed with water (2 × 50 mL). The organic layer was dried ($MgSO_4$), filtered and carefully concentred under reduced

pressure. Purification by column chromatography (5% Et_2O/pentane), gave **19** as a colourless oil (866 mg, 94%, 91/9 mixture of stereoisomers). Analytical data were in agreement with literature data [18].

(2*R*,3*S*,6*RS*)-3-Ethyl-2-((*E*)-2-iodovinyl)-6-methoxy-3,6-dihydro-2*H*-pyran (20): This compound was prepared according to reference [18].

A solution of the alkyne **19** (300 mg, 1.80 mmol) dans in anhydrous dichloromethane (4.2 mL) was added dropwise to a suspension of Cp_2ZrHCl (696 mg, 2.70 mmol, 1.5 equiv) in anhydrous dichloromethane (9 mL). After stirring at rt for 15 min, a solution of iodine (777 mg, 3.06 mmol, 1.7 equiv) in anhydrous dichloromethane (9 mL) was added dropwise until a light brown solution was obtained. The reaction mixture was hydrolyzed by successive addition of a saturated aqueous $Na_2S_2O_3$ solution (25 mL) and water (9 mL). The layers were separated and the organic layer was washed with water (9 mL). The combined aqueous layers were back-extracted with diethyl ether (2 × 40 mL). The combined organic layers were dried ($MgSO_4$), filtered and concentred under reduced pressure. Purification of the residue by column chromatography (2.5% Et_2O/pentane) gave **20** as a yellowish oil (347 mg, 65%, 91:9 mixture of steroisomers). Analytical data were in agreement with literature data [18].

Coupling reaction between vinyl iodide 20 and ketone 11b: A solution of the vinyl iodide **20** (283 mg, 0.962 mmol, 1.8 equiv) in anhydrous toluene (2 mL) was cooled to −78 °C, and a *n*-butyllithium solution (2.3 M in hexanes, 0.39 mL, 0.909 mmol, 1.7 equiv) was added dropwise. The solution was stirred for 30 min at −78 °C then a solution of ketone **11b** (215 mg, 0.535 mmol, 1 equiv) in toluene (3.8 mL) was slowly added. The reaction was stirred at −78 °C for 45 h than slowly warmed to rt over 20 h. The reaction as quenched by addition of a saturated aqueous NH_4Cl solution (3.8 mL). The layers were separated and the aqueous layer extracted with ethyl acetate (2 × 8 mL) and diethyl ether (2 × 8 mL). The combined organic layers were dried ($MgSO_4$), filtered and concentred under reduced pressure. Purification of the residue by column chromatography (20 to 30% AcOEt/cyclohexane) gave the coupling product **23** as an orange oil, which was carried into the next step without further characterization (140 mg, 46%).

Product **23** was redissolved in 96% EtOH (3.9 mL) and pyridinium *para*-toluenesulfonate (17 mg, 0.066 mmol, 0.25 equiv) was added. The reaction mixture was stirred at rt for 24 h then neutralized by addition of a few drops of a saturated sodium hydrogen carbonate solution. The solvents were removed under reduced pressure and the residue partioned between ethyl acetate (5 mL) and water (2.5 mL). The layers were separated and the aqueous layer extracted with ethyl acetate (3 × 5 mL) and diethyl ether (5 mL). The combined organic layers were dried ($MgSO_4$), filtered and concentred under reduced pressure to give the crude lactol **24** which was immediately engaged into the next reaction.

A solution of the above lactol (147 mg, 0.265 mmol) in acetone (6 mL) was cooled to 0 °C and a solution of the Jones reagent (2.2 M in water, 0.14 mL, 0.31 mmol, 1.15 equiv) was added. After stirring 15 min at 0 °C, the reaction was quenched by addition of a saturated aqueous sodium hydrogen carbonate solution (9 mL) and isopropanol (1.5 mL). The solvents were removed under reduced pressure and the residue partioned between ethyl acetate (11 mL) and water (5.5 mL). The layers were separated and the aqueous layer extracted with ethyl acetate (2 × 11 mL) and diethyl ether (2 × 11 mL). The combined organic layers were dried ($MgSO_4$), filtered and concentred under reduced pressure. Purification of the residue by column chromatography (25 to 40% AcOEt/cyclohexane) gave first the protected lactone **25** as a sticky yellow oil (42 mg, 29% over two steps), further elution with 100% AcOEt gave the unprotected alcohol **26** (18 mg, 17%).

***tert*-Butyl (6*R*)-5-((*E*)-2-((2*S*,3*S*)-3-ethyl-6-oxo-3,6-dihydro-2*H*-pyran-2-yl)vinyl)-5-hydroxy-6-(2-((triisopropylsilyl)oxy)ethyl)-1,2-oxazinane-2-carboxylate (25):** Data for **25**: R_f: 0.10 (30% AcOEt/cyclohexane); ^{1}H NMR (360 MHz, $CDCl_3$) δ 6.97 (dd, *J* = 9.7, 5.5 Hz, 1H), 6.05 (d, *J* = 9.7 Hz, 1H), 5.95 (dd, *J* = 15.5, 4.2 Hz, 1H), 5.82 (dd, *J* = 15.5, 1.4 Hz, 1H), 5.02 (ddd, app td, *J* = 4.2, 4.2, 1.4 Hz, 1H), 3.99–3.90 (m, 3H), 3.76–3.69 (m, 1H), 3.55 (td, *J* = 13.1, 2.7 Hz, 1H), 2.44–2.37 (m, 1H), 1.90–1.70 (m, 2H), 1.67–1.57 (m, 3H), 1.49 (s, 9H), 1.45–1.39 (m, 1H), 1.05 (m, 21H), 0.93 (t, *J* = 7.5 Hz, 3H) ppm; ^{13}C NMR (62,5 MHz, $CDCl_3$) δ 163.9, 155.1, 150.1, 135.5, 125.1, 121.0, 82.6, 81.8, 79.8, 70.8, 59.0, 42.3, 39.4, 35.9, 31.3, 28.4, 21.8, 18.1,12.0,11.1 ppm; HRMS (*m*/*z*): $[M + Na]^+$ calcd 576.3327; found, 576.3330; $[\alpha]_D^{20}$ +86.3 (*c* 1.1, CH_2Cl_2).

***tert*-Butyl (6*R*)-5-((*E*)-2-((2*S*,3*S*)-3-ethyl-6-oxo-3,6-dihydro-2*H*-pyran-2-yl)vinyl)-5-hydroxy-6-(2-hydroxyethyl)-1,2-oxazinane-2-carboxylate (26):** Data for **26**: R_f: 0.38 (80% AcOEt/cyclohexane); ^{1}H NMR (400 MHz, acetone-d_6) δ 7.09 (dd, *J* = 10.0, 5.2 Hz, 1H), 6.02 (dd, *J* = 15.6, 5.5 Hz, 1H), 5.97 (dd, *J* = 10.0, 1.2 Hz, 1H), 5.85 (dd, *J* = 15.6, 1.2 Hz, 1H), 5.06 (ddd, *J* = 5.5, 4.0,1.2 Hz, 1H), 4.27 (s, exchangeable with D_2O, 1H), 3.96–3.91 (m, 2H), 3.74–3.66 (m, 2H), 3.63–3.59 (m, 1H), 2.61–2.53 (m, 1H), 1.95–1.83 (m, 2H), 1.73–1.67 (m, 1H), 1.67–1.55 (m, 2H), 1.49 (s, 9H), 1.47–1.38 (m, 1H), 0.94 (t, *J* = 7.6 Hz, 3H) ppm; ^{13}C NMR (100 MHz, acetone-d_6) δ 163.83,

156.0, 151.0, 137.2, 126.1, 121.2, 84.0, 81.8, 80.7, 71.1, 59.5, 42.7, 40.0, 36.3, 31.3, 28.4, 22.2, 11.2 ppm; HRMS (m/z): $[M + Na]^+$ calcd 420.1993; found, 420.1970.

Funding

The authors thank CNRS and the Université Paris-Saclay for financial support of this research.

ORCID® iDs

Guillaume Vincent - https://orcid.org/0000-0003-3162-1320
Cyrille Kouklovsky - https://orcid.org/0000-0001-5399-9469

Preprint

A non-peer-reviewed version of this article has been previously published as a preprint: https://doi.org/10.3762/bxiv.2022.69.v1

References

1. Kohama, T.; Enokita, R.; Okazaki, T.; Miyaoka, H.; Torikata, A.; Inukai, M.; Kaneko, I.; Kagasaki, T.; Sakaida, Y.; Satoh, A.; Shiraishi, A. *J. Antibiot.* **1993,** *46,* 1503–1511. doi:10.7164/antibiotics.46.1503
2. Kohama, T.; Nakamura, T.; Kinoshita, T.; Kaneko, I.; Shiraishi, A. *J. Antibiot.* **1993,** *46,* 1512–1519. doi:10.7164/antibiotics.46.1512
3. Fushimi, S.; Nishikawa, S.; Shimazu, A.; Seto, H. *J. Antibiot.* **1989,** *42,* 1019–1025. doi:10.7164/antibiotics.42.1019
4. Fushimi, S.; Furihata, K.; Seto, H. *J. Antibiot.* **1989,** *42,* 1026–1036. doi:10.7164/antibiotics.42.1026
5. Teruya, T.; Simizu, S.; Kanoh, N.; Osada, H. *FEBS Lett.* **2005,** *579,* 2463–2468. doi:10.1016/j.febslet.2005.03.049
6. Kawada, M.; Kawatsu, M.; Masuda, T.; Ohba, S.-i.; Amemiya, M.; Kohama, T.; Ishizuka, M.; Takeuchi, T. *Int. Immunopharmacol.* **2003,** *3,* 179–188. doi:10.1016/s1567-5769(02)00231-x
7. Wang, Y.-G.; Takeyama, R.; Kobayashi, Y. *Angew. Chem., Int. Ed.* **2006,** *45,* 3320–3323. doi:10.1002/anie.200600458
8. Druais, V.; Hall, M. J.; Corsi, C.; Wendeborn, S. V.; Meyer, C.; Cossy, J. *Org. Lett.* **2009,** *11,* 935–938. doi:10.1021/ol8029142
9. Druais, V.; Hall, M. J.; Corsi, C.; Wendeborn, S. V.; Meyer, C.; Cossy, J. *Tetrahedron* **2010,** *66,* 6358–6375. doi:10.1016/j.tet.2010.05.050
10. König, C. M.; Gebhardt, B.; Schleth, C.; Dauber, M.; Koert, U. *Org. Lett.* **2009,** *11,* 2728–2731. doi:10.1021/ol900757k
11. Shibahara, S.; Fujino, M.; Tashiro, Y.; Okamoto, N.; Esumi, T.; Takahashi, K.; Ishihara, J.; Hatakeyama, S. *Synthesis* **2009,** 2935–2953. doi:10.1055/s-0029-1216930
12. Sarkar, S. M.; Wanzala, E. N.; Shibahara, S.; Takahashi, K.; Ishihara, J.; Hatakeyama, S. *Chem. Commun.* **2009,** 5907–5909. doi:10.1039/b912267b
13. Shimada, K.; Kaburagi, Y.; Fukuyama, T. *J. Am. Chem. Soc.* **2003,** *125,* 4048–4049. doi:10.1021/ja0340679
14. Miyashita, K.; Tsunemi, T.; Hosokawa, T.; Ikejiri, M.; Imanishi, T. *J. Org. Chem.* **2008,** *73,* 5360–5370. doi:10.1021/jo8005599
15. Moïse, J.; Sonawane, R. P.; Corsi, C.; Wendeborn, S. V.; Arseniyadis, S.; Cossy, J. *Synlett* **2008,** 2617–2620. doi:10.1055/s-0028-1083511
16. Greszler, S. N.; Malinowski, J. T.; Johnson, J. S. *Org. Lett.* **2011,** *13,* 3206–3209. doi:10.1021/ol2011192
17. Trost, B. M.; Biannic, B.; Brindle, C. S.; O'Keefe, B. M.; Hunter, T. J.; Ngai, M.-Y. *J. Am. Chem. Soc.* **2015,** *137,* 11594–11597. doi:10.1021/jacs.5b07438
18. Rousseau, A.; Buchotte, M.; Guillot, R.; Vincent, G.; Kouklovsky, C. *Eur. J. Org. Chem.* **2017,** 6804–6810. doi:10.1002/ejoc.201701336
19. Yamamoto, Y.; Yamamoto, H. *Eur. J. Org. Chem.* **2006,** 2031–2043. doi:10.1002/ejoc.200500847
20. Vogt, P. F.; Miller, M. J. *Tetrahedron* **1998,** *54,* 1317–1348. doi:10.1016/s0040-4020(97)10072-2
21. Iwasa, S.; Fakhruddin, A.; Nishiyama, H. *Mini-Rev. Org. Chem.* **2005,** *2,* 157–175. doi:10.2174/1570193053544445
22. Bodnar, B. S.; Miller, M. J. *Angew. Chem., Int. Ed.* **2011,** *50,* 5630–5647. doi:10.1002/anie.201005764
23. Galvani, G.; Lett, R.; Kouklovsky, C. *Chem. – Eur. J.* **2013,** *19,* 15604–15614. doi:10.1002/chem.201302905
24. Calogeropoulou, T.; Wiemer, D. F. *J. Org. Chem.* **1988,** *53,* 2295–2299. doi:10.1021/jo00245a030
25. Kouklovsky, C.; Pouilhès, A.; Langlois, Y. *J. Am. Chem. Soc.* **1990,** *112,* 6672–6679. doi:10.1021/ja00174a034
26. Lichtenthaler, F. W. *Chem. Rev.* **1961,** *61,* 607–649. doi:10.1021/cr60214a004
27. Hall, A.; Bailey, P. D.; Rees, D. C.; Rosair, G. M.; Wightman, R. H. *J. Chem. Soc., Perkin Trans. 1* **2000,** 329–342. doi:10.1039/a908333b
28. Cano, M. J.; Bouanou, H.; Tapia, R.; Alvarez, E.; Alvarez-Manzaneda, R.; Chahboun, R.; Alvarez-Manzaneda, E. *J. Org. Chem.* **2013,** *78,* 9196–9204. doi:10.1021/jo4014047
29. Barbier, J.; Gerth, K.; Jansen, R.; Kirschning, A. *Org. Biomol. Chem.* **2012,** *10,* 8298–8307. doi:10.1039/c2ob26256h
30. Trost, B. M.; Rudd, M. T. *J. Am. Chem. Soc.* **2005,** *127,* 4763–4776. doi:10.1021/ja043097o
31. Huang, W.; Zheng, P.; Zhang, Z.; Liu, R.; Chen, Z.; Zhou, X. *J. Org. Chem.* **2008,** *73,* 6845–6848. doi:10.1021/jo801210n
32. Lecomte, V.; Stéphan, E.; Jaouen, G. *Tetrahedron Lett.* **2002,** *43,* 3463–3465. doi:10.1016/s0040-4039(02)00597-x
33. Lawhorn, B. G.; Boga, S. B.; Wolkenberg, S. E.; Colby, D. A.; Gauss, C.-M.; Swingle, M. R.; Amable, L.; Honkanen, R. E.; Boger, D. L. *J. Am. Chem. Soc.* **2006,** *128,* 16720–16732. doi:10.1021/ja066477d
34. Shi, Y.; Wulff, W. D. *J. Org. Chem.* **1994,** *59,* 5122–5124. doi:10.1021/jo00097a005
35. Stadtmüller, H.; Vaupel, A.; Tucker, C. E.; Stüdemann, T.; Knochel, P. *Chem. – Eur. J.* **1996,** *2,* 1204–1220. doi:10.1002/chem.19960021006

BEILSTEIN JOURNAL OF ORGANIC CHEMISTRY

Solid-phase total synthesis and structural confirmation of antimicrobial longicatenamide A

Takumi Matsumoto, Takefumi Kuranaga*, Yuto Taniguchi, Weicheng Wang and Hideaki Kakeya*

Full Research Paper

Open Access

Address:
Department of System Chemotherapy and Molecular Sciences, Division of Medicinal Frontier Sciences, Graduate School of Pharmaceutical Sciences, Kyoto University, Yoshida, Sakyo-ku, Kyoto 606-8501, Japan

Email:
Takefumi Kuranaga* - tkuranaga@pharm.kyoto-u.ac.jp;
Hideaki Kakeya* - scseigyo-hisyo@pharm.kyoto-u.ac.jp

* Corresponding author

Keywords:
antimicrobial; longicatenamides; peptidic natural product; solid-phase synthesis; total synthesis

Beilstein J. Org. Chem. **2022,** *18,* 1560–1566.
https://doi.org/10.3762/bjoc.18.166

Received: 20 September 2022
Accepted: 09 November 2022
Published: 18 November 2022

This article is part of the thematic issue "Total synthesis: an enabling science".

Associate Editor: B. Nay

Abstract

Longicatenamides A–D are cyclic hexapeptides isolated from the combined culture of *Streptomyces* sp. KUSC_F05 and *Tsukamurella pulmonis* TP-B0596. Because these peptides are not detected in the monoculture broth of the actinomycete, they are key tools for understanding chemical communication in the microbial world. Herein, we report the solid-phase total synthesis and structural confirmation of longicatenamide A. First, commercially unavailable building blocks were chemically synthesized with stereocontrol. Second, the peptide chain was elongated via Fmoc-based solid-phase peptide synthesis. Third, the peptide chain was cyclized in the solution phase, followed by simultaneous cleavage of all protecting groups to afford longicatenamide A. Chromatographic analysis corroborated the chemical structure of longicatenamide A. Furthermore, the antimicrobial activity of synthesized longicatenamide A was confirmed. The developed solid-phase synthesis is expected to facilitate the rapid synthesis of diverse synthetic analogues.

Introduction

Naturally occurring bioactive compounds can serve as both drug leads and research tools for chemical biology [1]. Because the rediscovery rate of these compounds has increased in the last few decades, new approaches to explore natural products are in demand [2]. To this end, the combined-culture strategy has been applied to discover new natural products. For example, the mycolic acid-containing bacterium *Tsukamurella pulmonis* TP-B0596 can influence the biosynthesis of cryptic natural products [3]. Additionally, we have developed several highly sensitive labeling reagents to detect and identify scarce and cryptic natural products [4]. Integrating the combined-culture strategy and new labeling reagents has led to the detection and structural determination of several unprecedented secondary metabolites [5-7].

Longicatenamides A–D (**1**–**4**, Figure 1) are cyclic hexapeptides isolated from the combined-culture of *Streptomyces* sp. KUSC_F05 and *T. pulmonis* TP-B0596 [8]. The planar structures were determined by analyzing two-dimensional (2D) nuclear magnetic resonance (NMR) spectra and mass spectrometry (MS) data, and the absolute configurations of their component amino acids were elucidated by using highly sensitive reagents that we recently developed [4]. Among the isolated longicatenamides, compound **1** exhibits weak but preferential antimicrobial activity against *Bacillus subtilis*. Because peptides **1**–**4** are not detected in the monoculture broth of *Streptomyces* sp. KUSC_F05, they are key tools for understanding chemical communication in the microbial world. To elucidate the role of compounds **1**–**4** in the microbial world, developing a strategy to synthesize compounds **1**–**4**, including future derivatization to produce probe molecules, is required. Herein, we report the total synthesis of peptide **1** by Fmoc-based solid-phase peptide synthesis [9] and the evaluation of its antimicrobial activity. The present study confirmed our proposed structure of **1**, which was determined by the use of our original labeling reagents [4].

Results and Discussion

Although the solution-phase total synthesis of an analogue of longicatenamycin A has been reported [10], a solid-phase strategy can facilitate the production of a wider variety of analogous compounds than solution-phase synthesis [11]. Consequently, in this study, compound **1** was synthesized using a solid-phase strategy for future derivatization to produce probe molecules for deciphering microbial chemical communication.

The retrosynthesis of peptide **1** is displayed in Scheme 1. First, the cyclic peptide **1** was linearized by retrosynthesis, and acid-labile protecting groups were attached onto the reactive side chain. The biomimetic synthesis of cyclic peptides often enables efficient synthesis [12,13] and provides insights into the biosynthesis pathways of these peptides [14]. However, the biosynthetic gene clusters of compounds **1**–**4** remain unidentified. Therefore, the least sterically hindered amine, namely the amino group of glycine, was selected as a nucleophile of the cyclization reaction in this study. Second, to realize the solid-phase synthesis, the C-terminus of the linear peptide was connected to 2-chlorotrityl resin [15] to give resin-bound peptide **5**. Peptide **5** was divided into six building blocks **6**–**11** by retrosynthesis.

At the beginning of the total synthesis, commercially unavailable building blocks **7** and **10** were chemically constructed from readily available starting materials. The synthesis of building block **10** commenced with the synthesis of compound **15** through Wittig reaction of Garner's aldehyde (**13**) [16], which was readily obtained from *tert*-butyloxycarbonyl (Boc)-protected D-serine **12** (Scheme 2). Treatment of the olefin **15** with trifluoroacetic acid (TFA) cleaved the Boc protecting group and the acetonide to deliver unsaturated amino alcohol **16**. The amino group in **16** was protected by the fluorenylmethyloxycarbonyl (Fmoc) protecting group for solid-phase peptide synthesis, and then hydrogenation of the double bond in **17** provided intermediate **18**. Oxidation of the alcohol **18** to acid **10** was realized with the combination of Dess–Martin oxidation [17,18] and Pinnick oxidation [19].

Another unusual amino acid **7** was also synthesized from D-serine (**20**, Scheme 3). The $SnCl_2$-catalyzed coupling reaction [20] between **21** and **22** afforded β-keto ester **23**, which

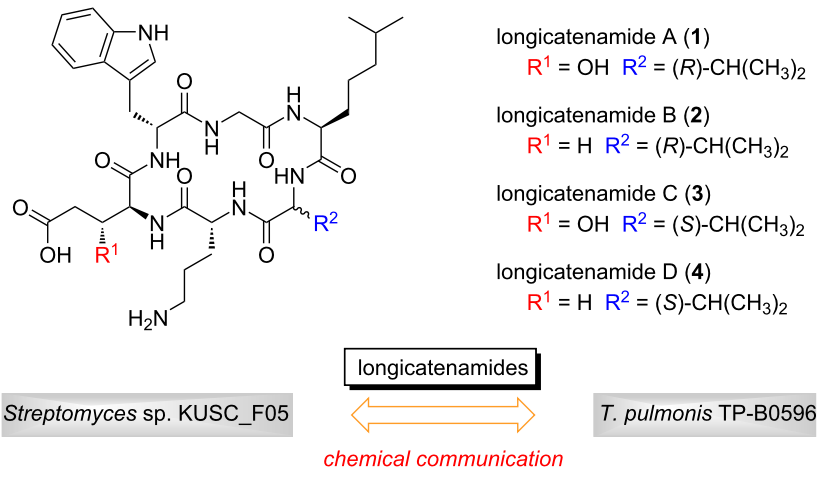

Figure 1: Structures of longicatenamides A–D (**1**–**4**).

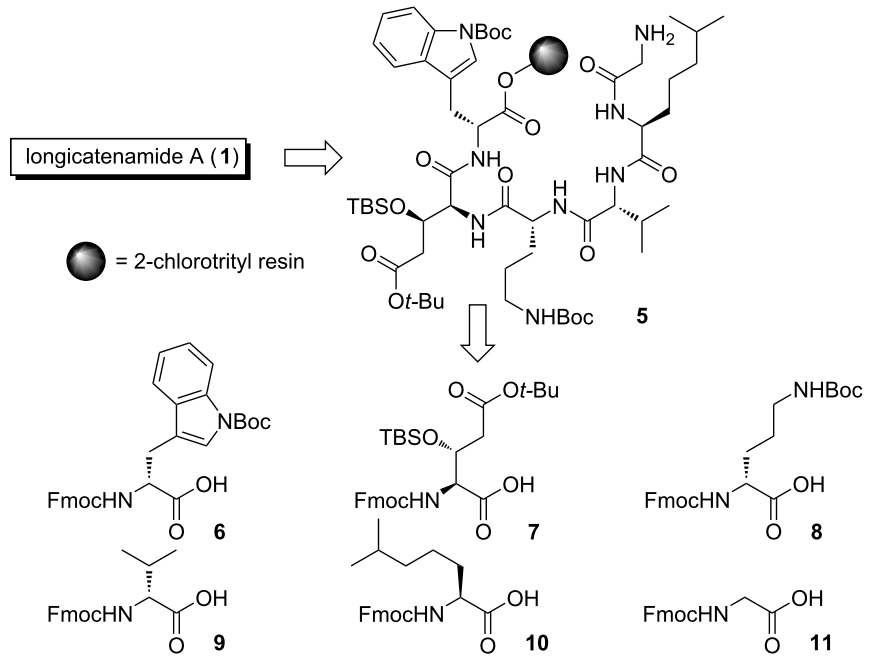

Scheme 1: Retrosynthesis of longicatenamycin A (**1**).

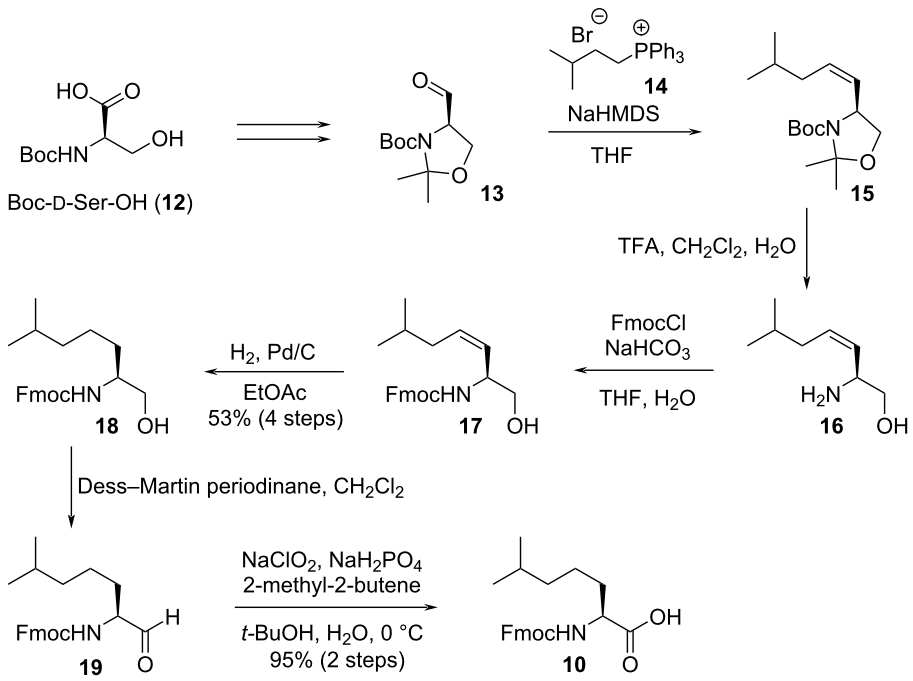

Scheme 2: Synthesis of building block **10**.

was then reduced to the corresponding β-hydroxy ester **24** by K-Selectride (dr > 20:1), and subsequent acidic removal of the acetonide furnished diol **25**. The stereochemistry of the newly generated hydroxy group was determined using the modified Mosher's method [21]. Protection of diol **25** by *tert*-butyl(dimethyl)silyl (TBS) group followed by selective depro-

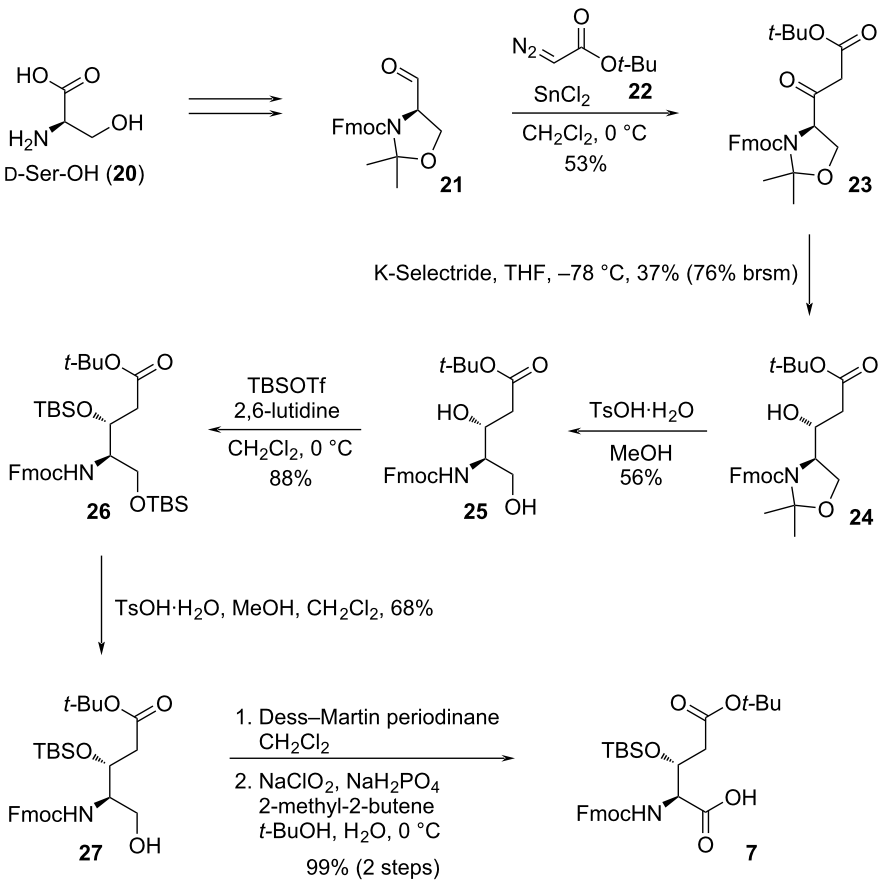

Scheme 3: Synthesis of building block **7**.

tection of the primary alcohol led to **27**. Finally, acid **7** was obtained from alcohol **27** through the same two-step oxidation used to obtain compound **10**.

Having synthesized the necessary building blocks, we turned our attention to construct resin-bound peptide **5** (Scheme 4). The assembly of this hexapeptide started with the loading of Fmoc-D-Trp(Boc)-OH (**6**) onto 2-chlorotrityl resin with iPr_2NEt, which was followed by piperidine treatment to liberate resin-bound amine **29**. Then, five rounds of DIC/Oxyma-mediated amidation [22] and N^{α}-deprotection with piperidine led to resin-bound peptide **5**. Treatment of **5** with TFA/CH_2Cl_2 1:99 released **30** into the solution without unmasking the acid-labile protecting groups of the side chains. Subsequently, peptide **30** was cyclized by the action of PyBOP/HOAt [23,24] followed by treatment with TFA/iPr_3SiH/H_2O 95:2.5:2.5 to provide crude **1**. After reversed-phase high-performance liquid chromatography (HPLC) purification, longicatenamide A (**1**) was obtained with 36% yield over 15 steps starting from **6**.

The NMR spectra of synthesized compound **1** agreed with those of natural **1**. At this stage the confirmation of the identity of natural and synthesized compounds by structural determination using NMR spectroscopy is often difficult because the NMR spectra of peptidic products vary depending on the conditions in the NMR tube [25-29], such as concentration, pH, and purity. Thus, analyses of the NMR spectra of peptides sometimes lead to incorrect structural determination even though total synthesis of the proposed structures is successful [30]. In this study, synthesized and natural **1** were compared by collecting LC–MS data. As displayed in Figure 2, the retention time of synthesized **1** was identical to that of natural **1**. These results confirmed total synthesis of **1** and supported our proposed structure of isolated natural **1**.

Total synthesis sometimes invalidates the reported biological activity of the isolated natural product, which could be due to the presence of uncharacterized impurities. To verify the bioactivity of **1**, the antimicrobial activity of synthesized **1** was preliminary tested in this study following a previously reported

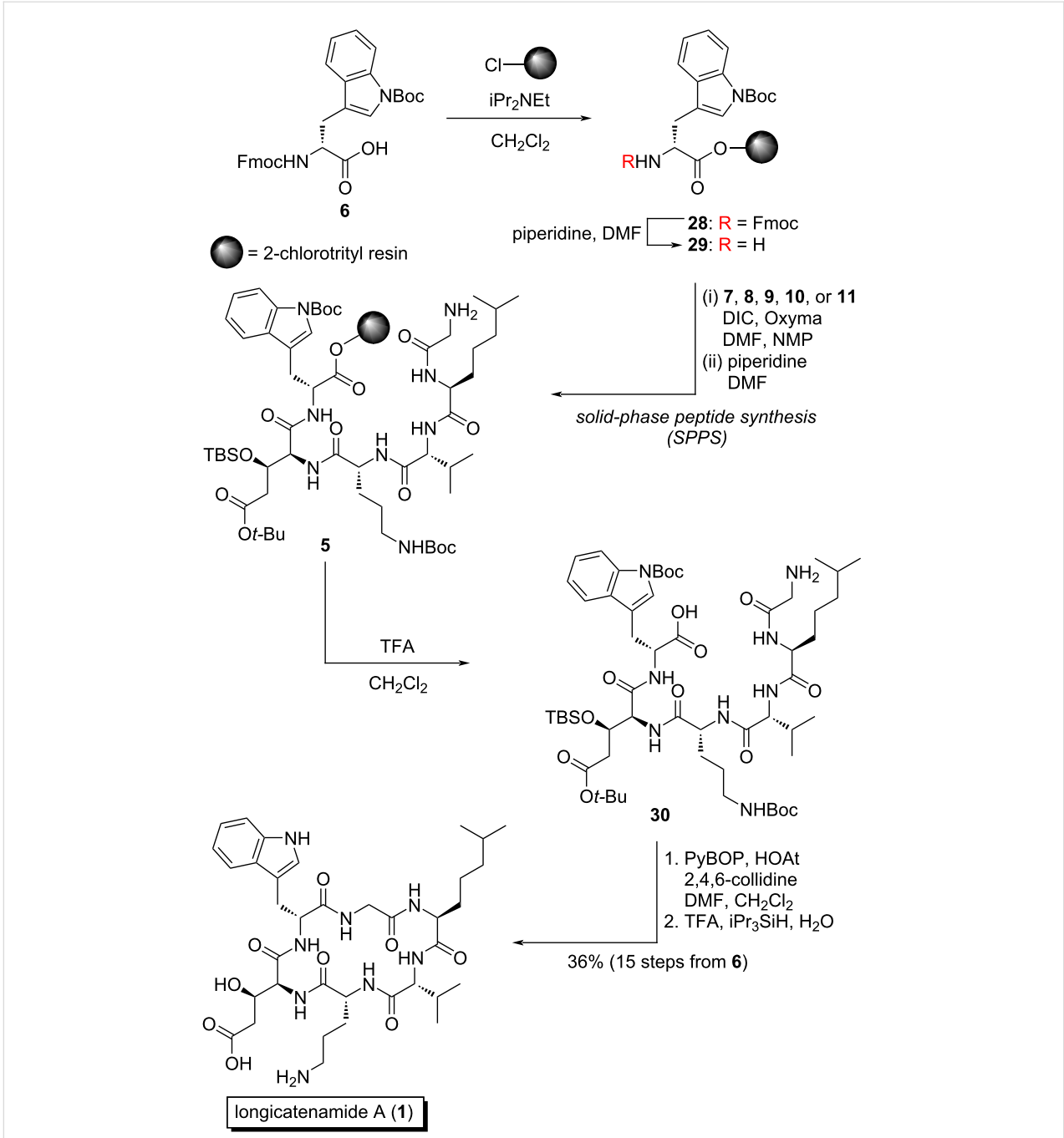

Scheme 4: Total synthesis of longicatenamycin A (**1**).

method [8], revealing that chemically synthesized **1** (minimum inhibitory concentration (MIC) = 50 μM) exhibited moderate but selective antimicrobial activity against *Bacillus subtilis* similar to natural **1** (MIC = 100 μM).

Conclusion

We accomplished solid-phase total synthesis of longicatenamide A (**1**). Initially, commercially unavailable building blocks **7** and **10** were chemically synthesized with stereocontrol. Then, the peptide chain was elongated by Fmoc-based solid-phase peptide synthesis. Finally, the cyclization of the peptide chain followed by simultaneous cleavage of all protecting groups in the solution phase afforded target compound **1**. The comparison of the chromatograms of synthesized and natural **1** corroborated the chemical structure of **1**. Further studies of the structure–activity relationship, identification of

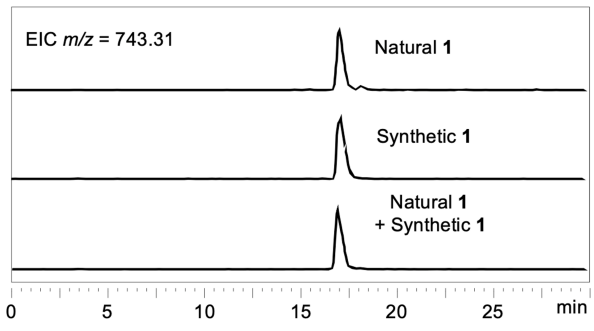

Figure 2: LC–MS extracted ion chromatograms (EICs) of synthesized and natural **1**. Column: Imtakt Cadenza CD-C18 3 × 150 mm; eluent: MeCN/H_2O/TFA 30:70:0.05, isocratic, 0.2 mL/min; 40 °C.

biosynthetic gene clusters, and detailed investigations of the combined-culture production of longicatenamides are currently underway in our laboratory.

Supporting Information

Supporting Information File 1

Experimental procedures and compound characterization data.
[https://www.beilstein-journals.org/bjoc/content/supplementary/1860-5397-18-166-S1.pdf]

Funding

This work was financially supported in part by a Grant-in-Aid for Scientific Research from the Ministry of Education, Culture, Sports, Science and Technology, Japan [17H06401 (H.K.), 18K14396 (T.K.), 19H02840 (H.K.), 22K05112 (T.K.)], in addition to the Platform Project for Supporting Drug Discovery and Life Science Research from the Japan Agency for Medical Research and Development (AMED) (H.K.). Contributions from the Takeda Science Foundation, The Tokyo Biochemical Research Foundation, and the foundation of Tokyo Chemical Industry to T.K. are greatly appreciated.

ORCID® iDs

Hideaki Kakeya - https://orcid.org/0000-0002-4293-7331

References

1. Kakeya, H. *Nat. Prod. Rep.* **2016,** *33,* 648–654. doi:10.1039/c5np00120j
2. Pye, C. R.; Bertin, M. J.; Lokey, R. S.; Gerwick, W. H.; Linington, R. G. *Proc. Natl. Acad. Sci. U. S. A.* **2017,** *114,* 5601–5606. doi:10.1073/pnas.1614680114
3. Onaka, H.; Mori, Y.; Igarashi, Y.; Furumai, T. *Appl. Environ. Microbiol.* **2011,** *77,* 400–406. doi:10.1128/aem.01337-10
4. Kuranaga, T.; Minote, M.; Morimoto, R.; Pan, C.; Ogawa, H.; Kakeya, H. *ACS Chem. Biol.* **2020,** *15,* 2499–2506. doi:10.1021/acschembio.0c00517
5. Pan, C.; Kuranaga, T.; Liu, C.; Lu, S.; Shinzato, N.; Kakeya, H. *Org. Lett.* **2020,** *22,* 3014–3017. doi:10.1021/acs.orglett.0c00776
6. Pan, C.; Kuranaga, T.; Cao, X.; Suzuki, T.; Dohmae, N.; Shinzato, N.; Onaka, H.; Kakeya, H. *J. Org. Chem.* **2021,** *86,* 1843–1849. doi:10.1021/acs.joc.0c02660
7. Kuranaga, T.; Tamura, M.; Ikeda, H.; Terada, S.; Nakagawa, Y.; Kakeya, H. *Org. Lett.* **2021,** *23,* 7106–7111. doi:10.1021/acs.orglett.1c02506
8. Jiang, Y.; Matsumoto, T.; Kuranaga, T.; Lu, S.; Wang, W.; Onaka, H.; Kakeya, H. *J. Antibiot.* **2021,** *74,* 307–316. doi:10.1038/s41429-020-00400-3
9. Sheppard, R. *J. Pept. Sci.* **2003,** *9,* 545–552. doi:10.1002/psc.479
10. von Nussbaum, F.; Anlauf, S.; Freiberg, C.; Benet-Buchholz, J.; Schamberger, J.; Henkel, T.; Schiffer, G.; Häbich, D. *ChemMedChem* **2008,** *3,* 619–626. doi:10.1002/cmdc.200700297
11. Behrendt, R.; White, P.; Offer, J. *J. Pept. Sci.* **2016,** *22,* 4–27. doi:10.1002/psc.2836
12. Kuranaga, T.; Enomoto, A.; Tan, H.; Fujita, K.; Wakimoto, T. *Org. Lett.* **2017,** *19,* 1366–1369. doi:10.1021/acs.orglett.7b00249
13. Kuranaga, T.; Matsuda, K.; Sano, A.; Kobayashi, M.; Ninomiya, A.; Takada, K.; Matsunaga, S.; Wakimoto, T. *Angew. Chem., Int. Ed.* **2018,** *57,* 9447–9451. doi:10.1002/anie.201805541
14. Matsuda, K.; Kobayashi, M.; Kuranaga, T.; Takada, K.; Ikeda, H.; Matsunaga, S.; Wakimoto, T. *Org. Biomol. Chem.* **2019,** *17,* 1058–1061. doi:10.1039/c8ob02867b
15. Chatzi, K. B. O.; Gatos, D.; Stavropoulos, G. *Int. J. Pept. Protein Res.* **1991,** *37,* 513–520. doi:10.1111/j.1399-3011.1991.tb00769.x
16. Garner, P. *Tetrahedron Lett.* **1984,** *25,* 5855–5858. doi:10.1016/s0040-4039(01)81703-2
17. Dess, D. B.; Martin, J. C. *J. Org. Chem.* **1983,** *48,* 4155–4156. doi:10.1021/jo00170a070
18. Dess, D. B.; Martin, J. C. *J. Am. Chem. Soc.* **1991,** *113,* 7277–7287. doi:10.1021/ja00019a027
19. Bal, B. S.; Childers, W. E., Jr.; Pinnick, H. W. *Tetrahedron* **1981,** *37,* 2091–2096. doi:10.1016/s0040-4020(01)97963-3
20. Holmquist, C. R.; Roskamp, E. J. *J. Org. Chem.* **1989,** *54,* 3258–3260. doi:10.1021/jo00275a006
21. Ohtani, I.; Kusumi, T.; Kashman, Y.; Kakisawa, H. *J. Am. Chem. Soc.* **1991,** *113,* 4092–4096. doi:10.1021/ja00011a006
22. Subirós-Funosas, R.; Prohens, R.; Barbas, R.; El-Faham, A.; Albericio, F. *Chem. – Eur. J.* **2009,** *15,* 9394–9403. doi:10.1002/chem.200900614
23. Coste, J.; Le-Nguyen, D.; Castro, B. *Tetrahedron Lett.* **1990,** *31,* 205–208. doi:10.1016/s0040-4039(00)94371-5
24. Carpino, L. A. *J. Am. Chem. Soc.* **1993,** *115,* 4397–4398. doi:10.1021/ja00063a082
25. Zou, B.; Long, K.; Ma, D. *Org. Lett.* **2005,** *7,* 4237–4240. doi:10.1021/ol051685g
26. Sugiyama, H.; Watanabe, A.; Teruya, T.; Suenaga, K. *Tetrahedron Lett.* **2009,** *50,* 7343–7345. doi:10.1016/j.tetlet.2009.10.059
27. Ma, B.; Litvinov, D. N.; He, L.; Banerjee, B.; Castle, S. L. *Angew. Chem., Int. Ed.* **2009,** *48,* 6104–6107. doi:10.1002/anie.200902425

28. Ma, B.; Banerjee, B.; Litvinov, D. N.; He, L.; Castle, S. L. *J. Am. Chem. Soc.* **2010,** *132,* 1159–1171. doi:10.1021/ja909870g
29. Kuranaga, T.; Sesoko, Y.; Sakata, K.; Maeda, N.; Hayata, A.; Inoue, M. *J. Am. Chem. Soc.* **2013,** *135,* 5467–5474. doi:10.1021/ja401457h
30. Kuranaga, T.; Mutoh, H.; Sesoko, Y.; Goto, T.; Matsunaga, S.; Inoue, M. *J. Am. Chem. Soc.* **2015,** *137,* 9443–9451. doi:10.1021/jacs.5b05550

License and Terms

BEILSTEIN JOURNAL OF ORGANIC CHEMISTRY

Formal total synthesis of macarpine via a Au(I)-catalyzed 6-*endo*-*dig* cycloisomerization strategy

Jiayue Fu[1,2,3], Bingbing Li[1,2,3], Zefang Zhou[1,2,3], Maosheng Cheng[1,3], Lu Yang*[1,2,3] and Yongxiang Liu*[1,2,3]

Letter

Open Access

Address:
[1]Key Laboratory of Structure-Based Drug Design and Discovery (Shenyang Pharmaceutical University), Ministry of Education, Shenyang 110016, P. R. China, [2]Wuya College of Innovation, Shenyang Pharmaceutical University, Shenyang 110016, P. R. China and [3]Institute of Drug Research in Medicine Capital of China, Benxi 117000, P. R. China

Email:
Lu Yang* - yanglusyphu@163.com; Yongxiang Liu* - yongxiang.liu@syphu.edu.cn

* Corresponding author

Keywords:
benzo[*c*]phenanthridine alkaloids; 1,5-enyne; formal total synthesis; gold catalysis; macarpine

Beilstein J. Org. Chem. **2022,** *18,* 1589–1595.
https://doi.org/10.3762/bjoc.18.169

Received: 12 September 2022
Accepted: 14 November 2022
Published: 23 November 2022

This article is part of the thematic issue "Total synthesis: an enabling science".

Associate Editor: B. Nay

Abstract

The formal total synthesis of macarpine was accomplished by the construction of a naphthol intermediate in Ishikawa's synthetic route with two different synthetic routes. The convergent synthetic strategies feature the utilization of Au(I)-catalyzed cycloisomerizations of a 1,5-enyne and alkynyl ketone substrates, which were prepared by Sonogashira coupling reactions.

Introduction

Benzo[*c*]phenanthridine alkaloids are an ancient and influential category of isoquinoline alkaloids, mainly found in Papaveraceae and Rutaceae (Scheme 1) [1,2]. According to their oxidation states, benzo[*c*]phenanthridine alkaloids can be divided into two types: partially hydrogenated base and fully aromatized base, in which natural fully aromatic alkaloids can be further classified into three subclasses: O_4-base, O_5-base, and O_6-base [3].

Among these alkaloids macarpine is the most oxidized tetracyclic alkaloid with many bioactivities, including anesthesia, anticancer, anti-inflammatory [4-8], insecticidal, fungicidal, etc [9]. In addition to the above-mentioned activities, macarpine was also used as a DNA probe for flow cytometry and fluorescence microscopy due to its fluorescent properties [10]. Despite some research on the activities of macarpine had been performed, a more in-depth evaluation of the biological activities was still limited due to the need of its isolation from natural sources. Inspired by the requirement of further biological evaluation, the chemical syntheses of macarpine have been developed rapidly in the last three decades.

The benzo[*c*]phenanthridine skeleton consists of a phenanthridine (rings A, B, C) and a benzene (ring D), and most of the

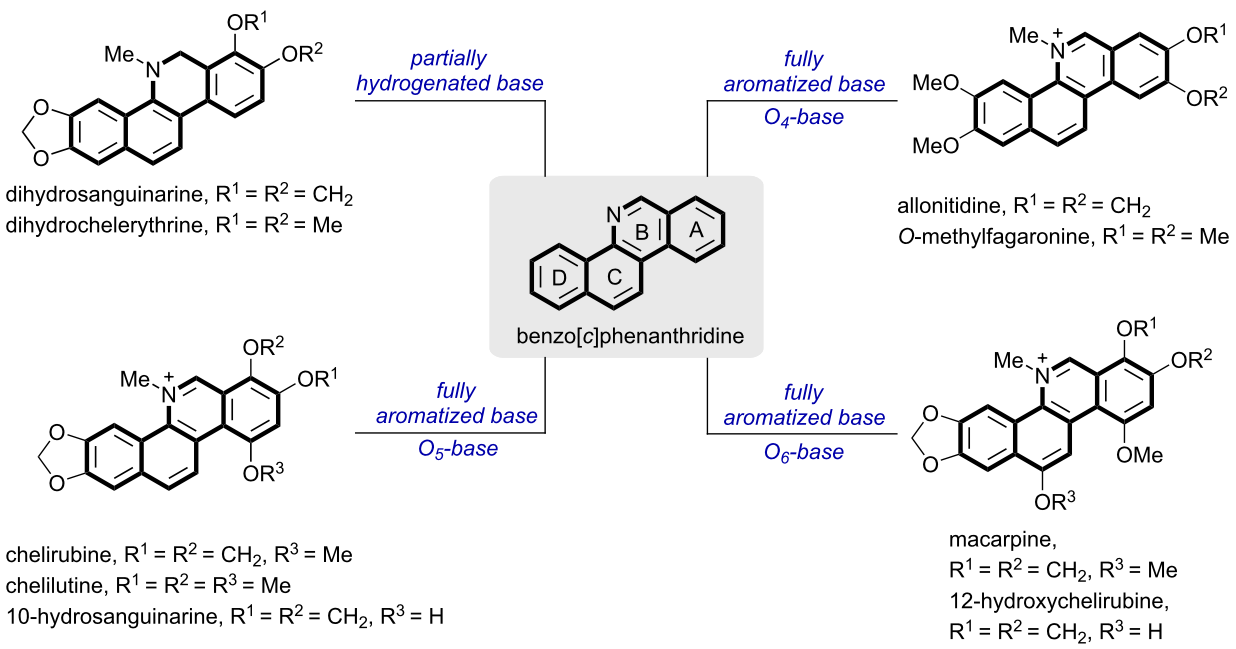

Scheme 1: Classification of benzo[*c*]phenanthridine alkaloids.

synthetic routes were completed in the last step by constructing ring B or ring C. Some representative examples and their key strategies are summarized in Scheme 2. In 1989, Hanaoka and co-workers developed the total synthesis of macarpine by Hofmann elimination from protoberberine by introducing rings B and C (Scheme 2a) [11]. In 1995, Ishikawa and co-workers accomplished the total synthesis via a Reformatsky reaction and aromatic nitrosation through the building of rings B and C (Scheme 2b) [12]. In 2010, Echavarren and co-worker completed the formal total synthesis via a Au(I)-catalyzed cyclization (Scheme 2c) [13]. In 2018, Pabbaraja and co-workers disclosed the synthesis of macarpine by constructing ring C through the domino Michael addition/S_NAr reaction of nitromethane to an ynone precursor (Scheme 2d) [14].

Results and Discussion

The efforts on developing efficient synthetic strategies to access macarpine never ceased during the last decades, and we have joined this meaningful research. Herein, a strategy involving the synthesis of an intermediate reported by Ishikawa in 1995 in the total synthesis of macarpine [12] is proposed via a Au(I)-catalyzed cycloisomerization reaction.

Retrosynthetically, the target molecule macarpine (**1**) could be disconnected into naphthol **12** (Scheme 3), a key intermediate reported by Ishikawa in the total synthesis of macarpine. This intermediate could be synthesized from silyl enol ether compound **10** via the Au(I)-catalyzed cycloisomerization reaction developed by our group [15]. The compound **10** could be constructed by the Sonogashira coupling reaction from readily prepared iodoarene **8** [12,16] and ketone **5**, which could be synthesized by using cheap 6-bromopiperonal (**2**) as the starting material.

To attempt the proposed synthetic strategy, ketone **5** and iodoarene **8** were prepared by following the synthetic route outlined in Scheme 4. Ketone **5** was prepared in a four-step procedure. Firstly, a Sonogashira coupling between 6-bromopiperonal (**2**) and trimethylsilylacetylene was performed to furnish aldehyde **3** [17,18] in 89% yield. A following nucleophilic addition reaction of aldehyde **3** by methylmagnesium bromide (MeMgBr) gave alcohol **4** in 99% yield, which was oxidized by pyridinium chlorochromate (PCC) leading to the formation of ketone compound and the deprotection of the silyl group was accomplished in the presence of potassium carbonate (K_2CO_3) and methanol to provide the terminal alkyne **5** in 96% yield in two steps. The iodoarene **8** [12,16] was facilely synthesized from sesamol (**6**) via methylation and iodination in an overall yield of 67%.

With the building blocks **5** and **8** in hand, ketone **9** was prepared via a palladium-catalyzed Sonogashira coupling reaction in a yield of 95%. The precursor **10** for the gold(I)-catalyzed [19-24] cycloisomerization was then synthesized by treating ketone **9** with sodium bis(trimethylsilyl)amide (NaHMDS) and *tert*-butyldimethylsilyl chloride (TBSCl) (Scheme 5).

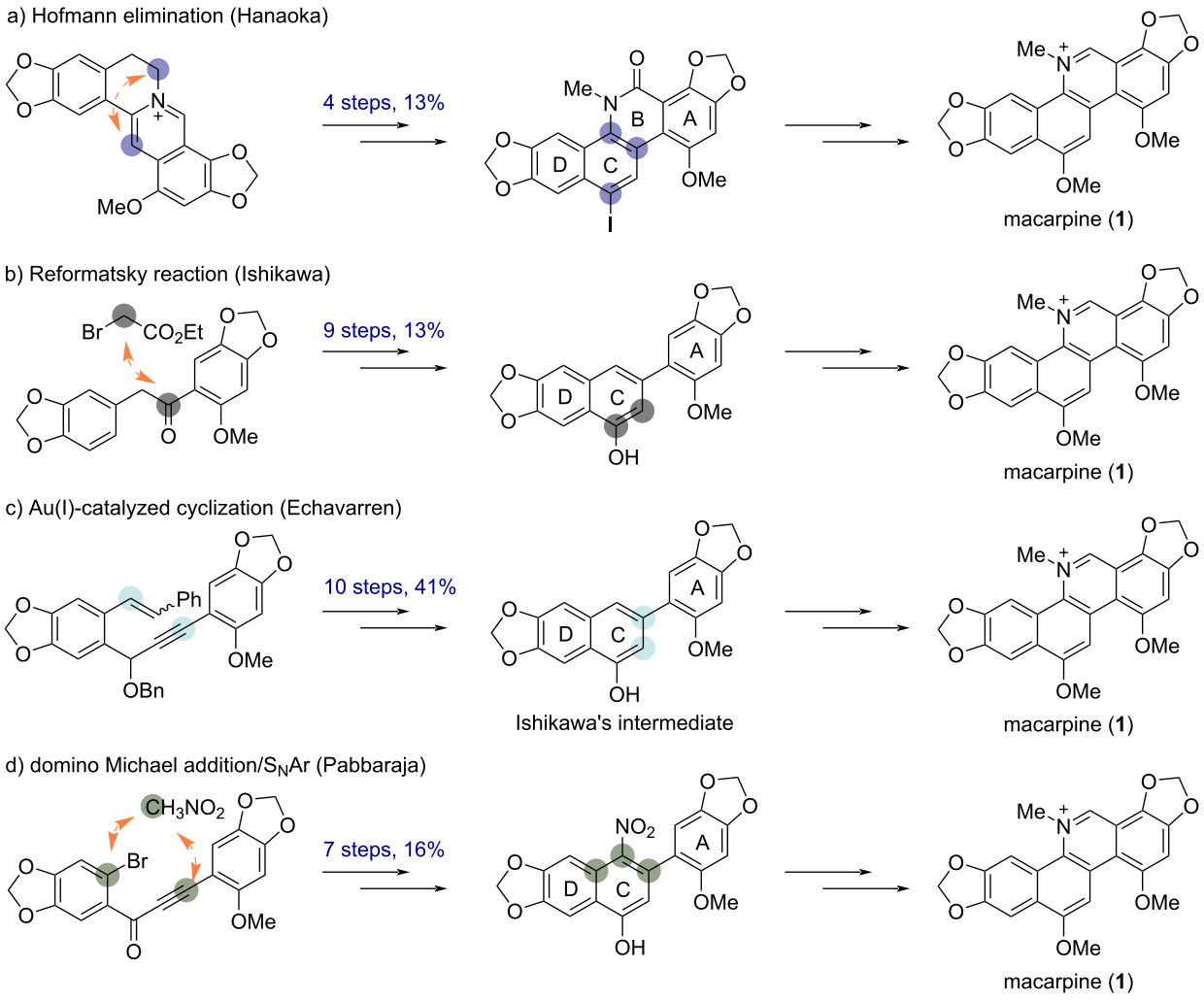

Scheme 2: Representative synthetic strategies for macarpine (**1**).

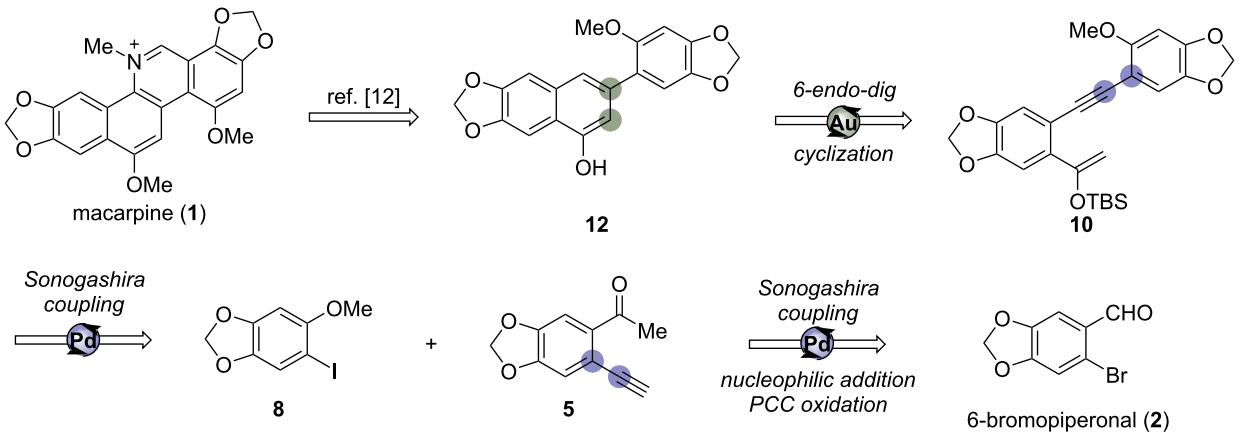

Scheme 3: Retrosynthetic analysis of marcarpine precursor **12** for a partial synthesis.

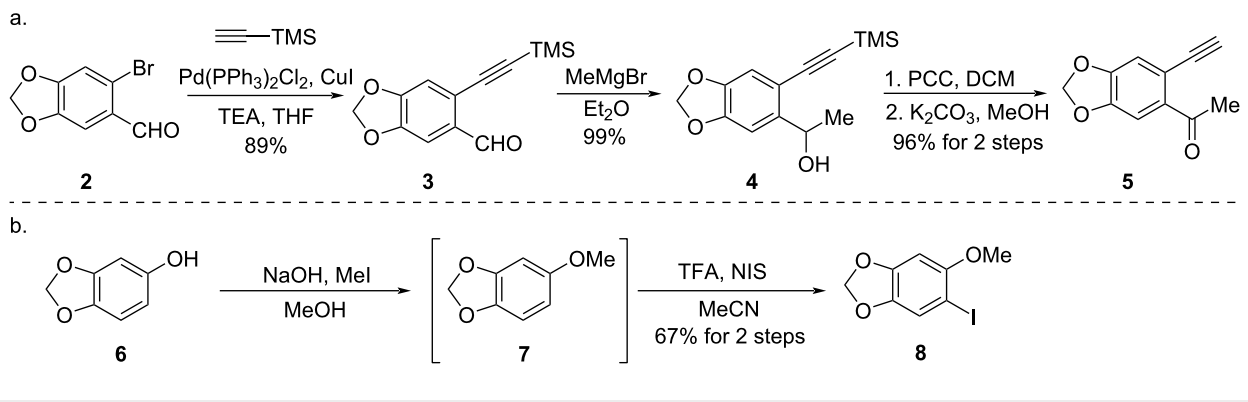

Scheme 4: Syntheses of precursors **5** and **8**.

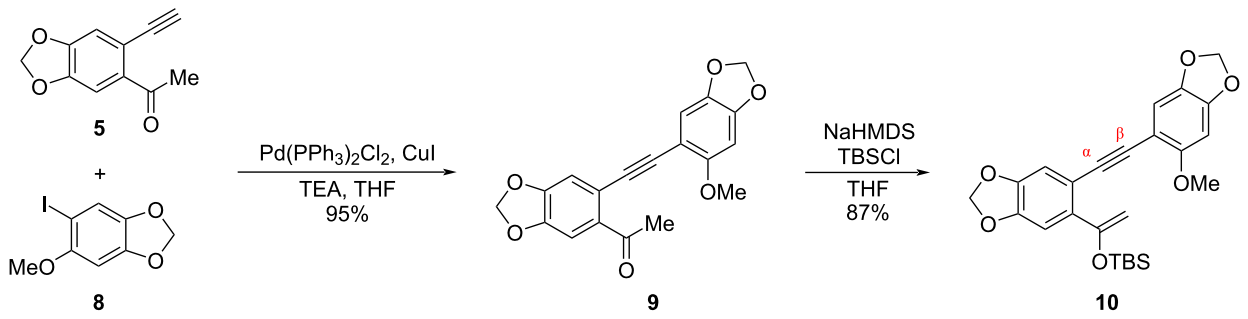

Scheme 5: Synthesis of enol silyl ether **10**.

To find the best cycloisomerization conditions, the 1,5-enyne substrate **10** was subjected to different reaction conditions as listed in Table 1. It was observed that [1,3-bis(2,6-diisopropylphenyl)imidazol-2-ylidene]gold(I) chloride (IPrAuCl) itself failed to catalyze the cycloisomerization (Table 1, entry 1). Evaluation of a number of silver salts illustrated that silver hexafluoroantimonate ($AgSbF_6$) was the optimal additive to activate the gold catalyst (Table 1, entries 2, 3, and 7). Screening of the other ligands of Au(I) catalysts, including triphenylphosphane (Ph_3P), [1,1'-biphenyl]-2-yl-di-*tert*-butylphosphane (JohnPhos) dicyclohexyl(2',4'-diisopropyl-3,6-dimethoxy-[1,1'-biphenyl]-2-yl)phosphane (BrettPhos) (Table 1, entries 4–6) revealed that 1,3-bis(2,6-diisopropylphenyl)imidazol-2-ylidene (IPr) was still the best one (Table 1, entry 7). Neither decreasing nor increasing the loading of the catalyst gave better yields (Table 1, entries 8 and 9). Examination of the reaction time showed that 2 h was the shortest reaction time and that extending the reaction time did not help to increase the yield (Table 1, entries 10 and 11). Lowering or raising the reaction temperature resulted in lower yields (Table 1, entries 12 and 13). The solvent had less effect on the reaction, and combining various factors, DCM was used for the reaction (Table 1, entries 14 and 15). When $AgSbF_6$ was utilized as the sole catalyst, not any product was generated indicating cationic Au(I) was the true catalyst (Table 1, entry 16). A control experiment using 2,6-di-*tert*-butylpyridine as a proton scavenger in the IPrAuCl/$AgSbF_6$ system provided the product in good yield, which excluded the influence of trace amounts of acids on the reaction (Table 1, entry 17).

The Au(I)-catalyzed cycloisomerization reaction of substrate **10** occurred under the catalysis of 5 mol % [1,3-bis(2,6-diisopropylphenyl)imidazol-2-ylidene]gold(I) chloride (IPrAuCl) and 5 mol % silver hexafluoroantimonate ($AgSbF_6$) [25,26] in anhydrous DCM at room temperature for 2 h forming a benzene ring smoothly, leading to the exclusive formation of biaryl intermediate **11** in a yield of 82%. It is worth noting that the methoxy substitution in the substrate played a crucial role in controlling the selectivity of the cycloisomerization according to our previous study [15]. It was rationalized that the electron-donating phenyl ring enabled the coordination of the alkyne with the Au^+ complex in the α-position, which promoted the silyl ether to attack the β-position of the alkyne to promote a 6-*endo*-*dig* cyclization. Next, compound **11** was subjected to a

Table 1: Optimization of the Au(I)-catalyzed cycloisomerization conditions.

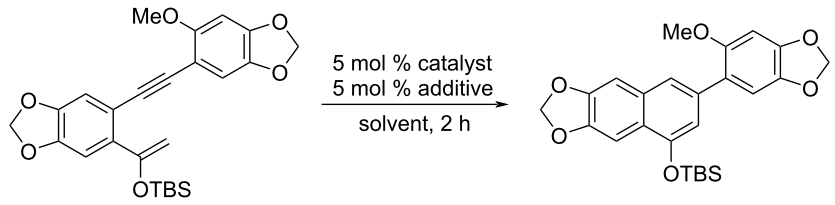

10 **11**

entry	catalyst	solvent	additive	*T* (°C)	yield (%)
1	IPrAuCl	DCM	–	23	0
2	IPrAuCl	DCM	AgOTf	23	61
3	IPrAuCl	DCM	$AgCO_2CF_3$	23	23
4	Ph_3PAuCl	DCM	$AgSbF_6$	23	77
5	JohnPhosMeCNAuSbF_6	DCM	–	23	64
6	BrettPhosAuCl	DCM	$AgSbF_6$	23	45
7	**IPrAuCl**	**DCM**	**$AgSbF_6$**	**23**	**82**
8	IPrAuCl	DCM	$AgSbF_6$	23	68[a]
9	IPrAuCl	DCM	$AgSbF_6$	23	82[b]
10	IPrAuCl	DCM	$AgSbF_6$	23	57[c]
11	IPrAuCl	DCM	$AgSbF_6$	23	81[d]
12	IPrAuCl	DCM	$AgSbF_6$	0	63
13	IPrAuCl	DCM	$AgSbF_6$	40	72
14	IPrAuCl	toluene	$AgSbF_6$	23	82
15	IPrAuCl	THF	$AgSbF_6$	23	80
16	–	DCM	$AgSbF_6$	23	0
17	IPrAuCl	THF	$AgSbF_6$	23	80[e]

[a]3 mol % IPrAuCl and 3 mol % $AgSbF_6$ were used. [b]10 mol % IPrAuCl and 10 mol % $AgSbF_6$ were used. [c]The reaction was run for 1 h. [d]The reaction was run for 3 h. [e]5 mol % 2,6-di-*tert*-butylpyridine was added. IPr = [1,3-bis(2,6-diisopropylphenyl)imidazol-2-ylidene]. JohnPhos = [[1,1'-biphenyl]-2-yldi-*tert*-butylphosphane]. BrettPhos = [dicyclohexyl(2',4'-diisopropyl-3,6-dimethoxy-[1,1'-biphenyl]-2-yl)phosphane].

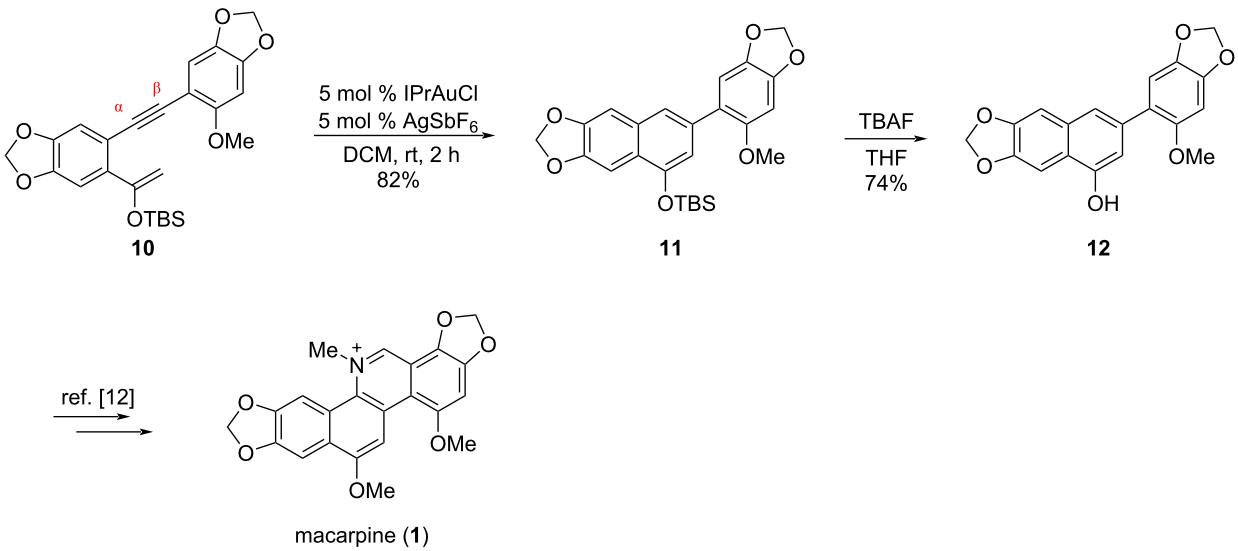

Scheme 6: Formal total synthesis of macarpine (**1**).

solution of tetrabutylammonium fluoride (TBAF) in tetrahydrofuran (THF), resulting in the formation of naphthol **12** [12,13], a key intermediate in the previous total synthesis of macarpine (**1**) reported by Ishikawa (Scheme 6).

To simplify the synthetic procedure, a more straightforward strategy was proposed by using alkynyl ketone **9** [27-29] as the substrate for the gold-catalyzed cycloisomerization in the presence of protonic acid. It was supposed that alkynyl ketone **9** would undergo enolization under the acidic conditions, followed by a gold-catalyzed cycloisomerization to provide the naphthol **12**.

To test the idea, alkynyl ketone **9** was subjected to different reaction conditions as listed in Table 2. It was observed that both the acids and the temperatures had a great influence on the cycloisomerization. An attempt was also made by using only *p*-toluenesulfonic acid (TsOH) in the cycloisomerization step, but no corresponding product was obtained. Finally, the optimal conditions for the Au(I)-catalyzed cycloisomerization of alkynyl ketone **9** were determined as to stir the substrate under the catalysis of 5 mol % IPrAuCl/$AgSbF_6$ with 2 equiv of TsOH as the additive at 70 °C for 2 h (Table 2, entry 3). It is notable that our synthetic route to naphthol **9** is shorter and proceeds with higher yield (5 steps, 59% yield) than Ishikawa's route (9 steps, 13% yield).

Conclusion

In summary, the formal total synthesis of the natural product macarpine was achieved through two synthetic routes by synthesizing Ishikawa's naphthol intermediate via Au(I)-catalyzed cycloisomerizations. Compared to the route reported in the literature, these routes are more concise and easier to perform. This gold-catalyzed strategy provides a new approach to macarpine and related benzo[*c*]phenanthridine alkaloids and the application of this strategy to access benzo[*c*]phenanthridine derivatives and further assessments of their bioactivities are currently in progress in our laboratory.

Supporting Information

Supporting Information File 1

Synthetic procedures and characterization data for compounds **3**–**5**, **8**–**12**, and their ^{1}H NMR and ^{13}C NMR spectra.
[https://www.beilstein-journals.org/bjoc/content/supplementary/1860-5397-18-169-S1.pdf]

Funding

Y.L. acknowledges the financial support from the National Natural Science Foundation of China (No. 21977073), Natural Science Foundation of Liaoning, China (No. 2022-MS-245) and the Liaoning Provincial Foundation of Educational Department (No. LJKZ0908). The authors would like to thank the Program for the Innovative Research Team of the Ministry of Education and the Program for the Liaoning Innovative Research Team in University.

Table 2: Reaction condition optimization of the cycloisomerization of alkynyl ketone **9**.

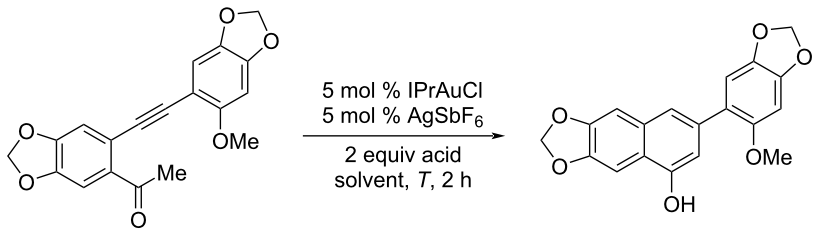

9 **12**

entry	acid	solvent	*T* (°C)	yield (%)
1	TsOH	DCM	23	0
2	TsOH	DCM	40	0
3	**TsOH**	**DCE**	**70**	**73**
4	TFA	DCE	70	50
5	AcOH	DCE	70	24
6	$PhCO_2H$	DCE	70	39

ORCID® iDs

Lu Yang - https://orcid.org/0000-0001-9727-4849
Yongxiang Liu - https://orcid.org/0000-0003-0364-0137

Preprint

A non-peer-reviewed version of this article has been previously published as a preprint: https://doi.org/10.3762/bxiv.2022.70.v1

References

1. Slaninová, I.; Slunská, Z.; Šinkora, J.; Vlková, M.; Táborská, E. *Pharm. Biol. (Abingdon, U. K.)* **2007,** *45,* 131–139. doi:10.1080/13880200601113099
2. Al-Snafi, A. E. *Indo Am. J. Pharm. Sci.* **2017,** *4,* 257–263.
3. Cheng, P.; Zeng, J. *Chin. J. Org. Chem.* **2012,** *32,* 1605–1619. doi:10.6023/cjoc201204008
4. Orhan, I.; Özçelik, B.; Karaoğlu, T.; Şener, B. *Z. Naturforsch., C: J. Biosci.* **2007,** *62c,* 19–26. doi:10.1515/znc-2007-1-204
5. Wang, Q.; Dai, P.; Bao, H.; Liang, P.; Wang, W.; Xing, A.; Sun, J. *Exp. Ther. Med.* **2017,** *13,* 263–268. doi:10.3892/etm.2016.3947
6. Balažová, A.; Urdová, J.; Forman, V.; Mučaji, P. *Molecules* **2020,** *25,* 1261. doi:10.3390/molecules25061261
7. Gaziano, R.; Moroni, G.; Buè, C.; Miele, M. T.; Sinibaldi-Vallebona, P.; Pica, F. *World J. Gastrointest. Oncol.* **2016,** *8,* 30–39. doi:10.4251/wjgo.v8.i1.30
8. Pica, F.; Balestrieri, E.; Serafino, A.; Sorrentino, R.; Gaziano, R.; Moroni, G.; Moroni, N.; Palmieri, G.; Mattei, M.; Garaci, E.; Sinibaldi-Vallebona, P. *Anti-Cancer Drugs* **2012,** *23,* 32–42. doi:10.1097/cad.0b013e32834a0c8e
9. Schmeller, T.; Latz-Brüning, B.; Wink, M. *Phytochemistry* **1997,** *44,* 257–266. doi:10.1016/s0031-9422(96)00545-6
10. Slaninová, I.; López-Sánchez, N.; Šebrlová, K.; Vymazal, O.; Frade, J. M.; Táborská, E. *Biol. Cell* **2016,** *108,* 1–18. doi:10.1111/boc.201500047
11. Hanaoka, M.; Cho, W. J.; Yoshida, S.; Fueki, T.; Mukai, C. *Heterocycles* **1989,** *29,* 857–860. doi:10.3987/com-89-4926
12. Ishikawa, T.; Saito, T.; Ishii, H. *Tetrahedron* **1995,** *51,* 8447–8458. doi:10.1016/0040-4020(95)00460-p
13. Solorio-Alvarado, C. R.; Echavarren, A. M. *J. Am. Chem. Soc.* **2010,** *132,* 11881–11883. doi:10.1021/ja104743k
14. Singh, S.; Samineni, R.; Pabbaraja, S.; Mehta, G. *Angew. Chem., Int. Ed.* **2018,** *57,* 16847–16851. doi:10.1002/anie.201810652
15. Fu, J.; Li, B.; Wang, X.; Liang, Q.; Peng, X.; Yang, L.; Wan, T.; Wang, X.; Lin, B.; Cheng, M.; Liu, Y. *Chin. J. Chem.* **2022,** *40,* 46–52. doi:10.1002/cjoc.202100582
16. Huang, Q.; Wang, P.; Tian, Y.; Song, N.; Ren, S.; Tao, J.; Hang, K.; Li, M. *Synlett* **2015,** *26,* 1385–1390. doi:10.1055/s-0034-1380520
17. Xie, F.; Zhang, B.; Chen, Y.; Jia, H.; Sun, L.; Zhuang, K.; Yin, L.; Cheng, M.; Lin, B.; Liu, Y. *Adv. Synth. Catal.* **2020,** *362,* 3886–3897. doi:10.1002/adsc.202000755
18. Liu, X.-J.; Zhou, S.-Y.; Xiao, Y.; Sun, Q.; Lu, X.; Li, Y.; Li, J.-H. *Org. Lett.* **2021,** *23,* 7839–7844. doi:10.1021/acs.orglett.1c02858
19. Hashmi, A. S. K.; Rudolph, M. *Chem. Soc. Rev.* **2008,** *37,* 1766–1775. doi:10.1039/b615629k
20. Rudolph, M.; Hashmi, A. S. K. *Chem. Soc. Rev.* **2012,** *41,* 2448–2462. doi:10.1039/c1cs15279c
21. Pflästerer, D.; Hashmi, A. S. K. *Chem. Soc. Rev.* **2016,** *45,* 1331–1367. doi:10.1039/c5cs00721f
22. Hashmi, A. S. K.; Frost, T. M.; Bats, J. W. *J. Am. Chem. Soc.* **2000,** *122,* 11553–11554. doi:10.1021/ja005570d
23. Hashmi, A. S. K.; Rudolph, M.; Siehl, H.-U.; Tanaka, M.; Bats, J. W.; Frey, W. *Chem. – Eur. J.* **2008,** *14,* 3703–3708. doi:10.1002/chem.200701795
24. Dankwardt, J. W. *Tetrahedron Lett.* **2001,** *42,* 5809–5812. doi:10.1016/s0040-4039(01)01146-7
25. Schießl, J.; Schulmeister, J.; Doppiu, A.; Wörner, E.; Rudolph, M.; Karch, R.; Hashmi, A. S. K. *Adv. Synth. Catal.* **2018,** *360,* 2493–2502. doi:10.1002/adsc.201800233
26. Schießl, J.; Schulmeister, J.; Doppiu, A.; Wörner, E.; Rudolph, M.; Karch, R.; Hashmi, A. S. K. *Adv. Synth. Catal.* **2018,** *360,* 3949–3959. doi:10.1002/adsc.201800629
27. Song, L.; Tian, G.; Van der Eycken, E. V. *Chem. – Eur. J.* **2019,** *25,* 7645–7648. doi:10.1002/chem.201901860
28. Guan, Y.; Lu, Z.; Yin, X.; Mohammadlou, A.; Staples, R. J.; Wulff, W. D. *Synthesis* **2020,** *52,* 2073–2091. doi:10.1055/s-0039-1690860
29. Makra, F.; Rohloff, J. C.; Muehldorf, A. V.; Link, J. O. *Tetrahedron Lett.* **1995,** *36,* 6815–6818. doi:10.1016/00404-0399(50)14035-

License and Terms

BEILSTEIN JOURNAL OF ORGANIC CHEMISTRY

Synthetic study toward the diterpenoid aberrarone

Liang Shi[‡1], Zhiyu Gao[‡1], Yiqing Li[1], Yuanhao Dai[1], Yu Liu[1], Lili Shi[*2] and Hong-Dong Hao[*1,2]

Letter

Open Access

Address:
[1]Department Shaanxi Key Laboratory of Natural Products & Chemical Biology, College of Chemistry & Pharmacy, Northwest A&F University, Yangling, Shaanxi 712100, China and [2]State Key Laboratory of Chemical Oncogenomics, Guangdong Provincial Key Laboratory of Chemical Genomics, Peking University Shenzhen Graduate School, Shenzhen, Guangdong 518055, China

Email:
Lili Shi[*] - shill@pkusz.edu.cn; Hong-Dong Hao[*] - hongdonghao@nwafu.edu.cn

* Corresponding author ‡ Equal contributors

Keywords:
aberrarone; C–H insertion; gold; Pauson–Khand; total synthesis

Beilstein J. Org. Chem. **2022,** *18,* 1625–1628.
https://doi.org/10.3762/bjoc.18.173

Received: 28 September 2022
Accepted: 16 November 2022
Published: 30 November 2022

This article is part of the thematic issue "Total synthesis: an enabling science".

Associate Editor: B. Nay

Abstract

An approach to aberrarone, an antimalarial diterpenoid natural product with tetracyclic skeleton is reported. Key to the stereoselective preparation of the 6-5-5 tricyclic skeleton includes the mediation of Nagata reagent for constructing the C1 all-carbon quaternary centers and gold-catalyzed cyclopentenone synthesis through C–H insertion.

Introduction

Marine natural products have found myriad use in new drug development, exemplified by ET-743 and eribulin [1]. Back in 1990s, Rodriguez and co-workers isolated a rich array of terpenoid natural products from the Caribbean sea whip, *Pseudopterogorgia elisabethae* with unprecedented carbon skeleton, most of which showed antitumor, antituberculosis and antimalarial activities [2-6]. Among these structurally intriguing natural products, aberrarone (**1**) shows antimalarial activity against the chloroquine-resistant strain of *Plasmodium falciparum* (IC_{50} = 10 μg/mL) [7]. Structurally, aberrarone possesses an unusual tetracyclic carbon skeleton yet-to-be found in *Pseudopterogorgia elisabethae* species, although related cyclohexane-angularly-fused triquinane systems have been found in waihoensene (**3**), conidiogenone (**4**), lycopodium alkaloids magellamine (**5**) and lycojaponicumin C (**6**) (Figure 1). Its seven stereogenic centers, including two all-carbon quaternary centers, together with the non-enolizable cyclic α-diketone moiety collectively render aberrarone as an attractive but challenging synthetic target. Its congener elisabanolide (**2**) with a lactone in the D ring shows their potential biosynthetic relationship [2]. These natural products have been popular synthetic targets mainly due to their intriguing structural features. For example, several total syntheses of **3**–**6** have been reported [8-29]. Previously, two synthetic studies of aberrarone were reported [30,31] and more recently, Carreira and co-workers reported [32] the first total synthesis of aberrarone through an impres-

sive cascade reaction including a gold-catalyzed Nazarov cyclization, a cyclopropanation followed by intramolecular aldol reaction to forge the A, B and D rings. Impressed by the structural features and biological profiles, our group embarked a project on the total synthesis of this natural product. Herein, we report our stereoselective synthesis of its 6-5-5 tricyclic skeleton.

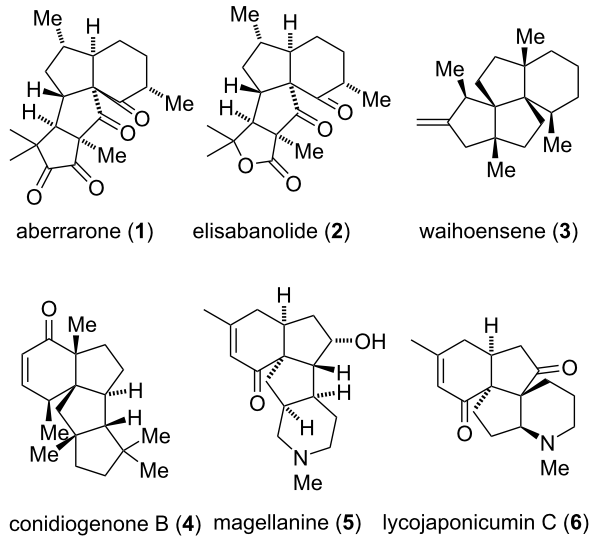

Figure 1: Selected representative natural products with 6-5-5 tricyclic skeleton.

Our retrosynthetic analysis is shown in Scheme 1. For the formation of the D ring with one quaternary carbon stereocenter and 1,2-dikeone moiety, Nazarov cyclization [33] of **7** was proposed for synthesizing this challenging moiety. The corresponding precursor cyclopentenone **8** may be prepared from alkynone **9** through a gold-catalyzed C–H insertion [34]. Alkynone **9** could be achieved through functional transformation from **10**, which itself would be prepared through methylation and conjugate addition from Pauson–Khand adduct **11**. This cyclopentenone could be readily accessed from 1,7-enyne **12** which could be obtained through the reported procedure [35] from the commercially available 5-hexenoic acid.

Results and Discussion

Our synthetic route commenced from known compound **12** which is readily accessed from 5-hexenoic acid through a reported procedure [35]. In the mediation of $Co_2(CO)_8$, the 6-5 bicyclic skeleton [36] was constructed with the right configuration at C6, and the explanation of this stereoselectivity is possible through the conformation of **14** where the OTBS group is in pseudoequatorial position (Scheme 2). Therefore, the Pauson–Khand reaction proceeded to afford **11** containing an α-H at C6. From this intermediate, to our delight, the stereoselective attachment of the requisite methyl group through the corresponding lithium enolate occurred from the convex face of the bicyclic ring system [37]. After these two continuous stereocenters were successfully installed, the expected challenging all-carbon quaternary center at C1 was constructed utilizing the Nagata reagent (Et_2AlCN). By using this strategy, the stereogenic center at C1 was synthesized, along with a smooth attachment of the cyanate group served for further functional group transformation to construct the C ring through C–H insertion. The stereochemistry finding of this conjugate addition from the convex face of the 6-5 ring system was further confirmed through X-ray crystallographic analysis.

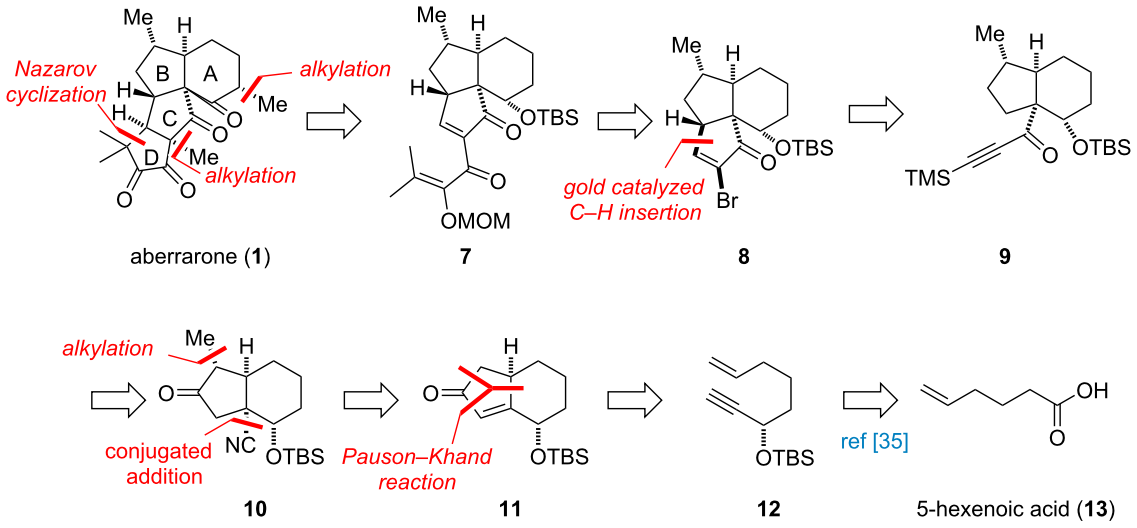

Scheme 1: Retrosynthetic analysis of aberrarone (**1**).

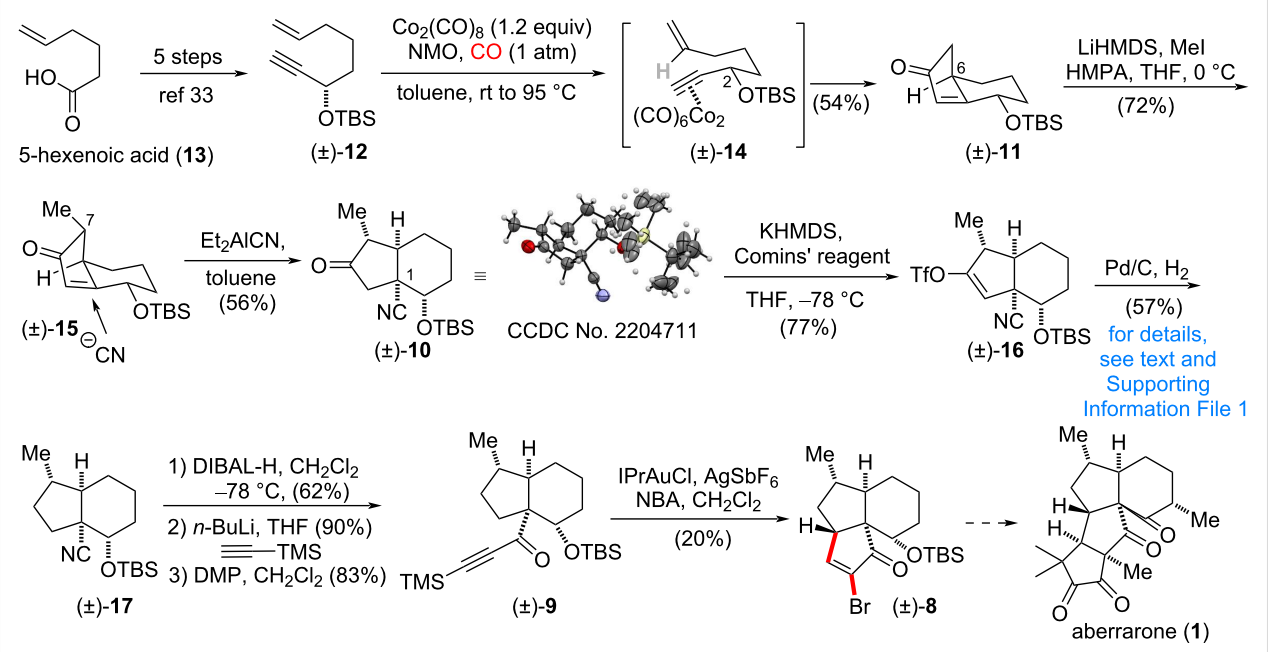

Scheme 2: Synthetic study toward aberrarone (**1**).

With the key intermediate **10** in hand, we were in a position to test the planned two-step transformation including the palladium-catalyzed reductive cross coupling with HCO_2H followed by Pd/C-catalyzed hydrogenation. To our surprise, the hydrogenation turned out to be a difficult transformation due to the steric hindered environment of the trisubstituted double bond, mainly caused by the bulky OTBS group. However, direct subjection of compound **16** to hydrogenation [38] afforded reduction of both triflate and double bond. The plausible pathway for this facile transformation might proceed with first hydrogenation followed by the substitution of the labile triflate ester (for details, see Supporting Information File 1). Moving forward, compound **17** was further converted into alkynone **9** through DIBAL-H reduction, nucleophilic addition and Dess–Martin oxidation. At this stage, the pivotal C–H insertion step was tried under the reported conditions [34], and cyclopentenone **8** was successfully obtained. Further study with cross coupling or halogen–magnesium exchange shows this moiety is inert for functional group transformation. The attempt for constructing the D ring is currently undergoing.

Conclusion

In summary, we have developed an approach to assemble the tricyclic skeleton of aberrarone through stereoselective methylation, conjugate addition and gold-catalyzed C–H insertion from the readily accessed cyclopentenone. Further work to access natural product aberrarone from the key intermediate cyclopentenone **8** is currently underway, and will be reported in due course.

Supporting Information

The crystallographic data of compound **10** (CCDC 2204711) has been deposited at the Cambridge Crystallographic Database Center (http://www.ccdc.cam.ac.uk).

Supporting Information File 1

Characterization data and ^{1}H NMR, ^{13}C NMR, and HRMS spectra of the compounds.
[https://www.beilstein-journals.org/bjoc/content/supplementary/1860-5397-18-173-S1.pdf]

Funding

We are grateful for financial support from Natural Science Foundation of China (Grant No. 21901211).

ORCID® iDs

Hong-Dong Hao - https://orcid.org/0000-0002-9236-3727

Preprint

A non-peer-reviewed version of this article has been previously published as a preprint: https://doi.org/10.3762/bxiv.2022.79.v1

References

1. Altmann, K.-H. *Chimia* **2017,** *71,* 646–652. doi:10.2533/chimia.2017.646

2. Rodríguez, A. D.; González, E.; Huang, S. D. *J. Org. Chem.* **1998,** *63,* 7083–7091. doi:10.1021/jo981385v
3. Rodríguez, A. D.; Ramírez, C. *Org. Lett.* **2000,** *2,* 507–510. doi:10.1021/ol991362i
4. Rodríguez, A. D.; Ramírez, C.; Rodríguez, I. I.; Barnes, C. L. *J. Org. Chem.* **2000,** *65,* 1390–1398. doi:10.1021/jo9914869
5. Rodríguez, A. D.; Ramírez, C.; Shi, Y.-P. *J. Org. Chem.* **2000,** *65,* 6682–6687. doi:10.1021/jo000875w
6. Wei, X.; Rodríguez, I. I.; Rodríguez, A. D.; Barnes, C. L. *J. Org. Chem.* **2007,** *72,* 7386–7389. doi:10.1021/jo070649n
7. Rodríguez, I. I.; Rodríguez, A. D.; Zhao, H. *J. Org. Chem.* **2009,** *74,* 7581–7584. doi:10.1021/jo901578r
8. Jeon, H.; Winkler, J. D. *Synthesis* **2021,** *53,* 475–488. doi:10.1055/s-0040-1705953
9. Lee, H.; Kang, T.; Lee, H.-Y. *Angew. Chem., Int. Ed.* **2017,** *56,* 8254–8257. doi:10.1002/anie.201704492
10. Qu, Y.; Wang, Z.; Zhang, Z.; Zhang, W.; Huang, J.; Yang, Z. *J. Am. Chem. Soc.* **2020,** *142,* 6511–6515. doi:10.1021/jacs.0c02143
11. Peng, C.; Arya, P.; Zhou, Z.; Snyder, S. A. *Angew. Chem., Int. Ed.* **2020,** *59,* 13521–13525. doi:10.1002/anie.202004177
12. Rosenbaum, L.-C.; Häfner, M.; Gaich, T. *Angew. Chem., Int. Ed.* **2021,** *60,* 2939–2942. doi:10.1002/anie.202011298
13. Wang, Y.-P.; Fang, K.; Tu, Y.-Q.; Yin, J.-J.; Zhao, Q.; Ke, T. *Nat. Commun.* **2022,** *13,* 2335. doi:10.1038/s41467-022-29947-5
14. Hou, S.-H.; Tu, Y.-Q.; Wang, S.-H.; Xi, C.-C.; Zhang, F.-M.; Wang, S.-H.; Li, Y.-T.; Liu, L. *Angew. Chem., Int. Ed.* **2016,** *55,* 4456–4460. doi:10.1002/anie.201600529
15. Hu, P.; Chi, H. M.; DeBacker, K. C.; Gong, X.; Keim, J. H.; Hsu, I. T.; Snyder, S. A. *Nature* **2019,** *569,* 703–707. doi:10.1038/s41586-019-1179-2
16. Xu, B.; Xun, W.; Su, S.; Zhai, H. *Angew. Chem., Int. Ed.* **2020,** *59,* 16475–16479. doi:10.1002/anie.202007247
17. Hirst, G. C.; Johnson, T. O., Jr.; Overman, L. E. *J. Am. Chem. Soc.* **1993,** *115,* 2992–2993. doi:10.1021/ja00060a064
18. Paquette, L. A.; Friedrich, D.; Pinard, E.; Williams, J. P.; St. Laurent, D.; Roden, B. A. *J. Am. Chem. Soc.* **1993,** *115,* 4377–4378. doi:10.1021/ja00063a072
19. Sha, C.-K.; Lee, F.-K.; Chang, C.-J. *J. Am. Chem. Soc.* **1999,** *121,* 9875–9876. doi:10.1021/ja992315o
20. Yen, C.-F.; Liao, C.-C. *Angew. Chem., Int. Ed.* **2002,** *41,* 4090–4093. doi:10.1002/1521-3773(20021104)41:21<4090::aid-anie4090>3.0.co;2-%23
21. Ishizaki, M.; Niimi, Y.; Hoshino, O.; Hara, H.; Takahashi, T. *Tetrahedron* **2005,** *61,* 4053–4065. doi:10.1016/j.tet.2005.02.044
22. Kozaka, T.; Miyakoshi, N.; Mukai, C. *J. Org. Chem.* **2007,** *72,* 10147–10154. doi:10.1021/jo702136b
23. Jiang, S.-Z.; Lei, T.; Wei, K.; Yang, Y.-R. *Org. Lett.* **2014,** *16,* 5612–5615. doi:10.1021/ol502679v
24. Lin, K.-W.; Ananthan, B.; Tseng, S.-F.; Yan, T.-H. *Org. Lett.* **2015,** *17,* 3938–3940. doi:10.1021/acs.orglett.5b01975
25. McGee, P.; Bétournay, G.; Barabé, F.; Barriault, L. *Angew. Chem., Int. Ed.* **2017,** *56,* 6280–6283. doi:10.1002/anie.201611606
26. Liu, J.; Chen, S.; Li, N.; Qiu, F. G. *Adv. Synth. Catal.* **2019,** *361,* 3514–3517. doi:10.1002/adsc.201900376
27. Huang, B.-B.; Lei, K.; Zhong, L.-R.; Yang, X.; Yao, Z.-J. *J. Org. Chem.* **2022,** *87,* 8685–8696. doi:10.1021/acs.joc.2c00871
28. Hou, S.-H.; Tu, Y.-Q.; Liu, L.; Zhang, F.-M.; Wang, S.-H.; Zhang, X.-M. *Angew. Chem., Int. Ed.* **2013,** *52,* 11373–11376. doi:10.1002/anie.201306369
29. Zheng, N.; Zhang, L.; Gong, J.; Yang, Z. *Org. Lett.* **2017,** *19,* 2921–2924. doi:10.1021/acs.orglett.7b01154
30. Srikrishna, A.; Neetu, G. *Tetrahedron* **2011,** *67,* 7581–7585. doi:10.1016/j.tet.2011.07.054
31. Kobayashi, T.; Tokumoto, K.; Tsuchitani, Y.; Abe, H.; Ito, H. *Tetrahedron* **2015,** *71,* 5918–5924. doi:10.1016/j.tet.2015.05.089
32. Amberg, W. M.; Carreira, E. M. *J. Am. Chem. Soc.* **2022,** *144,* 15475–15479. doi:10.1021/jacs.2c07150
33. Hoffmann, M.; Weibel, J.-M.; de Frémont, P.; Pale, P.; Blanc, A. *Org. Lett.* **2014,** *16,* 908–911. doi:10.1021/ol403663j
34. Wang, Y.; Zarca, M.; Gong, L.-Z.; Zhang, L. *J. Am. Chem. Soc.* **2016,** *138,* 7516–7519. doi:10.1021/jacs.6b04297
35. Cantagrel, G.; Meyer, C.; Cossy, J. *Synlett* **2007,** 2983–2986. doi:10.1055/s-2007-992366
36. Mukai, C.; Kozaka, T.; Suzuki, Y.; Kim, I. J. *Tetrahedron* **2004,** *60,* 2497–2507. doi:10.1016/j.tet.2004.01.041
37. Hog, D. T.; Huber, F. M. E.; Jiménez-Osés, G.; Mayer, P.; Houk, K. N.; Trauner, D. *Chem. – Eur. J.* **2015,** *21,* 13646–13665. doi:10.1002/chem.201501423
38. Jigajinni, V. B.; Wightman, R. H. *Tetrahedron Lett.* **1982,** *23,* 117–120. doi:10.1016/s0040-4039(00)97549-x

License and Terms

BEILSTEIN JOURNAL OF ORGANIC CHEMISTRY

Synthesis of (–)-halichonic acid and (–)-halichonic acid B

Keith P. Reber* and Emma L. Niner

Full Research Paper

Open Access

Address:
Department of Chemistry, Towson University, 8000 York Road, Towson, MD, 21252, USA

Email:
Keith P. Reber* - kreber@towson.edu

* Corresponding author

Keywords:
alkaloid; amino acid; aza-Prins reaction; cascade reaction; natural product

Beilstein J. Org. Chem. **2022,** *18,* 1629–1635.
https://doi.org/10.3762/bjoc.18.174

Received: 29 September 2022
Accepted: 17 November 2022
Published: 01 December 2022

This article is part of the thematic issue "Total synthesis: an enabling science".

Associate Editor: B. Nay

Abstract

The first syntheses of the amino acids (–)-halichonic acid and (–)-halichonic acid B have been achieved in ten steps starting from commercially available (−)-α-bisabolol. The optimized synthetic route includes a new purification method for isolating (−)-7-amino-7,8-dihydrobisabolene in enantiomerically pure form via recrystallization of its benzamide derivative. The key intramolecular aza-Prins reaction forms the characteristic 3-azabicyclo[3.3.1]nonane ring system of halichonic acid along with the lactonized form of halichonic acid B in an 8:1 ratio. Optical rotation measurements confirmed that these synthetic compounds were in fact the enantiomers of the natural products, establishing both the relative and absolute configurations of the halichonic acids.

Introduction

Marine sponges produce a large number of structurally diverse natural products, including many that exhibit biological activity [1-3]. In 2019, Tsukamoto and co-workers isolated the aminobisabolene sesquiterpenoid halichonic acid ((+)-**1**) from the sponge *Halichondra* sp. (Figure 1) [4]. This amino acid natural product features a rigid 3-azabicyclo[3.3.1]nonane ring system containing four stereogenic centers within the piperidine ring. In 2021, the same group re-isolated (+)-**1** from the sponge *Axinyssa* sp. along with the structurally related compound halichonic acid B ((+)-**2**) [5]. Structurally, (+)-**2** is a pipecolic acid derivative containing a cyclohexenyl ring as a substituent group. This compound also features four stereogenic centers (three of which are located within the piperidine ring) and a tertiary alcohol. The structures of compounds (+)-**1** and (+)-**2** were elucidated through a combination of HRMS and NMR spectroscopy, while the relative configuration of each compound was established through nuclear Overhauser effect (NOE) correlations. Additionally, the absolute configuration of each compound was determined based on calculated electronic circular dichroism (ECD) spectra that were compared to the experimental ECD spectra of (+)-**1** and (+)-**2**. Although these natural products did not exhibit antimicrobial activity or cytotoxicity against HeLa cells, their biological activities in other assays have not yet been investigated.

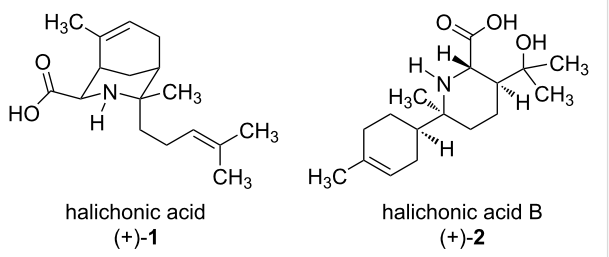

Figure 1: Structures of halichonic acid ((+)-**1**) and halichonic acid B ((+)-**2**).

Our group was particularly interested in the structure of halichonic acid ((+)-**1**), which shares the same bridged bicyclic ring system found in many of the *Aristotelia* alkaloids [6]. Since our lab recently reported a synthesis of the natural product aristoquinoline [7], we viewed the halichonic acids as ideal targets to extend the scope of our synthetic methodology. Given the structural similarity between compounds (+)-**1** and (+)-**2** (and the fact that they were co-isolated from the same sponge), Tsukamoto et al. proposed that these natural products could be derived from a common biosynthetic pathway starting from farnesyl pyrophosphate and glycine [5]. This prompted us to investigate a biomimetic synthesis in which the halichonic acids could be prepared from a common imine intermediate via divergent intramolecular aza-Prins cyclizations [8]. Herein, we report the first syntheses of the enantiomers of these natural products (i.e., (−)-**1** and (−)-**2**), confirming the structural assignments of the halichonic acids and establishing their absolute configurations.

Results

Our synthetic route began with the readily available sesquiterpenoid (−)-α-bisabolol (**3**), as shown in Scheme 1. In 2013, Shenvi and co-workers reported an operationally simple and high-yielding method for converting tertiary alcohols (including **3**) to the corresponding primary amines via the intermediacy of an isonitrile [9]. This four-step procedure was conveniently carried out on a multigram scale, affording (−)-7-amino-7,8-dihydrobisabolene (**4**) and its C7-epimer as an 83:17 mixture of diastereomers in 87% overall yield. Unfortunately, these diastereomers were not separable by conventional column chromatography. Although this diastereomeric mixture could be converted into a variety of amine derivatives (e.g., hydrochloride salt, mandelic acid salt, phthalimide, ketopinic acid amide, salicylaldehyde imine, *p*-toluenesulfonamide, acetamide, etc.), all attempts to separate the resulting isomers (which were oils) were similarly unsuccessful.

Seeking an alternative to column chromatography, we decided to prepare solid derivatives of **4** (and its C7-epimer) that could be purified by recrystallization. Although the α-bromoacet-

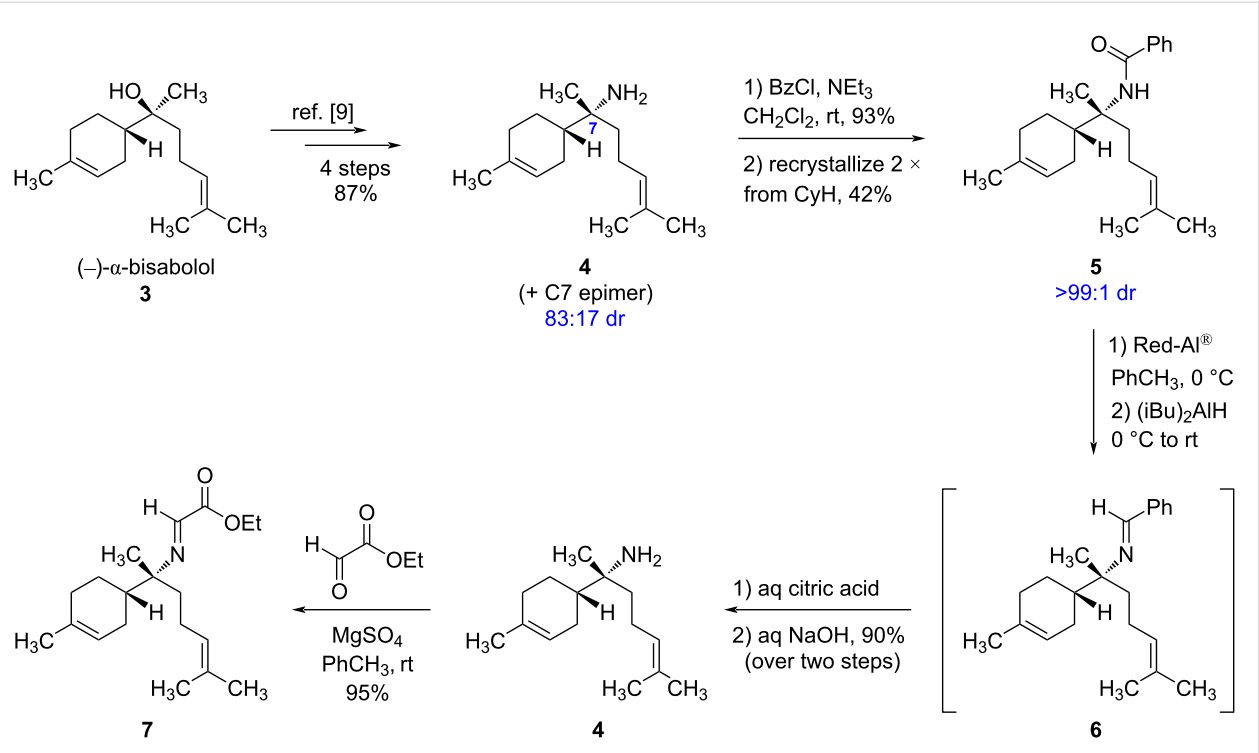

Scheme 1: Synthesis of (−)-7-amino-7,8-dihydrobisabolene (**4**) and its conversion to cyclization precursor **7**.

amide [10] and *p*-bromobenzamide derivatives of these amines are solids, no change in dr was observed upon recrystallization from a variety of solvents. Fortunately, we ultimately found success with the benzamide derivative **5**, which could be prepared from the mixture of **4** and its C7-epimer in 93% yield upon treatment with benzoyl chloride. Recrystallization of the resulting mixture of diastereomeric amides from cyclohexane improved the dr from 83:17 to 95:5 (as determined by ^{1}H NMR based on integration of the C7-methyl signals). A second recrystallization from cyclohexane afforded **5** as a single stereoisomer (>99:1 dr) with 42% overall recovery of material (corresponding to 51% recovery of the major diastereomer **5**).

Having finally separated the C7-diastereomers, we anticipated that the amide **5** could be hydrolyzed to give a single enantiomer of amine **4**. However, we found that amide **5** was remarkably resistant to hydrolysis, even under forcing conditions. For example, no amide hydrolysis was observed in concentrated aqueous NaOH solution at reflux (with or without an organic co-solvent), and slow decomposition occurred under acidic conditions at elevated temperatures. Alternative methods to cleave the benzamide using sodium peroxide [11] or triethyloxonium tetrafluoroborate [12] were also unsuccessful, giving either no reaction or significant decomposition, respectively. At this stage, we started to investigate alternative methods to cleave the amide via reduction. Achieving selective C–N-bond cleavage of amides under reductive conditions is still a largely unsolved problem since a C–O-bond cleavage is typically the preferred mode of reactivity, especially when using hydride reducing agents [13]. Nevertheless, specialized conditions for achieving C–N-bond cleavage of amides using SmI_2 [13], Tf_2O/Et_3SiH [14], and stoichiometric Schwartz's reagent [15] have been reported; however, none of these methods was successful in reducing amide **5** to the desired amine **4**.

Although there is one literature example of directly reducing a benzamide with diisobutylaluminum hydride (DIBAL) to achieve C–N-bond cleavage [16], we observed exclusive over-reduction of compound **5** under these conditions to form the corresponding *N*-benzylamine, even at −78 °C. We next investigated the reducing agent sodium bis(2-methoxyethoxy)aluminum hydride (Red-Al®), which is a convenient alternative to $LiAlH_4$ that exhibits high solubility in organic solvents and is also known to reduce amides [17]. When a solution of amide **5** in toluene was treated with an excess of Red-Al® at 0 °C, rapid gas evolution (likely H_2) occurred. However, no reduction of the amide was observed, even after stirring at room temperature for 24 hours. In an effort to "salvage" the reaction by reducing the amide to the corresponding *N*-benzylamine (which could potentially be oxidized to the corresponding imine with IBX [18] and subsequently hydrolyzed to give **4**), we added excess DIBAL and allowed the reaction mixture to stir at room temperature for an additional 24 hours. Upon quenching the reaction with a saturated aqueous solution of potassium sodium tartrate (Rochelle's salt), we were astonished to observe the clean formation of imine **6**. Presumably, the combination of Red-Al® and DIBAL reacts with amide **5** to form a stable tetrahedral intermediate that collapses to **6** upon aqueous workup. This type of direct amide semi-reduction using aluminum hydride reagents is, to the best of our knowledge, previously unknown within the chemical literature and is especially notable since it does not require cryogenic temperatures. Efforts to further investigate the scope of this unique transformation are currently underway in our laboratory and will be reported in due course.

Attempts to purify imine **6** by column chromatography on silica gel resulted in extensive decomposition. Therefore, the crude imine was immediately hydrolyzed using aqueous citric acid [14], affording (−)-7-amino-7,8-dihydrobisabolene (**4**) as a single stereoisomer in 90% yield over the two steps. The enantiomer of **4** is itself a natural product with cytotoxic, antifungal, and antimicrobial properties [10,19-22]. Notably, (+)-**4** was also co-isolated with compounds (+)-**1** and (+)-**2** in sponge extracts, suggesting that these compounds may share a common biosynthetic pathway [4,5]. Both enantiomers of **4** have been previously synthesized [9,23,24], and this compound has also been prepared in racemic form [25]. To supply the final two carbon atoms found in the halichonic acids, amine **4** was condensed with a solution of ethyl glyoxylate in toluene, giving imine **7** in 95% yield. We found that imine **7** could be purified by column chromatography on silica gel if the mobile phase contained approximately 2% triethylamine as a basic additive. However, it is also possible to use crude **7** in the subsequent cyclization step without significantly affecting isolated yields. ^{1}H NMR analysis showed that **7** was formed as a single geometrical isomer; although the imine configuration was not rigorously established, we have assigned it as the (*E*)-isomer, as is commonly observed in aldimine formation.

The stage was now set for the key intramolecular aza-Prins reaction that would form the bicyclic structures of the halichonic acids (Scheme 2). When a solution of imine **7** in chloroform was treated with a large excess (85–100 equiv) of formic acid at room temperature, we were pleased to observe the formation of bicyclic compound **8** as the major product in 64% yield. Notably, **8** is the ethyl ester of (−)-halichonic acid and features the characteristic 3-azabicyclo[3.3.1]nonane ring system found in this natural product. However, we were intrigued that a competing cyclization process also formed isomeric lactones **9** and **10** in 8% yield and 11% yield, respectively. ^{1}H NMR analysis confirmed that compounds **9** and **10**

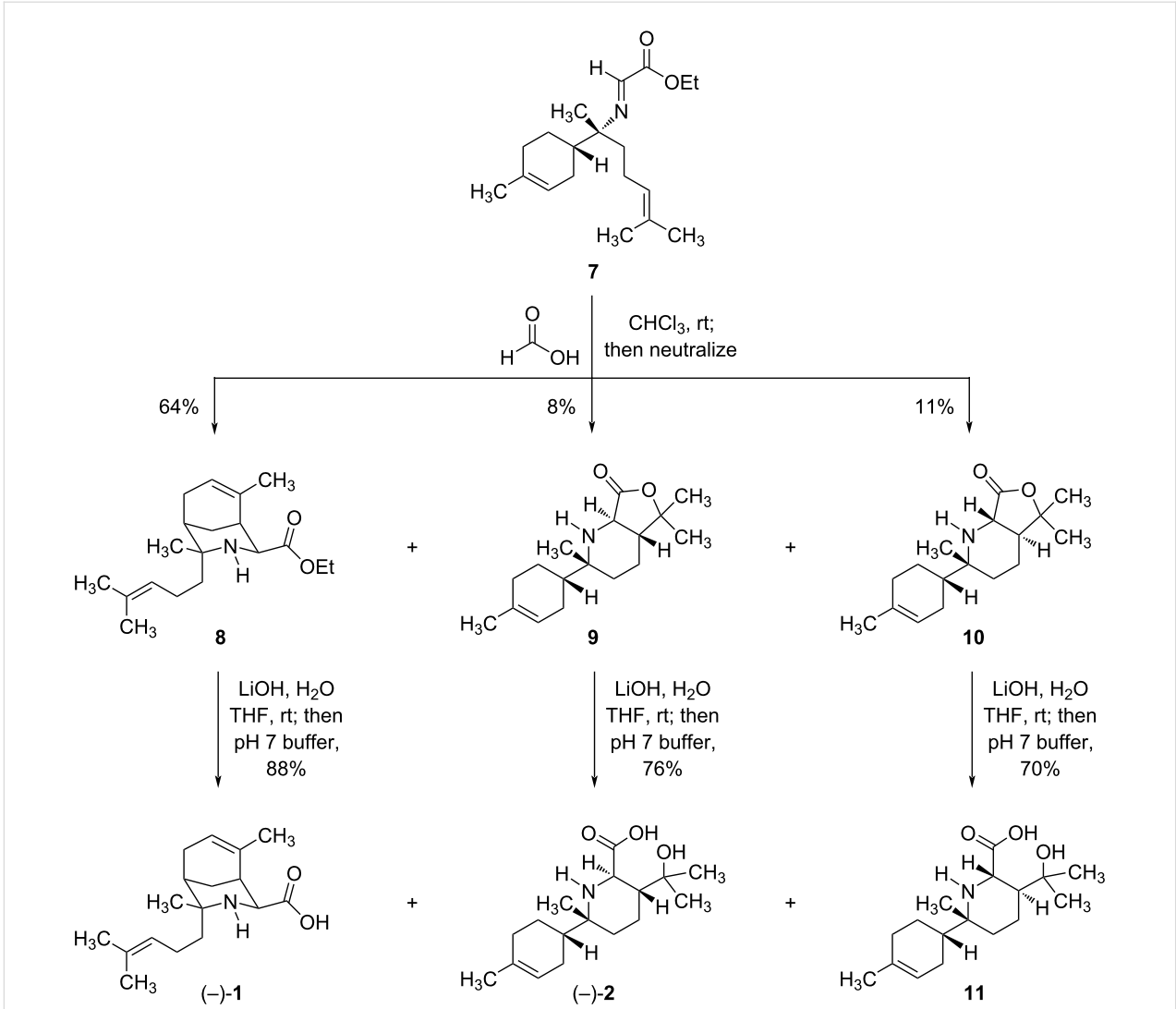

Scheme 2: Synthesis of the halichonic acids via a key intramolecular aza-Prins cyclization.

were both *trans*-fused 6/5 bicycles based on the magnitude of the vicinal coupling constant between the two methine hydrogens at the ring fusion (^3J = 12.9 Hz). The rigid nature of the *trans*-fused 6/5 ring system results in distinct conformers for **9** and **10**; fortunately, this allowed for the unambiguous assignment of the relative configurations of these diastereomers via NMR based on nuclear Overhauser effect (NOE) correlations (see the Supporting Information File 1 for additional details). This analysis showed that the minor product **9** corresponded to the lactone of (−)-halichonic acid B.

At this point, all that remained to complete the syntheses of the halichonic acids was hydrolysis of compounds **8** and **9** to form the corresponding amino acids. Thus, treating bicycle **8** with aqueous lithium hydroxide resulted in hydrolysis of the ethyl ester, and subsequent neutralization with pH 7 phosphate buffer afforded halichonic acid ((−)-**1**) in 88% yield after purification by column chromatography. Similarly, hydrolysis of lactone **9** under analogous conditions afforded halichonic acid B ((−)-**2**) in 76% yield. ^{1}H and ^{13}C NMR data for the synthetic compounds (−)-**1** and (−)-**2** were identical to those reported for the halichonic acids, confirming the proposed structures of these natural products. However, the observed optical rotations of these synthetic compounds were of opposite sign to those reported for the halichonic acids. Since we synthesized the enantiomers of these natural products, the absolute configurations of (+)-**1** and (+)-**2** assigned by Tsukamoto et al. have now been experimentally confirmed [4,5]. For the sake of comparison, the diastereomeric lactone **10** was also hydrolyzed under the same conditions to form the "unnatural" product **11** in 70% yield, which we have designated (−)-isohalichonic acid B. Although the NMR spectra of (−)-**2** and **11** are quite similar, we did note a

significant difference in the ^{13}C NMR chemical shift of the C7-methyl group, which appears at δ = 20.7 in (−)-**2** and δ = 14.5 in **11**.

Discussion

Rationalizing the outcome of the aza-Prins reaction leading to the formation of ethyl ester **8** and isomeric lactones **9** and **10** (Scheme 2) provides an interesting exercise in acyclic conformational analysis. Three divergent mechanistic pathways can be formulated by considering the different conformers of protonated imine **7**, namely iminium ions **12a–c** (Scheme 3). In each case, the chair-like transition state of the intramolecular aza-Prins reaction is controlled by the C7-stereogenic center, which bears a methyl group, the electrophilic site (the iminium ion), and two possible nucleophilic sites (a prenyl group and a trisubstituted alkene within a cyclohexene ring).

In conformer **12a**, the prenyl group occupies a pseudo-axial position, the methyl group occupies a pseudo-equatorial position, and the trisubstituted alkene within the six-membered ring serves as the nucleophile. It is important to note that in this chair-like conformer, the ethyl ester group at C2 assumes a pseudo-equatorial position. Although an alternative boat-like conformer is also possible (which would ultimately lead to the C2-epimer of **8**), the resulting transition state is presumably much higher in energy. In practice, the intramolecular aza-Prins reaction of **12a** forms a new carbon–carbon bond to generate a rigid 3-azabicyclo[3.3.1]nonane ring system (**13**). Although

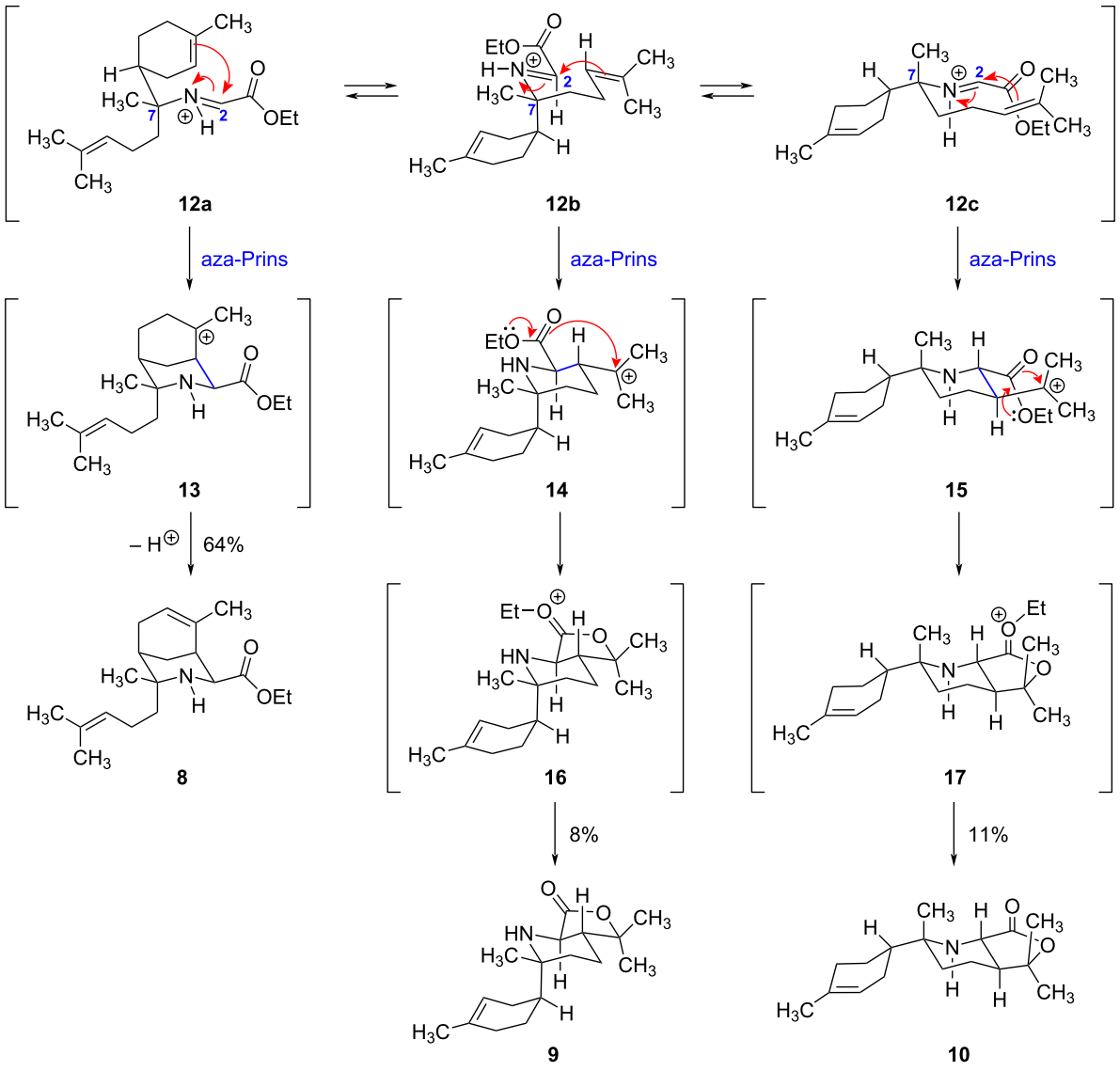

Scheme 3: Proposed intermediates for the intramolecular aza-Prins reaction leading to the formation of ethyl ester **8** and isomeric lactones **9** and **10**.

several different fates could be envisioned for this carbocation (e.g., a nucleophilic attack of formic acid to give a formate ester), only alkene formation was observed in this system. Interestingly, the deprotonation step is completely regioselective, giving the more highly substituted endocyclic trisubstituted alkene found in **8** as opposed to the isomeric exocyclic 1,1-disubstituted alkene [7,8]. Alternative mechanistic pathways involving (1) deprotonation to form a bridgehead alkene, or (2) intramolecular nucleophilic attack of the ethyl ester to form a lactone are not possible in this system due to the rigid geometric constraints of the 3-azabicyclo[3.3.1]nonane ring system. In any case, this aza-Prins reaction is by far the preferred mode of cyclization of iminium ion **12** based on the isolated yield of **8** (64%), ultimately leading to the carbon skeleton found in the natural product halichonic acid ((+)-**1**).

In conformer **12b**, the cyclohexenyl ring system occupies a pseudo-axial position, the methyl group occupies a pseudo-equatorial position, and the trisubstituted alkene of the prenyl group serves as the nucleophile. The chair-like transition state of the intramolecular aza-Prins reaction allows both the ethyl ester and the resulting tertiary carbocation to occupy equatorial positions (**14**), establishing the observed *trans*-relationship between these groups while simultaneously setting two new stereogenic centers. As before, one can envision several different fates for the tertiary carbocation present in **14**. Although elimination to form an alkene or intermolecular nucleophilic attack by formic acid (ultimately giving a formate ester) are reasonable mechanistically, only the intramolecular nucleophilic attack by the carbonyl group of the pendent ethyl ester was observed in this system to form the resonance-stabilized oxocarbenium ion **16**. Subsequent loss of the ethyl group (either as ethyl formate upon solvolysis with the formic acid co-solvent or as ethanol upon aqueous workup) gives lactone **9**, which features a strained *trans*-fused 6/5 ring system. Although this lactone survives aqueous workup at neutral pH, it is rapidly hydrolyzed under basic conditions (Scheme 2) to form the enantiomer of halichonic acid B ((−)-**2**). It is interesting to note that halichonic acid B exists exclusively as an open-chain 4-hydroxycarboxylic acid even though the corresponding γ-lactones typically form spontaneously. Indeed, no lactone formation was observed from (−)-**2** even upon purification by column chromatography on silica gel, reflecting the highly strained nature of *trans*-fused lactone **9**.

Finally, conformer **12c** is similar to **12b** in that the trisubstituted alkene of the prenyl group once again serves as the nucleophile; however, the methyl group now occupies a pseudo-axial position, and the cyclohexenyl ring system occupies a pseudo-equatorial position. In this case, the aza-Prins reaction forms *trans*-fused lactone **10** via an analogous intramolecular nucleophilic attack of the ethyl ester on the intermediate tertiary carbocation **15** to give oxocarbenium ion **17**. In comparing conformers **12b** and **12c**, it appears that the chair-like transition state **12c** should be lower in energy since the more sterically demanding cyclohexenyl ring is located in a pseudo-equatorial position. Although we did observe a slightly higher yield of **10** as compared to **9** (11% vs 8%), these values are sufficiently close to make any conclusions regarding the effects of conformational preferences on reactivity tenuous at best. However, it is interesting to note that the enantiomer of **11** has not been co-isolated as a natural product along with compounds (+)-**1** and (+)-**2**. If the biosyntheses of these natural products does occur through a common iminium ion intermediate, then our isolation of **11** suggests that the key aza-Prins cyclization is enzyme-mediated rather than spontaneous.

Conclusion

In summary, we have synthesized the enantiomers of halichonic acid and halichonic acid B in 10 steps starting from commercially available (−)-α-bisabolol (**3**). An important intermediate in our route was (−)-7-amino-7,8-dihydrobisabolene (**4**), which was prepared in enantiomerically pure form following recrystallization of a diastereomeric mixture of the corresponding benzamides. A common imine intermediate (**7**) underwent two different intramolecular aza-Prins reactions in the presence of formic acid to give the ethyl ester of (−)-**1** and the lactone of (−)-**2** in 64% yield and 8% yield, respectively. Subsequent hydrolysis of these intermediates under basic conditions afforded (−)-halichonic acid and (−)-halichonic acid B, confirming the proposed structures of the natural products. Efforts to investigate the biological activities of compounds (−)-**1** and (−)-**2** and their synthetic analogs are currently underway in our laboratory.

Supporting Information

The supporting information file contains detailed experimental procedures, full characterization data and copies of ^{1}H and ^{13}C NMR spectra for all new compounds, and complete NMR spectral assignments for compound (−)-**1**, (−)-**2**, **8**, **9**, **10**, and **11**. A tabular comparison between the NMR data reported for natural products (+)-**1** and (+)-**2** and that obtained for their synthetic enantiomers (−)-**1** and (−)-**2** is also provided.

Supporting Information File 1

Experimental procedures, characterization data and copies of ^{1}H and ^{13}C NMR spectra.
[https://www.beilstein-journals.org/bjoc/content/supplementary/1860-5397-18-174-S1.pdf]

Acknowledgements

We thank Dr. John Sivey (Towson University) for assisting with the collection of HRMS data.

Funding

Funding for this project was provided by the Fisher College of Science and Mathematics (Towson University) through an undergraduate research grant. This work was also supported by instrumentation provided through the National Science Foundation under grant Nos. 0923051 and 1531562.

ORCID® iDs

Keith P. Reber - https://orcid.org/0000-0003-0407-9281
Emma L. Niner - https://orcid.org/0000-0001-8126-8321

References

1. Mehbub, M. F.; Lei, J.; Franco, C.; Zhang, W. *Mar. Drugs* **2014,** *12,* 4539–4577. doi:10.3390/md12084539
2. Abdelaleem, E. R.; Samy, M. N.; Desoukey, S. Y.; Liu, M.; Quinn, R. J.; Abdelmohsen, U. R. *RSC Adv.* **2020,** *10,* 34959–34976. doi:10.1039/d0ra04408c
3. Shady, N. H.; El-Hossary, E. M.; Fouad, M. A.; Gulder, T. A. M.; Kamel, M. S.; Abdelmohsen, U. R. *Molecules* **2017,** *22,* 781. doi:10.3390/molecules22050781
4. Raiju, K.; Hitora, Y.; Kato, H.; Ise, Y.; Angkouw, E. D.; Mangindaan, R. E. P.; Tsukamoto, S. *Tetrahedron Lett.* **2019,** *60,* 1079–1081. doi:10.1016/j.tetlet.2019.03.030
5. Hitora, Y.; Ogura, K.; El-Desoky, A. H. H.; Ise, Y.; Angkouw, E. D.; Mangindaan, R. E. P.; Tsukamoto, S. *Chem. Pharm. Bull.* **2021,** *69,* 802–805. doi:10.1248/cpb.c21-00392
6. Bick, I. R. C.; Hai, M. H. *Aristotelia* Alkaloids. In *The Alkaloids;* Brossi, A., Ed.; Academic Press: New York, NY, USA, 1985; Vol. XXIV, pp 113–151.
7. Gujarati, P. D.; Reber, K. P. *Synthesis* **2022,** *54,* 1404–1412. doi:10.1055/s-0041-1737276
8. Argade, M. D.; Straub, C. J.; Rusali, L. E.; Santarsiero, B. D.; Riley, A. P. *Org. Lett.* **2021,** *23,* 7693–7697. doi:10.1021/acs.orglett.1c02057
9. Pronin, S. V.; Reiher, C. A.; Shenvi, R. A. *Nature* **2013,** *501,* 195–199. doi:10.1038/nature12472
10. Kitagawa, I.; Yoshioka, N.; Kamba, C.; Yoshikawa, M.; Hamamoto, Y. *Chem. Pharm. Bull.* **1987,** *35,* 928–931. doi:10.1248/cpb.35.928
11. Clerici, F.; Gelmi, M. L.; Gambini, A.; Nava, D. *Tetrahedron* **2001,** *57,* 6429–6438. doi:10.1016/s0040-4020(01)00534-8
12. Brummond, K. M.; Painter, T. O.; Probst, D. A.; Mitasev, B. *Org. Lett.* **2007,** *9,* 347–349. doi:10.1021/ol062842u
13. Szostak, M.; Spain, M.; Eberhart, A. J.; Procter, D. J. *J. Am. Chem. Soc.* **2014,** *136,* 2268–2271. doi:10.1021/ja412578t
14. Pelletier, G.; Bechara, W. S.; Charette, A. B. *J. Am. Chem. Soc.* **2010,** *132,* 12817–12819. doi:10.1021/ja105194s
15. Mai, T. T.; Viswambharan, B.; Gori, D.; Kouklovsky, C.; Alezra, V. *J. Org. Chem.* **2012,** *77,* 8797–8801. doi:10.1021/jo301588t
16. Mahrwald, R.; Quint, S. *Tetrahedron Lett.* **2001,** *42,* 1655–1656. doi:10.1016/s0040-4039(01)00012-0
17. Strouf, O.; Casensky, B.; Kubanek, V. *Sodium Dihydrido-Bis(2-methoxyethoxo)-Aluminate (SDMA): A Versatile Organometallic Hydride;* Journal of Organometallic Chemistry Library, Vol. 15; Elsevier: Amsterdam, Netherlands, 1985.
18. Nicolaou, K. C.; Mathison, C. J. N.; Montagnon, T. *Angew. Chem., Int. Ed.* **2003,** *42,* 4077–4082. doi:10.1002/anie.200352076
19. Sullivan, B. W.; Faulkner, D. J.; Okamoto, K. T.; Chen, M. H. M.; Clardy, J. *J. Org. Chem.* **1986,** *51,* 5134–5136. doi:10.1021/jo00376a014
20. Bensemhoun, J.; Bombarda, I.; Aknin, M.; Vacelet, J.; Gaydou, E. M. *Biochem. Syst. Ecol.* **2008,** *36,* 326–328. doi:10.1016/j.bse.2007.09.009
21. Jamison, M. T.; Macho, J.; Molinski, T. F. *Bioorg. Med. Chem. Lett.* **2016,** *26,* 5244–5246. doi:10.1016/j.bmcl.2016.09.053
22. Abdjul, D. B.; Kanno, S.-i.; Yamazaki, H.; Ukai, K.; Namikoshi, M. *Bioorg. Med. Chem. Lett.* **2016,** *26,* 315–317. doi:10.1016/j.bmcl.2015.12.022
23. Kochi, T.; Ellman, J. A. *J. Am. Chem. Soc.* **2004,** *126,* 15652–15653. doi:10.1021/ja044753n
24. Ota, K.; Hamamoto, Y.; Eda, W.; Tamura, K.; Sawada, A.; Hoshino, A.; Mitome, H.; Kamaike, K.; Miyaoka, H. *J. Nat. Prod.* **2016,** *79,* 996–1004. doi:10.1021/acs.jnatprod.5b01069
25. Ichikawa, Y. *Chem. Lett.* **1990,** *19,* 1347–1350. doi:10.1246/cl.1990.1347

BEILSTEIN JOURNAL OF ORGANIC CHEMISTRY

Total synthesis of grayanane natural products

Nicolas Fay‡, Rémi Blieck‡, Cyrille Kouklovsky and Aurélien de la Torre*

Review

Open Access

Address:
Institut de Chimie Moléculaire et des Matériaux d'Orsay (ICMMO), Université Paris-Saclay, CNRS, 15, rue Georges Clémenceau, 91405 Orsay Cedex, France

Email:
Aurélien de la Torre* - aurelien.de-la-torre@universite-paris-saclay.fr

* Corresponding author ‡ Equal contributors

Keywords:
enantioselectivity; grayananes; oxidation; 1,2-shift; total synthesis

Beilstein J. Org. Chem. **2022,** *18,* 1707–1719.
https://doi.org/10.3762/bjoc.18.181

Received: 08 September 2022
Accepted: 16 November 2022
Published: 12 December 2022

This article is part of the thematic issue "Total synthesis: an enabling science".

Associate Editor: B. Nay

Abstract

Grayananes are a broad family of diterpenoids found in *Ericaceae* plants, comprising more than 160 natural products. Most of them exhibit interesting biological activities, often representative of *Ericaceae* use in traditional medicine. Over the last 50 years, various strategies were described for the total synthesis of these diterpenoids. In this review, we survey the literature for synthetic approaches to access grayanane natural products. We will focus mainly on completed total syntheses, but will also mention unfinished synthetic efforts. This work aims at providing a critical perspective on grayanane synthesis, highlighting the advantages and downsides of each strategy, as well as the challenges remaining to be tackled.

Introduction

The *Ericaceae* are a large plant family, with over 4250 known species all around the world [1]. While *Ericaceae*'s toxicity has been known since at least 400 BC, barks, leaves and flowers from these plants are still commonly used in traditional medicine in Asia, Europe and America, mainly for their anti-inflammatory and analgesic properties, but also to treat different conditions (e.g. arthritis, hypertension, diabetes, lung, liver and gastrointestinal disorders), and for crop protection [2].

Among natural products formed by *Ericaceae*, grayananes are a wide diterpenoid family whose biological activities are often representative of *Ericaceae*'s use in traditional medicine [3-5]. In particular, many grayananes were found to have analgesic [6], antifeedant [7-9], antituberculosis [10], cytotoxic [11] and antioxidant [12] properties. The grayanane family comprises more than 160 natural products, and new members are isolated every year. For instance, 13 new grayanane natural products were reported since 2020 [13-16].

Grayanane diterpenoids all share the same tetracyclic skeleton, with 5, 7, 6 and 5-membered carbocycles commonly named A, B, C and D (Figure 1). The diversity in this family arises from different oxidation states at positions 2, 3, 5, 6, 7, 10, 14, 15, 16, and 17 which can bear free, acylated or glycosylated alcohol, olefin, ketone or epoxide functionalities.

From a biosynthetic point of view, grayananes arise from an oxidative rearrangement of the *ent*-kaurane skeleton (Scheme 1).

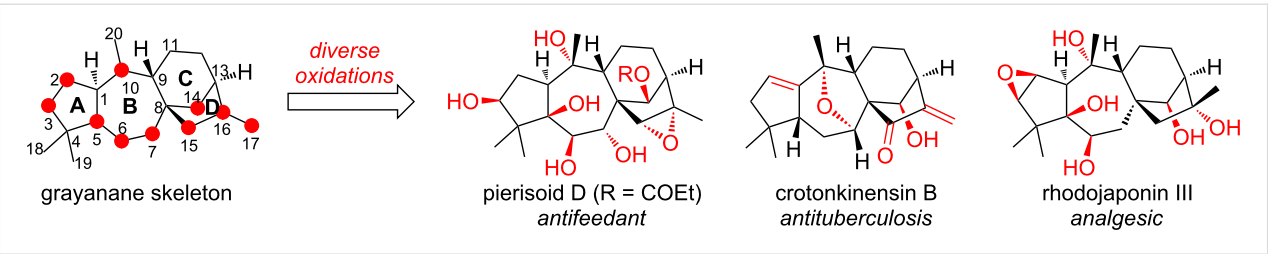

Figure 1: General structure of grayanane natural products.

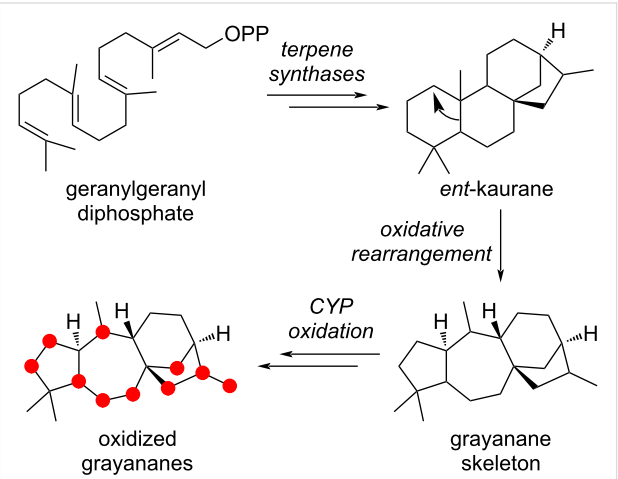

Scheme 1: Grayanane biosynthesis.

The diversity is generated by cytochromes P450 (CYP) enzymatic oxidation of the grayanane skeleton [17].

The biological activities and low extraction yields have prompted various research groups to undertake the total synthesis of grayanane natural products. In this work, we will survey the literature for synthetic routes to grayanane diterpenoids, including uncompleted approaches. The review is chronologically organized, starting from the earliest synthetic efforts from 1971 to the latest in 2022. In a last part we will present unfinished syntheses.

Review

Early syntheses by Matsumoto and Shirahama

The first synthetic approach towards a grayanane natural product was reported by Matsumoto in the 70s, using a relay approach. The authors first reported in 1972 the synthesis of grayanotoxin II from a degradation product **1** obtained in a few steps from grayanotoxin II itself (Scheme 2) [18]. Later on in 1976 [19], the same authors reported the synthesis of intermediate **1** from the known phenanthrene derivative **2** [20]. The tricyclic compound **2** was converted to **3** through a 6-step sequence involving reduction of the aromatic ring and oxidation of the enone to a dienone. The resulting dienone **3** underwent a key photoinduced santonin-like rearrangement in the presence of acetic acid, furnishing **4** in high yield. It should be noted that the group of Hiraoka had previously reported a similar rearrangement for the synthesis of a grayanane-type skeleton [21]. Further methylation and protecting group interconversions lead to an advanced tricyclic structure **5**, which could be further elaborated into relay intermediate **1**.

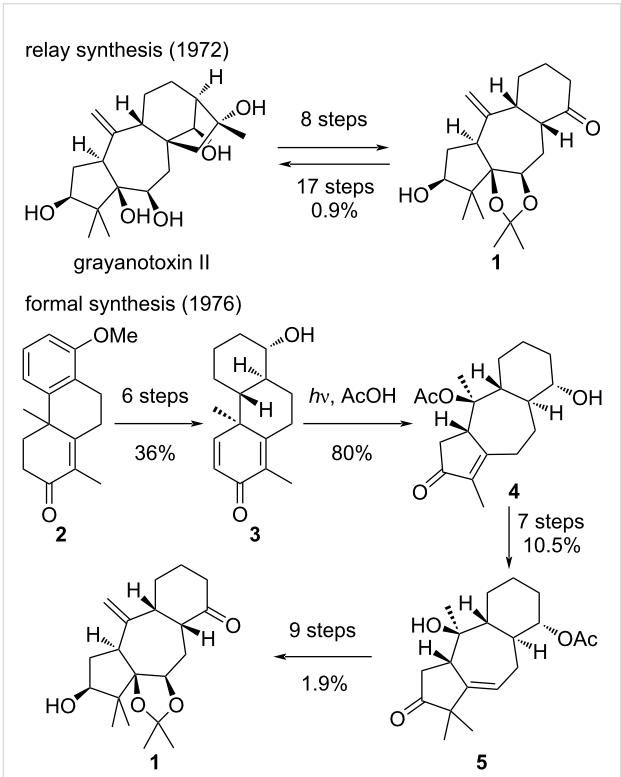

Scheme 2: Matsumoto's relay approach.

Although Matsumoto's approach does not fit with the requisites of modern organic synthesis, as it requires over 40 steps to synthesize grayanotoxin II and was performed in racemic form (in the case of the formal synthesis), it represents an impressive piece of synthetic work. Achieving the synthesis of such a com-

plex structure represented a challenging puzzle at that time, and was brilliantly solved by Matsumoto and co-workers.

Almost 20 years later, in 1994, Shirahama's group published the total synthesis of another member of the grayananes: grayanotoxin III [22]. One of the keys of their synthesis was the stereocontrolled 7-membered ring closure through a SmI_2-promoted pinacol coupling. This reaction had been previously described by the same group and proved to be highly effective [23]. For rings A, C and D, other SmI_2-promoted steps were employed, giving respectively the cyclopentane A ring moiety and the bicyclo[3.2.1]octane CD ring system with the correct configuration.

The synthesis started from commercially available (*S*)-2-((*p*-toluenesulfonyl)oxy)-1-propanol (**6**) which was converted to (*R*)-2-(benzyloxy)propionaldehyde (**7**) by a sequence involving formation of the a phenyl sulfide through an epoxide intermediate, protection of the secondary alcohol as a benzyl ether, oxidation of the sulfur and Pummerer rearrangement (Scheme 3). A

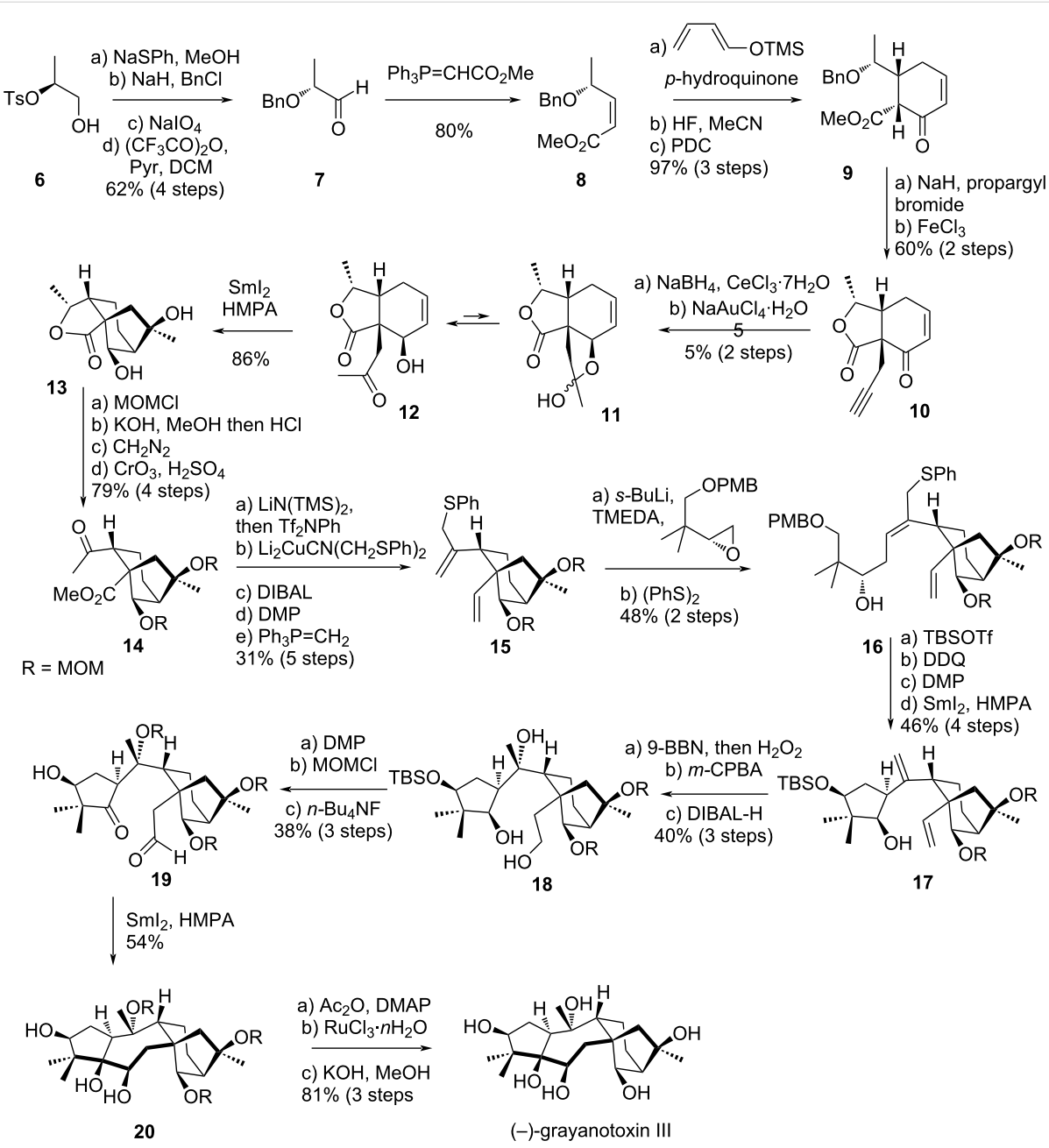

Scheme 3: Shirahama's total synthesis of (–)-grayanotoxin III.

Wittig reaction gave compounds **8**, as a 10:1 separable diastereomeric mixture. A diastereoselective Diels–Alder cycloaddition followed by oxidation of the resulting epimeric mixture gave substituted cyclohexanone **9**, corresponding to the future C ring [24]. After deprotonation, the C^3 position was stereoselectively alkylated using propargyl bromide, and the benzyl protecting group was cleaved with $FeCl_3$, leading to spontaneous lactone closure. A Luche reduction stereoselectively converted enone **10** to the corresponding allylic alcohol, followed by a Au-catalyzed alkyne hydration, providing hemiketal **11**. This intermediate was in equilibrium with hydroxy-ketone **12**, which was suitable for a SmI_2-promoted cyclization, affording intermediate **13** selectively, already bearing rings C and D. The selectivity was achieved by chelation of the Sm(III) intermediate with hydroxy groups present on the structure. As the direct coupling with the A-ring precursor failed, a strategy to build this part was developed, starting with a sequence involving a protection of the alcohols as MOM ethers, lactone hydrolysis, esterification, and Jones oxidation, affording intermediate **14** with a good 79% yield over 4 steps. Next, the methyl ketone was converted to an enol triflate, and then coupled with $Li_2CuCN(CH_2SPh)_2$. A reduction of the ester with DIBAL, followed by Dess–Martin oxidation and Wittig reaction lead to the formation of **15**. This intermediate was coupled with an (*R*)-epoxide in presence of *s*-BuLi, and intermediate **16** with *E* configuration was then obtained by a $(PhS)_2$-accelerated 1,3-sulfide shift. The A ring was then cyclized by a sequence consisting of protection of the alcohol, oxidative cleavage of the PMB protecting group, Dess–Martin oxidation, and SmI_2-induced cyclization. This last step was highly selective, giving solely the intermediate **17**. The synthesis was then pursued by the hydroboration–oxidation of the monosubstituted alkene, followed by stereoselective epoxidation of the 1,1-disubstituted olefin and reductive epoxide ring-opening giving triol **18**. After oxidation of the primary and the secondary alcohols with Dess–Martin periodinane, the remaining tertiary alcohol was protected as a MOM ether and the silyl ether protecting group was removed. The obtained intermediate **19** was then a suitable starting material for the SmI_2-promoted pinacol coupling, directed by the free hydroxy group, affording a complete selectivity in the formation of the 7-membered ring B. The synthesis of grayanotoxin III was then achieved by acetylation of the secondary alcohols, oxidative cleavage of the MOM protecting groups followed by hydrolysis of the acetyl protecting groups, affording the desired product with spectral data identical to reported natural samples.

Shirahama's synthesis was an illustrative example that rings A, B and the bicycle CD of grayananes could all be obtained by SmI_2-promoted steps, obtaining excellent selectivity in all cases. Alternatively, the same year, the authors published a vinyl radical cyclization occurring in presence of n-Bu_3SnH, providing a stereoselective access to the bicyclo[3.2.1]octane unit corresponding to the CD rings [25].

Newhouse's synthesis of principinol D

In 2019, Newhouse's group published a total synthesis of principinol D [26], a compound isolated from *Rhododendron principis* in 2014 [27,28]. Compared to grayanotoxin III, principinol D displays an inverse configuration at C^1 as well as an *exo*-olefin at C^{10}–C^{20}. The strategy developed by the group relied on the obtainment of two distinct fragments, a racemic bicyclo[3.2.1]octane unit **25** corresponding to rings C and D, and an enantioenriched cyclopentyl aldehyde derivative **29**, corresponding to ring A. These fragments were successfully coupled under basic conditions, and the ring B was later reductively closed using SmI_2.

The synthesis of fragment **25** began with commercially available cyclohexenone (**21**), which underwent a copper-catalyzed vicinal difunctionalization with vinylmagnesium bromide and DMPU and trapping using methyl cyanoformate, leading to the formation of ketoester **22** (Scheme 4). This intermediate was then allylated, the ester group selectively reduced with $Zn(TMP)_2$ and $LiBH_3NMe_2$ and the resulting primary alcohol was protected as a TBS ether, providing intermediate **23** as a single diastereomer. This key intermediate **23** was then submitted to a Ni-catalyzed α-vinylation and direct TBS deprotection giving the bicyclo[3.2.1]octane subunit with a good yield of 74%. A sequence involving diastereoselective reduction of ketone **24** with SmI_2, Appel reaction to convert the primary alcohol to the corresponding primary alkyl iodide followed by a MOM protection of the secondary alcohol afforded fragment **25** with 73% yield over 3 steps. On the other hand, the enantioenriched cyclopentyl aldehyde fragment **29** was obtained starting from commercially available 2,2-dimethylcyclopentane-1,3-dione (**26**). The dione was submitted to a sequence involving a monoreduction, protection of the alcohol as a TBS ether, α,β-desaturation, dithiane addition, MOM protection and dithiane deprotection.

The fragment **25** was lithiated with *t*-BuLi and the fragment **29** was then added, forming the coupling product as a 5:5:1:1 separable mixture of diastereomers (Scheme 5). The desired diastereomer **30** was isolated with a yield of 26%. The secondary alcohol was protected as a MOM ether and the allylic silyl ether was converted to an enone. A selective oxidative cleavage, only affecting the monosubstituted alkene, led to the formation of **31**, which underwent a key SmI_2-promoted seven-membered ring closure, giving a single diastereomer. The stereochemistry and absolute configuration of the obtained tetracyclic structure **32** was confirmed by NOESY NMR and X-ray crystallography.

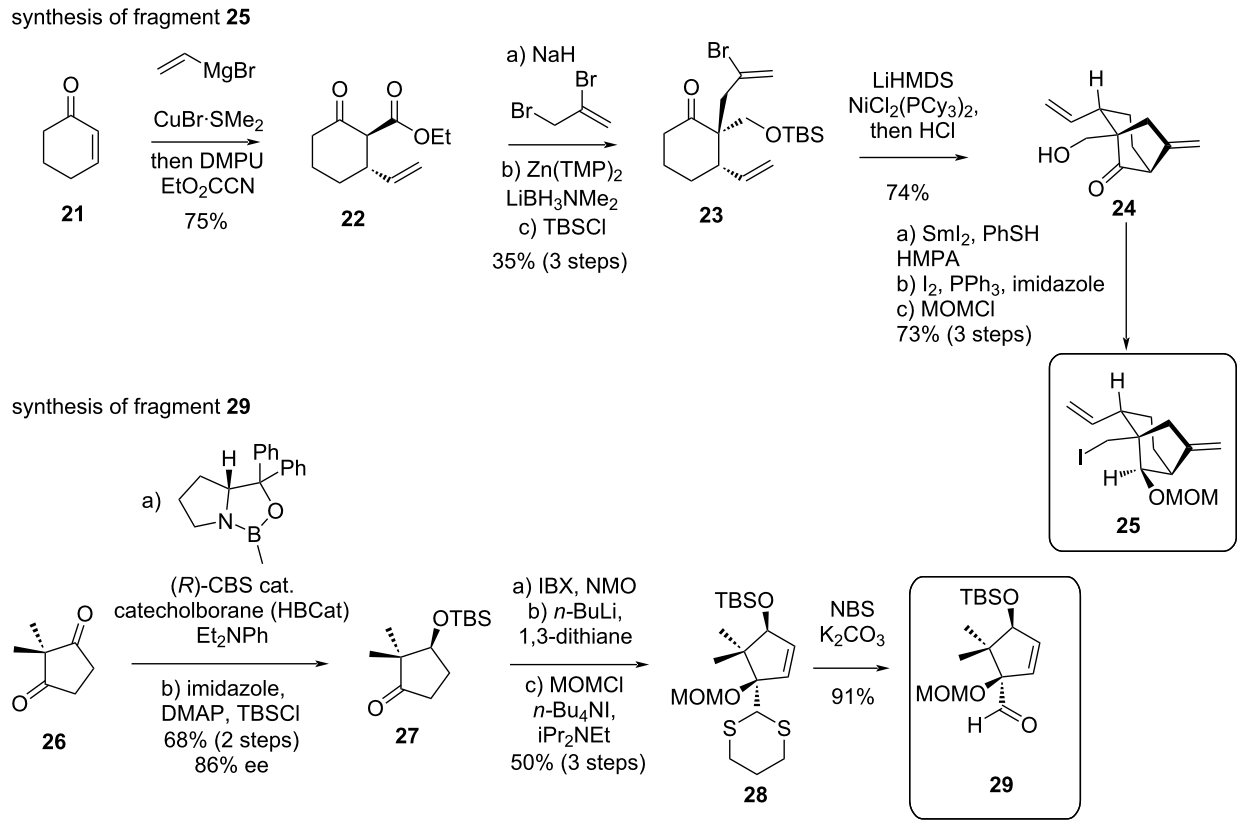

Scheme 4: Newhouse's syntheses of fragments **25** and **29**.

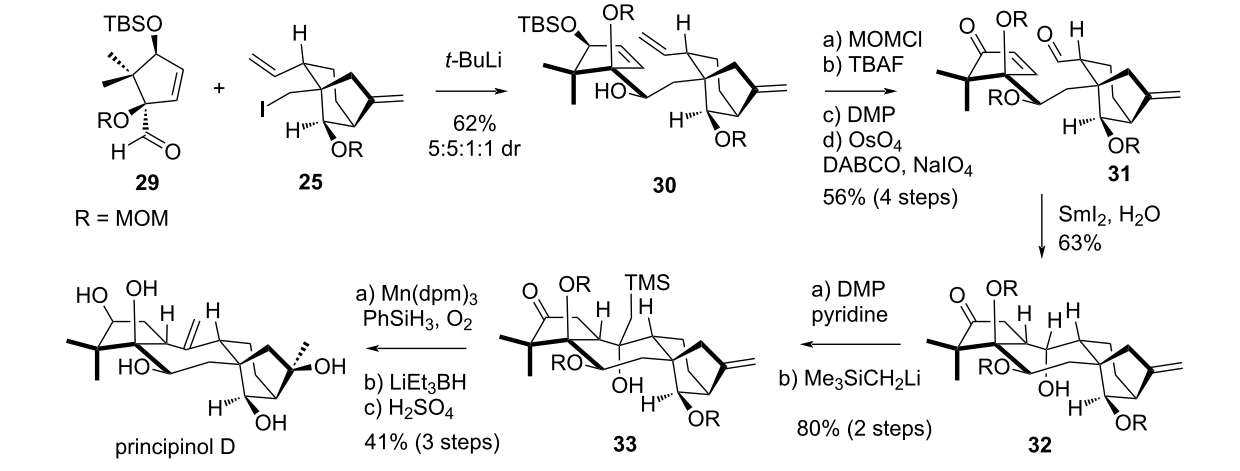

Scheme 5: Newhouse's total synthesis of principinol D.

Some additional modifications were required on the structure to synthesize principinol D: oxidation of the secondary alcohol to the corresponding ketone was achieved using Dess–Martin periodinane with a pyridine buffer. Addition of Me_3SiCH_2Li efficiently afforded the Peterson adduct **33**. The 1,1-disubtituted alkene was then submitted to Mukaiyma hydration to form the tertiary alcohol, in presence of $Mn(dpm)_3$, $PhSiH_3$ and O_2. Then, the ketone was selectively reduced in the presence of $LiEt_3BH$, while the Peterson adduct was eliminated concurrently, upon heating. Finally, treatment with H_2SO_4 allowed

total deprotection of the MOM ethers, leading to the formation of principinol D, in complete correspondence with reported spectral data.

Newhouse's synthesis represents an efficient access to grayananes, relying on two accessible fragments. Remarkably, although the strategy is different from that of Shirahama as it involves different retrosynthetic disconnections, it makes use of similar tactics through the use of a SmI_2-promoted cyclization. This first total synthesis of principinol D, in 19 steps as the longest linear sequence, is asymmetric even though a separation of the mixture of diastereomers resulting from fragment coupling is necessary. The SmI_2-mediated reductive ring-closure of the 7-membered ring is among the most remarkable steps of the synthesis, along with the Ni-catalyzed formation of the bicyclo[3.2.1]octane unit. It should be noted that due to the SmI_2-mediated ring-closure's stereochemical outcome, this synthesis can only be applied to compounds with an *R*-configured C^1 stereocenter, which are epimers of the vast majority of grayanane structures.

Ding's synthesis of rhodomolleins XX and XXII

Shortly after Newhouse's synthesis, Ding's group reported a synthetic strategy to access rhodomollein XX and XXII [29,30]. These natural products have the particularity of displaying an enone moiety on ring A. Ding's approach involves the construction of a tetracyclic structure where rings A and B had the correct arrangement, while rings C and D form a bicyclo[2.2.2]octane structure [31]. The correct bicyclo[3.2.1]octane structure was obtained after a key reductive epoxide opening/Dowd–Beckwith rearrangement cascade.

The synthesis started from 3-hydroxy-2-methoxybenzaldehyde (**34**), which was converted into Grignard reagent **35** and added onto 3-methylbut-2-enal (Scheme 6). A sequence involving Claisen rearrangement, Roskamp homologation, diazo transfer and intramolecular cyclopropanation led to intermediate **37**. The hydroxy group on C^6 was introduced after cyclopropane ring-opening, ketone protection, epoxidation and reductive ring-opening of the resulting epoxide. A one-pot β-keto phos-

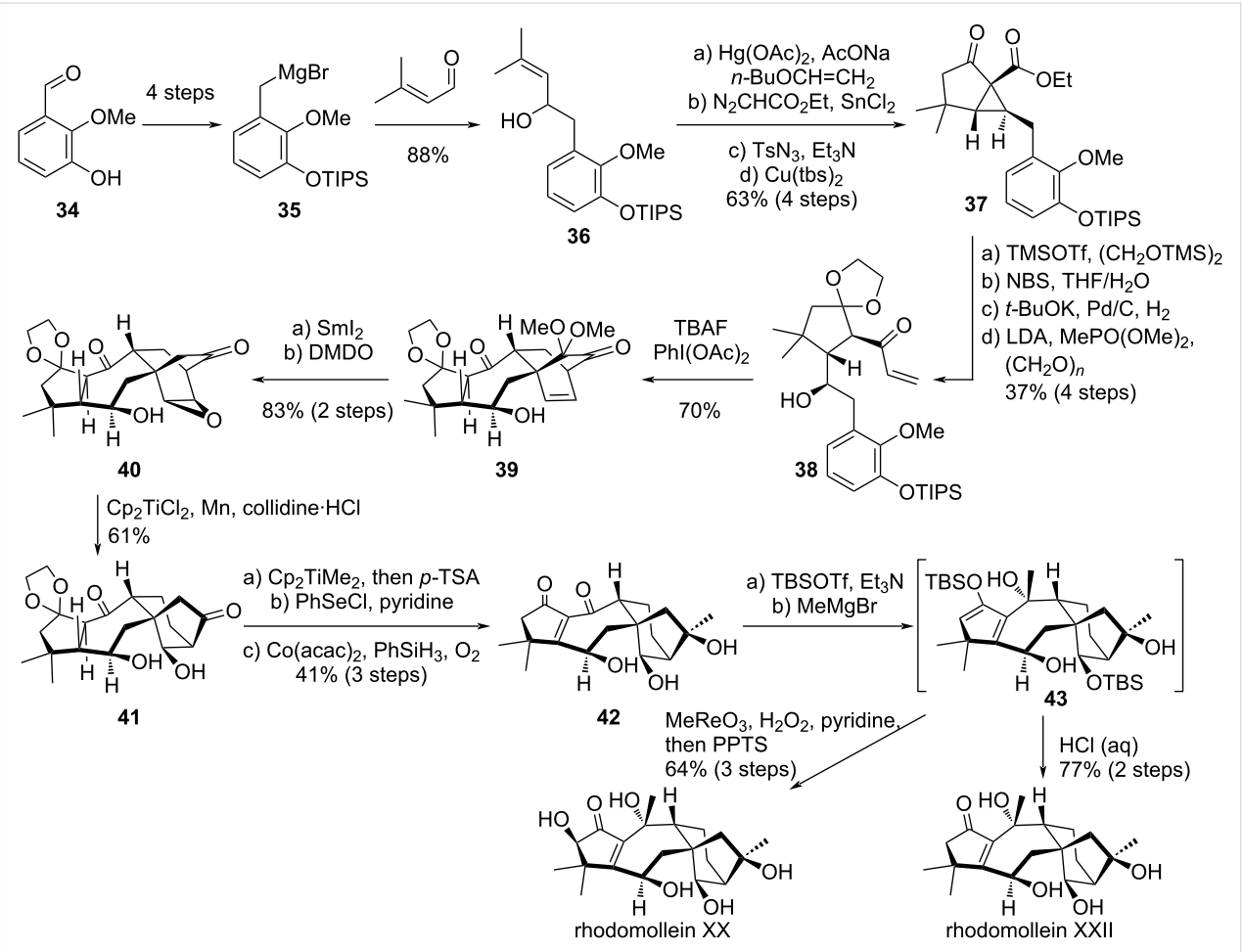

Scheme 6: Ding's total synthesis of rhodomolleins XX and XXII.

phonate formation/Horner–Wadsworth–Emmons reaction with formaldehyde afforded **38**, a precursor for the key oxidative dearomatization-induced Diels–Alder cycloaddition. Treatment of **38** with TBAF followed by $PhI(OAc)_2$ led to the formation of **39**, having the A and B ring correctly arranged. The product was obtained in 70% yield, along with 25% of an undesired diastereoisomer. The dimethoxy functionality was reduced in the presence of Kagan's reagent and DMDO could induce an epoxidation on the strained olefin. From intermediate **40**, the key reductive epoxide opening/Dowd–Beckwith rearrangement cascade could be performed in the presence of an in situ-generated Ti(III) catalyst. The main side-product of this reaction was due to a simple reductive opening of the epoxide (15%). From **41** having the correct tetracyclic skeleton, a transient protection followed by Petasis olefination, deprotection, selenide-mediated α,β-dehydrogenation and Mukaiyama oxidation afforded an advanced intermediate **42** bearing most of the target's functionalities. A sequence of enol-ether formation/Grignard addition lead to intermediate **43**, from which simple acidic treatment led to rhodomollein XXII, while α-oxidation in the presence of rhenium oxide followed by acidic work-up afforded rhodomollein XX.

Interestingly, Ding's synthesis constitutes an efficient approach (22 and 23 steps) to access grayananes with a cyclopentenone moiety on the A ring. It should be noted that although this is a racemic synthesis, intermediate **37** was also synthesized in enantioenriched form using a chiral copper catalyst for the cyclopropanation and a chiral auxiliary on the ester moiety. Moreover, the same group reported a related approach for the synthesis of various diterpenoids including rhodomollanol, an *abeo*-grayanane natural product [32,33].

Luo's synthesis of grayanotoxin III, principinol E and rhodomollein XX

In 2022, Luo et al. described an efficient and enantioselective synthetic route based on a convergent strategy to accomplish the synthesis of principinol E, grayanotoxin III and rhodomollein XX [34]. The key steps include i) a tandem reaction combining organocatalytic Mukaiyama aldol and intramolecular Hosomi–Sakurai reactions in a one-pot manner; ii) a 7-membered cyclization based on a bridgehead tertiary carbocation intermediate forging the B ring; iii) redox manipulations and a 1,2-migration as final steps. The synthesis started from (*S*)-ketone **44** which was prepared via asymmetric CBS reduction of diketone **26** (Scheme 7). Firstly, this (*S*)-ketone **44** was transformed into dimethylacetal **45** by Vilsmeier reaction followed by aldehyde protection in 54% yield over two steps. A Mukaiyama aldol reaction between trimethylsilyl enol ether **46** and dimethylacetal **45** followed by Sakurai cyclization provided an inseparable mixture of C^9 epimers (dr = 2:1). A catalyst optimization showed that chiral squaramide **47** developed by Jacobsen's group significantly accelerated the Mukaiyama reaction compared to TMSOTf or $TiCl_4$ thanks to chiral hydrogen bond-donor effect [35]. After Sakurai cyclization promoted by $EtAlCl_2$, the desired product **48** was obtained with the required diastereoselectivity in 58% on a 3 g scale.

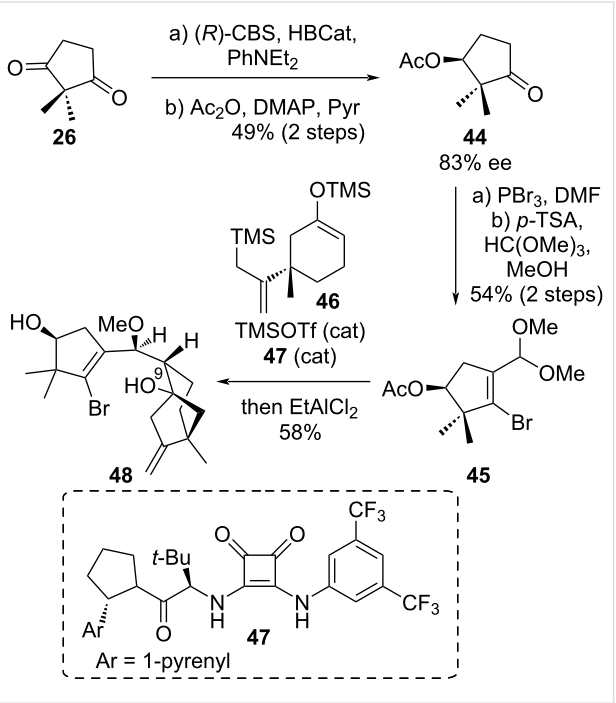

Scheme 7: First key step of Luo's strategy.

Subsequently, vinyl halide **48** was converted to diene **50** by Suzuki coupling with potassium vinyltrifluoroborate (**49**) in 90% yield (Scheme 8). The C^7–C^8 bond formation from a bridgehead carbocation was a real challenge to close the 7-membered ring. To achieve this, the secondary alcohol was oxidized by DMP, the tertiary alcohol was triflated, 4-phenylpyridine was added and the mixture was heated at 80 °C for 14 h. The intermediate carbocation was trapped by the terminal olefin, generating a dienone **51** after deprotonation at the relatively acidic position C^2. A singlet oxygen ene reaction involving the electron-rich olefin allowed the formation of an aldehyde, which was directly cleaved by an iridium-catalyzed deformylation, affording **52** in one-pot [36]. Deprotonation with KHMDS allowed the formation of an electron-rich diene which could again react with singlet oxygen by diastereoselective cycloaddition followed by C^{15}–C^{16} epoxidation with *m*-CPBA. Reductive cleavage of the O–O bond by Zn/AcOH treatment afforded epoxide **53** as a single diastereomer in two steps and 65% yield. The correct bicyclo[3.2.1]octane was obtained by Wagner–Meerwein epoxide rearrangement promoted by $EtAlCl_2$. Two separable alkene regioisomers **54** and **55** were

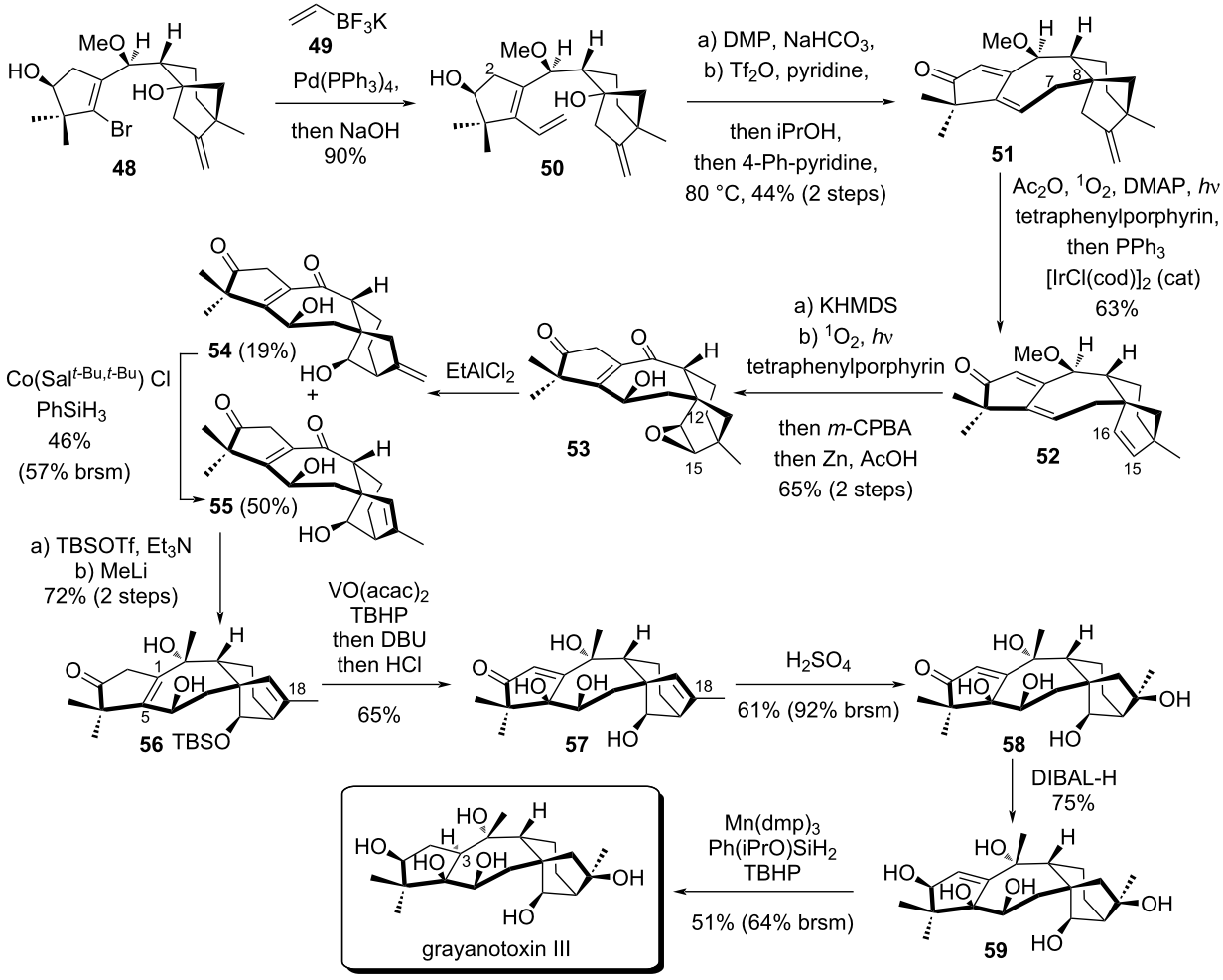

Scheme 8: Luo's total synthesis of grayanotoxin III.

obtained in 19% and 50% yield, respectively. A metal-catalyzed hydrogen atom transfer (MHAT) allowed **54** to be partially converted to **55** via Shenvi's isomerization [37]. Selective TBS protection on the bicyclo[3.2.1]octane moiety and ketone methylation gave access to **56**. Directed C^1–C^5 vanadium-mediated epoxidation followed by DBU treatment and TBS deprotection afforded **57** in one pot. The tertiary alcohol **58** was obtained as a single diastereomer after hydration of position C^{18}. Subsequent reduction with DIBAL-H gave the desired alcohol on the A ring in 75% yield. The C^3 epimer was also obtained in 4% yield and confirmed by X-ray diffraction. Hydrogenation of the sterically hindered C^1–C^2 alkene was accomplished using a combination of $Mn(dpm)_3$ and $Ph(iPrO)SiH_2$, providing grayanotoxin III in 51% yield.

The authors also achieved the synthesis of principinol E and rhodomoline XX by slight modifications of the late-stage functional group transformations. The synthesis of principinol E was performed in 6 steps starting from **60**, which was obtained by protection of **55** (Scheme 9). As before, directed epoxidation of C^1–C^5 in compound **60** was employed to form an α,β-epoxyketone intermediate which underwent SmI_2 reduction at −78 °C, giving access to the desired *syn* diastereomer with good selectivity (dr = 8.5:1). The free alcohol was then protected with an ethoxymethyl ether (EOM). Finally, Peterson olefination, stereoselective carbonyl reduction and TBS deprotection afforded principinol E in 53% yield over 4 steps. For the synthesis of rhodomollein XX, addition of methyllithium to **54** followed by Mukaiyama hydration using $Mn(dpm)_3$ afforded **62**. To access rhodomollein XX, an additional oxidation state at the C^2 position was required. Luo's team used Davis' oxaziridine followed by treatment with K_2CO_3 to equilibrate the hydroxyketone, delivering an inseparable epimeric mixture (1:3) of **63** in 31% overall yield. An additional TBS protection allowed

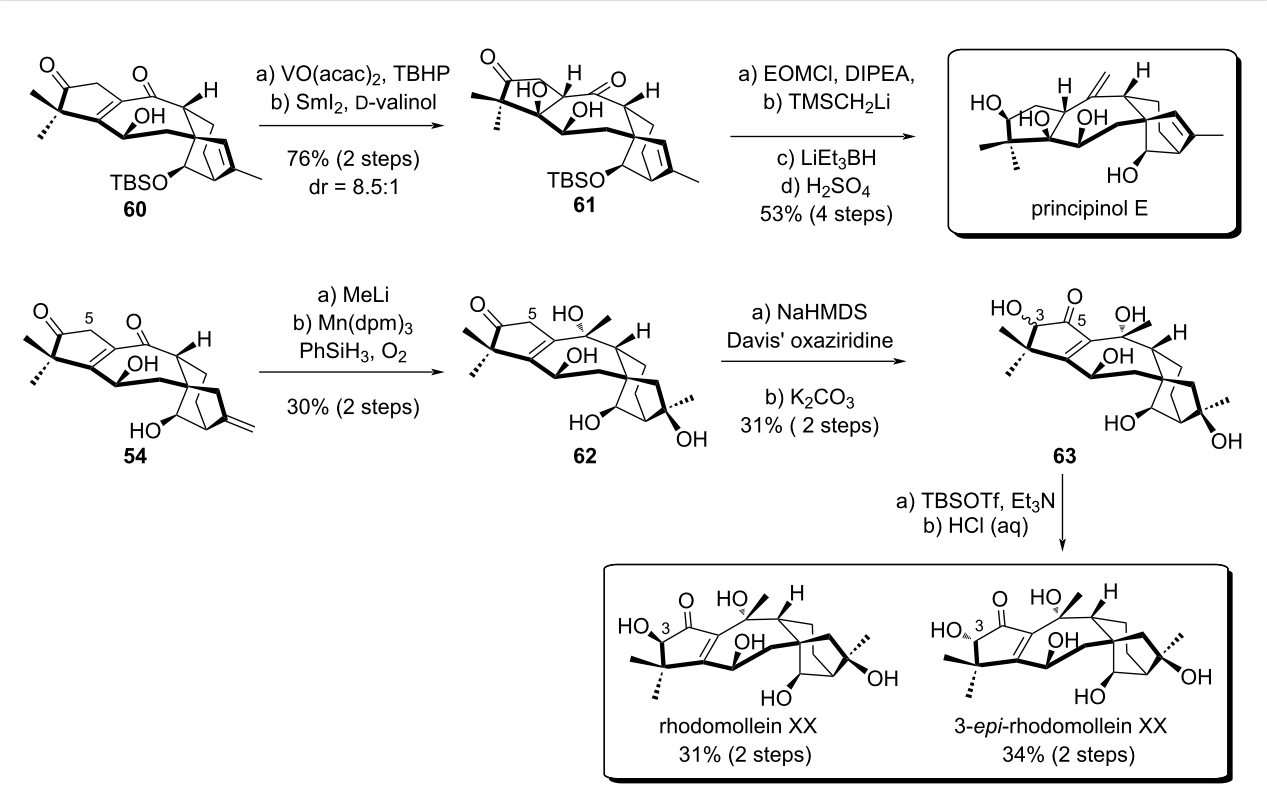

Scheme 9: Synthesis of principinol E and rhodomollein XX.

separation of the epimers. After acidic treatment, pure rhodomollein XX and 3-*epi*-rhodomollein were obtained in 31% and 34% yield in two steps, respectively.

Luo's synthetic work offers a powerful approach to synthesize grayanane natural products. The synthesis is both efficient (18 to 20 steps) and flexible, as demonstrated by the synthesis of 3 natural products, using pivotal intermediates **54** and **60**.

Other synthetic efforts

In 2011, Williams and co-workers reported an efficient synthetic route detailing the central core construction of pierisformaside C, which is the first grayanane isolated displaying three central double bonds (Scheme 10) [38]. The team's objective was to develop a synthetic pathway also giving access to several diterpene glycosides close to pierisformaside C in order to study the biological activity of this family. Their strategy was based on a common forward intermediate and a late construction of the central seven-membered ring.

In the beginning of the synthesis, the authors followed the strategy developed previously by Marinovi's group to form the bicyclo[3.2.1]octane moiety [39]. The synthesis started from **64** with a one-pot Birch reduction/alkylation with vinyl bromide **65**, affording **66** in 68% yield over two steps. Next the construction of the bicylo[3.2.1]octane **67** was achieved by a radical cyclization using *n*-Bu_3SnH in refluxing toluene. A sequence involving an ester reduction, Ley–Griffith oxidation and Seyferth–Gilbert homologation with Bestmann–Ohira reagent allowed to obtain the alkynyl bicylo[3.2.1]octane **69**. On the other hand, the five-membered triflate **71** was synthesized from diketone **26** in 5 steps and 37% overall yield. Both fragments were assembled by a Sonogashira cross-coupling, affording **72** in 72% yield. In a first attempt, TBS protection was considered on the bicylo[3.2.1]octane. However, later in the strategy, the deprotection presented some difficulties, and the authors decided to investigate the use of a free ketone. The partial hydrogenation of alkyne **72** proved to be inefficient, due to a lack of chemoselectivity involving competitive olefin reduction on the bicylo[3.2.1]octane. To overcome the over-oxidation, **72** was treated with *m*-CPBA, providing epoxide **73** as the main product in 71% yield (dr = 6:1). Lindlar hydrogenation of the alkyne and cyclization proceeded smoothly, and the tetracyclic skeleton **74** was obtained in moderate yield. However, the synthesis of pierisformaside C was never completed. The missing transformations include the removal of the ketone on the C ring, epoxide reductive opening, formation of the B ring *exo*-olefin, and glycosylation.

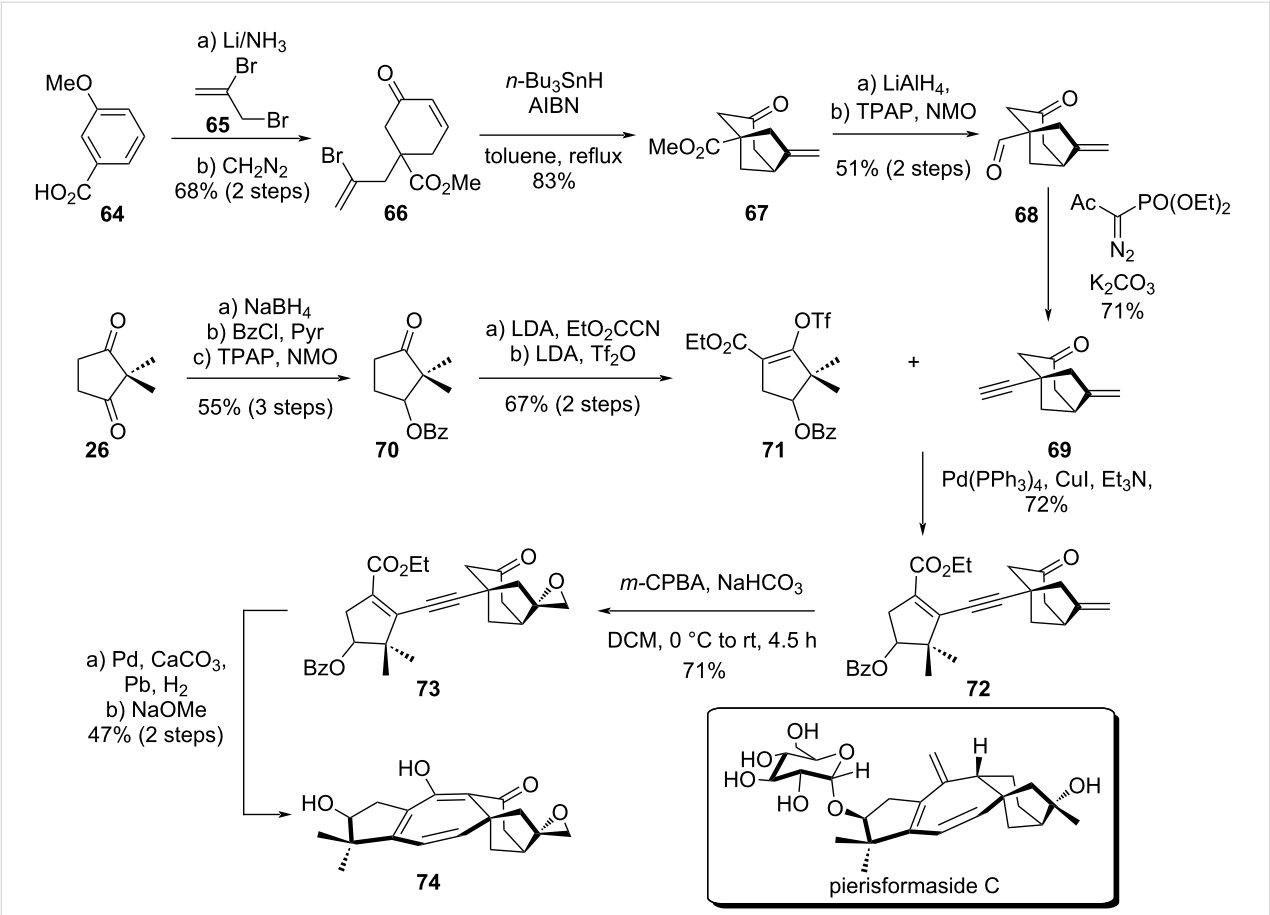

Scheme 10: William's synthetic effort towards pierisformaside C.

In 2021, Hong et al. presented a synthetic effort focused on the synthesis of rhodojaponin III B–C rings [40]. The authors employed a Mn(III)-mediated intramolecular radical cyclization of an alkynyl ketone as the key step.

The synthesis started by a Cu-catalyzed conjugate addition of the vinyl Grignard reagent, followed by TMS α-propargylation under basic conditions, affording the TMS-alkynyl ketone **76** as the major diastereomer (Scheme 11). Originally a Au-catalyzed Conia-ene-type cyclization, classically considered as a reliable method for the construction of bridged bicyclic structures [41], was envisaged. However, using a gold(I) catalyst the desired 5-*exo-dig* cyclization failed and only a 6-*endo-dig* cyclization was observed. Thus, Hong et al. explored a Mn(III)-mediated radical cyclization, an approach which had been previously reported by Jia and co-workers during the synthesis of glaucocalyxin A [42]. After treatment with $Mn(OAc)_3$, the desired 5-*exo-dig* cyclization product **77** was obtained in 43% yield as an *E*/*Z* mixture. The TMS group was removed under acidic conditions. Then, a wide range of reducing agents was explored for the stereoselective ketone reduction. However, only the undesired diastereomer was obtained. Knowing that the correct diastereomer could be obtained in the presence of a primary alcohol instead of the ester moiety, as described by Newhouse previously [26], the authors performed a complete reduction of the carbonyl moieties using $LiAlH_4$ and TBS protection of the primary alcohol, affording intermediate **78** with the wrong configuration at the secondary alcohol stereocenter. After reoxidation and deprotection of the primary alcohol, SmI_2 reduction finally afforded the desired diastereomer **79**. This synthetic work highlights again the challenge of the bicyclo[3.2.1]octane construction, especially regarding the diastereocontrol at the secondary alcohol moiety. To date, this approach towards rhodojaponin III was never concluded.

Conclusion

Over the past 50 years, the synthesis of grayanane natural products has attracted the interest of many synthetic chemists, leading to the development of five total synthesis approaches, as well as two unfinished syntheses [43]. Table 1 summarizes the completed total syntheses in terms of steps, yields, advantages and drawbacks. The clear superiority of recent syntheses beauti-

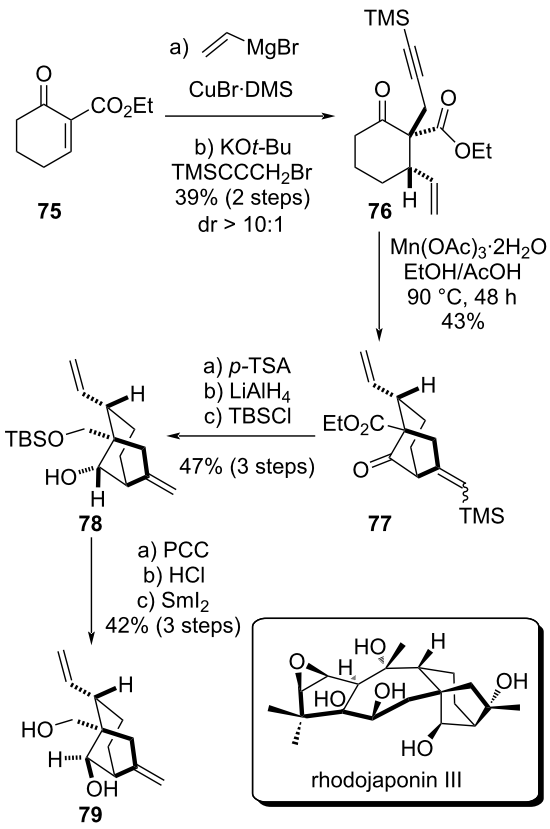

Scheme 11: Hong's synthetic effort towards rhodojaponin III.

fully showcases the progresses in the field of organic synthesis over the last decades. Among the last three syntheses, Newhouse's work has the huge advantage of being convergent, allowing a short synthesis (19 steps longest linear sequence). On the other hand, this strategy is limited to the synthesis of C^1 epimers of the grayanane general structure. Although linear and thus requiring a few more steps, Ding's syntheses still provide higher yields than Luo's and Newhouse's. Still, this strategy is also limited in terms of accessible structures, as only C^1–C^5 dehydrogenated natural products are obtained. It should be noted that despite this, a similar approach was applied by Ding's group to the synthesis of various diterpenoids. Finally, Luo's synthesis has the advantage of being more flexible, as it allows the synthesis of the general structure of grayananes. Nevertheless, this approach is somehow lower yielding than the previous ones. Regarding enantioselectivity, both Newhouse's and Luo's syntheses rely on an enantioenriched precursor obtained in 86% ee. On the other hand, while Ding's syntheses were performed in racemic form, the authors showed that a key intermediate could be obtained enantioselectively (93% ee) by a combination of a chiral catalyst and chiral auxiliary, although requiring extra steps for auxiliary installation and cleavage.

Scheme 12 summarizes the last 3 synthetic strategies for grayanane synthesis. Each group proposes different disconnections. Newhouse identified a C^1–C^{10} disconnection for a radical cyclization and a C^6–C^7 for an organolithium addition, allowing a convergent approach with A ring and C–D rings as key fragments. In this case, the bicyclo[3.2.1]octane is obtained by a Ni-catalyzed enolate/alkenyl bromide coupling. While both Ding and Luo propose a 1,2-shift relying on epoxide ring-opening as key step, each group proposes a different disconnection. For Ding, the rearrangement forms bond C^{13}–C^{16} through a Ti(III)-mediated reductive epoxide opening/Dowd–Beckwith rearrangement cascade. This allows to have a bicyclo[2.2.2]octane precursor, which can be obtained by a dearomatization/Diels–Alder cascade. For Luo, the 1,2-shift forms bond C^{12}–C^{13} through a cationic Wagner–Meerwein-type rearrangement. The B ring is obtained by a key bridgehead carbocation trapping, while the skeleton arises from an A ring fragment and a C ring fragment, assembled by a diastereoselective aldol/Sakurai cascade.

In recent years, important advances have been made regarding the synthesis of grayanane natural products, paving the way for deeper biological activity evaluation. Nevertheless, important challenges still need to be tackled. A highly enantioselective synthesis is still desirable, as the only synthesis offering >90% ee relies on the combination of chiral ligands and chiral auxiliary. Moreover, to date only 6 natural products from the

Table 1: Summary of previous syntheses.

Synthesis	Number of steps	Overall yield	Advantages	Drawbacks
Matsumoto (1972–1976) [18,19]	>40	<0.0005%	–	many steps, racemic
Shirahama (1994) [22]	38	0.05%	enantioselective	many steps
Newhouse (2019) [26]	19	0.4%	convergent, few steps	limited to C^1 epimers of the general structure
Ding (2019) [31]	22–23	1.2–1.4%	few steps, highest yielding	limited to C^1–C^5 dehydrogenated grayananes
Luo (2022) [34]	18–20	0.01–0.5%	few steps, flexible	lower yields

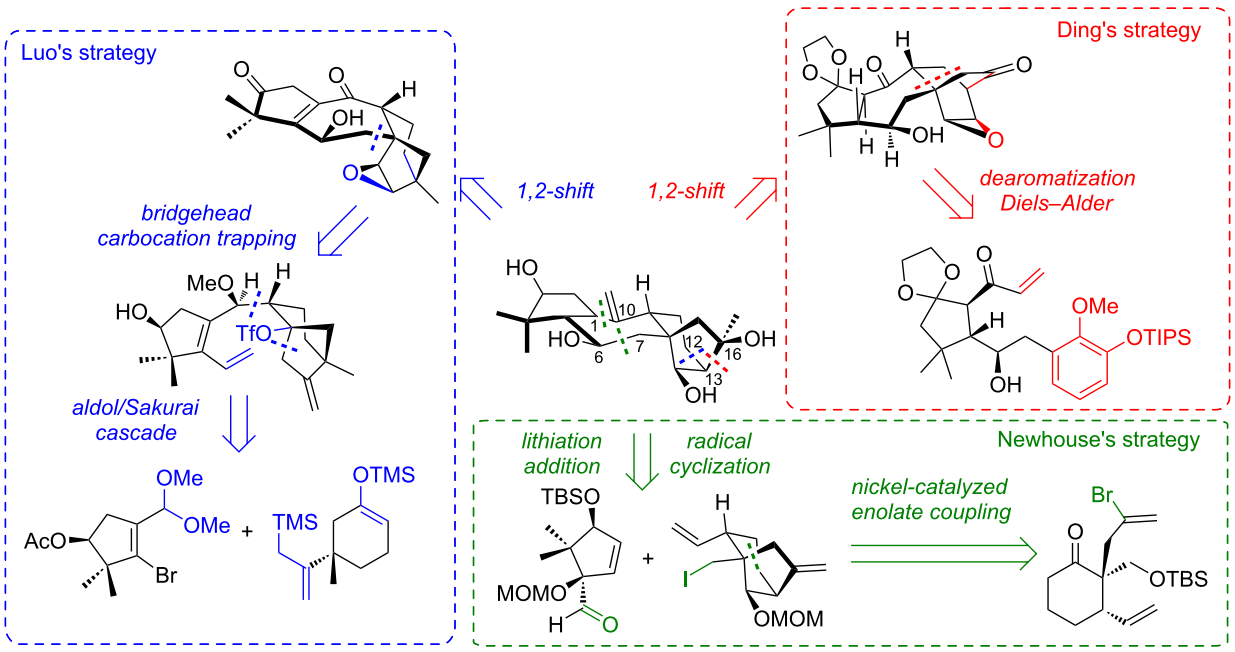

Scheme 12: Recent strategies for grayanane synthesis.

grayanane family were synthesized, out of the more than 160 compounds known to date. Thus, we anticipate that in the future, organic chemists will keep focusing on highly enantioselective, efficient and flexible synthetic strategies towards grayanane natural products.

Acknowledgements

The rhododendron photo in the graphical abstract is from Brian Taylor on Unsplash. The honeycomb photo in the graphical abstract is from Nathaniel Sison on Unsplash.

Funding

We would like to thank the Agence Nationale de la Recherche (ANR JCJC grant SynCol, ANR-19-CE07-0005), Université Paris-Saclay and Centre National de la Recherche Scientifique (CNRS) for funding.

ORCID® iDs

Nicolas Fay - https://orcid.org/0000-0002-6146-0823
Rémi Blieck - https://orcid.org/0000-0001-5100-5934
Cyrille Kouklovsky - https://orcid.org/0000-0001-5399-9469
Aurélien de la Torre - https://orcid.org/0000-0002-7909-0234

References

1. Christenhusz, M. J. M.; Byng, J. W. *Phytotaxa* **2016,** *261,* 201–217. doi:10.11646/phytotaxa.261.3.1
2. Popescu, R.; Kopp, B. *J. Ethnopharmacol.* **2013,** *147,* 42–62. doi:10.1016/j.jep.2013.02.022
3. Li, Y.; Liu, Y.-B.; Yu, S.-S. *Phytochem. Rev.* **2013,** *12,* 305–325. doi:10.1007/s11101-013-9299-z
4. Hanson, J. R. *Sci. Prog.* **2016,** *99,* 327–334. doi:10.3184/003685016x14720691270831
5. Li, C.-H.; Zhang, J.-Y.; Zhang, X.-Y.; Li, S.-H.; Gao, J.-M. *Eur. J. Med. Chem.* **2019,** *166,* 400–416. doi:10.1016/j.ejmech.2019.01.079
6. Gunduz, A.; Eraydin, I.; Turkmen, S.; Kalkan, O. F.; Turedi, S.; Eryigit, U.; Ayar, A. *Hum. Exp. Toxicol.* **2014,** *33,* 130–135. doi:10.1177/0960327113482693
7. Li, C.-H.; Niu, X.-M.; Luo, Q.; Xie, M.-J.; Luo, S.-H.; Zhou, Y.-Y.; Li, S.-H. *Org. Lett.* **2010,** *12,* 2426–2429. doi:10.1021/ol1007982
8. Li, Y.-P.; Li, X.-N.; Gao, L.-H.; Li, H.-Z.; Wu, G.-X.; Li, R.-T. *J. Agric. Food Chem.* **2013,** *61,* 7219–7224. doi:10.1021/jf401921x
9. Yi, X.; Zhao, H.; Dong, X.; Wang, P.; Hu, M.; Zhong, G. *PLoS One* **2013,** *8,* e77295. doi:10.1371/journal.pone.0077295
10. Jang, W. S.; Jyoti, M. A.; Kim, S.; Nam, K.-W.; Ha, T. K. Q.; Oh, W. K.; Song, H.-Y. *J. Nat. Med.* **2016,** *70,* 127–132. doi:10.1007/s11418-015-0937-1
11. Wang, S.; Lin, S.; Zhu, C.; Yang, Y.; Li, S.; Zhang, J.; Chen, X.; Shi, J. *Org. Lett.* **2010,** *12,* 1560–1563. doi:10.1021/ol1002797
12. Sahin, H.; Turumtay, E. A.; Yildiz, O.; Kolayli, S. *Int. J. Food Prop.* **2015,** *18,* 2665–2674. doi:10.1080/10942912.2014.999866
13. Li, Y.; Zhu, Y.; Zhang, Z.; Li, L.; Liu, Y.; Qu, J.; Ma, S.; Yu, S. *Acta Pharm. Sin. B* **2020,** *10,* 1073–1082. doi:10.1016/j.apsb.2019.10.013
14. Zheng, G.; Jin, P.; Huang, L.; Zhang, Q.; Meng, L.; Yao, G. *Bioorg. Chem.* **2020,** *99,* 103794. doi:10.1016/j.bioorg.2020.103794
15. Chai, B.; Li, Y.; Yu, S.-S. *J. Asian Nat. Prod. Res.* **2020,** *22,* 895–904. doi:10.1080/10286020.2020.1777545
16. Jin, P.; Zheng, G.; Yuan, X.; Ma, X.; Feng, Y.; Yao, G. *Bioorg. Chem.* **2021,** *111,* 104870. doi:10.1016/j.bioorg.2021.104870

17. Zhou, G.-L.; Zhu, P. *BMC Plant Biol.* **2020,** *20,* 414. doi:10.1186/s12870-020-02586-y
18. Hamanaka, N.; Matsumoto, T. *Tetrahedron Lett.* **1972,** *13,* 3087–3090. doi:10.1016/s0040-4039(01)85015-2
19. Gasa, S.; Hamanaka, N.; Matsunaga, S.; Okuno, T.; Takeda, N.; Matsumoto, T. *Tetrahedron Lett.* **1976,** *17,* 553–556. doi:10.1016/s0040-4039(00)77908-1
20. Shiozaki, M.; Mori, K.; Matsui, M. *Agric. Biol. Chem.* **1972,** *36,* 2539–2546. doi:10.1080/00021369.1972.10860565
21. Shiozaki, M.; Mori, K.; Matsui, M.; Hiraoka, T. *Tetrahedron Lett.* **1972,** *13,* 657–660. doi:10.1016/s0040-4039(01)84403-8
22. Kan, T.; Hosokawa, S.; Nara, S.; Oikawa, M.; Ito, S.; Matsuda, F.; Shirahama, H. *J. Org. Chem.* **1994,** *59,* 5532–5534. doi:10.1021/jo00098a009
23. Kan, T.; Matsuda, F.; Yanagiya, M.; Shirahama, H. *Synlett* **1991,** 391–392. doi:10.1055/s-1991-20737
24. Kan, T.; Oikawa, M.; Hosokawa, S.; Yanagiya, M.; Matsuda, F.; Shirahama, H. *Synlett* **1994,** 801–804. doi:10.1055/s-1994-23010
25. Kan, T.; Oikawa, M.; Hosokawa, S.; Yanagiya, M.; Matsuda, F.; Shirahama, H. *Synlett* **1994,** 805–808. doi:10.1055/s-1994-23011
26. Turlik, A.; Chen, Y.; Scruse, A. C.; Newhouse, T. R. *J. Am. Chem. Soc.* **2019,** *141,* 8088–8092. doi:10.1021/jacs.9b03751
27. Liu, C.-C.; Lei, C.; Zhong, Y.; Gao, L.-X.; Li, J.-Y.; Yu, M.-H.; Li, J.; Hou, A.-J. *Tetrahedron* **2014,** *70,* 4317–4322. doi:10.1016/j.tet.2014.05.019
28. Zhang, M.; Xie, Y.; Zhan, G.; Lei, L.; Shu, P.; Chen, Y.; Xue, Y.; Luo, Z.; Wan, Q.; Yao, G.; Zhang, Y. *Phytochemistry* **2015,** *117,* 107–115. doi:10.1016/j.phytochem.2015.06.007
29. Li, C.-J.; Liu, H.; Wang, L.-Q.; Jin, M.-W.; Chen, S.-N.; Bao, G.-H.; Qin, G.-W. *Acta Chim. Sin. (Chin. Ed.)* **2003,** *61,* 1153–1156.
30. Zhou, S.-Z.; Yao, S.; Tang, C.; Ke, C.; Li, L.; Lin, G.; Ye, Y. *J. Nat. Prod.* **2014,** *77,* 1185–1192. doi:10.1021/np500074q
31. Yu, K.; Yang, Z.-N.; Liu, C.-H.; Wu, S.-Q.; Hong, X.; Zhao, X.-L.; Ding, H. *Angew. Chem., Int. Ed.* **2019,** *58,* 8556–8560. doi:10.1002/anie.201903349
32. Gao, J.; Rao, P.; Xu, K.; Wang, S.; Wu, Y.; He, C.; Ding, H. *J. Am. Chem. Soc.* **2020,** *142,* 4592–4597. doi:10.1021/jacs.0c00308
33. Gao, K.; Hu, J.; Ding, H. *Acc. Chem. Res.* **2021,** *54,* 875–889. doi:10.1021/acs.accounts.0c00798
34. Kong, L.; Yu, H.; Deng, M.; Wu, F.; Jiang, Z.; Luo, T. *J. Am. Chem. Soc.* **2022,** *144,* 5268–5273. doi:10.1021/jacs.2c01692
35. Banik, S. M.; Levina, A.; Hyde, A. M.; Jacobsen, E. N. *Science* **2017,** *358,* 761–764. doi:10.1126/science.aao5894
36. Iwai, T.; Fujihara, T.; Tsuji, Y. *Chem. Commun.* **2008,** 6215–6217. doi:10.1039/b813171f
37. Iwasaki, K.; Wan, K. K.; Oppedisano, A.; Crossley, S. W. M.; Shenvi, R. A. *J. Am. Chem. Soc.* **2014,** *136,* 1300–1303. doi:10.1021/ja412342g
38. Chow, S.; Kreß, C.; Albæk, N.; Jessen, C.; Williams, C. M. *Org. Lett.* **2011,** *13,* 5286–5289. doi:10.1021/ol202147r
39. Marinovic, N. N.; Ramanathan, H. *Tetrahedron Lett.* **1983,** *24,* 1871–1874. doi:10.1016/s0040-4039(00)81793-1
40. Webster, C. G.; Park, H.; Ennis, A. F.; Hong, J. *Tetrahedron Lett.* **2021,** *71,* 153055. doi:10.1016/j.tetlet.2021.153055
41. Barabé, F.; Bétournay, G.; Bellavance, G.; Barriault, L. *Org. Lett.* **2009,** *11,* 4236–4238. doi:10.1021/ol901722q
42. Guo, J.; Li, B.; Ma, W.; Pitchakuntla, M.; Jia, Y. *Angew. Chem., Int. Ed.* **2020,** *59,* 15195–15198. doi:10.1002/anie.202005932
43. Ma, T.; Cheng, H.; Pitchakuntla, M.; Ma, W.; Jia, Y. *J. Am. Chem. Soc.* **2022,** *144,* 20196–20200. doi:10.1021/jacs.2c08694
See for a new total synthesis published by the group of Jia during the editing process of this article, following their work on the total synthesis of glaucocalyxin A [42].

License and Terms

BEILSTEIN JOURNAL OF ORGANIC CHEMISTRY

Synthetic study toward tridachiapyrone B

Morgan Cormier, Florian Hernvann and Michaël De Paolis*

Full Research Paper

Open Access

Address:
COBRA, Normandie University, 76000 Rouen, France

Email:
Michaël De Paolis* - michael.depaolis@univ-rouen.fr

* Corresponding author

Keywords:
α'-methoxy-γ-pyrone; 2,5-cyclohexadienone; oxy-Cope; quaternary carbon; Robinson-type annulation

Beilstein J. Org. Chem. **2022,** *18,* 1741–1748.
https://doi.org/10.3762/bjoc.18.183

Received: 10 October 2022
Accepted: 05 December 2022
Published: 19 December 2022

This article is part of the thematic issue "Total synthesis: an enabling science".

Associate Editor: B. Nay

Abstract

A convergent approach to the skeleton of tridachiapyrone B is described taking advantage of the desymmetrization of α,α'-dimethoxy-γ-pyrone leading to α-crotyl-α'-methoxy-γ-pyrone in one step. To construct the quaternary carbon of the 2,5-cyclohexadienone of the target, a strategy based on the Robinson-type annulation of an aldehyde derived from α-crotyl-α'-methoxy-γ-pyrone was applied. The grafting of the simplified target's side chain was demonstrated through an oxidative anionic oxy-Cope rearrangement of the tertiary alcohol arising from the 1,2-addition of a 1,3-dimethylallyl reagent to 2,5-cyclohexadienone connected to the α'-methoxy-γ-pyrone motif.

Introduction

The α'-methoxy-γ-pyrone motif is present in natural products and bioactive molecules [1-14]. Amidst these targets, a number contains a quaternary carbon vicinal to the scaffold, such as crispatene and photodeoxytridachione (Scheme 1a) [15]. These molecules feature a bicyclo[3.1.0]hexene core which photochemically arises from 1,3-cyclohexadiene precursors, tridachiapyrone A or 9,10-deoxytridachione, as demonstrated by Ireland [16,17]. In turn, the ring system arises from α-tetraenyl-α'-methoxy-γ-pyrone precursor **1a** upon heating through 6π-electrocyclization, as illustrated by Baldwin in the synthesis of 9,10-deoxytridachione [18]. In a further demonstration of the versatility of tetraenes connected to α'-methoxy-γ-pyrone, the synthesis of both crispatene and photodeoxytridachione was accomplished by Trauner through the Lewis acid-catalyzed 6π-disrotatory electrocyclization of compounds **1a** and **b** [19-22]. Interestingly, Baldwin and Moses demonstrated the irradiation or sunlight-promoted cycloisomerization of a similar tetraenyl framework into the bicyclo[3.1.0]hexane core through a 6π-conrotatory stereocontrol [23,24].

To date, the known strategies to install a quaternary carbon center connected to α'-methoxy-γ-pyrone therefore rely exclusively on the electrocyclization of tetraenes. With recently demonstrated potent antitumoral [25] and anti-HIV properties [26], aureothin is a natural product featuring the α'-methoxy-γ-pyrone motif connected to a chiral tetrahydrofuran

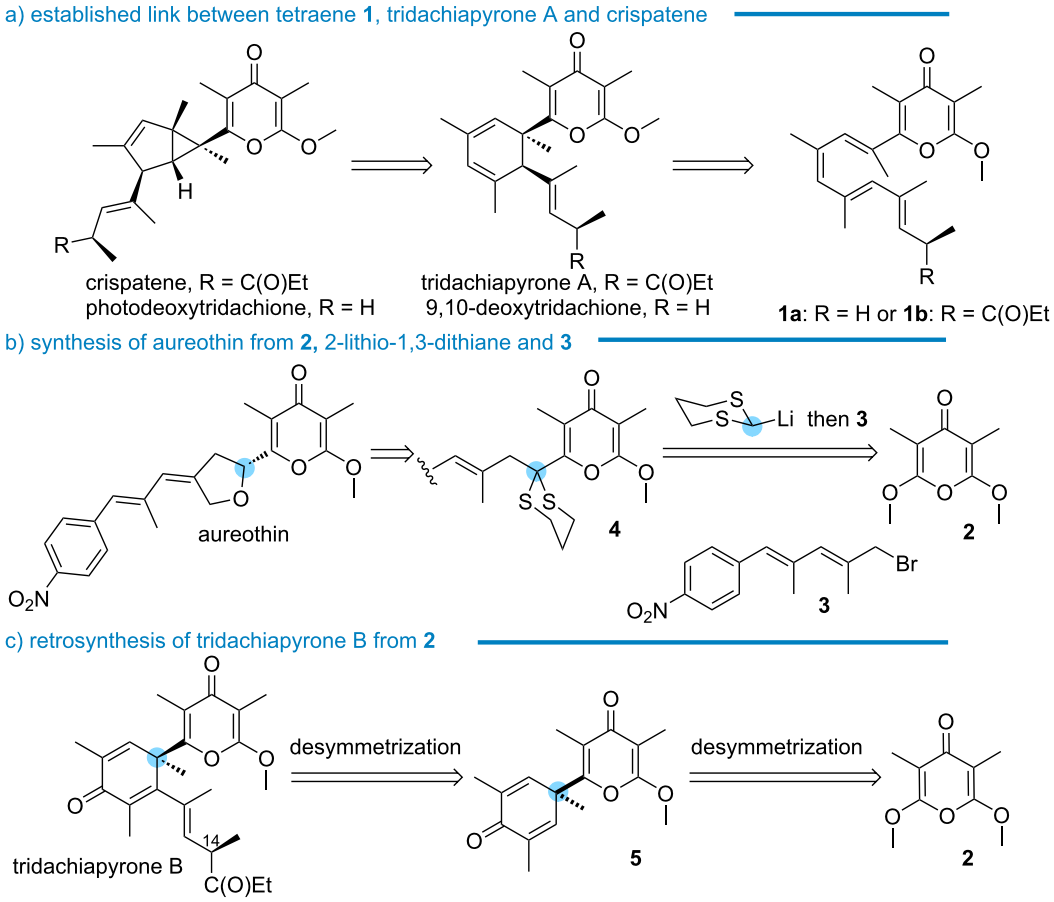

Scheme 1: Routes to crispatene, photodeoxytridachione, aureothin, and tridachiapyrone B.

(Scheme 1b). To assemble the skeleton of the natural product, we developed a new strategy in which the α,α'-dimethoxy-γ-pyrone motif **2** was first desymmetrized by a sequence encompassing the conjugate addition of 2-lithio-1,3-dithiane, elimination of methoxide lithium, and deprotonation of 2-(α'-methoxy-γ-pyrone)-1,3-dithiane. The resulting vinylogous enolate intermediate was trapped with the electrophile **3**, amounting to the one-pot preparation of compound **4**, having a masked carbonyl function connecting both key fragments [27,28].

Isolated and characterized by Schmitz [17], the metabolite tridachiapyrone B is related to tridachiapyrone A (Scheme 1c). As the 1,3-cyclohexadiene motif of the latest is oxidized into 2,5-cyclohexadienone, it is assumed that tridachiapyrone B arises from the ring opening of the epoxide (tridachiapyrone C) of tridachiapyrone A. To our knowledge, the synthesis of tridachiapyrone B was not investigated, even though it seems conceivable that the compound's stability to light, air or cytochrome would be higher than its 1,3-cyclohexadiene counterpart. As the molecule combines electron acceptor functions such as α'-methoxy-γ-pyrone and 2,5-cyclohexadienone, these considerations are advantageous with a view to evaluate the potential activity of tridachiapyrone B and analogues in biological electron transport processes.

With this context in mind, we sought to establish a straightforward access to the key 2,5-cyclohexadienone core connected to α'-methoxy-γ-pyrone by desymmetrization of α,α'-dimethoxy-γ-pyrone **2** through the addition of hindered nucleophiles to construct the vicinal quaternary carbon. In a subsequent and potentially enantioselective desymmetrization step, compound **5** would be converted into trichiachiapyrone B by 1,4-addition of the side chain to the 2,5-cyclohexadienone scaffold. Avoiding heat and light sensitive tetraenes, the convergent plan would also give the opportunity to assess an enantioselective synthesis of the targets, noting that the C^{14} epimeric product, isotridachiapyrone B, has also been isolated by Schmitz.

Results and Discussion

At first glance, the structure of 2,5-cyclohexadienone **5** suggests a disconnection involving the dearomative addition of 2,4,6-trimethylphenol to α,α'-dimethoxy-γ-pyrone **2** that we

eagerly sought to establish under basic activation of the nucleophile or by protonation of **2** (Scheme 2a). This ambitious coupling, however, met a dead-end and a less direct approach was explored. With a more reactive and less hindered nucleophile, we explored the coupling of lithiocyclopentadiene to compound **2**. After conjugate addition and elimination of lithium methoxide, the resulting **6a** would be deprotonated by lithiocyclopentadiene and the enolate intercepted with an alkylating reagent to build the quaternary carbon of **6b** (Scheme 2b). This one-pot procedure was reminiscent of our previous study describing the addition of an allylic carbanion, generated from allylstannane with *n*-BuLi, to **2** which was followed by the addition of an aldehyde resulting in a regioselective aldolization [29]. Thereafter, we hypothesized converting cyclopentadiene **6b** into 2,5-cyclohexadienone **5** by a sequence involving the oxidation into dialdehyde **7** and treatment with pentan-3-one to enable sequential steps of aldolization and crotonization. As an aromatic carbanion, it was unclear whether the addition of lithiocyclopentadiene to **2** would succeed [30].

Pleasingly though, the coupling was successful and moreover simply implemented by reacting lithiocyclopentadiene (2 equiv) with pyrone **2** at room temperature, no reaction occurring at lower temperature in contrast with the nucleophile 2-lithio-1,3-dithiane, and with acetic acid as electrophile (Scheme 3). Among the possible isomers that can be expected, a single one **6a'** was isolated in 49% yield after trituration, as it was found rather unstable on silica gel. While the addition of more reactive carbanions of 1,3-dithiane [27], allyl [27], and methyldienylbenzene groups [31] to compound **2** were demonstrated, this result amounts to the first grafting of an aromatic nucleophile to the motif.

The construction of the vicinal quaternary carbon of **6b** was next investigated by methylation of the highly delocalized enolate intermediate **6a·Li**. To that end, the addition of lithiocyclopentadiene to **2** was followed by the attendant quenching with a methylating reagent (MeI, Me_2SO_4, MeOTf) but a complex mixture of products was consistently obtained. To gather

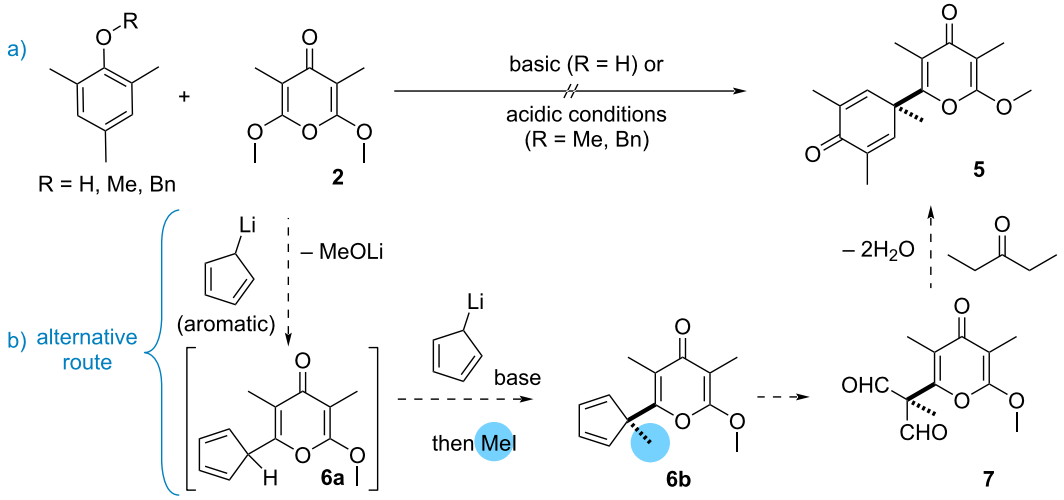

Scheme 2: Desymmetrization of **2**.

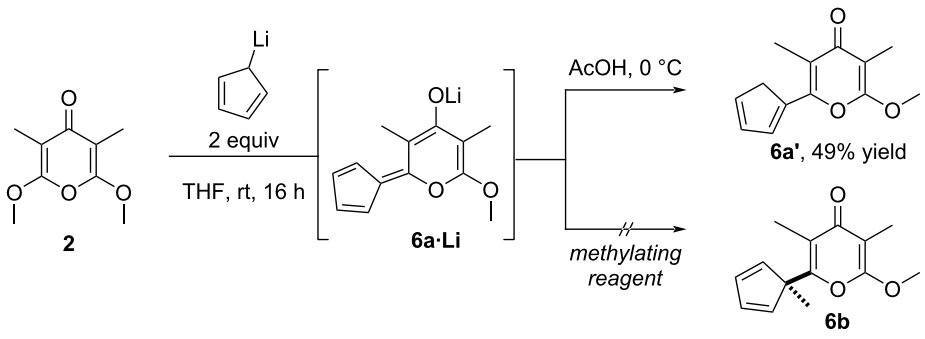

Scheme 3: Addition of lithiocyclopentadiene to pyrone **2**.

information on the reactivity of **6a·Li**, the stabilized enolate was treated with 4-nitrobenzaldehyde to promote the aldolization reaction but the corresponding alcohol was not observed, which confirmed the reluctance of **6a·Li** to react with other electrophiles than protons.

Unable to form the quaternary carbon of the target from this intermediate, the pathway to 2,5-cyclohexanedione **5** was accordingly updated and an approach to make use of the Robinson-type annulation was devised from aldehyde **9**, prepared by oxidation of α-crotyl-α'-methoxy-γ-pyrone **8** (Scheme 4). While its synthesis was initially investigated by the coupling of tri(*n*-butyl)crotylstannane to **2** in the presence of *n*-BuLi, the direct transfer of the crotyl appendage failed, likely compromised by the steric hindrance of the nucleophile [31].

To alleviate this shortcoming, the crotyl appendage of **8** was assembled by methylation of the allylic pyrone counterpart (Scheme 5). Implemented by exposing **2** to the combination of reagents tri(*n*-butyl)allylstannane/*n*-BuLi (2 equiv) followed by the treatment with MeI, the crotyl derivative **8** was directly isolated in 55–60% yield (5 g scale) via the regioselective methylation of the intermediate vinylogous enolate **10·Li**. The preparation of aldehyde **9** was carried out through a two-step sequence including dihydroxylation ($K_2OsO_4·H_2O$, 90% yield) of **8** and oxidative cleavage ($NaIO_4$, 91% yield) of the diol intermediate. Note that both ozonolysis and the one-pot Lemieux–Johnson oxidative cleavage process of **8** led instead to methyl ketone **11** in a significant amount (ca. 75% yield), probably by oxidation of the enol form of **9** [32]. The sensitive aldehyde was thus used without purification to investigate the Robinson-type annulation and a protocol was identified allowing the preparation of cyclohexenone **12** in 40% yield (2-step). Accordingly, the Michael addition of ethyl vinyl ketone (EVK), promoted by K_2CO_3 in a biphasic media (PhMe/H_2O), was followed by basic treatment (LiOH) of the keto aldehyde. Since compound **12**

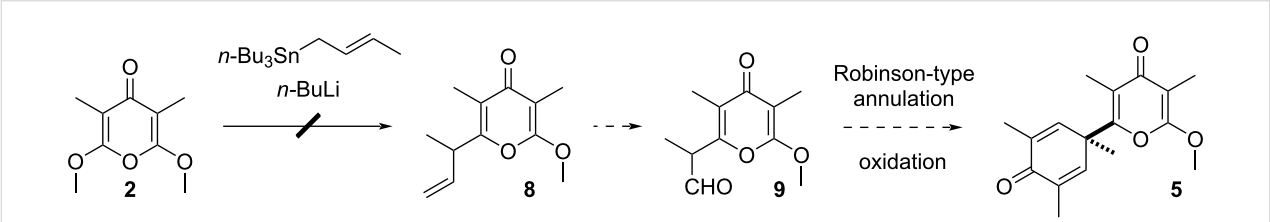

Scheme 4: Plan to reach 2,5-cyclohexadienone **5**.

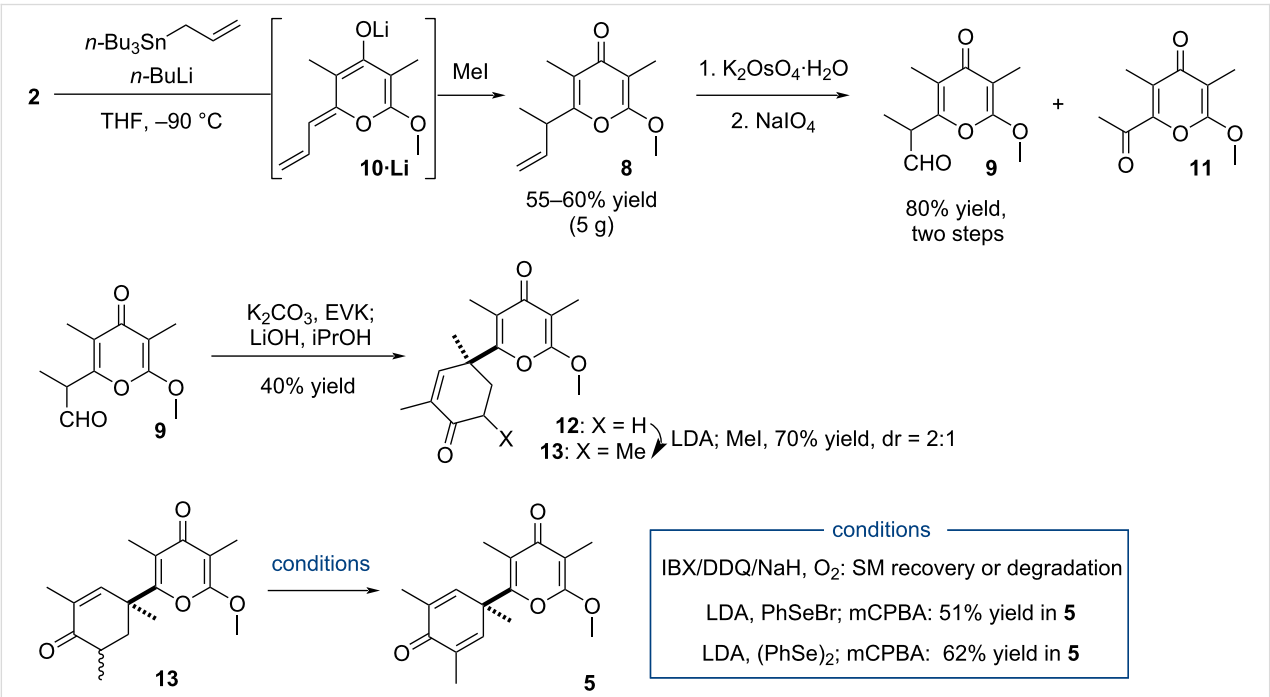

Scheme 5: Preparation of 2,5-cyclohexadienone **5**.

bears the desired quaternary carbon of this family of natural products, it was pleasing to reach this milestone, keeping in mind that the fair yield of this two-step transformation may be the consequence of the aldehyde's low stability.

Note that the Kotsuki method to perform the Robinson-type annulation of **9** with EVK, catalyzed by a combination of 1,2-cyclohexanediamine and 1,2-cyclohexanedicarboxylic acid, led to product **12** with higher yield but the scale-up of the reaction was less efficient [33]. It has to be underlined that all attempts, using either methods, to couple aldehyde **9** with 2-methylpent-1-en-3-one and directly produce **13** were unsuccessful. To achieve this goal a methylation step of **12** ($LiN(iPr)_2$ (LDA); MeI) was thus necessary (70% yield, 2:1 dr).

The desaturation of the enone compound was next examined and while exposure of **13** to oxidant (*o*-iodoxybenzoic acid (IBX) or 2,3-dichloro-5,6-dicyano-1,4-benzoquinone (DDQ)) left the starting materials unchanged, treatment with NaH in the presence of oxygen to induce the aerobic oxidation caused instead the degradation of **13**. An indirect approach was more rewarding as treatment of the enolate of **13** with PhSeBr led to 2,5-cyclohexadienone **5** in 51% yield after oxidation of the selenoether intermediate with *m*-chloroperoxybenzoic acid (*m*-CPBA). An appreciable increase of the yield was actually noted with $(PhSe)_2$ as electrophile, **5** being obtained in 62% yield, enabling thus an evaluation of the next desymmetrization step.

An overview of the scientific literature revealed that, while the asymmetric desymmetrization of prochiral 2,5-cyclohexadienones is a rich topic of investigation, it is mostly restricted to substrates bearing a tertiary alkoxy group [34]. Few examples of this intermolecular strategy actually involve substrates containing a quaternary carbon and the formation of a C–C bond [35,36]. Of note was the report of Takemoto and Iwata describing the 1,4-addition of $AlMe_3$ to 4,4-dimethyl-2,5-cyclohexadienone in the presence of a copper salt/chiral ligand and silylating reagent [37,38]. The racemic conjugate addition of nucleophiles to **5** was first investigated, starting with the Gilman reagent which was used in Takemoto and Iwata study (Scheme 6). In addition, a screening of various organocopper reagents (prepared from MeLi, EtMgBr, $ZnEt_2$ or $AlMe_3$ and copper halide or thiophene-2-carboxylate (CuTC)) was conducted, to no avail. In most cases, the starting material was recovered without indication that the pyrone ring interacted instead with the reagent. To decrease the steric hindrance of the electrophile and potentially facilitate the 1,4-addition, 2,5-cyclohexadienone **14**, deprived of a methyl group, was prepared and tested but the reactivity was not significantly improved compared to **5**. Both compounds appeared thus mostly reluctant to 1,4-addition and, when it was not the case, the process was poorly reproducible.

On the other hand, the 1,2-addition of Grignard reagents to **5** was observed, providing thus an alternative way of grafting a side chain. As summarized in Scheme 7a, this was envisaged through a sequence encompassing the 1,2-addition of the 1,3-dimethylallyl motif to **5** giving **17**, followed by the anionic oxy-Cope rearrangement of the dienol into cyclohexenone **18**. After desaturation, the resulting 2,5-cyclohexadienone **19** would provide a modular platform to construct the side chain of the target and analogues. Note that this updated route required the 1,2-addition of a rather hindered nucleophile to a carbonyl electrophile with low reactivity. Precedents were noted though, as Carreira used this strategy for the synthesis of indoxamycine B exploiting the reactivity of 1,3-dimethylallyltitanocene species [39]. The 1,2-addition of various allyltitanocene reagents to carbonyl compounds was described by Sato which were prepared from the corresponding allyl carbonates exposed to the combination of $[Cp_2TiCl_2]$/*n*-BuLi [40]. Pleasingly, conducting the coupling of carbonate **20** to **5** in conditions inspired from Carreira's study (Scheme 7b) led to the desired 1,2-adduct **17** in 50% yield [41].

To perform the anionic oxy-Cope rearrangement, alcohol **17** was exposed to *t*-BuOK, in the presence of 18-crown-6 ether (−78 °C to rt) [42].

However, these conditions did not trigger the rearrangement and the starting material was recovered. On the other hand, treatment with KH in DMSO at room temperature caused the

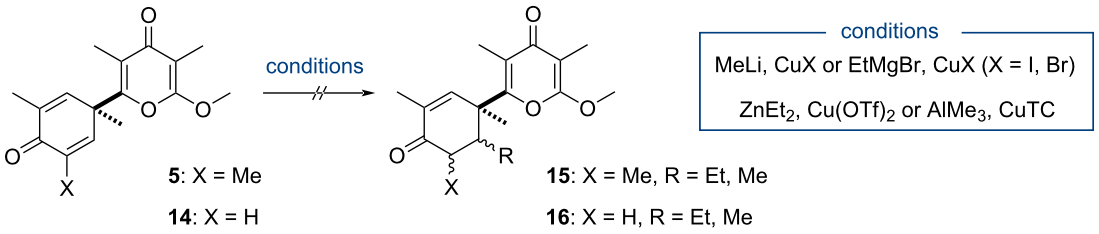

Scheme 6: Attempts to perform the conjugate addition.

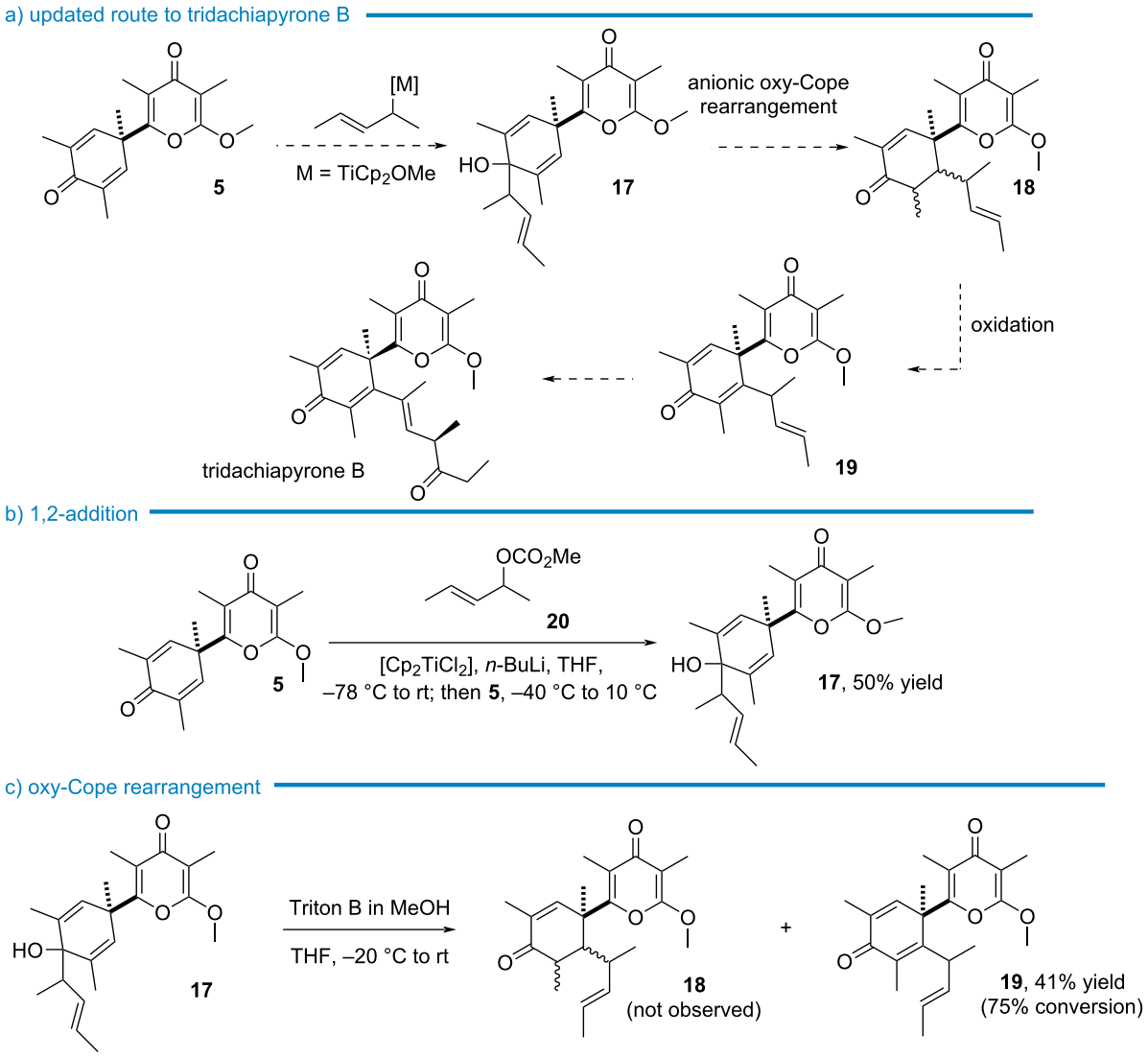

Scheme 7: Updated route to tridachiapyrone B.

degradation of **17**. Scarcely examined for this purpose, hydroxide of quaternary ammonium salt was next evaluated to promote the anionic oxy-Cope rearrangement with the prospect that non-coordinating organic cations could facilitate the transformation by destabilizing the negative charge of the anion (Scheme 7c). Simply generated with Triton B (benzyltrimethylammonium hydroxide), the alcoholate of **17** smoothly (−20 °C to rt) underwent the [3,3]-sigmatropic rearrangement (75% conversion) directly affording 2,5-cyclohexadienone *E*-**19** which was isolated in 41% yield [43] while cyclohexenone **18** was not observed in the crude reaction mixture (as analyzed by ^{1}H NMR spectroscopy). Even though the mechanism was not investigated, the presence of oxygen during the rearrangement step was suspected to account for the oxidation of the enolate intermediate, enabling thus a practical one-pot preparation of 2,5-cyclohexadienone **19** from **17**.

Conclusion

While the construction of the side chain's target remains to be completed, we developed a convergent access to a highly substituted 2,5-cyclohexadienone motif bearing a quaternary carbon connected to α'-methoxy-γ-pyrone, simplified analogues of tridachiapyrone B such as **19**. Without requiring the construction of polyenes, the route is enabled by key transformations such as the formal crotylation of α,α'-dimethoxy-γ-pyrone, the Robinson-type annulation of a sensitive aldehyde and 1,2-addition to 2,5-cyclohexadienone followed by an oxidative anionic oxy-Cope rearrangement promoted by hydroxide of

quaternary ammonium salt. Moreover, the coupling of lithiocyclopentadiene to α,α'-dimethoxy-γ-pyrone was demonstrated, enlarging the scope of nucleophiles grafted to the pharmaceutically relevant α'-methoxy-γ-pyrone motif. Drawing from this work, future studies will be focused on an enantioselective access to the target.

Supporting Information

Supporting Information File 1

Experimental details, ^{1}H and ^{13}C spectra of new compounds.
[https://www.beilstein-journals.org/bjoc/content/supplementary/1860-5397-18-183-S1.pdf]

Acknowledgements

Dr. Jacques Maddaluno is gratefully acknowledged for helpful discussions.

Funding

MC thanks Ministère de la Recherche et de l'Education Nationale for a Ph.D. fellowship. This work has been partially supported by CNRS, Normandie University, INSA Rouen, Labex SynOrg (ANR-11-LABX-0029) and Région Normandie (CRUNCh network).

ORCID® iDs

Morgan Cormier - https://orcid.org/0000-0002-2469-3345
Florian Hernvann - https://orcid.org/0000-0002-0590-2797
Michaël De Paolis - https://orcid.org/0000-0001-8139-3544

References

1. Sharma, P.; Powell, K.; Burnley, J.; Awaad, A. S.; Moses, J. E. *Synthesis* **2011,** 2865–2892. doi:10.1055/s-0030-1260168
2. Miller, A. K.; Trauner, D. *Synlett* **2006,** 2295–2316. doi:10.1055/s-2006-949627
3. Ui, H.; Shiomi, K.; Suzuki, H.; Hatano, H.; Morimoto, H.; Yamaguchi, Y.; Masuma, R.; Sunazuka, T.; Shimamura, H.; Sakamoto, K.; Kita, K.; Miyoshi, H.; Tomoda, H.; Ōmura, S. *J. Antibiot.* **2006,** *59,* 785–790. doi:10.1038/ja.2006.103
4. Wilk, W.; Waldmann, H.; Kaiser, M. *Bioorg. Med. Chem.* **2009,** *17,* 2304–2309. doi:10.1016/j.bmc.2008.11.001
5. Ishibashi, Y.; Ohba, S.; Nishiyama, S.; Yamamura, S. *Tetrahedron Lett.* **1996,** *37,* 2997–3000. doi:10.1016/0040-4039(96)00483-2
6. Garey, D.; Ramirez, M.-l.; Gonzales, S.; Wertsching, A.; Tith, S.; Keefe, K.; Peña, M. R. *J. Org. Chem.* **1996,** *61,* 4853–4856. doi:10.1021/jo960221g
7. Manzo, E.; Ciavatta, M. L.; Gavagnin, M.; Mollo, E.; Wahidulla, S.; Cimino, G. *Tetrahedron Lett.* **2005,** *46,* 465–468. doi:10.1016/j.tetlet.2004.11.085
8. Kim, Y.; Ogura, H.; Akasaka, K.; Oikawa, T.; Matsuura, N.; Imada, C.; Yasuda, H.; Igarashi, Y. *Mar. Drugs* **2014,** *12,* 4110–4125. doi:10.3390/md12074110
9. Inuzuka, T.; Yamamoto, K.; Iwasaki, A.; Ohno, O.; Suenaga, K.; Kawazoe, Y.; Uemura, D. *Tetrahedron Lett.* **2014,** *55,* 6711–6714. doi:10.1016/j.tetlet.2014.10.032
10. Fujimaki, T.; Saito, S.; Imoto, M. *J. Antibiot.* **2017,** *70,* 328–330. doi:10.1038/ja.2016.162
11. Wu, T.; Salim, A. A.; Bernhardt, P. V.; Capon, R. J. *J. Nat. Prod.* **2021,** *84,* 474–482. doi:10.1021/acs.jnatprod.0c01343
12. Leiris, S. J.; Khdour, O. M.; Segerman, Z. J.; Tsosie, K. S.; Chapuis, J.-C.; Hecht, S. M. *Bioorg. Med. Chem.* **2010,** *18,* 3481–3493. doi:10.1016/j.bmc.2010.03.070
13. Lin, Z.; Torres, J. P.; Ammon, M. A.; Marett, L.; Teichert, R. W.; Reilly, C. A.; Kwan, J. C.; Hughen, R. W.; Flores, M.; Tianero, M. D.; Peraud, O.; Cox, J. E.; Light, A. R.; Villaraza, A. J. L.; Haygood, M. G.; Concepcion, G. P.; Olivera, B. M.; Schmidt, E. W. *Chem. Biol.* **2013,** *20,* 73–81. doi:10.1016/j.chembiol.2012.10.019
14. De Paolis, M. *Targets Heterocycl. Syst.* **2016,** *20,* 63–84.
15. Ireland, C.; Faulkner, J. *Tetrahedron* **1981,** *37,* 233–240. doi:10.1016/0040-4020(81)85059-4
16. Ireland, C.; Scheuer, P. J. *Science* **1979,** *205,* 922–923. doi:10.1126/science.205.4409.922
17. Ksebati, M. B.; Schmitz, F. J. *J. Org. Chem.* **1985,** *50,* 5637–5642. doi:10.1021/jo00350a042
18. Moses, J. E.; Adlington, R. M.; Rodriguez, R.; Eade, S. J.; Baldwin, J. E. *Chem. Commun.* **2005,** 1687–1689. doi:10.1039/b418988d
19. Miller, A. K.; Trauner, D. *Angew. Chem., Int. Ed.* **2003,** *42,* 549–552. doi:10.1002/anie.200390158
20. Miller, A. K.; Byun, D. H.; Beaudry, C. M.; Trauner, D. *Proc. Natl. Acad. Sci. U. S. A.* **2004,** *101,* 12019–12023. doi:10.1073/pnas.0401787101
21. Beaudry, C. M.; Malerich, J. P.; Trauner, D. *Chem. Rev.* **2005,** *105,* 4757–4778. doi:10.1021/cr0406110
22. Zuidema, D. R.; Miller, A. K.; Trauner, D.; Jones, P. B. *Org. Lett.* **2005,** *7,* 4959–4962. doi:10.1021/ol051887c
23. Brückner, S.; Baldwin, J. E.; Moses, J.; Adlington, R. M.; Cowley, A. R. *Tetrahedron Lett.* **2003,** *44,* 7471–7473. doi:10.1016/j.tetlet.2003.08.021
24. Eade, S. J.; Walter, M. W.; Byrne, C.; Odell, B.; Rodriguez, R.; Baldwin, J. E.; Adlington, R. M.; Moses, J. E. *J. Org. Chem.* **2008,** *73,* 4830–4839. doi:10.1021/jo800220w
25. Henrot, M.; Jean, A.; Peixoto, P. A.; Maddaluno, J.; De Paolis, M. *J. Org. Chem.* **2016,** *81,* 5190–5201. doi:10.1021/acs.joc.6b00878
26. Herrmann, A.; Roesner, M.; Werner, T.; Hauck, S. M.; Koch, A.; Bauer, A.; Schneider, M.; Brack-Werner, R. *Sci. Rep.* **2020,** *10,* 1326. doi:10.1038/s41598-020-57843-9
27. Henrot, M.; Richter, M. E. A.; Maddaluno, J.; Hertweck, C.; De Paolis, M. *Angew. Chem., Int. Ed.* **2012,** *51,* 9587–9591. doi:10.1002/anie.201204259
28. De Paolis, M.; Rosso, H.; Henrot, M.; Prandi, C.; d'Herouville, F.; Maddaluno, J. *Chem. – Eur. J.* **2010,** *16,* 11229–11232. doi:10.1002/chem.201001780
29. Rosso, H.; De Paolis, M.; Collin, V. C.; Dey, S.; Hecht, S. M.; Prandi, C.; Richard, V.; Maddaluno, J. *J. Org. Chem.* **2011,** *76,* 9429–9437. doi:10.1021/jo201683u
30. Erker, G.; Kehr, G.; Fröhlich, R. *Organometallics* **2008,** *27,* 3–14. doi:10.1021/om7007666

31. Cormier, M.; Ahmad, M.; Maddaluno, J.; De Paolis, M. *Organometallics* **2017,** *36,* 4920–4927. doi:10.1021/acs.organomet.7b00765
32. Belotti, D.; Andreatta, G.; Pradaux, F.; BouzBouz, S.; Cossy, J. *Tetrahedron Lett.* **2003,** *44,* 3613–3615. doi:10.1016/s0040-4039(03)00695-6
33. Inokoishi, Y.; Sasakura, N.; Nakano, K.; Ichikawa, Y.; Kotsuki, H. *Org. Lett.* **2010,** *12,* 1616–1619. doi:10.1021/ol100350w
34. Kalstabakken, K. A.; Harned, A. M. *Tetrahedron* **2014,** *70,* 9571–9585. doi:10.1016/j.tet.2014.07.081
35. Zeng, X.-P.; Cao, Z.-Y.; Wang, Y.-H.; Zhou, F.; Zhou, J. *Chem. Rev.* **2016,** *116,* 7330–7396. doi:10.1021/acs.chemrev.6b00094
36. Miyamae, N.; Watanabe, N.; Moritaka, M.; Nakano, K.; Ichikawa, Y.; Kotsuki, H. *Org. Biomol. Chem.* **2014,** *12,* 5847–5855. doi:10.1039/c4ob00733f
37. Takemoto, Y.; Kuraoka, S.; Hamaue, N.; Iwata, C. *Tetrahedron: Asymmetry* **1996,** *7,* 993–996. doi:10.1016/0957-4166(96)00100-0
38. Takemoto, Y.; Kuraoka, S.; Hamaue, N.; Aoe, K.; Hiramatsu, H.; Iwata, C. *Tetrahedron* **1996,** *52,* 14177–14188. doi:10.1016/0040-4020(96)00869-1
39. Jeker, O. F.; Carreira, E. M. *Angew. Chem., Int. Ed.* **2012,** *51,* 3474–3477. doi:10.1002/anie.201109175
40. Kasatkin, A.; Nakagawa, T.; Okamoto, S.; Sato, F. *J. Am. Chem. Soc.* **1995,** *117,* 3881–3882. doi:10.1021/ja00118a030
41. Isolated as a single stereoisomer.
42. Paquette, L. A. *Tetrahedron* **1997,** *53,* 13971–14020. doi:10.1016/s0040-4020(97)00679-0
43. Isolated as a single stereoisomer. The dr of the reaction and the relative configuration of the product were not determined.

License and Terms

BEILSTEIN JOURNAL OF ORGANIC CHEMISTRY

Combining the best of both worlds: radical-based divergent total synthesis

Kyriaki Gennaiou‡, Antonios Kelesidis‡, Maria Kourgiantaki‡ and Alexandros L. Zografos*

Review

Open Access

Address:
Aristotle University of Thessaloniki, Department of Chemistry, Laboratory of Organic Chemistry, Thessaloniki, 54124, Greece

Email:
Alexandros L. Zografos* - alzograf@chem.auth.gr

* Corresponding author ‡ Equal contributors

Keywords:
biomimetic synthesis; cascades; common scaffold; hydrogen atom transfer; photoredox catalysis

Beilstein J. Org. Chem. **2023,** *19,* 1–26.
https://doi.org/10.3762/bjoc.19.1

Received: 09 September 2022
Accepted: 30 November 2022
Published: 02 January 2023

This article is part of the thematic issue "Total synthesis: an enabling science".

Associate Editor: B. Nay

Abstract

A mature science, combining the art of the total synthesis of complex natural structures and the practicality of delivering highly diverged lead compounds for biological screening, is the constant aim of the organic chemistry community. Delivering natural lead compounds became easier during the last two decades, with the evolution of green chemistry and the concepts of atom economy and protecting-group-free synthesis dominating the field of total synthesis. In this new era, total synthesis is moving towards natural efficacy by utilizing both the biosynthetic knowledge of divergent synthesis and the latest developments in radical chemistry. This contemporary review highlights recent total syntheses that incorporate the best of both worlds.

Introduction

Societal needs push sciences into new directions, as the urge for new pharmaceutical leads grows, in order to counteract global health challenges. Following this trend, total synthesis has been remodeled from the purely academic quest and display of human abilities to synthetically achieve natural complexity [1] to a modern science addressing the need for the supply of natural products and congeners for biological screening.

The era of scalability [2] in total synthesis prompts researchers in this field to make use of more direct retrosynthetic disconnections with the aid of “radical” retrosynthetic analysis, as the advancement in the area now allows to harness one-electron power in a highly chemoselective manner [3]. The development of persistent radicals [4] as synthons in chemical synthesis, coupled with the advancements in generating and manipulating transient radicals [5] as cross-coupling partners in an array of chemical reactions, gives access to a wide variety of “new” retrosynthetic disconnections. As radical disconnections are gaining ground, more sophisticated retrosyntheses of natural products are unlocked, enriching thus their synthetic scalability

[6,7]. A direct comparison of a classic vs a radical approach highlights the complementarity and, more often than not, the superiority of the latter, which is proven in the number of steps and the overall yield, hence establishing it as highly appealing for further development (Scheme 1).

In order to identify the new pharmaceutical leads of tomorrow, drug discovery relies on the available chemical space rising from existing chemical libraries. But how big should this chemical space be, so as to actually address our needs? A general consensus has emerged, supporting that "it is not actually the library size but rather the library diversity in terms of molecular structure and function which is fundamental for a successful drug discovery" [8]. And this is where divergent total synthesis might help. Divergent total synthesis is an old but yet underdeveloped strategy, utilizing the conceptual advantages of biosyn-

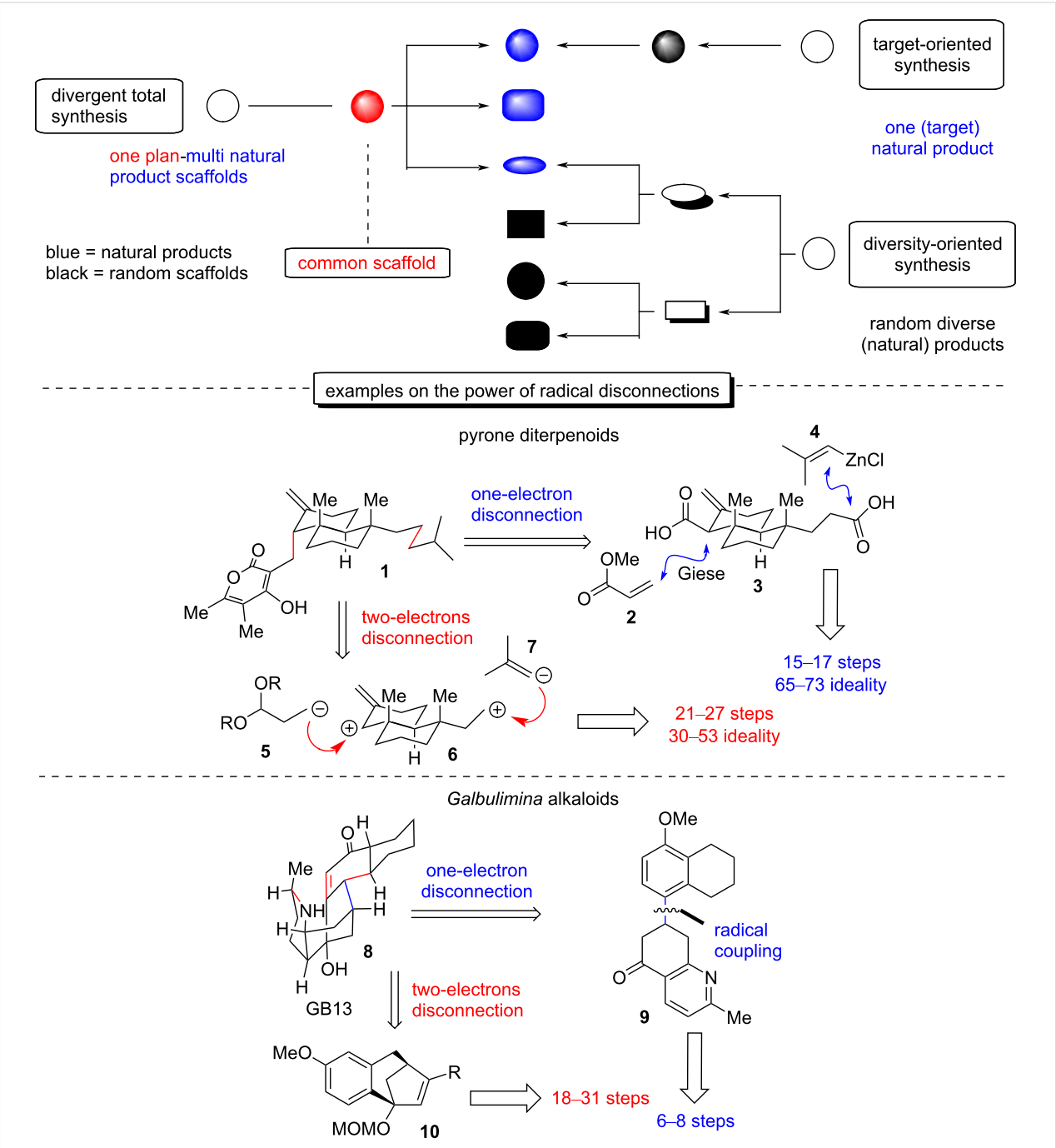

Scheme 1: The power of radical retrosynthesis and the tactic of divergent total synthesis.

thetic routes that allow multi-target natural product synthesis through a unified synthetic plan [9,10]. Based on the logic of divergent synthesis, common synthetic scaffolds, which are regarded as the points of diversity of the synthetic plan, lie at the heart of retrosynthetic design. Radical disconnections on common scaffolds, in accordance to the trends of green chemistry [11] and the concepts of atom economy [12] and protecting-group-free synthesis [13], are gradually drawing more and more the interest of organic chemists as a sustainable way to deliver structurally diverse chemical libraries for biological screening. The current review is focusing on selected examples utilizing a radical-based divergent total synthesis approach, excluding electrochemical methods for generating radicals. An exhaustive review on radical total synthesis or divergent total synthesis lies beyond the scope of this review, and the readers are advised to refer to excellent reviews on these topics [6,10,14]. This review covers the years 2018–2022.

Review

Radical-based divergent synthesis

Commonly, the most successful divergent plans apply where the natural molecular complexity is rich. Not surprisingly, most of the divergent total syntheses carried out thus far are performed on terpenoid and alkaloid targets, utilizing common synthetic intermediates closely related to the biosynthetic origins of the family. On the other hand, radical retrosynthetic disconnections on common scaffolds are much less predictable and rarely similar due to the plethora of radical chemical transformations available nowadays.

Although radicals stopped being confronted as “scientific curiosities” in the late 1960s, when radical initiators and organomercury reagents were developed as reliable reaction partners (Giese reaction) [15], it was not until the mid-1980s, at which point they appeared as key reaction players in total synthesis (Figure 1). The change in the perception that radicals cannot be selectively used took place with the introduction of tin hydrides in organic synthesis. Apart from the lower toxicity compared to organomercury reagents, the stability and longevity of tin-centered radicals allowed better propagation of radical chain reactions [16]. Based on their reactivity, major contributions in carbon-centered radical formation followed, consequently unlocking highly predictable intramolecular reactions, deoxygenation protocols (Barton–McCombie reaction) [17], etc. Other reagents that majorly contributed were samarium diiodide for the generation of radicals from carbonyl reduction [18] but also manganese(III) acetate as a convenient one-electron oxidant [19]. The next twenty years, the field continued to flourish mainly by way of the decipherment of hydrogen atom transfer (HAT) mechanisms, which led to the establishment of several reactions of transition metal hydrides (Fe, Co, Mn, etc) with alkenes (e.g., Mukaiyama hydration) [20].

The last decade saw the development of milder methods for generating carbon-centered radicals as the advancement of their reactivity in cross-coupling reactions, the concept of photoredox catalysis [21], and electrochemistry [22] all refuelled the field, allowing for more practical radical disconnections for total synthesis.

Divergent synthesis of pyrone diterpenes

(Baran 2018) [23]**:** The modestly sized family of pyrone diterpenes exhibits a wide range of bioactivities, ranging from immunosuppressive to hypertensive properties [24-26] depending on the subtle substituents in the periphery of a

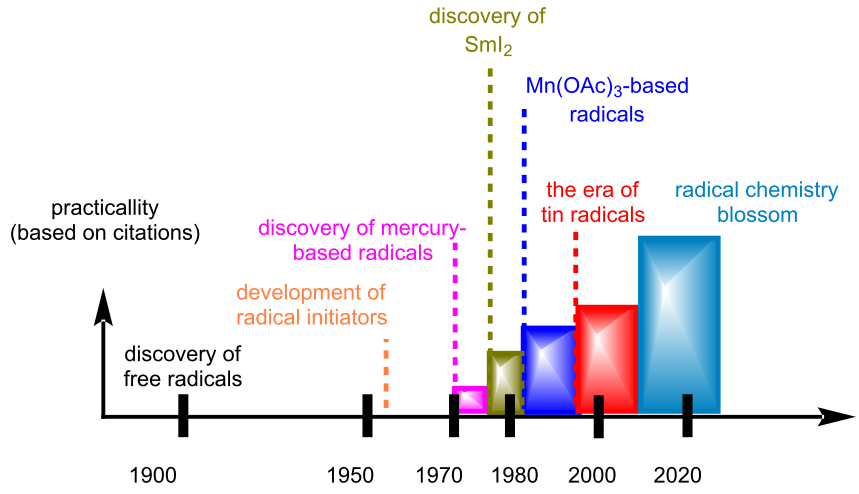

Figure 1: Evolution of radical chemistry for organic synthesis.

decalin core (Scheme 2). In 2018, the Baran group reported the divergent total synthesis of several pyrone diterpene natural products, relying solely on one-electron-based retrosynthesis. The group recognized the disadvantages that stemmed from prior 2-electron disconnections, namely the complicated C–C bond formations and the necessity for excessive functional group manipulations but also the unavailability of a unified divergent plan for this class of diterpenoids. As an alternative, they proposed nickel-mediated decarboxylative Giese reactions and decarboxylative radical zinc-mediated cross-coupling reactions of redox-active esters, established from previous works of the group [27,28], for the key C–C bonds of the diverse congeners. To this end, a hypothetical intermediate **3** was envisioned for their synthesis (Scheme 2). The synthetic variant of **3** was designed as the common scaffold **16**, bearing the appropriate substitution for sequential revelation of carboxylic acid moieties. The highly congested decalin core of common scaffold **16** was obtained by a modified electrochemical polycyclization of polyene **14** (prepared in two steps) in multigram quantities [23]. The reaction employed a divided cell with substoichiometric amounts of magnesium(II) acetate (0.5 equiv) and catalytic copper(II) 3,5-diisopropylsalicylate (0.02 equiv) to allow the redox radical cyclization of polyene in 42% yield. A Tsuji allylation using achiral H-PHOX followed to produce **16**,

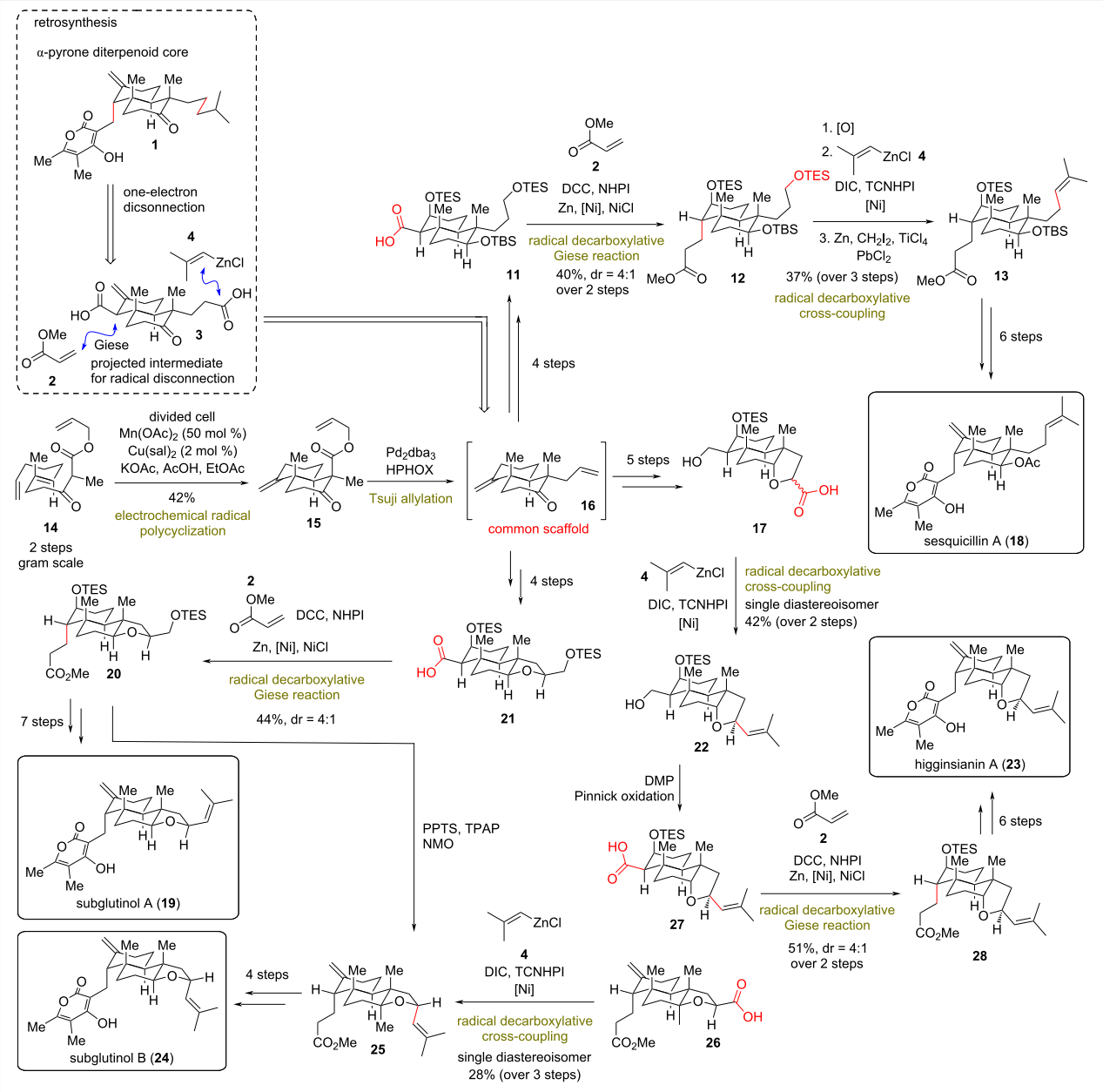

Scheme 2: Divergent total synthesis of α-pyrone-diterpenoids (Baran).

without being isolated. From this point of divergence, Baran's group managed to reveal the requisite phthalimide carboxylates for each precursor of the diverse natural products and transformed it carrying out Giese reactions or nickel-catalyzed radical coupling to **13**, **20**, **25**, and **28**, few steps away from the total syntheses of sesquicillin A (**18**), subglutinols A and B (**19** and **24**) and higginsianin A (**23**, Scheme 2).

Merged chemoenzymatic and radical synthesis of oxidized pyrone meroterpenoids

(Renata 2020) [29]**:** In 2020, a different approach was conceptualized by Renata's group to access various oxidized members of pyrone meroterpenoids. The divergent plan of Renata's group depended on the development of a highly chemoselective, chemoenzymatic 3-hydroxylation of sclareolide (**29**) and (−)-sclareol (**43**, Scheme 3 and Scheme 4). The group began by conducting a brief survey of several P450 BM3 mutants, deducing that the variant 1857 V328A (BM3 MERO1) was able to achieve high conversion of sclareolide (**29**) to the hydroxylated counterpart **30** in >95% yield. Based on this success, the group employed a radical disconnection approach of several 3-hydroxylated pyrone meroterpenoids on sclareolide (**29**). Key reaction of this strategy was the formal [3 + 3] cycloaddition, catalyzed by phosphoric acid **33**, followed by addition of a pyrone residue **32** to sclareolide-derived aldehyde **31**, which served as the common synthetic intermediate for the synthesis

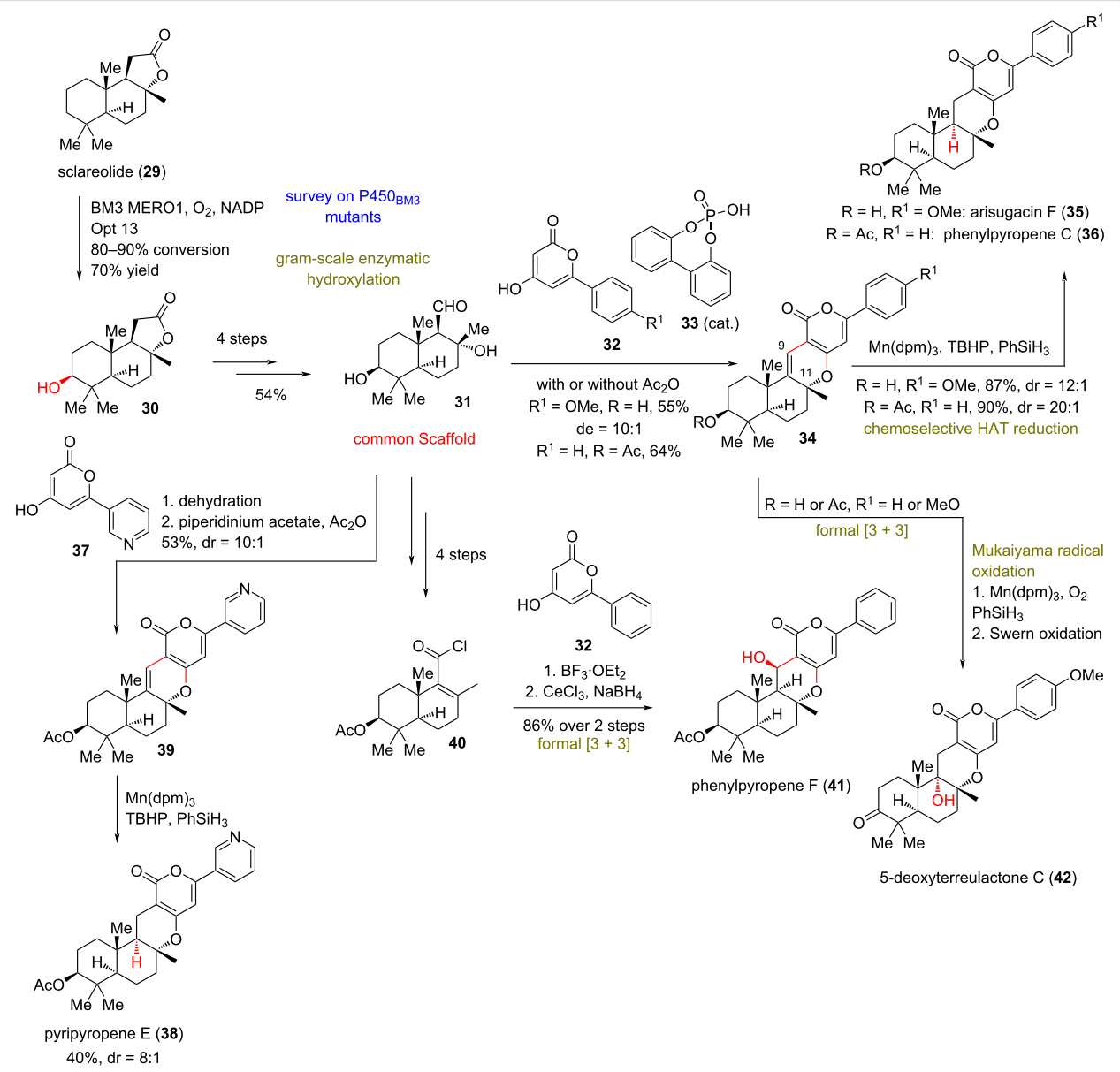

Scheme 3: Divergent synthesis of pyrone diterpenoids by merged chemoenzymatic and radical synthesis (part I, Renata).

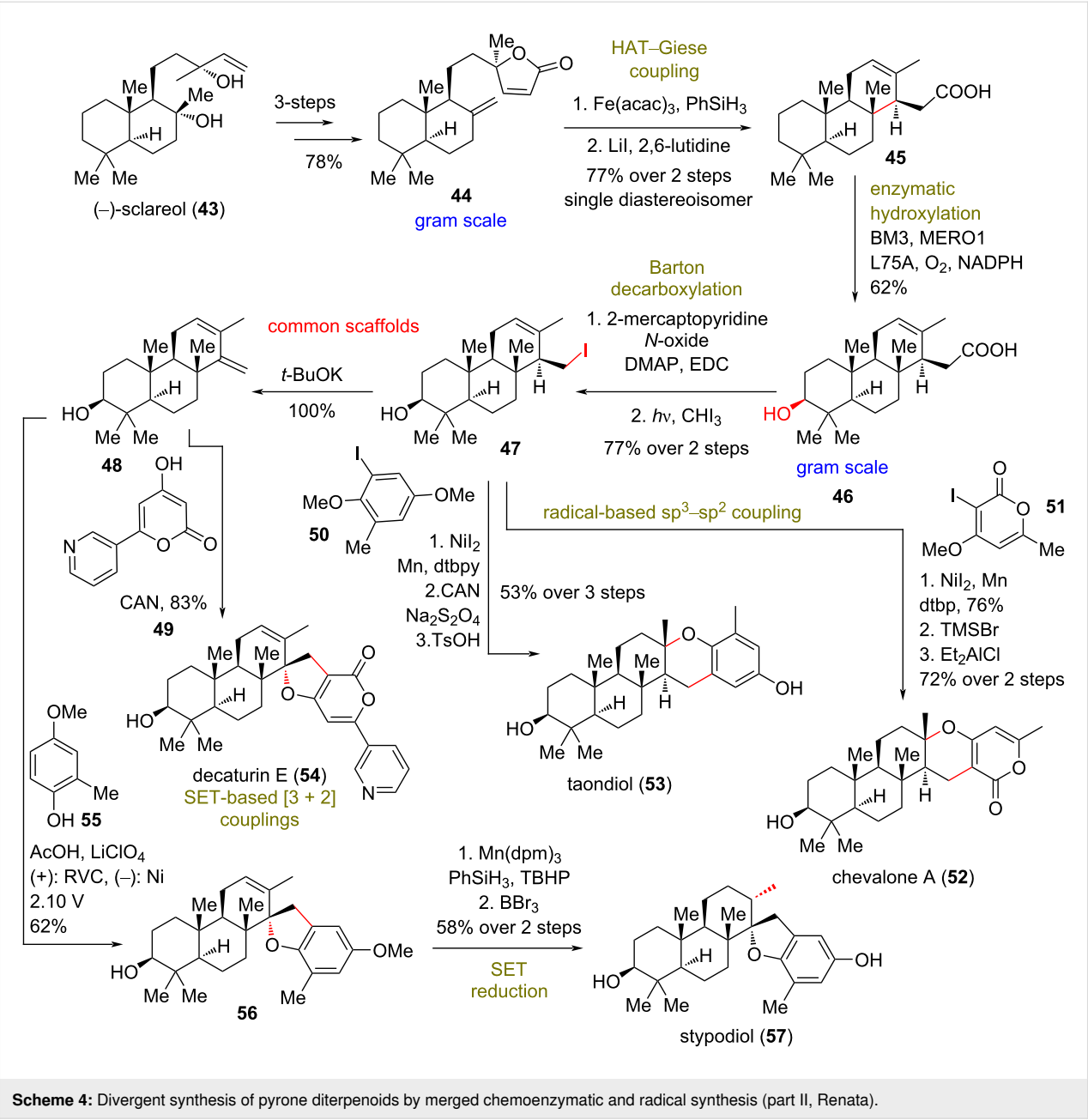

Scheme 4: Divergent synthesis of pyrone diterpenoids by merged chemoenzymatic and radical synthesis (part II, Renata).

(Scheme 3) [30]. HAT reductions of the C9–C11 alkene followed to deliver arisugacin F (**35**), phenylpyropene C (**36**), pyripyropene E (**38**), and phenylpyropene F (**41**). The steric bulk of the manganese catalyst employed suppressed the undesired reaction with tetrasubstituted alkenes and led to the exclusive reaction of the desired trisubstituted alkene due to stabilization of the incipient radical at C9. Furthermore, HAT reduction served to only deliver the thermodynamic product of the *trans*-decalin. Similarly, the C9–C11 alkene can serve as an ideal handle to C11-hydroxylated products, such as **42**, through a Mukaiyama hydration [20] to furnish natural complexity.

A similar approach was devised for the synthesis of modified meroterpenoids chevalone A (**52**), taondiol (**53**), decaturin E (**54**), and stypodiol (**57**, Scheme 4). For this purpose, tricycle **45** was prepared from compound **44** in gram-scale quantities by HAT–Giese coupling, followed by reductive cleavage of the lactone moiety with LiI. Enzymatic hydroxylation by the BM3 MERO1 variant worked equally well to provide the 3-hydroxylated product **46**. Photochemical radical decarboxylation of the formed mercaptopyridine derivative and radical capture by iodoform led to common scaffolds **47** and diene **48** after subsequent elimination. Those molecules serve as templates for Ni-based radical-based sp^3–sp^2 coupling and single-electron

transfer (SET)-based [3 + 2] coupling, respectively (Scheme 4). Initial attempts to realize the [3 + 2] radical coupling with CAN led to competitive oxidation of the C3 alcohol to the respective ketone. Increasing the equivalents of pyrone led to 83% of **54**. On the other hand, employment of the same conditions to phenol **55** resulted only in the oxidation of the phenol. A more controlled delivery of electrons was realized by applying an electrochemical method to provide the desired coupling towards **56** in 62% yield. Radical reduction by $Mn(dpm)_3$ afforded stypodiol (**57**) after BBr_3-mediated deprotection. Nickel-catalyzed coupling under a Weix procedure [31] was selected in order to elaborate the cores of taondiol (**53**) and chevalone A (**52**) as the radical cross-coupling employing redox-active esters of carboxylic acid **46** proved unsuccessful. The coupling was followed by an acid-catalyzed cyclization to yield the pyrone core of the natural products. The divergent plan described provided various meroterpenoids in 7–12 steps, comprising one of the most concise methods to attain this class of compounds, highlighting the power of merged biocatalytic and radical tactics [32].

(+)-Yahazunol (**61**) and related meroterpenoids

(Li 2018) [33]**:** In 2018, Li's group reported a divergent plan for the synthesis of drimane-type hydroquinone meroterpenoids. This class of compounds possesses versatile bioactivities, ranging from anticancer and anti-HIV to antifungal properties, with minor modifications on the decoration of either the hydroquinone or the terpene part of the secondary metabolite [34]. The group applied a semisynthetic plan starting from (−)-sclareol (**43**) to access the common synthetic intermediate of (+)-yahazunol (**61**), inspired by prior work of Baran's group on divergent synthesis of meroterpenoids utilizing boronosclareolide (Scheme 5) [35]. Li's group instead utilized compound **58**, readily available by the oxidative degradation of (−)-sclareol (**43**) [36] as the precursor to a photolabile Barton ester **59**. When the latter was irradiated at 250 W in the presence of benzoquinone, a decarboxylated coupling occurred, yielding semiquinone **60**, few steps away from the common scaffold **61**. Following this protocol, researchers managed to synthesize more than 4 g of the natural product (+)-yahazunol (**61**). (+)-Yahazunol (**61**) can be readily transformed to several members of meroterpenoids of the class, either by Friedel−Crafts reactions or common oxidative manipulations.

Total synthesis of dysideanone B (**75**) and dysiherbol A (**79**)

(Lu 2021) [37]**:** Dysideanone B (**75**), isolated from the South China Sea sponge *Dysidea avara*, possesses an unprecedented 6/6/6/6-fused tetracycle with interesting anticancer properties against HeLa and HepG2 cancer cell lines (Scheme 6) [38]. The structurally similar dysiherbols **79** and **80**, bearing a 6/6/5/6-fused tetracycle instead, were reported to possess NF-kB-inhibitory activity and anticancer activity against NCI H-929 cancer cell lines (Scheme 6) [39]. In 2021 Lu's group reported the total synthesis of members of both meroterpenoid families based on a highly chemoselective α-alkylation in the thermodynamic position of a Wieland−Miescher ketone derivative **68** with benzyl bromide **69**. Despite the challenging O- and C7-alkylations that required suppression, the desired C9-alkylation was achieved in 72% yield under thermodynamically controlled conditions (*t*-BuOK in THF at −40 °C). This coupled the terpene and the aromatic moieties present in these natural products and provided the common synthetic intermediate **70** (Scheme 6). The diverse tetracycles were accessed either via an intramolecular radical cyclization of the reduced congener **73** or through a Heck reaction of intermediate **71**. Reaction of **73** with Bu_3SnH in the presence of AIBN as initiator provided the tetracyclic core of dysideanones. The late introduction of an ethoxy group completed the total synthesis of dysideanone B (**75**) and "dysideanone F" (**76**). Ring closure to the dysiherbol scaffold was a much more challenging task as the classic conditions of the Heck reaction to common scaffold **70** proved unsuccessful. Screening of several reaction conditions on different analogues led to the conclusion that reduction of the C8-carbonyl side and acetal deprotection to **71** are essential in order to create the 6/6/5/6-carbocycle in the presence of $Pd_2(dba)_3$, SPhos, and Et_3N in 86% yield. Reduction of the double bond with Pd/C followed by dual Stille coupling for the introduction of two methyl groups and Mukaiyama hydration utilizing $Mn(dpm)_3$ and $PhSiH_3$ furnished the misassigned structure for dysiherbol A (**79**). A revised structure was finally assigned after deprotection with BBr_3 to complete the first total synthesis of dysiherbol A (**79**).

Total syntheses of (+)-jungermatrobrunin A (**89**) and related congeners

(Lei 2019) [40]**:** The *ent*-kaurane diterpenoids constitute a highly diverse class of structurally complex natural products possessing promising biological profiles, including anticancer, antifungal, and antiviral activities [41]. The highly diverse nature of the family makes a divergent synthesis extremely challenging, even for closely related members. Biosynthetically, the jungermannenone natural products have been proposed to derive from *ent*-kaurane diterpenoids through carbocationic rearrangements [42]. Jungermatrobrunin A (**89**) [43] bears a highly oxidized scaffold with a unique bicyclo[3.2.1]octene backbone and an unprecedented peroxide bridge (Scheme 7). Natural product (−)-1α,6α-diacetoxyjungermannenone C (**88**) [43] was projected by Lei's group as the common scaffold for the divergent synthesis of this class. Finally, the closely related

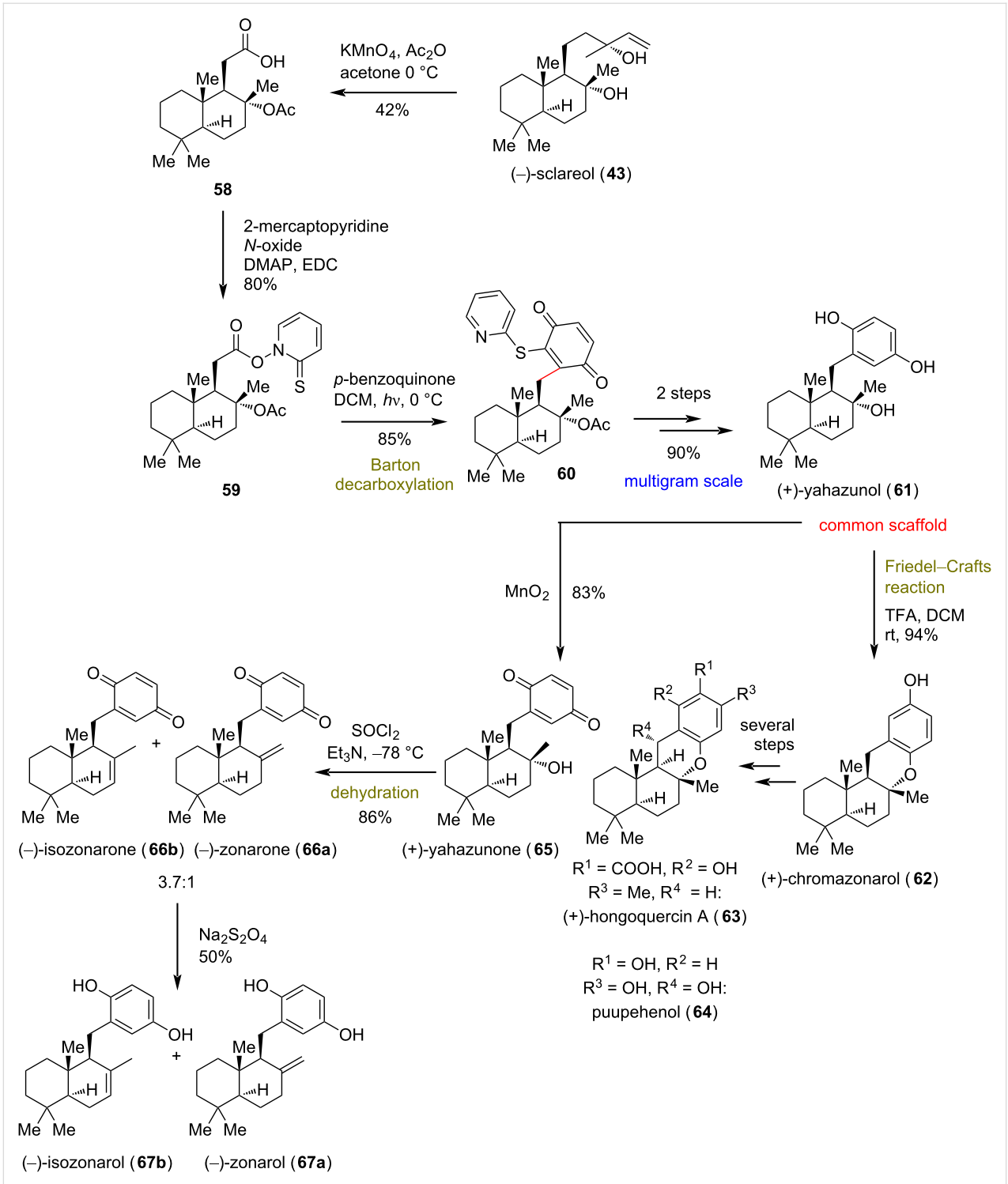

Scheme 5: Divergent synthesis of drimane-type hydroquinone meroterpenoids (Li).

congener **90** [43] was envisaged to originate by a radical rearrangement of the common scaffold **88**.

Initially, Lei's group unfolded the synthesis of **83** on a decagram scale, utilizing an asymmetric conjugate reaction of commercially available **81** and **82** using Fletcher's protocol (94% ee) [44]. A subsequent intramolecular arylation in the α-position of the ketone of **83**, catalyzed by a Pd(II)–NHC [45], followed by methylation, provided *cis*-decalin **84** (Scheme 7). Appropriate redox modifications allowed the delivery of *trans*-

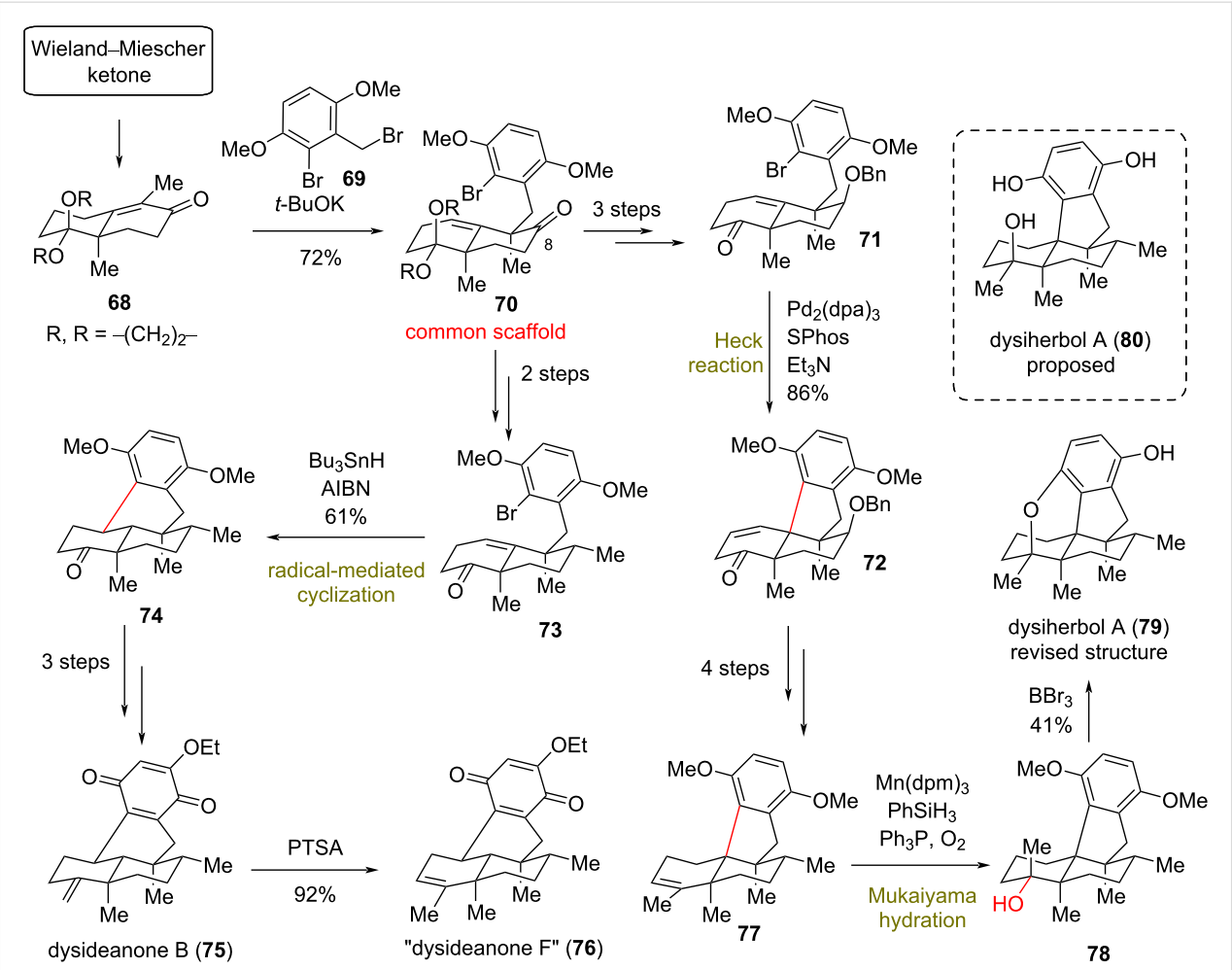

Scheme 6: Divergent synthesis of natural products isolated from *Dysidea avara* (Lu).

decalin **85** in a gram-scale quantity. Birch reduction of the electron-rich aromatic ring, followed by propargylic addition and functional group interconversion (FGI) provided dienyne **86**. Compound **86**, under the previously developed radical reductive cyclization for 1,6-dienyne cyclization (using Bu_3SnH and AIBN) [46], led to the construction of the key bicyclo[3.2.1]octene carbocyclic core of jungermatrobrunin, which was further elaborated to **87** in up to 61% yield, after alkene cleavage by OsO_4 and $NaIO_4$. The described reductive radical cyclization can be scaled up to 2 g without substantial decrease of the product yield. FGI, followed by methylenation provided the common scaffold **88**. Further elaboration of **88** to natural products **90** and **89** was accomplished by UV irradiation at 365 nm in MeOH and by utilizing singlet oxygen (using rose Bengal) in MeCN/pyridine, 40:1, respectively. Interestingly, irradiation at 365 nm even in the presence of photosensitizer and O_2 failed to furnish (+)-jungermatrobrunin A (**89**), and **90** was obtained as the sole product, albeit in low yield (14%). Attempts to optimize the yield always afforded recovered **88**, hinting at a potential equilibrium between **88** and **90**.

Total syntheses of magninoids and guignardones

(Lou 2021) [47]**:** Magninoids and guignardones are two classes of biogenetically related meroterpenoids, bearing a highly substituted cyclopentane moiety and a 6-oxabicyclo[3.2.1]octane fragment [48,49]. These classes exhibit diverse biological properties, such as potent inhibition of 11-β-hydroxysteroid dehydrogenase type I and inhibition of *Candida albicans* [48]. Although earlier syntheses have been reported recently for magninoids [50,51], Lou's group envisioned a divergent plan based on a late-stage bioinspired semipinacol rearrangement–cyclization of common synthetic intermediates **94** and **95** (Scheme 8). Compound **94** was obtained in three steps, with the key step being the Suzuki–Miyaura coupling of appropriately functionalized precursors **91** and **92** using Romo and co-worker's protocol [52]. Reaction of **94** under PPTS acidic

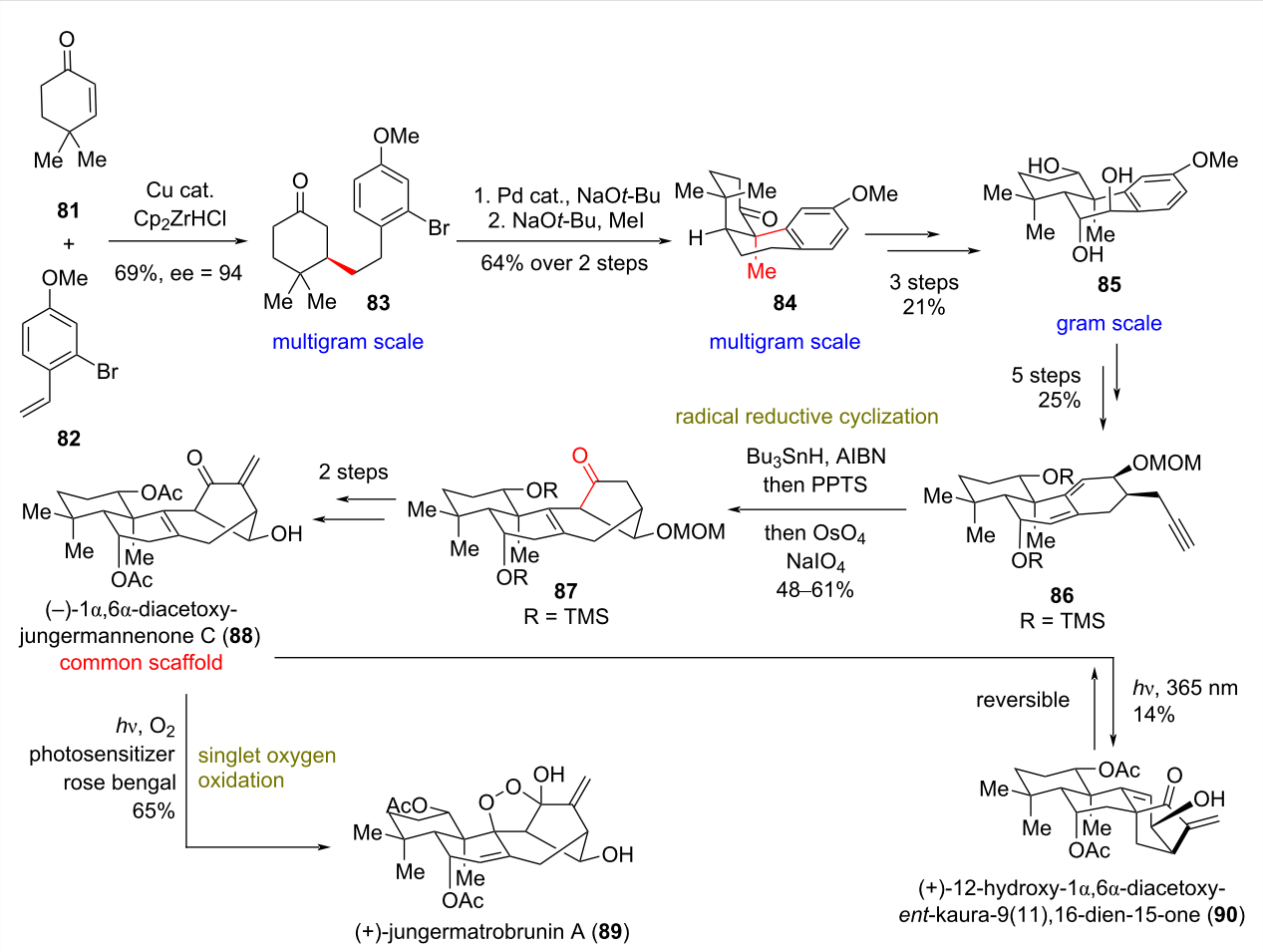

Scheme 7: Divergent synthesis of kaurene-type terpenoids (Lei).

conditions initiated a semipinacol rearrangement leading to **95**, followed by subsequent cyclization to natural products guignardone A (**96**) and C (**97**). This process involved 1,2-allyl migration and C–O bond formation through a semipinacol rearrangement and a cyclodehydration cascade reaction (Scheme 8).

Following the same rationale, **94** was diverted to produce **100** after basic deprotection of the nonisolated **95**. The radical oxidation of the former in the presence of dioxygen and sunlight or a catalytic amount of $Mn(OAc)_3$ led to the creation of the compounds **101** and **102**. FGI, followed by the cleavage of the hydroperoxide bond and final dehydration by Burgess reagent provided the total syntheses of magninoids A (**104**) and C (**103**, Scheme 8).

Divergent total synthesis of crinipellins

(Xie and Ding 2022) [53]**:** Crinipellins are highly congested tetraquinane natural products comprising 6–10 stereogenic centers, three of which are consecutive all-carbon quaternary carbon atoms [54-56]. Preliminary biological screening of this family revealed notable antibacterial and anticancer activities due to the α-methylene lactone moiety they bear [57]. Recently, in order to synthesize the common core present in crinipellins, Xie and Ding's groups developed an approach using an unprecedented ring distortion. Their strategy consisted of a metal-catalyzed HAT to the *exo*-Δ-alkene of the 5/5/6/5 tetracycle **109**, so as to subsequently favor a Dowd–Beckwith rearrangement [58] towards the tetraquinane skeleton of **112** (Scheme 9). The synthesis commenced with the generation of **107** from cyclopentenone **105** and aryl aldehyde **106** in a three-step sequence. An oxidative dearomatization induced a [5 + 2] cycloaddition–pinacol rearrangement of **107** to **109**, according to previous studies of the same group (Scheme 9) [59-61]. The key HAT-mediated rearrangement was realized in an impressive yield of 95% to obtain **112** on a gram-scale, when cobalt complex C6 was used in the presence of $PhSiH_3$ and TBHP in isopropanol. Further modifications of **112** led to the common scaffold **113** in 47% yield, which could be readily transformed to several crinipellin natural products by chemoselective redox reactions.

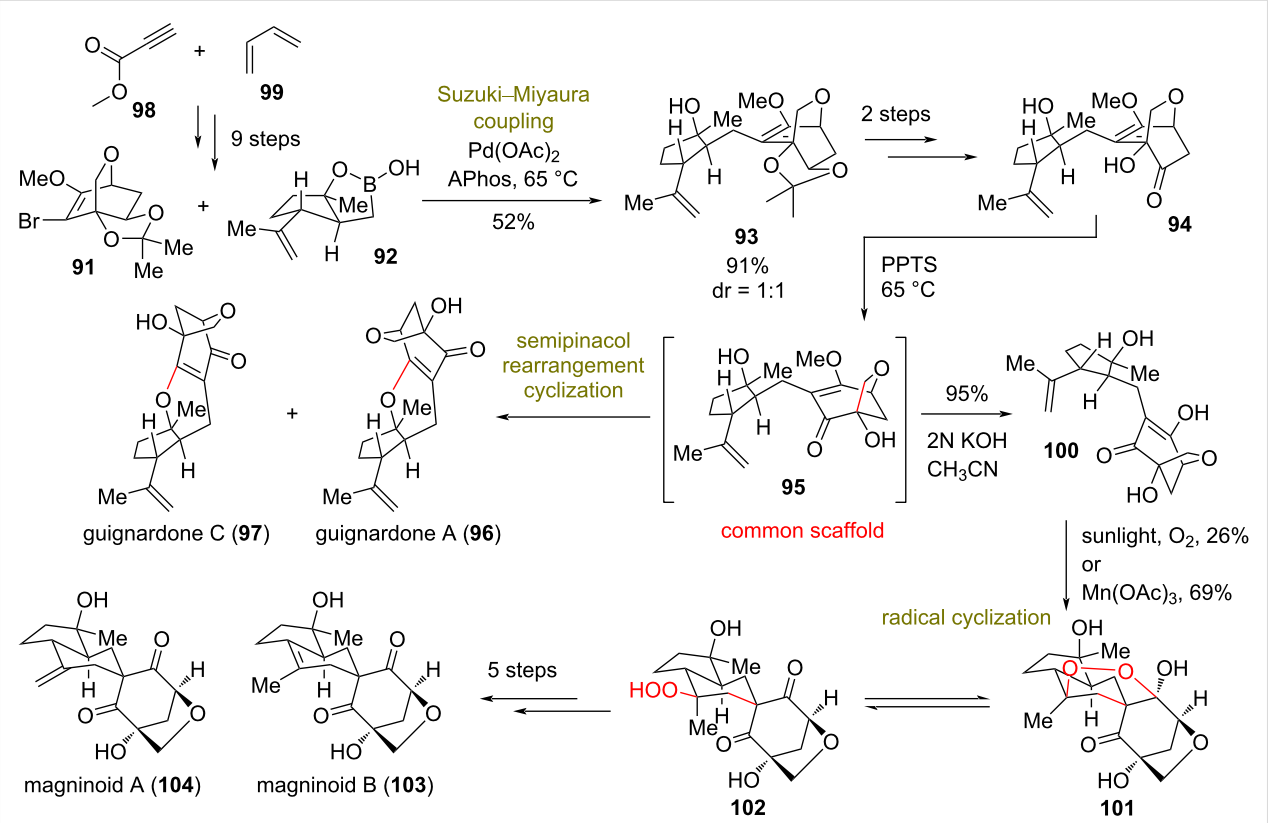

Scheme 8: Divergent synthesis of 6-oxabicyclo[3.2.1]octane meroterpenoids (Lou).

Divergent total synthesis of *Galbulimima* alkaloids

(Shenvi 2022) [62]**:** Members of the *Galbulimima* alkaloids extracted from rainforest canopy trees were found to possess neuroactive properties, such as antagonistic activity at muscarinic receptors [63], psychotropic activity, and antiplasmodic activity [64]. Their structural diversity, consisting of different connectivities between piperidine and decalin domains, is especially difficult to be divergently accessed. Shenvi's group recognized that an aromatic congener within this class could be traced back to aromatic common intermediate **9** (Scheme 10). Despite the simplicity, the most obvious disconnections, such as an anionic enone conjugated addition and a direct cationic Friedel–Crafts reaction failed. Highlighting the power of radical disconnection, the group thought of utilizing a β-keto carbon-centered radical to circumvent the unsuccessful Friedel–Crafts reaction. Prior reports implicated β-keto radical formation in the ring opening of siloxycyclopropanes with photoinduced electron transfer (PET) to 1,4-dicyanonaphthalene [65]. Inspired by reports on dual photoredox and Ni-catalytic cross-coupling platforms [66], the group considered a system in which a photoexcited catalyst oxidatively cleaves a siloxycyclopropane with endo selectivity [67], leading to aryl–nickel capture and reductive elimination. Thus, when substrates **121** and **122** were photoirradiated with blue LED light at 45 °C in the presence of lutidine base, 7 mol % organic photocatalyst 4CzIPN, 30 mol % $NiBr_2$, and 30 mol % bpy provided 57% of **9**. Intramolecular Friedel–Crafts reaction by Et_2AlCl and HFIP complex led to **123**, possessing the correct connectivity for the divergent synthesis of the family. Choreographically executed sequential reduction steps allowed the total synthesis of GB13 (**8**), himgaline (**126**), and GB22 (**125**) in only one third of the number of steps of prior syntheses (Scheme 10).

Concise syntheses of eburnane alkaloids

(Qin 2018) [68,69]**:** Eburnane indole alkaloids comprise a highly diverse class of natural products mainly distributed in Southeast Asia and China [70]. Compounds of this class are traditionally used for detoxification and as anti-inflammatory agents in Chinese medicine [71]. Qin and co-workers reported the asymmetric total syntheses of several eburnane alkaloids. Therein, they relied on one of their previous discoveries, namely a photoredox-catalytic nitrogen-centered radical cascade [72], which has resulted in the impressive collective total synthesis of 33 alkaloids of three different classes of indole natural products (please see the inset of Scheme 11 for concise representation). Specifically, this included (–)-eburnaminol (**132**), (+)-larutenine (**133**), (–)-terengganensine B (**134**), and

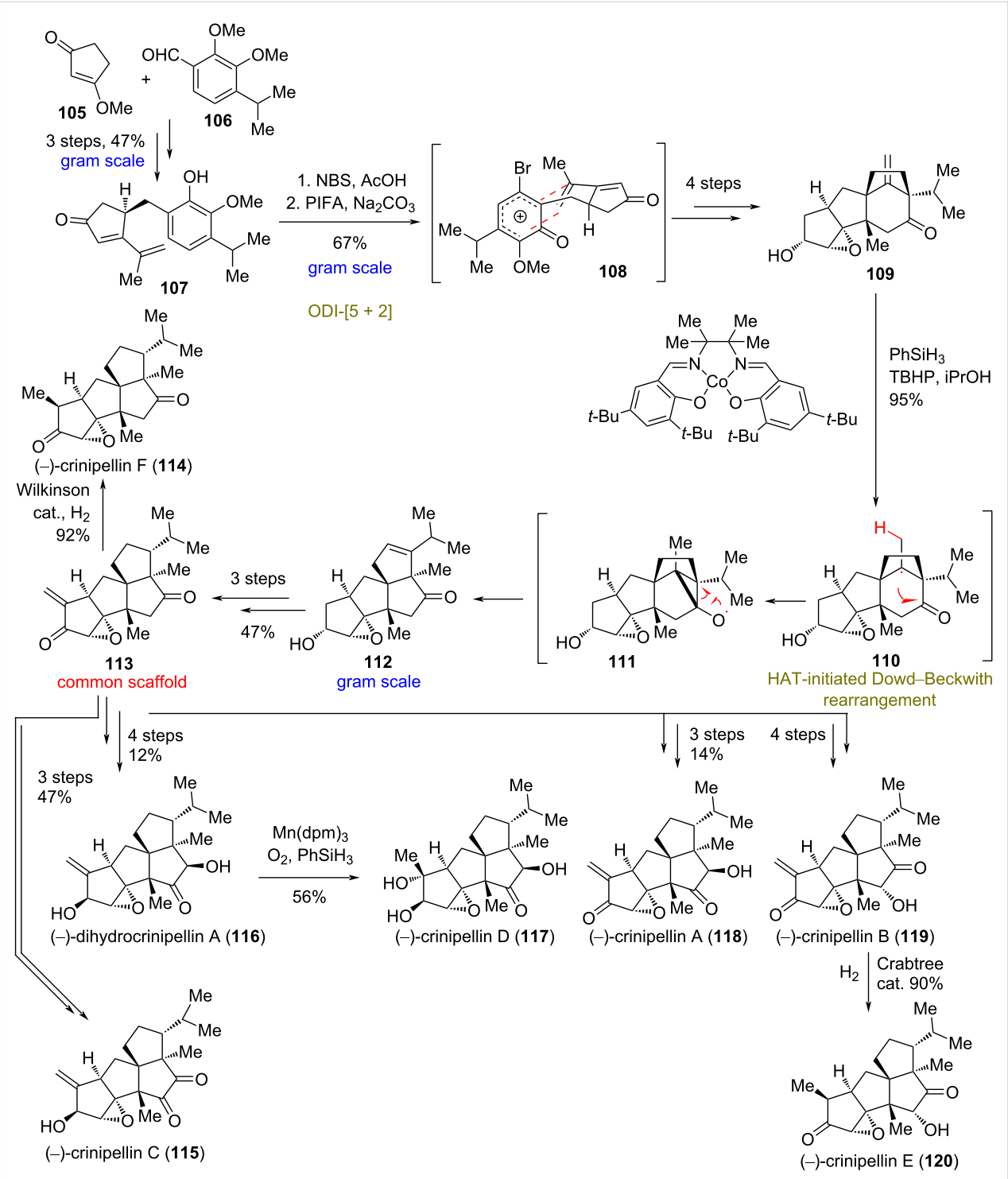

Scheme 9: Divergent synthesis of crinipellins by radical-mediated Dowd–Backwith rearrangement (Xie and Ding).

(–)-strempeliopine (**136**), as well as the asymmetric formal total synthesis of (–)-terengganensine A (not shown, Scheme 11). The requisite common synthetic intermediate **129** for the cascade was accessed by an acid-promoted condensation of chiral aldehyde **127** and Boc-protected amine **128**, followed by zinc reduction of the nitro group and subsequent protection of the amine by a tosyl group in 27% overall yield. Irradiating **129** with blue light at 30 W in the presence of 1 mol % of $[Ir(dtbbpy)(ppy)_2]PF_6$ and 5 equiv of $KHCO_3$ in THF resulted in the radical formation of the tetracyclic core of **130** in 75%

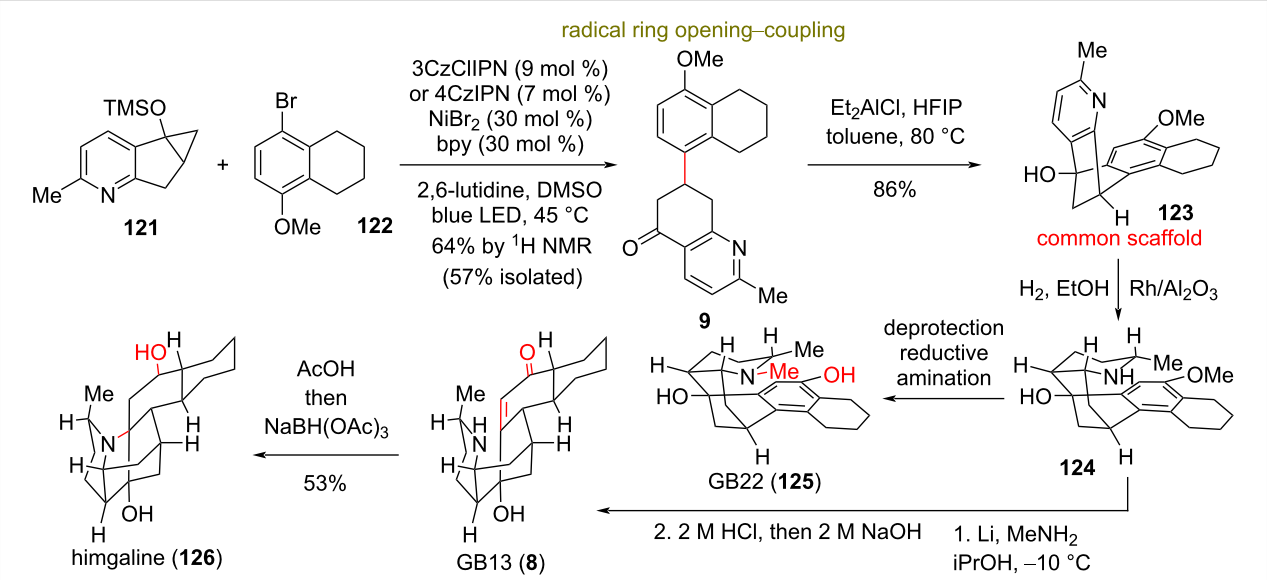

Scheme 10: Divergent total synthesis of *Galbulimima* alkaloids (Shenvi).

yield as a mixture of two diastereoisomers (dr = 3:2) that were both used to access natural products. Impressively, the protocol allowed the installation of three rings and the stereoselective introduction of chiral centers at C2 and C21 for the final targets. With regard to the mechanism, it is hypothesized that it commences with the formation of a nitrogen-centered radical. The carbon radical **139** is then formed after the aforementioned nitrogen radical attacks the enamide group. The α-amide positioning is theorized to improve drastically the radical stability, nucleophilicity, and selectivity of **139** [73]. Furnishing of the common scaffold **130** can be carried out via an attack of intermediates of this type (e.g., **139**) on Michael acceptors. Tosyl group deprotection of **130**, followed by selenium anhydride oxidation and catalytic reduction of the amide using Wilkinson's catalyst provided diastereoisomeric indole **131**. Careful manipulation of the nitrile and alcohol side chains allowed selective cyclizations to the nitrogen atom of the indole core to conclude the total syntheses of **132**–**134**. Samarium diiodide-mediated reductive cyclization of aldehyde **135**, obtained also from **131**, provided the pentacyclic core of (−)-strempeliopine (**136**) as a single diastereoisomer in 65% yield. Then, Barton's radical deoxygenation resulted in the total synthesis of **136**. Further, FGI of both diastereoisomers of **130** allowed the formal synthesis of (−)-terengganensine A (not shown) under the same divergent plan (Scheme 11).

Divergent total synthesis of (−)-pseudocopsinine (**149**) and (−)-minovincinine (**150**)

(Boger 2020) [74]**:** (−)-Pseudocopsinine (**149**) was isolated from *Vinca erecta*, with a structure related to the *Aspidosperma* alkaloids, containing an additional C20–C2 bond (Scheme 12) [75]. In 2020, Boger's group reported the first total synthesis of (−)-pseudocopsinine (**149**) and (−)-minovincinine (**150**) from a common intermediate **146**, featuring a late-stage HAT strategy to assemble the highly congested carbocyclic core of these natural products (Scheme 12). Based on earlier studies of the group on the total synthesis of vinblastine and related natural congeners [76], the authors realized that a late-stage formation of the C20–C2 bond would be highly strategic to provide the greatest simplification to these targets. The *Aspidosperma* skeleton **146** of both natural products was accessed in a single step from **145** through a scalable tandem [4 + 2]–[3 + 2] cascade in 74–84% yield in gram-scale quantities, known from previous studies [77]. Compound **145** was readily prepared in four steps from *N*-benzyltryptamine and 4-(2-*t*-butyldimethylsilyloxy)pent-4-enoic acid, requiring only two purification steps [77]. FGI of **146** led to (−)-enantiomer **147**, which serves as the radical point od divergence of this plan. HAT-initiated transannular free-radical cyclization of (−)-enantiomer **147** according to Baran's protocols [78] provided the benzyl-protected (−)-pseudocopsinine **148** in 60% yield, when **147** was treated with $PhSiH_3$ in the presence of $Fe(acac)_3$. Notably, the reaction provided a diastereoselectivity of 3:1 for the formation of the C20-stereocenter and exclusive formation of the C3-center. Key to this success is the low level of Fe(III)–H generation, thus minimizing intermediate radical reduction. The observed diastereoselectivity can be rationalized by referring to earlier mechanistic studies [79]. The same (−)-configured intermediate **147** was utilized in a HAT-initiated oxidation to access (−)-minovincinine (**150**) in 38% yield after deprotection (Scheme 12). Interestingly, the classic Mukaiyama conditions

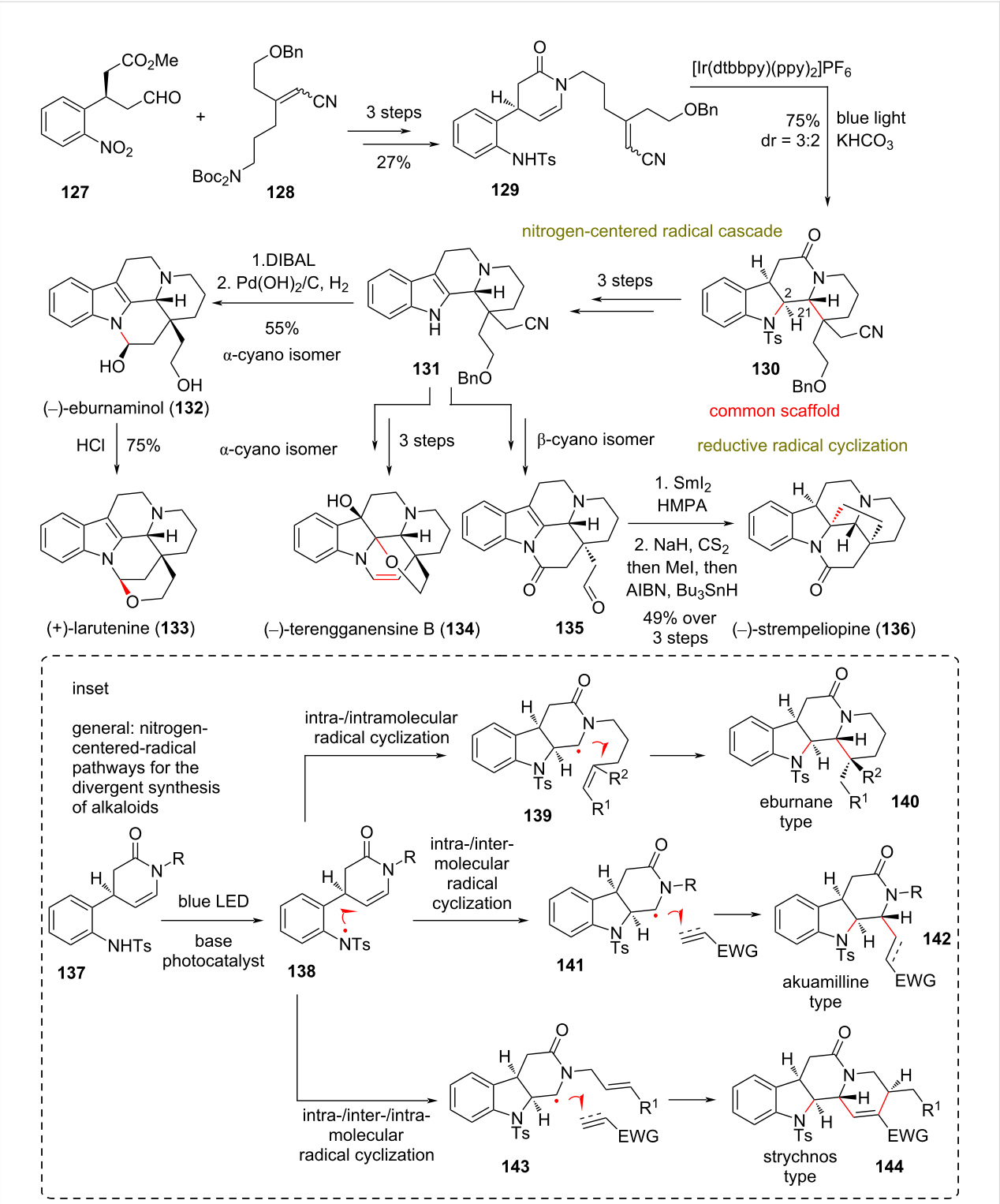

Scheme 11: Divergent synthesis of eburnane alkaloids (Qin).

using $Co(acac)_2$ with $PhSiH_3$ provided compound **152** as the only isomer which, upon reduction, led to the exclusive formation of the compound *epi*-minovincinine (**151**). Replacement of $Co(acac)_2$ with Co complex **A** suppressed the formation of **152** and provided the desired **150** and the isomer as an almost 1:1 mixture.

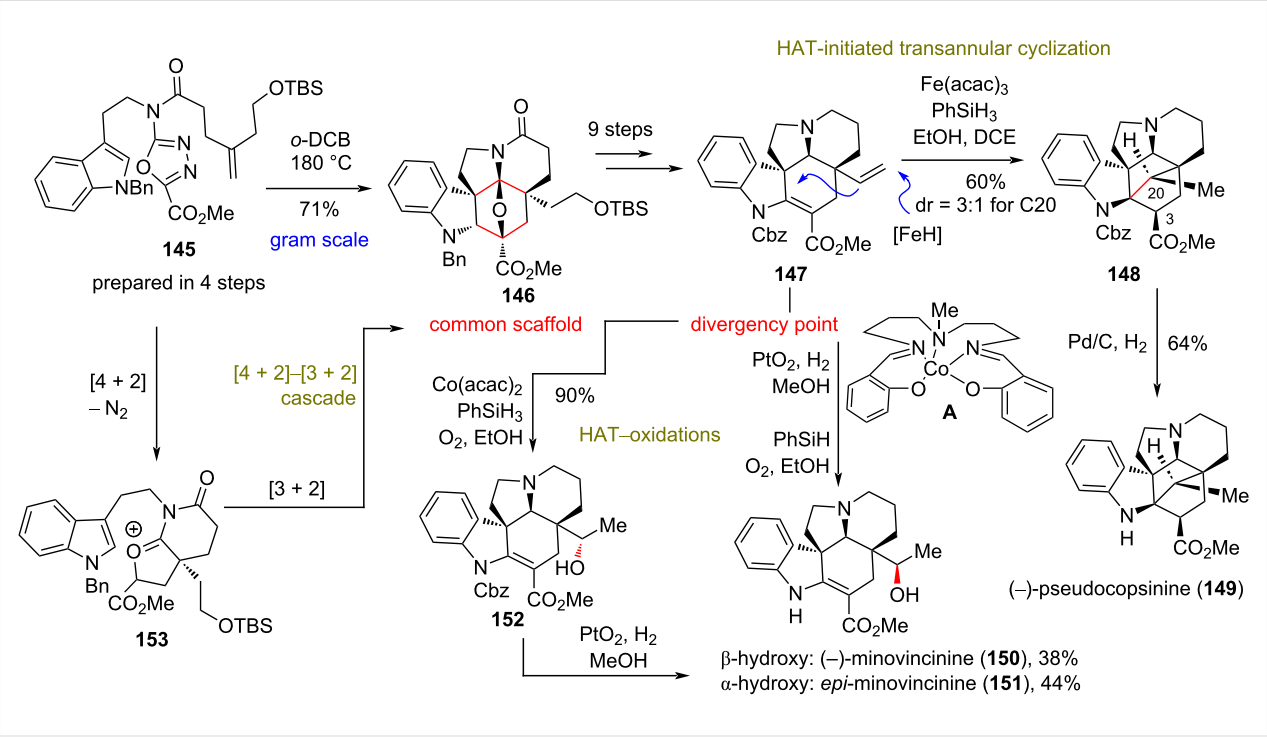

Scheme 12: Divergent synthesis of *Aspidosperma* alkaloids (Boger).

Syntheses of (–)-FR901483 (**160**) and (+)-TAN1251C (**162**)

(Gaunt 2020) [80]**:** Nitrogen-spirocyclic natural products consist a common class of important pharmaceutical candidates. FR901483, which was isolated from the fermentation broth of *Cladobotryum sp.* No. 11231, exhibits impressively potent immunosuppressant activity. This has resulted in extensive synthetic efforts towards the compound, in order to meet the needs for the supply as a potential therapeutic for the treatment of arthritis, Crohn's disease, and organ transplant rejection [81]. The TAN1251 natural products, on the other hand, show potent activity as muscarinic antagonists, with potential applications as antispasmodic and antiulcer agents [82]. Despite the synthetic efforts on these natural products [83-86], in 2020, Gaunt's group recognized a novel common synthetic intermediate in the structure of spirolactam **157** to access the family (Scheme 13). To synthesize it, they conjectured that a tyrosine amino acid, a cyclohexadione derivative, and a nonracemic dehydroalanine derivative could be effectively combined to build the core structure, using an already known iridium-photocatalyzed radical reaction [87]. Indeed, when L-tyrosine methyl ester (**154**), 1,4-cyclohexanedione monoethylene acetal (**155**), and dehydroalanine derivative **156** were allowed to react in the presence of TFA, molecular sieves, 1 mol % of *fac*-Ir(ppy)$_3$, and Hantzsch ester under blue LED irradiation at 40 W, this resulted in the formation of spirolactam **157** in 73% yield (Scheme 13). The reaction is estimated to take place initially with the one electron reduction to α-amino radical **164**. This step is thought to be facilitated after TFA protonates the formed imine. Afterwards, radical addition of **164** to **156**, generates an α-carbonyl species. A HAT from Hantzsch ester, which takes place diastereoselectively from the more accessible face, afforded the lactone **158**. Spirolactam **157** can effortlessly be produced after the cyclization of the aforementioned lactone. Redox manipulations from this point on brought about the total synthesis of (−)-FR901483 (**160**) through an aldol reaction, and an intramolecular condensation resulted in the synthesis of (+)-TAN1251C (**162**, Scheme 13).

Divergent synthesis of bipolamine alkaloids

(Maimone 2022) [88]**:** Bipolamines were isolated from the fungi *Curvularia sp.* IFB Z10 and *Bipolaris maydis* in 2014 and were reported to possess antibacterial activity against a small panel of both gram-positive and -negative bacteria [89,90]. Interestingly, their chemical structure bears no resemblance to recognize antibiotics and their mechanism of action remains unknown. Based on the knowledge gained from the first total synthesis of (−)-curvulamine (**171**) [91], Maimone's group leveraged their plan for accessing several members of this class (Scheme 14). The challenge this group had to address in this particular case was the high acid sensitivity and oxidative fragility of pyrrole intermediates. As common synthetic intermediate, the group utilized compound **170**, readily available in gram-scale quantity, through a modified previously reported se-

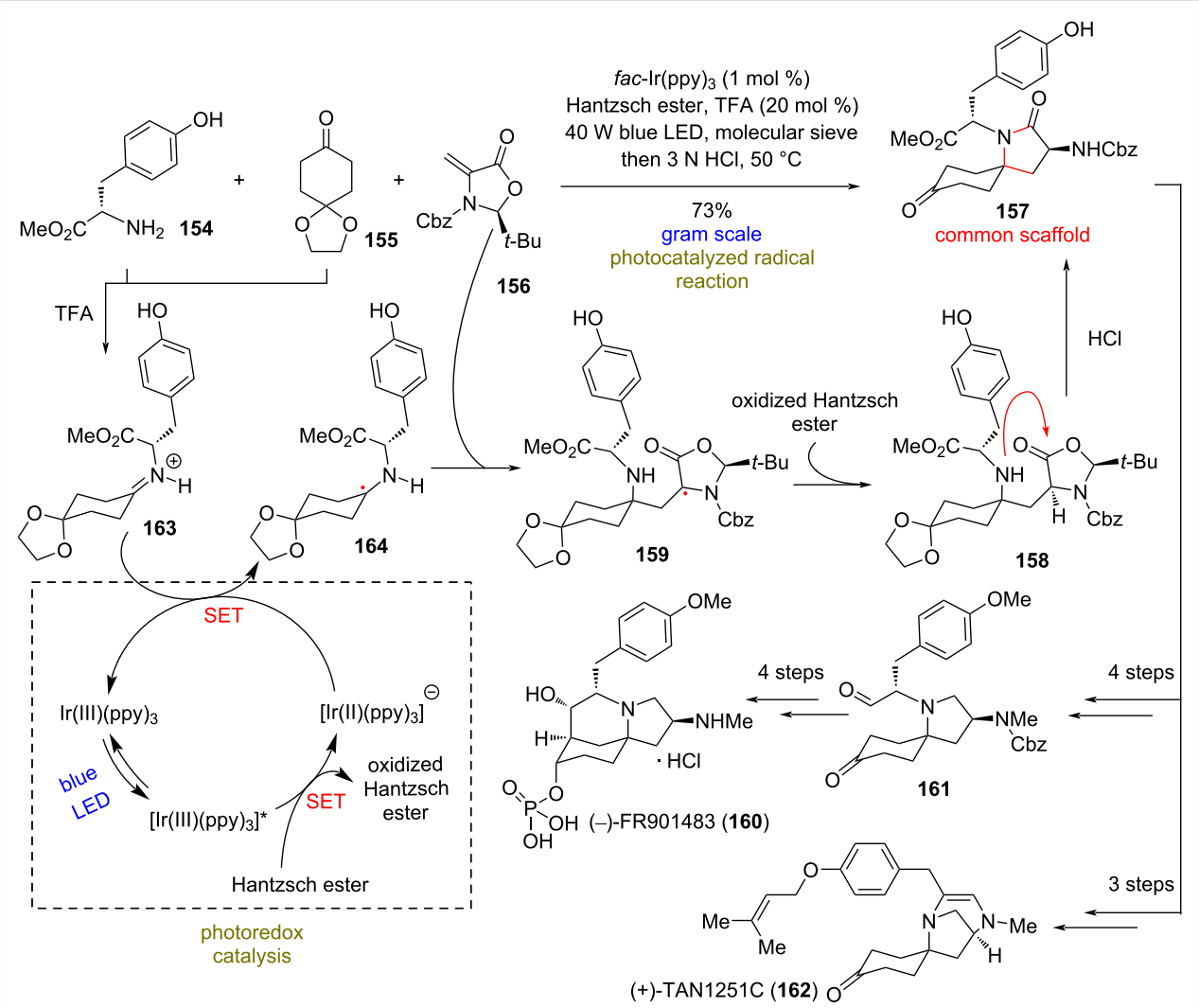

Scheme 13: Photoredox based synthesis of (–)-FR901483 (**160**) and (+)-TAN1251C (**162**, Gaunt).

quence [91]. The synthesis of the sterically constrained tetracyclic core of **170** relied initially on the photochemical radical cyclization of iodide **167** at 390 nm in the presence of $NaHCO_3$ in CH_3CN/*t*-BuOH, 5:1 to provide **168** in 55% yield (Scheme 14) [91]. Alkylation of the tetracycle, followed by epimerization of the C2 center and radical deoxygenation, or alternatively S_N2 etherification, provided the common scaffold **170**. The latter can serve as ideal diversification point to access (−)-curvulamine (**171**) by CBS reduction, bipolamines D (**173**) and E (**172**) by additional BH_3·DMS hydroboration, and bipolamine G (**174**) initially by dihydroxylation of the alkene moiety with osmium tetroxide, followed by acidic etherification and reduction. Finally, bipolamine I (**176**) was obtained from **169** via a samarium diiodide reduction of the mesylate, followed by sodium borohydride reduction of the ketone, hydroboration, and base-mediated cyclization.

Flow-controlled divergent synthesis of aporphine and morphinandienone natural products

(Felpin 2022) [92]**:** Reticuline-type alkaloid oxidative coupling is a well-established biosynthetic pathway that produces important pharmaceutical structures [93], such as (+)-corytuberine, (−)-codeine, (−)-morphine, (+)-sebiferine (**181**), etc., depending on the regioselectivity of the coupling (Scheme 15) [94]. During this process, two major families of natural compounds are formed, namely the aporphine and the morphinandienone alkaloids. Mimicking the selectivity of the natural process in laboratory setups commonly proves tricky, producing an irreproducible yield of isomers for both classes. Recently, Felpin's group reported the flow-controlled divergent synthesis of aporphine and morphinandienone alkaloids based on biomimetic common scaffolds (e.g., **180**) using hypervalent iodine(III) reagents. Capitalizing on previously reported mechanistic inves-

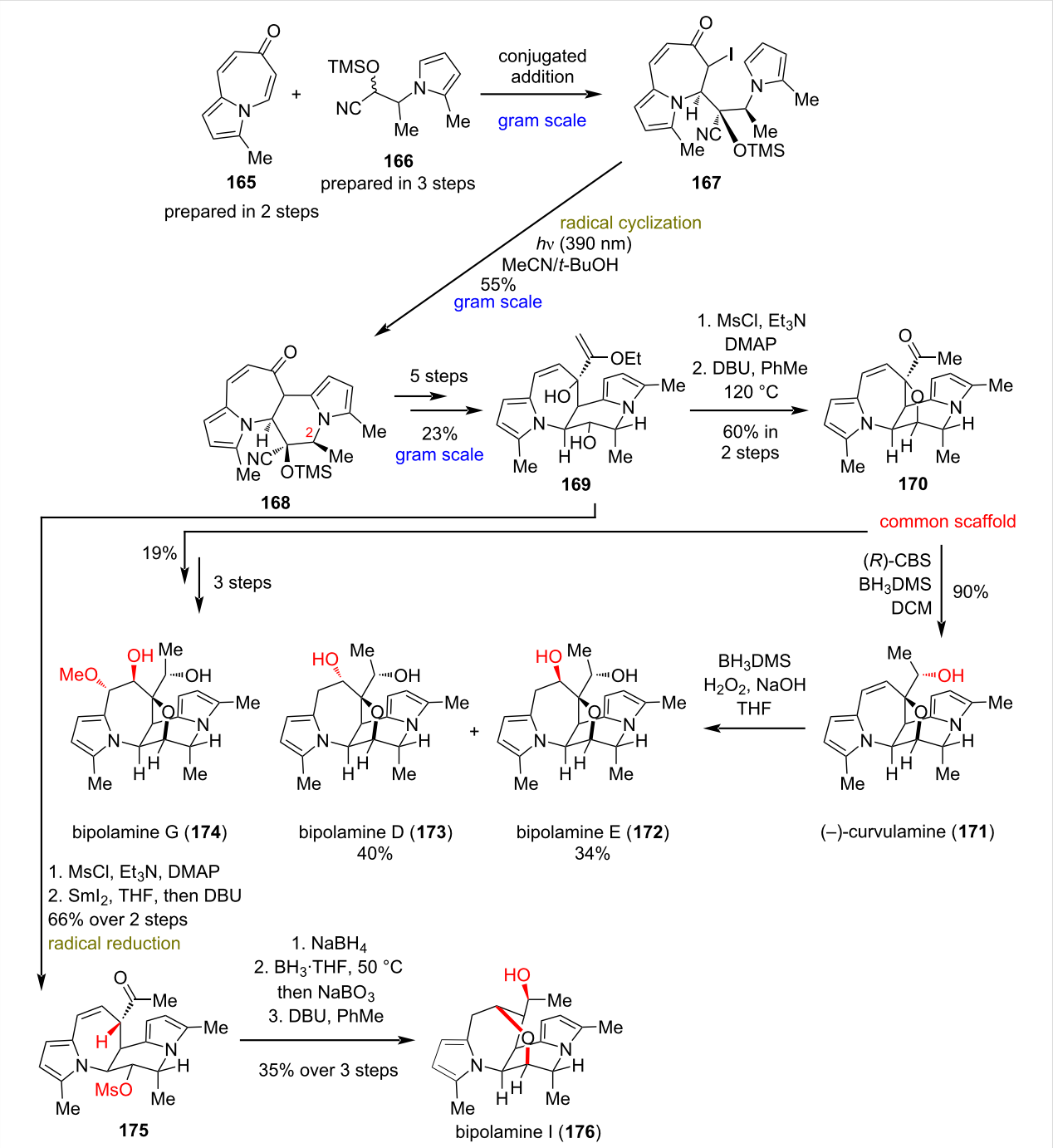

Scheme 14: Divergent synthesis of bipolamines (Maimone).

tigations, they assumed that **180** can rearrange to glaucine (**183**) through the erythrinadienone intermediate **182**. On contrary, common scaffold **180** should hydrolyze to sebiferine-type scaffolds in the presence of water. Taking these results into account, the group exploited the ability of HFIP to stabilize the radical cation formed by PIFA and $BF_3{\cdot}EtO_2$ [95,96] to selectively produce aporphine natural products, while the use of PIDA or PIFA in the presence of $BF_3{\cdot}OEt$ or TMSOTf in wet CH_3CN allows to diverge the synthesis to morphinandienone natural products (e.g., **181**, Scheme 15). The flow reaction was performed in a reaction coil at room temperature. Two reaction loops were used. The first one was loaded with the substrate and the second with PIFA and $BF_3{\cdot}EtO_2$, while HFIP was used as the solvent. The two streams were mixed in a T-mixer, equipped with a 250 µL frit, to ensure efficient mixing. Under the optimized conditions, the method provided aporphine prod-

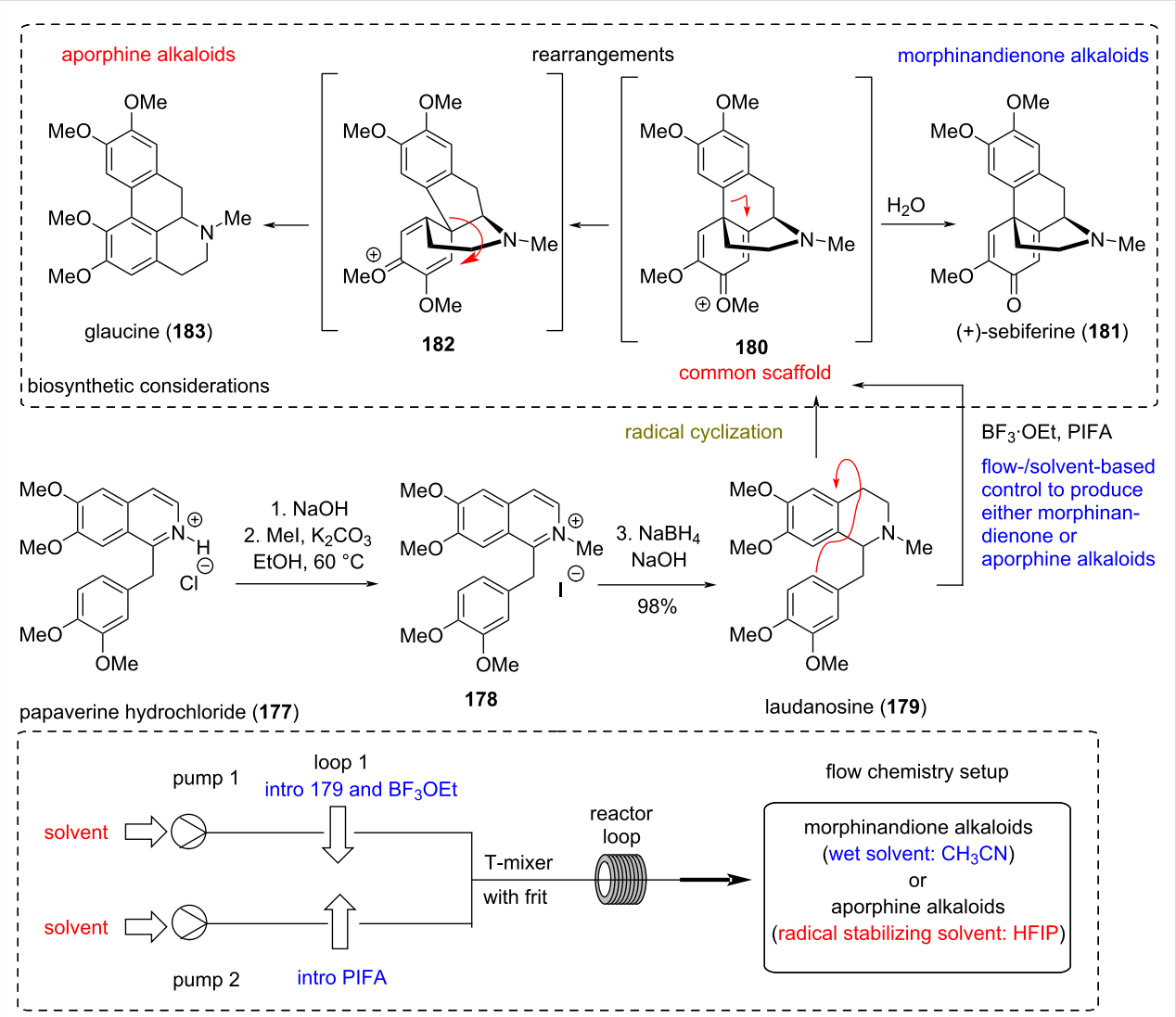

Scheme 15: Flow chemistry divergency between aporphine and morphinandione alkaloids (Felpin).

ucts in good to moderate yield, depending on the substrates used. Altering the solvent to wet CH_3CN allowed the efficient delivery of morphindienone compounds.

Pyrroloazocine natural products

(Echavarren 2018) [97]**:** In 2018, Echavarren's group reported the divergent synthesis of several pyrroloazocine alkaloids [98-100]. Preliminary biological screening indicates that members of this class are able to overcome multidrug resistance in vincristine resistant cells [98-100]. To access the common scaffold **188**, the group relied on an intramolecular gold-photocatalyzed radical-mediated cyclization of an α-keto radical to the pendant indole core, reported earlier in the total synthesis of lundurines A–C (Scheme 16) [101]. The authors postulate that photoexcitation of $[(dppmAuCl)_2]$ with 365 nm light serves as initiator for radical generation in the brominated position of **186**, prepared after following a 7-step sequence. The cyclization of the formed radical is 6-*exo-trig* and leads to the formation of a benzyl radical that is further oxidized to **188**. From this common scaffold, the group managed to access several natural products of the class, majorly by utilizing the ability of conjugated alkenes to be further oxidized, and thus producing the respective benzylic cation. Intramolecular cyclization in the cationic position under participation of the methyl ester function provided the core for (+)-grandilodine C (**191**) and (+)-lapidilectine B (**192**), while allylation of the benzylic position allowed oxidative decomposition to the core of **194** and **195**. FGI followed to complete targets **196**–**200** (Scheme 16).

Pyrroloindoline natural products

(Knowles 2018) [102]**:** In 2018, Knowles' group demonstrated the ability of TEMPO to act as a trap for radical cations arising

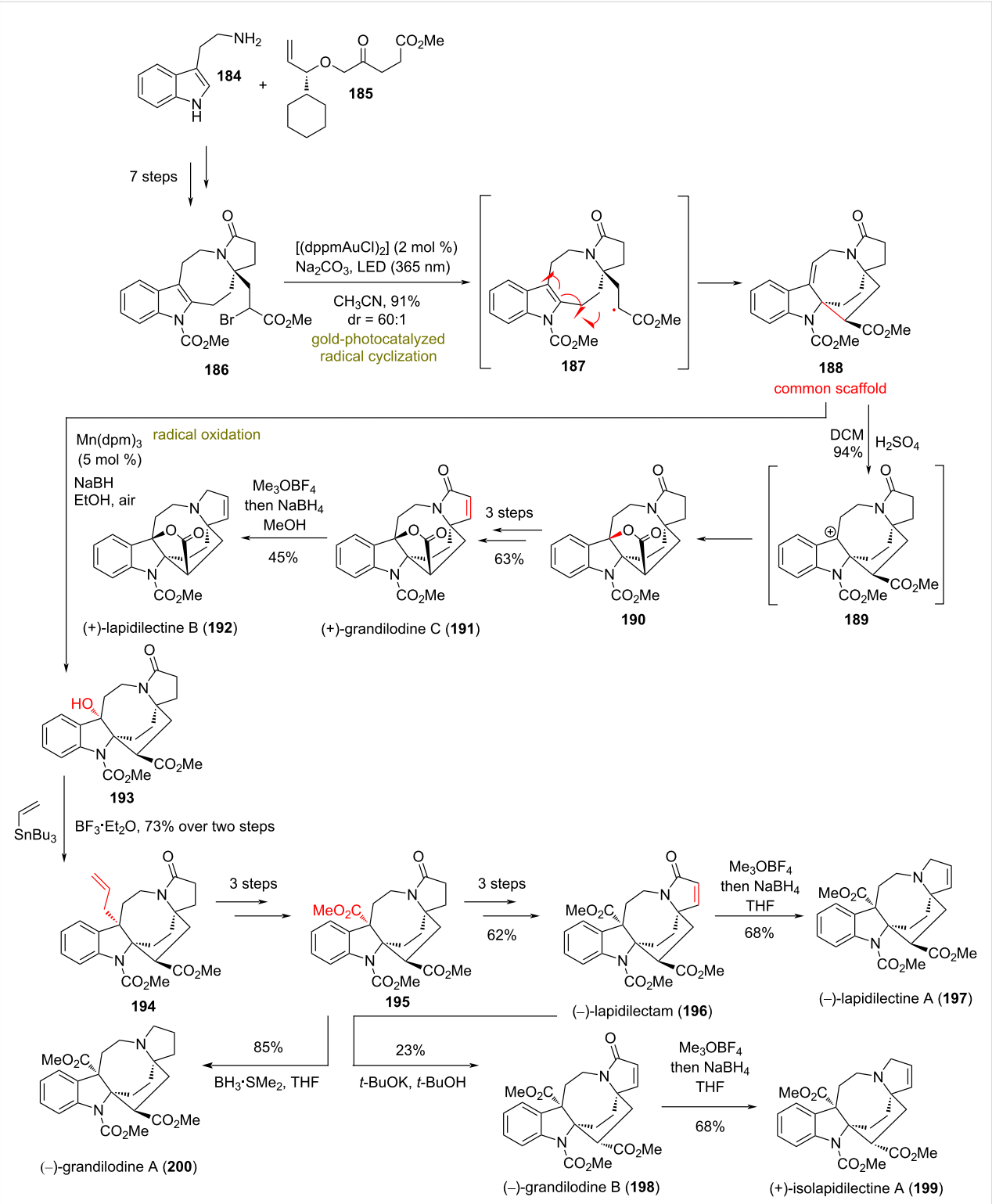

Scheme 16: Divergent synthesis of pyrroloazocine natural products (Echavarren).

from the single-electron oxidation of protected tryptamine starting materials. The utilization of a chiral phosphate base is essential for the formation of a hydrogen bond between phosphate and tryptamines, allowing the decrease of the oxidation potential. This concept was used for the synthesis of pyrroloindoline natural products (Scheme 17). Thus, upon irradiation,

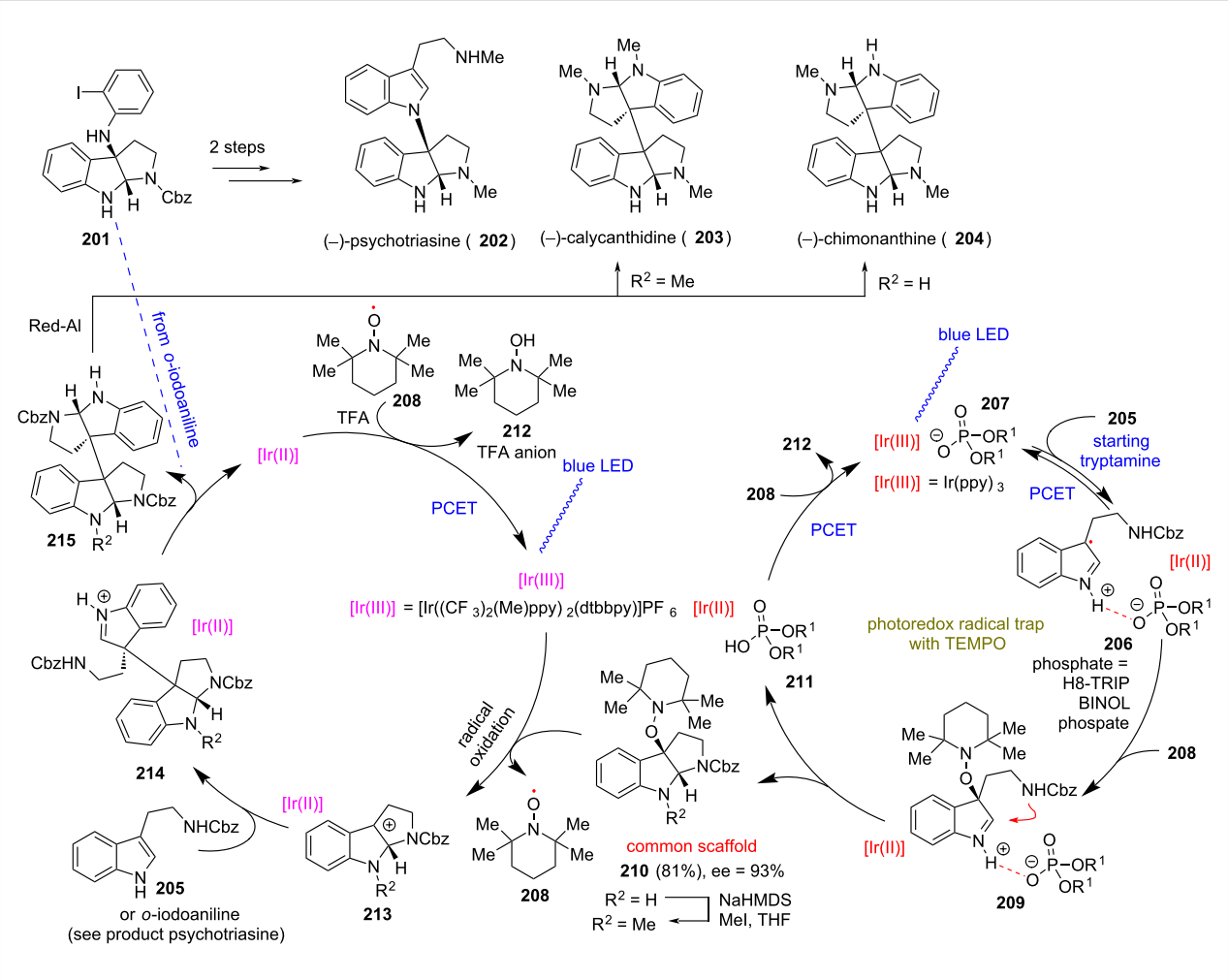

Scheme 17: Using TEMPO to stabilize radicals for the divergent synthesis of pyrroloindoline natural products (Knowles).

iridium polypyridyl photocatalyst allowed the oxidation of the phosphate complex **207** to radical cation **206**, which can be readily trapped by TEMPO, and hence stabilizing the imine and allowing cyclization with the pendant amine to form the pyrroloindoline core **210** in 81% yield and 93% ee. The latter can serve as a common scaffold to access an array of pyrroloindoline natural products but also synthetic analogues (Scheme 17). Oxidation of **210** by a second iridium photocatalyst yields benzyl cation **213**, which can undergo nucleophilic attack by tryptamine derivatives to allow the total synthesis of (−)-psychotriasine (**202**), (−)-calycanthidine (**203**), and (−)-chimonanthine (**204**).

Synthesis of structurally diverse lignans

(Zhu, 2022) [103]**:** Lignans are structurally diverse natural compounds generated biosynthetically by the oxidative dimerization of phenylpropanoids [104]. Despite the wide oxidative diversity, classic lignans bearing a C8–C8’ bond can be biosynthetically traced back to coniferyl alcohol (Scheme 18). Commonly, lignans possess important pharmacological properties including antimicrobial, anti-inflammatory, immunosuppressive activities, etc. [105]. At the same time, some members have been recognized as potent topoisomerase inhibitors and have been used as anticancer drugs [106]. To access the rich diversity of this class, Zhu’s group recently applied a Fukuzumi salt ([Mes–Acr–Me]BF_4)-mediated photochemical oxidation of dicinnamyl ether derivative **225** in the presence of appropriate additives (Scheme 18). According to the postulated mechanism, the reaction is initiated by an SET of the dicinnamyl ether substrate to Fukuzumi’s salt **233**, leading to radical cation **216**. Earlier findings of the same group [107] revealed that substitution on the aryl groups is the determinant factor for either 8,8’-*cis*- or 8,8’-*trans*-cyclization to furan heterocycle cation **218**, which serves as the hypothetical common scaffold of the plan. Diverting this mechanistic route to different lignans is possible by introducing nucleophilic additives (e.g., MeOH), oxidants (e.g., $Cu(OTFA)_2$), or quenchers (e.g., PhSSPh) to the reaction mixture. When monosubstitution of the aryl group is present,

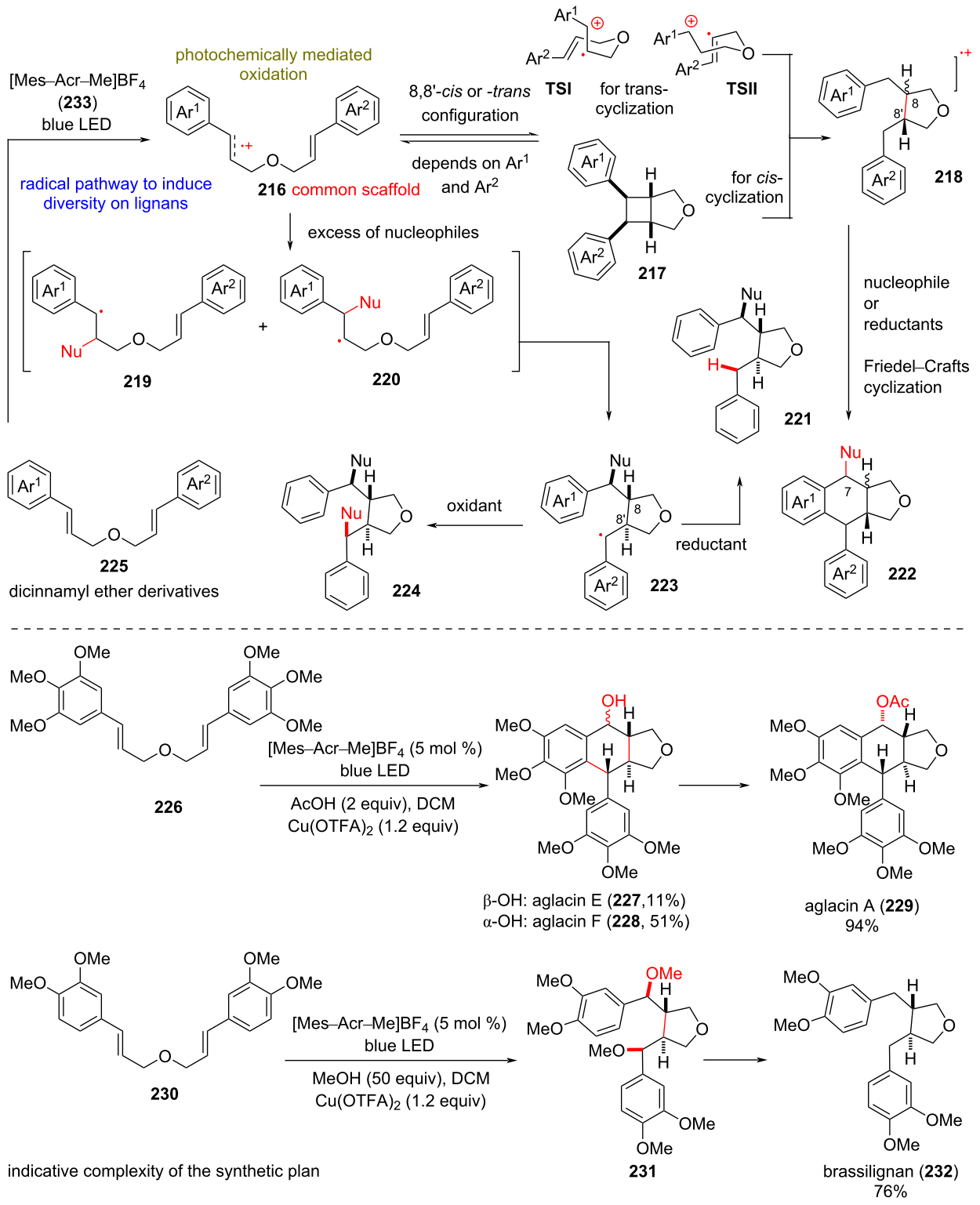

Scheme 18: Radical pathway for preparation of lignans (Zhu).

the formed radical cation, the product of the photooxidation of the cinnamyl ether, readily cyclizes to cyclobutene radical cation **217**. The latter cleaves the benzylic C–C bond to produce the 1,4-radical cation *cis*-**218**. On the other hand, when polysubstitution with methoxy groups is present, the cation in **216** is delocalized, inhibiting the production of cyclobutene **217**. Thus,

radical cyclization according to the Beckwith–Houk model [108,109] via transition states **TSI** and **TSII** would take place, leading to the intermediate *trans*-**218**. In the presence of external nucleophiles (e.g., MeOH), the cation can be trapped, leading to substitution in the 7-position, while the radical is postulated to be oxidized to a cation, followed by a Friedel–Crafts reaction to the final product **222**. When an excess of nucleophile is employed, radical **223** is favored, leading to either monosubstitution or disubstitution with external nucleophiles, depending on the presence of oxidant or reductant in the reaction mixture. Based on this plan, Zhu's group managed to synthesize a rich number of lignans and congeners, such as aglacin A (**229**), β-OH-aglacin E (**227**), α-OH-aglacin F (**228**), brassilignan (**232**), etc.

Diverse synthesis of highly oxidized dibenzocyclooctadiene (DBCOD)-type lignans

Lumb (2021) [110]**:** Extracts of *Schisandraceae* are rich sources of highly oxidized DBCOD lignans with interesting biological properties [111]. Designing their divergent plan on postulated biosynthetic steps, Lumb's group managed to efficiently prepare DBCOD derivatives **238** bearing the appropriate handles for late-stage radical formation (Scheme 19). Their success relied on the strategic design of linear precursors

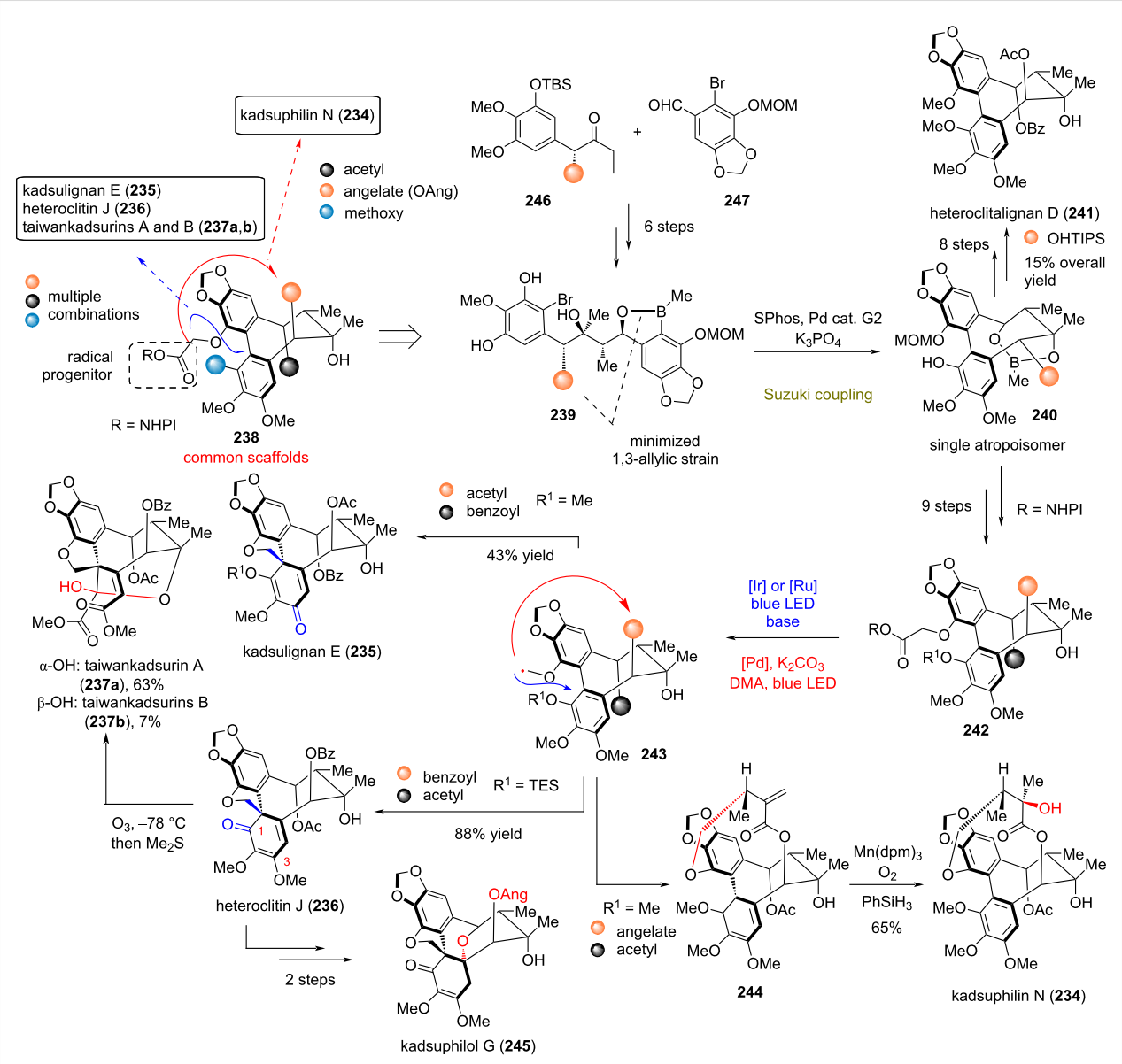

Scheme 19: Divergent synthesis of DBCOD lignans (Lumb).

239, bearing the appropriate substitution for the minimization of 1,3-allylic strain to enable Suzuki coupling for biaryl formation as a single atropisomer. The optimized conditions for this transformation utilize Buchwald's catalyst (SPhos and Pd-based G2 precatalyst) in conjunction with K_3PO_4. With DBCOD bearing carboxylic acid handles at the 19-position in hands, the group proceeded with the generation of requisite radical **243** from the respective phthalimide ester under photocatalyzed conditions, either with $[Ir(dtbpy)(ppy)_2](PF_6)$ or $[Ru(bpy)_3](PF_6)_2$ in the presence of base. The reaction provided a good yield of the cyclized products kadsulignan E (**235**) and heteroclitin J (**236**) depending on the appropriate substitution of DBCODs. Selection of radical termination at the 3- and 1-positions, respectively, can be engineered by the strategic incorporation of a TES protecting group at the 1-position (see **243**) for heteroclitin J (**236**). Further treatment of heteroclitin J (**236**) with ozone provided the selective formation of taiwankadsurins A and B (**237a**,**b**) by initial oxidative cleavage of the electron-rich aromatic ring and subsequent formation of the lactole ring. Heteroclitin J (**236**) has also been transformed to kadsuphilol G (**245**) by basic deprotection of the acetyl and benzoyl groups, followed by intramolecular cyclization and angelate esterification. Also, the differently redox-active DBCOD bearing an angelate functional group enabled the synthesis of kadsuphilin N (**234**). The synthetic sequence utilizes Fu's protocol for palladium-mediated photocatalysis (using $Pd(PPh_3)_2Cl_2$ in combination with xantphos) [112] towards **244**, followed by Mukaiyama hydration with the aid of $Mn(dpm)_3$, dioxygen, and $PhSiH_3$ for the synthesis of kadsuphilin N (**234**).

Conclusion

The utility of radical retrosynthetic disconnections in natural product synthesis is highlighted in practice, day after day, when shorter and scalable syntheses are coming into light. Combining these advantages with the power of divergent synthesis provides a yet underdeveloped strategy to address the challenges that insufficient supply of pharmaceutical leads poses, enriching the chemical libraries with natural scaffolds for biological screening. The evidenced increase of divergent radical syntheses in the last few years indicates that this approach is here to change the way chemists will practice total synthesis in the future.

Funding

This work was supported by the project "OPENSCREEN-GR" (MIS 5002691), which is implemented under the Action "Reinforcement of the Research and Innovation Infrastructure", funded by the Operational Program "Competitiveness, Entrepreneurship and Innovation" (NSRF 2014-2020) and cofinanced by Greece and the European Union (European Regional Development Fund).

ORCID® iDs

Alexandros L. Zografos - https://orcid.org/0000-0002-1834-2100

References

1. Nicolaou, K. C.; Vourloumis, D.; Winssinger, N.; Baran, P. S. *Angew. Chem., Int. Ed.* **2000,** *39,* 44–122. doi:10.1002/(sici)1521-3773(20000103)39:1<44::aid-anie44>3.0.co;2-l
2. Kuttruff, C. A.; Eastgate, M. D.; Baran, P. S. *Nat. Prod. Rep.* **2014,** *31,* 419–432. doi:10.1039/c3np70090a
3. Smith, J. M.; Harwood, S. J.; Baran, P. S. *Acc. Chem. Res.* **2018,** *51,* 1807–1817. doi:10.1021/acs.accounts.8b00209
4. Leifert, D.; Studer, A. *Angew. Chem., Int. Ed.* **2020,** *59,* 74–108. doi:10.1002/anie.201903726
5. Romero, K. J.; Galliher, M. S.; Pratt, D. A.; Stephenson, C. R. J. *Chem. Soc. Rev.* **2018,** *47,* 7851–7866. doi:10.1039/c8cs00379c
6. Bonjoch, J.; Diaba, F. *Eur. J. Org. Chem.* **2020,** 5070–5100. doi:10.1002/ejoc.202000391
7. Hung, K.; Hu, X.; Maimone, T. J. *Nat. Prod. Rep.* **2018,** *35,* 174–202. doi:10.1039/c7np00065k
8. Follmann, M.; Briem, H.; Steinmeyer, A.; Hillisch, A.; Schmitt, M. H.; Haning, H.; Meier, H. *Drug Discovery Today* **2019,** *24,* 668–672. doi:10.1016/j.drudis.2018.12.003
9. Anagnostaki, E. E.; Zografos, A. L. *Chem. Soc. Rev.* **2012,** *41,* 5613–5625. doi:10.1039/c2cs35080g
10. Li, L.; Chen, Z.; Zhang, X.; Jia, Y. *Chem. Rev.* **2018,** *118,* 3752–3832. doi:10.1021/acs.chemrev.7b00653
11. Li, C.-J.; Trost, B. M. *Proc. Natl. Acad. Sci. U. S. A.* **2008,** *105,* 13197–13202. doi:10.1073/pnas.0804348105
12. Gaich, T.; Baran, P. S. *J. Org. Chem.* **2010,** *75,* 4657–4673. doi:10.1021/jo1006812
13. Young, I. S.; Baran, P. S. *Nat. Chem.* **2009,** *1,* 193–205. doi:10.1038/nchem.216
14. Galliher, M. S.; Roldan, B. J.; Stephenson, C. R. J. *Chem. Soc. Rev.* **2021,** *50,* 10044–10057. doi:10.1039/d1cs00411e
15. Giese, B.; Meister, J. *Chem. Ber.* **1977,** *110,* 2588–2600. doi:10.1002/cber.19771100717
16. Giese, B.; Rupaner, R. *Synthesis* **1988,** 219–221. doi:10.1055/s-1988-27517
17. Herrmann, J. M.; König, B. *Eur. J. Org. Chem.* **2013,** 7017–7027. doi:10.1002/ejoc.201300657
18. Nicolaou, K. C.; Ellery, S. P.; Chen, J. S. *Angew. Chem., Int. Ed.* **2009,** *48,* 7140–7165. doi:10.1002/anie.200902151
19. Snider, B. B. *Chem. Rev.* **1996,** *96,* 339–364. doi:10.1021/cr950026m
20. Shevick, S. L.; Wilson, C. V.; Kotesova, S.; Kim, D.; Holland, P. L.; Shenvi, R. A. *Chem. Sci.* **2020,** *11,* 12401–12422. doi:10.1039/d0sc04112b
21. Pitre, S. P.; Overman, L. E. *Chem. Rev.* **2022,** *122,* 1717–1751. doi:10.1021/acs.chemrev.1c00247
22. Novaes, L. F. T.; Liu, J.; Shen, Y.; Lu, L.; Meinhardt, J. M.; Lin, S. *Chem. Soc. Rev.* **2021,** *50,* 7941–8002. doi:10.1039/d1cs00223f
23. Merchant, R. R.; Oberg, K. M.; Lin, Y.; Novak, A. J. E.; Felding, J.; Baran, P. S. *J. Am. Chem. Soc.* **2018,** *140,* 7462–7465. doi:10.1021/jacs.8b04891
24. Engel, B.; Erkel, G.; Anke, T.; Sterner, O. *J. Antibiot.* **1998,** *51,* 518–521. doi:10.7164/antibiotics.51.518
25. Uchida, R.; Imasato, R.; Yamaguchi, Y.; Masuma, R.; Shiomi, K.; Tomoda, H.; Ōmura, S. *J. Antibiot.* **2005,** *58,* 804–809. doi:10.1038/ja.2005.107

26. Lee, J. C.; Lobkovsky, E.; Pliam, N. B.; Strobel, G.; Clardy, J. *J. Org. Chem.* **1995,** *60,* 7076–7077. doi:10.1021/jo00127a001
27. Qin, T.; Cornella, J.; Li, C.; Malins, L. R.; Edwards, J. T.; Kawamura, S.; Maxwell, B. D.; Eastgate, M. D.; Baran, P. S. *Science* **2016,** *352,* 801–805. doi:10.1126/science.aaf6123
28. Qin, T.; Malins, L. R.; Edwards, J. T.; Merchant, R. R.; Novak, A. J. E.; Zhong, J. Z.; Mills, R. B.; Yan, M.; Yuan, C.; Eastgate, M. D.; Baran, P. S. *Angew. Chem., Int. Ed.* **2017,** *56,* 260–265. doi:10.1002/anie.201609662
29. Li, J.; Li, F.; King-Smith, E.; Renata, H. *Nat. Chem.* **2020,** *12,* 173–179. doi:10.1038/s41557-019-0407-6
30. Hubert, C.; Moreau, J.; Batany, J.; Duboc, A.; Hurvois, J.-P.; Renaud, J.-L. *Adv. Synth. Catal.* **2008,** *350,* 40–42. doi:10.1002/adsc.200700375
31. Everson, D. A.; Shrestha, R.; Weix, D. J. *J. Am. Chem. Soc.* **2010,** *132,* 920–921. doi:10.1021/ja9093956
32. Hyster, T. K. *Synlett* **2020,** *31,* 248–254. doi:10.1055/s-0037-1611818
33. Zhang, S.; Wang, X.; Hao, J.; Li, D.; Csuk, R.; Li, S. *J. Nat. Prod.* **2018,** *81,* 2010–2017. doi:10.1021/acs.jnatprod.8b00310
34. Shan, W.-G.; Ying, Y.-M.; Ma, L.-F.; Zhan, Z.-J. Drimane-Related Merosesquiterpenoids, a Promising Library of Metabolites for Drug Development. In *Studies in Natural Products Chemistry;* Attar-ur-Rahman, Ed.; Elsevier: Amsterdam, Netherlands, 2015; Vol. 45, pp 147–215. doi:10.1016/b978-0-444-63473-3.00006-x
35. Dixon, D. D.; Lockner, J. W.; Zhou, Q.; Baran, P. S. *J. Am. Chem. Soc.* **2012,** *134,* 8432–8435. doi:10.1021/ja303937y
36. Barrero, A. F.; Alvarez-Manzaneda, E. J.; Chahboun, R.; Arteaga, A. F. *Synth. Commun.* **2004,** *34,* 3631–3643. doi:10.1081/scc-200031056
37. Chong, C.; Zhang, Q.; Ke, J.; Zhang, H.; Yang, X.; Wang, B.; Ding, W.; Lu, Z. *Angew. Chem., Int. Ed.* **2021,** *60,* 13807–13813. doi:10.1002/anie.202100541
38. Jiao, W.-H.; Xu, T.-T.; Yu, H.-B.; Chen, G.-D.; Huang, X.-J.; Yang, F.; Li, Y.-S.; Han, B.-N.; Liu, X.-Y.; Lin, H.-W. *J. Nat. Prod.* **2014,** *77,* 346–350. doi:10.1021/np4009392
39. Jiao, W.-H.; Shi, G.-H.; Xu, T.-T.; Chen, G.-D.; Gu, B.-B.; Wang, Z.; Peng, S.; Wang, S.-P.; Li, J.; Han, B.-N.; Zhang, W.; Lin, H.-W. *J. Nat. Prod.* **2016,** *79,* 406–411. doi:10.1021/acs.jnatprod.5b01079
40. Wu, J.; Kadonaga, Y.; Hong, B.; Wang, J.; Lei, X. *Angew. Chem., Int. Ed.* **2019,** *58,* 10879–10883. doi:10.1002/anie.201903682
41. Sun, H.-D.; Huang, S.-X.; Han, Q.-B. *Nat. Prod. Rep.* **2006,** *23,* 673–698. doi:10.1039/b604174d
42. Li, L.-M.; Li, G.-Y.; Xiao, W.-L.; Zhou, Y.; Li, S.-H.; Huang, S.-X.; Han, Q.-B.; Ding, L.-S.; Lou, L.-G.; Sun, H.-D. *Tetrahedron Lett.* **2006,** *47,* 5187–5190. doi:10.1016/j.tetlet.2006.05.025
43. Qu, J.-B.; Zhu, R.-L.; Zhang, Y.-L.; Guo, H.-F.; Wang, X.-N.; Xie, C.-F.; Yu, W.-T.; Ji, M.; Lou, H.-X. *J. Nat. Prod.* **2008,** *71,* 1418–1422. doi:10.1021/np8003062
44. Maksymowicz, R. M.; Roth, P. M. C.; Fletcher, S. P. *Nat. Chem.* **2012,** *4,* 649–654. doi:10.1038/nchem.1394
45. Xiao, Z.-K.; Shao, L.-X. *Synthesis* **2012,** *44,* 711–716. doi:10.1055/s-0031-1289698
46. Liu, W.; Li, H.; Cai, P.-J.; Wang, Z.; Yu, Z.-X.; Lei, X. *Angew. Chem., Int. Ed.* **2016,** *55,* 3112–3116. doi:10.1002/anie.201511659
47. Zong, Y.; Xu, Z.-J.; Zhu, R.-X.; Su, A.-H.; Liu, X.-Y.; Zhu, M.-Z.; Han, J.-J.; Zhang, J.-Z.; Xu, Y.-L.; Lou, H.-X. *Angew. Chem., Int. Ed.* **2021,** *60,* 15286–15290. doi:10.1002/anie.202104182
48. Chen, K.; Zhang, X.; Sun, W.; Liu, J.; Yang, J.; Chen, C.; Liu, X.; Gao, L.; Wang, J.; Li, H.; Luo, Z.; Xue, Y.; Zhu, H.; Zhang, Y. *Org. Lett.* **2017,** *19,* 5956–5959. doi:10.1021/acs.orglett.7b02955
49. Yuan, W. H.; Liu, M.; Jiang, N.; Guo, Z. K.; Ma, J.; Zhang, J.; Song, Y. C.; Tan, R. X. *Eur. J. Org. Chem.* **2010,** 6348–6353. doi:10.1002/ejoc.201000916
50. Yan, Z.; Zhao, C.; Gong, J.; Yang, Z. *Org. Lett.* **2020,** *22,* 1644–1647. doi:10.1021/acs.orglett.0c00241
51. Zhang, Y.-A.; Milkovits, A.; Agarawal, V.; Taylor, C. A.; Snyder, S. A. *Angew. Chem., Int. Ed.* **2021,** *60,* 11127–11132. doi:10.1002/anie.202016178
52. Tao, Y.; Reisenauer, K.; Taube, J. H.; Romo, D. *Angew. Chem., Int. Ed.* **2019,** *58,* 2734–2738. doi:10.1002/anie.201812909
53. Zhao, Y.; Hu, J.; Chen, R.; Xiong, F.; Xie, H.; Ding, H. *J. Am. Chem. Soc.* **2022,** *144,* 2495–2500. doi:10.1021/jacs.1c13370
54. Anke, T.; Heim, J.; Knoch, F.; Mocek, U.; Steffan, B.; Steglich, W. *Angew. Chem., Int. Ed. Engl.* **1985,** *24,* 709–711. doi:10.1002/anie.198507091
55. Li, Y.-Y.; Shen, Y.-M. *Helv. Chim. Acta* **2010,** *93,* 2151–2157. doi:10.1002/hlca.200900470
56. Rohr, M.; Oleinikov, K.; Jung, M.; Sandjo, L. P.; Opatz, T.; Erkel, G. *Bioorg. Med. Chem.* **2017,** *25,* 514–522. doi:10.1016/j.bmc.2016.11.016
57. Kupka, J.; Anke, T.; Oberwinkler, F.; Schramm, G.; Steglich, W. *J. Antibiot.* **1979,** *32,* 130–135. doi:10.7164/antibiotics.32.130
58. Dowd, P.; Zhang, W. *Chem. Rev.* **1993,** *93,* 2091–2115. doi:10.1021/cr00022a007
59. He, C.; Hu, J.; Wu, Y.; Ding, H. *J. Am. Chem. Soc.* **2017,** *139,* 6098–6101. doi:10.1021/jacs.7b02746
60. Gao, J.; Rao, P.; Xu, K.; Wang, S.; Wu, Y.; He, C.; Ding, H. *J. Am. Chem. Soc.* **2020,** *142,* 4592–4597. doi:10.1021/jacs.0c00308
61. Wang, B.; Liu, Z.; Tong, Z.; Gao, B.; Ding, H. *Angew. Chem., Int. Ed.* **2021,** *60,* 14892–14896. doi:10.1002/anie.202104410
62. Landwehr, E. M.; Baker, M. A.; Oguma, T.; Burdge, H. E.; Kawajiri, T.; Shenvi, R. A. *Science* **2022,** *375,* 1270–1274. doi:10.1126/science.abn8343
63. Miller, J. H.; Aagaard, P. J.; Gibson, V. A.; McKinney, M. *J. Pharmacol. Exp. Ther.* **1992,** *263,* 663–667.
64. Collins, D. J.; Culvenor, C. C. J.; Lamberton, J. A.; Loder, J. W.; Price, J. R. *Plants for Medicines: A Chemical and Pharmacological Survey of Plants in the Australian Region;* CSIRO Publishing: Clayton, Australia, 1990. doi:10.1071/9780643101203
65. Rinderhagen, H.; Waske, P. A.; Mattay, J. *Tetrahedron* **2006,** *62,* 6589–6593. doi:10.1016/j.tet.2006.03.060
66. Milligan, J. A.; Phelan, J. P.; Badir, S. O.; Molander, G. A. *Angew. Chem., Int. Ed.* **2019,** *58,* 6152–6163. doi:10.1002/anie.201809431
67. Varabyeva, N.; Barysevich, M.; Aniskevich, Y.; Hurski, A. *Org. Lett.* **2021,** *23,* 5452–5456. doi:10.1021/acs.orglett.1c01795
68. Liu, X.-Y.; Qin, Y. *Acc. Chem. Res.* **2019,** *52,* 1877–1891. doi:10.1021/acs.accounts.9b00246
69. Zhou, Q.; Dai, X.; Song, H.; He, H.; Wang, X.; Liu, X.-Y.; Qin, Y. *Chem. Commun.* **2018,** *54,* 9510–9512. doi:10.1039/c8cc05374j
70. Kam, T.-S. Alkaloids from Malaysian Flora. In *Alkaloids: Chemical and Biological Perspectives;* Pelletier, S. W., Ed.; Pergamon Press: Oxford, UK, 1999; p 350.
71. Yap, W.-S.; Gan, C.-Y.; Sim, K.-S.; Lim, S.-H.; Low, Y.-Y.; Kam, T.-S. *J. Nat. Prod.* **2016,** *79,* 230–239. doi:10.1021/acs.jnatprod.5b00992

72. Wang, X.; Xia, D.; Qin, W.; Zhou, R.; Zhou, X.; Zhou, Q.; Liu, W.; Dai, X.; Wang, H.; Wang, S.; Tan, L.; Zhang, D.; Song, H.; Liu, X.-Y.; Qin, Y. *Chem* **2017,** *2,* 803–816. doi:10.1016/j.chempr.2017.04.007
73. Alabugin, I. V.; Harris, T. *Chem* **2017,** *2,* 753–755. doi:10.1016/j.chempr.2017.05.018
74. Zeng, X.; Shukla, V.; Boger, D. L. *J. Org. Chem.* **2020,** *85,* 14817–14826. doi:10.1021/acs.joc.0c02493
75. Abdurakhimova, N.; Yuldashev, P. K.; Yunusov, S. Y. *Chem. Nat. Compd.* **1967,** *3,* 263–266. doi:10.1007/bf00574630
76. Ishikawa, H.; Colby, D. A.; Seto, S.; Va, P.; Tam, A.; Kakei, H.; Rayl, T. J.; Hwang, I.; Boger, D. L. *J. Am. Chem. Soc.* **2009,** *131,* 4904–4916. doi:10.1021/ja809842b
77. Campbell, E. L.; Zuhl, A. M.; Liu, C. M.; Boger, D. L. *J. Am. Chem. Soc.* **2010,** *132,* 3009–3012. doi:10.1021/ja908819q
78. Lo, J. C.; Kim, D.; Pan, C.-M.; Edwards, J. T.; Yabe, Y.; Gui, J.; Qin, T.; Gutiérrez, S.; Giacoboni, J.; Smith, M. W.; Holland, P. L.; Baran, P. S. *J. Am. Chem. Soc.* **2017,** *139,* 2484–2503. doi:10.1021/jacs.6b13155
79. Kim, D.; Rahaman, S. M. W.; Mercado, B. Q.; Poli, R.; Holland, P. L. *J. Am. Chem. Soc.* **2019,** *141,* 7473–7485. doi:10.1021/jacs.9b02117
80. Reich, D.; Trowbridge, A.; Gaunt, M. J. *Angew. Chem., Int. Ed.* **2020,** *59,* 2256–2261. doi:10.1002/anie.201912010
81. Sakamoto, K.; Tsujii, E.; Abe, F.; Nakanishi, T.; Yamashita, M.; Shigematsu, N.; Izumi, S.; Okuhara, M. *J. Antibiot.* **1996,** *49,* 37–44. doi:10.7164/antibiotics.49.37
82. Shirafuji, H.; Tsubotani, S.; Ishimaru, T.; Harada, S. Compound tan-1251, its derivatives, their production and use. WO Patent WO1991013887, Sept 19, 1991.
83. Scheffler, G.; Seike, H.; Sorensen, E. J. *Angew. Chem., Int. Ed.* **2000,** *39,* 4593–4596. doi:10.1002/1521-3773(20001215)39:24<4593::aid-anie4593>3.0.co;2-x
84. Ousmer, M.; Braun, N. A.; Bavoux, C.; Perrin, M.; Ciufolini, M. A. *J. Am. Chem. Soc.* **2001,** *123,* 7534–7538. doi:10.1021/ja016030z
85. Carson, C. A.; Kerr, M. A. *Org. Lett.* **2009,** *11,* 777–779. doi:10.1021/ol802870c
86. Snider, B. B.; Lin, H. *Org. Lett.* **2000,** *2,* 643–646. doi:10.1021/ol991401q
87. Trowbridge, A.; Reich, D.; Gaunt, M. J. *Nature* **2018,** *561,* 522–527. doi:10.1038/s41586-018-0537-9
88. Xuan, J.; Machicao, P. A.; Haelsig, K. T.; Maimone, T. J. *Angew. Chem., Int. Ed.* **2022,** *61,* e202209457. doi:10.1021/ol991401q
89. Han, W. B.; Lu, Y. H.; Zhang, A. H.; Zhang, G. F.; Mei, Y. N.; Jiang, N.; Lei, X.; Song, Y. C.; Ng, S. W.; Tan, R. X. *Org. Lett.* **2014,** *16,* 5366–5369. doi:10.1021/ol502572g
90. Han, W. B.; Zhang, A. H.; Deng, X. Z.; Lei, X.; Tan, R. X. *Org. Lett.* **2016,** *18,* 1816–1819. doi:10.1021/acs.orglett.6b00549
91. Haelsig, K. T.; Xuan, J.; Maimone, T. J. *J. Am. Chem. Soc.* **2020,** *142,* 1206–1210. doi:10.1021/jacs.9b12546
92. Tra, B. B. J.; Abollé, A.; Coefard, V.; Felpin, F.-X. *Eur. J. Org. Chem.* **2022,** e202200301. doi:10.1002/ejoc.202200301
93. Phillipson, J. D.; Roberts, M. F.; Zenk, M. H., Eds. *The Chemistry and Biology of Isoquinoline Alkaloids;* Springer: Berlin, Heidelberg, 1985. doi:10.1007/978-3-642-70128-3
94. Beaudoin, G. A. W.; Facchini, P. J. *Planta* **2014,** *240,* 19–32. doi:10.1007/s00425-014-2056-8
95. Dohi, T.; Ito, M.; Yamaoka, N.; Morimoto, K.; Fujioka, H.; Kita, Y. *Tetrahedron* **2009,** *65,* 10797–10815. doi:10.1016/j.tet.2009.10.040
96. Dohi, T.; Yamaoka, N.; Kita, Y. *Tetrahedron* **2010,** *66,* 5775–5785. doi:10.1016/j.tet.2010.04.116
97. Miloserdov, F. M.; Kirillova, M. S.; Muratore, M. E.; Echavarren, A. M. *J. Am. Chem. Soc.* **2018,** *140,* 5393–5400. doi:10.1021/jacs.7b13484
98. Awang, K.; Sévenet, T.; Hamid, A.; Hadi, A.; David, B.; Païs, M. *Tetrahedron Lett.* **1992,** *33,* 2493–2496. doi:10.1016/s0040-4039(00)92223-8
99. Awang, K.; Sévenet, T.; Païs, M.; Hadi, A. H. A. *J. Nat. Prod.* **1993,** *56,* 1134–1139. doi:10.1021/np50097a018
100. Yap, W.-S.; Gan, C.-Y.; Low, Y.-Y.; Choo, Y.-M.; Etoh, T.; Hayashi, M.; Komiyama, K.; Kam, T.-S. *J. Nat. Prod.* **2011,** *74,* 1309–1312. doi:10.1021/np200008g
101. Kirillova, M. S.; Muratore, M. E.; Dorel, R.; Echavarren, A. M. *J. Am. Chem. Soc.* **2016,** *138,* 3671–3674. doi:10.1021/jacs.6b01428
102. Gentry, E. C.; Rono, L. J.; Hale, M. E.; Matsuura, R.; Knowles, R. R. *J. Am. Chem. Soc.* **2018,** *140,* 3394–3402. doi:10.1021/jacs.7b13616
103. Xiang, J.-C.; Fung, C.; Wang, Q.; Zhu, J. *Nat. Commun.* **2022,** *13,* 3481. doi:10.1038/s41467-022-31000-4
104. Teponno, R. B.; Kusari, S.; Spiteller, M. *Nat. Prod. Rep.* **2016,** *33,* 1044–1092. doi:10.1039/c6np00021e
105. Saleem, M.; Kim, H. J.; Ali, M. S.; Lee, Y. S. *Nat. Prod. Rep.* **2005,** *22,* 696–716. doi:10.1039/b514045p
106. Zhang, X.; Rakesh, K. P.; Shantharam, C. S.; Manukumar, H. M.; Asiri, A. M.; Marwani, H. M.; Qin, H.-L. *Bioorg. Med. Chem.* **2018,** *26,* 340–355. doi:10.1016/j.bmc.2017.11.026
107. Xiang, J.-C.; Wang, Q.; Zhu, J. *Angew. Chem., Int. Ed.* **2020,** *59,* 21195–21202. doi:10.1002/anie.202007548
108. Beckwith, A. L. J.; Schiesser, C. H. *Tetrahedron* **1985,** *41,* 3925–3941. doi:10.1016/s0040-4020(01)97174-1
109. Spellmeyer, D. C.; Houk, K. N. *J. Org. Chem.* **1987,** *52,* 959–974. doi:10.1021/jo00382a001
110. Huang, Z.; Lumb, J.-P. *Nat. Chem.* **2021,** *13,* 24–32. doi:10.1038/s41557-020-00603-z
111. Zhu, P.; Li, J.; Fu, X.; Yu, Z. *Phytomedicine* **2019,** *59,* 152760. doi:10.1016/j.phymed.2018.11.020
112. Wang, G.-Z.; Shang, R.; Fu, Y. *Org. Lett.* **2018,** *20,* 888–891. doi:10.1021/acs.orglett.8b00023

License and Terms

BEILSTEIN JOURNAL OF ORGANIC CHEMISTRY

Total synthesis of insect sex pheromones: recent improvements based on iron-mediated cross-coupling chemistry

Eric Gayon*[1], Guillaume Lefèvre*[2], Olivier Guerret[1], Adrien Tintar[1,2] and Pablo Chourreu[1,2]

Perspective

Open Access

Address:
[1]M2i Development, Bâtiment ChemStart'Up, 64170 Lacq, France and [2]i-CLeHS, UMR 8060, CNRS Chimie ParisTech 11, rue Pierre et Marie Curie, 75005 Paris, France

Email:
Eric Gayon* - eric.gayon@m2i-group.fr; Guillaume Lefèvre* - guillaume.lefevre@chimieparistech.psl.eu

* Corresponding author

Keywords:
catalysis; cross-coupling; insect pheromones; iron

Beilstein J. Org. Chem. **2023,** *19,* 158–166.
https://doi.org/10.3762/bjoc.19.15

Received: 12 December 2022
Accepted: 27 January 2023
Published: 14 February 2023

This article is part of the thematic issue "Total synthesis: an enabling science".

Associate Editor: B. Nay

Abstract

In the current ecological context, use of insect sex pheromones as an alternative to conventional pesticides is in constant growth. In this report, we discuss the recent contributions brought by our groups in the field of iron-catalyzed cross-couplings applied to the synthesis of insect pheromones. The pivotal question of the development of sustainable synthetic procedures involving cheap, non-toxic and efficient additives is also discussed, as well as the mechanistic features guiding the reactivity of such catalytic systems.

Introduction

Public health issues related to environmental problems, particularly pollution and soil persistence, led in recent years to a decrease in the use of so-called conventional protection products for the protection of crops and plants. Some of these synthetic pesticides, such dimethoate (pesticides for the protection of cherry crops) or chlordecone (pesticides for the protection of banana crops) [1], have recently been forbidden in the EU. In this context, the development of eco-friendlier solutions for the protection of crops and plants is a major challenge. This is why biocontrol (that is: all plant protection methods that use natural mechanisms to help regulate/balance the populations of harmful species rather than eradicating them) based on the use of insect pheromones [2-5] is an eco-friendly solution for the protection of a wide range of crops and plants against pests. Indeed, those chemical mediators, which are emitted by insects from a given species, trigger a specific reaction, such as sexual attraction, on an individual of the same species and represent very selective intraspecific means of communication. Used in crop protection,

synthetic pheromones can disturb communication between individuals in order to prevent their reproduction and then limit their proliferation, finally lowering the damages caused by pests to the crops. Moreover, those molecules are totally biodegradable, harmless to Humans and don't interact with non-targeted insects [6].

However, at this time, few pathways for the synthesis of insect pheromones reported in the literature are applicable on an industrial scale, which slows the widespread application of this solution. As a matter of fact, the key step of the synthesis of such compounds, which is the introduction of C=C unsaturations, traditionally involves expensive, toxic and low atom economy methodologies. The synthesis of the sex pheromone of the horse-chestnut leaf miner (*Cameraria ohridella*), (8*E*,10*Z*)-tetradecadienal (**1**, Scheme 1) perfectly illustrates this issue: the main synthetic pathways reported in the literature until now (Svatoš, 1999 [7]; Francke, 2002 [8], Grodner, 2009 [9]) are linear syntheses involving a great number of steps and purifications as well as cryogenic temperatures. Moreover, the introduction of the C=C unsaturation is achieved via a Wittig reaction or a Pd-catalyzed Sonogashira cross-coupling followed by a reduction by a borane reagent, methods which lead to overall processes with a low atom economy, generating a significant amount of chemical waste, and which can be expensive when noble metals such as palladium salts are required (Scheme 1).

The high efficiency of transition-metal-catalyzed cross-coupling methods in C–C bond formation processes constitutes an extremely powerful tool in total synthesis. In order to reach sustainable and economically appealing conditions, the quest for the substitution of palladium by non-noble metals has been investigated for more than four decades. To address this issue, new eco-friendly synthetic routes relying on carbon–carbon iron-catalyzed cross coupling as a key step were developed, capitalizing on the low toxicity and the cheap cost of this abundant metal [10]. For instance, in 1971, Kochi developed an iron-catalyzed alkyl–alkenyl cross-coupling reaction between aliphatic Grignard reagents and vinyl bromides, using $FeCl_3$ as the catalyst, in order to obtain cross-coupling products with yields between 64 and 83% (Scheme 2a) [11]. Drawing his inspiration from Kochi, Cahiez reported that using *N*-methyl-2-pyrrolidone or NMP as a co-solvent drastically improved the efficiency of the iron-catalyzed alkyl–alkenyl cross coupling reaction developed by Kochi, leading to better yields, with no need to use an excess of one of the coupling partners (Scheme 2b) [12]. The yields obtained using this ligand-free method are comparable to those obtained in recent palladium-mediated alkyl–vinyl cross-couplings using exogenous N- or P-based ligands, highlighting the efficiency of iron as a credible alternative to noble metal catalysis in cross-coupling chemistry [13]. Cahiez' pioneering work highlighted the potential of iron catalysis in organic chemistry and generated a new interest for the study of iron-catalyzed reactions, which witnessed considerable development in the last two decades [14], several cross-coupling methodologies involving soft nucleophiles, such as iron-mediated Suzuki–Miyaura cross-couplings, being reported [15].

The introduction of alkyl–alkenyl linkage by means of iron-catalyzed cross-coupling reactions thus appears as an appealing tool for the synthesis of insect pheromones, which often display linear chains involving C=C unsaturations with a well-defined stereochemistry (Scheme 1). Therefore, we aimed at developing this strategy for the design of high-scale, eco-friendly and economic new synthetic procedures applied to obtain a variety of insect pheromones. The present report summarizes the recent progresses made in insect sex pheromone synthetic applications in our group, with a particular focus on the quest for non-toxic and sustainable catalytic platforms developed in the iron-catalyzed cross-coupling field.

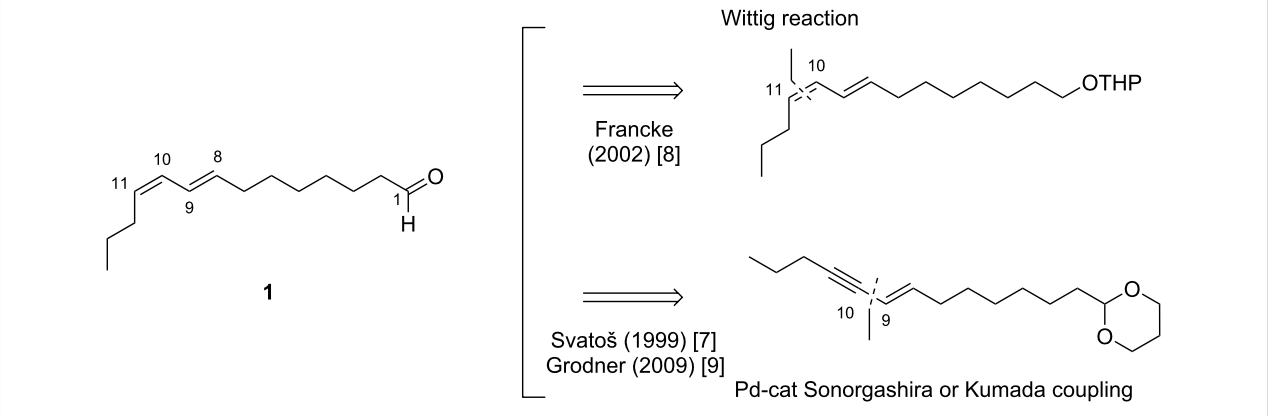

Scheme 1: Structure of the (8*E*,10*Z*)-tetradecadienal (**1**, sex pheromone of the horse-chestnut leaf miner) and reported retrosynthetic pathways.

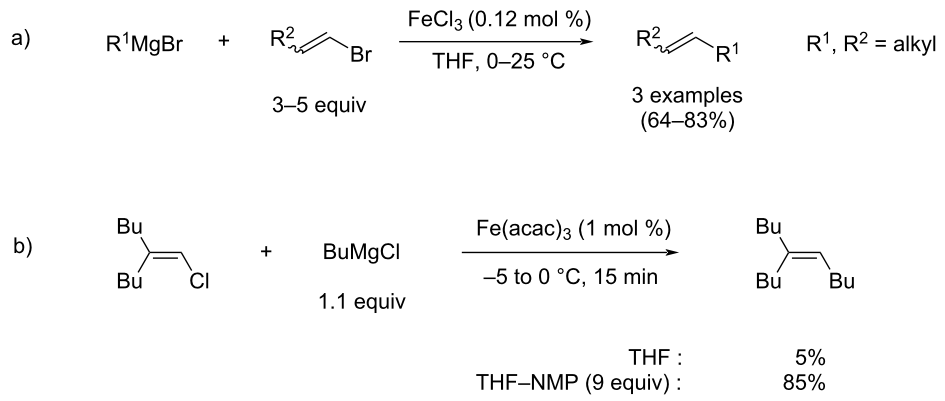

Scheme 2: a) Alkyl–vinyl seminal cross-coupling reaction by Kochi; b) improved procedure described by Cahiez.

Discussion

The quest for non-toxic and efficient additives for iron-mediated cross-coupling reactions

Co-solvents used as NMP surrogates

In spite of the very good yields and soft conditions provided by Cahiez' method (Scheme 2b), a major drawback of the latter is the requirement of NMP as a co-solvent. Indeed, NMP recently proved to be of very high concern due to its acute toxicity, since it was classified as a reprotoxic reagent [16,17]. In order to circumvent this matter and develop new non-toxic and sustainable iron-mediated coupling transformations, efforts were put in the quest for suitable additives as surrogates of NMP. Szostak and Bisz reported in 2019 that *N*-methyl-ε-caprolactame (NMCPL) could be used as an alternative solvent, and sp^3–sp^2 cross-coupling reactions proceeding with good to excellent yields were reported. Alkyl Grignard reagents could thus be used in combination with a variety of alkenyl chlorides and (hetero)aryl chlorides [18].

Importance of the leaving groups: use of enol phosphates

In order to overcome the delicate choice of either NMP or one of its surrogates as a suitable co-solvent, it has also been demonstrated that amide-free catalytic procedures could afford satisfying coupling yields by a suitable variation of the nature of the leaving group. In 2008, Cahiez reported an iron-catalyzed alkenylation of organomagnesium reagents with enol phosphates as electrophiles, instead of alkenyl halides [19]. In this case, when reactive enol phosphates derived from aldehydes were used, excellent coupling yields were obtained in THF, with no need of NMP additive (Table 1, entries 1 and 2). However, less reactive α,β-disubstituted enol phosphates required the presence of NMP (Table 1, entry 3) or even *N*,*N*′-dimethylpropyleneurea (DMPU) (Table 1, entry 4) as a co-solvent.

Nevertheless, capitalizing on these results, Cahiez further developed this iron-catalyzed cross coupling reaction with dienol phosphates as electrophiles, which are thermally more stable than dienyl halides [20]. It was found that when dienol phosphates were used as electrophiles, the presence of NMP is actually detrimental. Indeed, for the cross coupling reaction of octylmagnesium chloride with 1-butadienyl phosphate in THF at −20°C in the presence of 1% $Fe(acac)_3$ and 9 equivalents of NMP, the resulting 1,3-dodecadiene cross-coupling product was only obtained with a 54% yield, whereas when the reaction was performed in THF alone (at 20 °C), the yield improved significantly (92%, Scheme 3).

The efficient iron-mediated alkylation of dienyl phosphates, proceeding with an excellent retention of stereochemistry, was then successfully used in the introduction of the alkyl–alkenyl linkage of several insect pheromones. Cahiez paved the way of this strategy in 2008, showing that (*E*)-dodeca-9,11-dien-1-yl acetate (**2**), the sex pheromone of red bollworm moth (*Diparopsis castanea*), which contains a terminal diene, could be obtained at a laboratory scale (ca. 200 mg) by means of iron-mediated cross-coupling (77% yield for the coupling step, Scheme 4a) [20]. In this cross-coupling, an α,ω-difunctionalized Grignard reagent bearing a magnesium alkoxide moiety at the end of the aliphatic chain is used as a coupling partner. Following in those footsteps, similar syntheses of other insect pheromones involving a key alkyl–alkenyl linkage introduction by iron-catalyzed cross-coupling reactions of α,ω-difunctionalized alkyl Grignard reagents with stereochemically pure dienyl phosphates were successfully performed at higher scales, in order to be successfully implemented in industrial processes. (7*E*,9*Z*)-Dodeca-7,9-dien-1-yl acetate (**3**), the sex pheromone of European grapevine moth (*Lobesia botrana*), was thus obtained at a 14 g scale, with an overall 85% yield for the one-pot sequence involving the iron-catalyzed cross coupling followed by acetylation with Ac_2O (Scheme 4b) [21]. Illustrating the appli-

Table 1: Iron-catalyzed alkenylation of enol phosphates by Grignard reagents by Cahiez.

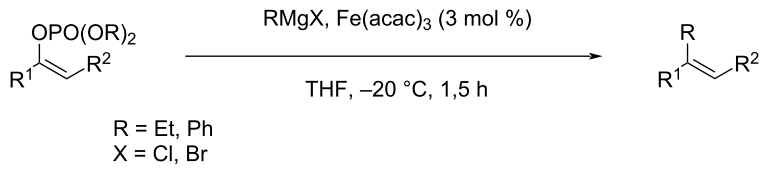

R = Et, Ph
X = Cl, Br

Entry	Enol phosphate (*E*:*Z*)	Product (*E*:*Z*)	Solvent	Yield (%)
1	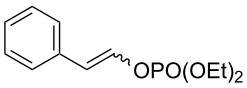 (86:14)	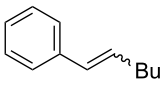 (90:10)	THF	87
2	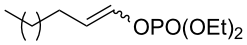 (70:30)	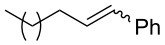 (85:15)	THF	81
3	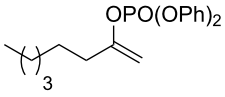	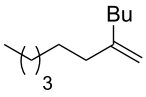	THF + NMP	75
4	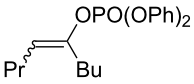 (68:32)	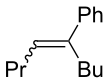 (94:6)	THF + DMPU	70

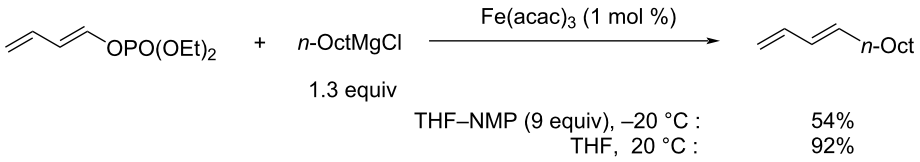

Scheme 3: Iron-catalyzed cross-coupling of *n*-OctMgCl with a 1-butadienyl phosphate.

cability of this process to large industrial scales, a synthesis of 50 kg of pheromone **3** was performed using this method [22,23]. Similarly, a 40 g batch of (8*E*,10*Z*)-tetradeca-8,10-dienal (**1**), the sex pheromone of horse-chestnut leaf miner (*Cameraria ohridella*) was obtained following an analogous procedure (Scheme 4c) [24]. It is of note that a low 0.1 mol % catalytic loading could be used for the latter coupling, which is thus particularly appealing for high-scale applications. In this context, the procedure described in Scheme 4c is currently used for industrial medium-scale synthesis of **1** by the M2i Company.

Magnesium alkoxides used as additives

Although it can lead to efficient NMP-free cross-coupling procedures, the use of enol phosphates as coupling electrophiles also brings several issues for efficient and sustainable procedures meant to be carried out at large scales. First, dialkyl phosphates used as leaving groups lead to overall transformations which display a poor atom economy. Moreover, diethyl chlorophosphate (DCP), used as a classic starting material in the dienol phosphates synthesis, is also registered under REACH regulation, and its use brings several toxicity issues for living organisms [25,26]. Additionally, the classic stereoselective synthesis of dienol phosphates requires cryogenic temperatures (−78 °C) as well as NMP-based methodologies [27]. Therefore, motivated by those considerations, we sought a suitable efficient and non-toxic additive which would allow the use of alkenyl halides as cross-coupling partners in the absence of NMP.

A remarkable feature of the alkyl–dienyl cross-coupling reactions displayed in Scheme 4 is the implication of α,ω-difunctionalized Grignard reagents, bearing a magnesium alkoxide moiety at the end of the chain. Magnesium alkoxides exhibit

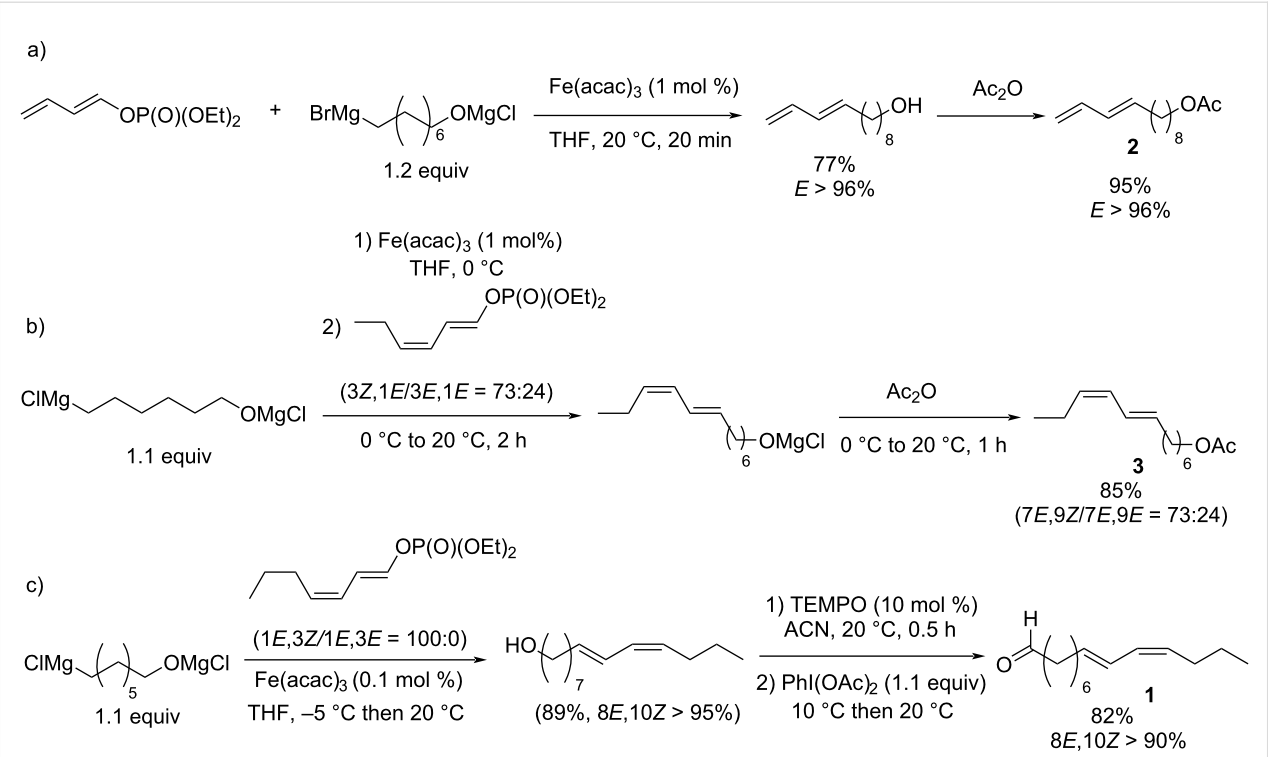

Scheme 4: Synthesis of several insect sex pheromones (a) red bollworm moth, b) European grapevine moth, c) horse-chestnut leaf miner) involving a key alkyl–alkenyl iron-mediated cross-coupling between a dienol phosphate and an α,ω-difunctionalized Grignard reagent.

strong σ-donating properties, given the high nucleophilicity of the alkoxide moiety. Moreover, the beneficial effect of molecular σ-donating additives on the yields and selectivities of iron-mediated cross-coupling reactions had already been reported in the literature. Nakamura thus described an elegant aryl–aryl cross-coupling procedure suppressing the formation of Grignard homocoupling byproducts relying on the use of FeF_3 as catalyst, associated with strong N-heterocyclic carbenes (NHCs) and a source of fluoride anions [28]. A similar procedure involving sodium alkoxide additives and NHCs was also described by Duong for the aryl–aryl cross coupling [29]. Alkoxide salts appear as good alternatives to NMP or phosphate-based additives, since several classic alcohol sources display low toxicities and can also come from renewable resources [30].

In this context, Cahiez and Lefèvre developed an eco-friendlier, and easily scalable iron-catalyzed cross-coupling method between alkyl Grignard reagents and C_{sp2} (alkenyl or aryl) organic halides [31]. By combining a catalytic charge of $FeCl_3$ with alkoxide magnesium salts such as EtOMgCl in THF, complete conversion of the alkenyl/aryl halides was observed and the cross-coupling products were afforded in good to excellent yields (Scheme 5). Moreover, this reaction can also be carried out at the gram scale (up to 50 mmol for alkyl–alkenyl coupling reactions, up to 10 mmol for alkyl–aryl couplings). Alkoxide salts, such as EtOMgCl, are cheaper and much less toxic than NMP, making this method particularly eco-friendly. Moreover, this method also provides results equivalent to those obtained using NMP-based cross-coupling reactions. Again, no exogenous nor expensive ligands are required, leading to an overall economically viable process. Those results clearly demonstrate that magnesium alkoxide additives per se can play a beneficial role in alkyl–alkenyl iron-mediated cross-coupling reactions, similarly to the results observed when NMP is used as a co-solvent (Scheme 2b).

Therefore, targeting applications in pheromone synthesis, we aimed at combining the advantages brought by those additives with the atom-economy offered by the use of organic electrophiles bearing halide leaving groups (better than that obtained with phosphates leaving groups, Scheme 4). We thus investigated the development of pheromone synthesis involving cross-coupling methods using Grignard reagents bearing terminal alkoxide magnesium moieties and dienyl halides. This strategy is moreover particularly appealing since the magnesium alkoxide additive used in the cross-coupling is also a part of the final synthetic target. The oxygen atom of the -OMgX functionality indeed affords the terminal oxidized function of the pheromone molecule (alkoxy acetate in **2** or **3**, Scheme 4a and 4b, or formyl group in **1**, Scheme 4c).

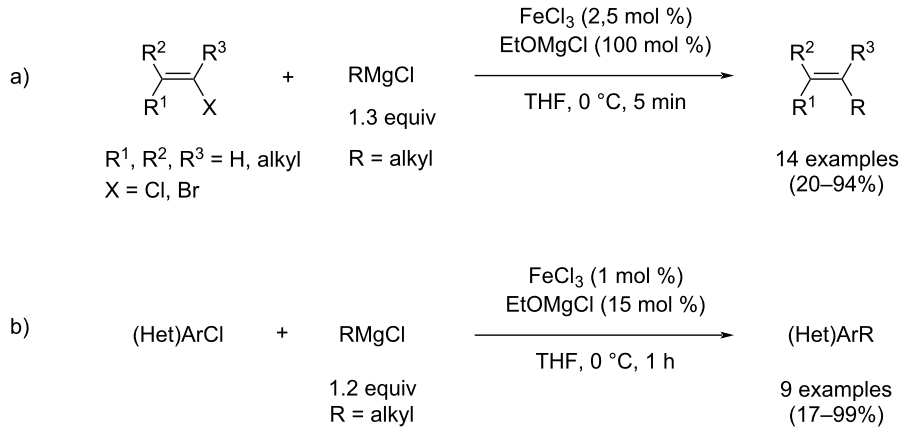

Scheme 5: Cross-coupling of alkyl Grignard reagents with a) alkenyl or b) aryl halides involving EtOMgCl as additive.

As a representative target, we developed the total synthesis of the codling moth sex pheromone, (8*E*,10*E*)-dodecadien-1-ol (**4**), featuring the introduction of the C_7–C_8 linkage by a key iron-mediated cross-coupling sequence between the suitable α,ω-difunctionalized Grignard reagent and 1-bromopenta-1,3-diene as the electrophile (Scheme 6) [32].

A classic drawback of the use of dienyl halides as coupling partners is their intrinsic thermal instability. Dienyl halides indeed tend to polymerize at low temperatures, and drastic storage conditions must be applied. For example, chloroprene, a well-known precursor of isoprene polymers, must be transported under inert atmosphere below −10 °C, and an inhibitor must be added to prevent polymerization. Cross-coupling systems involving this reagent are thus particularly scarce, and few examples are reported, using for some of them Ni-based catalysts [33].

1-Bromopenta-1,3-diene used in the synthesis of **4** (Scheme 6) is not an exception. The expected (*E*,*E*) isomer was easily obtained from sorbic acid, a renewable C_6 synthon, by a Hunsdiecker–Borodin bromodecarboxylation, adapting the recent micellar conditions developed by Rajanna for the synthesis of alkenyl halides starting from α,β-unsaturated acids [34]. However, purification and concentration of 1-bromopenta-1,3-diene proved to only promote its degradation, likely by polymerization. To circumvent this matter, we developed a workup procedure allowing to directly obtain THF solutions of 1-bromopenta-1,3-diene in the 0.4–0.7 M concentration range, and no further purification was required. Those solutions can be directly used in a subsequent iron-mediated cross-coupling procedure. We demonstrated that the alkyl–dienyl cross coupling of those solutions of 1-bromopenta-1,3-diene with α,ω-difunctionalized Grignard reagents afforded the coupling product **4** with an excellent 94% yield and a total retention of stereochem-

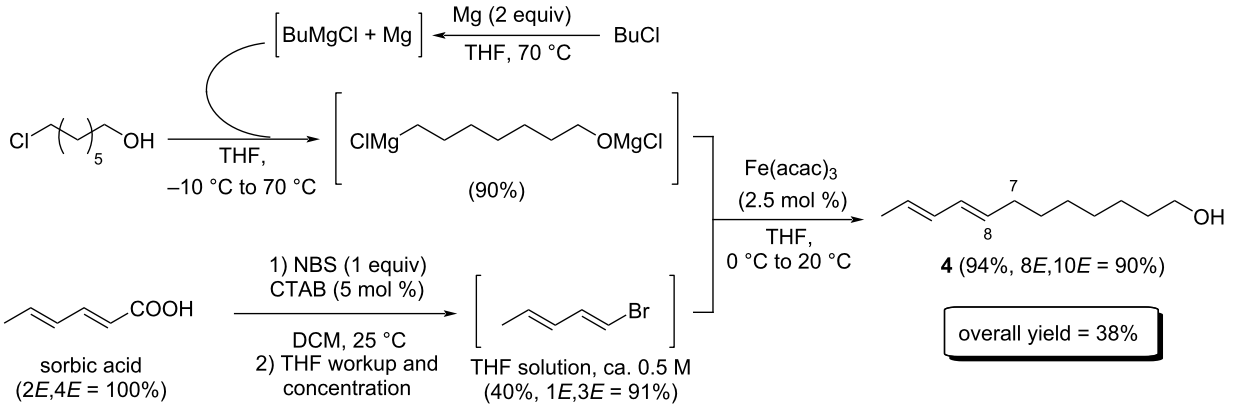

Scheme 6: Total synthesis of codling moth sex pheromone **4** using an iron-mediated cross-coupling between an α,ω-difunctionalized Grignard reagent and a dienyl bromide.

istry (Scheme 6). Overall, sex pheromone **4** can be obtained in a convergent total synthesis with a key iron-mediated cross coupling starting from sorbic acid and a commercially available α,ω-chloroalcohol in 4 steps, with an overall 38% yield.

This method can also be used for the alkylation of dienyl bromides by classic aliphatic or aromatic Grignard reagents which do not bear ω-magnesium alkoxide functionalities: in that case, EtOMgX can be used as an external additive to enhance the cross-coupling selectivity, in line with the alkyl–alkenyl and aryl–alkenyl cross-coupling methods discussed earlier (Scheme 5) [32].

The beneficial role of magnesium alkoxide salts in the outcome of iron-mediated alkyl–alkenyl cross-coupling reactions can thus display a double interest for the total synthesis of insect pheromones. Indeed, α,ω-difunctionalized Grignard reagents featuring a terminal magnesium alkoxide group can be used as both nucleophilic partners and as a magnesium alkoxide additive source, enabling the development of iron-mediated cross-coupling procedures with alkenyl or dienyl halides, requiring neither heavy alkyl phosphate leaving groups nor toxic solvents such as NMP. Moreover, those procedures can be carried out at large industrial kilogram scales, leading to green, efficient and economically viable processes.

Mechanistic considerations

The improvements of the initial cross-coupling conditions developed by Kochi (Scheme 2a) discussed in this report have high potent synthetic applications since they do not require well-defined iron precursors stabilized by highly functionalized ligands, the high price of the latter often precluding their use in high-scale syntheses. On the other hand, the exact role played at a molecular level by the additives discussed herein (NMP or one of its surrogates, magnesium alkoxides, phosphate leaving groups, etc.) is still an unclear question, even if the latter species proved to have an unambiguous beneficial effect on the cross-coupling yields and selectivities. Several recent literature results which enlighten the role of those additives, either brought by external reagents or by in situ-formed intermediates, are gathered in Table 2.

The beneficial role of the NMP co-solvent on the alkyl–alkenyl cross-coupling yield reported by Cahiez (Scheme 2b) and considerably used ever since was explained at a molecular level by Neidig in 2018. It was demonstrated that NMP did not act as a ligand to the iron center in alkyl–alkenyl cross-coupling reactions featuring Grignard reagents, but was involved in the formation of the bulky dication $[Mg(NMP)_6]^{2+}$, the presence of the latter contributing to the kinetic stabilization of the on-cycle active species $[Me_3Fe^{II}]^-$ (Table 2, entry 1) [35]. The exact nature of the interaction between the active *ate*-ferrous complex and the NMP-ligated magnesium cation is so far unknown. Although often neglected in the mechanistic analysis of a cross-coupling system, the importance of the coordination sphere of the main-group cation brought by the nucleophilic partner R[M] in a cross-coupling has been reported in the recent literature. It was indeed shown that some ligands (such as diphosphines) used in Fe-catalyzed Negishi cross-coupling reactions (R[M] = RZnX) were actually involved in the coordination of the Zn^{II} cation in a key on-cycle transmetallation step, and not in the coordination of the iron-containing intermediates [36,37].

Table 2: Selected additives used in iron-mediated cross-coupling procedures and their role at a molecular level.

	Nucleophile	Electrophile	Additive	Molecular effect of the additive	Reference
1	MeMgBr	PhCH=CHBr	NMP	formation of $[Mg(NMP)_6]^{2+}$; stabilization of $[Me_3Fe^{II}]^-$	[12,35]
2	AlkylMgBr ArMgBr	 R^1, R^2, R^3 = H, alkyl X = Cl, Br (Het)ArCl	EtOMgX	formation of [Mg]-OEt adducts, stabilization of $[Me_3Fe^{II}]^-$ (high RMgX:EtOMgX ratio); and/or $[Fe^{II}]$-OEt intermediates (low RMgX:EtOMgX ratio)	[38]
3	AlkylMnBr MesMgBr	 R^1 = alkyl, (Het)aryl	RS^-	formation of Mes-$[Fe^{II}]$-SEt adducts	[39]
4	AlkylMgBr	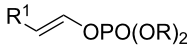 R^1 = alkyl, alkenyl	phosphate group	unknown	[20-24]

The use of magnesium alkoxide salts, either as an ω-functionalization of the nucleophilic partner (Scheme 4) or as an external molecular additive such as EtOMgCl (Scheme 5), also likely proceeds similarly to the NMP, as demonstrated by recent studies by Neidig and Lefèvre (Table 2, entry 2) [38]. No alteration of the structure of the active species $[Me_3Fe^{II}]^-$ is observed in the presence of an excess of EtOMgCl, suggesting that the alkoxide additives solely bind to the magnesium cations. However, for very low RMgX:EtOMgX ratios, minor species possibly featuring alkoxide stabilized ferrous $[Fe^{II}]$-OEt intermediates were observed by paramagnetic ^{1}H NMR spectroscopy.

In line with this result, Fleischer and Lefèvre also recently demonstrated that the anionic thiolate leaving group EtS^- released in Fukuyama cross-coupling reactions between alkylmanganese nucleophiles AlkylMnX and thioesters RC(O)SEt using $Fe(acac)_3$ as catalyst could act as a ligand to on-cycle organoiron(II) intermediates (Table 2, entry 3) [39]. This behaviour opens the door to interesting synthetic perspectives, since it suggests that leaving groups can act as stabilizing additives to on-cycle organometallic intermediates in cross-coupling procedures. Given that the quantity of free anionic leaving groups, released at each turnover cycle, increases upon completion of the coupling process, it means that the catalyst resting state strongly benefits from the leaving group ligation at the latest stages of the cross coupling. This is particularly interesting since it can hamper the usual decomposition of the iron catalyst, which tends to afford unreactive reduced aggregates at the end of the catalytic transformation, when the coupling kinetics is slowed down due to the drop of the concentration of coupling reagents. The affinity of ferrous precatalysts for thiolate ligands had also been reported by Cahiez earlier in the cross coupling of alkyl Grignard reagents with alkenyl halides, 2-naphthylthiolates being used as additives [40]. No in-depth mechanistic studies were so far reported regarding the reactivity of the enol phosphate electrophiles (Scheme 3 and Scheme 4, and Table 2, entry 4). Phosphate free anions released at each catalytic cycle could act either as NMP or alkoxides, that is, as ligands to the magnesium cations, or as thiolate leaving groups, and stabilize at a molecular level active Fe^{II} species. In both cases, a beneficial effect should be observed at a molecular level on the stabilization and/or the reactivity of on-cycle species, given that phosphate electrophiles proved to afford satisfying coupling yields in the absence of other additives.

Conclusion

In conclusion, iron-mediated cross-coupling reactions between Grignard reagents and alkenyl organic electrophiles prove to be an efficient method for the introduction of the key alkyl–alkenyl linkages in insect sex pheromones total synthesis. This method has been applied to a variety of targets, and has witnessed important improvements since the seminal reports by Cahiez and Kochi. To date, alternatives to the use of reprotoxic additives such as NMP have been reported (involving, e.g., phosphate leaving groups, or magnesium alkoxide additives), and can be efficiently applied at large industrial scales.

Extension of such methods to more challenging hybridization patterns in cross-coupling chemistry applied to synthesis of other insect pheromones is currently investigated in our groups.

Funding

The M2i Company is thanked for its financial support (CIFRE Grant Program for P.C. and A.T.) in the frame of the M2i–CNRS Joint Research Program “PheroChem”. The IRP “IrMaCAR” (CNRS program) is thanked for financial support.

ORCID® iDs

Guillaume Lefèvre - https://orcid.org/0000-0001-9409-5861

References

1. Guzelian, P. S. *Annu. Rev. Pharmacol. Toxicol.* **1982,** *22,* 89–113. doi:10.1146/annurev.pa.22.040182.000513
2. Rossi, R. *Synthesis* **1977,** 817–836. doi:10.1055/s-1977-24592
3. Henrick, C. A. *Tetrahedron* **1977,** *33,* 1845–1889. doi:10.1016/0040-4020(77)80372-4
4. Rossi, R. *Synthesis* **1978,** 413–434. doi:10.1055/s-1978-24768
5. Witzgall, P.; Kirsch, P.; Cork, A. *J. Chem. Ecol.* **2010,** *36,* 80–100. doi:10.1007/s10886-009-9737-y
6. Kirsch, P. *Am. J. Altern. Agric.* **1988,** *3,* 83–97. doi:10.1017/s0889189300002241
7. Svatoš, A.; Kalinová, B.; Hoskovec, M.; Kindl, J.; Hovorka, O.; Hrdý, I. *Tetrahedron Lett.* **1999,** *40,* 7011–7014. doi:10.1016/s0040-4039(99)01426-4
8. Francke, W.; Franke, S.; Bergmann, J.; Tolasch, T.; Subchev, M.; Mircheva, A.; Toshova, T.; Svatoš, A.; Kalinová, B.; Kárpáti, Z.; Szőcs, G.; Tóth, M. Z. *Z. Naturforsch., C: J. Biosci.* **2002,** *57,* 739–752. doi:10.1515/znc-2002-7-832
9. Grodner, J. *Tetrahedron* **2009,** *65,* 1648–1654. doi:10.1016/j.tet.2008.12.044
10. Bedford, R. B.; Brenner, P. B. The development of iron catalysts for cross-coupling reactions. In *Iron Catalysis II;* Bauer, E., Ed.; Topics in Organometallic Chemistry, Vol. 50; Springer: Cham, Switzerland, 2015; pp 19–46. doi:10.1007/3418_2015_99
11. Tamura, M.; Kochi, J. K. *J. Am. Chem. Soc.* **1971,** *93,* 1487–1489. doi:10.1021/ja00735a030
12. Cahiez, G.; Avedissian, H. *Synthesis* **1998,** 1199–1205. doi:10.1055/s-1998-2135
13. Krasovskiy, A. L.; Haley, S.; Voigtritter, K.; Lipshutz, B. H. *Org. Lett.* **2014,** *16,* 4066–4069. doi:10.1021/ol501535w
14. Bauer, I.; Knölker, H.-J. *Chem. Rev.* **2015,** *115,* 3170–3387. doi:10.1021/cr500425u
Section 2.4.1. See for a complete review on Fe-catalyzed cross-couplings.

15. O'Brien, H. M.; Manzotti, M.; Abrams, R. D.; Elorriaga, D.; Sparkes, H. A.; Davis, S. A.; Bedford, R. B. *Nat. Catal.* **2018,** *1,* 429–437. doi:10.1038/s41929-018-0081-x
16. Åkesson, B. *N-Methyl-2-Pyrrolidone;* World Health Organization, 2001.
17. Reprotoxic Category 2, R61, *Official Journal of the European Union*, December 31, 2008, European regulation No. 1272/2008.
18. Bisz, E.; Podchorodecka, P.; Szostak, M. *ChemCatChem* **2019,** *11,* 1196–1199. doi:10.1002/cctc.201802032
19. Cahiez, G.; Gager, O.; Habiak, V. *Synthesis* **2008,** 2636–2644. doi:10.1055/s-2008-1067194
20. Cahiez, G.; Habiak, V.; Gager, O. *Org. Lett.* **2008,** *10,* 2389–2392. doi:10.1021/ol800816f
21. Cahiez, G.; Guerret, O.; Moyeux, A.; Dufour, S.; Lefèvre, N. *Org. Process Res. Dev.* **2017,** *21,* 1542–1546. doi:10.1021/acs.oprd.7b00206
22. Dufour, S.; Guerret, O. Nouveau procédé de fabrication du (E,Z)-7,9-dodécandiényl-1-acétate. WO Pat. Appl WO2016001383A1, Jan 7, 2016.
23. Pucheault, M.; Liautard, V.; Guerret, O.; Guillonneau, L. Nouvelle composition d'isomeres du 7,9-dodécadiényl-1-acétate et son procede de fabrication. WO Pat. Appl. WO2018162739A1, Sept 13, 2018.
24. Chourreu, P.; Guerret, O.; Guillonneau, L.; Gayon, E.; Lefèvre, G. *Org. Process Res. Dev.* **2020,** *24,* 1335–1340. doi:10.1021/acs.oprd.0c00191
25. Yang, F.; Li, J.; Pang, G.; Ren, F.; Fang, B. *Molecules* **2019,** *24,* 2003. doi:10.3390/molecules24102003
26. ECHA, European Chemicals Agency. https://echa.europa.eu/fr.
27. Cahiez, G.; Habiak, V.; Gager, O. *J. Org. Chem.* **2008,** *73,* 6871–6872. doi:10.1021/jo800865z
28. Hatakeyama, T.; Nakamura, M. *J. Am. Chem. Soc.* **2007,** *129,* 9844–9845. doi:10.1021/ja073084l
29. Chua, Y.-Y.; Duong, H. A. *Chem. Commun.* **2014,** *50,* 8424–8427. doi:10.1039/c4cc02930e
30. Oklu, N. K.; Matsinha, L. C.; Makhubela, B. C. E. Bio-Solvents: Synthesis, Industrial Production and Applications. In *Solvents, Ionic Liquids and Solvent Effects;* Glossman-Mitnik, D.; Maciejewska, M., Eds.; IntechOpen: London, UK, 2020. doi:10.5772/intechopen.86502
31. Cahiez, G.; Lefèvre, G.; Moyeux, A.; Guerret, O.; Gayon, E.; Guillonneau, L.; Lefèvre, N.; Gu, Q.; Zhou, E. *Org. Lett.* **2019,** *21,* 2679–2683. doi:10.1021/acs.orglett.9b00665
32. Chourreu, P.; Guerret, O.; Guillonneau, L.; Gayon, E.; Lefèvre, G. *Eur. J. Org. Chem.* **2021,** 4701–4706. doi:10.1002/ejoc.202100844
33. Tamao, K.; Sumitani, K.; Kiso, Y.; Zembayashi, M.; Fujioka, A.; Kodama, S.-i.; Nakajima, I.; Minato, A.; Kumada, M. *Bull. Chem. Soc. Jpn.* **1976,** *49,* 1958–1969. doi:10.1246/bcsj.49.1958
34. Rajanna, K. C.; Reddy, N. M.; Reddy, M. R.; Saiprakash, P. K. *J. Dispersion Sci. Technol.* **2007,** *28,* 613–616. doi:10.1080/01932690701282690
35. Muñoz, S. B., III; Daifuku, S. L.; Sears, J. D.; Baker, T. M.; Carpenter, S. H.; Brennessel, W. W.; Neidig, M. L. *Angew. Chem., Int. Ed.* **2018,** *57,* 6496–6500. doi:10.1002/anie.201802087
36. Messinis, A. M.; Luckham, S. L. J.; Wells, P. P.; Gianolio, D.; Gibson, E. K.; O'Brien, H. M.; Sparkes, H. A.; Davis, S. A.; Callison, J.; Elorriaga, D.; Hernandez-Fajardo, O.; Bedford, R. B. *Nat. Catal.* **2019,** *2,* 123–133. doi:10.1038/s41929-018-0197-z
37. Wowk, V.; Lefèvre, G. *Dalton Trans.* **2022,** *51,* 10674–10680. doi:10.1039/d2dt00871h
38. Bakas, N. J.; Chourreu, P.; Gayon, E.; Lefèvre, G.; Neidig, M. L. *Chem. Commun.* **2023,** in press. doi:10.1039/d2cc06257g
39. Geiger, V. J.; Lefèvre, G.; Fleischer, I. *Chem. – Eur. J.* **2022,** *28,* e202202212. doi:10.1002/chem.202202212
40. Cahiez, G.; Gager, O.; Buendia, J.; Patinote, C. *Chem. – Eur. J.* **2012,** *18,* 5860–5863. doi:10.1002/chem.201200184

License and Terms

BEILSTEIN JOURNAL OF ORGANIC CHEMISTRY

Identification and determination of the absolute configuration of amorph-4-en-10β-ol, a cadinol-type sesquiterpene from the scent glands of the African reed frog *Hyperolius cinnamomeoventris*

Angelique Ladwig, Markus Kroll and Stefan Schulz*

Full Research Paper

Open Access

Address:
Institute of Organic Chemistry, Technische Universität Braunschweig, Hagenring 30, 38106 Braunschweig, Germany

Email:
Stefan Schulz* - stefan.schulz@tu-braunschweig.de

* Corresponding author

Keywords:
Anura; chiral gas chromatography; enantioselective synthesis; GC/MS; semiochemicals

Beilstein J. Org. Chem. **2023,** *19,* 167–175.
https://doi.org/10.3762/bjoc.19.16

Received: 14 November 2022
Accepted: 25 January 2023
Published: 16 February 2023

This article is part of the thematic issue "Total synthesis: an enabling science".

Associate Editor: B. Nay

Abstract

Hyperolid reed frogs are one of the few families of Anurans known to possess glands that emit volatile compounds used in chemical communication. *Hyperolius cinnamomeoventris*, a model species, possesses a gular gland on its vocal sac that emits chemicals, and sends visual and auditory signals during calling. Previous investigations have shown that the glandular compounds are typically macrocyclic lactones. However, in this work, we show that another major constituent of the male specific gland is (10*R*,1*S*,6*R*,7*R*,10*R*)-amorph-4-ene-10β-ol [(1*R*,4*R*,4a*R*,8a*S*)-4-isopropyl-1,6-dimethyl-1,2,3,4,4a,7,8,8a-octahydronaphthalen-1-ol]. This compound was synthesized for the first time and has the opposite configuration to amorph-4-ene-10β-ol known from plants. A short synthesis using an organocatalytic approach through a tandem Mannich/intramolecular Diels–Alder reaction led to a mixture of cadinols, which was used for the assignment of the natural cadinol structures and their stereoisomers.

Introduction

Hyperolius cinnamomeoventris (Figure 1) is one of the largest species of reed frogs (Hyperoliidae), which are commonly found in Africa, south of the Sahara. Males of the Hyperoliidae possess a characteristic yellow gular patch on their vocal sac that also serves as a gland which emits volatile organic compounds during calling [1]. These courtship calls are trimodal, consisting of calls, yellow flashing signals, and volatile chemicals released from the gland [2]. The semiochemical signal, the glandular secretion, seems to be used for species recognition and mate choice. In the related frog family Mantellidae such

functions of volatiles from males have been demonstrated [3], but no behavioral experiments involving semiochemicals have been performed so far within the hyperolid family.

Figure 1: Calling male *Hyperolius cinnamomeoventris* with exposed vocal sac carrying the yellow gular gland. Figure 1 was reprinted from [2], I. Starnberger et al., "Take time to smell the frogs: vocal sac glands of reed frogs (Anura: Hyperoliidae) contain species-specific chemical cocktails", Biological Journal of the Linnean Society, 2013, 110, 828–838, by permission of the Biological Journal of the Linnean Society published by John Wiley & Sons Ltd on behalf of The Linnean Society of London (© 2013 The Authors, Biological Journal of the Linnean Society; distributed under the terms of the Creative Commons Attribution-NonCommercial-NoDerivatives 4.0 International License, https://creativecommons.org/licenses/by-nc-nd/4.0/). This content is not subject to CC-BY-4.0.

H. cinnamomeoventris also served as a model species for the investigation of the gular gland compound composition of hyperolids. The macrolides (*Z*)-tetradec-5-en-13-olide (**D**) [4], frogolide (**E**) [5], and cinnamomeoventrolide (**B**) [6] have been identified in earlier works as gular gland constituents of this species (Figure 2). Macrolides are commonly found as scent constituents of hyperolids, but also in scent-emitting femoral glands of the Mantellinae [7]. Contrary to mantellines, whose scent gland secretions are dominated by macrolides and secondary alcohol derivatives, hyperolid secretions additionally contain sesquiterpenes, such as constituents **A** and **C** (Figure 3).

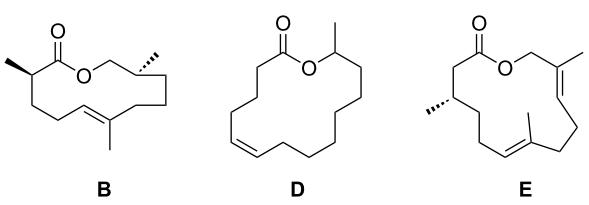

Figure 2: Macrolides identified in gular glands of male *Hyperolius cinnamomeoventris*.

As biological material is scarce and the amount of analytes is low, GC–MS trace analytical methods are performed to investigate extracts from the glands of individual frogs to identify their constituents. The analysis of MS and GC–IR data as well as gas chromatographic retention indices and microderivatization of extracts finally lead to structural proposals that have to be verified by synthesis. On this way a large variety of hyperolid and mantellid frog gland constituents have been identified [3-9]. Herein, we report on the structural elucidation of sesquiterpene **A**, including spectral analysis and synthesis to determine its constitution and absolute configuration.

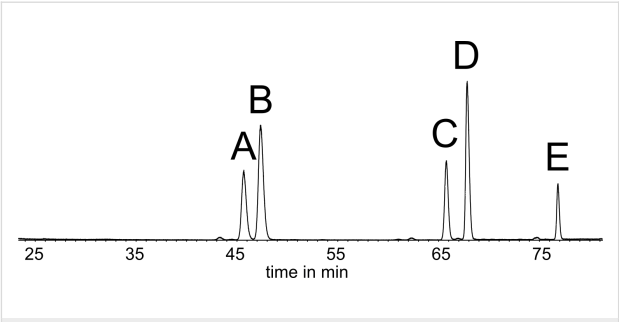

Figure 3: Total ion chromatogram (TIC) of a gular gland extract of *Hyperolius cinnamomeoventris* on a polar DB-wax GC phase. **A**, **C**: sesquiterpenes; **B**: cinnamomeoventrolide; **D**: (*Z*)-tetradec-5-en-13-olide; **E**: frogolide.

Results and Discussion

High-resolution mass spectrometry (HRMS) revealed both compounds **A** and **C** to be likely sesquiterpenes because of their molecular formula of $C_{15}H_{26}O$ (*m/z* 222.1977, calcd for 222.1984) and $C_{15}H_{22}O$ (*m/z* 216.1514, calcd for 216.1514), respectively, as well as the general appearance of their EI mass spectra. The mass spectrum of compound **A** (Figure 4) showed similarity to that of δ-cadinol (**12**) [10], but the linear gas chromatographic retention index [11] I = 1596 on an apolar DB-5 phase differed from the literature value of 1645 reported for compound **12** [12]. As no reference material was available, a problem hindering identification of sesquiterpenes in general, we planned to synthesize **12** and its seven diastereomers. Therefore, we adapted a synthesis of **12** originally developed by Taber and Gunn [13], using a Diels–Alder reaction as the key step, as it would allow access to several cadinol diastereomers, in line with a diversity-oriented synthetic plan.

The synthesis began with enamine formation of isovaleraldehyde (**1**) and piperidine (**2**) to give enamine **3** that was reacted in a Michael addition with methyl acrylate, affording aldehyde **4** (Scheme 1). Instead of the original Wittig reaction [13], a Horner–Wadsworth–Emmons reaction using diethyl (2-methylallyl)phosphonate and BuLi led to a higher yield and formation of the pure (*E*)-isomer **5**. The required phosphonate was cleanly obtained in 75% yield from triethyl phosphite and 3-chloro-2-methylpropene by addition of NaI [14]. Subsequent reduction of

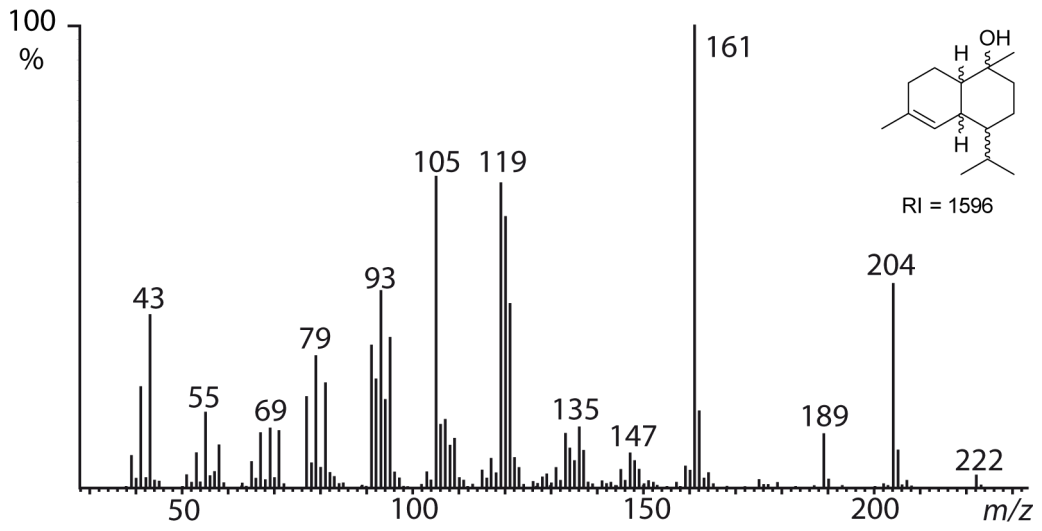

Figure 4: Mass spectrum of sesquiterpene **A** (*I* = 1596) from the gular gland extract of male *Hyperolius cinnamomeoventris,* identified to be amorph-4-en-10β-ol (**14**).

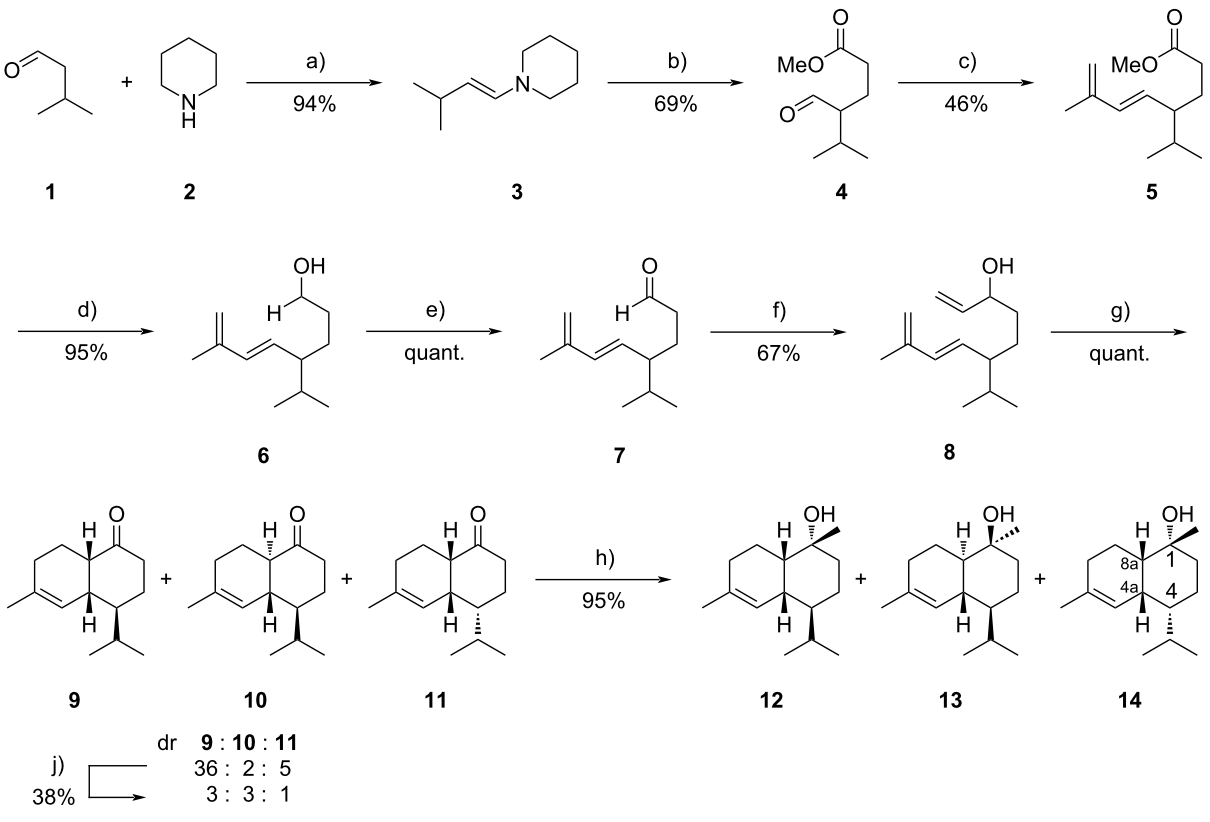

Scheme 1: Racemic synthesis of cadinols modified from Taber and Gunn [13]. Conditions a) i) K_2CO_3 (0.35 equiv), 0 °C, 1 h, ii) rt, 2.5 h; b) i) methyl acrylate (1.3 equiv), MeCN, 90 °C, 42.5 h, ii) dest. H_2O, AcOH, reflux, 1 h; c) i) diethyl (2-methylallyl)phosphonate (1.3 equiv), *n*-BuLi (1.3 equiv), THF, −78 °C, 35 min, ii) **4** (1.0 equiv), THF, −78 °C, 1 h, iii) rt, 1.5 h; d) i) $LiAlH_4$ (1.2 equiv), Et_2O, 0 °C, 15 min ii) rt, 45 min; e) IBX (3.0 equiv), EtOAc, reflux, 3 h; f) i) CH_2=CHMgBr (1.5 equiv) Et_2O, 0 °C, ii) rt, 20 min; g) IBX (3.0 equiv), EtOAc, reflux, 6 h; h) i) MeMgBr (1.5 equiv) Et_2O, 0 °C, ii) rt, 30 min; j) NaOMe (25.0 equiv), MeOH, rt, 60 h.

the ester with $LiAlH_4$ and oxidation with IBX gave aldehyde **7** in 95% yield. Grignard addition of vinylmagnesium bromide afforded the alcohol **8**, which comprised the desired triene system for an intramolecular Diels–Alder reaction. Oxidation of **8** with IBX changed the electronic properties of the system implementing an electron-deficient double bond suitable for a heat-induced intramolecular Diels–Alder reaction. The higher reaction temperature compared to the original synthesis by Taber that used dichromate as an oxidant [13] led to a less diastereoselective reaction furnishing the three ketones **9**, **10**, and **11** in a ratio of 36:2:5. The *cis*-conformation of the decalin backbone of **9** and **11** originates from the *endo*-selectivity of the Diels–Alder reaction and the boat conformation of the transition state. A chair transition state is less preferred because of inherent non-bonding interactions of some hydrogens. This has been discussed in detail in the original publication by Taber and Gunn, favoring **9** as the main diastereomer [13]. Our results confirm these data. To increase the ratio of the minor diastereomers, the ketone mixture was treated with NaOMe, resulting in epimerization of **9**, arriving at a 3:3:1 mixture of **9**, **10**, and **11**. Unfortunately, a moderate amount of material was lost due to competing aldol reactions of the ketones. While compound **9** was epimerized to a large extent into **10**, the isomer **11** could not be converted into the respective trans-fused compound. This inseparable ketone mixture was then quantitatively converted into the target cadinols by addition of methylmagnesium bromide [15]. Major compounds were cedrelanol or τ-cadinol (**13**) and δ-cadinol (**12**) (for mass spectra see Supporting Information File 1). A minor diastereomer **14** was obtained in 9% yield after isolation by RP-HPLC using a LiChroPrep RP-18 phase because conventional column chromatography did not allow for good separation from the major products. Only one face of the carbonyl groups underwent nucleophilic attack, leading the formation of the three desired compounds.

The diastereomer **14** showed the same linear retention index I = 1596 and the same mass spectrum as **A**. After detailed NMR analysis, the relative configuration of the natural product could be determined. The most stable conformation was determined by calculation using force field methods (MMFF94 [16]) and is shown in Figure S2 of Supporting Information File 1. Key NOE couplings were observed between bridgehead H-8a, H-4a and H-4. The latter also couples with the methyl group at C-1, indicating a *cis*-decalin configuration with an equatorial isopropyl group and axial OH in compound **14**. A more detailed description showing the relevant NOESY correlations is given in Supporting Information File 1.

Compound **14** proved to be identical to amorph-4-en-10β-ol, which is a rare natural product, known from the wood oil of *Cryptomeria japonica* [17], the essential oil from *Aglaia odorata* [18], and from vetiver oil (*Vetiveria zizanioides*) [19]. Nevertheless, the absolute configuration of the natural compound remained unknown [18].

Having established the constitution and relative configuration of **A**, we then determined the absolute configuration. Controlling the stereogenic center C-4 of **4** would allow access to the respective enantiomers. Unfortunately, enantiomerically pure **4** is not easily available, in contrast to ketone **17**. This compound can be obtained in high optical purity using Jørgensen's organocatalyst **16** [20,21]. In addition, such a synthetic approach would shorten the synthesis from eight to four steps and allow access to both enantiomers of the compounds **12**–**14**.

The synthesis started with an enantioselective Michael addition of aldehyde **1** to methyl vinyl ketone (**15**) catalyzed by (*S*)-Jørgensen's organocatalyst *S*-**16**, to define the first stereogenic center at the isopropyl group, which becomes C-4 in the final products. Both *S*- and *R*-**16** were used to obtain the respective products in high ee and high yields (*R*-**17** = 87%, 98% ee, *S*-**17** = 87%, 99% ee) (Scheme 2) [20].

As in the racemic synthesis (Scheme 1), a HWE reaction using diethyl (2-methylallyl)phosphonate gave diene ketone *S*-**18** [13]. Here, we envisioned that a Mannich reaction would introduce the required α,β-unsaturated carbonyl system needed for the following intramolecular Diels–Alder reaction, that likely would proceed directly under these conditions. This concept proved to be difficult to achieve, but by optimization of different parameters of this Domino reaction, the required enantiomerically almost pure ketones **9**–**11** were obtained (Table 1). The Mannich reaction worked best using diisopropylammonium trifluoroacetate as the catalyst [22]. The isolation of *S*-**19** was attempted (Table 1, entry 1) but proved not to be necessary as the intramolecular Diels–Alder reaction proceeded readily during the reaction. Other conditions using an excess of formaldehyde, paraformaldehyde, or gaseous formaldehyde (Table 1, entries 2–4) were unsuccessful, mostly due to slow reaction, but a 37% solution of formaldehyde in water/methanol proved to be successful (Table 1, entries 5–10). Nevertheless, two problems were encountered. First, the Diels–Alder products **9**–**11** proved to be also active Mannich acceptors, leading to the unwanted unsaturated ketone **20**, a double Mannich product. To avoid this second addition, an excess or equimolar amounts of formaldehyde were avoided (Table 1, entries 6–10). The best result was achieved by adding only 0.4 equivalents formaldehyde to obtain products *S*-**9**–**11** (Table 1, entries 9 and 10). The stereochemical descriptors *S* and *R* in compound numbers indicate the stereochemistry at C-4 in the cadinane system (Scheme 2) in the following discussion. Secondly, unreacted starting material **18** was not separable from

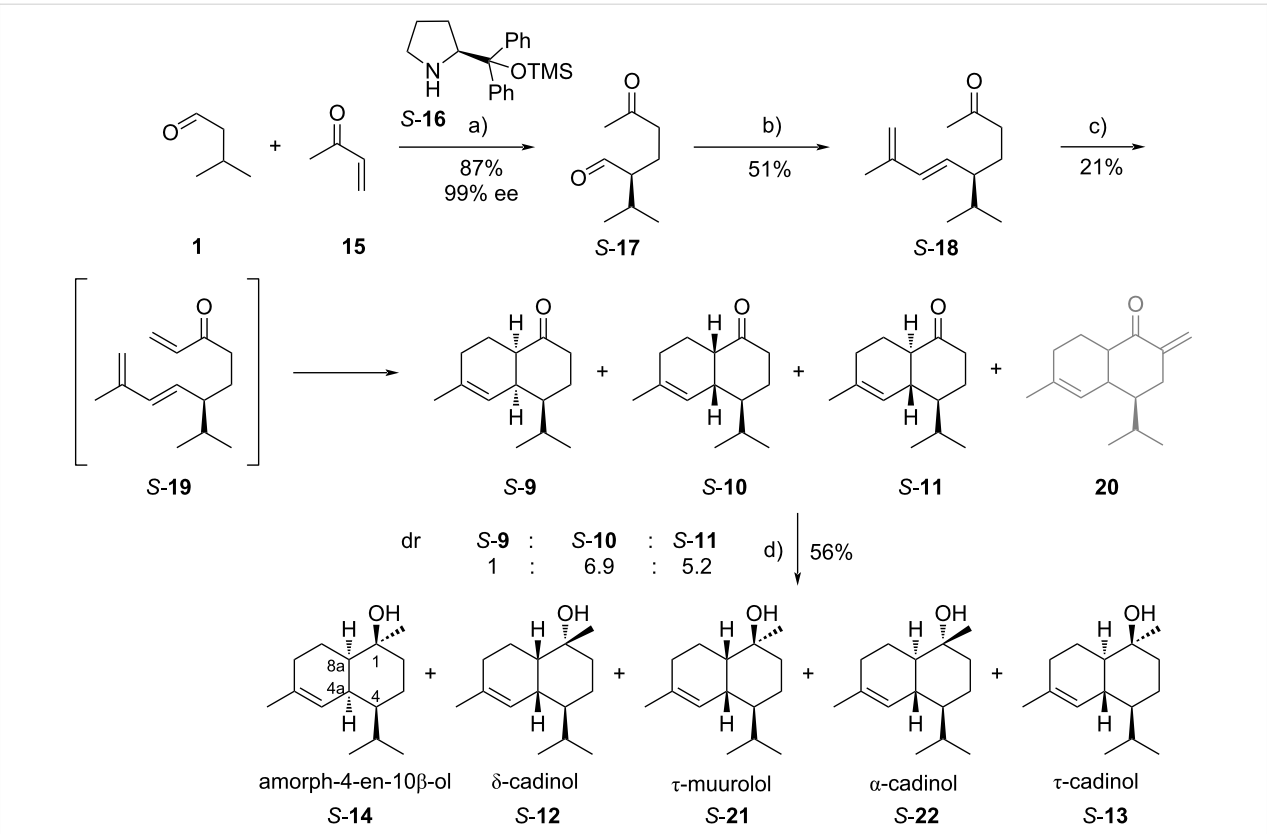

Scheme 2: Enantioselective synthesis with (*S*)-Jørgensen's organocatalyst *S*-**16**. Conditions: a) *S*-**16** (5 mol %), ethyl 3,4-dihydroxybenzoate (0.2 equiv), 4 °C, 36 h; b) i) diethyl (2-methylallyl)phosphonate (1.5 equiv), THF, −78 °C, 10 min, ii) *n*-BuLi (1.5 equiv), THF, −78 °C, 1 h, iii) *S*-**17** (1.0 equiv), −78 °C, 10 min, rt, 8 h; c) i) formaldehyde (0.4 equiv), diisopropylamine (0.4 equiv), TFA (0.1 equiv), THF, reflux, 3 d, ii) maleic anhydride (1.2 equiv), reflux, 16 h; d) MeMgBr (3.0 equiv), THF, reflux, 4 h.

Table 1: Screening of different reaction conditions with the (*S*)-Jørgensen's organocatalyst *S*-**16** for the key Domino reaction, consecutive Mannich and intramolecular Diels–Alder reactions. DIA TFA: diisopropylammonium trifluoroacetate.

entry	reagent	base	solvent (reflux)	reaction time	result
1[a]	formaldehyde (11.8 equiv)	piperidine (0.13 equiv)	MeOH	1 d	*S*-**8** 23%
2[b]	paraformaldehyde (2.0 equiv, cracked in reaction mixture)	DIA TFA (2.0 equiv)	THF	10 d	*S*-**12**
3[b]	paraformaldehyde (1.0 equiv, cracked in reaction mixture)	DIA TFA (1.0 equiv)	THF	10 d	mixture
4[b]	paraformaldehyde (1.0 equiv cracked in a separate flask)	DIA TFA (1.0 equiv)	THF	10 d	mixture
5[b]	formaldehyde (37%) (1.0 equiv)	DIA TFA (2.0 equiv)	toluene	1 d	*S*-**12**
6[b]	formaldehyde (37%) (0.75 equiv)	DIA TFA (0.75 equiv)	toluene	12 h	*S*-**12**
7[b]	formaldehyde (37%) (0.6 equiv)	DIA TFA (0.6 equiv)	toluene	8 h	*S*-**12**
8[b]	formaldehyde (37%) (0.5 equiv)	DIA TFA (0.5 equiv)	toluene	8 h	*S*-**12**
9[b]	formaldehyde (37%) (0.4 equiv)	DIA TFA (0.4 equiv)	toluene	3 d	*S*-**9**–*S*-**11** 21%
10[b]	formaldehyde (37%) in methanol (0.4 equiv)	DIA TFA (0.4 equiv)	THF	3 d	*S*-**9**–*S*-**11** 21%

[a]With AcOH (0.22 equiv) [23], [b]with TFA (0.1 equiv) [22].

the products by column chromatography. Therefore, maleic anhydride was added at the end of the reaction to form a Diels–Alder adduct with **18** that was readily separable from the target ketones. Following the optimization of reaction conditions, a change of solvent to THF was shown to be as equally effective as toluene (Table 1, entry 10).

The ketones *S*-**9**, *S*-**10**, and *S*-**11** were obtained in a ratio of 1:6.9:5.2, indicating a higher degree of epimerization at C-8a or a less selective Diels–Alder reaction compared to the racemic synthesis. Similar results were obtained within the *R*-series, starting with *R*-**17**. A final Grignard reaction using both ketone stereoisomeric mixtures with methylmagnesium bromide led to the *R*- and *S*-enantiomers of amorph-4-en-10β-ol (**14**), δ-cadinol (**12**), *epi*-α-muurolol or τ-muurolol (**21**), α-cadinol (**22**), and 10-*epi*-α-cadinol or τ-cadinol (**13**), respectively.

The isolation of product **14** proved unsuccessful due to the inseparability from the other cadinols. Nevertheless, with this material in hand, the absolute configuration of the sesquiterpene **A** was elucidated by enantioselective gas chromatography. The enantiomers of the alcohols could be separated on a Hydrodex β-6TBDM phase (Figure 5). This allowed to determine the absolute configuration of the sesquiterpene **A**. A coinjection of a gland extract with both the synthetic *R*- and *S*-samples would confirm the stereochemistry (Figure 6).

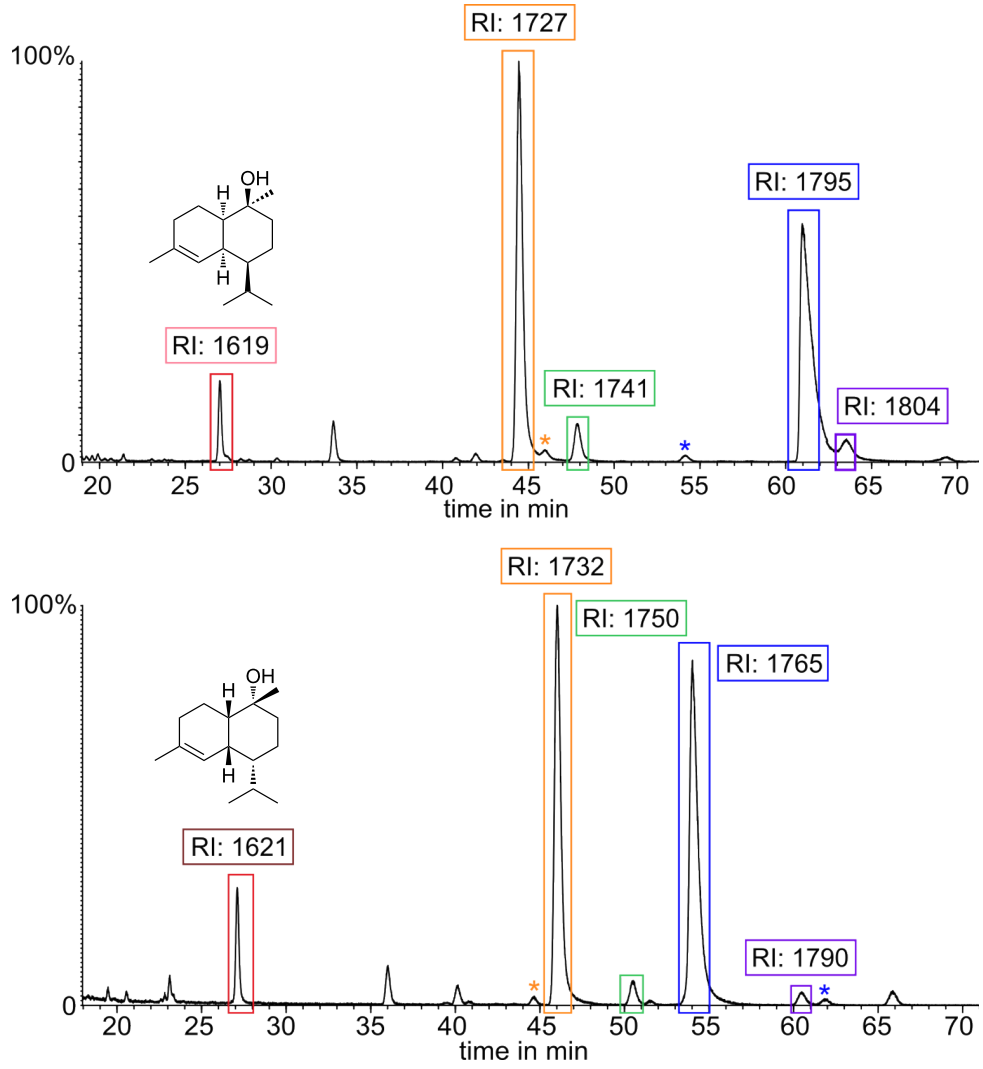

Figure 5: TIC and gas chromatographic Kovats retention indices RI [24] values determined on a Hydrodex β-6TBDM phase. The compounds are color-coded with the respective mass spectra in Figure 7 of each cadinol-type. Orange: δ-cadinol; blue: τ-cadinol; red: amorph-4-en-10β-ol; violet: α-cadinol. Upper trace: (4*S*)-diastereomers; lower trace: (4*R*)-diastereomers. *Corresponding enantiomers.

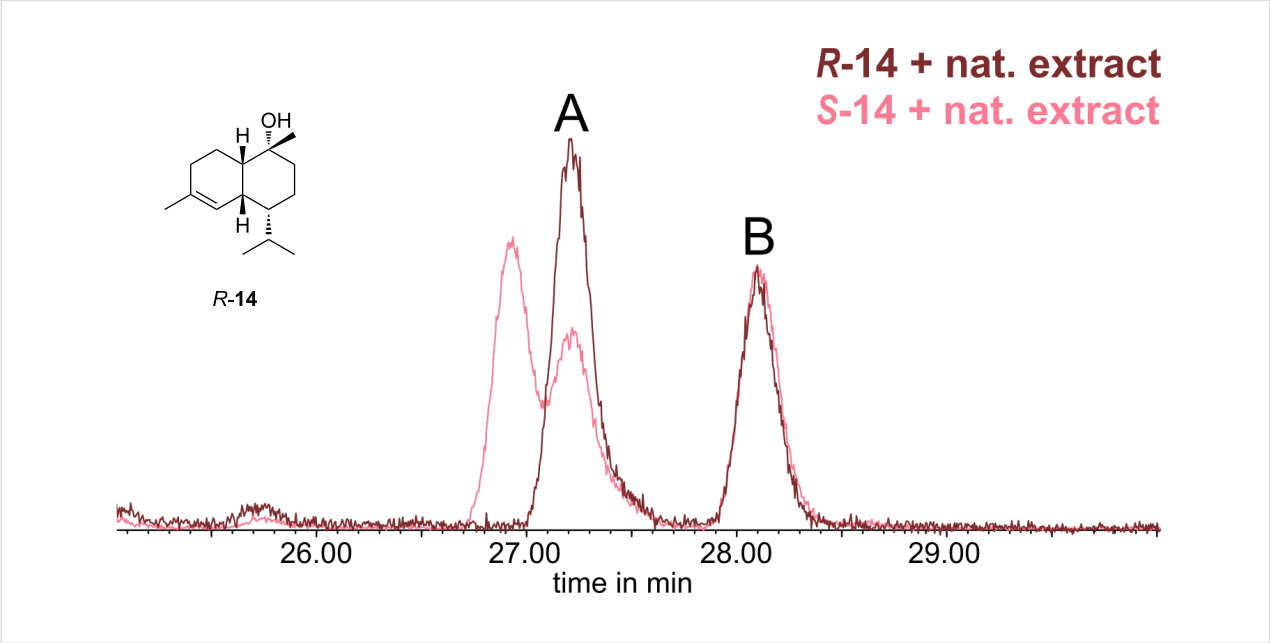

Figure 6: Coinjection of *R*-**14** and *S*-**14** with a gular gland extract of *Hyperolius cinnamomeoventris* performed with a Hydrodex β-6TBDM column. Compound **B** serves as relative standard to target compound **A**.

The coinjection of **A** with of *R*-**14** showed only one peak with increased intensity, while two peaks were observed with *S*-**14**. Therefore, the natural compound **A** is (1*R*,4*R*,4a*R*,8a*S*)-4-isopropyl-1,6-dimethyl-1,2,3,4,4a,7,8,8a-octahydronaphthalen-1-ol) (*R*-**14**) or, according to the nomenclature used initially [17,18], (10*R*,1*S*,6*R*,7*R*,10*R*)-amorph-4-ene-10β-ol (see Figure S3 in Supporting Information File 1 for a comparison of compound numbering). To the best of our knowledge, this is the first determination of the absolute configuration of amorph-4-en-10β-ol (**14**) from a natural source. Alcohol **14** has been isolated before [17,18] or obtained by rearrangement from (+)-α-ylangene [25]. In the latter case the (4*S*)-stereoisomer of **14** was formed, as the isopropyl group is not affected by the rearrangement (see Figure S3 in the Supporting Information File 1). The same enantiomer was isolated from the wood oil of *Cryptomeria japonica* [17]. Therefore, the enantiomer *R*-**14** from the frogs is different to the plant compound. This finding may point to a biosynthesis of **14** by the frogs themselves or by associated microorganisms, although uptake from the arthropod diet also may be possible, but less likely. The diet is varying. In addition, some arthropods can produce terpenes but they are not regarded as prolific producers of sesquiterpenes. The analysis of several *H. cinnamomeoventris* individuals from different locations showed a consistent composition of the gular gland blend, including always **14**. Diet-dependent uptake of compounds by frogs usually results in individual differences in compound composition, as has been observed, e.g., for skin alkaloids of Madagascan poison frogs [26]. Finally, experiments with mantellines showed that at least scent gland macrolides can be biosynthesized by the frogs [7], although the macrolides are produced from the fatty acid biosynthetic pathway.

The gas chromatographic separation obtained with the chiral phase also allowed the determination of the identity of the minor diastereomers formed during the reaction. This was not possible on a conventional DB-5-MS GC phase, because of overlapping peaks. Next to the major diastereomers **12**, **13** and **14**, *epi*-α-muurolol or τ-muurolol (**21**), and α-cadinol (**22**) were identified by their mass spectra [10,27] (Figure 7). After publication of this article, mass spectra and *I* of **12** and **14**, not present in the NIST 17 database will be made publically available in computer readable format through the open access mass spectra data base MACE [28].

Conclusion

In this work, we have characterized compound **A** to be (10*R*,1*S*,6*R*,7*R*,10*R*)-amorph-4-ene-10β-ol or (1*R*,4*R*,4a*R*,8a*S*)-4-isopropyl-1,6-dimethyl-1,2,3,4,4a,7,8,8a-octahydronaphthalen-1-ol (*R*-**14**) as part of the semiochemical mixture released by gular glands of the African reed frog *Hyperolius cinnamomeoventris*. This establishes the importance of sesquiterpenes for reed frogs, alongside macrocyclic lactones [2]. The total synthesis and characterization showed that this compound is the opposite enantiomer of **14** known from plants. This may indicate biosynthesis in the frog, but more work has to be performed to establish this. Furthermore, a short diversity-oriented synthesis based on the work of Taber and Gunn [13] enabled mass spectrometric and gas chromatographic data to be

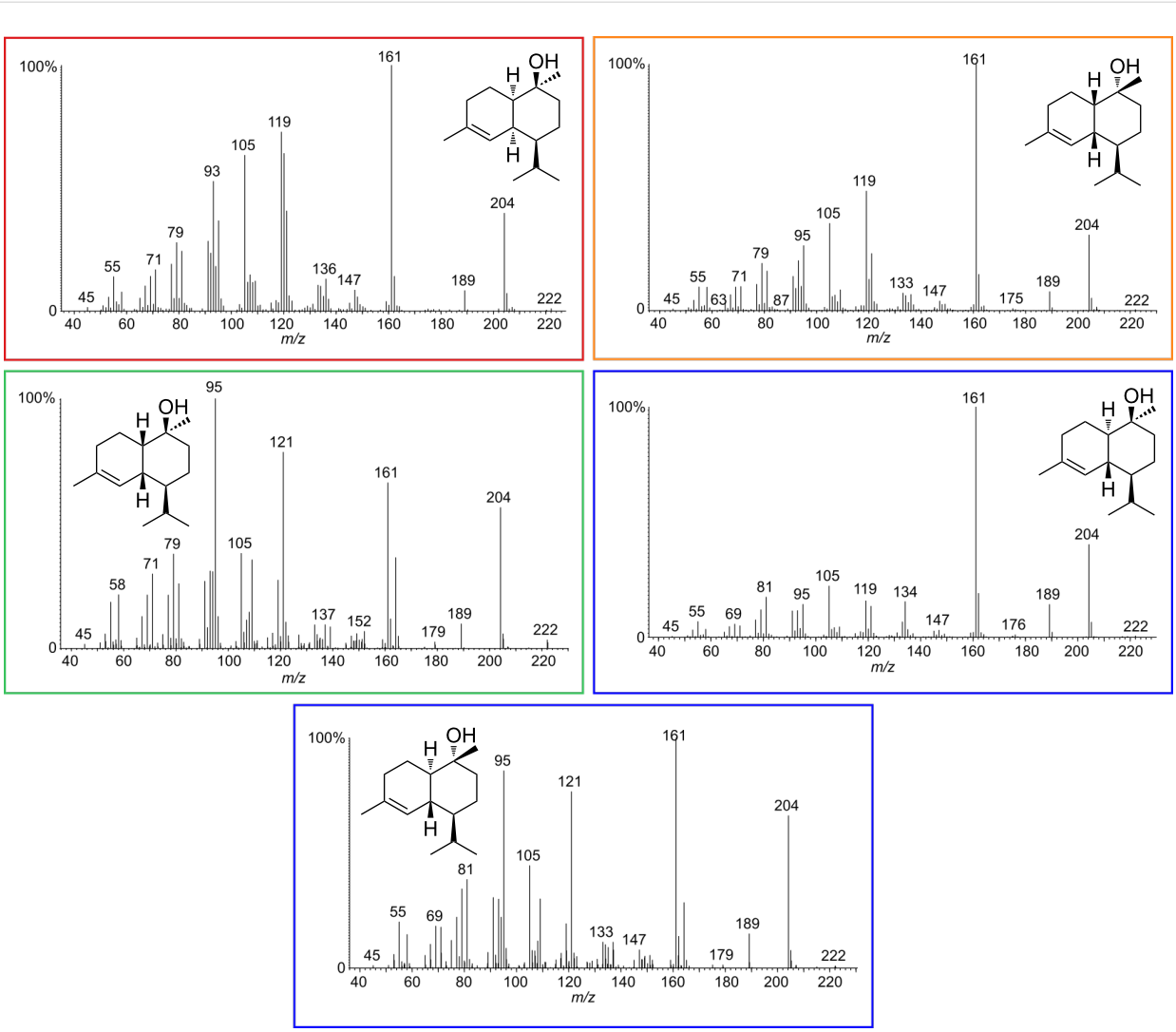

Figure 7: Mass spectra of each cadinol-type diastereomer. The box colors refer to the peaks and compounds in Figure 5.

acquired, clarifying the identity and stereochemistry of several cadinols.

Supporting Information

Supporting Information File 1

Numbering scheme, experimental procedures, ^{1}H, ^{13}C and 2D NMR spectra, and mass spectra.
[https://www.beilstein-journals.org/bjoc/content/supplementary/1860-5397-19-16-S1.pdf]

Acknowledgements

We thank Serdar Dilek for technical assistance and Miguel Vences for fruitful discussions. Furthermore, we would like to thank Dr. Christian Schlawis for performing calculations with the MMFF94 method. We also thank Dr. Matthew Stell for language improvement of the manuscript.

Funding

We thank the Deutsche Forschungsgemeinschaft for grant Schu 984/10-2.

ORCID® iDs

Angelique Ladwig - https://orcid.org/0000-0003-2924-1150
Markus Kroll - https://orcid.org/0000-0003-3336-6917
Stefan Schulz - https://orcid.org/0000-0002-4810-324X

References

1. Starnberger, I.; Preininger, D.; Hödl, W. *J. Comp. Physiol., A* **2014,** *200,* 777–787. doi:10.1007/s00359-014-0923-1

2. Starnberger, I.; Poth, D.; Peram, P. S.; Schulz, S.; Vences, M.; Knudsen, J.; Barej, M. F.; Rödel, M.-O.; Walzl, M.; Hödl, W. *Biol. J. Linn. Soc.* **2013,** *110,* 828–838. doi:10.1111/bij.12167
3. Poth, D.; Wollenberg, K. C.; Vences, M.; Schulz, S. *Angew. Chem., Int. Ed.* **2012,** *51,* 2187–2190. doi:10.1002/anie.201106592
4. Menke, M.; Peram, P. S.; Starnberger, I.; Hödl, W.; Jongsma, G. F. M.; Blackburn, D. C.; Rödel, M.-O.; Vences, M.; Schulz, S. *Beilstein J. Org. Chem.* **2016,** *12,* 2731–2738. doi:10.3762/bjoc.12.269
5. Menke, M.; Melnik, K.; Peram, P. S.; Starnberger, I.; Hödl, W.; Vences, M.; Schulz, S. *Eur. J. Org. Chem.* **2018,** 2651–2656. doi:10.1002/ejoc.201800199
6. Kuhn, J.; Schulz, S. *J. Chem. Ecol.* **2022,** *48,* 531–545. doi:10.1007/s10886-022-01370-6
7. Schulz, S.; Poth, D.; Peram, P. S.; Hötling, S.; Menke, M.; Melnik, K.; Röpke, R. *Synlett* **2021,** *32,* 1683–1701. doi:10.1055/a-1381-2881
8. Poth, D.; Peram, P. S.; Vences, M.; Schulz, S. *J. Nat. Prod.* **2013,** *76,* 1548–1558. doi:10.1021/np400131q
9. Melnik, K.; Menke, M.; Rakotoarison, A.; Vences, M.; Schulz, S. *Org. Lett.* **2019,** *21,* 2851–2854. doi:10.1021/acs.orglett.9b00852
10. *NIST 17 mass spectral library;* John Wiley & Sons: Hoboken, NJ, USA, 2017.
11. van den Dool, H.; Kratz, P. *J. Chromatogr.* **1963,** *11,* 463–471. doi:10.1016/s0021-9673(01)80947-x
12. Salido, S.; Altarejos, J.; Nogueras, M.; Sánchez, A.; Pannecouque, C.; Witvrouw, M.; De Clercq, E. *J. Ethnopharmacol.* **2002,** *81,* 129–134. doi:10.1016/s0378-8741(02)00045-4
13. Taber, D. F.; Gunn, B. P. *J. Am. Chem. Soc.* **1979,** *101,* 3992–3993. doi:10.1021/ja00508a061
14. Nishikawa, K.; Nakahara, H.; Shirokura, Y.; Nogata, Y.; Yoshimura, E.; Umezawa, T.; Okino, T.; Matsuda, F. *J. Org. Chem.* **2011,** *76,* 6558–6573. doi:10.1021/jo2008109
15. Daub, M. E.; Prudhomme, J.; Ben Mamoun, C.; Le Roch, K. G.; Vanderwal, C. D. *ACS Med. Chem. Lett.* **2017,** *8,* 355–360. doi:10.1021/acsmedchemlett.7b00013
16. Halgren, T. A. *J. Comput. Chem.* **1996,** *17,* 490–519. doi:10.1002/(sici)1096-987x(199604)17:5/6<490::aid-jcc1>3.0.co;2-p
17. Nagahama, S.; Tazaki, M.; Nomura, H.; Nishimura, K.; Tajima, M.; Iwasita, Y. *Mokuzai Gakkaishi* **1996,** *42,* 1127–1133.
18. Weyerstahl, P.; Marschall, H.; Son, P. T.; Giang, P. M. *Flavour Fragrance J.* **1999,** *14,* 219–224. doi:10.1002/(sici)1099-1026(199907/08)14:4<219::aid-ffj815>3.0.co;2-#
19. Weyerstahl, P.; Marschall, H.; Splittgerber, U.; Wolf, D.; Surburg, H. *Flavour Fragrance J.* **2000,** *15,* 395–412. doi:10.1002/1099-1026(200011/12)15:6<395::aid-ffj930>3.0.co;2-9
20. Chen, K.; Ishihara, Y.; Galán, M. M.; Baran, P. S. *Tetrahedron* **2010,** *66,* 4738–4744. doi:10.1016/j.tet.2010.02.088
21. Franzén, J.; Marigo, M.; Fielenbach, D.; Wabnitz, T. C.; Kjærsgaard, A.; Jørgensen, K. A. *J. Am. Chem. Soc.* **2005,** *127,* 18296–18304. doi:10.1021/ja056120u
22. Bugarin, A.; Jones, K. D.; Connell, B. T. *Chem. Commun.* **2010,** *46,* 1715–1717. doi:10.1039/b924577d
23. Gembus, V.; Bonnet, J.-J.; Janin, F.; Bohn, P.; Levacher, V.; Brière, J.-F. *Org. Biomol. Chem.* **2010,** *8,* 3287–3293. doi:10.1039/c004704j
24. Kováts, E. *Helv. Chim. Acta* **1958,** *41,* 1915–1932. doi:10.1002/hlca.19580410703
25. Ohta, Y.; Hirose, Y. *Bull. Chem. Soc. Jpn.* **1973,** *46,* 1535–1539. doi:10.1246/bcsj.46.1535
26. Daly, J. W.; Garraffo, H. M.; Spande, T. F.; Giddings, L.-A.; Saporito, R. A.; Vieites, D. R.; Vences, M. *J. Chem. Ecol.* **2008,** *34,* 252–279. doi:10.1007/s10886-007-9396-9
27. König, W. A.; Hochmuth, D.; Joulain, D. *Massfinder 3;* Dr. Hochmuth scientific consulting: Hamburg, Germany, 2005.
28. Schulz, S.; Möllerke, A. *J. Chem. Ecol.* **2022,** *48,* 589–597. doi:10.1007/s10886-022-01364-4

License and Terms

BEILSTEIN JOURNAL OF ORGANIC CHEMISTRY

Strategies to access the [5-8] bicyclic core encountered in the sesquiterpene, diterpene and sesterterpene series

Cécile Alleman[1], Charlène Gadais[1], Laurent Legentil[2] and François-Hugues Porée[*1]

Review

Open Access

Address:
[1]Université Rennes, Faculté de Pharmacie, CNRS ISCR UMR 6226, F-35000 Rennes, France and [2]Université Rennes, Ecole Nationale Supérieure de Chimie de Rennes, CNRS, ISCR – UMR 6226, F-35000 Rennes, France

Email:
François-Hugues Porée[*] - francois-hugues.poree@univ-rennes.fr

* Corresponding author

Keywords:
5-8 bicycle; cyclization strategies; terpenes

Beilstein J. Org. Chem. **2023,** *19,* 245–281.
https://doi.org/10.3762/bjoc.19.23

Received: 12 December 2022
Accepted: 13 February 2023
Published: 03 March 2023

This article is part of the thematic issue "Total synthesis: an enabling science".

Associate Editor: B. Nay

Abstract

Terpene compounds probably represent the most diversified class of secondary metabolites. Some classes of terpenes, mainly diterpenes (C20) and sesterterpenes (C25) and to a lesser extent sesquiterpenes (C15), share a common bicyclo[3.6.0]undecane core which is characterized by the presence of a cyclooctane ring fused to a cyclopentane ring, i.e., a [5-8] bicyclic ring system. This review focuses on the different strategies elaborated to construct this [5-8] bicyclic ring system and their application in the total synthesis of terpenes over the last two decades. The overall approaches involve the construction of the 8-membered ring from an appropriate cyclopentane precursor. The proposed strategies include metathesis, Nozaki–Hiyama–Kishi (NHK) cyclization, Pd-mediated cyclization, radical cyclization, Pauson–Khand reaction, Lewis acid-promoted cyclization, rearrangement, cycloaddition and biocatalysis.

Introduction

Terpene compounds represent the largest and most diversified class of secondary metabolites. They are present in all organisms and their structure can vary from simple terpenes (C10 skeleton) to polymers (example of rubber) thanks to iterative addition of geranyl (C10) or farnesyl (C15) building blocks derived from isoprene as starting unit and further structure rearrangement and functionalization [1]. This ubiquitous distribution highlights their pivotal role in living systems such as cell wall structural agent or ecological mediator [2]. In several cases, terpenes possess a complex polycyclic framework which challenged the chemistry community over the years to develop efficient approaches and methodologies to access them. Indeed, some classes of terpenes, mainly diterpenes (C20) and sesterterpenes (C25) and to a lesser extent sesquiterpenes (C15), share a common bicyclo[3.6.0]undecane core which is characterized by the presence of a cyclooctane ring fused to a cyclopentane ring

i.e., a [5-8] bicyclic ring system (Figure 1). In most cases, additional rings are present and original strategies have been considered to construct this bicyclic system.

This review focuses on the different strategies elaborated to build this [5-8] bicyclic ring system and their applications in the total synthesis of terpenes over the last two decades [3]. We are not providing here a comprehensive collection of the literature. When appropriate, the reader will be referred to specific reviews on a particular class of terpenes. Rather, we try to present the portfolio of available methods used nowadays to build this motif.

Accordingly, in most cases the overall approaches involve construction of the 8-membered ring from an appropriate cyclopentane precursor. The proposed strategies include metathesis, Nozaki–Hiyama–Kishi (NHK) cyclization, Pd-mediated cyclization, radical cyclization (including SmI_2), Pauson–Khand reaction, Lewis acid-promoted cyclization, rearrangement, cycloaddition, and biocatalysis. In particular, the purpose will focus on the following criteria: position/stage of the key cyclooctane ring formation in the synthesis plan, the selectivity, and the opportunity for late-stage functionalization.

Review

1 Metathesis: ring-closing metathesis and related methods

The metathesis reaction, first discovered by serendipity in the 1950s, has turned into one of the most used and powerful reactions in organic synthesis, and allows the formation of functionalized double or triple bonds. Over the time, this reaction drew more and more scientists' attention, with increasing numbers of publications on this topic [4-6]. Proof of this success, Chauvin, Schrock and Grubbs were awarded the Nobel Prize in 2005 for their improvements in metathesis reactions [5,6]. Key to success of the metathesis reaction arises from its broad spectrum of application, its functional groups tolerance, its versatility, and its mild reaction conditions [4-9]. Metathesis reactions take place by the means of a metallic catalyst. Firstly, olefin metathesis was achieved with an air-sensitive tungsten complex [8]. An important focus on air-stable catalyst design was undertaken and contributed to the popularization of the reaction. Thus, Grubbs catalysts of 1st and 2nd generation (G-I and G-II, respectively) as well as more recent Hoveyda–Grubbs 1st or 2nd generation (HG-I and HG-II, respectively) (Figure 2) are now commercially available. Today,

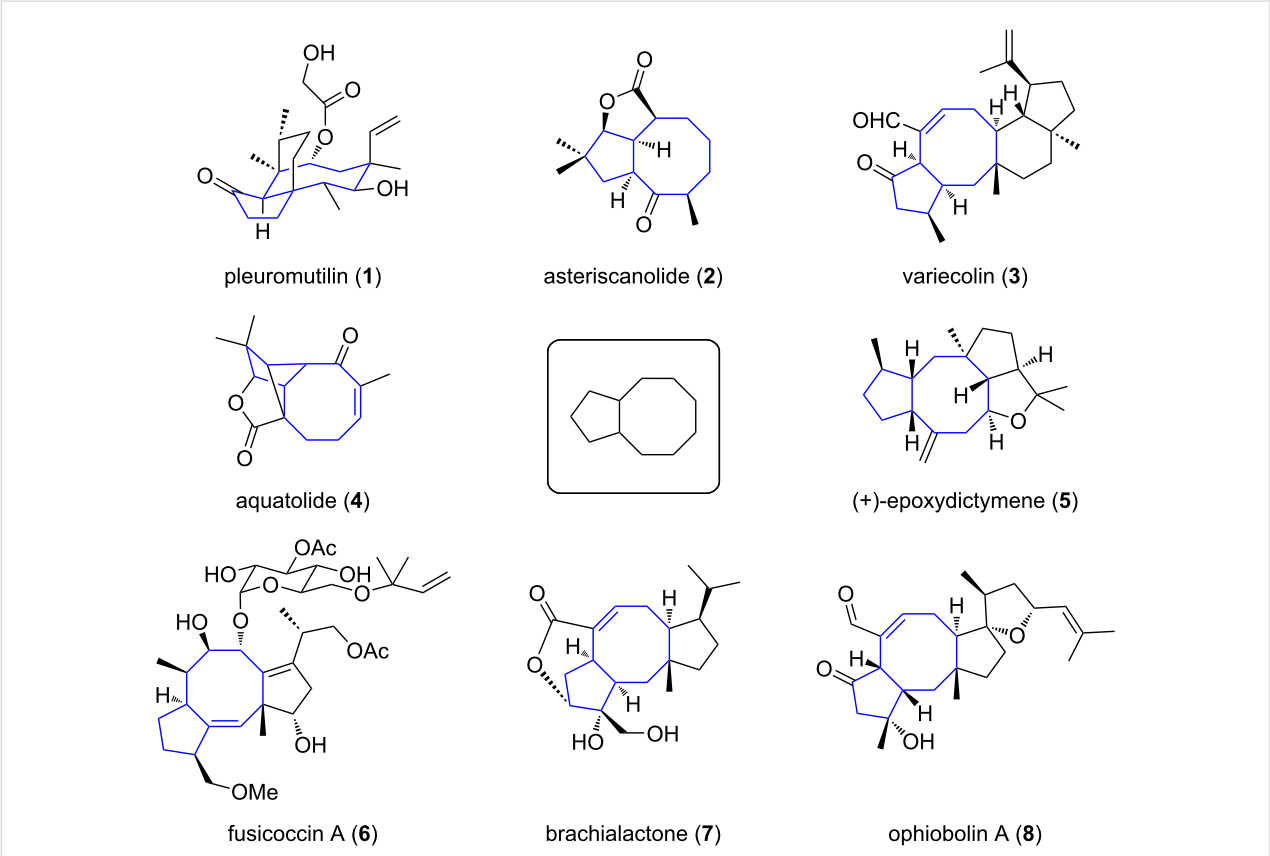

Figure 1: Examples of terpenes containing a bicyclo[3.6.0]undecane motif.

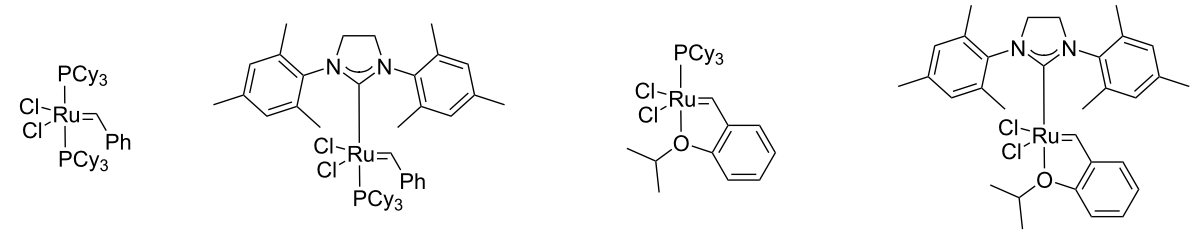

Figure 2: Commercially available first and second generation Grubbs and Hoveyda–Grubbs catalysts.

the design of new efficient catalysts is at the heart of research [4-7,9-12].

The synthesis of five- and six-membered rings can be readily achieved through ring-closing metathesis (RCM), but the synthesis of eight-membered rings has been carried out later [13,14]. In this part, we will focus on the use of RCM to achieve total syntheses of natural products or to access the carbon skeleton of natural products, and more particularly to construct the cyclooctane ring that is part in these motifs.

1.1 Ring-closing metathesis (RCM)

Among all metathesis reactions available in the chemist's toolbox, ring-closing metathesis (RCM) is nowadays one of the most popular and has been used several times as a key-step to synthesize the cyclooctanoid ring that is part of the sesterterpenoid family.

1.1.1 Syntheses of fusicoccans and ophiobolins: Fusicoccanes and ophiobolins represent an important class of natural diterpenes, whose principal members are fusicoccin A (**6**) and ophiobolin A (**8**), respectively (Figure 1). Both families share the same core structure bearing a fused [5-8-5] tricyclic skeleton and they vary within their decorative functional groups.

Over the years, many different syntheses to access compounds from the fusicoccan and ophiobolin family have been reported, with two strategies standing out. The first one (strategy 1, Figure 3) consists in the successive formation of the eight-membered ring B followed by construction of the five-membered ring C: i.e., the cyclooctene ring is built first from a suitably substituted cyclopentane substrate, which then serves as a precursor for the cyclopentane ring C formation. In the second strategy (strategy 2, Figure 3), both cyclopentane rings A and C are formed first, and the eight-membered ring B is introduced at a late stage.

1.1.1.1 Strategy 1: Successive introduction of rings B and C starting from cyclopentene via the [5-8] bicyclic structure to the final [5-8-5] tricyclic core:

The synthesis of the core bicyclic structure **12** of ophiobolin M (**13**) isolated from the fungus *Cochliobolus heterostrophus* and cycloaraneosene (**14**) firstly isolated in 1975 from the fungus *Sordaria araneosa*, was undertaken by Williams et al. in 2002 [15]. Compound **14** shares the common [5-8-5] tricyclic framework emblematic of the fusicoccan series, albeit cycloaraneosene (**14**) does not have any heteroatom (Scheme 1) [16]. Focusing on the B–C bicyclic fragment, they used diene **10**, readily available from cyclopentane-1,3-dione (**9**), as the precursor for installing the eight-membered ring by RCM (Scheme 1). Optimization of the reaction parameters (temperature, solvent, concentration, and catalyst amount) was carried out with G-I catalyst. Indeed, the authors noticed that high temperatures improved the reaction conversion, and dichloromethane seemed to furnish clean reaction and easy work-up. Thus, the final conditions were determined as 8–10 mol % of G-I catalyst loading in refluxing dichloromethane, albeit C5-C8 bicycle **11** was formed in modest yields and incomplete conver-

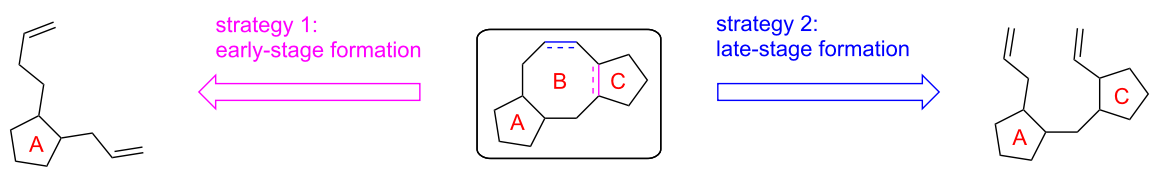

Figure 3: Examples of strategies to access the fusicoccan and ophiobolin tricyclic core structure by RCM.

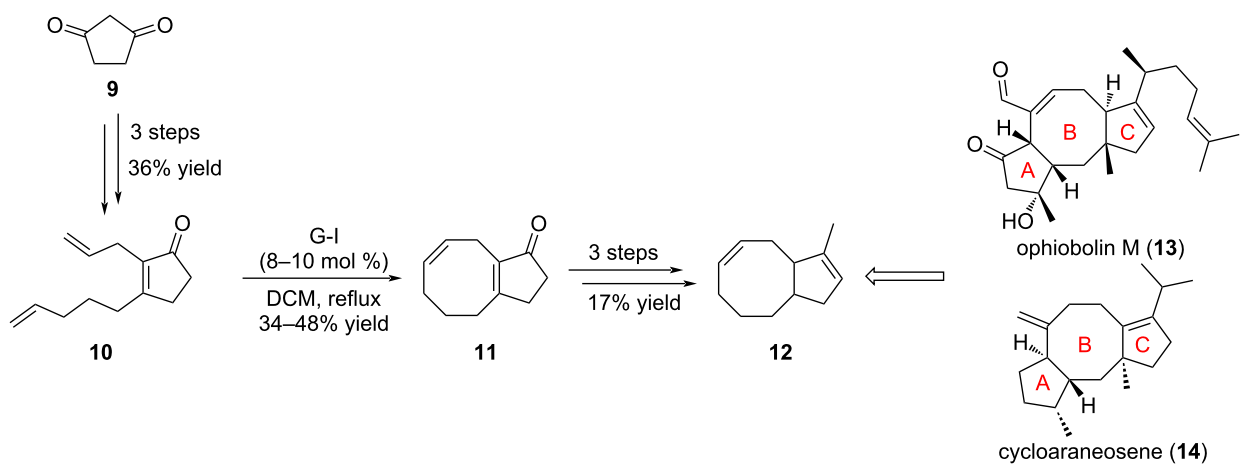

Scheme 1: Synthesis of bicyclic core structure **12** of ophiobolin M (**13**) and cycloaraneosene (**14**).

sion. Interestingly, use of G-II catalyst, known to give better results, did not improve the yield nor the bicycle-to-monocycle ratio.

In 2005, Michalak et al. examined the synthesis of the dicyclopenta[*a*,*d*]cyclooctane structure present in ophiobolins and fusicoccanes by the means of a ring-closing metathesis reaction [17]. The metathesis substrate **17** was readily prepared in four steps from accessible methylcyclopentenone **16** (Scheme 2). The sequence included a Mukaiyama–Michael reaction with silyl enol **15** followed by a Tsuji alkylation. With diene **17** in hands, the RCM reaction was performed by addition of G-II

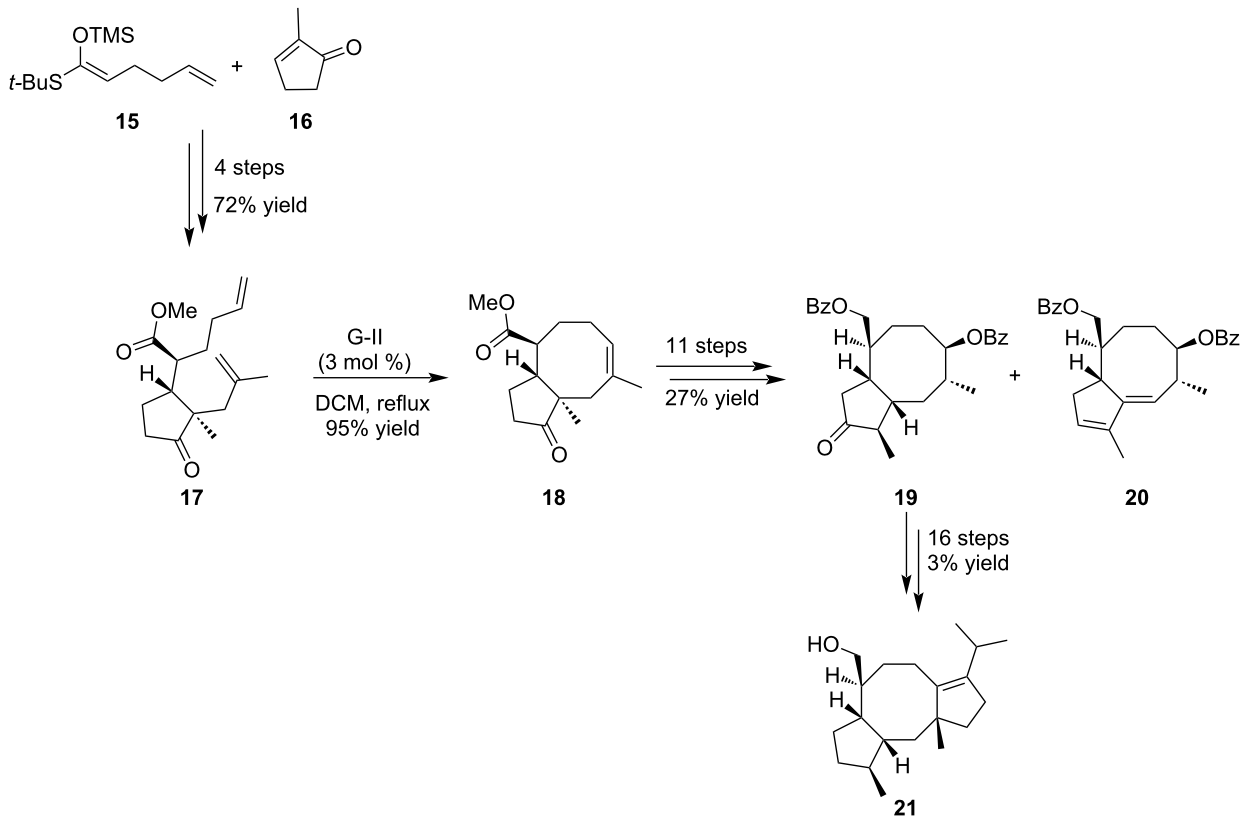

Scheme 2: Synthesis of the core structure **21** of ophiobolins and fusicoccanes.

catalyst and furnished the expected C5-C8 bicyclic framework **18** in 95% yield [17,18]. This key intermediate was then converted into ketone **19** in 11 steps leading to the desired dicyclopenta[*a,d*]cyclooctane structure **21** [19].

As explained by the authors, the RCM reaction was not as easy as expected and extensive work was necessary to accomplished the construction of this eight-membered ring. Indeed, in the initial strategy, thioester **22** was the first substrate subjected to the cyclization. In the presence of G-I catalyst, the reaction delivered the dimeric compound **23** whereas [5-7] bicycle **24** was formed in the presence of the G-II catalyst (Scheme 3). The formation of compound **24** was rationalized by an isomerization of the double bond prior to the cyclization step.

Isolated from the Ecuadorian liverwort *Anastrophyllum auritum* in 1994, *ent*-fusicoauritone (**28**) is a diterpene presenting a fusicoccan skeleton with a β-hydroxyketone on the A-ring and 5 stereogenic centers [20]. Its total synthesis was explored by Srikrishna and Nagaraju in 2012 using a linear strategy (Scheme 4) [20]. Thus, menthene **25** was converted in 16 steps into cyclopentane **26** presenting two unsaturated lateral chains. This compound was then treated with G-I catalyst to give the corresponding [5-8] cyclooctene **27** in very high yield. The final stages of the synthesis corresponded to the elaboration of the second cyclopentenone ring allowing access to *ent*-fusicoauritone (**28**) in 24 steps.

1.1.1.2 Strategy 2: Late-stage formation of the 8-membered ring:

Ophiobolins belong to the family of sesterterpenoids which displays around 50 members [21]. All these molecules share a similar [5-8-5] tricyclic structure (A-B-C ring system), with different decorating groups. The first congener to be isolated was ophiobolin A (**8**), which is present in the fungus *Ophiobolus miyabeanus* [22]. Other fungal species were found to produce ophiobolin A (**8**), and many other ophiobolin congeners such as ophiobolin B (**29**), ophiobolin C (**30**), and ophiobolin M (**13**) were also isolated (Figure 4) [23].

This natural products family is of high interest because of its broad spectrum of biological activities ranging from anti-infectious to anticancer properties [21,24,25]. Indeed, access to the ophiobolin structure is crucial to study their biological activities in detail. Many synthetic approaches have emerged for the synthesis of ophiobolins and total syntheses of some congeners have also been reported [21,24].

Nakada and co-workers reported in 2011 the first enantioselective total synthesis of (+)-ophiobolin A (**8**), involving a RCM approach to form the central eight-membered ring [24]. In this way, their total synthesis involved the enantioselective preparation of the C-D spiro bicyclic ring system **33** in 21 steps from diester **31** and oxazolidinone **32** (Scheme 5) [26]. Subsequently,

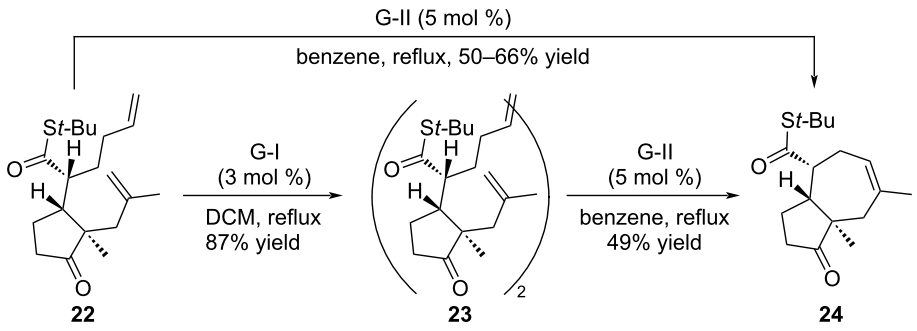

Scheme 3: Ring-closing metathesis attempts starting from thioester **22**.

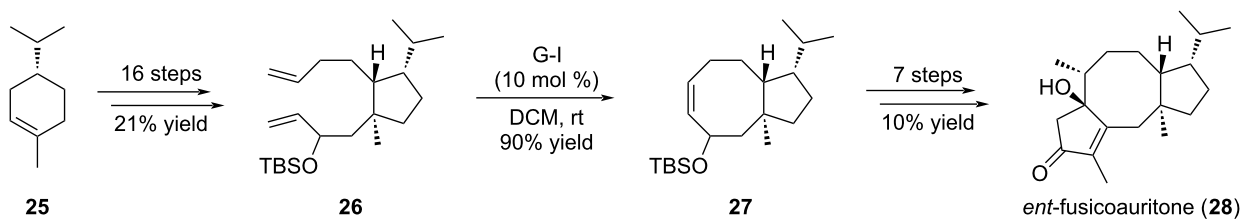

Scheme 4: Total synthesis of *ent*-fusicoauritone (**28**).

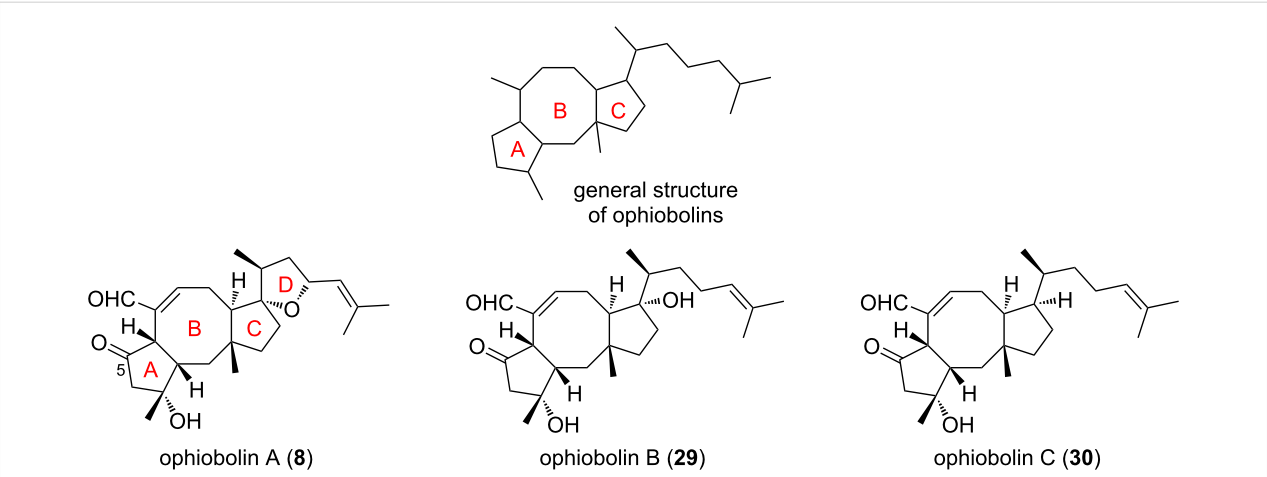

Figure 4: General structure of ophiobolins and congeners.

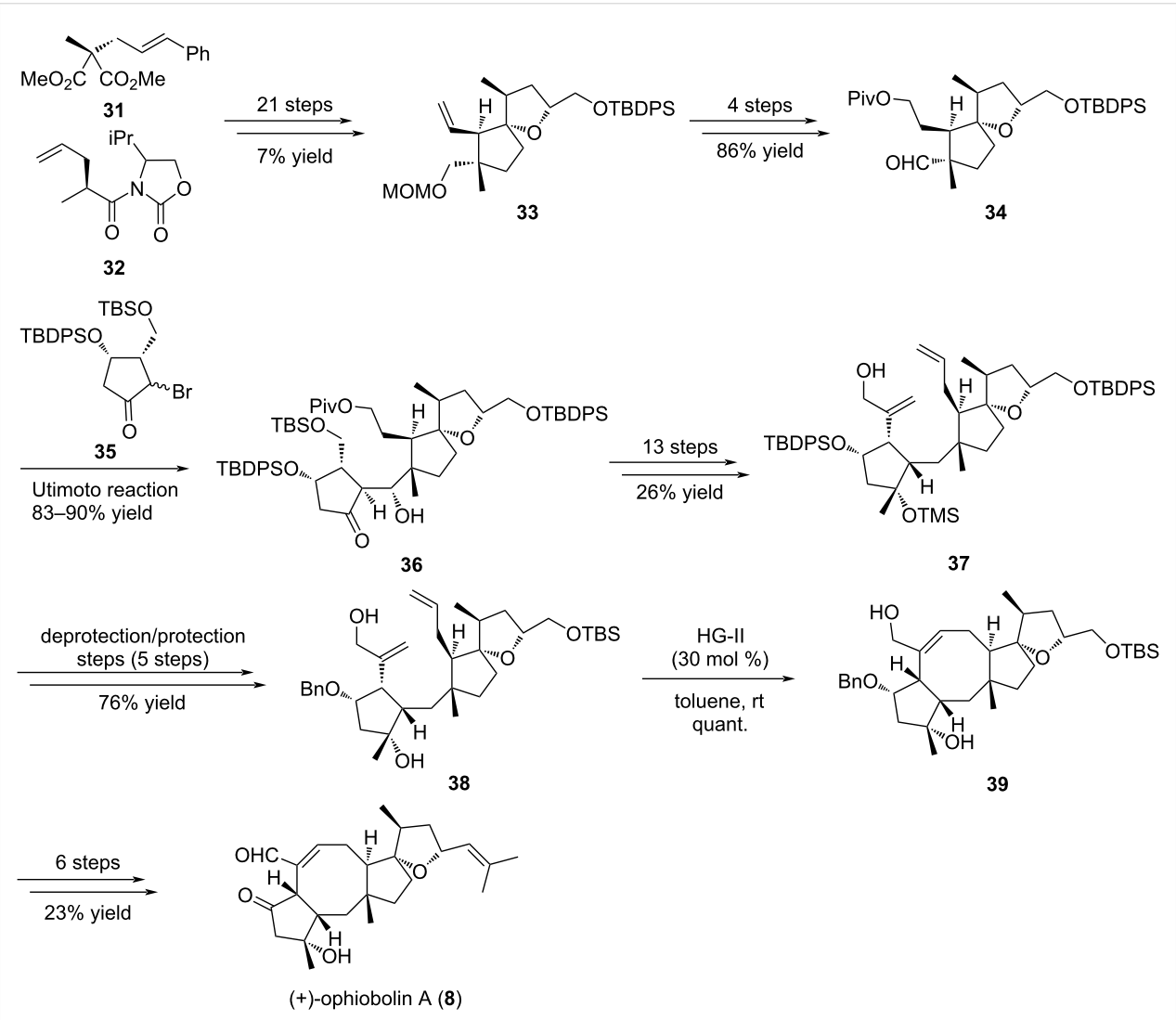

Scheme 5: Total synthesis of (+)-ophiobolin A (**8**).

compound **33** was converted in four steps into aldehyde **34** which was engaged in a coupling reaction with bromoketone **35** according to Utimoto conditions to furnish the A-C-D adduct **36** as a single stereoisomer in high yield. Of note, the Utimoto reaction has never been used in the synthesis of natural products before this report, and no β-elimination of the silyloxy group was observed, although this often occurs in such systems [26]. The installation of the two alkenes in **37** required 13 additional steps, and further protecting group manipulations were necessary to give compound **38** as a precursor for the late-stage RCM cyclization. This ring formation was very challenging and necessitated extended optimization. Indeed, during the course of the RCM a dramatic effect of the OH-protecting group on the cyclopentane unit was observed. The presence of a TBDPS substituent in compound **40** was assumed unfavorable, since this bulky residue generates a steric hindrance precluding the cyclization (Scheme 6, path A) [27]. Its replacement by a sterically less demanding benzyl protecting group (compound **44**) allowed the reaction to occur (Scheme 6, path B). It also appeared that the RCM depended on the substrate core structure and the presence of a protected allylic alcohol prevented the cyclization to take place. Taking these observations into account, the tricyclic [5-8-5] ring system **45** was obtained using the HG-II catalyst in refluxing toluene. Further functionalization steps finally furnished (+)-ophiobolin A (**8**).

In the fusicoccanes family, cotylenol (**50**), the aglycon of cotylenin A (**131**) (see section 3.1), is a fungal metabolite which displays various interesting biological activities [28]. For example, it expresses a moderate cytotoxicity against human myeloid leukemia cells, and stabilizes the 14-3-3 – TASK3 protein–protein interaction [29,30]. Sugita et al. investigated the synthesis of the core structure of cotylenol (**50**) first through an RCM approach on the advanced intermediate **47** (Scheme 7) [31]. Despite many attempts, the authors could not obtain the desired tricyclic compound possessing the required eight-membered ring, but instead they recovered the starting material **47**, together with a dimeric product or an eleven-membered ring resulting from a RCM and a retro-aldol reaction. Assuming that the allylic alcohol may induce a steric hindrance, alcohol **47** was converted into triene **48** upon dehydration, and further engaged in the RCM reaction. In this case, the use of HG-II catalyst proved to be the best choice to achieve cyclooctene ring formation giving rise to intermediate **49**, providing entries for further functionalization and access to cotylenin A aglycon **50**.

Other examples of fusicoccan derivatives are represented by alterbrassicicene D (**54**) and 3(11)-epoxyhypoestenone (**55**), recently isolated from *Hypoestes verticillaris* [32]. Structurally, alterbrassicicene D (**54**) comprises an α,β-unsaturated ketone C-ring, and a single hydroxy group on the central eight-membered ring and 3(11)-epoxyhypoestenone (**55**) shows a surprising oxa-bridge between the A and C rings, an α,β-unsaturated ketone on ring C, and an *endo*-alkene into the cyclooctene ring. Recently, Chen et al. reported the synthesis of the tricyclic

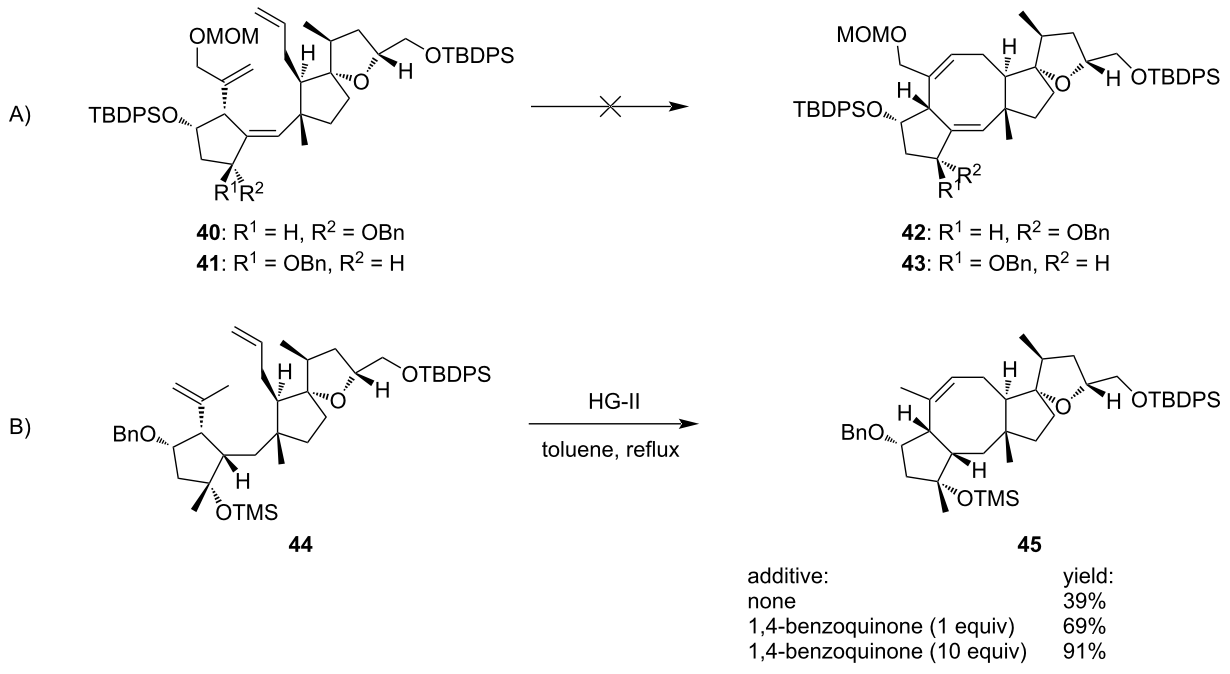

Scheme 6: Investigation of RCM for the synthesis of ophiobolin A (**8**). Path A) RCM with TBDPS-protected alcohol. Path B) RCM with benzyl-protected alcohol.

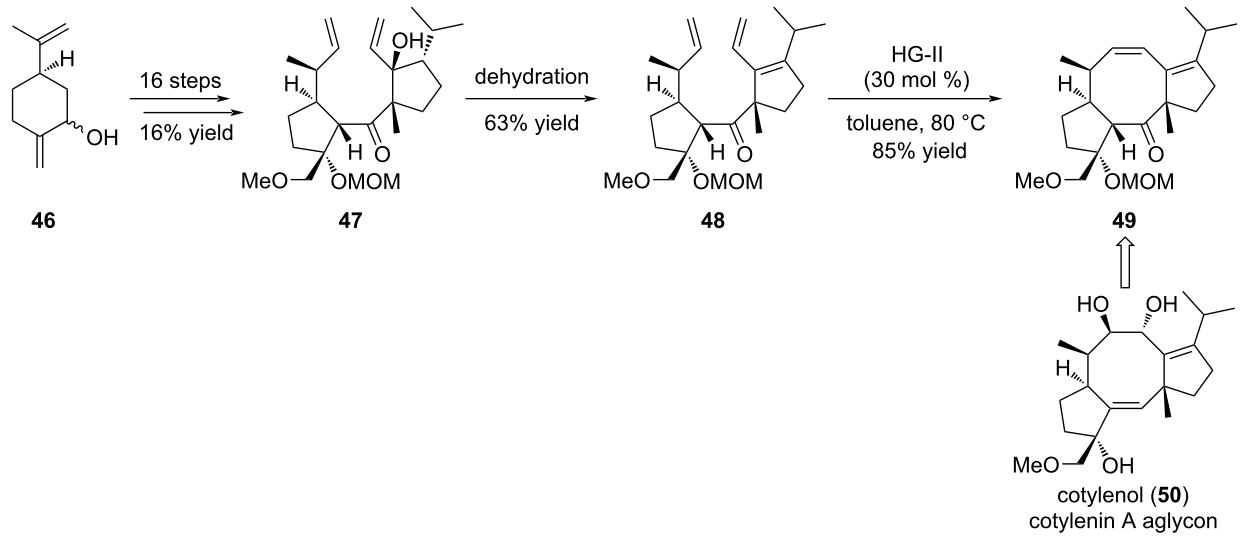

Scheme 7: Synthesis of the core structure of cotylenin A aglycon, cotylenol (**50**).

core structure of the fusicoccane skeleton **53** using a RCM approach (Scheme 8) [33]. The key RCM reaction was envisioned on precursor **52** corresponding to the A-C rings of the tricyclic backbone. In this case, G-II catalyst was used and the expected product **53** was obtained in high yields. Interestingly, the tricyclic intermediate **53** could be obtained in only 8 steps and at a large scale. Validation of this strategy allowed the authors to extend this approach to the total synthesis of alterbrassicicene D (**54**) and 3(11)-epoxyhypoestenone (**55**).

1.1.2 Other chemical series possessing a [5-8] unit;

1.1.2.1 Early-stage introduction of the eight-membered ring: (−)-Teubrevin G (**59**) is an example of a C5-C8 bicycle in which the C5 unit corresponds to a furan ring (Scheme 9) [34]. Indeed, this compound isolated from aerial parts of *Teucrium brevifolium* has a unique structure composed of a cyclooctanone, fused with a furan ring, and bearing a spirolactone. As illustrated with the previous examples, access to the final cyclooctane ring was envisioned through a RCM reaction from an appropriate precursor. In a first attempt, compound **57**, prepared from oxazole **56**, was heated in the presence of G-I catalyst but yielded bicycle **58** only in modest amounts even after extensive reaction times (more than 3 days) and high catalyst loadings (30–35 mol %). After reaction optimization, use of G-II catalyst allowed formation of cyclooctene **58** in excellent 90% yield. This compound could ultimately be advanced to **59** in 8 steps.

Exhibiting a [5-8-5] tricyclic framework, the basmane family of terpenes differs from the fusicoccans by the arrangement of the

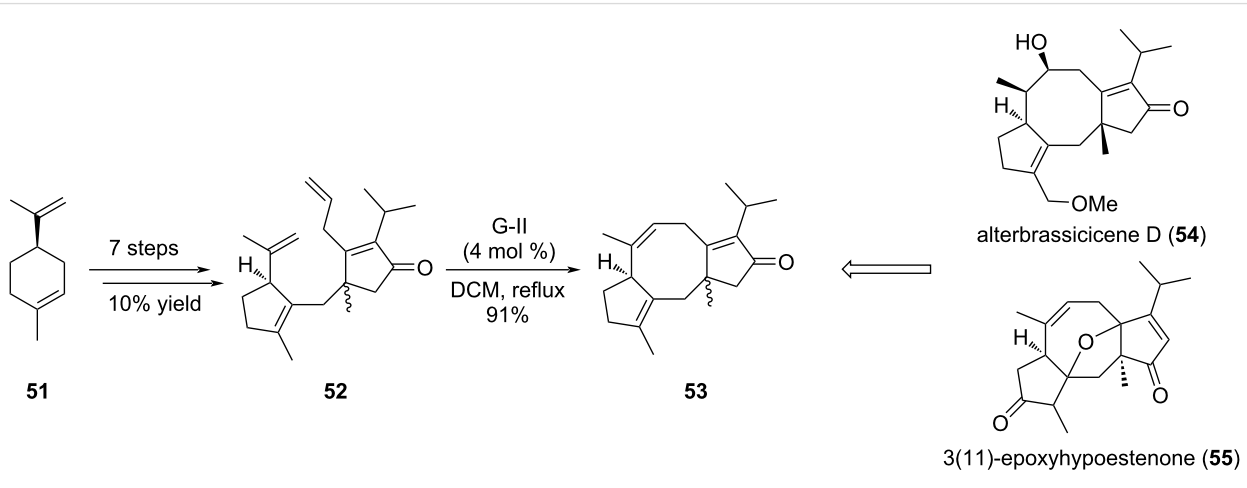

Scheme 8: Synthesis of tricyclic core structure of fusicoccans.

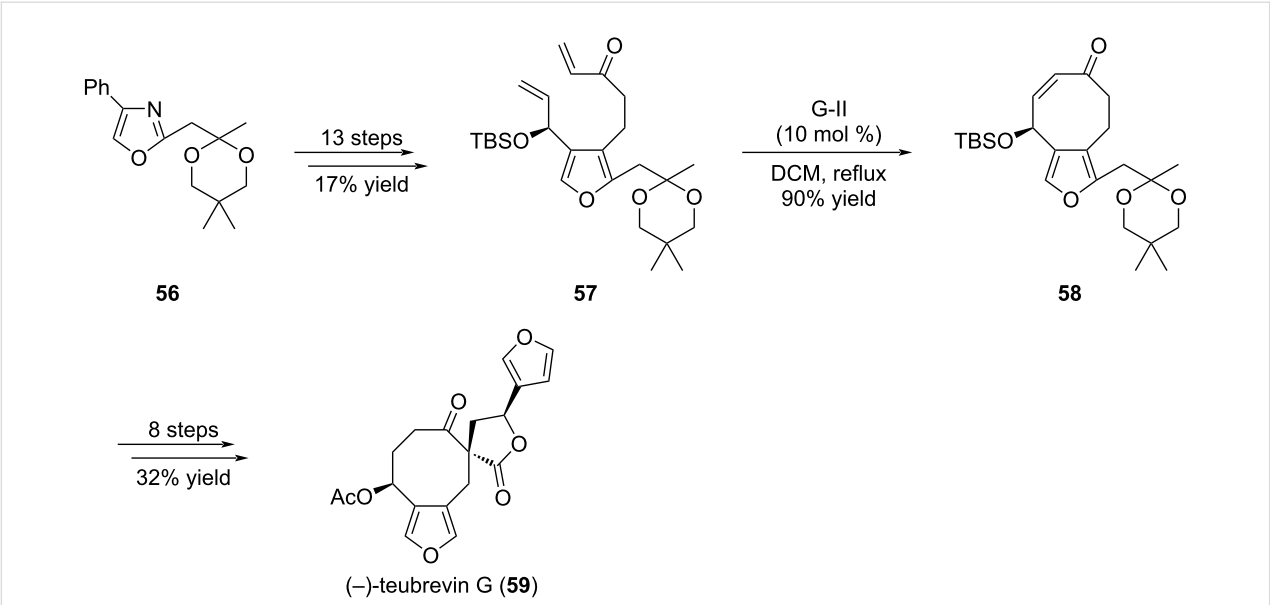

Scheme 9: Total synthesis of (–)-teubrevin G (**59**).

cycles, especially the position of the shared C–C bond between ring B and ring C (Scheme 10). In 2010, Ravi et al. investigated the synthesis of the core skeleton of this family [35]. Dihydrolimonene **25** was converted in 9 steps into compound **60** before subsequent RCM. As the authors knew G-I catalyst isomerizes β,γ-unsaturated ketones, G-II catalyst was chosen to produce bicyclic compound **61**. Several additional steps were necessary to forge the last ring and obtain the core structure **63** of this series.

Schindilactone A (**68**) is a nortriterpenoid isolated from *Schisandraceae* plant family which displayed interesting biological activities in cancer and anti-infectious axis. However, access to this compound is limited because it possesses a very complex structure composed of a highly oxygenated backbone with 8 fused rings, a unique [7-8] bicyclic motif, an oxa-bridge over the cyclooctane ring, and the presence of 12 stereogenic centers [36].

The strategy proposed by the authors was to carry out a RCM reaction to elaborate the cyclooctene ring from functionalized intermediate **66**, prepared as a diastereomeric mixture (α-position of the lactone, OTES) (Scheme 11) [36]. Interestingly, in this transformation the G-II-mediated ring formation was performed in the presence of $MgBr_2$, which acted as an epimerization agent at the lactol position yielding compound **67** as a single diastereomer in 65% yield. Of note, this compound entails the oxabicyclo[4.2.1]nonane core present in schindilactone A (**68**). The synthesis of schindilactone A (**68**) was achieved in 29 steps (0.11% overall yield).

1.1.2.2 Late-stage introduction of cyclooctene: The marine sesquiterpene dactylol (**72**), isolated from both sea hare *Aplysia dactylomela* and red seaweed *Laurencia poitei*, bears a rare rearranged *trans*-bicyclo[6.3.0]undecane isoprenoid skeleton. Its structure is – only – composed of a bicyclic ring with fused five- and eight-membered rings, with a hydroxy group at the

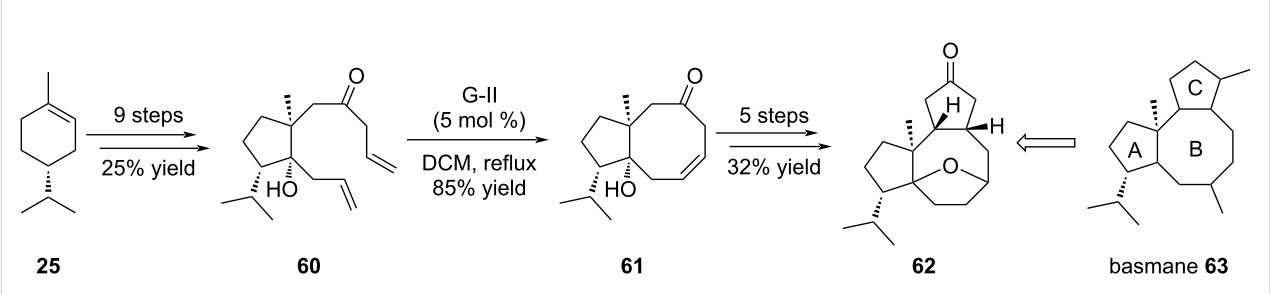

Scheme 10: Synthesis of the core skeleton **63** of the basmane family.

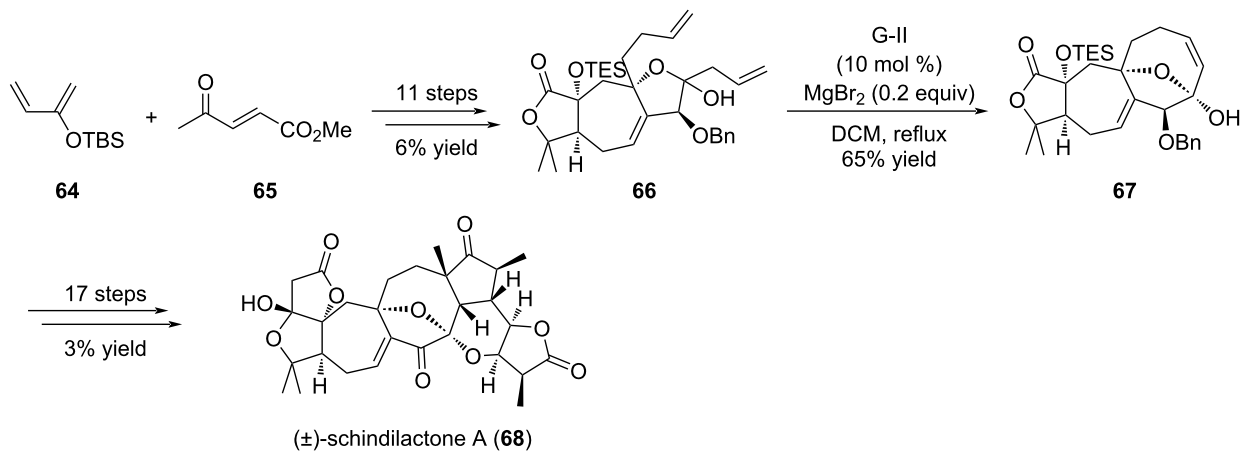

Scheme 11: Total synthesis of (±)-schindilactone A (**68**).

junction cycle [37,38]. In 1996, Fürstner and Langemann reported an efficient and short total synthesis of the natural product dactylol (**72**) (Scheme 12) [37]. The main originality of this work was the use of the Schrock molybdenum carbene catalyst **73** for the ring-closing metathesis reaction. The metathesis precursor **70** was obtained in 4 steps from commercial cyclopentenone **69**. Protection of the alcohol function was mandatory prior to the cyclization as the free alcohol substrate failed to cyclize. As proposed by the authors, interaction between the free alcohol **70** and the molybdenum metal center may explain the reaction inhibition. Thus, after protection of the alcohol function as a silyl ether leading to diene **71**, the RCM was performed in refluxing hexane and dactylol (**72**) was isolated in 17% overall yield after silyl ether removal [18,37].

Asteriscanolide (**2**), isolated in 1985 from the hexane extract of the plant *Astericus aquaticus*, is a sesquiterpene with a unique framework. Indeed, this natural compound has a rare [6.3.0] carbocyclic backbone with a bridging butyrolactone, and possesses five *cis* stereocenters [39,40]. This compound, in a racemic version, has been studied by Krafft, Cheung and Abboud (Scheme 13) [39]. The initial strategy relied on an intramolecular RCM reaction on compound **74** between the two terminal olefins, that could lead to the formation of a trisubstituted double bond (compound **75**), and further access to the required α-methyl ketone. However, despite many attempts, no cyclization occurred. Indeed, the disubstituted methylene in compound **74** and the formation of a trisubstituted alkene in **75** were assumed to cause an important steric hindrance unfavor-

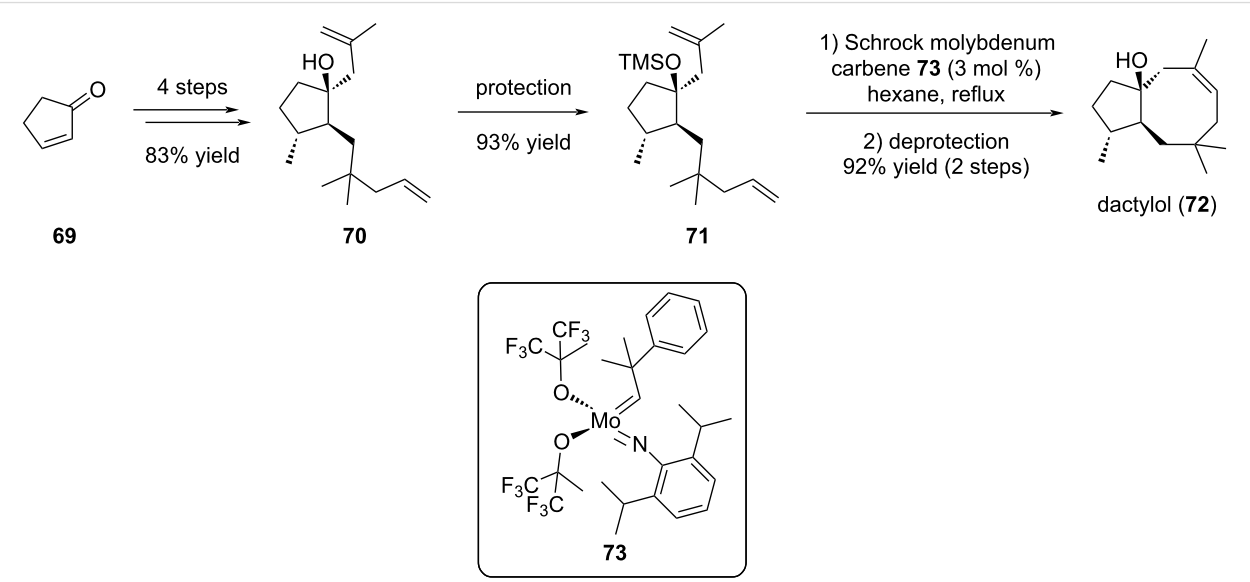

Scheme 12: Total synthesis of dactylol (**72**).

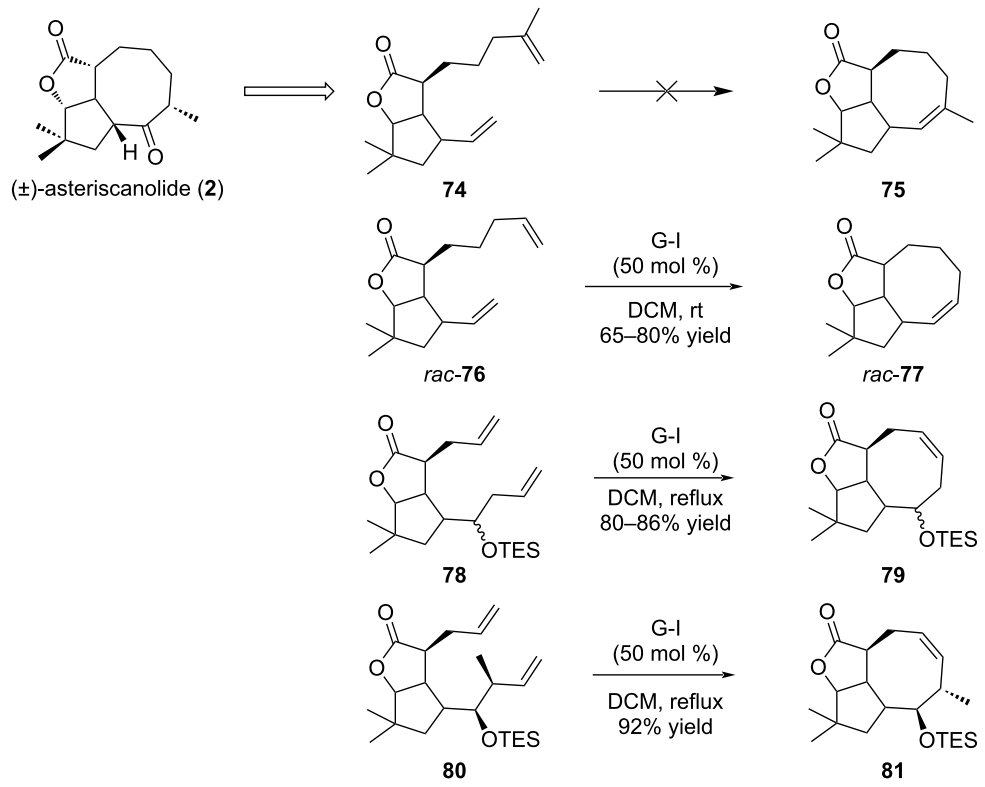

Scheme 13: Ring-closing metathesis for the total synthesis of (±)-asteriscanolide (**2**).

able for the cyclization process. As a solution, the RCM was envisaged on **76** which possesses two terminal double bonds and successfully produced cyclooctene **77** in 65–80% yield with G-I catalyst in dichloromethane at room temperature. Diene **78** was also designed, with the two alkene side chains closer in length, and the cyclization produced tricyclic **79** in higher yields (80–86%). Finally, diene **80** bearing a functionalized lateral chain was submitted to RCM conditions and delivered cyclooctene **81**, an advanced intermediate in the synthesis of (±)-asteriscanolide (**2**).

Pleuromutilin (**1**) is the flagship representative of a recent class of antibiotics which displays a propellane-like structure (Scheme 14) [41-44]. Indeed, these compounds possess a compact tricyclic backbone resulting from the fusion of a five-, six- and eight-membered ring in which the three rings share a

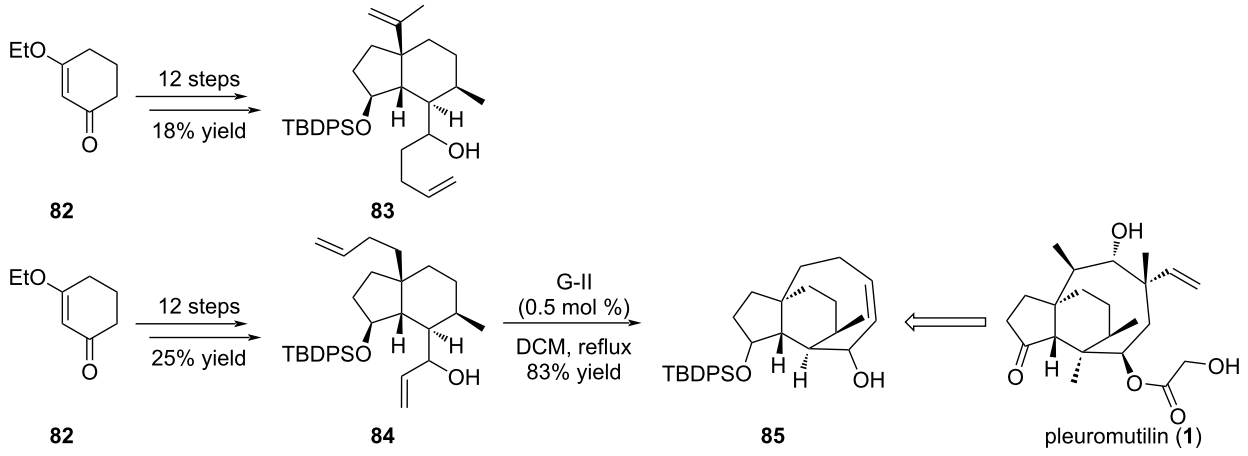

Scheme 14: Synthesis of the simplified skeleton of pleuromutilin (**1**).

common carbon–carbon bond. Its core structure was investigated in 2011 through the ring-closing metathesis of intermediate **83** [45]. However, the isopropenyl group seemed too hindered and the cyclization could not proceed in any investigated conditions. In a second strategy, the design of diene **84** allowed the RCM to happen and furnished tricyclic compound **85** in good yields, an advanced intermediate to the synthesis of pleuromutilin (**1**).

Nitidasin (**93**) is a pentacyclic sesterterpenoid bearing a [5-8-6-5] tetracyclic all-carbon system with 10 stereogenic centers (Scheme 15). This natural product was isolated from two *Gentianella* plant species, namely *G. nitida* and *G. alborosea* used in Peruvian traditional medicine. The first report of its synthesis was given in 2014 by Hog and co-workers [46,47]. In this work, the RCM was envisaged at a late stage on advanced intermediate **90** to forge the central eight-membered ring. The synthesis begins with known hydrindanone **86** (Scheme 15). This compound was converted in 12 steps into derivative **87**, allowing introduction of a methylallyl lateral chain in α-position to the keto function. This terminal double bond prefigures the late RCM cyclization. *trans*-Hydrindanone **87** was isolated as a single diastereomer and possesses 5 out of the 10 stereogenic centers of nitidasin (**93**). In parallel, (−)-citronellene (**88**) was converted into derivative **89** possessing a terminal alkene and a vinyl iodide moiety in 9 steps. This compound can be considered as a difunctionalized compound. Indeed, the vinyl iodide function will be engaged first in a coupling reaction with hydrindanone **87** and the terminal alkene will be involved in the key RCM reaction to ensure formation of the central eight-membered ring. To achieve this goal, a model study was first conducted to define the best reaction conditions. Thus, coupling of the lithio-derivative of **89** to hydrindanone **87** proceeded smoothly to furnish the expected tertiary alcohol **90** with a high stereo- and diastereoselectivity. In a first attempt, the RCM reaction was envisioned prior to the epoxide formation. Unfortunately, no reaction occurred probably due to the presence of the tetrasubstituted olefin. Therefore, this olefin was converted into epoxide **91** and further RCM in the presence of G-II catalyst delivered the expected tetracyclic

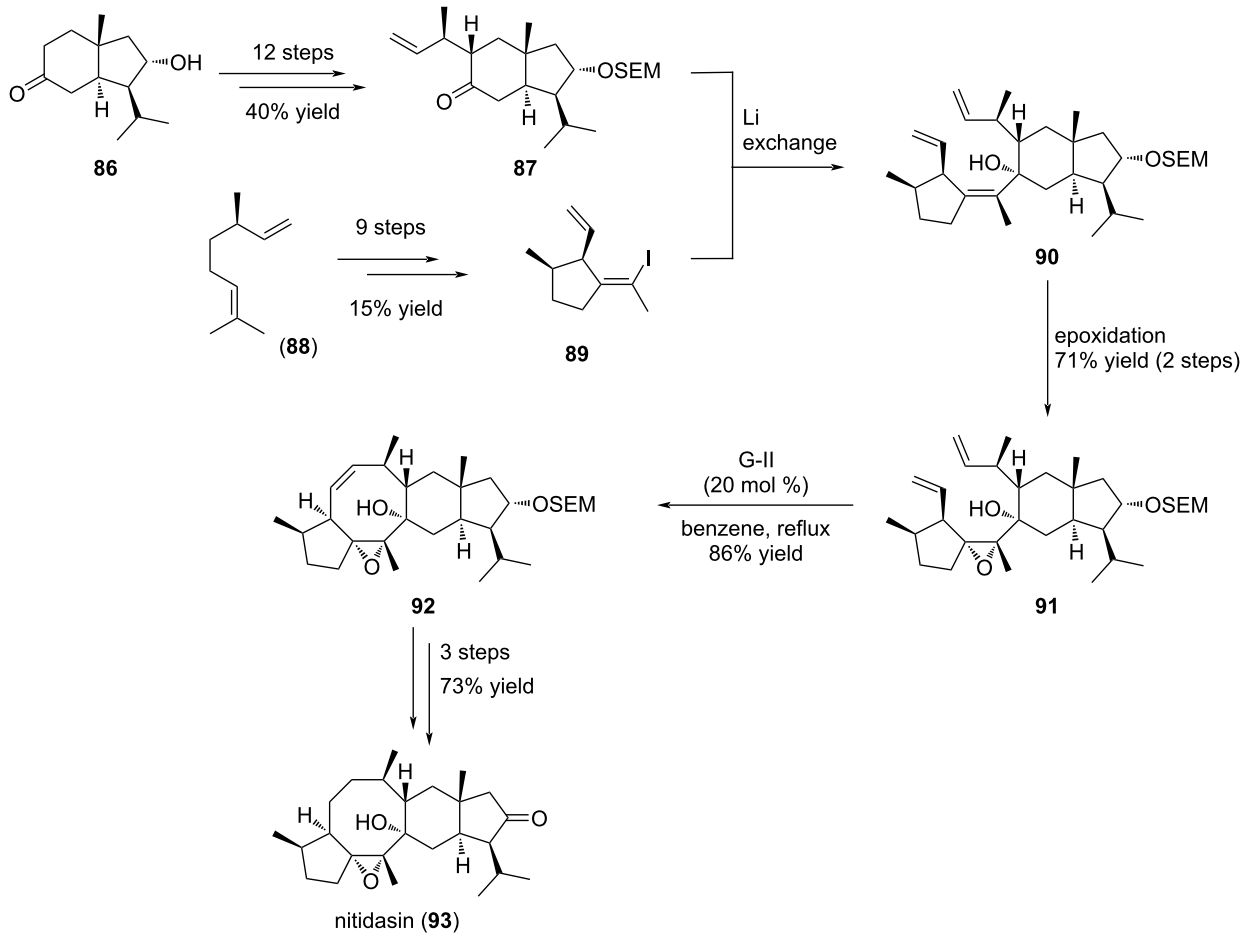

Scheme 15: Total synthesis of (−)-nitidasin (**93**) using a ring-closing metathesis to construct the eight-membered ring.

cyclooctane-bearing product **92** in high yield (86%). Of note, this cyclization occurred on a highly functionalized substrate. All the carbons of the cyclooctene ring were stereogenic, except the two of the double bond, and the precursor possesses both a hydrindane and a cyclopentane unit. The final steps of this synthesis involved alcohol deprotection, double bond hydrogenation and oxidation, and allowed the total synthesis of (−)-nitidasin (**93**) in 27 steps.

Naupliolide (**97**) was first isolated from the aerial parts of *Nauplius graveolens* in 2006. This tetracyclic natural product displays a similar backbone as asteriscanolide (**2**), with an α,β-unsaturated ketone on the eight-membered ring, fused with a γ-butyrolactone and a cyclopentane, onto which a cyclopropane is also grafted [48]. The total synthesis of (±)-naupliolide (**97**) reported by Ito et al. constituted another example of the usefulness of the RCM to construct a cyclooctane ring fused to a cyclopentane unit and presenting a *trans*-ring junction (Scheme 16) [48]. The synthesis started from compound **94** which was converted in 16 steps into derivative **95**, the precursor of the RCM. The cyclization was performed in refluxing toluene in the presence of G-II catalyst and provided tetracyclic compound **96** with 50% yield. In this case, the RCM involved a terminal diene and a disubstituted diene. Further oxidation of the secondary alcohol furnished naupliolide (**97**).

1.2 Enyne ring-closing metathesis

The enyne ring-closing metathesis (EYRCM) reported by Katz in 1985, represents an attractive variant of the classical RCM with the replacement of one of the alkenes by an alkyne function. Thus, EYRCM is atom economic and provides a 1,3 diene, which constitutes an ideal partner for further functionalization, typically a Diels–Alder process [4,8,10].

In 2008, Patrick et al. investigated the access to bicyclic structure **100** mimicking the A-B ring system of the fusicoccane series (Scheme 17) [49]. Starting from lactone **98**, enyne **99** was prepared in 23 steps. The EYRCM was planned at the final stage allowing an access to compound **100**. Despite the relative simplicity of substrate **99**, the reaction was running in the exclusive presence of G-II catalyst and necessitated a high catalyst loading (30 mol %) to eventually furnish modest yields. The presence of two major byproducts was also noticed, namely the cross metathesis adduct resulting from 2 equivalents of **99** and the cross metathesis adduct resulting from **99** and a styrene unit coming from the catalyst. In addition, the corresponding RCM on the alkene analogue of **99** did not proceed either with G-II or Schrock catalysts, showcasing the substrate sensitivity of this reaction.

1.3 Tandem ring-closing metathesis

The tandem ring-closing metathesis (TRCM) approach offers the opportunity to form two contiguous cycles in one step from a well-designed precursor. To this end, the starting substrate should integrate a dienyne moiety in its backbone. One of the olefins reacts first with the alkyne to form a carbocycle possessing a vinyl moiety, which in turn reacts with the second alkene, thus producing the expected bicyclic structure in a tandem process.

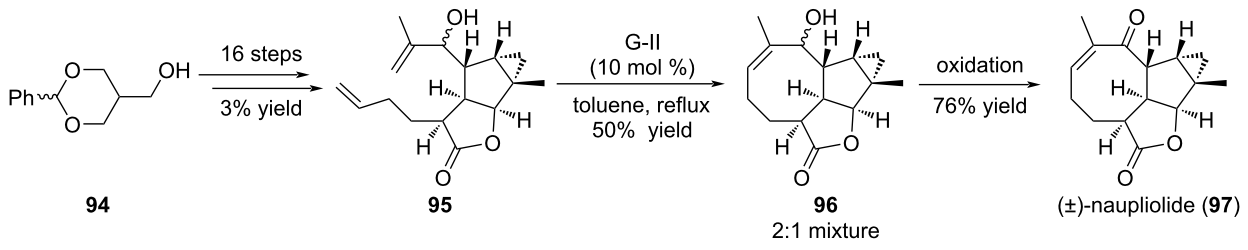

Scheme 16: Total synthesis of (±)-naupliolide (**97**).

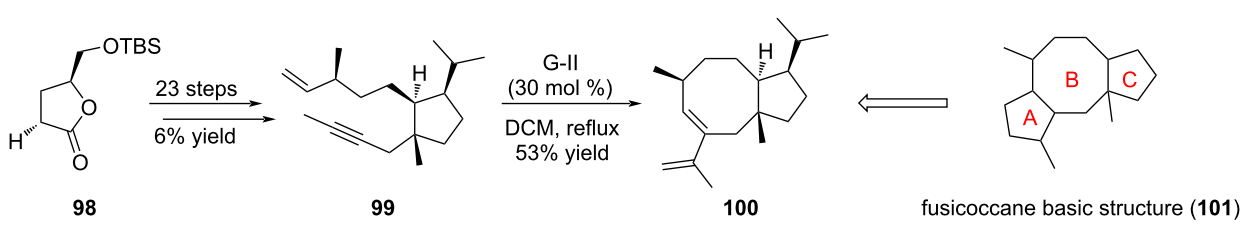

Scheme 17: Synthesis of the A-B ring structure of fusicoccane (**101**).

Ophiobolin A (**8**), one of the representatives of the ophiobolin family, contains a [5-8-5] tricyclic backbone with a side chain on the D-ring. It was isolated in 1958 from the fungus *Ophiobolus miyabeanus*, and displayed a remarkable cytotoxicity against several cancer cell lines [50]. Meanwhile, variecolin (**3**) was isolated from the fermentation broth of the fungus *Aspergillus variecolor* in 1991, and it appears to be a potent immunosuppressant. Structurally, variecolin (**3**) has a complex tetracyclic backbone with a fused [5-8-6-5] skeleton, with 8 stereocenters, 4 of them being contiguous and located on the C-ring [50]. The synthesis of the core structures of ophiobolin A (**8**) and variecolin (**3**) was undertaken by Gao and his group who used this strategy to construct both A and B rings (Scheme 18) [50]. 2-Methylcyclopentenone **16** was selected as a suitable A-ring starting material for the synthesis of ophiobolin A (**8**) (Scheme 18). Sequential modulations resulted in dienyne intermediates **102** and **103**, the latter presenting a functionalized alkyne moiety prefiguring the aldehyde function of ophiobolin A (**8**). These two compounds were submitted to the EYRCM in the presence of G-II catalyst and furnished two different outcomes. Indeed, compound **102** gave the expected product **104** in 78% yield, whereas precursor **103**, bearing hindered *gem*-dimethyl and benzyl protecting group, did not undergo the tandem process and furnished the monocyclized product **105**.

To circumvent this monocyclization reaction, Gao and co-workers decided to simplify the *gem*-dimethyl group by a methyl residue and prepared the analogous compounds of **102** and **103**, namely **106** and **107**, respectively (Scheme 19). With these compounds in hand, terminal alkyne **106** provided the desired product **108** as previously observed with **102**, while the protected alkyne **107** furnished a 1:1.7 mixture of monocyclized **109** and the expected product **110** in overall good yield. This study highlighted that a less-hindered olefin facilitated the second enyne metathesis of this tandem reaction.

The same strategy was applied for the synthesis of the variecolin [5-8-6-5] skeleton (Scheme 20). Dienynes **112** and **113** were first prepared from methyl ketone **111** and subsecuently submitted to the metathesis conditions in the presence of G-II catalyst. Interestingly, in both cases the expected compounds resulting from the TRCM were obtained in good yields. Of particular interest, precursor **113** furnished **115** as the sole product.

1.4 Allylsilane ring-closing metathesis

As demonstrated above and in the literature [4-10], the RCM reaction constitutes a powerful tool to construct rings of various sizes. In 2009, Vanderwal and Dowling extended this process to the use of allylsilane derivatives which can be further submitted to an electrophilic desilylation reaction [51-54] giving an access to *exo*-methylene [38,55]. This concept was exemplified with the synthesis of poitediol (**118**) (Scheme 21), a bicyclopentacyclooctane compound isolated from the red seaweed *Laurencia poitei* in 1978. This sesquiterpene bearing a [5-8] bicyclic structure includes an *exo*-methylidene moiety on the eight-membered ring [38,55]. Thus, allylsilane diene **116** prepared from cyclopentenone **69** as a 4:1 diastereomeric mixture was submitted to RCM conditions in the presence of G-II catalyst in

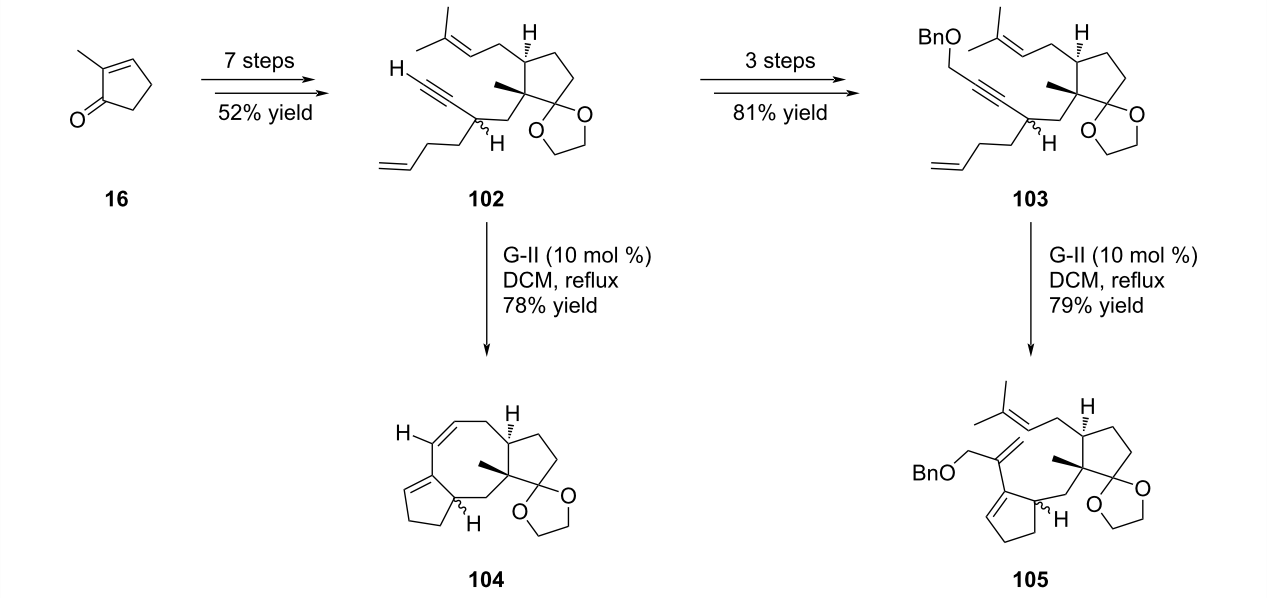

Scheme 18: First attempts of TRCM of dienyne substrates.

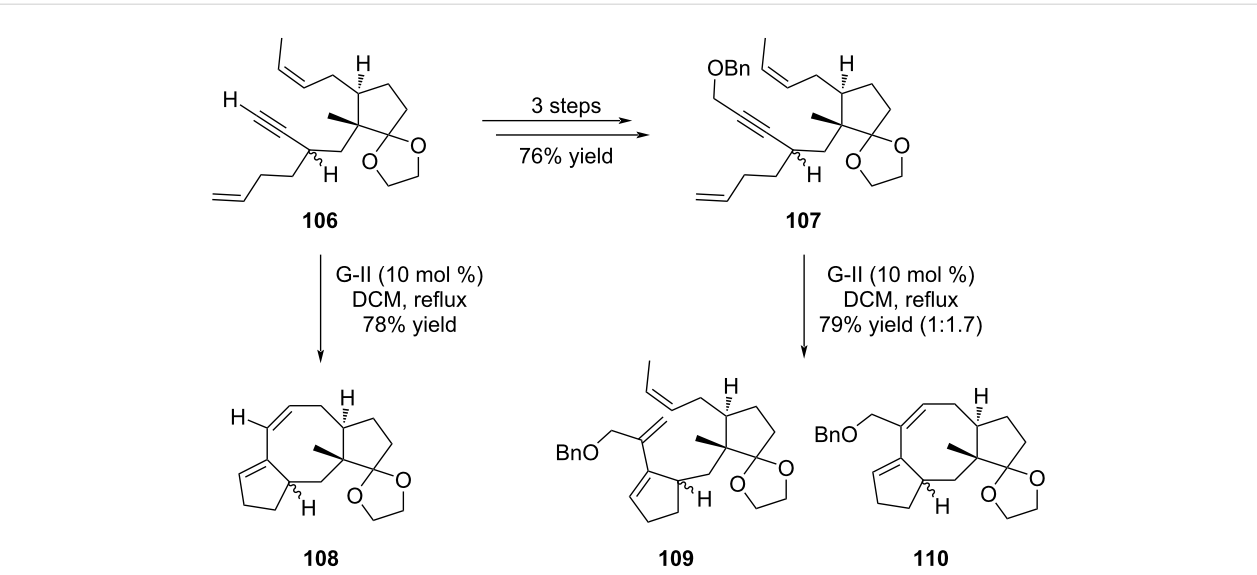

Scheme 19: TRCM on optimized substrates towards the synthesis of ophiobolin A (**8**).

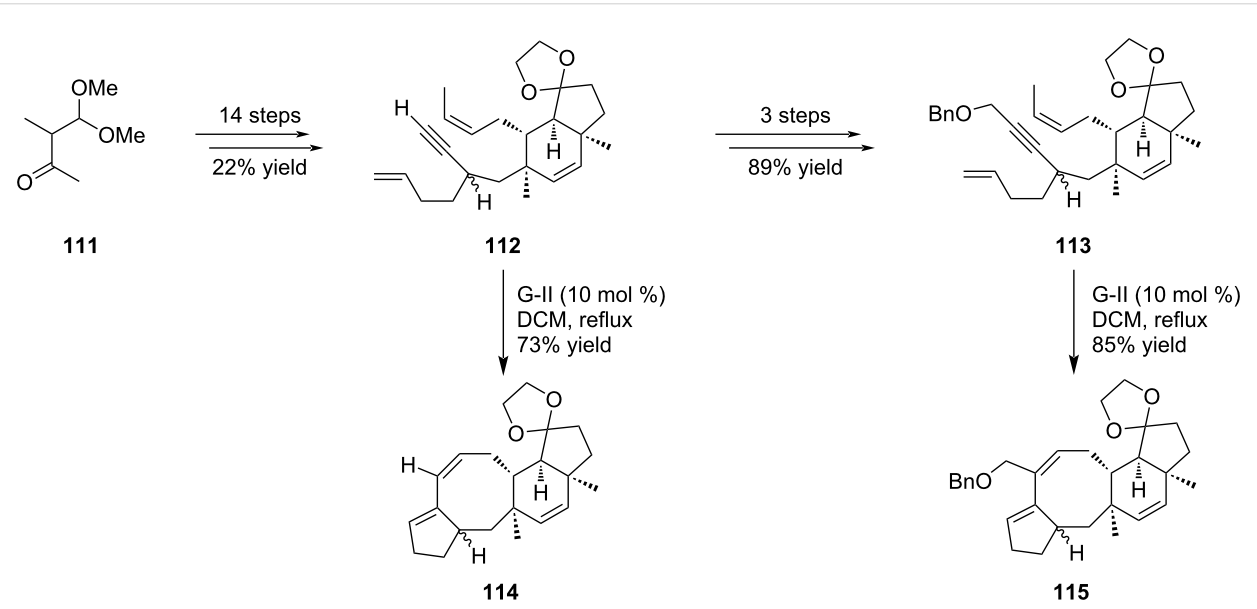

Scheme 20: Tandem ring-closing metathesis for the synthesis of variecolin intermediates **114** and **115**.

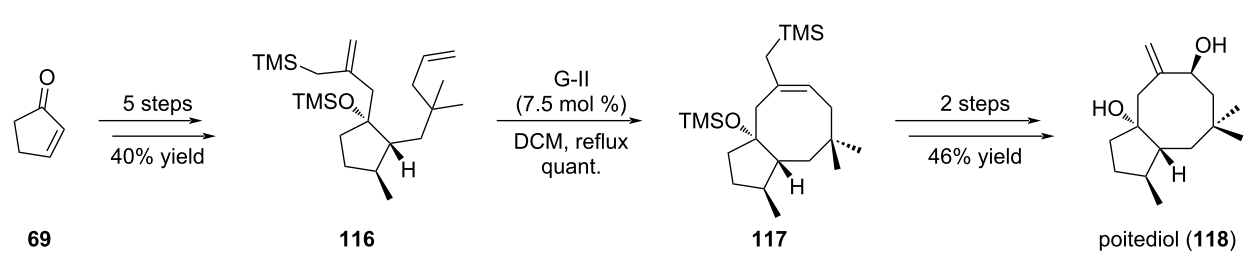

Scheme 21: Synthesis of poitediol (**118**) using the allylsilane ring-closing metathesis.

refluxing dichloromethane. The bicyclic product **117** was obtained in quantitative yield. Given the amount of electrophilic desilylation agents which can be used, a large diversity of compounds can be accessible through this method [51,52]. Oxidation followed by desilylation with fluoride source produces the natural product poitediol (**118**) in overall good yield.

2 Nozaki–Hiyama–Kishi (NHK) cyclization

The Nozaki–Hiyama–Kishi (NHK) reaction is an interesting coupling reaction involving the addition of a halogeno derivative (either bromide or iodide) to an aldehyde in the presence of nickel and chromium salts, typically $NiCl_2/CrCl_2$, generating an alcohol. In its original version, the stereochemistry of the adduct was not controlled, yielding a mixture of stereoisomers. Recent developments were undertaken to propose an asymmetric version [56,57].

In its intramolecular version, the NHK reaction was successfully applied by Kishi in 1989 to forge the cyclooctane ring of ophiobolin C (**30**) [5-8-5] framework, thus opening the door for further applications [58]. Indeed, several groups included this method at a late stage in their synthetic plan.

2.1 Synthesis of pleuromutilin

The purpose of Sorensen's work was to design an efficient strategy allowing a rapid access to the pharmacophoric core of pleuromutilin, e.g., compound **122** for further derivatization and structure–activity relationship (SAR) studies [59]. In this case, an intramolecular NHK was carried out on compound **120** prepared from 3-allylcyclopent-2-enone (**119**) to give the tricyclic compound **121** possessing the eight-membered ring in 73% yield as the major compound. The diastereoselectivity was modest with a dr of 3:2. Esterification of the secondary alcohol followed by silyl removal gave access to the key scaffold **122** (Scheme 22).

2.2 Synthesis of aquatolide (**4**): Late-stage NHK medium-ring formation

Aquatolide (**4**) is a sesquiterpene lactone isolated from *Astericus aquaticus* (Asteraceae) which possesses a unique backbone featuring a cyclobutane moiety fused to a cyclopentane ring, a γ-lactone, and an eight-membered enone [60,61]. Zhang and Gu achieved its preparation through the use of a late-stage intramolecular NHK reaction (Scheme 23) [62]. Thus, when compound **123** was treated with $CrCl_2$ in the presence of a catalytic amount of $NiCl_2$ in DMSO and further oxidized under Swern conditions, aquatolide (**4**) was obtained in 43% yield over the two steps along with 50% recovery of the starting material **123**.

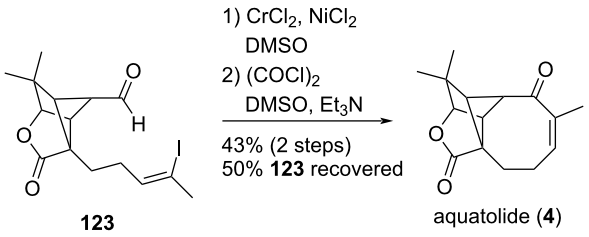

Scheme 23: Key step to construct the [5-8] bicyclooctanone core of aquatolide (**4**).

Of note, the initial strategy involved an intramolecular hydroacylation on alkynyl compound **124** to construct the cyclooctanone unit. Despite several attempts, no cyclization occurred (Scheme 24).

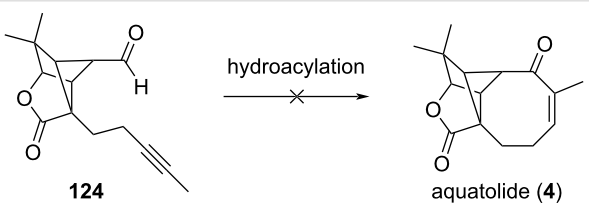

Scheme 24: Initial strategy to access aquatolide (**4**).

3 Pd-mediated cyclization

3.1 Pd-promoted intramolecular alkenylation of methyl ketone: synthesis of cotylenin A (**130**)

Nakada exploited the usefulness of a Pd-promoted intramolecular alkenylation of methyl ketone to forge in the late-stage of

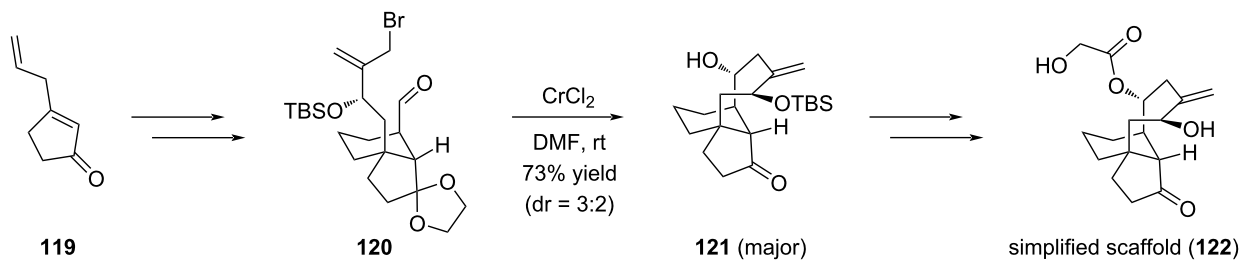

Scheme 22: Access to scaffold **122** by a NHK coupling reaction.

the synthesis the eight-membered ring of cotylenin A (**130**) [63]. To this end, the two cyclopentane units of the tricyclic core of cotylenin A were prepared separately and first assembled by an Utimoto coupling reaction to give after additional functionalization steps the key intermediate **128**. This compound constituted the substrate for the Pd-promoted intramolecular cyclization. In this case, an enol triflate was used instead of an alkenyl halide which required the presence of an electron-rich phosphine, a lower temperature (50 °C instead of 100 °C) to avoid C-7 epimerization, and two equivalents of the Pd complex. The cycloadduct **129** was obtained in very high yield and could be converted to cotylenin A (**130**) in 5 steps. This work constituted an enantioselective total synthesis of cotylenin A (**130**) (Scheme 25).

3.2 Intramolecular Mizoroki–Heck reaction: construction of the [5-8] bicyclic ring system of brachialactone

A study of the versatility of the Mizoroki–Heck reaction in an intramolecular version was recently described by Nishikawa to elaborate the eight-membered ring of brachialactone (**7**) (fusicoccane series) from an advanced cyclopentane intermediate accessed from (*S*)-limonene [64]. Several cyclopentane precursors were prepared to investigate the importance of the alkene functionalization on the cyclization. Thus, the reaction proceeded in the presence of silylated allylic alcohol **131**, producing **132** albeit in low yield. The presence of a terminal methyl ketone function did not influence the reaction outcome as compound **133** produced cycloadduct **134** in the same low-moderate yield. Interestingly, the reaction was highly selective and only one single diastereomer was formed (Scheme 26). However, replacement of the allylic alcohol by a vinyl ketone (compound **135**) or a butenolide (compound **137**) moiety dramatically influenced the outcome of the reaction and no cycloadduct was observed in both cases (Scheme 27).

4 Radical cyclization (including SmI_2)

Introduced by Kagan more than four decades ago, samarium diiodide (SmI_2) has found multiple applications in natural product synthesis [65]. Employed in C–C bond-formation reactions, this single-electron reducing agent has been particularly useful for five- to eight-membered ring cyclizations [65]. Its tunable reactivity opens access to both radical and anionic processes, hence favoring reactivity with various types of substrates, ranging from halides to carbonyls and alkenes/alkynes. It is comprehensible that this reagent attracted early interest in natural product synthesis and more precisely on medium-sized ring formation.

4.1 SmI_2-mediated Barbier-type ring annulation towards variecolin synthesis

Following Kagan's work, Molander's group thoroughly investigated the potential of SmI_2-mediated intramolecular ring closure. Among the approaches they studied, the Barbier-type cyclization rapidly gained popularity for five-to-eight-membered ring formation. Based on a reductive addition of an alkyl halide to a carbonyl group, implementation of the Barbier-type ring closure relied thus on the preliminary introduction of both

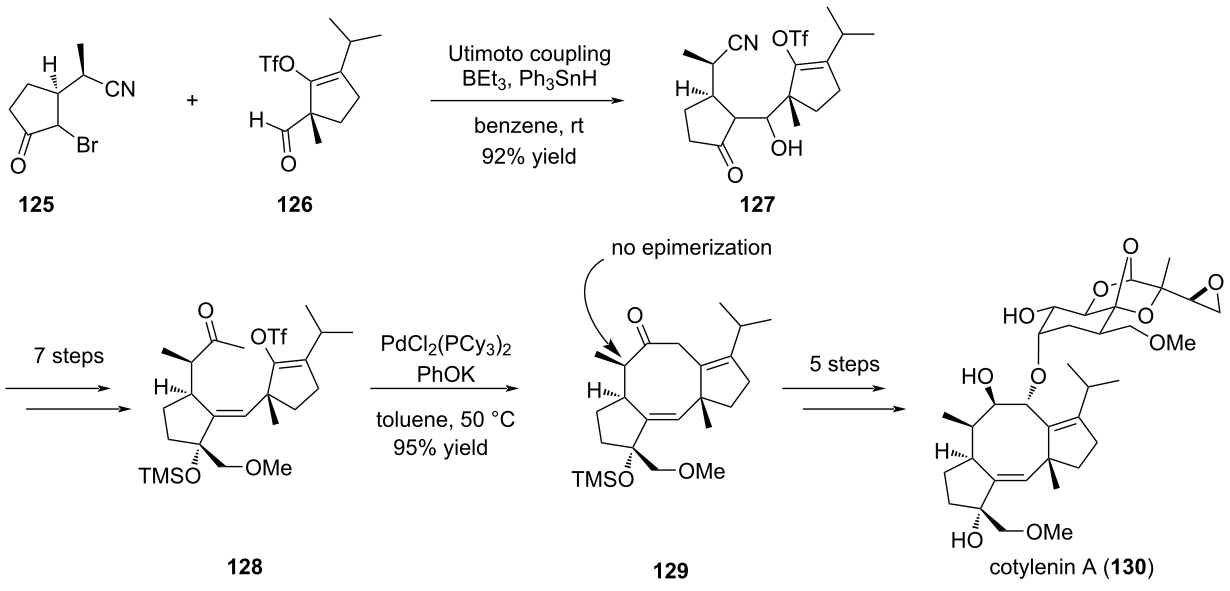

Scheme 25: Synthetic plan to cotylenin A (**130**).

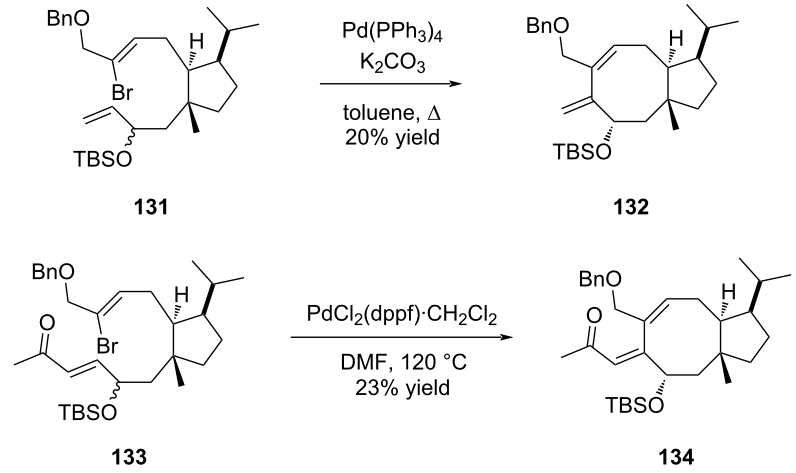

Scheme 26: [5-8] Bicyclic structure of brachialactone (**7**) constructed by a Mizoroki–Heck reaction.

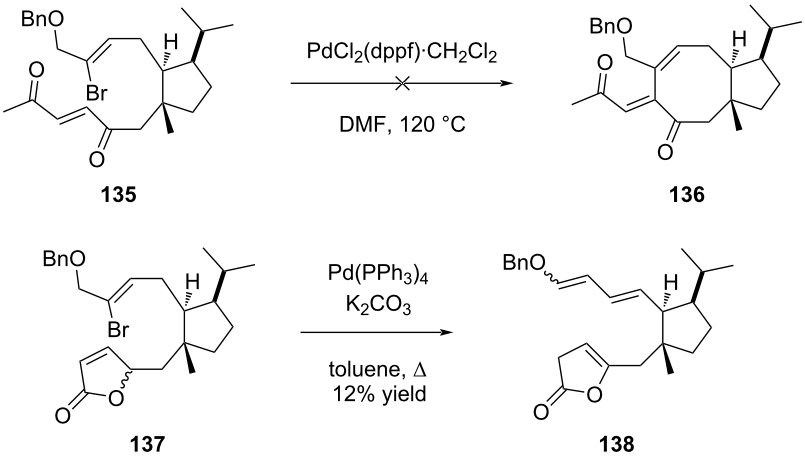

Scheme 27: Influence of the replacement of the allylic alcohol moiety.

aldehyde and alkyl halide functional groups on a suitable substrate. The mechanism was first thought to involve the coupling of an alkyl radical and a ketyl radical, but is now assumed to proceed through the formation of an organosamarium intermediate, resulting from two successive single-electron reductions [66]. This strategy was successfully applied to the construction of variecolin intermediate **140** possessing a [5-8] ring system in its backbone (Scheme 28). Interestingly, the reaction was carried out under UV irradiation and in the presence of catalytic nickel diiodide allowing formation of the expected compound in 63% yield [67].

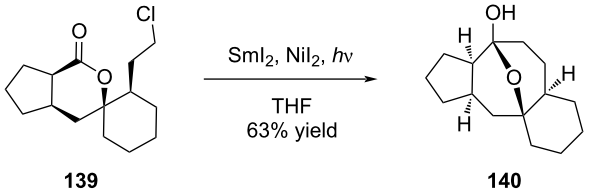

Scheme 28: Formation of variecolin intermediate **140** through a SmI_2-mediated Barbier-type reaction.

4.2 SmI_2-mediated ketyl addition: discussion around pleuromutilin scaffold access

Despite the promising results of the SmI_2-mediated ketyl addition, one would have to wait almost two decades before employing it again in eight-membered ring closure. Among the diterpenes and sesterterpenes featuring a cyclooctane framework, (+)-pleuromutilin (**1**) was recently targeted by Reisman's group through an elegant approach involving a SmI_2-mediated cyclization as a key step of the synthesis [68]. Indeed, this pivotal annulation step was conducted on aldehyde **142** pre-

pared from (+)-*trans*-dihydrocarvone (**141**) and yielded the expected complex tricyclic [5-8-6] alcohol **144** in 93% with a high diastereoselectivity (dr 23:1). Of note, the reaction conditions were subjected to extensive studies for optimization. The intermediate hydrindanone enal fragment **142**, bearing both an aldehyde and an alkene function, was subjected to rigorously anaerobic conditions, in the presence of 3 equivalents of SmI_2, 6 equivalents of H_2O, and TMSCl as a quenching agent (Scheme 29).

In their discussion, the authors highlighted the differences with previously reported SmI_2-mediated eight-membered ring closure in pleuromutilin (**1**) synthesis. Indeed, in 2013, Procter's group was actually the first to report a 34-step enantiospecific total synthesis of (+)-pleuromutilin (**1**), where the eight-membered ring was accessed through a SmI_2-mediated cyclization cascade reaction of a dialdehyde [69]. In this approach, an original way was proposed to form in a single step the tricyclic core of pleuromutilin (**1**) with a stereocontrol at the four contiguous stereocenters [69,70]. The dialdehyde was obtained from *trans*-dihydrocarvone (**141**) and treated early in the sequence (step 13/34) by SmI_2. The authors assumed that the cascade reaction was initiated with the left-hand aldehyde ketyl formation **146** which further attacked the alkene and oriented the *anti*-5-*exo*-*trig*-cyclization toward (*Z*)-Sm^{III} enolate **147**. The cyclooctane ring was then accessed through the (*Z*)-Sm^{III} enolate aldol cyclization. The different organosamarium species generated during the cascade cyclization mechanism were hypothesized to drive the diastereoselectivity on each of the stereocenters created during the process (Scheme 30).

4.3 Nickel-catalyzed reductive cyclization: mutilin and pleuromutilin C12-epimers access

In view of maximizing the scope of accessible pleuromutilin epimers from one single synthetic pathway, Herzon's group reported a modular and convergent route, where the eight-membered ring was built intramolecularly in a late-stage step (Scheme 31A) [71,72]. With this strategy, the authors intended to benefit from the pre-installed quarternary carbon centers or sp^2-hybridized carbons to limit the number of rotatable bonds and transannular *syn*-pentane-type interactions, hence to lower the entropic penalty associated to ring closure. To reach this goal, they first dedicated efforts in optimal syntheses of an electrophilic enimide **151** [73] and its conjunctive reagent, the neopentyl iodide **153**. Both fragments were then engaged in a two-fold neopentylic fragment coupling, giving a bicyclic intermediate which after appropriate modification led to the alkynyl aldehyde cyclization precursor **154**. The ring closure was performed under catalytic reductive conditions in the presence of $Ni(cod)_2$ and ligand **155** as the catalytic system, and triethylsilane as a reductant. The expected cycloadduct was obtained as a single diastereomer (dr > 20:1) in 60% yield [71]. This intermediate allowed then access to several members of the mutilin/pleuromutilin family: total syntheses of (+)-12-*epi*-mutilin,

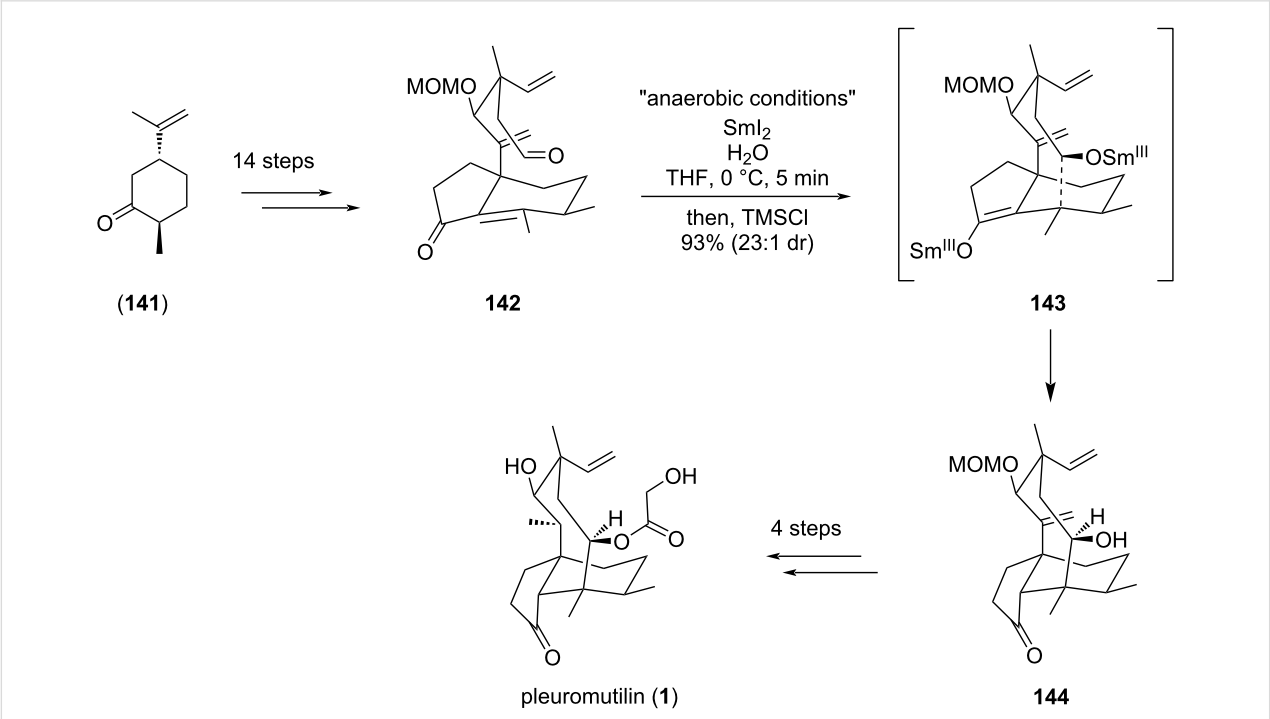

Scheme 29: SmI_2-mediated ketyl addition. Pleuromutilin (**1**) eight-membered ring closure via C^5–C^{14} bond formation.

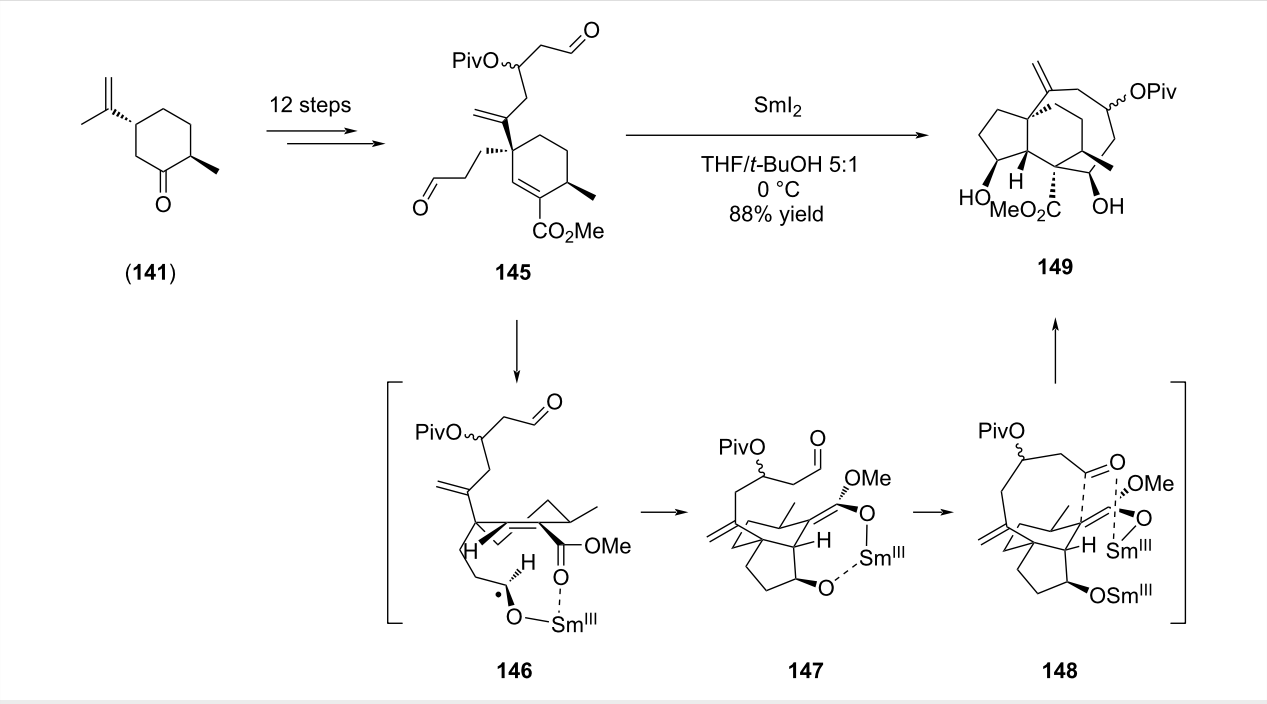

Scheme 30: SmI_2-mediated dialdehyde cyclization cascade of [5-8-6] pleuromutilin scaffold **149**.

(+)-11,12-di-*epi*-mutilin, (+)-12-*epi*-pleuromutilin, (+)-11,12-di-*epi*-pleuromutilin, and (+)-pleuromutilin (**1**) itself were there described in 17 to 20 steps [71,72]. The series was later extended via a revised and improved synthetic strategy toward the tricyclic [5-8-6]-pleuromutilin platform [74], allowing access to remarkable chemical diversity for pleuromutilin derivatives which were evaluated against a panel of Gram-positive and Gram-negative bacteria (Scheme 31B).

4.4 Photocatalyzed oxidative ring expansion: alternative radical chemistry for pleuromutilin scaffold construction

Following the advent of photoredox catalysis in ring-opening and ring-expansion chemistry [75], a new route was proposed by Foy and Pronin to access the cyclooctane unit of the pleuromutilin scaffold [76]. In this very recent paper, the authors implemented adequately chosen tactics allowing the completion of the 15-step and 16-step synthesis of mutilin and pleuromutilin (**1**), respectively. To access the terpenoid core, the synthetic pathway was articulated around a ring expansion of a fused cyclobutane/perhydroindanone fragment, leading to the cyclooctane motif. Interestingly, and unlike the previously reported strategies, the perhydroindanone precursor was prepared starting from achiral building blocks **157** and **158**. They were engaged in a selective *exo* Diels–Alder cycloaddition, which resulted in compound **159**. The enol ether was oxidized by ceric ammonium nitrate (CAN) to deliver intermediate **160**, which was further subjected to an iron-catalyzed hydrogen atom transfer generating tricyclic intermediate **161**. Further functionalization permitted the formation of the fused cyclobutane acid **162** as the desired precursor for the cyclooctane formation. The ring expansion was achieved in the presence of an iridium catalyst and under blue LED irradiation, via the trapping by TEMPO or O_2 of the cyclobutyl radical resulting from decarboxylation, which allowed a Criegee- or a Grob-type fragmentation to generate cyclooctadione **163**. Pleuromutilin (**1**) was then accessed in 4 additional steps (Scheme 32).

4.5 Reductive radical cascade cyclization: toward total synthesis of (–)-6-*epi*-ophiobolin N (**168**) and (+)-6-*epi*-ophiobolin A (**173**)

Despite indisputable success of the radical approach in the formation of the eight-membered ring of pleuromutilin (**1**), the chemistry was scarcely extended to other terpenoid molecules. Only ophiobolin synthetic strategy was implemented with an 8-*endo*/5-*exo* radical cascade cyclization by Maimone's group [77]. Inspired by the cyclase-mediated polyterpene cyclization mechanism, they proposed a rapid 9-step strategy starting from abundant monoterpene farnesol (**164**), chemically converted into cyclopentanol **165** bearing a trichloroketone function that is a well-known radical precursor. The authors found that the correct stereochemistry of the stereogenic centers formed during the cascade cyclization was secured by the use of benzothiophene-based TADDOL thiol **166** as chiral catalyst. They obtained in one single step a 5.3:1 and 3.4:1 diastereomeric ratio for C14 and C15, respectively, while forming the desired

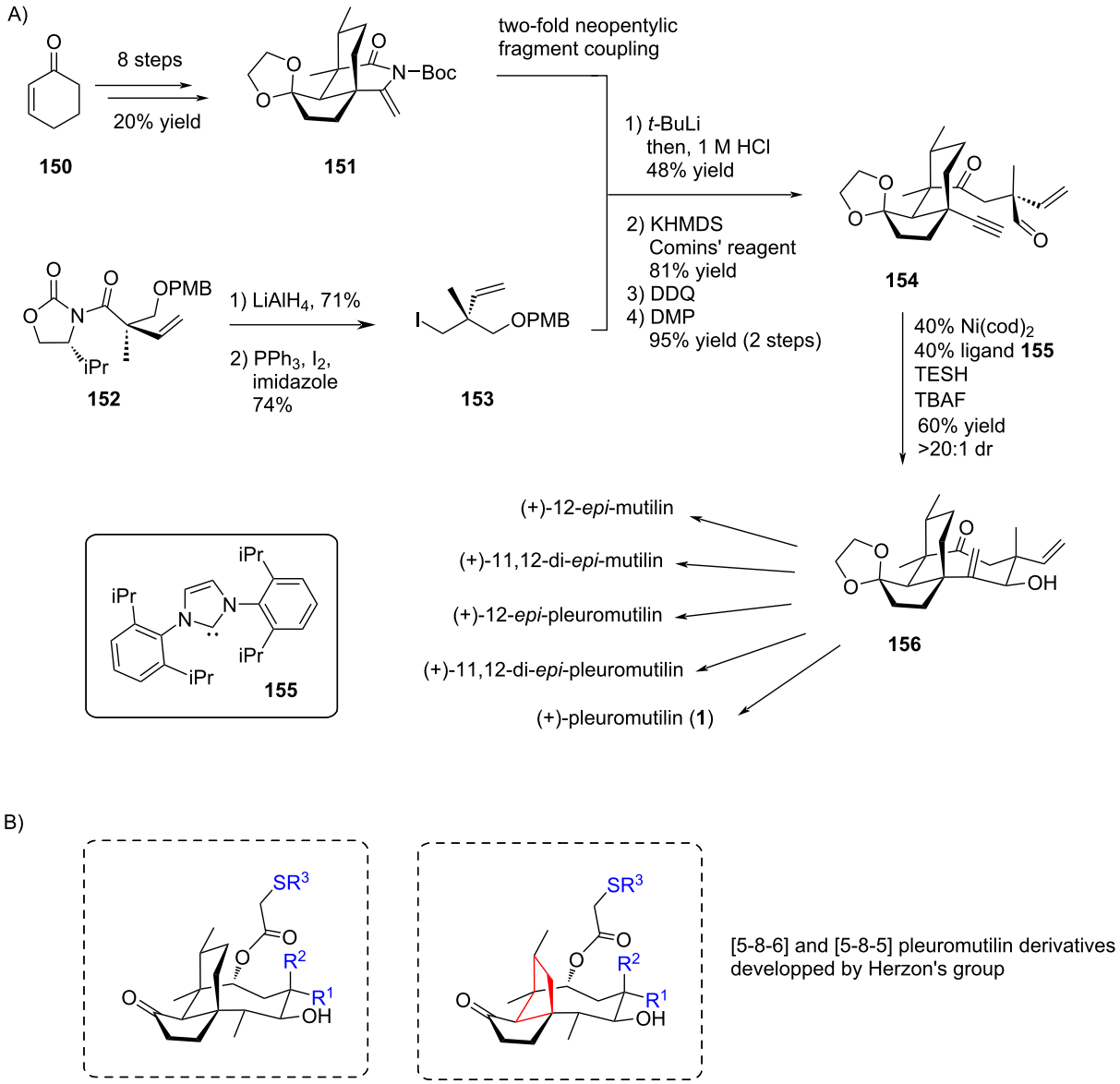

Scheme 31: A) Modular synthetic route to mutilin and pleuromutilin family members by Herzon's group. B) Scaffolds of pleuromutilin derivatives reported by Herzon's group.

trans [5-8] ring junction in C10-C11 (Scheme 33). (−)-6-*epi*-Ophiobolin N (**168**) was then accessible with four additional steps.

Following the extensive work they dedicated to (−)-6-*epi*-ophiobolin N (**168**), Maimone's group reused one of the investigated cyclization conditions for the total synthesis of (+)-6-*epi*-ophiobolin A (**173**), which was then described in a 14-step strategy, starting from geraniol (**169**) [78]. Unlike compound **168**, the installation of stereogenic centers at C14 and C15 was not sought at the 8-5 cyclization stage of the strategy, since formation of the tetrasubstituted alkene provided an adequate precursor towards the tetrahydrofuran-ring formation. The intramolecular atom-transfer radical cyclization was thus carried out with achiral di-*tert*-butylbipyridine-ligated Cu^{I} **171** to generate the [5-8-5] scaffold **172** in 55% yield, while securing the C10 stereocenter in the required configuration and providing a suitable alkene bond for further functionalization. (+)-6-*epi*-Ophiobolin A (**173**) was eventually accessed with 9 additional steps (Scheme 34).

4.6 Other radical approaches towards eight-membered ring closure

As seen above, radical-based pathways proved to be efficiently implemented in peculiar pleuromutilin tricyclic scaffold construction. Alternative reagents were thus explored to close the

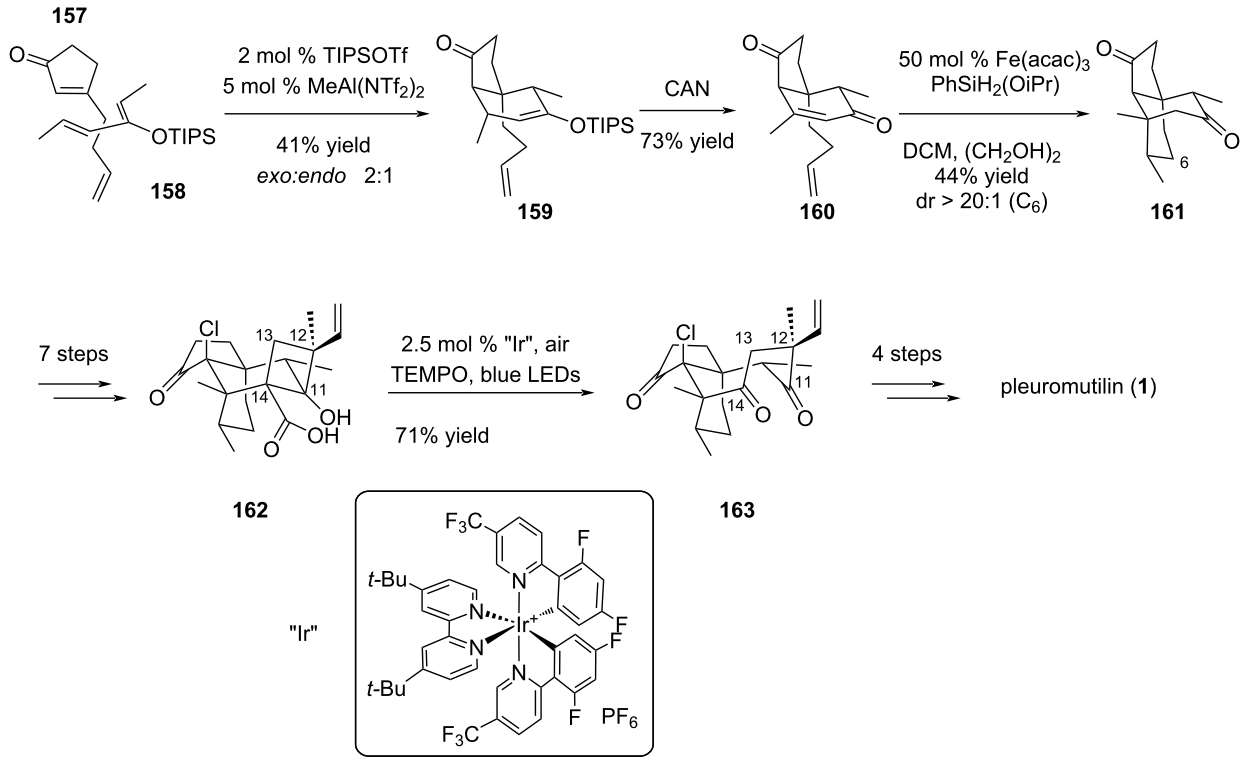

Scheme 32: Photocatalyzed oxidative ring expansion in pleuromutilin (**1**) total synthesis.

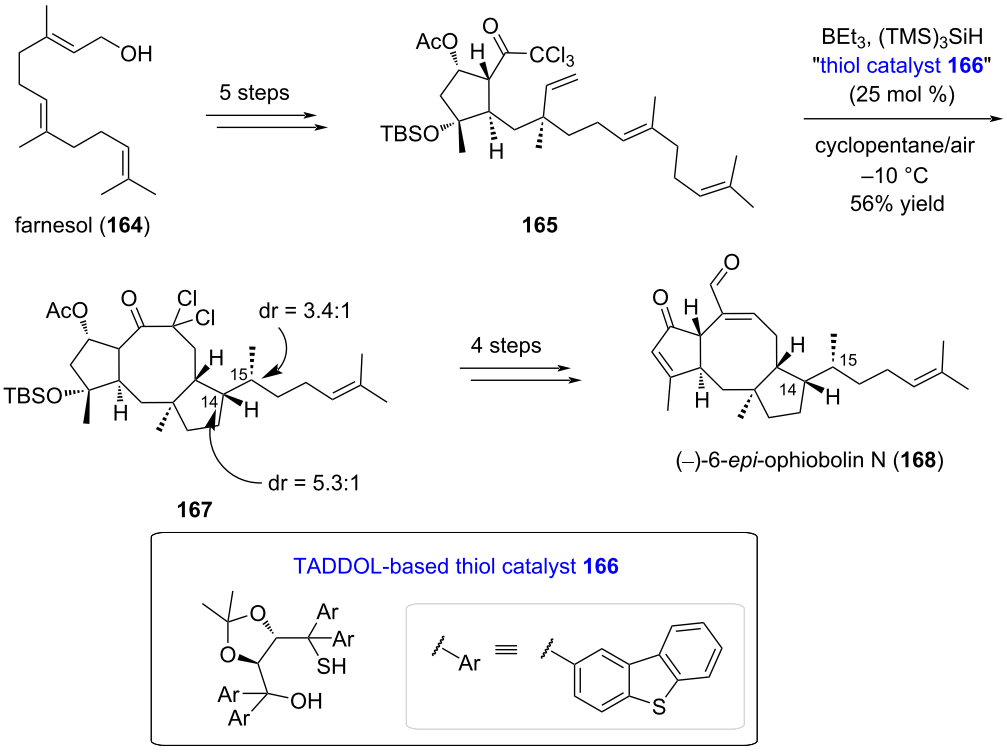

Scheme 33: Reductive radical cascade cyclization route towards (–)-6-*epi*-ophiobolin N (**168**).

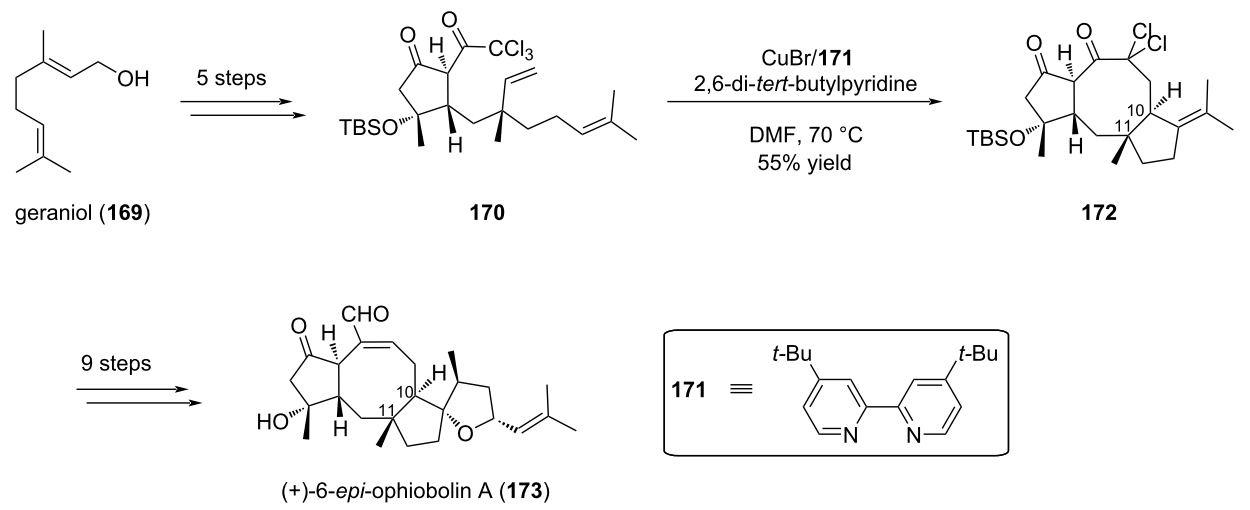

Scheme 34: Reductive radical cascade cyclization route towards (+)-6-*epi*-ophiobolin A (**173**).

eight-membered ring via initial radical genesis. For instance, Bacqué et al. reported the insertion in the cyclization precursors of functional groups prone to form radicals (Scheme 35). In their investigations toward pleuromutilin scaffold synthesis, they proposed to perform a radical 8-*endo*-*trig*-cyclization of a xanthate precursor. The xanthate group was quantitatively installed on an adequately functionalized hydrindanone starting moiety **175**, obtained in 10 steps from ethyl *m*-toluate (**174**), which was then refluxed in the presence of a small amount of dilauroyl peroxide (DLP) as radical initiator. The eight-membered ring **176** was obtained in 60% yield as a single diastereomer [79].

5 Pauson–Khand reaction

Discovered in the seventies [80], the Pauson–Khand reaction has been widely used for the formation of cyclopentenone motifs, by reaction of an alkene, alkyne, and carbon monoxide. This is only recently, in April 2022, that this reaction was reported to allow the formation of an eight-membered ring [81]. Indeed, Li and co-workers employed the Pauson–Khand reaction in order to undertake the total synthesis of hypoestin A (**177**), albolic acid (**178**), and ceroplastol II (**179**) (Figure 5) bearing the same [5-8-5] tricyclic core structure.

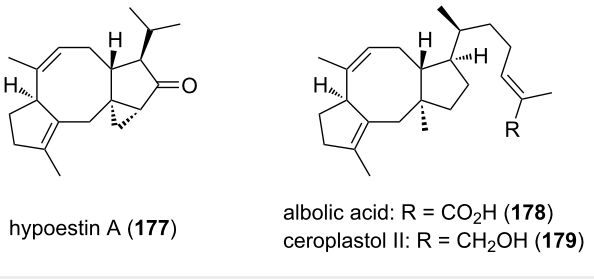

Figure 5: Structural representations of hypoestin A (**177**), albolic acid (**178**), and ceroplastol II (**179**) bearing the same [5-8-5] core structure.

Belonging to the fusicoccane diterpenoid family, hypoestin A (**177**) (Figure 5) can play an important role in cardiovascular and neurological diseases by its inhibitory activity of the $Ca_v3.1$ calcium channel. From a chemical point of view, hypoestin A

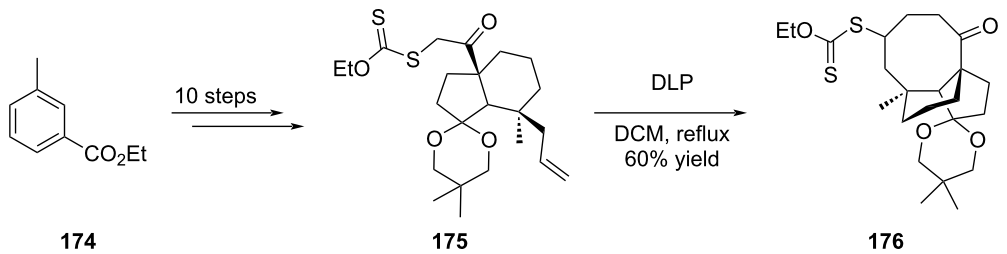

Scheme 35: Radical 8-*endo*-*trig*-cyclization of a xanthate precursor.

(**177**) presents a complex structure: it is composed of a [5-8-5-3] tetracyclic core skeleton, with five stereogenic centers, whose four of them are contiguous. Before their work, no asymmetric total synthesis of hypoestin A (**177**) has been reported. During this study, they also looked into the asymmetric total synthesis of albolic acid (**178**) and ceroplastol II (**179**). Only one paper reported their total synthesis, using a reductive coupling of aldehydes for the synthesis of the eight-membered ring with an excellent yield of 96% [82]. However, the total synthesis included 24 steps, with an overall yield of 5% and 4% for albolic acid (**178**) and ceroplastol II (**179**), respectively. To synthesize these 3 complex natural products, they used the same method to access the [5-8-5] tricyclic advanced intermediate **184**. After that, different strategies allowed the functionalization for each natural product. Their general method consisted in using an intramolecular Pauson–Khand reaction catalyzed by a rhodium complex from an allene-yne substrate to build the eight-membered ring, which was quite challenging.

Starting from commercial (*R*)-limonene (**51**), Li and co-workers synthesized allene-yne intermediate **182** (Scheme 36) in 7 steps, with a 16% overall yield. To access the allene moiety **182**, they first tried addition of propadienyllithium to aldehyde **180**, but they obtained a complex mixture of allenic alcohol and homopropargylic alcohol. Then, they were inspired by Corey's work [83] and formed this key function through the addition of propargylborane **181** to aldehyde **180**, with a good 80% yield. Protection of the obtained alcohol was also necessary. All these 7 first steps set the stereochemistry of the methyl group on the further eight-membered ring and the hydrogen atom at the junction of the five- and eight-membered rings.

The next step of the synthesis was the key formation of the eight-membered ring and several attempts were necessary in order to determine the optimal conditions. They first explored the nature of the catalyst among different rhodium-based catalysts and 5% of $[Rh(CO)_2Cl]_2$ were found to be the best catalyst loading (28% yield). The addition of a silver additive, to make the reaction quicker and to remove a CO ligand, appeared to be useless in this case, with no reaction, and the use of 50% dppp as ligand allowed the formation of the product but with lower yields (25%). The effect of the concentration was also important, since increasing or lowering the concentration from 0.01 M resulted in lower yields. The same trend was observed when the temperature was varied. Finally, the amount of catalyst was explored: increasing from 5 mol % to 10 mol % almost doubled the yield (respectively 38% and 60% yield), and no significant increase in the yield was found when using 20% of catalyst (62% yield). Thus, the use of 10 mol % of $[Rh(CO)_2Cl]_2$ catalyst in toluene at 110 °C and under CO atmosphere yielded the cyclized compound **183** in 56%, even at large scale (2 g). Having this tricyclic structure in hands, several more steps were needed to access advanced intermediate **184** for the synthesis of both natural products. Thus, they first selectively hydrogenated the double bond on the eight-membered ring, and ketone reduction allowed to install the cyclopropane ring thanks to the allylic alcohol. The latter was submitted to Ley oxidation, then deprotection and removal of the obtained alcohol gave the [5-8-5] advanced intermediate **184** (Scheme 36).

The stage was set for the further functionalization to synthesize hypoestin A (**177**), albolic acid (**178**), and ceroplastol II (**179**)

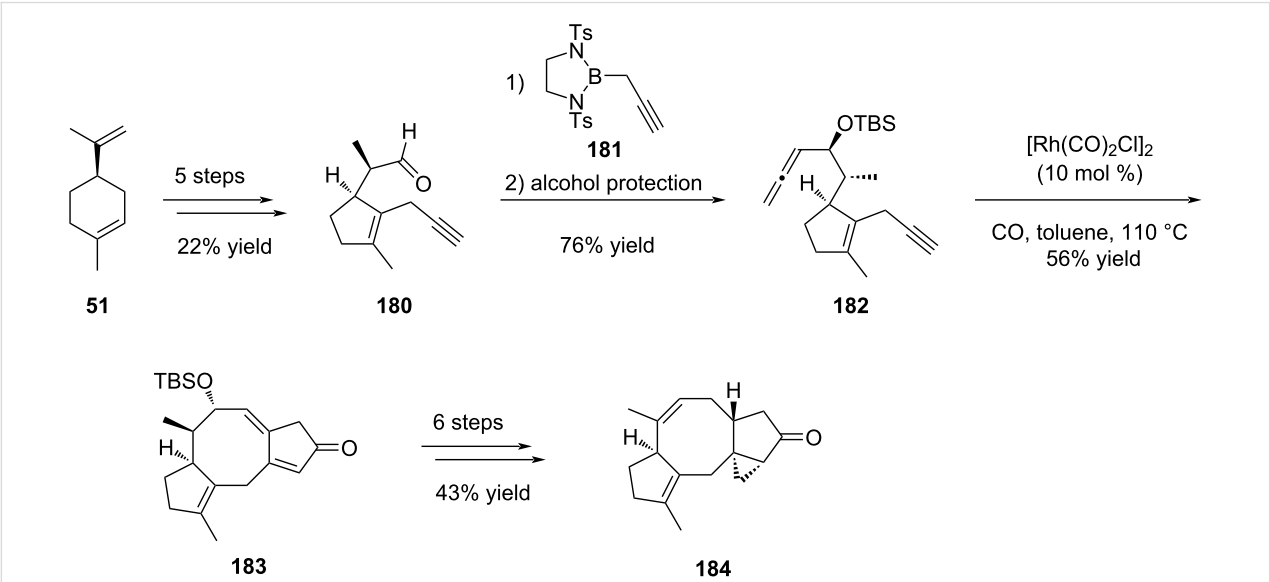

Scheme 36: Synthesis of the common [5-8-5] tricyclic intermediate of hypoestin A (**177**), albolic acid (**178**), and ceroplastol II (**179**).

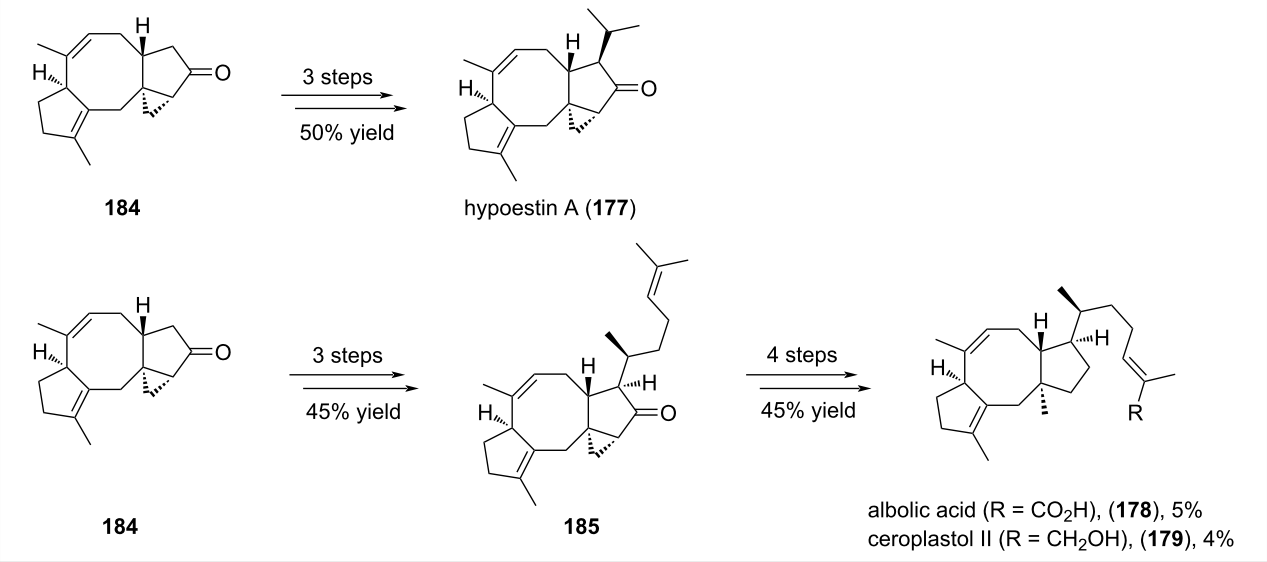

Scheme 37: Asymmetric synthesis of hypoestin A (**177**), albolic acid (**178**), and ceroplastol II (**179**).

(Scheme 37). For the synthesis of hypoestin A (**177**), the side chain was introduced by selective deprotonation of **184**, addition of acetaldehyde, dehydration and conjugated addition of Me_2CuLi. These three last steps provided the desired product **177** in 50% overall yield. For the synthesis of albolic acid (**178**) and ceroplastol II (**179**), the side chain was introduced by deprotonation and addition of the corresponding aldehyde. After dehydration of the subsequent alcohol and conjugated addition of Me_2CuLi, the regioselective reductive opening of cyclopropane **185** was performed with lithium in liquid ammonia in order to introduce the angular methyl group. In the same time, the ketone was reduced into an alcohol, which one was submitted to Barton deoxygenation. The alkene side chain underwent a metathesis reaction with methyl methacrylate to introduce an ester. Finally, this latter was hydrolyzed or reduced to respectively provide albolic acid (**178**) and ceroplastol II (**179**).

The scope of the reaction was also extended to various products containing the [X-8-5] tricyclic system (Figure 6). Several functionalized terminal alkynes succeeded in the Pauson–Khand cyclization (**186**), with moderate yields ranging from 40 to 61%. It was also possible to change the alcohol protecting group (**187**) without significant change in yields (45–62%). The addition of a methyl group on the eight-membered cycle (**188**) was also possible through the functionalization of the internal position of the allene (51%). In the same conditions, an excellent yield (86%) was obtained for the synthesis of a precursor of schindilactone A (**189**) containing a [5-7-8-5] ring structure.

6 Lewis-acid-promoted cyclization

Several Lewis acid-promoted intramolecular cyclization reactions of appropriate substrates were proposed to access the [5-8] bicyclic scaffold including the Nazarov cyclization, the Nicholas reaction or a Mukaiyama-type aldolization.

6.1 Synthesis of fusicoauritone: Nazarov cyclization

In the case of fusicoauritone (**28**), Williams envisaged a Nazarov cyclization to construct the bicyclo[3.6.0]undecane

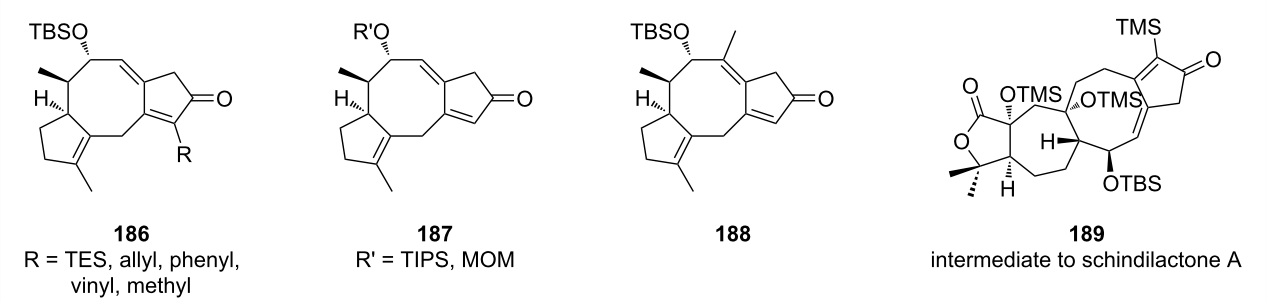

Figure 6: Scope of the Pauson–Khand reaction.

ring system in one step from an advanced intermediate [84]. The strategy proposed here was inspired by biogenetic considerations. Indeed, intermediate **191** possessing an eleven-membered ring could be considered as an equivalent of 3,7-dolabelladiene, the key biogenetic precursor of fusicoccanes, neodolabellanes as well as clavulananes. Following this hypothesis, exposure of compound **191**, prepared in 11 steps from cyclopentenol **190**, to $BF_3{\cdot}OEt_2$ induced an intramolecular five-membered ring formation revealing the central cyclooctane ring of fusicoauritone (**192**) in 77% yield (Scheme 38).

This approach was further extended to compound **193** which was cyclized in the presence of *p*-toluenesulfonic acid to furnish the corresponding tricyclic compound **194** in 92% yield. The latter was finally converted to fusicoauritone (**28**) upon direct oxidative treatment with *tert*-butyl hypochlorite in 40% yield (Scheme 39).

6.2 Synthesis of epoxydictymene (**5**): Nicholas reaction

In the synthesis of (+)-epoxydictymene (**5**), Schreiber proposed an elegant sequence involving a Nicholas cyclization followed by a Pauson–Khand reaction to build the overall tetracyclic backbone [85,86]. The Nicholas reaction took place on allylsilane **196** prepared from (*R*)-pulegone (**195**). After complexation of the triple bond with dicobalt octacarbonyl, the resulting red organometallic cluster underwent a cyclization in the presence of Et_2AlCl to give the fused [5-8] ring system **197** in 82% yield over two steps and a high degree of stereoselectivity. Compound **197** was then engaged in a Pauson–Khand reaction to finalize the construction of the sesquiterpene core which ultimately lead to epoxydictymene (**5**) (Scheme 40).

6.3 Synthesis of aquatolide: Mukaiyama-type aldolisation

The synthetic plan reported by Hiemstra to synthesize aquatolide (**4**) takes advantage of their previous work on a photochemical [2 + 2]-cycloaddition to access the crucial bicyclo[2.2.1] hexane core and a late-stage intramolecular Mukaiyama-type aldol reaction to form the eight-membered ring [87]. To this end, ketone **201** was regioselectively converted to the enol silyl ether and directly subjected to cyclization upon exposure to $BF_3{\cdot}OEt_2$ to give a mixture of stereoisomers. Final treatment with TsOH in refluxing toluene afforded aquatolide (**4**) as a crystalline product in 59% yield over the three step sequence (Scheme 41).

7 Rearrangement: synthesis of variecolin (**3**) with tandem Wolff/Cope rearrangement

Stoltz reported a stereoselective access to the bicyclo[3.6.0]undecane core through a tandem Wolff/Cope rearrangement approach [88]. The strategy was first designed in a racemic version and further developed in an asymmetric fashion. The prerequisite for the rearrangement was the presence of a diazocyclobutyl ketone as represented by compound **203**. When this strained bicycle was heated under microwave irradiation, the tandem Wolff/Cope rearrangement occurred to furnish the corresponding fused [5-8] carbocycle **204** in very high yield (Scheme 42).

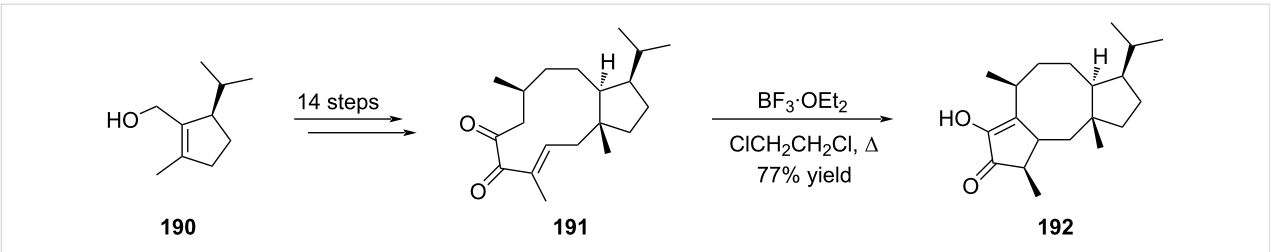

Scheme 38: Nazarov cyclization revealing the fusicoauritone core structure **192**.

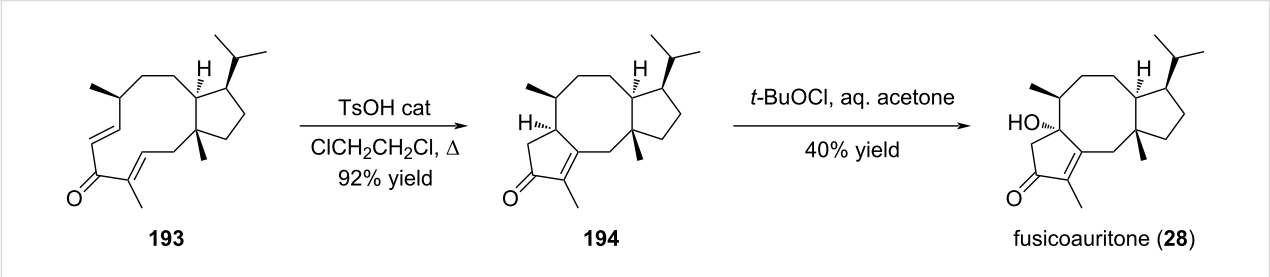

Scheme 39: Synthesis of fusicoauritone (**28**) through Nazarov cyclization.

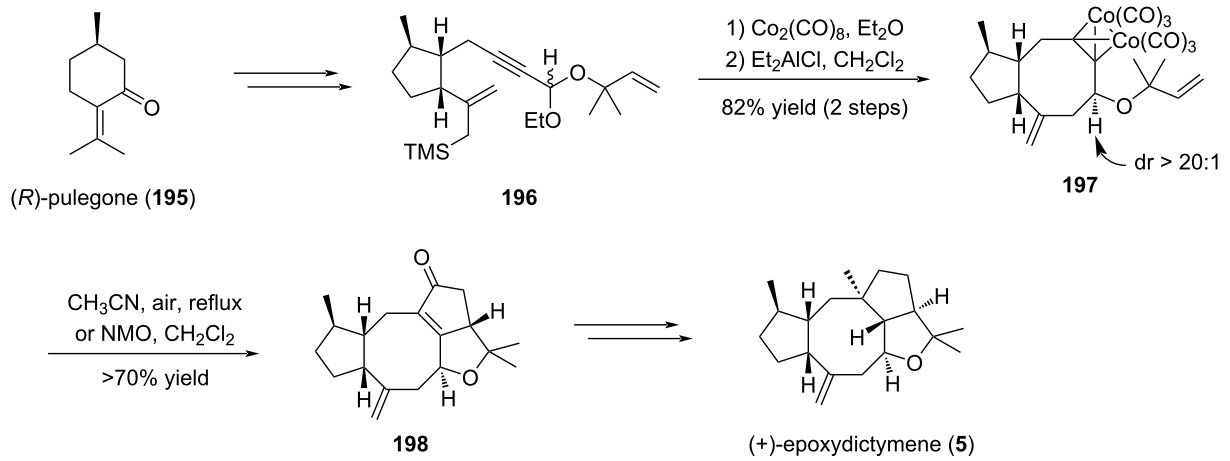

Scheme 40: (+)-Epoxydictymene (**5**) synthesis through a Nicholas cyclization followed by a Pauson–Khand reaction to build the overall tetracyclic backbone.

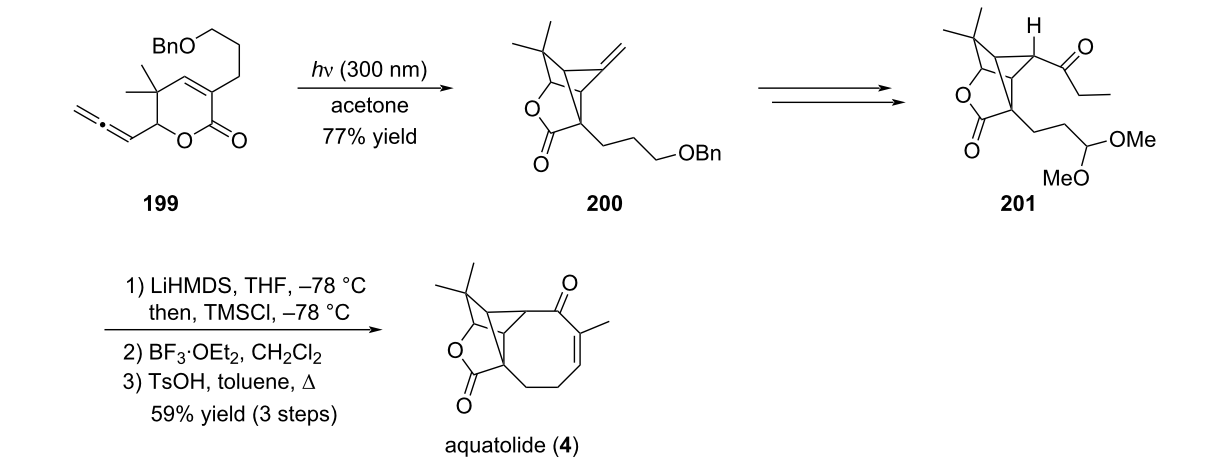

Scheme 41: Synthesis of aquatolide (**4**) by a Mukaiyama-type aldolisation.

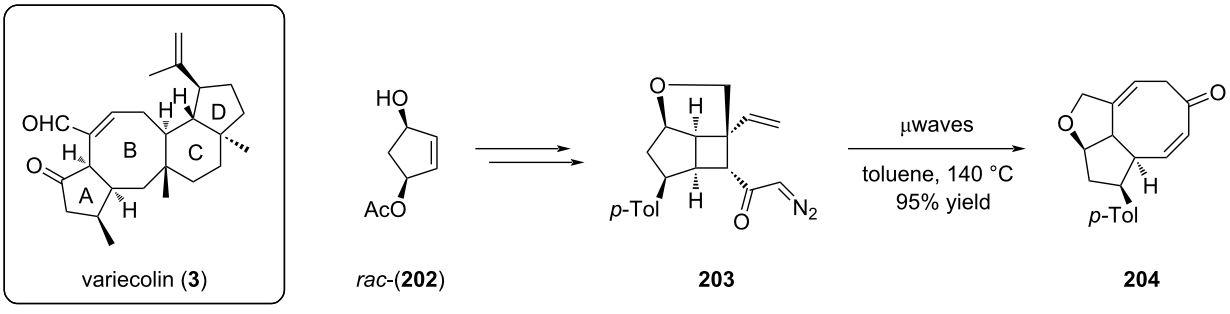

Scheme 42: Tandem Wolff/Cope rearrangement furnishing the A-B bicyclic moiety **204** of variecolin.

Extension to the asymmetric version corresponding to the A-B ring of variecolin (**3**) demonstrated the importance of non-polar solvents for this tandem reaction. Thus, replacement of toluene by heptane improved the yield of the reaction in the presence of an additional methyl substituent (**206**, 26% to 42%) (Scheme 43).

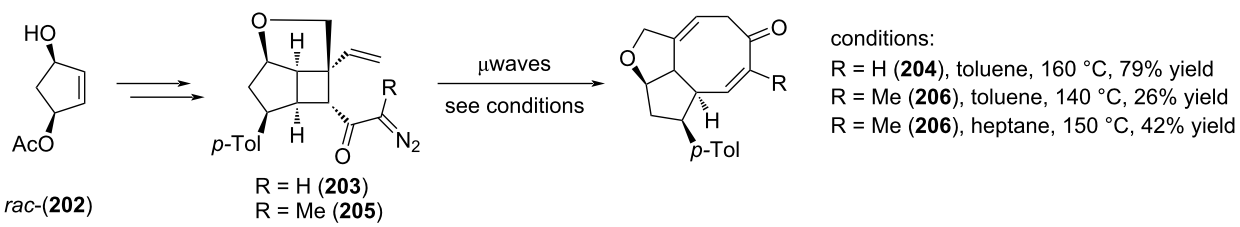

Scheme 43: Asymmetric synthesis of the A-B bicyclic core **205** and **206** of variecolin.

8 Cycloaddition reactions

As exemplified above, access to fused bicycles with one cyclooctanoid ring suffers from major drawbacks including ring strains, disfavored enthalpy and entropy, and transannular hindrance. Among the available methods described in the literature, cycloaddition reactions constitute an efficient route that combines both one-pot cascade and good stereocontrol of the newly formed asymmetric centers. Three types of cycloadditions have recently been reported depending on the nature of the activation, thermal, metal-catalyzed, or photocatalyzed.

8.1 Cycloadditions under thermal activation

Recently, an efficient synthesis of [5-8] fused oxabridged cyclooctanoids was reported by Radhakrishnan et al. [89]. They described the first [6 + 3] cycloaddition reaction between 6,6-diarylfulvene **209** and the betaine 3-oxidopyrylium (**208**) to give intermediate **210** that rearranged itself upon 1,5-hydrogen shift into **212** (Scheme 44). The reaction turned out to be regioselective and ab initio calculations rationalized a stereoselective *endo*-approach between the diene and the dienophile leading to the formation of $C2_{(fulvene)}$–$C2_{(betaine)}$ and $C6_{(fulvene)}$–$C6_{(betaine)}$ bonds [90]. The scope of the reaction was successfully extended to diaryl, dialkyl (including cycloalkyl), and aryl alkyl fulvenes. In the last examples, the stereogenicity of the C6 center of the newly formed cyclooctanoid ring was not controlled. Interestingly the [5-8]-fused ring scaffold possessed functions like an oxabridge, an α,β-unsaturated ketone and cyclopentadiene that can be derivatized at will [91]. For example, the dipolar cycloaddition on the olefin part of the enone allowed the synthesis of a [5-8-5] system while reduction gave access to either allylic alcohol **213** or ketone **214**.

Ghosh also reported a rapid access to the [5-8-6] ring system of variecolin (**3**) through an intramolecular Diels–Alder approach [92]. The key annulation step was achieved on compound **215** which was prepared from the carbohydrate chiral pool. The cycloaddition proceeded upon heating in a sealed tube over two days to give tricycle **216** in 60% yield (Scheme 45). The stereoselectivity of the reaction was controlled by the chiral pentoside unit. Interestingly, compound **216** possesses suitable function for further derivatization into variecolin (**3**). This study highlighted once again the potency of the Diels–Alder reaction in synthesis with the formation of a fused [6-8] ring system.

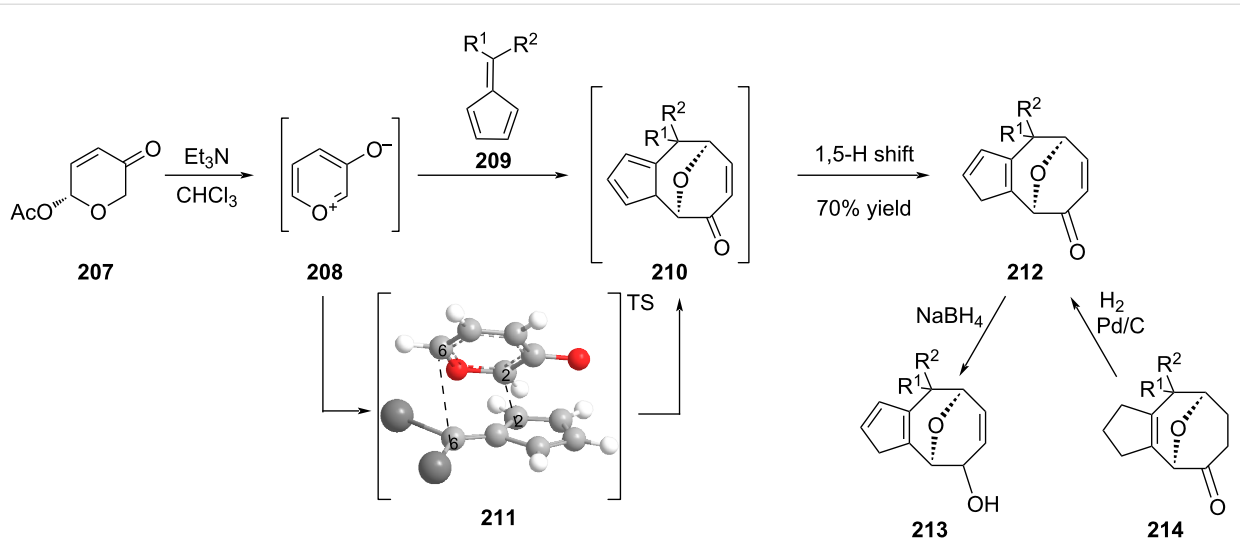

Scheme 44: Formation of [5-8]-fused rings by cyclization under thermal activation.

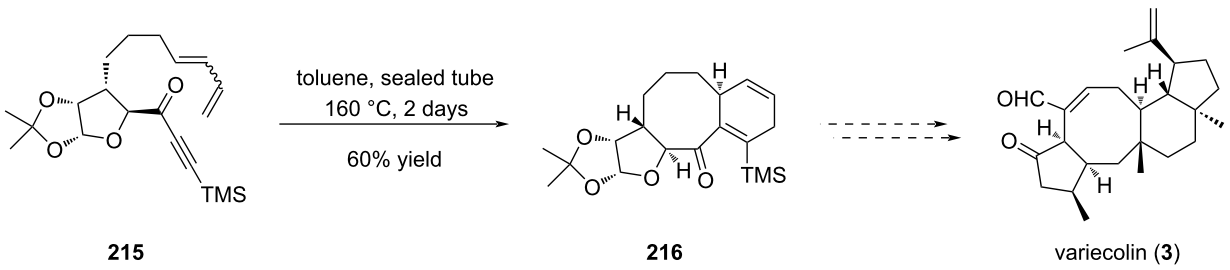

Scheme 45: Construction of the [5-8-6] tricyclic core structure of variecolin (**3**) by Diels–Alder reaction.

8.2 Metal-catalyzed cycloadditions

The efficient use of transition-metal catalysis to perform the direct formation of a [5-8-5] tricyclic skeleton was described in the context of the ophiobolan core synthesis. Previous work highlighted the efficient cyclocarbopalladation of propargylic diol **217** in the presence of vinylstannane **218** followed by a 6π electrocyclization to give the unusual tricyclic system [93]. Using stannylated dienes **218**, the same cascade involving 4-*exo*-*dig* cyclization followed by a Stille coupling provided tetraene intermediates **219** (Scheme 46) [94]. In this case the 6π electrocyclization was unfavored as the resulting spirocyclic diene **220** was too strained. Instead, an 8π electrocyclization occurred to lead to the corresponding tetracyclic triene **221** as a pure diastereomer. Overheating of the reaction media caused the 4π electrocyclic ring opening of **221a** followed by a 1,5-hydrogen shift to provide ketoallylic alcohol **222**. Interestingly, using six-membered ring diols allowed to efficiently access in one pot the stable [6-4-8-5]-tetracyclic system **221b**.

Another metal-catalyzed cycloaddition was also reported in the course of the synthesis of the asteriscan family. The first total synthesis of the asteriscanolide (**2**) intricate natural product was described by Wender and co-workers in the late 90's [95]. They employed a Ni(0)-catalyzed intramolecular [4 + 4] cycloaddition as the key step toward the tricyclic core. Later on, Yu et al. reported the one-pot rhodium(I)-catalyzed [(5 + 2) + 1] cycloaddition of a tethered ene-vinylcyclopropane in the presence of CO [96]. They argued that while reductive elimination (RE) of the rhodium intermediate **224** was unfavored, the introduction of a CO unit in the catalytic step followed by migratory reductive elimination (MRE) would be easier (Scheme 47). Indeed, the cycloaddition of the ene-vinyl cyclopropane **223** in the pres-

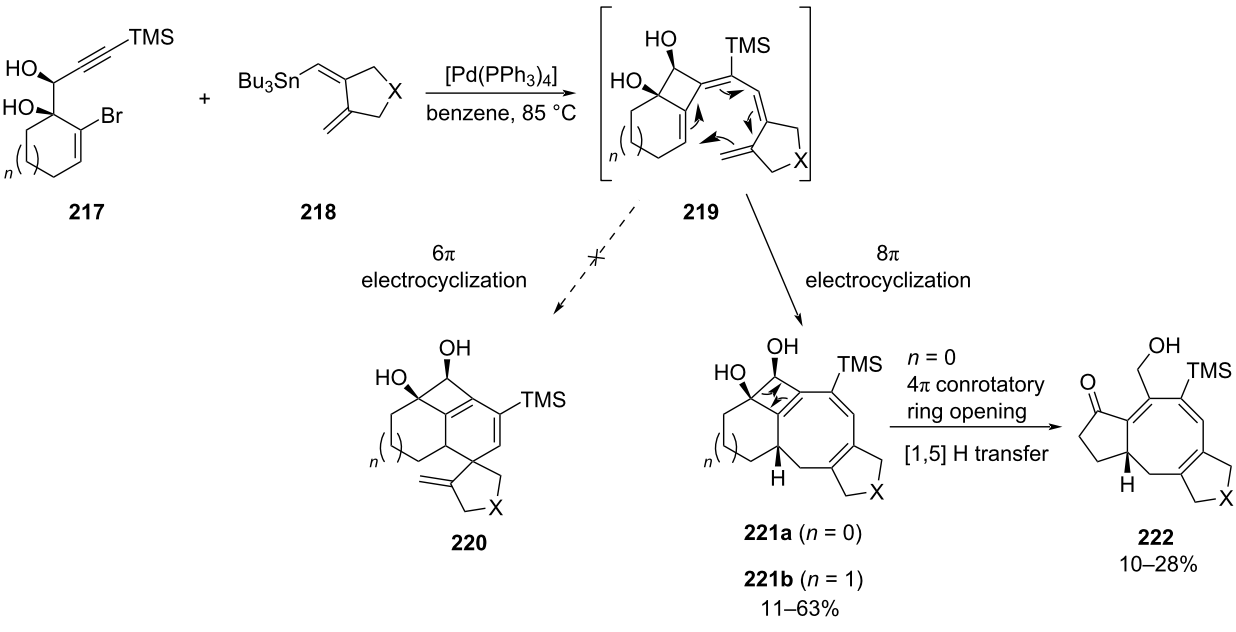

Scheme 46: Synthesis of the [6-4-8-5]-tetracyclic skeleton by palladium-mediated cyclization.

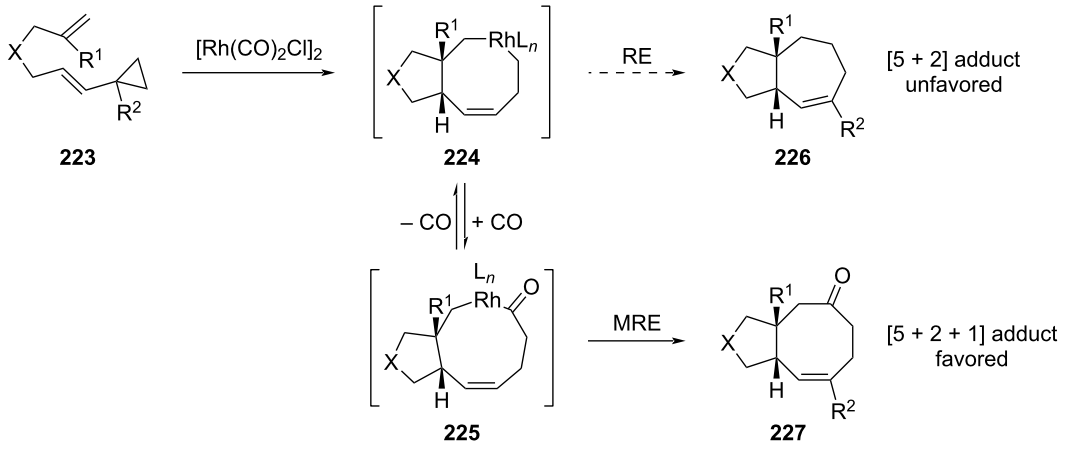

Scheme 47: Access to the [5-8] bicyclic core structure of asteriscanolide (**227**) through rhodium-catalyzed cyclization.

ence of $[Rh(CO)_2Cl]_2$ and 1 atm of CO gave cycloadduct **227** as a single diastereomer with more than 70% yield. Interestingly, this reaction was tolerant to geminal function as well as heteroatoms. Also, the geometry of the double bond in **223** influenced the *cis–trans* ratio of the final products.

This powerful strategy was then applied to the stereoselective total synthesis of (±)-asterisca-3(15),6-diene (**230**) and (+)-asteriscanolide (**2**). The simpler [5-6] bicycle was obtained from bicyclic *cis*-cyclooctenone **229** that arose from a previous [(5 + 2) + 1] cycloaddition of ene-vinylcyclopropane **228** (Scheme 48) [97]. A hydroxy group was then introduced thanks to a hydroboration reaction. Isomerization of position C7 was performed in acidic conditions to provide the targeted compound **230** with 14% overall yield over seven steps. The unusual [6.3.0] carbocyclic system bridged by a butyrolactone was the object of a more complex strategy. Selection of the appropriate ene-vinylcyclopropane substrate led to extensive work which ultimately allowed to consider enantiopure precursor **231** for the rhodium(I)-catalyzed cycloaddition [98]. Thus, exposure of **231** to $[Rh(CO)_2Cl]_2$ complex in toluene under controlled CO/N_2 atmosphere yielded cyclooctenone **232** in 70% yield and high diastereoselectivity (>95:5). The presence of the TBS protecting group was critical for the stereoselectivity and the use of toluene rather than dioxane as initially described allowed to improve the yield from 30% to 70%. Moreover, the *cis* ring junction was in accordance with the configuration of the natural product. Density functional theory calculations were also undertaken to support the observed diastereoselectivity (Scheme 48) [40]. Interestingly, none of the other envisaged ene-vinylcyclopropanes were able to cyclize, highlighting the fact that preexisting five-membered rings were

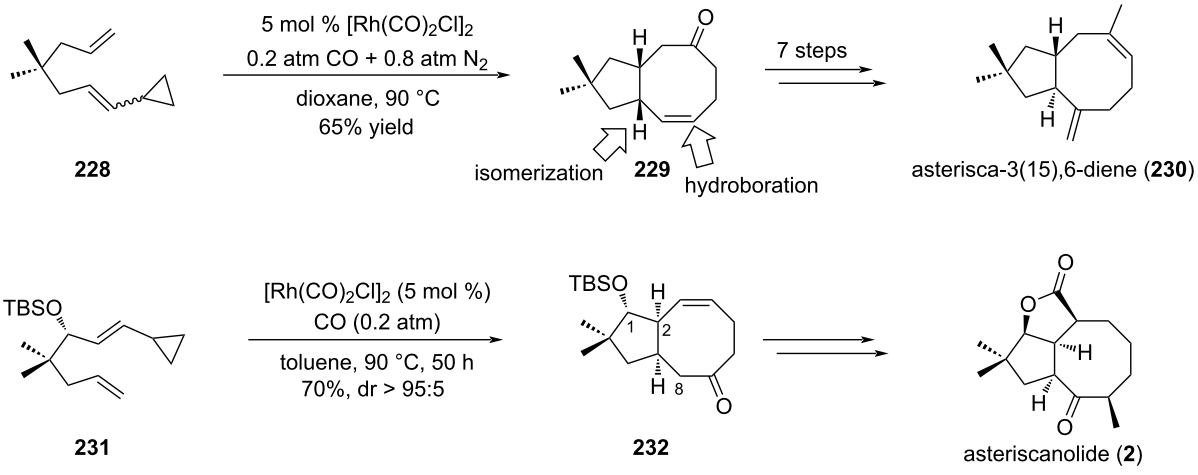

Scheme 48: Total syntheses of asterisca-3(15),6-diene (**230**) and asteriscanolide (**2**) with a Rh-catalyzed cyclization as the key step.

not suitable for this [(5 + 2) + 1] cycloaddition. Having intermediate **232** in hands, further transformations were performed: introduction of a hydroxy group at C8 following a 3-step procedure (enolization, iron-catalyzed cross-coupling and epoxidation); inversion of the configuration at C1 by an oxidation–reduction sequence and construction of the butyrolactone ring by free radical annulation of seleno carbonate.

8.3 Photocyclizations

Historically, the first attempt to attain the fusicoccan ring thanks to photocyclization started from linked 2-pyridones **233** (Scheme 49). Under irradiation provided by a 450 W mercury lamp, smooth conversion to dicyclopenta[*a*,*d*]cyclooctane was observed [99]. The intramolecular [4 + 4] cycloaddition allowed to control the stereoselectivity of C11 under the influence of C3 and C12. As for C7, the possibility to form H-bonds with the solvent greatly influences its stereogenicity. In the absence of *N*-methyl groups, polar solvents where strong H-bond networks exist lead to the *trans*-diastereomer **235** mainly, while non-polar solvents (like benzene) exclusively gave the *cis* isomer **234** [100]. This last compound quickly underwent irreversible Cope rearrangement at room temperature. To avoid this side reaction and to provide the targeted cyclooctane ring, a subsequent epoxidation was performed to give the corresponding epoxide **237**. Remarkably, such epoxidation reaction is both facial and site selective. Finally, selective reductive opening of one lactam ring was performed after activation as urea to provide the corresponding carbinol.

Another straightforward access to the [5-8-5]-fused tricycle of the humulane core (see aquatolide (**4**)) has been reported using light-assisted cycloaddition. The humulane core was synthesized according to different methods including Mukaiyama aldol reaction [87] or intramolecular NHK strategy [62]. Recently, an elegant transannular [2 + 2] "crossed" cycloaddition was described by the group of Takao to obtain selectively (+)-aquatolide (**4**) from the asteriscanolide-type precursor **245** (Scheme 50) [101]. This is one of the first examples of a biomimetic transannulation strategy. It relied on the pioneering work of Li and co-workers on the isomerization of eleven-membered ring humulanes under irradiation [102]. In the report from Takao et al., the [2 + 2] photocycloaddition was performed starting from the same humulane ring using a high pressure mercury lamp (100 W) with a wide range of wavelengths to give the [5-5-4-8] ring system with moderate yield. The eleven-membered ring precursor **241** was obtained thanks to a ring-opening/ring-closing/cross-metathesis (ROM/RCM/CM) cascade followed by intramolecular Nozaki–Kishi reaction starting from the cyclobutenecarboxylate **238**. Remarkably, compound **241** was obtained as a single diastereomer owing to the fact that the pseudoequatorial hydroxy group is favored in the NHTK reaction [103]. Interestingly, the intermediate, humulene lactone **241**, is common to related natural products. Success of the crucial [2 + 2] cycloaddition was obtained after masking of the double bond C7–C8 to prevent simple isomerization. Transformation into an epoxide lead to the alternative parallel cycloaddition to give the regioisomer of aquatolide

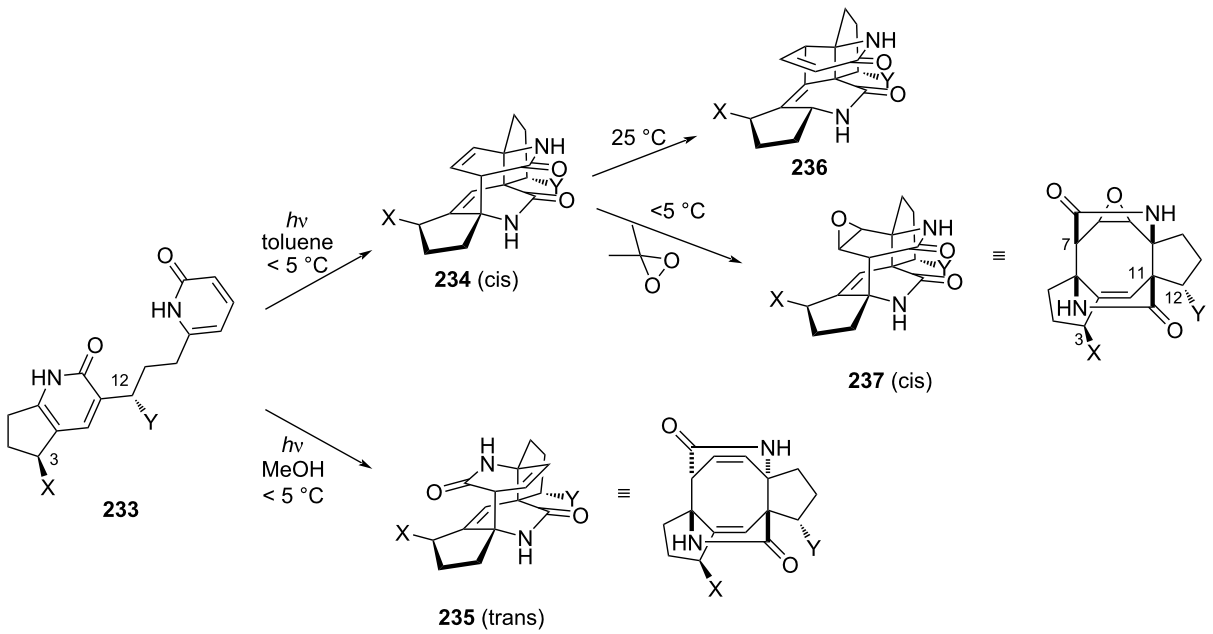

Scheme 49: Photocyclization of 2-pyridones to access the [5-8-5] backbone of fusicoccanes.

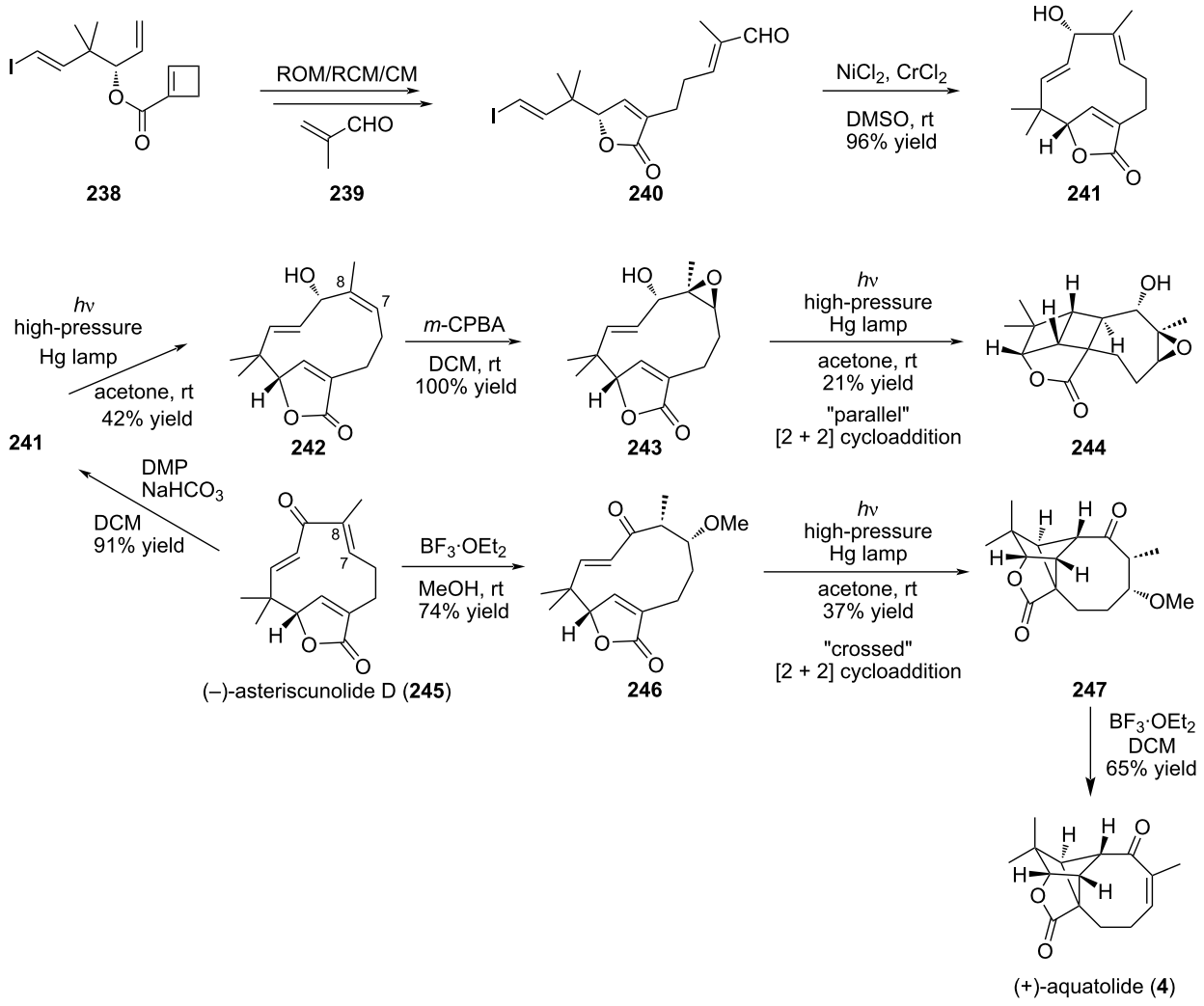

Scheme 50: Total synthesis of (+)-asteriscunolide D (**245**) and (+)-aquatolide (**4**) through photocyclization.

244 but after masking the olefin as methyl ether the bicyclo[2.1.1]hexane **247** was obtained with 37% yield. Elimination of methanol under acidic conditions gave the corresponding aquatolide (**4**). It confirms the crucial role of the alcohol or thiol function at position C6 in the natural precursor to provide the aquatolide skeleton by the plant. Conformational analyses confirmed the preferred cross-path adopted by intermediate **246**. It is in accordance with the fact that intramolecular [2 + 2] photocycloadditions prefer to form five-membered ring regioisomers [104].

9 Miscellaneous

9.1 Biocatalysis

Despite cutting-edge organic methods available nowadays for the production of fused bicycle cyclooctatin, numerous drawbacks remain including lengthy synthetic pathways, adequate control of the stereochemistry and low yields. The diversity of enzymes involved in the biosynthetic pathway could constitute an alternative to a total synthesis approach. Significant advantages of such a process are the high selectivity of the enzyme towards the substrate and the clean conversion to one and only one product. Thus, it reduces drastically the number of steps involved, the amount of waste generated and the need for purification. As many enzymes work in aqueous media under mild conditions, often at room temperature, the fingerprint on the environment is low and the amount of energy used is minimal. Biosynthetic pathways toward terpene cyclization are now well documented [105,106] but only two terpene cyclases involved in the [5-8-5]-fused ring structure have been reported so far [107,108]. They both used geranylgeranyl diphosphate (GGDP **248**; C20) as precursor. Recently, the group of Oikawa managed to rebuild the biosynthetic pathway of brassicicenes

thanks to the heterologous expression of eight genes including a *N*-terminal terpene cyclase BscA [109]. Earlier on, Kuzuyama et al. deciphered the mechanism involved in the biosynthesis of cyclooctat-9-en-7-ol **255** thanks to the combination of theoretical calculations, in vivo studies using ^{13}C-labeled glucose and in vitro reaction with deuterated GGDP [110,111]. They showed that the reaction cascade catalyzed by the cyclooctat-9-en-7-ol synthase CotB2, a class I terpene cyclase derived from *Streptomyces*, was divided in 3 parts (Scheme 51); i) the ring construction that involved the formation of carbocation and subsequent electrophilic cyclization to provide the bicyclic cationic intermediate **249**. Hydride-shift cascade gave the core tricyclic [5-8-5] fused ring structure **250**, ii) long-range cation transfer via multiple hydride migration to generate carbocation **252**, and iii) carbon–carbon bond rearrangement through the formation of cyclopropylcarbinyl cations **253** and **254**. Finally, attack of water on the cyclopropyl gave the targeted monounsaturated cyclooctenol **255**.

Remarkably, conformation of the starting GGDP (**248**) within the catalytic pocket as well as the cyclization mechanism described succinctly above allowed the strict control of the 6 stereocenters of **255** starting from the achiral C_{20} allylic diphosphate GGDP (**248**). This specificity for one single product was further diverted for the biocatalyzed synthesis of non-natural analogs of **255**. Site-saturation mutagenesis of CotB2 allowed to identify two mutants that catalyzed the conversion of GGDP into hitherto unknown fusicoccane macrocycles **256** and **257** (Scheme 52) [112]. In both mutants, swapping the hydrophobic amino acids phenylalanine 149 and 107, involved in the catalytic pocket, with shorter leucine and alanine, respectively modified either the spatial constraints or the charge profile of the active pocket.

To conclude this part, biocatalysis using mutated versions of cyclooctanol synthase constitutes an elegant and efficient alternative to classical multistep synthesis. The cost associated to GGDP (**248**) is now lifted thanks to the development of alternative production systems and it therefore paves the way to an innovative eco-friendly synthesis of [5-8-5] fusicoccane scaffolds.

Conclusion

The [5-8] bicyclic motif encountered in the sesquiterpene, diterpene, and sesterterpene series has stimulated the chemistry

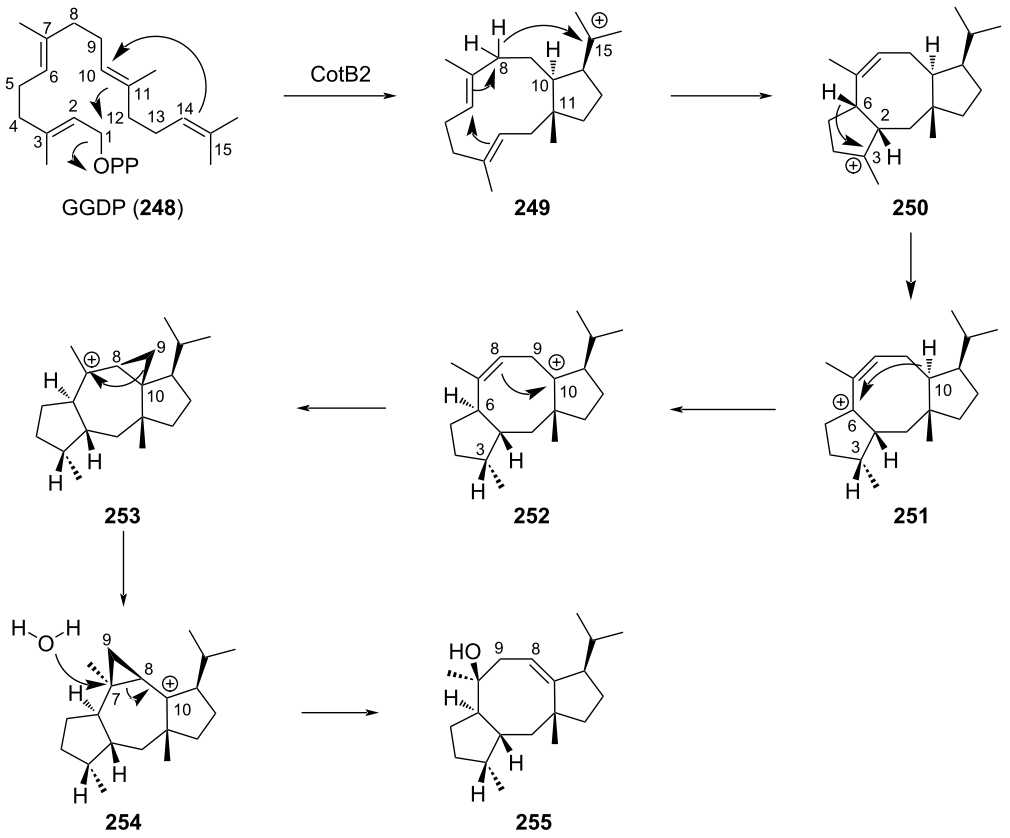

Scheme 51: Biocatalysis pathway to construct the [5-8-5] tricyclic scaffold of brassicicenes.

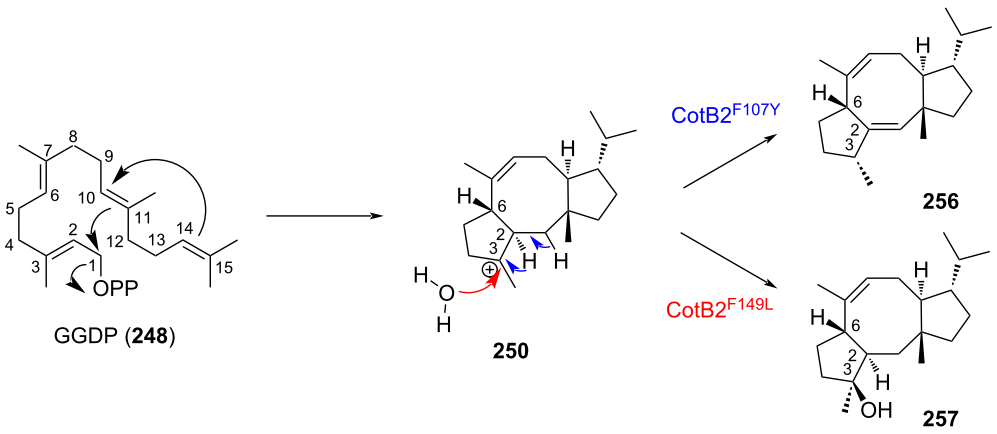

Scheme 52: Influence of the CotB2 mutant over the cyclization's outcome of GGDP.

community to develop efficient and straightforward synthetic methods, the main challenge consisting in the construction of the eight-membered ring. The intramolecular ring-closing metathesis (RCM) has attracted considerable attention due to its versatility, functional group tolerance and mild reaction conditions and represents the method of choice to access this scaffold. Indeed, two strategies have been designed to construct the eight-membered ring: early- or late-stage cyclization. The Grubbs II (G-II) catalyst appears to be the most versatile catalyst for this transformation. However, Grubbs I (G-I) and Hoveyda–Grubbs II (HG-II) catalysts were also used in some situations. Of particular interest, the tandem ring closing metathesis, allowing the formation of the [5-8] motif in a single step, constitutes a very powerful method. Among the most recent approaches described, the intramolecular radical cyclization proves to be very attractive and several groups focused on this strategy. Interestingly, radical-promoted intramolecular eight-membered ring-closing methodologies were successfully applied on advanced intermediates, delivering the cyclic compounds in high yields and high stereoselectivity. Thus, elaboration of pleuromutilin (**1**) and several analogs constituted a representative example showcasing the usefulness of this strategy. Also, cycloaddition reactions, either under thermal activation, metal-promoted or under photoactivation have been explored. However, applications are mainly confined to the preparation of a [5-8] bicyclic model mimicking the natural product. Finally, exploration of the biogenetic pathways allowed to propose some elegant biocatalytic approaches which pave the way to innovative eco-friendly syntheses.

Appendix

Abbreviations used in text, figures and schemes are collected in Table 1.

Table 1: List of abbreviations.

Ac	acetate
acac	acetylacetone
aq	aqueous
BEt_3	triethylborane
Bn	benzyl
Boc	*tert*-butyloxycarbonyl
Bz	benzoate
CAN	ceric ammonium nitrate
Cat	catalytic
CM	cross metathesis
cod	cyclooctadiene
Cy	cyclohexane
DA	Diels–Alder
DCM	dichloromethane
DDQ	2,3-dichloro-5,6-dicyano-1,4-benzoquinone
DFT	density functional theory
DLP	dilauroyl peroxide
DMF	dimethylformamide
DMSO	dimethyl sulfoxide
DMP	Dess–Martin periodinane
dppf	diphenylphosphinoferrocene
dppp	bis(diphenylphosphino)propane
dr	diastereoisomeric ratio
E	electrophile
Et	ethyl
Et_2O	diethyl ether
Et_3N	triethylamine
EtOAc	ethyl acetate
EYRCM	enyne ring-closing metathesis
GGDP	geranylgeranyl diphosphate
HIV1	Human Immunodeficiency Virus 1
HMPA	hexamethylphosphoramide
iPr	isopropyl

Table 1: List of abbreviations. (continued)

LED	light-emitting diode
m-CPBA	*m*-chloroperoxybenzoic acid
M	mol/L
Me	methyl
MeOH	methanol
MOM	methoxymethyl
MRE	migratory reductive elimination
NHC	N-heterocyclic carbene
NHK	Nozaki–Hiyama–Kishi
NMO	*N*-methylmorpholine *N*-oxide
Ph	phenyl
PhH	benzene
PhOK	potassium phenolate
Piv	pivaloyl
PMB	*para*-methoxybenzyl
PP	pyrophosphate
p-Tol	*p*-tolyl
quant	quantitative
Rac	racemic
RCM	ring-closing metathesis
RE	reductive elimination
ROM	ring-opening metathesis
rt	room temperature
SAR	structure–activity relationship
SE	electrophilic substitution
SEM	trimethylsilylethoxymethyl
TADDOL	α,α,α',α'-tetraaryl-2,2-disubstituted 1,3-dioxolane-4,5-dimethanol
TBAF	tetrabutylammonium fluoride
TBDPS	*tert*-butyldiphenylsilyl
TBS	*tert*-butyldimethylsilyl
t-Bu	*tert*-butyl
t-BuOH	*tert*-butanol
t-BuLi	*tert*-butyllithium
TEMPO	(2,2,6,6-tetramethylpiperidin-1-oxyl
TES	triethylsilyl
Tf	triflate
THF	tetrahydrofuran
TIPS	triisopropylsilyl ether
TMS	trimethylsilyl
TMSCl	trimethylsilyl chloride
TRCM	tandem ring closing metathesis
Ts	tosyl
TsOH	*p*-toluenesulfonic acid
UV	ultraviolet
W	Watt

ORCID® iDs

Cécile Alleman - https://orcid.org/0000-0003-1353-1292
Charlène Gadais - https://orcid.org/0000-0002-6061-0420
François-Hugues Porée - https://orcid.org/0000-0003-3344-5260

References

1. Dewick, P. *Medicinal Natural Products: A Biosynthetic Approach,* 3rd ed.; John Wiley & Sons: Chichester, UK, 2009. doi:10.1002/9780470742761
2. Gershenzon, J.; Dudareva, N. *Nat. Chem. Biol.* **2007,** *3,* 408–414. doi:10.1038/nchembio.2007.5
3. Urabe, D.; Asaba, T.; Inoue, M. *Chem. Rev.* **2015,** *115,* 9207–9231. doi:10.1021/cr500716f
4. Nicolaou, K. C.; Bulger, P. G.; Sarlah, D. *Angew. Chem., Int. Ed.* **2005,** *44,* 4490–4527. doi:10.1002/anie.200500369
5. Lozano-Vila, A. M.; Monsaert, S.; Bajek, A.; Verpoort, F. *Chem. Rev.* **2010,** *110,* 4865–4909. doi:10.1021/cr900346r
6. Alcaide, B.; Almendros, P.; Luna, A. *Chem. Rev.* **2009,** *109,* 3817–3858. doi:10.1021/cr9001512
7. Trnka, T. M.; Grubbs, R. H. *Acc. Chem. Res.* **2001,** *34,* 18–29. doi:10.1021/ar000114f
8. López, J. C.; Plumet, J. *Eur. J. Org. Chem.* **2011,** 1803–1825. doi:10.1002/ejoc.201001518
9. Grubbs, R. H. *Tetrahedron* **2004,** *60,* 7117–7140. doi:10.1016/j.tet.2004.05.124
10. Mori, M. *Adv. Synth. Catal.* **2007,** *349,* 121–135. doi:10.1002/adsc.200600484
11. Ogba, O. M.; Warner, N. C.; O'Leary, D. J.; Grubbs, R. H. *Chem. Soc. Rev.* **2018,** *47,* 4510–4544. doi:10.1039/c8cs00027a
12. Müller, D. S.; Baslé, O.; Mauduit, M. *Beilstein J. Org. Chem.* **2018,** *14,* 2999–3010. doi:10.3762/bjoc.14.279
13. Mehta, G.; Singh, V. *Chem. Rev.* **1999,** *99,* 881–930. doi:10.1021/cr9800356
14. Michaut, A.; Rodriguez, J. *Angew. Chem., Int. Ed.* **2006,** *45,* 5740–5750. doi:10.1002/anie.200600787
15. Ruprah, P. K.; Cros, J.-P.; Pease, J. E.; Whittingham, W. G.; Williams, J. M. J. *Eur. J. Org. Chem.* **2002,** 3145–3152. doi:10.1002/1099-0690(200209)2002:18<3145::aid-ejoc3145>3.0.co;2-3
16. Kato, N.; Tanaka, S.; Takeshita, H. *Chem. Lett.* **1986,** *15,* 1989–1992. doi:10.1246/cl.1986.1989
17. Michalak, K.; Michalak, M.; Wicha, J. *Molecules* **2005,** *10,* 1084–1100. doi:10.3390/10091084
18. Touré, B. B.; Hall, D. G. *Chem. Rev.* **2009,** *109,* 4439–4486. doi:10.1021/cr800296p
19. Michalak, M.; Michalak, K.; Urbanczyk-Lipkowska, Z.; Wicha, J. *J. Org. Chem.* **2011,** *76,* 7497–7509. doi:10.1021/jo201357p
20. Srikrishna, A.; Nagaraju, G. *Synlett* **2012,** 123–127. doi:10.1055/s-0031-1290095
21. Tao, Y.; Reisenauer, K. N.; Masi, M.; Evidente, A.; Taube, J. H.; Romo, D. *Org. Lett.* **2020,** *22,* 8307–8312. doi:10.1021/acs.orglett.0c02938
22. Ishibashi, K.; Nakamura, R. *Nippon Nogei Kagaku Kaishi* **1958,** *32,* 739–744.
23. Nozoe, S.; Morisaki, M.; Tsuda, K.; Iitaka, Y.; Takahashi, N.; Tamura, S.; Ishibashi, K.; Shirasaka, M. *J. Am. Chem. Soc.* **1965,** *87,* 4968–4970. doi:10.1021/ja00949a061
24. Tsuna, K.; Noguchi, N.; Nakada, M. *Angew. Chem., Int. Ed.* **2011,** *50,* 9452–9455. doi:10.1002/anie.201104447
25. Tian, W.; Deng, Z.; Hong, K. *Mar. Drugs* **2017,** *15,* 229. doi:10.3390/md15070229
26. Noguchi, N.; Nakada, M. *Org. Lett.* **2006,** *8,* 2039–2042. doi:10.1021/ol060437x

27. Tsuna, K.; Noguchi, N.; Nakada, M. *Chem. – Eur. J.* **2013,** *19,* 5476–5486. doi:10.1002/chem.201204119
28. Kato, N.; Okamoto, H.; Takeshita, H. *Tetrahedron* **1996,** *52,* 3921–3932. doi:10.1016/s0040-4020(96)00059-2
29. Huffman, T.; Kuroo, A.; Sato, R.; Shenvi, R. *ChemRxiv* **2022**. doi:10.26434/chemrxiv-2022-dcbd8
30. Jiang, Y.; Renata, H. *ChemRxiv* **2022**. doi:10.26434/chemrxiv-2022-7nvn3
31. Kuwabara, M.; Matsuo, A.; Kamo, S.; Matsuzawa, A.; Sugita, K. *Synthesis* **2021,** *53,* 2092–2102. doi:10.1055/s-0040-1706684
32. Omole, R. A.; Moshi, M. J.; Heydenreich, M.; Malebo, H. M.; Gathirwa, J. W.; Ochieng', S. A.; Omosa, L. K.; Midiwo, J. O. *Phytochem. Lett.* **2019,** *30,* 194–200. doi:10.1016/j.phytol.2019.02.019
33. Chen, B.; Wu, Q.; Xu, D.; Zhang, X.; Ding, Y.; Bao, S.; Zhang, X.; Wang, L.; Chen, Y. *Angew. Chem., Int. Ed.* **2022,** *61,* e202117476. doi:10.1002/anie.202117476
34. Efremov, I.; Paquette, L. A. *J. Am. Chem. Soc.* **2000,** *122,* 9324–9325. doi:10.1021/ja002450x
35. Srikrishna, A.; Nagaraju, G.; Ravi, G. *Synlett* **2010,** 3015–3018. doi:10.1055/s-0030-1259073
36. Xiao, Q.; Ren, W.-W.; Chen, Z.-X.; Sun, T.-W.; Li, Y.; Ye, Q.-D.; Gong, J.-X.; Meng, F.-K.; You, L.; Liu, Y.-F.; Zhao, M.-Z.; Xu, L.-M.; Shan, Z.-H.; Shi, Y.; Tang, Y.-F.; Chen, J.-H.; Yang, Z. *Angew. Chem., Int. Ed.* **2011,** *50,* 7373–7377. doi:10.1002/anie.201103088
37. Fürstner, A.; Langemann, K. *J. Org. Chem.* **1996,** *61,* 8746–8749. doi:10.1021/jo961600c
38. Dowling, M. S.; Vanderwal, C. D. *J. Org. Chem.* **2010,** *75,* 6908–6922. doi:10.1021/jo101439h
39. Krafft, M. E.; Cheung, Y. Y.; Abboud, K. A. *J. Org. Chem.* **2001,** *66,* 7443–7448. doi:10.1021/jo010623a
40. Liang, Y.; Jiang, X.; Fu, X.-F.; Ye, S.; Wang, T.; Yuan, J.; Wang, Y.; Yu, Z.-X. *Chem. – Asian J.* **2012,** *7,* 593–604. doi:10.1002/asia.201100805
41. Kavanagh, F.; Hervey, A.; Robbins, W. J. *Proc. Natl. Acad. Sci. U. S. A.* **1951,** *37,* 570–574. doi:10.1073/pnas.37.9.570
42. Birch, A. J.; Holzapfel, C. W.; Rickards, R. W. *Tetrahedron* **1966,** *22,* 359–387. doi:10.1016/s0040-4020(01)90949-4
43. Rittenhouse, S.; Biswas, S.; Broskey, J.; McCloskey, L.; Moore, T.; Vasey, S.; West, J.; Zalacain, M.; Zonis, R.; Payne, D. *Antimicrob. Agents Chemother.* **2006,** *50,* 3882–3885. doi:10.1128/aac.00178-06
44. Fazakerley, N. J.; Procter, D. J. *Tetrahedron* **2014,** *70,* 6911–6930. doi:10.1016/j.tet.2014.05.092
45. Findley, T. J. K.; Sucunza, D.; Miller, L. C.; Helm, M. D.; Helliwell, M.; Davies, D. T.; Procter, D. J. *Org. Biomol. Chem.* **2011,** *9,* 2433–2451. doi:10.1039/c0ob01086c
46. Hog, D. T.; Huber, F. M. E.; Mayer, P.; Trauner, D. *Angew. Chem., Int. Ed.* **2014,** *53,* 8513–8517. doi:10.1002/anie.201403605
47. Kawahara, N.; Nozawa, M.; Flores, D.; Bonilla, P.; Sekita, S.; Satake, M.; Kawai, K.-i. *Chem. Pharm. Bull.* **1997,** *45,* 1717–1719. doi:10.1248/cpb.45.1717
48. Abe, H.; Morishita, T.; Yoshie, T.; Long, K.; Kobayashi, T.; Ito, H. *Angew. Chem., Int. Ed.* **2016,** *55,* 3795–3798. doi:10.1002/anie.201600055
49. Dake, G. R.; Fenster, E. E.; Patrick, B. O. *J. Org. Chem.* **2008,** *73,* 6711–6715. doi:10.1021/jo800933f
50. Li, K.; Wang, C.; Yin, G.; Gao, S. *Org. Biomol. Chem.* **2013,** *11,* 7550–7558. doi:10.1039/c3ob41693c
51. Fleming, I.; Barbero, A.; Walter, D. *Chem. Rev.* **1997,** *97,* 2063–2192. doi:10.1021/cr941074u
52. Fleming, I.; Dunoguès, J.; Smithers, R. *Org. React.* **1989,** *37,* 57–575. doi:10.1002/0471264180.or037.02
53. Chabaud, L.; James, P.; Landais, Y. *Eur. J. Org. Chem.* **2004,** 3173–3199. doi:10.1002/ejoc.200300789
54. Masse, C. E.; Panek, J. S. *Chem. Rev.* **1995,** *95,* 1293–1316. doi:10.1021/cr00037a008
55. Dowling, M. S.; Vanderwal, C. D. *J. Am. Chem. Soc.* **2009,** *131,* 15090–15091. doi:10.1021/ja906241w
56. Hargaden, G. C.; Guiry, P. J. *Adv. Synth. Catal.* **2007,** *349,* 2407–2424. doi:10.1002/adsc.200700324
57. Tian, Q.; Zhang, G. *Synthesis* **2016,** *48,* 4038–4049. doi:10.1055/s-0036-1589457
58. Rowley, M.; Tsukamoto, M.; Kishi, Y. *J. Am. Chem. Soc.* **1989,** *111,* 2735–2737. doi:10.1021/ja00189a069
59. Lotesta, S. D.; Liu, J.; Yates, E. V.; Krieger, I.; Sacchettini, J. C.; Freundlich, J. S.; Sorensen, E. J. *Chem. Sci.* **2011,** *2,* 1258–1261. doi:10.1039/c1sc00116g
60. Lodewyk, M. W.; Soldi, C.; Jones, P. B.; Olmstead, M. M.; Rita, J.; Shaw, J. T.; Tantillo, D. J. *J. Am. Chem. Soc.* **2012,** *134,* 18550–18553. doi:10.1021/ja3089394
61. San Feliciano, A.; Medarde, M.; Miguel del Corral, J. M.; Aramburu, A.; Gordaliza, M.; Barrero, A. F. *Tetrahedron Lett.* **1989,** *30,* 2851–2854. doi:10.1016/s0040-4039(00)99142-1
62. Wang, B.; Xie, Y.; Yang, Q.; Zhang, G.; Gu, Z. *Org. Lett.* **2016,** *18,* 5388–5391. doi:10.1021/acs.orglett.6b02767
63. Uwamori, M.; Osada, R.; Sugiyama, R.; Nagatani, K.; Nakada, M. *J. Am. Chem. Soc.* **2020,** *142,* 5556–5561. doi:10.1021/jacs.0c01774
64. Hirata, Y.; Nakazaki, A.; Nishikawa, T. *Tetrahedron Lett.* **2022,** *90,* 153608. doi:10.1016/j.tetlet.2021.153608
65. Nicolaou, K. C.; Ellery, S. P.; Chen, J. S. *Angew. Chem., Int. Ed.* **2009,** *48,* 7140–7165. doi:10.1002/anie.200902151
66. Curran, D. P.; Fevig, T. L.; Jasperse, C. P.; Totleben, M. J. *Synlett* **1992,** 943–961. doi:10.1055/s-1992-21544
67. Molander, G. A.; Quirmbach, M. S.; Silva, L. F.; Spencer, K. C.; Balsells, J. *Org. Lett.* **2001,** *3,* 2257–2260. doi:10.1021/ol015763l
68. Farney, E. P.; Feng, S. S.; Schäfers, F.; Reisman, S. E. *J. Am. Chem. Soc.* **2018,** *140,* 1267–1270. doi:10.1021/jacs.7b13260
69. Fazakerley, N. J.; Helm, M. D.; Procter, D. J. *Chem. – Eur. J.* **2013,** *19,* 6718–6723. doi:10.1002/chem.201300968
70. Helm, M. D.; Da Silva, M.; Sucunza, D.; Findley, T. J. K.; Procter, D. J. *Angew. Chem., Int. Ed.* **2009,** *48,* 9315–9317. doi:10.1002/anie.200905490
71. Murphy, S. K.; Zeng, M.; Herzon, S. B. *Science* **2017,** *356,* 956–959. doi:10.1126/science.aan0003
72. Zeng, M.; Murphy, S. K.; Herzon, S. B. *J. Am. Chem. Soc.* **2017,** *139,* 16377–16388. doi:10.1021/jacs.7b09869
73. Murphy, S. K.; Zeng, M.; Herzon, S. B. *Org. Lett.* **2017,** *19,* 4980–4983. doi:10.1021/acs.orglett.7b02476
74. Goethe, O.; DiBello, M.; Herzon, S. B. *Nat. Chem.* **2022,** *14,* 1270–1277. doi:10.1038/s41557-022-01027-7
75. Xuan, J.; Lu, L.-Q.; Chen, J.-R.; Xiao, W.-J. *Eur. J. Org. Chem.* **2013,** 6755–6770. doi:10.1002/ejoc.201300596
76. Foy, N. J.; Pronin, S. V. *J. Am. Chem. Soc.* **2022,** *144,* 10174–10179. doi:10.1021/jacs.2c04708
77. Brill, Z. G.; Grover, H. K.; Maimone, T. J. *Science* **2016,** *352,* 1078–1082. doi:10.1126/science.aaf6742

78. Thach, D. Q.; Brill, Z. G.; Grover, H. K.; Esguerra, K. V.; Thompson, J. K.; Maimone, T. J. *Angew. Chem., Int. Ed.* **2020,** *59,* 1532–1536. doi:10.1002/anie.201913150
79. Bacqué, E.; Pautrat, F.; Zard, S. Z. *Org. Lett.* **2003,** *5,* 325–328. doi:10.1021/ol027312m
80. Blanco-Urgoiti, J.; Añorbe, L.; Pérez-Serrano, L.; Domínguez, G.; Pérez-Castells, J. *Chem. Soc. Rev.* **2004,** *33,* 32–42. doi:10.1039/b300976a
81. Wang, Y.-Q.; Xu, K.; Min, L.; Li, C.-C. *J. Am. Chem. Soc.* **2022,** *144,* 10162–10167. doi:10.1021/jacs.2c04633
82. Kato, N.; Kataoka, H.; Ohbuchi, S.; Tanaka, S.; Takeshita, H. *J. Chem. Soc., Chem. Commun.* **1988,** 354–356. doi:10.1039/c39880000354
83. Corey, E. J.; Yu, C. M.; Lee, D. H. *J. Am. Chem. Soc.* **1990,** *112,* 878–879. doi:10.1021/ja00158a064
84. Williams, D. R.; Robinson, L. A.; Nevill, C. R.; Reddy, J. P. *Angew. Chem., Int. Ed.* **2007,** *46,* 915–918. doi:10.1002/anie.200603853
85. Jamison, T. F.; Shambayati, S.; Crowe, W. E.; Schreiber, S. L. *J. Am. Chem. Soc.* **1994,** *116,* 5505–5506. doi:10.1021/ja00091a079
86. Jamison, T. F.; Shambayati, S.; Crowe, W. E.; Schreiber, S. L. *J. Am. Chem. Soc.* **1997,** *119,* 4353–4363. doi:10.1021/ja970022u
87. Saya, J. M.; Vos, K.; Kleinnijenhuis, R. A.; van Maarseveen, J. H.; Ingemann, S.; Hiemstra, H. *Org. Lett.* **2015,** *17,* 3892–3894. doi:10.1021/acs.orglett.5b01888
88. Krout, M. R.; Henry, C. E.; Jensen, T.; Wu, K.-L.; Virgil, S. C.; Stoltz, B. M. *J. Org. Chem.* **2018,** *83,* 6995–7009. doi:10.1021/acs.joc.7b02972
89. Radhakrishnan, K. V.; Syam Krishnan, K.; Bhadbhade, M. M.; Bhosekar, G. V. *Tetrahedron Lett.* **2005,** *46,* 4785–4788. doi:10.1016/j.tetlet.2005.05.042
90. Krishnan, K. S.; Sajisha, V. S.; Anas, S.; Suresh, C. H.; Bhadbhade, M. M.; Bhosekar, G. V.; Radhakrishnan, K. V. *Tetrahedron* **2006,** *62,* 5952–5961. doi:10.1016/j.tet.2006.04.017
91. Krishnan, K. S.; Smitha, M.; Suresh, E.; Radhakrishnan, K. V. *Tetrahedron* **2006,** *62,* 12345–12350. doi:10.1016/j.tet.2006.09.102
92. Hossain, M. F.; Ghosh, S. *ChemistrySelect* **2021,** *6,* 12209–12211. doi:10.1002/slct.202103501
93. Salem, B.; Klotz, P.; Suffert, J. *Org. Lett.* **2003,** *5,* 845–848. doi:10.1021/ol0274965
94. Salem, B.; Suffert, J. *Angew. Chem., Int. Ed.* **2004,** *43,* 2826–2830. doi:10.1002/anie.200453773
95. Wender, P. A.; Ihle, N. C.; Correia, C. R. D. *J. Am. Chem. Soc.* **1988,** *110,* 5904–5906. doi:10.1021/ja00225a055
96. Wang, Y.; Wang, J.; Su, J.; Huang, F.; Jiao, L.; Liang, Y.; Yang, D.; Zhang, S.; Wender, P. A.; Yu, Z.-X. *J. Am. Chem. Soc.* **2007,** *129,* 10060–10061. doi:10.1021/ja072505w
97. Fan, X.; Zhuo, L.-G.; Tu, Y. Q.; Yu, Z.-X. *Tetrahedron* **2009,** *65,* 4709–4713. doi:10.1016/j.tet.2009.04.020
98. Liang, Y.; Jiang, X.; Yu, Z.-X. *Chem. Commun.* **2011,** *47,* 6659–6661. doi:10.1039/c1cc11005e
99. Sieburth, S. M.; McGee, K. F.; Al-Tel, T. H. *J. Am. Chem. Soc.* **1998,** *120,* 587–588. doi:10.1021/ja973422q
100. Sieburth, S. M.; McGee, K. F., Jr.; Al-Tel, T. H. *Tetrahedron Lett.* **1999,** *40,* 4007–4010. doi:10.1016/s0040-4039(99)00671-1
101. Takao, K.-i.; Kai, H.; Yamada, A.; Fukushima, Y.; Komatsu, D.; Ogura, A.; Yoshida, K. *Angew. Chem., Int. Ed.* **2019,** *58,* 9851–9855. doi:10.1002/anie.201904404
102. Han, J.-c.; Li, F.; Li, C.-c. *J. Am. Chem. Soc.* **2014,** *136,* 13610–13613. doi:10.1021/ja5084927
103. Gil, A.; Albericio, F.; Álvarez, M. *Chem. Rev.* **2017,** *117,* 8420–8446. doi:10.1021/acs.chemrev.7b00144
104. Srinivasan, R.; Carlough, K. H. *J. Am. Chem. Soc.* **1967,** *89,* 4932–4936. doi:10.1021/ja00995a018
105. Smanski, M. J.; Peterson, R. M.; Huang, S.-X.; Shen, B. *Curr. Opin. Chem. Biol.* **2012,** *16,* 132–141. doi:10.1016/j.cbpa.2012.03.002
106. Zhang, Q.; Tiefenbacher, K. *Nat. Chem.* **2015,** *7,* 197–202. doi:10.1038/nchem.2181
107. Kim, S.-Y.; Zhao, P.; Igarashi, M.; Sawa, R.; Tomita, T.; Nishiyama, M.; Kuzuyama, T. *Chem. Biol.* **2009,** *16,* 736–743. doi:10.1016/j.chembiol.2009.06.007
108. Minami, A.; Tajima, N.; Higuchi, Y.; Toyomasu, T.; Sassa, T.; Kato, N.; Dairi, T. *Bioorg. Med. Chem. Lett.* **2009,** *19,* 870–874. doi:10.1016/j.bmcl.2008.11.108
109. Tazawa, A.; Ye, Y.; Ozaki, T.; Liu, C.; Ogasawara, Y.; Dairi, T.; Higuchi, Y.; Kato, N.; Gomi, K.; Minami, A.; Oikawa, H. *Org. Lett.* **2018,** *20,* 6178–6182. doi:10.1021/acs.orglett.8b02654
110. Meguro, A.; Motoyoshi, Y.; Teramoto, K.; Ueda, S.; Totsuka, Y.; Ando, Y.; Tomita, T.; Kim, S.-Y.; Kimura, T.; Igarashi, M.; Sawa, R.; Shinada, T.; Nishiyama, M.; Kuzuyama, T. *Angew. Chem., Int. Ed.* **2015,** *54,* 4353–4356. doi:10.1002/anie.201411923
111. Sato, H.; Teramoto, K.; Masumoto, Y.; Tezuka, N.; Sakai, K.; Ueda, S.; Totsuka, Y.; Shinada, T.; Nishiyama, M.; Wang, C.; Kuzuyama, T.; Uchiyama, M. *Sci. Rep.* **2015,** *5,* 18471. doi:10.1038/srep18471
112. Görner, C.; Häuslein, I.; Schrepfer, P.; Eisenreich, W.; Brück, T. *ChemCatChem* **2013,** *5,* 3289–3298. doi:10.1002/cctc.201300285

License and Terms

BEILSTEIN JOURNAL OF ORGANIC CHEMISTRY

Asymmetric synthesis of a stereopentade fragment toward latrunculins

Benjamin Joyeux[‡1], Antoine Gamet[‡1], Nicolas Casaretto[2] and Bastien Nay[*1]

Letter

Open Access

Address:
[1]Laboratoire de Synthèse Organique, Ecole Polytechnique, CNRS, ENSTA, Institut Polytechnique de Paris, 91128 Palaiseau, France and [2]Laboratoire de Chimie Moléculaire, Ecole Polytechnique, CNRS, Institut Polytechnique de Paris, 91128 Palaiseau, France

Email:
Bastien Nay[*] - bastien.nay@polytechnique.edu

* Corresponding author ‡ Equal contributors

Keywords:
allylation; aldol reaction; latrunculins; stereocontrol; total synthesis

Beilstein J. Org. Chem. **2023,** *19,* 428–433.
https://doi.org/10.3762/bjoc.19.32

Received: 15 December 2022
Accepted: 27 March 2023
Published: 03 April 2023

This article is part of the thematic issue "Total synthesis: an enabling science".

Associate Editor: D. Y.-K. Chen

Abstract

Latrunculins are marine toxins used in cell biology to block actin polymerization. The development of new synthetic strategies and methods for their synthesis is thus important in order to improve, modulate or control this biological value. The total syntheses found in the literature all target similar disconnections, especially an aldol strategy involving a recurrent 4-acetyl-1,3-thiazolidin-2-one ketone partner. Herein, we describe an alternative disconnection and subsequent stereoselective transformations to construct a stereopentade amenable to latrunculin and analogue synthesis, starting from (+)-β-citronellene. Key stereoselective transformations involve an asymmetric Krische allylation, an aldol reaction under 1,5-*anti* stereocontrol, and a Tishchenko–Evans reduction accompanied by a peculiar ester transposition, allowing to install key stereogenic centers of the natural products.

Introduction

Latrunculins constitute a class of marine polyketide natural products isolated from Sponges like *Negombata* (= *Latrunculia) magnifica* [1,2]. They are characterized by the presence of an unsaturated fourteen- or sixteen-membered macrolactone decorated by an L-cysteine-derived 2-oxo-1,3-thiazolidin-4-yl substitutent, and the presence of five stereogenic centers forming a 1,2,4,6,9-stereopentade (Figure 1). In latrunculins A (**1**) and B (**2**) three of them are embedded in a lactol ring, while latrunculin C (**3**) lacks this ring due to the reduction of C-15. The biological activities of latrunculins A and B have early been reported [3]. These compounds induce important but reversible morphological changes on mouse neuroblastoma and fibroblast cells at low concentrations such as 50 ng/ mL [2]. It was rapidly demonstrated that the toxins target the cytoskeleton and inhibit the actin polymerization by specifically sequestering the G-actin monomers with a high affinity [4], unlike cytochalasin D that targets the actin filament [5]. Structure–activity relationships have also been demonstrated thanks to the synthesis of an-

alogues, which hardly superseded the natural product properties, highlighting the importance of the macrocycle and of the lactol ring for this biological activity (**3** is inactive) [6,7].

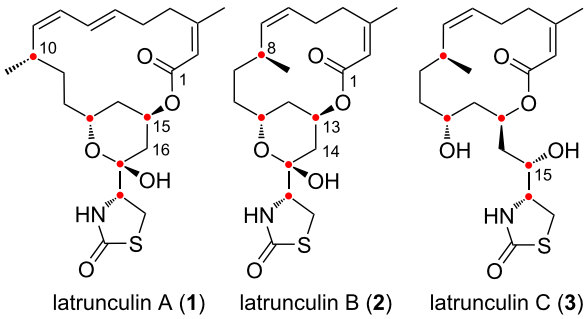

Figure 1: Structure of latrunculins (the red dots show the natural product stereopentade).

Considering the structural features of these toxins and their valuable biological properties (**1** and **2** are nowadays commercially available as tools for cell biology), latrunculins have been appealing targets for synthetic studies. Several total syntheses of latrunculins were reported by Smith III [8-10], White [11], Fürstner [6,12] and Watson [13]. These syntheses involved similar disconnection strategies for the macrocycle or the lactol formation (Figure 2, left), and for the aldol reaction leading to **4**, using a 4-acetyl-1,3-thiazolidin-2-one **5** as ketone partner (Figure 2, route A). Strikingly, this last disconnection was adopted in all previous syntheses to form the (15,16)- or the (13,14)-bond of **1** and **2**, respectively. Conversely, we envisaged an alternative disconnection to form the (16,17)- or the (14,15)-bond of **1** and **2**, through an aldol reaction of aldehyde **8** readily available from L-cysteine, leading to aldol adduct **7** (Figure 2, route B). The methyl ketone partner **9** could be formed by the oxidation of an allyl moiety introduced by the asymmetric allylation of an aldehyde derived from (+)-β-citronellene. At this stage, we can speculate that the stereocontrol of this reaction could either follow a polar Felkin–Anh model [14-16] based on chiral aldehyde partner **8** [17], or a 1,5-*anti* induction of the aldol reaction [18-20] based on chiral alkoxy partner **9**. Furthermore, it could be envisaged to reduce the resulting β-hydroxyketone **7** in a diastereoselective manner to obtain a 1,3-diol.

This synthetic strategy could thus bring new stereochemical opportunities to synthesize latrunculin analogues for chemical biology studies. In particular, our initial goal was to protect an inactive lactol-opened form of latrunculins, which could cyclize in vivo upon deprotection under a specific stimulus (light or enzyme, for instance) for biological applications. This challenge precluded the installation of the pyran ring – and the use of its well-known isomerization to set up important stereocenters

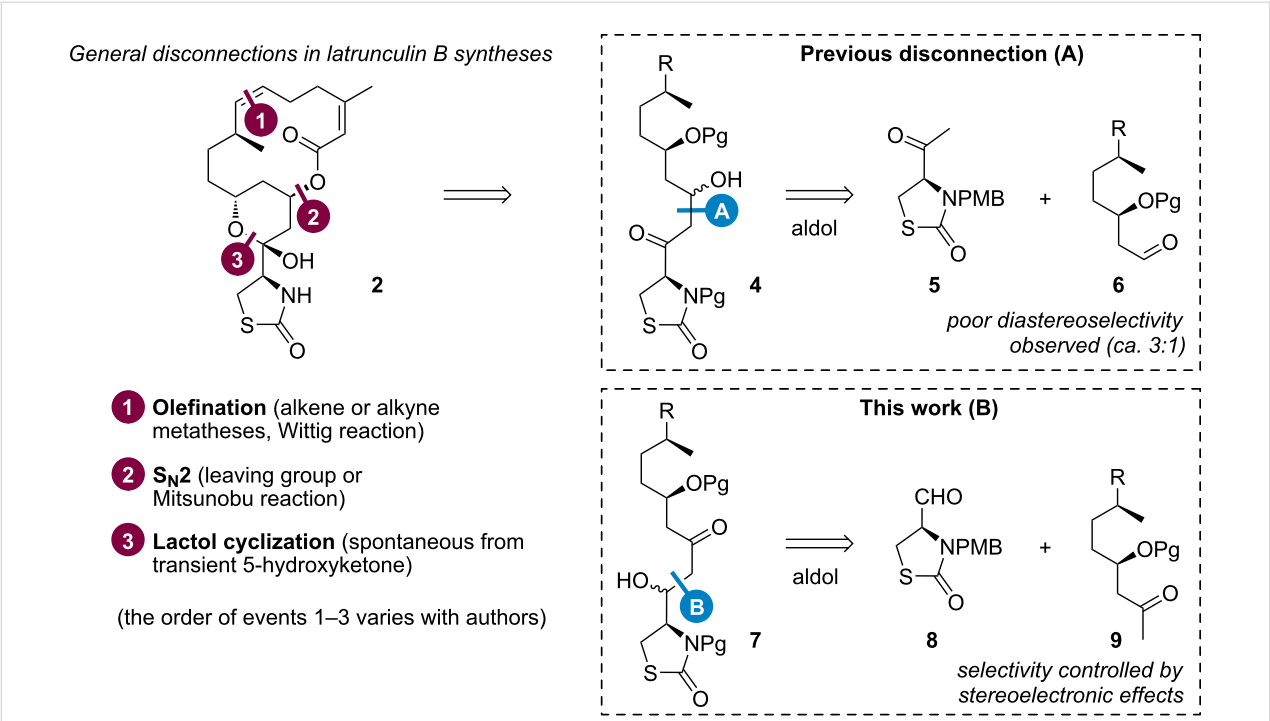

Figure 2: General strategy for latrunculin cycle disconnections (left), previous works towards linear precursor **4** (A), and our alternative disconnection of **7** through the aldol reaction (B).

[6,9] –, thus imposing the anticipated construction of key asymmetric centers. The following discussion will deal with the stereoselective synthesis of a stereopentade amenable to such latrunculin synthesis and the encountered difficulties thereof.

Results and Discussion

Our synthesis started from commercially available (+)-β-citronellene (**10**). The ozonolysis of the trisubstituted double bond followed by a reductive treatment with $NaBH_4$ chemoselectively afforded primary alcohol **11** in 78% yield (Scheme 1). Due to easier purification, this alcohol was preferred to the aldehyde in our synthetic route, allowing a key stereoselective Krische allylation [21,22] to be envisaged. Applying reported conditions for this allylation – in presence of allyl acetate (10 equiv), $[Ir(COD)Cl]_2$ (2.5 mol %), (*S*)-SEGPHOS (5 mol %), 3-nitrobenzoic acid (10 mol %), Cs_2CO_3 (20 mol %) in THF at 100 °C for 24 hours – we obtained homoallylic alcohol **12** in a good 86% yield, with a diastereomeric ratio (dr) of 93:7 deduced from the NMR analysis of the methyl substituent signals in CD_3OD (NMR spectra compared to those of a 50:50 mixture of diastereoisomers, obtained from the addition of allylmagnesium bromide onto the corresponding aldehyde). The stereochemistry of the resulting secondary alcohol was expected to be (*R*) according to Krische's studies involving (*S*)-SEGPHOS [22]. This result was secured by the NMR analysis of Mosher's esters made from (*R*)-(+)- and (*S*)-(−)-α-methoxy-α-trifluoromethylphenylacetic acid (MTPA) (see Supporting Information File 1) [23-25], confirming the installation of the C-11 stereocenter of latrunculins.

The next steps consisted in the functionalization of **12**, in view of its coupling to **8**. We first relied the chemoselective epoxidation of the homoallylic alcohol, done in presence of $VO(OiPr)_3$ (20 mol %) and *t*-BuOOH to afford epoxide **13**, in 86% yield and a dr of 75:25 (measured by NMR, presumably resulting from the major diastereoisomer of **13**; minor isomers were not identified), when the reaction was performed at room temperature during 6 hours. This vanadium catalyst superseded $VO(acac)_2$ in terms of yields [26,27]. Additional epoxidation attempts allowed to improve the dr to 82:18 (82% yield) when the reaction was left at −30 °C for 6 days. Unfortunately, it was not possible to set up an appropriate nucleophile through the umpolung of aldehyde **8** to react with this epoxide, which led us to envisage the following aldol strategy through ketone **15**. Attempts of Wacker reactions to produce **15** were unsuccessful on **12**, presumably due to a competition between the two olefinic parts. After protection of the secondary alcohol as a *para*-methoxybenzyl (PMB) ether (78% yield of **14**), the ketone (**15**) was installed in two steps from the epoxide (direct rearrangement attempts of the epoxide to form the ketone were unsuccessful). Thus, the epoxide was first reduced on its primary carbon in presence of $LiAlH_4$, and the resulting secondary alcohol was oxidized in presence of Dess–Martin periodinane (DMP), giving ketone **15** in 78% yield over the two steps. This six-step sequence to **15** was performed in a 35% overall yield from starting material **10**.

The aldehyde partner (**8**) for the aldol reaction brings the thiazolidinone heterocycle of the natural product. It was synthesized in four steps from L-cysteine ester derivative **16**, first reacting with carbonyldiimidazole (CDI) to afford thiazolidinone **17** in 85% yield (Scheme 2). The nitrogen atom was protected with a PMB group in 72% yield (**18**), after deprotonation with NaH and reaction with PMBBr. The ester moiety of **18** was then

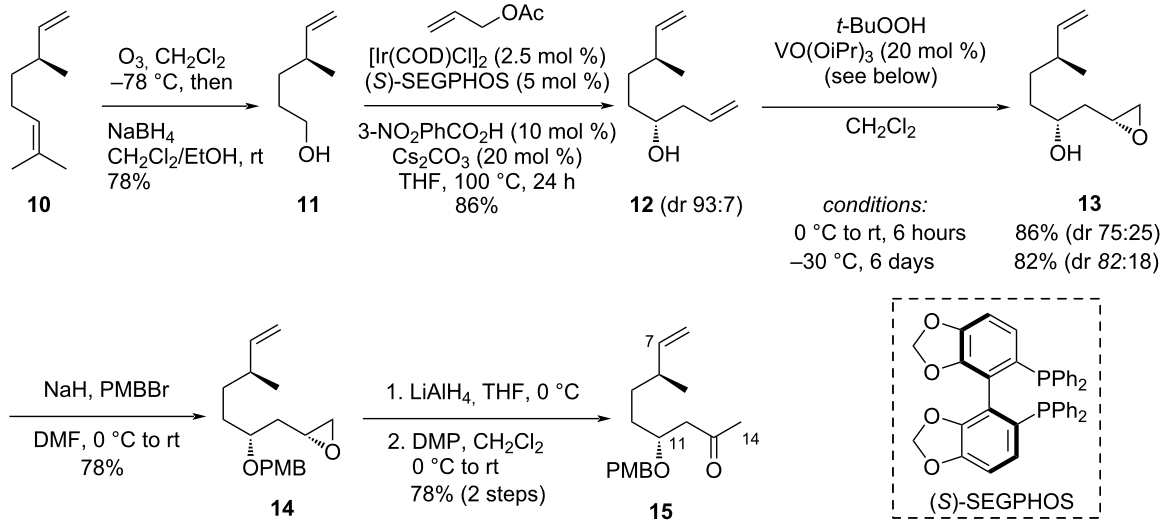

Scheme 1: Synthesis of fragment **15** from (+)-β-citronellene (**10**).

chemoselectively reduced into alcohol **19** in 90% yield, in presence of $LiBH_4$ to avoid the reduction of the thiazolidinone part. Finally, the aldehyde (**8**) was generated in 78% yield by oxidation in presence of DMP.

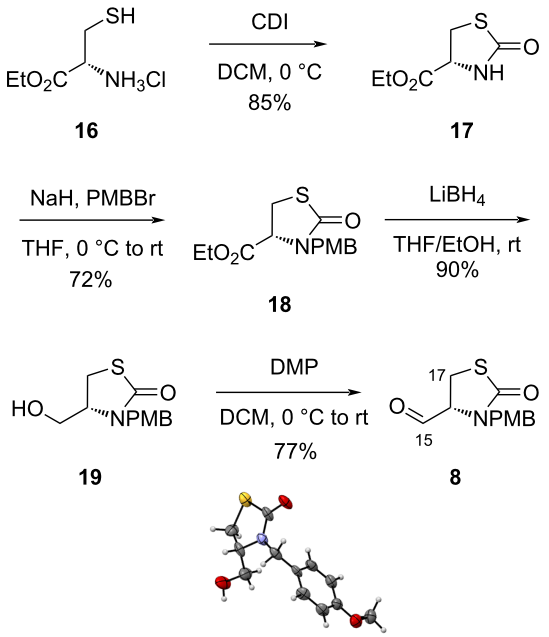

Scheme 2: Synthesis of fragment **8** from L-cysteine ethyl ester hydrochloride (**16**).

The assembly of aldehyde **8** and methyl ketone **15** was envisaged through a stereoselective aldol reaction. After unsuccessful attempts of Mukaiyama aldol reactions with silyl enol ethers [28], we found that dicyclohexylboron enolate **20**, made in situ from ketone **15** and Cy_2BCl in presence of DIPEA, performed well in the aldol reaction to furnish product **21** in 55% yield with a good dr of 91:9 (Scheme 3).

The stereocontrol of the reaction could be envisaged through two principal mechanisms. A remote stereocontrol by the nucleophile could first be expected [29], through a 1,5-*anti*-induction of the aldol stereocenter by β-alkoxy ketone **9**, leading to an (*S*)-configuration [18-20]. This control is supposed to follow a boat transition state **A** stabilized by a formyl hydrogen bond [30]. It is known to be dependent on the nature of the β-alkoxy substituent, being particularly favoured by the PMB and other aromatic groups, while being disfavoured by silyl protecting groups. Alternatively, an (*R*)-configuration of C-15 could result from a polar Felkin–Anh model controlled by aldehyde **8** through chair-transition state **B** [14-16]. To determine the configuration of C-15, we initially relied on the comparative NMR analysis of Mosher's esters [23]. Despite clear ^1H NMR spectra, irregular values of $\Delta\delta^{S-R}$ precluded the unambiguous determination of the C-15 stereocenter [24]. These difficulties were attributed to the hindered character of this secondary alcohol, substituted by the thiazolidinone ring, possibly leading to a strong conformational distortion of Mosher's model. The question of the resulting stereoselectivity was thus left open for later resolution.

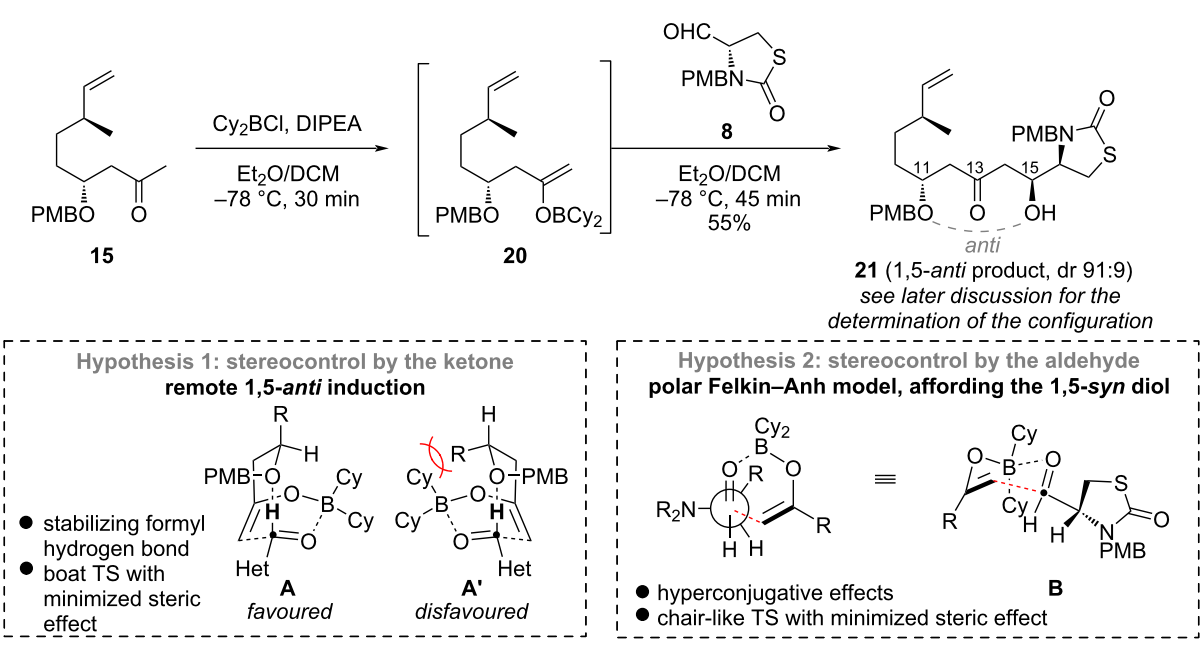

Scheme 3: Synthesis of fragment **21** through a stereoselective aldol reaction.

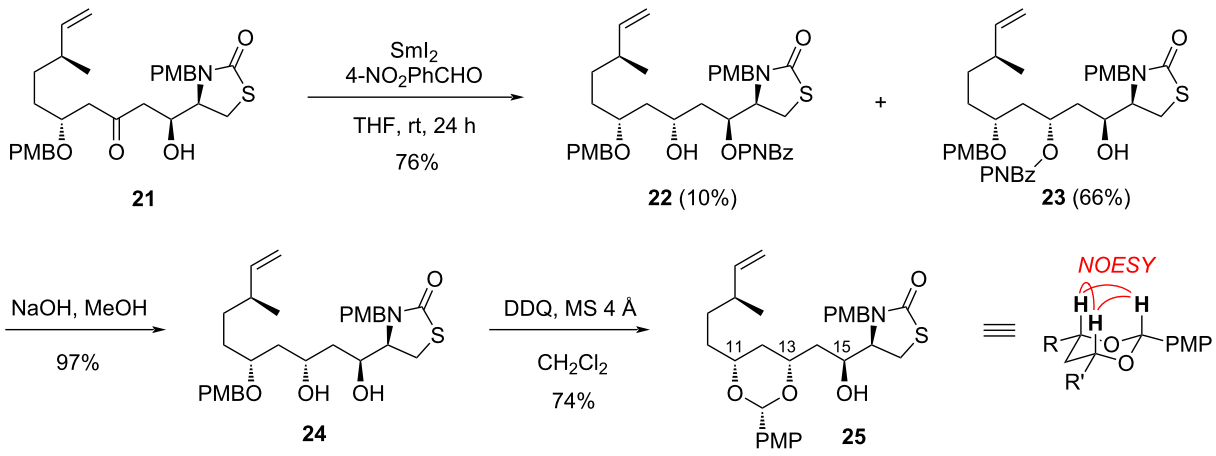

Scheme 4: 1,3-*Anti*-diastereoselective reduction of **21** with PNBz transposition, and final determination of the relative stereochemistry by NOESY experiment on **25**.

To complete this study, the 1,3-*anti*-diastereoselective reduction of β-hydroxyketone **21** was undertaken through the Evans–Tishchenko method [31,32], in presence of SmI_2 and an aldehyde (Scheme 4). *para*-Nitrobenzaldehyde was used [33] to introduce a labile *para*-nitrobenzoate on the product, planning an easy deprotection of the alcohol. This would also pave the way to an orthogonal manipulation of protecting groups on the stereopentade, in view of designing molecular tools for biological purpose. The reduction took place in 76% yield with complete stereoselectivity. However, a mixture of two inseparable products was obtained, containing the expected but minor alcohol **22** (10%), and more surprisingly the major isomer **23** (66%). This compound results from the transposition of the *para*-nitrobenzoyl (PNBz) group onto the 13-OH, which could be favoured by the steric hindrance of C-15 and a possible π–π stacking with the OPMB group.

These PNBz esters were readily hydrolyzed to furnished diol **24** in 97% yield. The oxydation of the PMB group, in presence of DDQ under anhydrous conditions [18], gratifyingly afforded acetal **25** in 74% yield, whose stereochemical assignment by NOESY NMR experiment showed the *syn* stereochemistry of the acetal. By deduction, it was confirmed that the asymmetric boron aldol reaction between **8** and **15** proceeded through a 1,5-*anti* induction by the ketone to form **21**. Most importantly, compounds **22**–**25** bear the (11*R*,13*R*) configuration of latrunculins (**1** and **2**).

Conclusion

A straightforward synthesis of a stereopentade intermediate towards latrunculins and lactol-opened analogues was achieved with high stereoselectivity. Starting from the chiral pool bringing the 8-methyl substituent, the secondary alcohol on C-11 was stereoselectively introduced by the Krische allylation of alcohol **11**. The next key step consisted in an aldol reaction of ketone **15** onto aldehyde **8**, which proceeded with a high stereocontrol resulting from a 1,5-*anti* induction by the nucleophile leading to product **21**, and excluding a Felkin–Anh control by the aldehyde. This reaction validates a unique disconnection among latrunculin synthetic strategies and avoids the construction of a 4-acetyl-1,3-thiazolidin-2-one. Finally, this β-hydroxyketone was submitted to the SmI_2-mediated Evans–Tishchenko reduction, which was performed with full 1,3-*anti*-stereocontrol but surprisingly resulted in the ester transposition to predominantly form alcohol **23** in good yields. This last reduction allowed to install the key (11*R*,13*R*) configuration of latrunculins.

Supporting Information

Crystallographic data of compound **19** were deposited in the Cambridge Crystallographic Data Center under the CCDC number 2225628.

Supporting Information File 1

Experimental procedures, compound characterizations and spectra.
[https://www.beilstein-journals.org/bjoc/content/supplementary/1860-5397-19-32-S1.pdf]

Supporting Information File 2

Crystallographic Information File of compound **19**.
[https://www.beilstein-journals.org/bjoc/content/supplementary/1860-5397-19-32-S2.cif]

Funding

We are grateful to CNRS, Ecole Polytechnique, and ANR (project N°ANR-22-CE44-0006) for financial supports. BJ and AG respectively acknowledge receipt of a Ph.D. grant from Ecole Polytechnique (2019-2022) and of a master internship grant from Labex CHARM3AT (2022).

ORCID® iDs

Antoine Gamet - https://orcid.org/0009-0001-7919-4324
Nicolas Casaretto - https://orcid.org/0000-0003-0636-983X
Bastien Nay - https://orcid.org/0000-0002-1209-1830

References

1. Kashman, Y.; Groweiss, A.; Shmueli, U. *Tetrahedron Lett.* **1980,** *21,* 3629–3632. doi:10.1016/0040-4039(80)80255-3
2. Groweiss, A.; Shmueli, U.; Kashman, Y. *J. Org. Chem.* **1983,** *48,* 3512–3516. doi:10.1021/jo00168a028
3. Spector, I.; Shochet, N. R.; Kashman, Y.; Groweiss, A. *Science* **1983,** *219,* 493–495. doi:10.1126/science.6681676
4. Coué, M.; Brenner, S. L.; Spector, I.; Korn, E. D. *FEBS Lett.* **1987,** *213,* 316–318. doi:10.1016/0014-5793(87)81513-2
5. Spector, I.; Shochet, N. R.; Blasberger, D.; Kashman, Y. *Cell Motil. Cytoskeleton* **1989,** *13,* 127–144. doi:10.1002/cm.970130302
6. Fürstner, A.; Kirk, D.; Fenster, M. D. B.; Aïssa, C.; De Souza, D.; Nevado, C.; Tuttle, T.; Thiel, W.; Müller, O. *Chem. – Eur. J.* **2007,** *13,* 135–149. doi:10.1002/chem.200601136
7. Amagata, T.; Johnson, T. A.; Cichewicz, R. H.; Tenney, K.; Mooberry, S. L.; Media, J.; Edelstein, M.; Valeriote, F. A.; Crews, P. *J. Med. Chem.* **2008,** *51,* 7234–7242. doi:10.1021/jm8008585
8. Zibuck, R.; Liverton, N. J.; Smith, A. B. *J. Am. Chem. Soc.* **1986,** *108,* 2451–2453. doi:10.1021/ja00269a056
9. Smith, A. B., III; Noda, I.; Remiszewski, S. W.; Liverton, N. J.; Zibuck, R. *J. Org. Chem.* **1990,** *55,* 3977–3979. doi:10.1021/jo00300a006
10. Williams, B. D.; Smith, A. B., III. *J. Org. Chem.* **2014,** *79,* 9284–9296. doi:10.1021/jo501733m
11. White, J. D.; Kawasaki, M. *J. Am. Chem. Soc.* **1990,** *112,* 4991–4993. doi:10.1021/ja00168a071
12. Fürstner, A.; De Souza, D.; Parra-Rapado, L.; Jensen, J. T. *Angew. Chem., Int. Ed.* **2003,** *42,* 5358–5360. doi:10.1002/anie.200352413
13. She, J.; Lampe, J. W.; Polianski, A. B.; Watson, P. S. *Tetrahedron Lett.* **2009,** *50,* 298–301. doi:10.1016/j.tetlet.2008.10.144
14. Chérest, M.; Felkin, H.; Prudent, N. *Tetrahedron Lett.* **1968,** *9,* 2199–2204. doi:10.1016/s0040-4039(00)89719-1
15. Anh, N. T.; Eisenstein, O. *Nouv. J. Chim.* **1977,** *1,* 61–70.
16. Mengel, A.; Reiser, O. *Chem. Rev.* **1999,** *99,* 1191–1224. doi:10.1021/cr980379w
17. Cee, V. J.; Cramer, C. J.; Evans, D. A. *J. Am. Chem. Soc.* **2006,** *128,* 2920–2930. doi:10.1021/ja0555670
18. Paterson, I.; Gibson, K. R.; Oballa, R. M. *Tetrahedron Lett.* **1996,** *37,* 8585–8588. doi:10.1016/0040-4039(96)01962-4
19. Evans, D. A.; Coleman, P. J.; Côté, B. *J. Org. Chem.* **1997,** *62,* 788–789. doi:10.1021/jo962417m
20. Dias, L. C.; Aguilar, A. M. *Chem. Soc. Rev.* **2008,** *37,* 451–469. doi:10.1039/b701081h
21. Kim, I. S.; Ngai, M.-Y.; Krische, M. J. *J. Am. Chem. Soc.* **2008,** *130,* 6340–6341. doi:10.1021/ja802001b
22. Kim, I. S.; Ngai, M.-Y.; Krische, M. J. *J. Am. Chem. Soc.* **2008,** *130,* 14891–14899. doi:10.1021/ja805722e
23. Dale, J. A.; Mosher, H. S. *J. Am. Chem. Soc.* **1973,** *95,* 512–519. doi:10.1021/ja00783a034
24. Seco, J. M.; Quiñoá, E.; Riguera, R. *Chem. Rev.* **2004,** *104,* 17–118. doi:10.1021/cr000665j
25. Hoye, T. R.; Jeffrey, C. S.; Shao, F. *Nat. Protoc.* **2007,** *2,* 2451–2458. doi:10.1038/nprot.2007.354
26. Mihelich, E. D.; Daniels, K.; Eickhoff, D. J. *J. Am. Chem. Soc.* **1981,** *103,* 7690–7692. doi:10.1021/ja00415a067
27. Zhang, W.; Yamamoto, H. *J. Am. Chem. Soc.* **2007,** *129,* 286–287. doi:10.1021/ja067495y
28. Matsuo, J.-i.; Murakami, M. *Angew. Chem., Int. Ed.* **2013,** *52,* 9109–9118. doi:10.1002/anie.201303192
29. Roush, W. R. *J. Org. Chem.* **1991,** *56,* 4151–4157. doi:10.1021/jo00013a015
30. Paton, R. S.; Goodman, J. M. *Org. Lett.* **2006,** *8,* 4299–4302. doi:10.1021/ol061671q
31. Evans, D. A.; Hoveyda, A. H. *J. Am. Chem. Soc.* **1990,** *112,* 6447–6449. doi:10.1021/ja00173a071
32. Ralston, K. J.; Hulme, A. N. *Synthesis* **2012,** *44,* 2310–2324. doi:10.1055/s-0032-1316544
33. Jiang, Y.; Hong, J.; Burke, S. D. *Org. Lett.* **2004,** *6,* 1445–1448. doi:10.1021/ol049701h